UNIVERSITY OF CALIFORNIA
RIVERSIDE

Systematic Research on Minute Litter Bugs Dipsocoromorpha With Emphasis on Schizopteridae (Hemiptera: Heteroptera)

A Dissertation submitted in partial satisfaction
of the requirements for the degree of

Doctor of Philosophy

in

Entomology

by

Alexander Knyshov

December 2018

Dissertation Committee:

Dr. Christiane Weirauch, Chairperson
Dr. John Heraty
Dr. Timothy Paine
Dr. Mark Springer

The Dissertation of Alexander Knyshov is approved:

Committee Chairperson

University of California, Riverside

Acknowledgments

I would to thank the following individuals and institutions who have kindly loaned or donated the material for my research: Ruth Salas and Toby Schuh (AMNH), Mick Webb (BMNH), Vasily Grebennikov (CNC), Pavel Štys (CUNI), James Boone, Rebekah Baquiran, and Margaret Thayer (FMNH), Susan Halbert (FSCA), Jim Lewis (INBio), Giar-Ann Kung (LACM), Peter Schwendinger and John Hollier (MHNG), Edward Riley (TAMU), Steve Heydon (UCD), Tom Henry (USNM), Serguei V. Triapitsyn and Doug Yanega (UCRC), Edward Riley (TAMU), Fedor Konstantinov (ZISP), Michael Ivie (MTEC), Christopher Grinter (CAS), Norm Penny and Brian Fisher (CAS), Simon van Noort (SAM), Daniela Takiya (UFRJ), and Thailand Inventory Group for Entomological Research (TIGER) Project. Robin Delapena (FMNH) and Walter Winn (FSCA) helped with sorting lots of bulk samples and recovering many of the specimens used in this study. I am grateful to Serguei Triapitsyn and Vladimir Berezovskiy (UCR) for training me and helping with permanent slide-mounting of specimens and István Mikó (Penn State) for advice on confocal microscopy.

I thank the Heteropteran Systematics Lab undergraduates Bridget Gonzales, Walena Logan, Brian Vanderveer, Christy Hoong, Ishani Richardson, Joanna Mai, Michelle Ly, Kyle Whorrall for their help with specimen processing, including sorting and databasing. Members of the Weirauch lab, including Rochelle Hoey-Chamberlain, Stephanie Leon, Michael Forthman, Junxia Zhang, Eric Gordon, Paul Masonick, Madison Hernandez, Carlos Rosas, Samantha Smith, Stephanie Castillo, are acknowledged for help throughout my PhD and comments and suggestions on the manuscript drafts. Additionally, members

of the Heraty lab are thanked for reviewing some of my manuscripts. I am very grateful to Rochelle Hoey-Chamberlain and Eric Gordon for a lot of help with specimen processing and various research ideas.

I would also like to thank my dissertation committee members, Dr. John Heraty, Dr. Timothy Paine, and Dr. Mark Springer, for their guidance and help. Especially, I would like to thank Dr. Christiane Weirauch for all the help and support she provided to me during my time at UCR. I am thankful that she has given me an opportunity to extend my PhD research beyond what was originally proposed and experiment with new research ideas.

The following funding sources are acknowledged: the US National Science Foundation grant "ARTS: Litter Bugs: revisionary and phylogenetic research on the least studied true bug infraorder (Insecta: Hemiptera: Dipsocoromorpha)" project (DEB-1257702), awarded to Christiane Weirauch; the UCR seed grant "Unlocking the Vault of SoCal Biota" awarded to Christiane Weirauch, Amy Litt, and John Heraty; a Dean's Distinguished Fellowship, a Dr. Mir S. Mulla and Lelia Mulla Endowed Scholarship, and a UCR Dissertation Research Grant awarded to me.

The text of this dissertation, in part or in full, is a reprint of the material as it appears in Knyshov *et al.* (2016) and Knyshov *et al.* (2018). The co-author Christiane Weirauch listed in those publications directed and supervised the research which forms the basis for this dissertation.

ABSTRACT OF THE DISSERTATION

Systematic Research on Minute Litter Bugs Dipsocoromorpha With Emphasis on Schizopteridae (Hemiptera: Heteroptera)

by

Alexander Knyshov

Doctor of Philosophy, Graduate Program in Entomology
University of California, Riverside, December 2018
Dr. Christiane Weirauch, Chairperson

Dipsocoromorpha, or the minute litter bugs, are a poorly studied and minuscule group of true bugs (Hemiptera: Heteroptera) with uncertain phylogenetic position, often bizarre morphology, and substantial undescribed biodiversity. A combination of taxonomic revisions, comparative morphological studies, and phylogenetic analyses based on both morphological and molecular data is employed to advance our knowledge of the group. The first chapter taxonomically revises the New World genus *Chinannus* and describes 26 new species. The second chapter develops and tests a cost-efficient DNA sequencing method for archival specimens. The third chapter uses and refines this method to conduct a comprehensive phylogenetic analysis of a very diverse group of dipsocoromorphans, the *Corixidea* genus group. The fourth chapter taxonomically revises the genus *Voragocoris* that belongs to the *Corixidea* genus group, building on the phylogeny inferred in chapter three, and describing seven new species. The fifth chapter conducts a

comparative study of abdominal morphology in Dipsocoromorpha, and both standardizes the terminology and proposes primary homology hypotheses, that could be used for a phylogenetic reconstruction. The sixth, and last, chapter presents a comprehensive phylogenetic analysis of Dipsocoromorpha based on both morphological and molecular data.

Table of contents

List of Tables

List of Figures

Introduction

The infraorder Dipsocoromorpha, or minute litter bugs, is the least studied of the seven infraorders of Heteroptera. Representatives of the infraorder are small, typically 1-2 mm true bugs that mostly inhabit tropical regions of the world with few species living in temperate climates. The group includes ~435 described species (Costas *et al.* 2015; Hill 2013, 2014; Hoey-Chamberlain & Weirauch 2016; Josifov 1967; Knyshov *et al.* 2016; Leon & Weirauch 2016b; a; Linnavuori 1966, 1974; Makhan 2013b; a; Poinar & Brown 2014; Ren & Zheng 1992; Štys 1983; Weirauch 2012; Weirauch *et al.* 2017, 2018; Weirauch & Frankenberg 2015; Weirauch & Štys 2014) in five families: Ceratocombidae, Dipsocoridae, Hypsipterygidae, Schizopteridae, and Stemmocryptidae. The families are morphologically distinctive, but most members share the following diagnostic features: small body size (under 2.5 mm), long and thin flagellomeres with long setae, membranous forewings, and, except some Ceratocombidae and Dipsocoridae, metacoxal adhesive pads (Schuh & Slater 1995; Štys 1970, 1983). A unique modification of the excretory system (Miyamoto 1961) and the structure of the egg (Cobben 1968) were also claimed to be unique among Heteroptera, but were studied only for one genus (the former), and five genera in three families (the latter). The families Hypsipterygidae (Drake 1961) and Stemmocryptidae (Štys 1983), with five and one species, respectively, were described relatively recently from the tropics of the Old World (Drake 1961; Rédei 2007; Štys 1970, 1983). Dipsocoridae are found in all biogeographic regions and include three genera and ~30 described species (Henry 1988b; Kerzhner 1995), with approximately half of the species known from temperate zones. Ceratocombidae contain

seven genera and ~50 species and inhabit all biogeographic regions, with about one third of the species known from temperate climates (Henry 1988a; Kerzhner 1995). Lastly, Schizopteridae is the largest family with ~60 genera and ~355 species that are primarily found in the tropics with only four species known from temperate zones (Drake 1961; Emsley 1969; Henry 1988c; Hill 2013, 2014, 2015; Hoey-Chamberlain & Weirauch 2016; Kerzhner 1995; Knyshov *et al.* 2016; Leon & Weirauch 2016b; a; Linnavuori 1966, 1974; Makhan 2013b; a; Poinar & Brown 2014; Ren & Zheng 1992; Štys 1970, 1982, 1985; Weirauch 2012; Weirauch *et al.* 2017, 2018; Weirauch & Frankenberg 2015; Weirauch & Štys 2014). Minute litter bugs are primarily collected in leaf litter and soil detritus, but have also been found on vegetation, under tree bark, in the interstitial zone of streams, and even in mangroves (Emsley 1969; McAtee & Malloch 1925). Collection-method data summarized based on samples sorted in the Weirauch lab (Knyshov *et al.* 2016; Leon & Weirauch 2016b; Weirauch & Frankenberg 2015) indicates that besides leaf litter sifting, other methods such as Malaise traps, flight intercept traps, and pan traps are effective in catching minute litter bugs.

The small body size of litter bugs and their cryptic habits are the primary reasons why the infraorder is so poorly studied. Despite the modest number of described species, a large undescribed diversity, particularly in the tropics, remains to be documented. Even taxonomic studies that have focused on very restricted geographic areas have revealed astounding species-level diversity, e.g., Emsley (1969) who described 28 out of 64 species in the genus *Schizoptera* Fieber from the island of Trinidad. Similarly, a number of new species was recently added (Hill 1990a; b, 1992; Rédei 2008; Rédei *et al.* 2012;

Štys 1985) to genera that had been described in the middle of 20th century based on one or few species (e.g., *Ogeria* Distant, *Kokeshia* Miyamoto, *Pachyplagia* Gross, *Pachyplagioides* Gross). In the genus *Hypselosoma* Reuter with 18 previously known species, 19 new species were described from New Caledonia (Hill 2013). One of the most recent taxonomic studies on Schizopteridae revised the genus *Silhouettanus* and increased the number of species from one to 10 (Hill 2014). Additionally, the material assembled in the Weirauch lab also shows substantial undescribed diversity of Dipsocoromorpha and has so far resulted in several taxonomic publications, significantly increasing the number of described species (Hoey-Chamberlain & Weirauch 2016; Knyshov *et al.* 2016; Leon & Weirauch 2016b; a; Weirauch *et al.* 2017, 2018; Weirauch & Frankenberg 2015).

The diversity of structural features in minute litter bugs is astounding and includes variation in head and labium morphology, forewing venation, male genitalia, but also so-called "male-specific organs". Male-specific organs have only been documented for a few genera of Schizopteridae (some Hypselosomatinae, *Chinannus*, *Ogeria*, *Pachyplagioides*, *Kaimon* Hill, and *Voragocoris* Weirauch), are restricted to the males, and refer to an assemblage of non-homologous morphological features that can be located on the head, thorax, wings, or abdomen (China 1946; Hill 1984, 1990b, 1992, 2004, 2013; Weirauch 2012). The term "organ" is here used in combination with the body part on which the structure is located, following Hill, e.g., "vertex organ" (Hill 2004) or "labral organ" (Hill 2013). Typically, these structures with unknown functions were documented only as line drawings, but Hill (1992) and Weirauch (2012) provided scanning electron micrographs for the male-specific organ in *Pachyplagioides* and

Voragocoris, respectively. In some cases, the presence of male-specific organs was used as a species or genus delimiting character (i.e., in *Membracioides* McAtee and Malloch and *Voragocoris*). No study has so far attempted a detailed comparative morphological documentation of these structures. The material assembled at UCR shows that many undescribed species in the subfamilies Hypselosomatinae, Ogeriinae, and the *Corixidea* genus group have such organs. Moreover, male-specific organs can have similar location in species belonging to taxonomically distant groups (Knyshov *et al.* unpublished). Homology hypotheses of the vertex organs (between *Kaimon* and the *Corixidea* group), the pronotal organs (between the *Corixidea* group and undescribed Hypselosomatinae), the wing organs (e.g., between *Ogeria* and undescribed New World Ogeriinae) were never tested.

Another morphological feature of Dipsocoromorpha in general, and Schizopteridae in particular, is the variation of wing structure and the sexual dimorphism that can be associated with the former. Most species of litter bugs have fore- and hind wings that are fully developed in both sexes, with forewings being membranous (Schuh & Slater 1995). The forewings in Hypsipterygidae show a unique venation within the infraorder. Several species of Ceratocombidae and Dipsocoridae have brachypterous wings in both sexes, and in the ceratocombid tribe Issidomimini striking sexual dimorphism is known with macropterous males and coleopteroid females. Coleopteroid females have convex beetle-like elytra that are usually heavily sclerotized, and their hind wings are always absent. In Schizopteridae, the number of different wing type combinations across sexes is even higher (Knyshov *et al.* unpublished), with both males and females displaying a range

from macroptery to brachyptery and coleopteroidy. In certain genera (e.g., *Chinannus*) all species exhibit coleopteroidy, whereas in others (e.g., the *Corixidea* genus group or *Schizoptera*) only some do (Leon & Weirauch 2017). However, no study has formally analyzed the distribution of different wing types across the infraorder or tested the hypothesis of multiple origins of coleopteroidy in Dipsocoromorpha.

Distribution patterns of Dipsocoromorpha are poorly documented (e.g., Schuh & Slater 1995). Species are known from all continents except Antarctica for each of the three larger families. Within families, at least some genera appear to be distributed across several continents. In Ceratocombidae, two out of seven described genera are distributed worldwide, one is confined to the Old World tropics, two are known only from the Afrotropical region, and two are restricted to the Indo-Pacific region. One out of the three Dipsocoridae genera, *Alpagut* Kiyak is confined to the Palearctic, *Pachycoleus* Fieber – to the Palearctic and Afrotropical regions, whereas species of *Cryptostemma* Herrich-Schaeffer occur worldwide. In Schizopteridae, almost all genera are restricted to one biogeographic region: approximately 45% of the genera are known only from the Indo-Pacific region, 40% occur in the New World tropics, and about 15% are described from the Afrotropical region. Exceptions include the genus *Pinochius* Carayon that was recorded from Southeast Asia in addition to the Afrotropical region (Rédei 2008) and the genus *Kokeshia* that is known from Africa and Southeast Asia (Weirauch *et al.* unpublished). Known distribution ranges for tropical species are often small or even restricted to the type locality (Emsley 1969; Leon & Weirauch 2016b; Weirauch & Frankenberg 2015). Many Ceratocombidae, Dipsocoridae, and Schizopteridae from

temperate zones appear to have fairly wide ranges (Henry *et al.* 2010; Hoffman *et al.* 2007), although this may be an artifact resulting from poorly diagnosed and delimited species that actually represent groups of closely related species. Male genitalia that supply excellent species-diagnostic features in many taxa have only been documented for one out of four species of North American Schizopteridae and have not been studied for the single North American ceratocombid species. Species may therefore have smaller ranges, similar to the situation seen in tropical litter bugs.

My dissertation includes two taxonomic projects, two phylogenetic studies, a research project aimed at adopting a previously developed method for DNA sequencing for use on small archival insect specimens, and a comparative morphological study. Chapter one focuses on a taxonomic revision of the genus *Chinannus*. The genus *Chinannus* currently accommodates two species, *Chinannus bierigi* Wygodzinsky and *Chinannus trinitatis* (China) from Costa Rica and Trinidad, respectively (China 1946; Wygodzinsky 1948). Unique morphological features, uncertain phylogenetic placement, and tremendous undescribed diversity (26 new species were discovered in the assembled material) made the genus important for a taxonomic study.

Gathering genetic data for rare species is one of the biggest remaining obstacles in modern phylogenetics, particularly for megadiverse groups such as arthropods. Next generation sequencing techniques allow for sequencing of short DNA fragments contained in preserved specimens >20 years old, but approaches such as whole genome sequencing are often too expensive for projects including many taxa. The second chapter explores utilization of in-house generated DNA baits to capture commonly utilized

mitochondrial and ribosomal DNA loci from insect museum specimens of various age and preservation types without the a priori need to know the sequence of the target loci.

The third chapter applies a protocol of sequencing archival specimens refined in chapter two to the *Corixidea* genus group. The group currently contains six described genera and 18 species from Central and South America. Generic limits within the group continue to be unsatisfactory, which became evident upon examination of >2,000 specimens assembled at UCR. This collection also shows enormous undescribed diversity of the *Corixidea* group, with ~150 undescribed species. Cost-efficient DNA sequencing is used to produce a comprehensive dataset and involve as much material of suboptimal quality (i.e. old point-mounted and trap residue-derived samples) as possible. The obtained phylogeny is instrumental for the upcoming taxonomic revisions of the group.

The fourth chapter utilizes the phylogenetic reconstruction, obtained in the chapter three, to revise one of the genera of the *Corixidea* genus group, the genus *Voragocoris*. This recently described genus previously contained only two species known from Peru and Suriname, respectively, however seven more species were discovered, significantly extending both our knowledge of the distribution ranges and variation of male-specific morphology.

The fifth chapter of my dissertation focuses on the study of male genitalia across Dipsocoromorpha. Male genitalic characters in litter bugs are known to be diagnostic for genera or generic groups within Dipsocoromorpha (Emsley 1969; Štys 1970). At the same time, male genitalia demonstrate a strong degree of asymmetry, and a presence of processes and appendages on pregenital and postgenital abdominal segments, both highly

unusual within Heteroptera. Moreover, the homology of pregenital and postgenital abdominal processes can be hard to discern, as similar processes can be actually formed by different segments. Few studies have so far included a comparative survey of male genitalic structures across the family or infraorder (i. e., Emsley 1969; Štys 1970), and none were comprehensive or attempted to test the homology of male abdominal structures.

In the last chapter, a phylogenetic analysis of the infraorder Dipsocoromorpha is performed. The current classification of the infraorder was proposed more than 30 years ago (Štys 1983) based on morphological evidence, and the proposed decisions remain untested. The involvement of contemporary phylogenetic methods will allow to propose and objectively test the relationships within Dipsocoromorpha, as well as subsequently inform the classification. The analysis will use molecular and morphological data, and focus on addressing problematic points in the classification, including the unresolved relationships between families (Štys 1983), and between schizopterid subfamilies (e.g., Hill 2004). It will also test the monophyly of all family-, subfamily-, and tribal-level taxa within the infraorder, as well as the proposed groups of genera within Schizopteridae (Emsley 1969).

References

China, W.E. (1946) New Cryptostemmatidae (Hemiptera) from Trinidad, British West Indies. *Proceedings of the Royal Entomological Society of London (B)* 15, 148–154.

Cobben, R.H. (1968) *Evolutionary Trends in Heteroptera. Part I. Eggs. Architecture of the Eggs, Architecture of the Shell, Gross Embryology and Eclosion. R. H. Cobben.* Centre for Agricultural Publications and Documentation, Wageningen, The Netherlands, 1968. viii + 476 pp.

Costas, M., Lopez, T. & Vazquez, M.A. (2015) Parque Nacional de la Isla de Coiba, Panamá. *Heteropterus Revista de Entomologia* 15, 101–109.

Drake, C.J. (1961) A new subfamily, genus and two new species of Dipsocoridae (Hemiptera). *Publicacoes Culturais da Companhia de Diamantes de Angola*, 77–80.

Emsley, M.G. (1969) The Schizopteridae (Hemiptera: Heteroptera) with the descriptions of new species from Trinidad. *Memoirs of the American Entomological Society* 25, 1–154.

Henry, T.J. (1988a) Family Ceratocombidae Fieber, 1861. The ceratocombids. In: *Catalog of the Heteroptera, or true bugs, of Canada and the continental United States.* E.J. Brill, Leiden, New York etc., pp. 61–63.

Henry, T.J. (1988b) Family Dipsocoridae Dohrn, 1859 (=Cryptostemmatidae McAtee and Malloch, 1925). The dipsocorids. In: *Catalog of the Heteroptera, or true bugs, of Canada and the continental United States.* E.J. Brill, Leiden, New York etc., pp. 130–131.

Henry, T.J. (1988c) Family Schizopteridae Reuter, 1891. The Schizopterids. *Catalog of the Heteroptera, or True Bugs, of Canada and the Continental United States. EJ Brill, Leiden*, 682–683.

Henry, T.J., Hevel, G.F. & Chordas, S.W. (2010) Additional records of the little-known *Corixidea major* (Heteroptera: Schizopteridae) from Arkansas and Oklahoma. *Proceedings of the Entomological Society of Washington* 112, 475–477.

Hill, L. (1984) New genera of Hypselosomatinae (Heteroptera: Schizopteridae) from Australia. *Australia Journal of Zoology, Supplementary Series* 103, 1–55.

Hill, L. (1990a) A revision of Australian *Pachyplagia* Gross (Heteroptera: Schizopteridae). *Invertebrate Systematics* 3, 605–617.

Hill, L. (1990b) Australian *Ogeria* Distant (Heteroptera: Schizopteridae). *Invertebrate Systematics* 4, 697–720.

Hill, L. (1992) A revision of *Pachyplagioides* Gross (Heteroptera: Schizopteridae). *Invertebrate Systematics* 6, 245–260.

Hill, L. (2004) *Kaimon* (Heteroptera: Schizopteridae), a new, speciose genus from Australia. *Memoirs of the Queensland Museum* 49, 603–647.

Hill, L. (2013) A revision of *Hypselosoma* Reuter (Insecta: Heteroptera: Schizopteridae) from New Caledonia. *Memoirs of the Queensland Museum* 56, 407–455.

Hill, L. (2014) Revision of *Silhouettanus* with description of nine new species (Hemiptera: Heteroptera: Schizopteridae). *Zootaxa* 3815, 353–385.

Hill, L. (2015) Three new genera of Schizopteridae from Australia with description of six new species (Hemiptera: Heteroptera: Schizopteridae). *Zootaxa* 3990, 73–96.

Hoey-Chamberlain, R. & Weirauch, C. (2016) Two new genera of big-eyed minute litter bugs (Hemiptera, Schizopteridae, Hypselosomatinae) from Brazil and the Caribbean. *ZooKeys*, 79–102.

Hoffman, R.L., Roble, S.M. & Henry, T.J. (2007) First records of the rarely collected bug *Nannocoris arenarius* from Georgia, North Carolina, and Virginia (Heteroptera: Schizopteridae). *Banisteria* 30, 38–39.

Josifov, M. (1967) Zur Systematik der Gattung *Cryptostemma* H.-S. (Heteroptera). *Annales Zoologici Warszawa* 25, 215–226.

Kerzhner, I.M. (1995) Infraorder Dipsocoromorpha. In: *Catalogue of Palearctic Heteroptera. Volume 1: general introduction: Enicocephalomorpha & Dipsocoromorpha, Nepomorpha, Gerromorpha & Leptopodomorpha.* Netherlands Entomological Society, pp. 6–12.

Knyshov, A., Leon, S., Hoey-Chamberlain, R. & Weirauch, C. (2016) *Pegs, pouches, and spines: systematics and comparative morphology of the New World litter bug genus Chinannus Wygodzinsky, 1948*. Entomological Society of America, Annapolis, MD.

Leon, S. & Weirauch, C. (2016a) Scratching the surface? Taxonomic revision of the subgenus *Schizoptera* (*Odontorhagus*) reveals vast undocumented biodiversity in the largest litter bug genus *Schizoptera* Fieber (Hemiptera: Dipsocoromorpha). *Zootaxa* 4184, 30.

Leon, S. & Weirauch, C. (2016b) Small Bugs, Big Changes: Taxonomic Revision of *Orthorhagus* McAtee & Malloch. *Neotropical Entomology*, 1–14.

Leon, S. & Weirauch, C. (2017) Molecular phylogeny informs generic and subgeneric concepts in the *Schizoptera* Fieber genus group (Heteroptera: Schizopteridae) and reveals multiple origins of female-specific elytra. *Invertebrate Systematics* 31, 191–207.

Linnavuori, R. (1966) Two new Heteroptera species from Egypt. *Suomen Hyonteistieteellinen Aikakauskirja* 32, 263–264.

Linnavuori, R. (1974) Hemiptera of the Sudan, with remarks on some species of the adjacent countries. Families Cryptostemmatidae, Cimicidae, Polyctenidae, Joppeicidae, Reduviidae, Pachynomidae, Nabidaea, Leptopodidae, Saldidae, Henicocephalidae and Berytidae. *Annales Entomologici Fennici* 42, 116–138.

Makhan, D. (2013a) *Voragocoris amrishi* sp. nov., a new Schizopterinae (Hemiptera: Heteroptera: Schizopteridae) from Suriname. *Calodema* 293, 1–4.

Makhan, M. (2013b) *Soekhnandanius aschne* gen. et sp. nov., Schizopterinae (Hemiptera: Heteroptera: Schizopteridae) from Suriname. *Calodema* 291, 1–3.

McAtee, W.L. & Malloch, J.R. (1925) Revision of bugs of the family Cryptostemmatidae in the collection of the United States National Museum. *Proceedings of the United States National Museum* 67, 1–42.

Miyamoto, S. (1961) Comparative morphology of alimentary organs of Heteroptera, with the phylogenetic consideration. *Sieboldia* 2, 197–260.

Poinar, G.J. & Brown, A. (2014) New genera and species of Jumping Ground Bugs (Hemiptera: Schizopteridae) in Dominican and Burmese amber, with a description of a meloid (Coleoptera: Meloidae) triungulin on a Burmese specimen. *Annales de la Société entomologique de France (N.S.): International Journal of Entomology* 50, 372–381.

Rédei, D. (2007) A new species of the family Hypsipterygidae from Vietnam, with notes on the hypsipterygid fore wing venation (Heteroptera, Dipsocoromorpha). *Deutsche Entomologische Zeitschrift* 54, 43–50.

Rédei, D. (2008) Two new species of *Kokeshia* from India and Thailand (Hemiptera: Heteroptera: Schizopteridae). *Acta Entomologica Musei Nationalis Pragae* 48, 241–250.

Rédei, D., Ren, S. & Bu, W. (2012) Two new species of *Kokeshia* from China (Hemiptera: Heteroptera: Schizopteridae). *Zootaxa* 3497, 29–36.

Ren, S. & Zheng, L. (1992) New species and new record of Dipsocoromorpha (Hemiptera: Heteroptera) from China. *Entomotaxonomia* 14, 187–196.

Schuh, R.T. & Slater, J.A. (1995) *True bugs of the world (Hemiptera: Heteroptera): classification and natural history*. Comstock Publishing Associates, Cornell University Press.

Štys, P. (1970) On the morphology and classification of the family Dipsocoridae s. lat., with particular reference to the genus *Hypsipteryx* Drake (Heteroptera). *Acta Entomologica Bohemoslovaca* 67, 21–46.

Štys, P. (1982) A new genus and species of Schizopteridae with porrect head from Papua New Guinea (Heteroptera). *Acta Entomologica Bohemoslovaca* 79, 450–456.

Štys, P. (1983) A new family of Heteroptera with dipsocoromorphan affinities from Papua New Guinea. *Acta Entomologica Bohemoslovaca* 80, 256–292.

Štys, P. (1985) Two new species of *Kokeshia* (Heteroptera, Schizopteridae) from Nepal and appraisal of alleged synapomorphies of Paraneoptera. *Acta Entomologica Bohemoslovaca* 82, 187–205.

Weirauch, C. (2012) *Voragocoris schuhi*, a new genus and species of Neotropical Schizopterinae (Hemiptera: Schizopteridae). *Entomologia Americana* 118, 285–294.

Weirauch, C. & Frankenberg, S. (2015) From "insect soup" to biodiversity discovery: taxonomic revision of *Peloridinannus* Wygodzinsky, 1951 (Hemiptera: Schizopteridae), with description of six new species. *Arthropod Systematics and Phylogenetics* 73(3), 457–475.

Weirauch, C., Knyshov, A. & Hoey-Chamberlain, R. (2017) *Machadonannus brailovskyi*, n. sp., a new species of Schizopteridae from the Afrotropical region. *Dugesiana* 24, 279–286.

Weirauch, C. & Štys, P. (2014) Litter bugs exposed: phylogenetic relationships of Dipsocoromorpha (Hemiptera: Heteroptera) based on molecular data. *Insect Systematics & Evolution* 45, 351–370.

Weirauch, C., Whorrall, K., Knyshov, A. & Hoey-Chamberlain, R. (2018) Giant among dwarfs: *Meganannus lewisi*, gen. n. and sp. n., a new genus and species of minute litter bugs from Costa Rica (Hemiptera: Schizopteridae). *Zootaxa* 4370, 156–170.

Wygodzinsky, P. (1948) On two new genera of Schizopterinae (Cryptostemmatidae) from the Neotropical region (Hemiptera). *Revista Brasileira de Biologia* 8, 143–155.

Chapter 1: Systematics of the genus *Chinannus* Wygodzinsky

Abstract

Dipsocoromorpha, the minute litter bugs, are poorly studied and minuscule true bugs (Hemiptera: Heteroptera) with uncertain phylogenetic position, often bizarre morphology, and substantial undescribed biodiversity. Schizopteridae, the largest family within Dipsocoromorpha, comprise 56 described genera and more than 250 species with primarily tropical distribution. Taxonomic research on the Neotropical fauna has all but ceased since the last third of the 20th century, but recent sorting of >950 residue samples from 30 countries across the New World indicates that the true species-level diversity is tremendous. We here taxonomically revise the genus *Chinannus* Wygodzinsky, 1948 (Dipsocoromorpha: Schizopteridae: Ogeriinae), previously known from two strongly sexually dimorphic species from Costa Rica and Trinidad, describing 26 species as new and expanding the known natural range of species in the genus to span most countries between Nicaragua and Bolivia. A revised diagnosis of the genus and thorough documentation of male and female habitus as well as genital and wing morphology are presented. Male genitalic and pregenitalic modifications of *Chinannus* spp. are species-diagnostic and we here use a combination of confocal microscopy, scanning electron microscopy and macrophotography to document these features and resolve homology issues. Males possess a unique modification of the forewing M vein, the so-called "wing organ" of unknown function, that provides additional species-level diagnostic features. Sexual dimorphism is extreme in *Chinannus*; we here use geographic information and molecular data (CO1) to match macropterous males with the strongly coleopteroid

females. To evaluate the monophyly and phylogenetic position of *Chinannus*, we generated and analyzed a molecular dataset (partial 28S and 18S rDNA, CO1). The genus is recovered as monophyletic with high branch support and nested amongst mostly undescribed Old and New World taxa currently classified as "Ogeriinae", which we here show to be paraphyletic. We claim that applying a similar combination of morphological and molecular approaches while examining large numbers of specimens will greatly advance knowledge of the biodiversity of Neotropical Schizopteridae.

Introduction

The infraorder Dipsocoromorpha, the litter bugs, comprises five morphologically distinctive families (~320 species) of mostly minuscule and poorly studied true bugs (Weirauch & Štys 2014) with uncertain phylogenetic position within Heteroptera (Wheeler *et al.* 1993; Xie *et al.* 2008; Li *et al.* 2012, Weirauch & Štys 2014). Litter bugs mostly inhabit tropical regions around the world, but a few species occur in temperate (Hill 1980) or even arid climates (Uhler 1904). With more than 250 species in 56 extant and fossil genera (Linnavuori 1974; Weirauch 2012; Makhan 2013; Weirauch and Štys 2014; Poinar and Brown 2014; Hill 2015), the family Schizopteridae contains the bulk of species and shows a tremendous array of morphological variation ranging from extreme genital and wing modifications to an assortment of specialized structures on head, thorax, and wings (Emsley 1969; Štys 1970; Weirauch and Štys 2014).

Amongst extant Schizopteridae, 20 genera are restricted to the New World, show greatest species diversity in the Neotropical region, and are classified in the subfamilies Hypselosomatinae (three genera), Ogeriinae (one genus), and Schizopterinae (16 genera)

(Weirauch & Fernandes 2015; Makhan 2013). Taxonomic research on the Neotropical schizopterid fauna started during the 19th century with publications by Fieber (1860) and Reuter (1882), followed by a monograph published by McAtee and Malloch (1925) that heavily focused on the Caribbean region and Central America and some excellent treatments by Wygodzinsky (1947, 1948, 1950a, 1951), mostly based on material from Argentina, Brazil, and Costa Rica. Emsley (1969) monographed the fauna of the small continental island of Trinidad that at that point was known to harbor only two species of Schizopteridae (China 1946) and described an astounding 46 species as new, a sign that the true species diversity across the poorly sampled Neotropics could be extremely high. After a gap of 40 years, taxonomic publications on Neotropical Schizopteridae have only recently started to appear with descriptions of new genera from Argentina and Peru (Carpintero & Dellapé 2006; Weirauch 2012) and a revision of *Peloridinannus* Wygodzinsky (Weirauch & Frankenberg 2015). Sorting of material acquired from residue samples (e.g., Malaise and Berlese trap bulk samples) as part of a United States National Science Foundation grant on Dipsocoromorpha (led by C. Weirauch; 2013-2016) shows that large numbers of species and several genera of Neotropical Schizopteridae are left to be described. Focusing on the only described New World Ogeriinae, the genus *Chinannus* Wygodzinsky, 1948 (two described species), we here show that combining the study of large series of specimens, with cutting-edge morphological documentation as well as molecular and phylogenetic approaches, has the potential to eventually reveal the true diversity of Neotropical litter bugs.

Although comprising only two valid species, the taxonomic history of *Chinannus* is intriguing and exemplifies challenges that are also encountered in other groups of litter bugs. China (1946) described the first species of *Chinannus* as *Ptenidiophyes trinitatis* China, 1946 from the Central ranges in Trinidad, placing it in a genus that had been created by Reuter (1891) for a species from Southern Brazil. Females of both, *Ptenidiophyes mirabilis* Reuter, 1891 and the species described by China, are coleopteroid, i.e. their wings are heavily sclerotized, curved to dorsally enclose the abdomen, lack conspicuous venation, but carry numerous small punctures. This extreme coleopteroidy is fairly rare amongst Neotropical Schizopteridae, explaining why China (1946) may have used it as a diagnostic feature to classify his new species in *Ptenidiophyes*. Males of the monotypic *Ptenidiophyes* are unknown, but China (1946) studied two male specimens that were collected with the female holotype in Trinidad. Despite striking differences, most importantly the well-developed membranous wings in the male and the modified vein M referred to as "wing organ", he recognized these specimens as conspecific and provided a description for the male. Wygodzinsky (1948) re-visited existing data and concluded that *P. trinitatis* and *P. mirabilis* are not congeneric, even though it is unclear if he examined specimens of either species. To formalize his decision that was mostly based on the length of the labium and details of the wing in females, Wygodzinsky (1948) described and diagnosed the new genus *Chinannus*, transferred China's species, and described a second species from Costa Rica while providing detailed morphological documentation of males and females of this new species, *Chinannus bierigi* Wygodzinsky, 1948. Štys (1975) re-discovered the holotype

of *P. mirabilis* and corroborated Wygodzinsky's assessment. To date, *C. bierigi* is only known from the mid-elevation rainforest at the type locality in the province of Cartago in Costa Rica. While studying litter bugs in Trinidad, Emsley (1969) collected additional specimens of *C. trinitatis* (China, 1946) from across the island (Northern, Central, and Southern ranges) and indicated that this species represents the most widely distributed species of Schizopteridae on that island. No new records of *Chinannus* spp. have become available since. By sorting > 950 bulk samples from 23 countries in the New World ranging from the United States in the North to Argentina in the South and including most major Caribbean island groups, we have recovered 420 specimens of *Chinannus* from 77 samples and 12 countries between Nicaragua and Bolivia. With the exception of one female that may be conspecific with a Peruvian species and that we here treat as *Chinannus* sp. and two undetermined nymphs, these specimens represent 28 species, 26 of which we here describe as new.

Most Heteroptera possess male genitalia that are composed of a genital capsule or pygophore (segment IX), an aedeagus that can be variously modified in different families, and parameres that range from symmetrical (most families; e.g. Pentatomidae and most Reduviidae) to slightly or even dramatically (e.g., Cimicidae, Miridae) asymmetrical (Singh-Pruthi 1925; Schuh & Slater 1995). In addition to the above outlined bauplan male Schizopteridae feature an astounding variety of modifications that range from asymmetrical processes on certain pregenital sternites to unique appendages on segments VIII and IX and a great diversity of shapes and sizes of the vesica and parameres (Emsley 1969; Štys 1970). Judging from published illustrations (China 1946;

Wygodzinsky 1948), the right side of the sternites III-VI is strongly asymmetrical in the two described species of *Chinannus*, the parameres are asymmetrical, the genital capsule appears to carry an appendage, and the vesica either consist of two (*C. bierigi*) or eight coils (*C. trinitatis*). Based on this limited published documentation, we propose that genitalic morphology will likely provide a wealth of both genus- and species-level diagnostic features for *Chinannus* spp. Intrigued by the pronounced differences of the vesica in the two described species, we also speculate that their length might be correlated with the length of the female spermathecal duct. Unfortunately, China (1946) and Wygodzinsky (1948) did not document female internal genitalia, but thorough documentation of female spermathecae in the present study will enable us to test this hypothesis. Besides extensively documenting male and female genitalic morphology, we also closely examined the wing organ. This structure is restricted to males and consists of a strongly inflated and sclerotized M vein with underlying cavity and peg-like structures along the opening of the cavity. China (1946) first described this structure and suggested that it might be a stridulatory organ, although there is no direct evidence for such a function. Wygodzinsky (1948) mentioned species-specific differences in the wing organ between *C. bierigi* and *C. trinitatis* and we here show that this complex structure indeed provides good species-diagnostic features across the genus.

One of the challenges for documenting the biodiversity and describing new species of *Chinannus* is the strong sexual dimorphism in this genus. Where only one species is present at a given locality, as was the case for the two previously described species, and both male and female specimens are available, the sexes can be (at least tentatively)

associated based on geographic information and to a certain degree on size and color pattern. However, where multiple male-based morphospecies co-occur with one or multiple female-based morphospecies, male-female associations cannot be unambiguously resolved. Matching dimorphic sexes using molecular markers has become a standard technique in insect systematics (Pilgrim & Pitts 2006; Kathirithamby *et al.* 2010; Zhang & Weirauch 2011; Park *et al.* 2011; Forthman *et al.* 2015) and we here use this approach with the caveat that molecular data may remain unavailable for rare taxa, species only represented by dry specimens that we were unable to sequence, and/or specimens that were preserved in low-percentage ethanol.

As part of the present monograph, we also test if *Chinannus* is monophyletic, evaluate its phylogenetic position amongst Schizopteridae, and provide a first insight into relationships within the genus. At the time of the description of *Chinannus* the higher-level classification of Dipsocoromorpha was poorly developed (see McAtee and Malloch [1925] and discussion in Emsley [1969]), and the genus was initially accommodated in the subfamily Schizopterinae within the Cryptostemmatidae (China 1946), disregarding Reuter (1910) who had previously elevated Schizopterinae to family status. The suprageneric classification within the Schizopteridae started with Esaki and Miyamoto (1959), who moved the genus *Hypselosoma* Reuter, 1891 into a separate tribe that was later elevated to subfamily level. Hypselosomatinae are recognized by large compound eyes, a well-developed ovipositor, and numerous veins on the forewing (Esaki & Miyamoto 1959; Emsley 1969). Emsley (1969) split the remainder of the family into the Schizopterinae and Ogeriinae and diagnosed the latter by the four segmented labium,

variable tarsal formula, genitalic features and three pairs of abdominal spiracles. Based on the Oriental and Australian genus *Ogeria* Distant, 1913, Emsley (1969) moved four additional genera to this new subfamily, *Pachyplagia* Gross, 1951 from Australia, *Luachimonannus* Wygodzinsky, 1950 from Africa, *Kokeshia* Miyamoto, 1960 from the Oriental region, and *Chinannus* as the only Neotropical representative of the group. Later, Hill (2004) included *Kaimon* Hill, 2004 from Australia into the Ogeriinae and indicated that the concept and diagnosis of the subfamily should be revisited. Ogeriinae have not been universally recognized (e.g., Štys in Schuh and Slater 1995), but the subfamily was recovered as monophyletic with fairly high branch support in a recent molecular phylogenetic analysis (Weirauch & Štys 2014). However, only three specimens representing one undescribed species of *Ogeria* from Borneo and two species of *Chinannus* were included in that analysis thus limiting the implication of this result. The present study is not designed to evaluate the monophyly and composition of the Ogeriinae in a comprehensive way: a phylogenetic study that includes additional taxa and characters would be required to do so. Nevertheless, we aim on testing the monophyly of *Chinannus* and on generating hypotheses on close relatives. In addition to *Chinannus* and various outgroups, we include representatives of *Kaimon*, *Kokeshia*, an undescribed species of Ogeriinae from Colombia, and two undescribed Ogeriinae from Cameroon in our analyses.

We here redescribe and rediagnose *Chinannus* and the two previously described species, describe 26 species as new, and provide keys to and distribution maps for all species. To complement habitus images and genitalic illustrations, the unique morphology of

Chinannus with special emphasis on the enigmatic wing organ is explored using scanning electron and confocal microscopy. The DNA of twenty-five specimens representing 11 species of *Chinannus* are sequenced to match males and females and to reveal relationships within the genus and these taxa are included in a larger dataset to test monophyly and phylogenetic relationships of the genus amongst Schizopteridae.

Material and Methods

Material

We examined 420 *Chinannus* specimens total, 99 of which were point- or card-mounted and 321 preserved in EtOH. Specimens that are deposited at UCR (University of California, Riverside) were collected during field trips of the Weirauch and Heraty labs, or were donated from several institutions. Other specimens were taken on loan and will be deposited in the following institutions:

AMNH American Museum of Natural History, New York, USA

BMNH Natural History Museum, London, UK

CNC The Canadian National Collection, Ottawa, Canada

CUNI Charles University, Prague, Czech Republic

FMNH The Field Museum of Natural History, Chicago, USA

FSCA Florida State Collection of Arthropods, Gainesville, USA

IAvH Instituto de Investigación de Recursos Biológicos Alexander von Humboldt, Bogotá, Colombia

INBIO Instituto Nacional de Biodiversidad, San Jose, Costa Rica

INPA Instituto Nacional de Pesquisas da Amazônia, Manaus, Brazil

MHNG Muséum d'Histoire Naturelle, Geneva, Switzerland

MNHN Muséum national d'histoire naturelle, Paris, France

MUSM Museo de Historia Natural, Universidad Nacional Mayor de San Marcos, Lima, Peru

QCAZ El Museo de Zoología de la Pontificia Universidad Católica del Ecuador, Quito, Ecuador

TAMU Texas A&M University, College Station, USA

UCD University of California, Davis, USA

USNM National Museum of Natural History, USA

Dipsocoromorpha were removed from bulk samples at the FMNH and FSCA by Robin Delapena and Walter Winn as part of the NSF-funded ARTS Dipsocoromorpha grant. Material from AMNH (dry), BMNH (dry), CUNI (dry), USNM (EtOH bulk samples), and MHNG (EtOH bulk samples) was presorted by one of us during visits at these institutions and processed further at UCR. INBIO, TAMU, and UCD loaned the available dry material.

All specimens were assigned a unique specimen identifier (USI) and specimen locality and identification information was digitized in the Planetary Biodiversity Inventory locality database (http://research.amnh.org/pbi/locality/). The USI is printed as a matrix code label with an alphanumeric string (i.e., UCR_ENT 00020590) and mounted together with the insect. USI numbers usually identify single specimens, however, in one case 41 specimens were represented by a single number; the total number of specimens examined reflects this as 41 individual counts. Locality data was geo-referenced using gazetteers,

atlases and Google Earth. The associated information is available on the website of the Planetary Biodiversity Inventory Project (http://research.amnh.org/pbi/heteropteraspeciespage/) and accessed through the www.discoverlife.org website. Voucher specimens for molecular study were also given an internal identification number. These numbers are reflected in Fig. 1.20 as well as in Table 1.2. The association of voucher specimens with USI's is given in Table 1.2.

Nomenclatural Acts

This publication and the nomenclatural acts it contains have been registered in ZooBank, the online registration system for the ICZN. The ZooBank LSIDs can be resolved by appending them to the web address "http://zoobank.org/". The LSID for this publication is urn:lsid:zoobank.org:pub:B9CBBA22-CC58-4C2F-A80F-ED3AAC2AB95C. The LSIDs for nomenclatural acts can be found in corresponding sections of the paper.

Terminology

The terminology used in taxonomic descriptions of Dipsocoromorpha is currently unstable, wing venation hypotheses differ dramatically between researchers (e.g., compare Wygodzinsky 1960; Emsley 1969; Hill 1987; Rédei 2008b), and no comprehensive review of details of dipsocoromorphan genitalia (in particular the intromittent organ) has been published (Štys 1970). The present paper utilizes a set of terms derived from different sources that seems optimal for the taxon studied and justified based on overall homology hypotheses. Median posterior projection of the metasternum is referred to as **metendosternite** following Emsley (1969) and Hill (2015). Wing venation homology hypotheses follow Rédei (2008b), who made great progress in

studying venation of different groups of Dipsocoromorpha, especially Old World Ogeriinae (Rédei 2007, 2008b, 2008a; Rédei *et al.* 2012). The modified M-vein of the forewing in *Chinannus* males is here referred to as the "**wing organ**" following Hill (2004, 2013), who used the general term "organ" for a variety of male-specific structures of Hypselosomatinae and Ogeriinae ("vertex organ", "labral organ"). Details of the wing organ cavity are described with respect to the body axis and when wings are at rest. Terminology of genitalic structures follows Štys (1970) and Emsley (1969), with some modifications. We here define several ambiguous terms as follows: **subgenital plate** – enlarged sternite VII in males that ventrally covers the pygophore; **pygophore** (=genital capsule) – segment IX, containing the intromittent organ; **appendage of tergite VIII** – a movable appendage associated with tergite of segment VIII; **process of tergite VIII** – unarticulated projection of tergite VIII. The term **parasternite** is used here after Wygodzinsky (1948) to define the subdivided lateral portions of sternites IV, V, VI, and VII.

We recognize that sclerites observed in *Chinannus* and termed "parasternites" by Wygodzinsky (1948) are not homologous to parasternites sensu Heymons (1899), originally used for the connexival sclerites of Heteroptera. The term parasternite in its original meaning, together with the more frequently used terms laterotergite and paratergite, was criticized as being confusing, since it names a structure that is not a subdivision of either tergite or sternite, but rather a fusion of one of them with the pleurite (Sweet 1996). Sweet (1996) proposed the use of the terms epipleurite and hypopleurite for the connexival sclerites and suggested to limit the use of the terms

laterotergite and parasternite to secondary subdivisions of the tergites and sternites. According to Sweet (1996), true parasternites are clearly distinguished from pleural sclerite by featuring muscle attachments. In *Chinannus*, the subdivided ventral sclerites show muscle attachments, only occur on certain abdominal segments, and in many species are present only on the right side of the abdomen. In addition, spiracles of segments VI and VII are located on the lateral edges of these ventral sclerites and we take this as an indication that they may be fused sternites and hypopleurites. However, Sweet (1996) indicated that spiracles "may readily shift" from the hypopleurite to the sternite, and therefore the spiracle position itself does not shed light on the situation in *Chinannus*. Based on the above mentioned arguments, we are confident that the subdivided sclerites in *Chinannus* are either parts of the sternites or a fusion of sternites and hypopleurites, but not the hypopleurites alone. We will therefore continue to use the term parasternite sensu Wygodzinsky (1948), as a secondary subdivision of the sternite sensu Sweet (1996).

The postgenital abdomen in Schizopteridae is here considered to be comprised of segments X and XI following Rédei (2008b) and Rédei *et al.* (2012). The sclerite of segment X is here referred to as **anophore** following Wygodzinsky (1950b), but not Emsley (1969), who considered the anophore to be part of segment IX. In *Chinannus*, the anophore bears an unarticulated projection that we call **anophoric process** (sensu Wygodzinsky 1950b) and not anophoric appendage (sensu Emsley 1969). The membranous portion of segment X together with segment XI form a tube here termed **anal tube** (following Weirauch 2012; Emsley 1969).

The structure of the dipsocoromorphan **aedeagus** varies widely within the infraorder, and terminology used to describe sub-structures are in need of a comprehensive review. Here we refer to the basal portion of the aedeagus as **basal plates** and its apical portion as **vesica**, following most other dipsocoromorphan researchers (Emsley 1969; China 1946; Hill 2004; Rédei 2008b; Wygodzinsky 1948; Weirauch 2012). The most problematic part of the aedeagus is the middle portion that lies between the basal plates and the vesica. It is termed phallotheca in most Heteroptera (Schuh & Slater 1995), but in Dipsocoromorpha it was either not named at all, or the following names were applied: phallotheca (Štys 1970), phallosoma (Wygodzinsky 1948), or conjunctiva (Emsley 1969). The term conjuctiva does not appear appropriate, since it usually defines membranous parts of the aedeagus that carry spicules, and the middle portion of the aedeagus in *Chinannus* is well sclerotized and devoid of spicules. The term phallotheca assumes the presence of a sheath for an eversible vesica, and this condition is not found in Schizopteridae. The present paper does not aim to develop a definitive term for this part of the aedeagus, since a much broader taxon sampling would be required for adequate evaluation. We therefore use the neutral "**middle portion**" as a placeholder for the time being.

For female internal genitalic structures, we adopt the following terminology: **spermathecal complex** – spermatheca and its ducts; **spermathecal duct** – a duct that runs from the spermatheca to the external opening in the genital chamber (position of segments – proximal or distal – are given with respect to the spermathecal reservoir); **spermathecal reservoir** – a spherical or elongated capsule connected to the spermathecal

duct; **spermathecal gland duct** – a duct in between the spermathecal reservoir and the spermathecal gland.

We use the following abbreviations: 1AN – first anal vein; 2AN – second anal vein; ac – anal cell; ano – anophore; ap – anophoric process; aph – apophysis of the appendage of tVIII; app tVIII – appendage of tergite VIII; at – anal tube; bb – basal bump; bp – basal plates; C– costa; Cu – cubitus; cub – cubital cell; cun – cuneus; DAG – dorsal abdominal scent gland scars; dc – discal cell; lp – left paramere; M – media; m1 – protractor of the appendage of tVIII; m2 – retractor of the appendage of tVIII; mem – membranous area posteriorly of the distal portion of 1AN vein; mpa – middle portion of aedeagus; oud – outbranching duct; peg – wing organ peg; po – peg opening; pstIV – parasternite IV; pp – preapical projection on a tip of vesica; ptVIII – process of tergite VIII; pstV – parasternite V; py – pygophore; R – radius; rp – right paramere; Sc – subcosta; sp –spine of parasternite V; spdd – distal segment of spermathecal duct; spdp – proximal segment of spermathecal duct; spgd– spermathecal gland duct; spgl – spermathecal gland; spr – spermathecal reservoir; stII+stIII – fused sternites II and III; stIV – sternite IV; stV – sternite V; stVI – sternite VI; stVII – subgenital plate; tc – trapezoidal cell; tVII – tergite VII; tVIII – tergite VIII; v – vesica.

Methods

Dorsal and lateral habitus images were taken using a Leica DFC 450 C Microsystems system (Leica, Wetzlar, Germany) with Planapo 1.0x or 2.0x objectives and stacked using Leica Application Suite V4.3. Wing photos were acquired on a Zeiss Axioskop 2 compound microscope (Oberkochen, Germany) using Archimed V5.4.1 (Microvision)

and stacked using Zerene Stacker V1.02 (Zerene Systems). Confocal pictures of wings and genitalia were taken on a Leica SP5 Inverted confocal microscope (Leica, Wetzlar, Germany) taking advantage of cuticular auto fluorescence excited by 488nm and 543nm lasers and collected by detectors in diapasons of 500-535nm (green in figures) and 555-700nm (red in figures). The resulting confocal images were rendered using Imaris V7.6.4 (Bitplane). For the study of genitalia, the male abdomen was either separated from the thorax and cleared by immersion into hot 10% KOH, or left intact after DNA extraction (see below). Line drawings were made using a Nikon Eclipse 80i compound microscope (Nikon, Tokio, Japan) with a camera lucida. For the study of female genitalia, the abdomen was separated from the remainder of the body, cleared in KOH if no DNA extraction was performed for the specimen, and placed in Chlorazol Black E for 10 to 20 seconds. The female internal reproductive system was then removed from the abdomen, placed on a microscope slide and imaged using a Zeiss Axioskop 2 compound microscope. Scanning electron micrographs of selected morphological characters were acquired on a Hitachi S-4700 scanning electron microscope (Hitachi, Tokio, Japan) at the UCR Central Facility for Advanced Microscopy and Microanalysis (http://cfamm.ucr.edu/) after sputter-coating on a Cressington 108 auto sputter coater (Cressington, Watford, UK). Maps were prepared in SimpleMappr (http://www.simplemappr.net/) using the coordinates exported from the PBI database. All images were edited and assembled into image plates in Adobe Photoshop CS4.

The molecular dataset included 45 taxa, 25 of which are specimens that represent 11 species of *Chinannus*. The relatively low number of species included in the molecular

phylogenetic analysis was due to limited availability of fresh material well-preserved in ethanol. We used a comprehensive sample of Dipsocoridae, Ceratocombidae, Hypselosomatinae, Schizopterinae, and other Ogeriinae as outgroups (20 specimens). DNA extraction was performed using a Qiagen DNeasy Blood and Tissue Kit (Qiagen, Hilden, Germany). Amplification of the D2 and D3-D5 regions of 28S rDNA, a portion of 18S rDNA, and COI was performed using the primers listed in Table 1.1. Sequencing was done at the Genomics Core of UCR's Institute for Integrative Genome Biology (http://genomics.ucr.edu/). Sequences are available in GenBank with accession numbers listed in Table 1.2. The acquired sequences were assembled and edited in Sequencher V4.8 (Gene Codes Corporation, Ann Arbor, MI) and aligned in MAFFT (http://mafft.cbrc.jp/alignment/server/) using the E-INS-i algorithm. Alignment was manually corrected and trimmed in Bioedit V7.2.5 (Ibis Biosciences). All gene sequences were concatenated into a single matrix with SequenceMatrix V1.7.8 (Vaidya *et al.* 2011). Missing data were spread unevenly across the matrix, with 18S sequences available for 21 out of 45 specimens (mostly for the outgroups), COI sequences for 17 specimens (mostly for the ingroup), 28S D2 sequences for 33 specimens, and 28S D3-D5 sequences for 40 specimens (see Table 1.2). Phylogenetic analysis using maximum likelihood was performed using RAxML-HPC2 (Stamatakis *et al.* 2008). The matrix was divided into three partitions (18S, 28S, and COI), the outgroup set to "Cryptostemma_251", the model to GTRCAT, and the number of bootstrap replicates to 1000.

COI sequences were used for male-female association. Uncorrected pairwise distances were computed using TaxonDNA Species Identifier (Meier *et al.* 2006), the smallest

distances between males and females were calculated and compared to the distances of the next closest sequence (Zhang & Weirauch 2011).

Measurements were performed on habitus images. Only the total body length and the width of the pronotum were measured, as they are easy to document in a comparable way for all specimens in dorsal view. All measurements are in mm. The descriptions of species were prepared and organized using mx (mx.phenomix.org). The initial matrix contained 39 characters including eight habitus characters, 16 wing characters, seven male pregenital abdomen characters, five male genitalia characters, and four female genitalia characters. After coding, the matrix-based descriptions were exported from mx as a text file (Mikó *et al.* unpublished). The exported descriptions were then edited manually and some additional character descriptions were added as needed. The genus description was assembled manually.

Results and Discussion

Systematics

Chinannus Wygodzinsky, 1948

Type species: *C. bierigi* Wygodzinsky, 1948 (original designation)

Diagnosis. The genus is distinguished from other Schizopteridae by the following combination of characters: males always with membranous forewings, females always with elytrous forewings (coleopteroid) (Figs 1.1-5); male forewings of all species except *C. perplexus* with wing organ (Figs 1.12, 1.13); hindwings present only in males (Fig. 1.13); eyes small, not overlapping margins of prothorax (Figs 1.1-5); ocelli present in males (Figs 1.7A, 1.7C), absent in females (Figs 1.9A, 1.9B); labium clearly four

segmented, as thick as tibiae, surpassing hind coxae, gradually tapering in lateral view (Figs 1.5, 1.7C, 1.7E); labial segments forming straight line on ventral (= morphological dorsal) surface (Figs 1.5, 1.7C); pronotal collar distinct (Figs 1.7A, 1.7B); five to six veins emanating from trapezoidal cell (Figs 1.12, 1.13) with the difference being due to M-vein topography: M-vein can be connected to trapezoidal cell through m-cu crossvein, or can run directly through trapezoidal cell (compare *C. advenus* and *C. bierigi* on Fig. 1.12); tarsal formula 3-3-2 in males, 2-2-2 in females; three pairs of abdominal spiracles in adults, located on stVI, stVII, tVIII; right, or both left and right abdominal parasternites IV in males modified; male subgenital plate large, entirely covering pygophore from below; tVIII usually with movable appendage attached to left side or with a process on the right side; pygophore simple, without processes; parameres asymmetrical but almost equal in size, elongate (Fig. 1.11H, lp, rp); aedeagus without spicules (Fig. 1.11I); vesica (v) thin, short to very long (one and a half to more than 10 coils); anophore well sclerotized, with a prominent process on the right side (Fig. 1.11C, 1.11D, ap); female ovipositor vestigial.

Males most closely resemble *Itagunannus* Wygodzinsky, 1948 in dorsal habitus, particularly in having similar looking thickened and darkened vein on forewings. However *Chinannus* is strikingly different in having long labium, smaller eyes, thickened and darkened M-vein (versus Cu-vein in *Itagunannus*), large subgenital plate, and relatively long and thin vesica. Females of *Chinannus* can be confused with coleopteroid representatives of other schizopterid genera, but differ in having small eyes, long and apically tapering labium, and lacking explanate costal margins of forewings.

Redescription. *Male*. COLORATION (Figs 1.1-4). General color brown to dark brown; head, thorax dark brown; labium yellow; hemelytra with pale transverse band running between middle and apical portion of clavus (Figs 1.12, 1.13); C+Sc and R+M darkened (Figs 1.12, 1.13); legs yellow; abdomen brown. SURFACE AND VESTITURE (Figs 1.7-8, 1.10). Head, pronotum, scutellum, thoracic pleura, and exposed parts of abdomen covered with sparse setae and dense microtrichia; surface of mouthparts, antennae, legs, and covered parts of thorax and abdomen without microtrichia; muscle scars on head and pronotum represented by groups of small rounded smooth patches (Fig. 1.7B); clypeus with simple setae of same size; second antennal segment with circle of setae at apex (Figs 1.7C, 1.7E); metanotum with wrinkles (Fig. 1.7H). STRUCTURE. Body elongate; head flattened longitudinally, as long as wide; eyes relatively small, somewhat elongated dorsoventrally, with convex ommatidia; interocular distance large; ocelli present, roughly equal in size to a compound eye ommatidium, closely situated to margin of compound eye (Figs 1.7B, 1.7C); antenna extending to one third or half of body length, first and second antennal segments relatively short and almost equal in length (Fig. 1.7E); buccula narrow (Figs 1.7D, 1.7F); maxillary plates small (Figs 1.7D, 1.7F); mandibular plates indistinct (Figs 1.7D, 1.7F); labium straight, long, extending beyond hind coxae, consisting of four segments that form straight line on ventral (= morphological dorsal) surface (Figs 1.7C, 1.7E); first segment wide and short; second, third and fourth segments roughly equal in width, fourth segment tapering; pronotum with curved frontal and caudal margins and straight lateral margins (Fig. 1.7A); pronotal collar well-developed (Figs 1.7A, 1.7B); mesoscutum covered by pronotum; scutellum small, not reaching

posterior margin of metanotum, triangular, with rounded apex, and two pits in middle (Figs 1.7H, 1.7I); metanotum with wrinkled sculpture in its posterior portion (Fig. 1.7H); hypopleural lobes not developed; propleuron cleft, projecting forward below eye (Fig. 1.7C); prosternum triangular, steeply inclined; mesopleura cleft, caudal portion with small lobe-like projection; mesosternal and metasternal processes absent, posterior margin of metendosternite blunt (Fig. 1.8A; Fig. 1.9J for female); joint between thorax and abdomen simple, modifications described for some other Ogeriinae (Hill 1990, 2004) absent; protibia with preapical comb (Figs 1.8C, 1.8D); metatibia with a small preapical comb (Fig. 1.8F); pro- and mesotibia slightly curved, metatibia straight; tarsal formula 3-3-2 (Figs 1.8C, 1.8F); pro- and mesopretarsus with inflatable arolia (Figs 1.8G, 1.8H); pretarsal claws with series of adpressed microtrichia on outer claw surface, with more numerous microtrichia on prolegs, and fewer on meso- and metalegs (Figs 1.8G, 1.8H, 1.8I); forewing reaching or surpassing tip of abdomen; venation as Figs 1.12, 1.13; part of M-vein in all except *C. perplexus* modified into wing organ, i.e. thickened, darkened, and more sclerotized, with cavity with peg-like structures (see discussion for more details); hindwings well-developed, with three lobes (Fig. 1.13); abdomen with five visible sternites corresponding to segments II through VII (Figs 1.16-18); sternite I membranous; sternites II and III fused together with trace of intersegmental suture; right side of sternite II+III usually prolonged caudally; sternites IV, V, VI and VII with well-developed parasternites, separated by membrane; parasternites usually present only on right side, but in *C. bispinosus* parasternites IV through VI developed on both sides; parasternite IV in all species except *C. inermis* with pouch (concave sclerite) and,

usually, with spine-like process oriented anteriorly; in four species parasternite IV with flattened process, and in *C. inermis* parasternite IV slender with elongated process (Fig. 1.11G); parasternites V, VI, and VII simple, sometimes V fused with IV; sternite VII modified into large rounded subgenital plate; sternite VIII small, not visible from outside, fused with pygophore; tergites of pregenital abdomen membranous except for VII, VIII, and rarely VI; tergite VII with prominent DAG scars on anterior margin; tergite VIII in all species except *C. deformis* with movable appendage at left corner or process at right corner; spiracles present on sides of sternites VI, VII and sides of tergite VIII; pygophore small, simple, completely submerged in subgenital plate at rest; aedeagus without spicules, consisting of basal plates, middle portion, and vesica; basal plates consisting of curved transverse band; vesica uniformly thin, short or long, coiled; parameres elongated, asymmetrical, nearly equal in size; anophore well sclerotized, with process on right side. *Female*. COLORATION. Coloration same as in male; transverse pale band on forewings present in some but not all species (Figs 1.1-5). SURFACE AND VESTITURE. Same as in male (Fig. 1.9). STRUCTURE. Body oval, less elongate than in male; ocelli absent (Figs 1.9A, 1.9B); eyes slightly smaller than in male, more rounded (Fig. 1.5); metapleura and sides of abdomen visible in lateral view, not hidden by forewings; tarsal formula 2-2-2, arolia absent (Figs 1.9F, 1.9G, 1.9H); forewings slightly overlapping, with punctures or areolae, costal margin not explanate (Figs 1.9D, 1.9E); with obsolete or sometimes visible venation; hindwings absent; tip of abdomen frequently exposed in lateral view (Fig. 1.5); tergites of abdomen membranous except VIII and IX. GENITALIA. Gonapophyses vestigial, genital opening in form of transverse slit between

last visible sternite (VII) and last large tergite (IX) (Fig. 1.9K); genital chamber membranous (Fig. 1.19); spermathecal complex always present but weakly pigmented and barely visible without staining; spermathecal reservoir and spermathecal gland of various shape and relative size (Fig. 1.19); spermathecal duct thin, short or long, connects to genital chamber in form of spiral (Figs 1.12I, 1.19).

Nymph. COLORATION (Figs 1.4-5). Generally paler than adults; head, pronotum, propleuron, mesonotum, mesopleuron, metanotum, metapleuron, wing buds, and midline of abdominal dorsum brown; abdominal sides, ventral surface, and appendages pale. SURFACE AND VESTITURE. Dorsum covered with macrosetae. STRUCTURE. See Figs 1.4, 5.

Distribution. Central America and northern part of South America, from Nicaragua in the north to Bolivia in the south (Fig. 1.7).

Collecting methods. Collecting data associated with the specimens examined by us indicate that the most productive methods for collecting *Chinannus* specimens are Malaise traps, flight intercept traps, and different methods of leaf litter extraction (Table 1.3). Flight intercept and light traps collected almost only males, whereas Malaise traps and pan traps recovered both sexes, however with a bias towards males. Leaf litter extractions usually provided almost equal numbers of males and females.

Discussion. *Wing organ structure*. The wing organ is restricted to males and located on the vein that runs from the trapezoidal cell to the costal margin of the wing. The vein is here considered to be M as it is apparently homologous to that vein in *Kokeshia* (Rédei 2008b; Rédei *et al.* 2012). The wing organ vein is inflated and strongly sclerotized. It has

a cavity that is typically located in the middle portion, but in *C. caudalis* (Fig. 1.14E) is found on the caudal side (with respect to the body axis when wings are at rest). Small tubular structures, or so called pegs, are situated in this cavity. The numbers, shapes, and locations of the pegs are variable across the genus and provide good diagnostic characters for many species. However, peg numbers can vary to some degree between specimens or sometimes even between left and right wings of a given specimen, especially in species that have wing organs with more than eight pegs. We indicate numbers observed in the studied specimens in the following descriptions. The internal structure of pegs and wing organ was not studied in the present paper, but judging from the presence of wing organs only in males and the hollow structure of the pegs that also have distal openings, we speculate that this structure may have a glandular function, and if so the secretion would likely be male-specific.

Dorsal abdominal gland scars. Adult specimens of all species have prominent DAG scars situated on the anterior margin of tergite VII. The DAG orifices are usually represented by a large wide central scar, a series of five-six small round scars and two large round scars on each side of the tergite.

Male abdomen. The apical portion of male abdomen of *Chinannus* includes two types of elongated processes or appendages besides the aedeagus – projections of segment VIII and projections of segment X.

Appendage and processes of tVIII. Most species (23) have a movable appendage associated with segment VIII. The appendage has a condyle distally to its base, the condyle is inserted in between tergites VII and VIII, and a spiracle is located either on the

base of the appendage or on the membrane near it. The apophysis of the appendage is flattened and provides attachment for two muscles, a large protractor and a small retractor. The protractor (m1) is attached to the anterior side of the apophysis and to the anterior margin of tergite VII. The retractor (m2) is attached to the ventral side of the basal portion of the pygophore. Judging from the position of the condyle, muscles and a spiracle, we assert that this appendage belongs to segment VIII. In the four species that lack this appendage, tergite VIII is relatively long, more than half of the length of tergite VII, and in three out of the four species bear a process on the right side. In *C. deformis*, the tergite VIII lacks both appendages and processes (Figs 1.11D, 1.11E).

Anophoric processes. Segment X is roughly cylindrical and attached to the median membranous area of the pygophore. The proximal part of segment X is sclerotized on both dorsal and ventral sides and this sclerite is the anophore. In all species, the anophore bears a prominent process on the right side that can take on various shapes. In many cases, the anophoric process is what we call "claw-shaped": if the anophore opening (of anal tube) is directed strictly posteriorly, the process will resemble a claw curved anteriorly. It is T-shaped in cross section with the "main" surface facing the same way as the anophore opening and a "keel" that is located underneath the "main" surface. The "main" surface is broad at its base, but strongly tapering at the apex, and the keel can be sharp or rounded. Thus depending on the position of the anophore with respect to the rest of abdomen, the drawings of genitalia may depict different planes of the anophoric process.

Parameres and aedeagus. Parameres at rest sit deeply in the pygophore, such that only a small portion is visible externally. Because the shape of the parameres is not essential for species identification, we have not documented them for all species. However, in the taxa examined both parameres have a characteristic basal bump (Fig. 1.11H, bb). Parameres are connected to the basal plates, which are fused together forming a U-shaped transverse band. The middle portion of the aedeagus of *Chinannus* is complex (Fig. 1.11I, mpa) and it is difficult to propose decisive homology hypotheses. The vesica is thick at the base but thin along most of its length, and forms between one and a half to more than 10 coils. The vesica of *C. duopaxillatus* bears series of small preapical projections (Fig. 1.10K, pp).

Female genitalia. External female genitalia of *Chinannus* are vestigial. Internally, the genitalia are extremely membranous and delicate, and their fine-structure was not examined in the present study. The spermathecal complex consists of the spermathecal duct, spermathecal reservoir, and spermathecal gland duct leading to the spermathecal gland. All components are surprisingly variable across the genus, but conservative within a species. The spermathecal duct usually consists of several segments that differ in thickness and shape. In several species there is a small duct originating from the middle portion of the main duct. The spermathecal duct connects to the genital chamber approximately in its center, and the connection is made by way of a spiral (Fig. 1.11J). The shape of this spiral connection and the size of its aperture are good species diagnostic characters (Fig. 1.19). The length of the spermathecal duct does not seem to be correlated with the length of the vesica: in the species with the longest vesica (around 10 coils) the spermathecal duct is much shorter (compare Fig. 1.8M and Fig. 1.19 *C. trinitatis*); in the

species with the longest spermathecal duct the vesica is relatively short (two and a half coils, compare Fig. 1.16 *C. advenus* and Fig. 1.19 *C. advenus*).

Key to species of *Chinannus* (males):

1 Wing organ absent (Fig. 1.13 *C. perplexus*) ..... *C. perplexus*, sp.n.

–Wing organ present (Fig. 1.12 *C. advenus*) 2

2 (1) Wing organ with caudal peg cavity (Fig. 1.14E) ..... *C. caudalis*, sp.n.

– Wing organ with middle peg cavity (Fig. 1.14A).....3

3 (2) Parasternites IV developed on both left and right side of the body, both with pouch and spine (Fig. 1.16 *C. bispinosus*). Panama ..... *C. bispinosus*, sp.n.

– Parasternite IV developed only on right side of the body (Figs 1.16-18).....4

4 (3) Forewing with large membranous area posteriorly of the distal portion of 1AN vein (Fig. 1.12 *C. advenus*).....14

– Forewing with reduced membranous area posteriorly of the distal portion of 1AN vein (Fig. 1.12 *C. areolatus*).....5

5 (4) Parasternite IV slender (Fig. 1.11G), with long thin process (Fig. 1.17 *C. inermis*); parasternite V and VI membranous; apical veins fused; wing organ with six pegs. Peru .....*C. inermis*, sp.n.

– Parasternite IV large, with pouch and spine (Fig. 1.11D); parasternite V and VI sclerotized 6

6 (5) Distal portion of forewing darkened, heavily sclerotized, all veins widened (Fig. 1.12, *C. latus*, Fig. 1.13 *C. nicaraguensis*) 7

– Distal portion of forewing not darkened, at least Cu and 1AN are thin (Fig. 1.12 *C. advenus*) 8

7 (6) Wing organ with eight pegs (Fig. 1.15C). Nicaragua ..... *C. nicaraguensis*, sp.n.

– Wing organ with 10 pegs (Fig. 1.14O). Panama, Costa Rica ..... *C. latus*, sp.n.

8 (6) Wing organ with transparent patch at apex (Fig. 1.12 *C. areolatus*, Fig. 1.13 *C. translucidus*). Ecuador 9

– Wing organ uniformly colored (Fig. 1.12 *C. advenus*).....10

9 (8) Wing organ with nine pegs (Fig. 1.15J), body length 0.76 ..... *C. translucidus*, sp.n.

– Wing organ with 11 pegs (Fig. 1.14B), body length 0.87 ..... *C. areolatus*, sp.n.

10 (8) Appendage of tVIII long and reaching the base of abdomen (Fig. 1.16 *C. grandis*). Peru 11

– Appendage of tVIII short or absent 12

11 (10) Wing organ with six pegs (Fig. 1.14L), body length 1.24 ..... *C. grandis*, sp.n.

– Wing organ with four pegs (Fig. 1.14P), body length 1.03 ..... *C. lewisi*, sp.n.

12 (10) Appendage of tVIII as well as right process of tVIII absent (Fig. 1.11D, 1.11E); wing organ elongate, with six pegs (Fig. 1.14G). Ecuador..... *C. deformis*, sp.n.

– Appendage of tVIII segment present (Fig. 1.11C); wing organ oval, with less than six pegs (Fig. 1.12 *C. dissimilis*) 13

13 (12) Wing organ with three pegs located in three deep sockets (Fig. 1.15E). Brazil .....*C. parvithecatus*, sp.n.

– Wing organ with five pegs, of which four aligned in one line and fifth peg slightly above that line and oriented at angle in respect to other pegs (Fig. 1.14I). Bolivia .....*C. dissimilis*, sp.n.

14 (4) Wing organ oval and short, less than 2x as long as wide (Fig. 1.12 *C. duopaxillatus*) 15

– Wing organ elongate, more than 3x as long as wide (Fig.12 *C. advenus*).....18

15 (14) Wing organ with two pegs located in individual deep sockets (Fig. 1.10G, 1.14K); parasternite IV with spine (Fig. 1.10I, 1.17 *C. duopaxillatus)*; appendage of tVIII present. Brazil, French Guiana, Peru .....*C. duopaxillatus*, sp.n.

– Wing organ with more than two pegs; appendage of tVIII absent (Fig. 1.11F); parasternite IV with blunt process (Fig. 1.11F) 16

16 (15) Wing organ with three pegs (Fig. 1.15G); anophoric process long and oriented anteriad (Fig. 1.11F). Ecuador .....*C. pecki*, sp.n.

– Wing organ with three to four pegs (Figs 1.15A, 1.15F); anophoric process short and oriented laterally (Fig. 1.18 *C. paveli*).....17

17 (16) Wing organ cavity with four pegs aligned in one line (Fig. 1.15F). Bolivia .....*C. paveli*, sp.n.

– Wing organ cavity with three or four pegs, of which two or three aligned in one line and one peg below that line and oriented at angle in respect to other pegs (Fig. 1.15A). Peru .....*C. loretensis*, sp.n.

18 (14) Appendage of tVIII distinctly elbowed with twist (Fig. 1.16 *C. advenus*) 19

– Appendage of tVIII not elbowed with twist (Fig. 1.16 *C. delapenae*) 23

19 (18) Apex of appendage of tVIII modified into cylinder with serrated walls; wing organ with eight pegs (Fig. 1.14A); large species, body length 1.22. Venezuela, one record from Canada..... *C. advenus*, sp.n.

– Apex of appendage of tVIII simple, tapering (Fig. 1.17 *C. monteverdensis*).....20

20 (19) Anophoric process as long as the width of pygophore, wide at base and tapering, with a hook at apex (Fig. 1.17 *C. monteverdensis*); wing organ with nine pegs (Fig. 1.15B). Costa Rica ..... *C. monteverdensis*, sp.n.

– Anophoric process smaller, without a hook at the apex (Fig. 1.17 *C. duckensis*) 21

21 (20) Wing organ with seven pegs (Fig. 1.14J); appendage of tVIII is short, not reaching apex of spine of parasternite IV (Fig. 1.17 *C. duckensis*); small species, body length 0.88. Brazil.....*C. duckensis*, sp.n.

– Wing organ with eight or more pegs; appendage of tVIII is long, reaching or surpassing apex of spine of parasternite IV (Fig. 1.16 *C. bierigi*); larger, body length 0.98-1.2.....22

22 (21) Length of the portion of appendage of tVIII distally of the twist is greater than width of tVII (Fig. 1.16 *C. bierigi*); distal portion of appendage of tVIII curved medially; wing organ with 9-10 pegs (Fig. 1.14C). Costa Rica, Panama.....*C. bierigi* Wygodzinsky

– Length of the portion of appendage of tVIII distally of the twist is equal to width of tVII (Fig. 1.16 *C. communis*); distal portion of appendage of tVIII straight; wing organ with 8-10 pegs (Fig. 1.14F). Colombia..... *C. communis*, sp.n.

23 (18) Parasternite IV large with long thin spine (Fig. 1.16 *C. delapenae*); right side of sternite II+III reaching abdominal segment VII; apex of appendage of tVIII strongly curved caudally; wing organ with 10 pegs (Fig. 1.14H). Ecuador ..... *C. delapenae*, sp.n.

– Parasternite IV small with short rounded spine (Fig. 1.18 *C. schuhi*); right side of sternite II+III reaching abdominal segments V or VI at most; apex of appendage of tVIII straight.....24

24 (23) Anophoric process hook-shaped, widened at base with rounded apex (Fig. 1.18 *C. scudderi*); wing organ with 10 pegs (Fig. 1.15I). Ecuador ..... *C. scudderi*, sp.n.

– Anophoric process elongated, stick-shaped (Fig. 1.18 *C. schuhi*).....25

25 (24) Appendage of tVIII has a characteristic bend at proximal portion (Fig. 1.17 *C. iquitosensis*); parasternites IV and V fused together; anophoric process slightly curved anteriorly; wing organ with seven pegs (Fig. 1.14N). Peru ..... *C. iquitosensis*, sp.n.

– Appendage of tVIII with straight proximal portion (Fig. 1.18 *C. trinitatis*); parasternite V is free (Fig. 1.18 *C. trinitatis*) 26

26 (25) Wing organ cavity curved, with 10-11 pegs (Fig. 1.15K); anophoric process medially constricted (Fig. 1.11C, Fig. 1.18 *C. trinitatis*). Trinidad and Tobago *C. trinitatis* (China)

– Wing organ cavity straight, with seven or less pegs (Fig. 1.15H); anophoric process without constriction (Fig. 1.18 *C. schuhi*) 27

27 (26) Wing organ with six pegs (Fig. 1.15H); anophoric process slightly curved posteriorly (Fig. 1.18 *C. schuhi*). Brazil ..... *C. schuhi*, sp.n.

– Wing organ with seven pegs (Fig. 1.15D); anophoric process straight (Fig. 1.18 *C. parvioculatus*). Venezuela ..... *C. parvioculatus*, sp.n.

Key to species of *Chinannus* (females):

1 Forewing with pale band (Fig. 1.1 *C. advenus*).....2

– Forewing without pale band, uniformly colored (Figs 1.1-2 *C. deformis*).....6

2 (1) Forewing strongly areolate, with prominent round cell at apex (Fig. 1.1 *C. areolatus*, Fig. 1.5 *C. areolatus*); spermathecal reservoir C-shaped; spermathecal gland same width as reservoir (Fig. 1.19 *C. areolatus*). Ecuador.....*C. areolatus*, sp.n.

– Forewing not areolate (Fig. 1.1 *C. advenus*), if yes, then no prominent round cell at apex; spermathecal reservoir comma-shaped 3

3 (2) Spermathecal reservoir with basal portion as wide as middle portion (Fig. 1.19 *C. advenus*); proximal segment of spermathecal duct long and coiled. Venezuela .....*C. advenus*, sp.n.

– Spermathecal reservoir with enlarged basal portion (Fig. 1.19 *C. monteverdensis*); proximal segment of spermathecal duct short, not coiled.....4

4 (3) Forewing with acute apex (Fig. 1.3 *C. monteverdensis*). Costa Rica .....*C. monteverdensis*, sp.n.

– Forewing with blunt or rounded apex (Fig. 1.1 *C. bierigi*).....5

5 (4) Forewing areolate (Fig. 1.2 *C. delapenae*); spermathecal gland of same width as reservoir (Fig. 1.19 *C. delapenae*). Ecuador.....*C. delapenae*, sp.n.

– Forewing punctate (Fig. 1.1 *C. bierigi*). Panama isthmus .....Complex of species (*C. bierigi* Wygodzinsky, *C. bispinosus* sp.n., *C. latus* sp.n., *C. nicaraguensis* sp.n.)

6 (1) Forewing with prominent spine on dorsal surface, as well as with apical spine (Fig. 1.4 *C.* sp. Peru, Fig. 1.5 *C.* sp. Peru).....*C.* sp. Peru

– No spines on the forewing surface.....7

7 (6) Eyes very small, equal in width to first antennal segment (Fig. 1.5 *C. parvioculatus*). Venezuela .....*C. parvioculatus*, sp.n.

– Eyes larger 8

8 (7) Venation distinct (Fig. 1.5 *C. deformis*); spermathecal gland large, equal or larger than width of spermathecal reservoir (Fig. 1.19 *C. deformis*); spermathecal gland duct extremely short. Ecuador .....*C. deformis*, sp.n.

– Venation indistinct.....9

9 (8) Spermathecal reservoir very small, the gland much smaller than gland duct (Fig. 1.19 *C. parvithecatus*). Brazil.....*C. parvithecatus*, sp.n.

– Spermathecal reservoir larger, not spherical (Fig. 1.19 *C. trinitatis*), or if spherical, then greater in diameter than gland duct (Fig. 1.19 *C. dissimilis*).....10

10 (9) Spermathecal reservoir spherical (Fig. 1.19 *C. dissimilis*).....11

– Spermathecal reservoir not spherical (Fig. 1.19 *C. trinitatis*).....13

11 (10) Spermathecal duct wide, same width or wider than spermathecal gland (Fig. 1.19 *C. iquitosensis*). Peru .....*C. iquitosensis*, sp.n.

– Spermathecal duct narrower than spermathecal gland (Fig. 1.19 *C. dissimilis*).....12

12 (11) Punctation weak (Fig. 1.5 *C. duopaxillatus*); body length 1.07. Brazil, French Guiana, Peru.....*C. duopaxillatus*, sp.n.

– Punctation strong (Fig. 1.5 *C. dissimilis*); body length 0.93. Bolivia...*C. dissimilis*, sp.n.

13 (10) Spermathecal reservoir T-shaped (Fig. 1.19 *C. trinitatis*); spermathecal duct coiled. Trinidad and Tobago .....*C. trinitatis* (China)

– Spermathecal reservoir C-shaped (Fig. 1.19 *C. inermis*); spermathecal duct not coiled. Peru 14

14 (13) Connection of spermathecal duct to genital chamber in form of narrow prominent spiral, center of spiral wide (Fig. 1.19 *C. inermis*) .....*C. inermis*, sp.n.

– Connection of spermathecal duct to genital chamber in form of wide lightly sclerotized spiral, center of spiral narrow (Fig. 1.19 *C. lewisi*) .....*C. lewisi*, sp.n.

***Chinannus advenus* sp. n.**

(Figs 1.1, 1.5, 1.12, 1.14A, 1.16, 1.19)

(urn:lsid:zoobank.org:act:913D7166-51C9-429B-90A9-B9C45894DFE0)

HOLOTYPE: 1 ♂, VENEZUELA, Aragua, Rancho Grande, 15 km N Maracay, 9.16667°N 64.61667°W, 1000 m, 19 – 27-II-71, S. B. Peck (UCR_ENT 00090588) (FMNH).

PARATYPES: 1 ♂(UCR_ENT 00020590), CANADA, British Columbia, Greater Vancouver Regional District Co., Pacific Spirit Regional Park, 49.25337°N 123.22192°W, 26 Jun 1997, J. Lea, A. Klimaszewski (CNC); 2 ♂ (UCR_ENT 00095646, UCR_ENT 00095645), 5 ♀ (UCR_ENT 00095637, UCR_ENT 00095638, UCR_ENT 00095640, UCR_ENT 00095642, UCR_ENT 00095643), VENEZUELA, Aragua, Tiara, 50 km SW of Caracas, 10.13217°N 67.15624°W, 2000 m, 22-II-71, S. Peck (CUNI); 2 ♂ (UCR_ENT 00098862, UCR_ENT 00097843), 2 ♀ (UCR_ENT 00098863, UCR_ENT 00096938) (FMNH), 1 ♂ (UCR_ENT 00097844) (AMNH), Rancho Grande, 15 km N Maracay, 9.16667°N 64.61667°W, 1000 m, 19 – 27-II-71, S. B. Peck.

Diagnosis. The species can be distinguished by the following combination of characters: forewing with well-developed membranous area posteriorly of the distal portion of 1AN; wing organ with middle cavity with eight pegs; parasternite IV with pouch and spine; appendage of tVIII elbowed with twist and serrated cylindrical apex; anophoric process narrowed at base, slightly widened in the middle, and tapering at apex; female forewing heavily punctate, with pale band; spermathecal reservoir comma-shaped, not inflated at base; proximal segment of spermathecal duct long and coiled.

The apical structure of the appendage of tVIII clearly separates males of the species from other species. The unique shape of the spermathecal reservoir and the coiled proximal segment of the spermathecal duct distinguish females of the species.

Description. *Male*. Total length: 1.22 mm; width across pronotum: 0.58 mm. COLORATION (Fig. 1.1). General color brown; costal cell of forewing darkened compared to the rest of corium; veins same color as membrane; apex of wing organ same color as the rest of wing organ. SURFACE AND VESTITURE. As in generic description. STRUCTURE. Macropterous, with well-developed membranous area posteriorly of the distal portion of 1AN (Fig. 1.12); veins (except for those forming costal cell) not widened; wing organ more than two thirds as long as discal cell; wing organ with middle cavity, almost equal in length to wing organ; wing organ cavity with eight pegs (Fig. 1.14A); wing organ pegs longer than wide. ABDOMEN AND GENITALIA (Fig. 1.16). Sternite II+III on right side reaching sternite V; parasternite IV relatively small, with pouch and spine; parasternites V and VI roughly equal in length to corresponding sternites; tVIII with movable appendage on left side, without process on

right side, half as long as tVII; appendage of tVIII elbowed with twist, its apex with serrated cylinder; vesica relatively short, two and a half coils; anophore tube-like, slightly asymmetrical with right side being little longer than left; anophoric process narrowed at base, slightly widened medially, and tapering at apex.

Female. Total length: 1.11 mm; width across pronotum: 0.52 mm. COLORATION (Figs 1.1, 1.5). General color brown; forewing brown with transverse pale band that strongly widens medially. SURFACE AND VESTITURE. Forewing heavily punctate. STRUCTURE. Compound eye wider than first antennal segment; apex of forewing rounded. GENITALIA (Fig. 1.19). Spermathecal reservoir comma-shaped, its basal portion as wide as middle portion; spermathecal duct long, more than three length of reservoir, consists of two segments with small outbranching duct in between; proximal segment of spermathecal duct long and coiled; spermathecal gland diameter equal to spermathecal reservoir width; spermathecal gland duct relatively long.

Etymology. Named for the fact that one of the specimens of this species was collected in Canada, with the remaining 13 specimens known from Venezuela. The epithet is an adjective after the Latin “advenus” meaning foreign or alien.

Distribution. Known from two localities in Venezuela at elevations of 1000m and 2000m. Also known from a single specimen collected in Vancouver, British Columbia, Canada.

Discussion. The first record of the species was reported by Scudder (2010) from Vancouver, British Columbia, Canada. A single male specimen was collected at a forest edge by extracting leaf litter close to a wood-processing facility that also imported

tropical wood (A. Klimaszewski and G. Scudder, pers. com.). Subsequent collecting attempts by two of us around Vancouver have not brought about any additional specimens. A morphological assessment of the specimen revealed strong similarities in wing and genitalic structures to specimens of a species that is otherwise known from Venezuela. Although four species of Schizopteridae occur in the northern Nearctic and have been recorded from as far north as Virginia (US), all records are from the central and eastern parts of North America. Given that the distribution ranges of other *Chinannus* species reach their northern limits in Nicaragua and the fact that the single Vancouver specimen was collected close to a disturbed area, we propose that this record from the West Coast of the United States is most likely due to an introduction event.

***Chinannus areolatus* sp. n.**

(Figs 1.1, 1.5, 1.12, 1.14B, 1.16, 1.19)

(urn:lsid:zoobank.org:act:B5835D11-2FD2-41E9-B72A-826DD3A6D944)

HOLOTYPE: 1 ♂ ECUADOR, Pastaza, 25 km N Puyo, 1.2855°S 78.02291°W, 1000 m, 13-VII-76, S. B. Peck (UCR_ENT 00090653) (FMNH).

PARATYPES: 1 ♀(UCR_ENT 00090662), ECUADOR, Pastaza, 25 km N Puyo, 1.2855°S 78.02291°W, 1000 m, 13-VII-76, S. B. Peck (FMNH).

Diagnosis. The species can be distinguished by the following combination of characters: forewing with reduced membranous area posteriorly of the distal portion of 1AN; wing organ with middle cavity, 11 pegs and transparent patch at apex; parasternite IV with pouch and spine; appendage of tVIII elbowed with twist, distal portion straight and

tapering at apex; anophoric process claw-shaped; female forewing strongly areolate, with pale band and round apical cell; spermathecal reservoir C-shaped, slightly inflated at base.

The species is most similar to *C. translucidus* in having a transparent patch on the wing organ and similar shape of spine of parasternite IV and appendage of tVIII. *C. areolatus* can be distinguished from *C. translucidus* by the longer wing organ with more pegs in it. Females of *C. areolatus* can be easily distinguished from other species by strongly areolate forewings with round apical cell.

Description. *Male*. Total length: 0.87 mm; width across pronotum: 0.46 mm. COLORATION (Fig. 1.1). General coloration brown; costal cell of forewing darkened compared to the rest of corium; veins same color as membrane; apex of wing organ with transparent patch at apex. SURFACE AND VESTITURE. As in generic description. STRUCTURE. Submacropterous, with reduced membranous area posteriorly of the distal portion of 1AN (Fig. 1.12); veins (except for those forming costal cell) not widened; wing organ more than four fifths as long as discal cell; wing organ with middle cavity, almost equal in length to wing organ; wing organ cavity with 11 pegs (Fig. 1.14B); wing organ pegs longer than wide at apex of wing organ or roughly as wide as long, blunt at base of wing organ. ABDOMEN AND GENITALIA (Fig. 1.16). Sternite II+III on right side reaching posterior margin of sternite IV; parasternite IV relatively large, with large pouch and small spine; parasternite V half as long as sternite V; parasternite VI roughly equal in length to sternite VI; tVIII with movable appendage on left side, without process on right side, less than half as long as tVII; appendage of tVIII elbowed with twist, distal

portion straight and tapering at apex; vesica relatively short, two and a half coils; anophore tube-like, almost symmetrical; anophoric process claw-shaped.

Female. Total length: 0.87 mm; width across pronotum: 0.47 mm. COLORATION (Figs 1.1, 1.5). General color brown; forewing brown with transverse pale band that slightly widens medially. SURFACE AND VESTITURE. Forewing strongly areolate. STRUCTURE. Compound eye slightly wider than first antennal segment; apex of forewing rounded with slight incision and prominent round cell. GENITALIA (Fig. 1.19). Spermathecal reservoir C-shaped, with slightly inflated basal portion; spermathecal duct short, two to three lengths of reservoir, consists of two segments with no outbranching ducts in between; proximal segment of spermathecal duct short, not coiled; spermathecal gland diameter equal to spermathecal reservoir width; spermathecal gland duct relatively short.

Etymology. The species is named for the strongly areolate forewings of the female, an adjective derived from the Latin noun “areola” meaning “small space” (between wing veins).

Distribution. The species is known from one locality in Pastaza, Ecuador.

***Chinannus bierigi* Wygodzinsky, 1948**

(Figs 1.1, 1.5, 1.10A-E, 1.11I, 1.11J, 1.12, 1.14C, 1.16, 1.19)

Chinannus bierigi Wygodzinsky, 1948: 147 (original description)

HOLOTYPE: 1 ♂, COSTA RICA, Cartago, Turrialba Co., Chitaría, 9.9369°N 83.59093°W, 760 m, 26-III-44 or 07 – 11-IV-44, Bierig (Instituto de Ecologia e Experimentação Agrícola), not studied

PARATYPES: 1 ♂ (UCR_ENT 00069182), 1 ♀(UCR_ENT 00069183), COSTA RICA, Cartago, Turrialba Co., Chitaría, 9.9369°N 83.59093°W, 760 m, 26-III-44, Bierig (BMNH); 1 ♀(AMNH_IZC 00150697) (AMNH), 1 ♀ (UCR_ENT 00026772) (USNM), 07 – 11-IV-44, A. Bierig.

Diagnosis. The species can be distinguished by the following combination of characters: forewing with well-developed membranous area posteriorly of the distal portion of 1AN; wing organ with middle cavity with nine or 10 pegs; parasternite IV with pouch and spine; appendage of tVIII elbowed with twist, distal portion curved medially and tapering at apex; anophoric process claw-shaped; female forewing heavily punctate, with pale band; spermathecal reservoir comma-shaped, inflated at base.

Along with *C. bierigi*, several other *Chinannus* species are known from the region, namely *C. bispinosus*, *C. latus*, *C. monteverdensis*, *C. perplexus*, and *C. nicaraguensis*. Males of *C. bierigi* clearly differs from all of them: from *C. latus*, *C. nicaraguensis* and *C. perplexus* by having wings with fully developed membrane, and from *C. monteverdensis* and *C. bispinosus* by shape of genitalia. Females of *C. bierigi* can be distinguished from *C. monteverdensis* by the blunt apex of forewings, however it is very difficult to tell apart *C. bierigi*, *C. nicaraguensis* and *C. bispinosus*, although our phylogenetic analysis showed difference between *C. bierigi* and *C. nicaraguensis*. The other species, to which *C. bierigi* is similar, is *C. communis* from Colombia. Male

specimens of *C. bierigi* are similar to *C. communis* in general habitus, having the same or almost the same number of pegs in the wing organ, and general shape of genitalia. Males of *C. bierigi* can be distinguished from *C. communis* by the shape of appendage of tVIII, which is longer and curved medially distally of the twist, and by a larger anophoric process.

Redescription. *Male*. Total length: 1.20 mm; width across pronotum: 0.54 mm. COLORATION (Fig. 1.1). General color brown to black; costal cell of forewing darkened compared to the rest of corium; veins same color as membrane; apex of wing organ same color as the rest of wing organ. SURFACE AND VESTITURE. As in generic description. STRUCTURE. Macropterous, with well-developed membranous area posteriorly of the distal portion of 1AN (Fig. 1.12); veins (except for those forming costal cell) not widened; wing organ almost equal in length to discal cell; wing organ with middle cavity, almost equal in length to wing organ; wing organ cavity with nine pegs (Fig. 1.14C); wing organ pegs longer than wide. ABDOMEN AND GENITALIA (Fig. 1.16). Sternite II+III on right side reaching the middle of sternite V; parasternite IV relatively small, with pouch and spine; parasternite V half as long as sternite V; parasternite VI slightly shorter than length of sternite VI; tVIII with movable appendage on left side, without process on right side, half as long as tVII; appendage of tVIII elbowed with twist, distal portion curved medially and tapering at apex; vesica short, two and a half coils; anophore tube-like, slightly asymmetrical with right side being longer than left; anophoric process claw-shaped.

Female. Total length: 0.88 mm; width across pronotum: 0.49 mm. COLORATION (Figs 1.1, 1.5). General color black; forewing brown with transverse pale band that slightly widens medially. SURFACE AND VESTITURE. Forewing heavily punctate. STRUCTURE. Compound eye slightly wider than first antennal segment; apex of forewing abrupt. GENITALIA (Fig. 1.19). Spermathecal reservoir comma-shaped, with enlarged basal portion; spermathecal duct short, two to three length of reservoir, consists of two segments with small outbranching duct in between; proximal segment of spermathecal duct short, not coiled; spermathecal gland diameter smaller than spermathecal reservoir width; spermathecal gland duct relatively short.

Distribution. The species is known from many localities across Costa Rica.

Other Specimens Examined. COSTA RICA: Cartago: Paraiso Co.: 1♂ (UCR_ENT 00014569), Est. Tapanti, Sendero Arboles Caidos, 9.75942°N 83.82102°W, 1100 m, 29-III-2011 – 19-II-2012, R. Zuniga, C. Mora (INBIO); 1♀ (UCR_ENT 00014790), Parque Nacional Tapanti. Send. Pava-Catarata., 9.73207°N 83.78013°W, 1300 m, 6 – 8-XII-2008, M. Solis & S. Meueses (INBIO); 3♂ (UCR_ENT 00089319-UCR_ENT 00089321), 3♀ (UCR_ENT 00089322-UCR_ENT 00089324), Turrialba, CATIE natural forest, 9.89656°N 83.65745°W, 560 m, 11-IX-78, P. Werner (MHNG); 1♂ (UCR_ENT 00089600), 24-IX-78, P. Werner, (MHNG); 1♂ (UCR_ENT 00014555), Turrialba. R.F. Rio Pacuare, P.N. Barbilla, Est. Barbilla, 9.97992°N 83.45232°W, 600 m, 19 Jan 2001, W. Arana. Tp. Mantillo (INBIO); Heredia: Sarapiqui Co.: 1♂ (UCR_ENT 00014580), La Virgen, La Isla, 10.41411°N 84.12805°W, 100 m, 5-XI-2011 – 7-XII-2011, I. Chacon (INBIO); 3♂ (UCR_ENT 00014563, UCR_ENT 00014566, UCR_ENT 00014515), 4♀

(UCR_ENT 00014793, UCR_ENT 00014792, UCR_ENT 00014794, UCR_ENT 00014795), P.N. Braulio Carrillo, 16 Km SSE La Virgen, 10.26784°N 84.084°W, 1050 m, 20 – 23-II-2001, INBio-OET-ALAS (INBIO); 1♂ (UCR_ENT 00014560), 2♀ (UCR_ENT 00014796, UCR_ENT 00014797), 23-II-2001, INBio-OET-ALAS (INBIO); 4♂ (UCR_ENT 00014553, UCR_ENT 00014557, UCR_ENT 00014565, UCR_ENT 00014516), 13♀ (UCR_ENT 00014592-UCR_ENT 00014597, UCR_ENT 00014602, UCR_ENT 00014598, UCR_ENT 00014600, UCR_ENT 00014601, UCR_ENT 00014599, UCR_ENT 00014603, UCR_ENT 00014604), 14 – 17-III-2001, INBio-OET-ALAS (INBIO); 4♂ (UCR_ENT 00014558, UCR_ENT 00014561, UCR_ENT 00014564, UCR_ENT 00014514), 5♀ (UCR_ENT 00014587-UCR_ENT 00014591), 17-III-2001, INBio-OET-ALAS (INBIO); 4♀ (UCR_ENT 00014798, UCR_ENT 00014799, UCR_ENT 00014605, UCR_ENT 00014606), 19 – 22-III-2001, INBio-OET-ALAS (INBIO); 2♂ (UCR_ENT 00014559, UCR_ENT 00014562), 6♀ (UCR_ENT 00014581-UCR_ENT 00014586), 22-III-2001, INBio-OET-ALAS (INBIO); 1♀ (UCR_ENT 00090862), 16 km N Volcán Barba, 10.00444°N 84.00139°W, 1020 m, 9-VII-86, J. T. Longino (FMNH); 2♂ (UCR_ENT 00093429, UCR_ENT 00093428), 16 km SSE La Virgen, 10.26666°N 84.08333°W, 1150 m, 9-II-2001 – 14-III-2001, E. G. Riley (TAMU); 2♂ (UCR_ENT 00120608, UCR_ENT 00120609), La Selva Biological Station, 10.42256°N 84.00144°E, 49 m, 12 – 13-VIII-2010, Heraty & Mottern (UCR); 4♂ (UCR_ENT 00077038, UCR_ENT 00082324, UCR_ENT 00082335, UCR_ENT 00082336), La Selva Biological Station, River Station, 10.43°N 84.00472°W, 60 m, 22 – 23-V-2011, J. Heraty & E. Murray (UCR); 1♂ (UCR_ENT 00109099), La Selva

Biological Station, nr Puerto Viejo, 10.43086°N 84.00647°W, 52 m, 5-II-98, INBio-OET-ALAS, Light Trap (INBIO); 1♂ (UCR_ENT 00109100), 30-III-99, INBio-OET-ALAS, Light Trap (INBIO); 3♂ (UCR_ENT 00109094-UCR_ENT 00109096), 2♀ (UCR_ENT 00109097, UCR_ENT 00109098), 21-VI-99, D. Brenes (INBIO); 1♂ (UCR_ENT 00109091), 2♀ (UCR_ENT 00109092, UCR_ENT 00109093), 25-VI-99, D. Brenes, (INBIO); 1♂ (UCR_ENT 00077351), 4♀ (UCR_ENT 00004804, UCR_ENT 00004789, UCR_ENT 00119031, UCR_ENT 00119032), 9 – 15-VIII-2010, OTS Heteroptera course (UCR); Puntarenas: 1♀ (UCR_ENT 00014556), Golfito, Res Ftal Golfo Dulce, ESt Agujas, 8.63879°N 83.16668°W, 250 m, 22-XII-99, A. Azofeifa (INBIO); 1♀ (UCR_ENT 00090602), OTS Station finca Las Cruces, San Vito, 8.76666°N 82.96666°W, 1219 m, 19-III-73, J. A. Wagner, J. B. Kethley (FMNH); Costa Rica, unknown locality: 1♂ (UCR_ENT 00088879), 2♀ (UCR_ENT 00088891, UCR_ENT 00088895) (MHNG), 1♀ (UCR_ENT 00088881) (MHNG), 1♀ (UCR_ENT 00089336) (MHNG), 6♀ (UCR_ENT 00088882-UCR_ENT 00088887) (MHNG), 2♀ (UCR_ENT 00089637, UCR_ENT 00089638) (MHNG), 1♂ (UCR_ENT 00089310), 1♀ (UCR_ENT 00089311) (MHNG).

***Chinannus bispinosus* sp. n.**

(Figs 1.1, 1.5, 1.12, 1.14D, 1.16, 1.19)

(urn:lsid:zoobank.org:act:62296F67-E6E4-485B-9825-2471076759B4)

HOLOTYPE: 1 ♂ PANAMA, Colon, 2 km S of Sabanitas, 9.32194°N 79.79833°W, 120 m, 15 – 19-VII-99, A. Gillogly & J.B. Woolley (UCR_ENT 00094267) (TAMU).

PARATYPES: 2 ♀ (UCR_ENT 00094268, UCR_ENT 00094269), PANAMA: Colon: 2 km S of Sabanitas, 9.32194°N 79.79833°W, 120 m, 15 – 19-VII-99, A. Gillogly & J.B. Woolley (TAMU); 1♀ (UCR_ENT 00030205), Panama, Barro Colorado Island, 9.15676°N 79.84703°W, I-II-45, Zelek (USNM).

Diagnosis. This species can be distinguished by the following combination of characters: forewing with well-developed membranous area posteriorly of the distal portion of 1AN; wing organ with middle cavity with 10 pegs; abdomen with parasternites on both sides of segments IV, V, and VI; parasternites IV with pouch and spine, symmetrical; appendage of tVIII elbowed with twist, distal portion curved laterally and tapering at apex; anophoric process claw-shaped; female forewing heavily punctate, with pale band; spermathecal reservoir comma-shaped, inflated at base.

Males of *C. bispinosus* resemble *C. bierigi*, but can be identified by having both sides of the abdomen with modified parasternites, and by the shape of the distal portion of the appendage of tVIII. Females are difficult to identify.

Description. *Male*. Total length: 0.92 mm; width across pronotum: 0.46 mm. COLORATION (Fig. 1.1). General color black; costal cell of forewing darkened compared to the rest of corium; veins same color as membrane; apex of wing organ same color as the rest of wing organ. SURFACE AND VESTITURE. As in generic description. STRUCTURE. Macropterous, with well-developed membranous area posteriorly of the distal portion of 1AN (Fig. 1.12); veins (except for those forming costal cell) not widened; wing organ almost equal to the length of discal cell; wing organ with middle cavity, almost equal in length to wing organ; wing organ cavity with 10 pegs (Fig.

1.14D); wing organ pegs longer than wide. ABDOMEN AND GENITALIA (Fig. 1.16). Sternite II+III on sides reaching the middle of sternite V; parasternites IV relatively small, with pouch and spine; parasternites V half as long as sternite V; parasternites VI slightly shorter than length of sternite VI, left one smaller than right one; tVIII with movable appendage on left side, without process on right side, half as long as tVII; appendage of tVIII elbowed with twist, distal portion curved laterally and tapering at apex; vesica relatively short, two coils; anophore tube-like, almost symmetrical; anophoric process claw-shaped.

Female. Total length: 0.82 mm; width across pronotum: 0.44 mm. COLORATION (Figs 1.1, 1.5). General color black; forewing brown with transverse pale band that slightly widens medially. SURFACE AND VESTITURE. Forewing heavily punctate. STRUCTURE. Compound eye slightly wider than first antennal segment; apex of forewing rounded. GENITALIA (Fig. 1.19). Spermathecal reservoir comma-shaped, with enlarged basal portion; spermathecal duct short, two to three length of reservoir, consists of two segments with small outbranching duct in between; proximal segment of spermathecal duct short, not coiled; spermathecal gland diameter smaller than spermathecal reservoir width; spermathecal gland duct relatively short.

Etymology. The species is named for the unique feature of having parasternites with one spine on each side of the abdomen, an adjective derived from the Latin prefix “bi-” and the noun “spina”, meaning “bearing two spines”.

Distribution. The species is known from two localities in Panama.

Discussion. The modification of the left side of the abdomen is unique amongst described species of Schizopteridae. In some other genera with modified pregenital abdomen (*Itagunannus*, *Vilhenannus* Wygodzinsky, 1950, *Machadonannus* Wygodzinsky, 1950, *Dundonannus* Wygodzinsky, 1950, and *Semangananus* Štys, 1974) only the right side has appendages or processes, with the left side being unmodified. In *C. bispinosus*, parasternites IV are modified on both sides into spine and pouch sclerites, with the appendage of tVIII and anophoric process retaining dextral orientation. This fact might cast doubt on speculations about the association between the asymmetry of segments VIII and X and asymmetry of segment IV. The observed condition in *C. bispinosus* could be due to teratology of a particular specimen, or due to an unusual but normal species morphology. This is currently hard to prove or disprove since only one male specimen was collected. However, it is important to mention that despite equal development of parasternites IV and V in *C. bispinosus*, parasternite VI is smaller on the left side, and parasternite VII is absent on the left side but present on the right. When sorting through the material of Dipsocoromorpha assembled at UCR we found multiple specimens of one yet undescribed species of the *Corixidea* genus group from Ecuador that has pregenital processes on both sides of abdomen. Interestingly, similar to the situation in *C. bispinosus*, in *Corixidea* specimens the basal portion of the abdomen carries processes on both sides, while the apical portion has only right side processes.

***Chinannus caudalis* sp. n.**

(Figs 1.1, 1.12, 1.14E, 1.16)

(urn:lsid:zoobank.org:act:CEE0245E-9DC4-4960-B844-8AC4EAEDF175)

HOLOTYPE: 1 ♂ COLOMBIA, Putumayo, Parque Nacional La Paya Cabaña Chagra, 0.11666°S 74.93333°W, 320 m, 1 – 15-XI-2001, R. Cobete (UCR_ENT 00076318) (IAvH).

PARATYPES: 1 ♂ (UCR_ENT 00076331), COLOMBIA, Putumayo, Parque Nacional La Paya Cabaña Chagra, 0.11666°S 74.93333°W, 320 m, 1 – 15-XI-2001, R. Cobete (IAvH).

Diagnosis. The species can be distinguished by the following combination of characters: forewing with reduced membranous area posteriorly of the distal portion of 1AN; wing organ with caudal cavity with two pegs; parasternite IV with pouch and flattened apex, spine absent; tVIII with process on right side, movable appendage absent; anophoric process long and thin, directed anteriorly.

The species can be easily distinguished from all species by caudal position of cavity in wing organ.

Description. *Male*. Total length: 0.88 mm; width across pronotum: 0.37 mm. COLORATION (Fig. 1.1). General color brown; costal cell of forewing darkened compared to the rest of corium; veins same color as membrane; apex of wing organ same color as the rest of wing organ. SURFACE AND VESTITURE. As in generic description. STRUCTURE. Submacropterous, with reduced membranous area posteriorly of the distal portion of 1AN (Fig. 1.12); veins (except for those forming costal cell) not

widened; wing organ more than four fifths as long as discal cell; wing organ with small caudal cavity; wing organ cavity with two pegs (Fig. 1.14E); wing organ pegs roughly as wide as long, and rounded. ABDOMEN AND GENITALIA (Fig. 1.16). Sternite II+III on right side reaching posterior margin of sternite IV; parasternite IV relatively large, with pouch and flattened apex; parasternite V fused with parasternite IV; parasternite VI roughly equal in length to sternite VI; tVIII without movable appendage on left side, with short wide tapering process on right side, almost half as long as tVII; vesica very short, one and a half coil; anophore tube-like, almost symmetrical; anophoric process long and thin, directed anteriorly.

Female. Unknown.

Etymology. The species is named for the caudal position of the cavity of the wing organ (when wings are at rest), which is a unique feature amongst species in the genus. An adjective derived from the Latin noun "cauda" meaning "tail".

Distribution. The species is known from one locality in Putumayo, Colombia.

Chinannus communis **sp. n.**

(Figs 1.1, 1.11A, 1.11B, 1.11H, 1.12, 1.14F, 1.16)

(urn:lsid:zoobank.org:act:3FB6E89A-2A4E-4FA5-A68B-9C1E34DEB547)

HOLOTYPE: 1 ♂ COLOMBIA, Cauca, PNN Gorgona, Alto el Mirador, 2.96666°N 78.18333°W, 180 m, 10 - 26-VI-2000, H. Torres (UCR_ENT 00081362) (IAvH).

PARATYPES: 1 ♂ (UCR_ENT 00076302), COLOMBIA: Boyacá: La Planada, Santuario de Flora y Fauna de Iguaque, 5.41666°N 73.45°W, 2850 m, 19-IV-2000 – 6-V-

2000, P. Reina (IAvH); 2 ♂ (UCR_ENT 00076298, UCR_ENT 00076272), SFF Iguaque La Planada, 5.7°N 73.45°W, 2850 m, 19-IV-2000 – 6-V-2000, P. Reina (IAvH); 1 ♂ (UCR_ENT 00078119), Cauca, PNN Gorgona, Alto el Mirador, 2.96666°N 78.18333°W, 180 m, 3 – 16-VIII-2000, H. Torres (IAvH); 7 ♂ (UCR_ENT 00115570-UCR_ENT 00115573, UCR_ENT 00115576, UCR_ENT 00115596, UCR_ENT 00115597), 6 – 23-X-2000, R. Duque (IAvH); 23 ♂ (UCR_ENT 00106835, UCR_ENT 00106844, UCR_ENT 00106848, UCR_ENT 00106849, UCR_ENT 00106856-UCR_ENT 00106859, UCR_ENT 00106877-UCR_ENT 00106879, UCR_ENT 00106883, UCR_ENT 00106900, UCR_ENT 00106901, UCR_ENT 00106906, UCR_ENT 00106909, UCR_ENT 00106911, UCR_ENT 00106912, UCR_ENT 00106920, UCR_ENT 00106921, UCR_ENT 00106925, UCR_ENT 00106940, UCR_ENT 00106943), 30-XI-2000 – 18-XII-2000, H. Torres (IAvH); 1 ♂ (UCR_ENT 00109001), PNN Gorgona, Antigua Laguna, 2.96667°N 78.18333°W, 70 m, 18-XII-2000 – 3-I-2001, H. Torres (IAvH); 3 ♂ (UCR_ENT 00112576-UCR_ENT 00112578), PNN Gorgona, El Helechal, 2.96667°N 78.18333°W, 30 m, 22-III-2001 – 13-IV-2001, R. Duque (IAvH); 1 ♂ (UCR_ENT 00092752), 23-VI-2001 – 15-VII-2001, H. Torres (IAvH); 2 ♂ (UCR_ENT 00099917, UCR_ENT 00099922), 27-VIII-2001 – 12-IX-2001, H. Torres (IAvH); 1 ♂ (UCR_ENT 00074605), PNN Gorgona El Saman, 2.96667°N 78.18333°W, 5 m, 12-VI-2001 – 27-VI-2001, H. Torres (IAvH); 1 ♂ (UCR_ENT 00099280), Parque Nacional Gorgona El Saman, 2.96667°N 78.18333°W, 5 m, 21-V-2001 – 12-VII-2001, H. Torres (IAvH); 1 ♂ (UCR_ENT 00074538), Parque Nacional Gorgona Mancora, 2.96666°N 78.18333°W, 60 m, 8 – 30-XI-2000, H. Torres (IAvH); 1 ♂ (UCR_ENT

00100863), Cundinamarca: PNN Chingaza La Siberia, 4.51667°N 73.75°W, 3170 m, 13 – 15-VII-2001, L. Cifuentes (IAvH).

Diagnosis. The species can be distinguished by the following combination of characters: forewing with well-developed membranous area posteriorly of the distal portion of 1AN; wing organ with middle cavity with eight to 10 pegs; parasternite IV with pouch and spine; appendage of tVIII elbowed with twist, distal portion straight and tapering at apex; anophoric process claw-shaped.

The species resembles *C. bierigi* in general habitus and shape of genitalia, for differences see *C. bierigi* discussion.

Description. *Male*. Total length: 0.98 mm; width across pronotum: 0.49 mm. COLORATION (Fig. 1.1). General color brown to black; costal cell of forewing darkened compared to the rest of corium; veins same color as membrane; apex of wing organ same color as the rest of wing organ. SURFACE AND VESTITURE. As in generic description. STRUCTURE. Macropterous, with well-developed membranous area posteriorly of the distal portion of 1AN (Fig. 1.12); veins (except for those forming costal cell) not widened; wing organ almost equal in length to discal cell; wing organ with middle cavity, almost equal in length to wing organ; wing organ cavity with 8-10 pegs (Fig. 1.14F); wing organ pegs longer than wide. ABDOMEN AND GENITALIA (Fig. 1.16). Sternite II+III on right side reaching the middle of sternite V; parasternite IV relatively small, with pouch and spine; parasternite V half as long as sternite V; parasternite VI roughly equal in length to sternite VI; tVIII with movable appendage on left side, without process on right side, half as long as tVII; appendage of tVIII elbowed

with twist, distal portion straight and tapering at apex; vesica relatively short, two and a half coils; anophore tube-like, almost symmetrical; anophoric process claw-shaped.

Female. Unknown.

Etymology. The species is named for being one of the three most commonly collected species of *Chinannus*, after *C. bierigi* and *C. trinitatis*. A Latin adjective "communis" meaning "common".

Distribution. The species is known from several localities in Colombia, comprising mountain ranges of Boyaca and Cundinamarca and Gorgona Island.

Discussion. Most specimens we have seen had either eight or 10 pegs. In both regions (mountain ranges and Gorgona Island), specimens with both eight and 10 pegs were collected. Our molecular analysis (only 28S rDNA due to poor specimen quality) grouped specimens based on geographic area rather than peg number, and the species was recovered as monophyletic. Genitalia of all studied specimens did not reveal any differences. Thus, in absence of additional morphological or molecular diagnostic features, we treat the specimens with eight and 10 pegs as one species.

***Chinannus deformis* sp. n.**

(Figs 1.1, 1.2, 1.5, 1.11D, 1.11E, 1.12, 1.14G, 1.16, 1.19)

(urn:lsid:zoobank.org:act:FDCE2B9E-8B0A-4589-8BAC-C4D4C9ED9462)

HOLOTYPE: 1 ♂ ECUADOR, Pichincha, 16 km NE Santo Domingo, Tinalandia, 0.16694°S 79.07194°W, 700 m, 5-VI-76, S. B. Peck (UCR_ENT 00090524) (FMNH).

PARATYPES: 2 ♂ (UCR_ENT 00090527, UCR_ENT 00090528), 1 ♀(UCR_ENT

00090518), ECUADOR, Pichincha, 16 km NE Santo Domingo, Tinalandia, 0.16694°S 79.07194°W, 700 m, 5-VI-76, S. B. Peck (FMNH); 1 ♂ (UCR_ENT 00090456), 2 ♀ (UCR_ENT 00090377, UCR_ENT 00090514), 5-VI-76, S. B. Peck (FMNH); 5 ♂ (UCR_ENT 00096989-UCR_ENT 00096993) (FMNH), 2 ♂ (UCR_ENT 00096994, UCR_ENT 00096995) (AMNH) 16 km S Santo Domingo, Tinalandia, 1.66444°S 77.01139°W, 680 m, 15-VI-75, S.B. Peck.

Diagnosis. This species can be distinguished by the following combination of characters: forewing with reduced membranous area posteriorly of the distal portion of 1AN; wing organ with middle cavity with six pegs; parasternite IV with pouch and spine; appendage and process of tVIII absent; anophoric process claw-shaped; female forewing heavily punctate or weakly areolate, uniformly colored; spermathecal reservoir comma-shaped, inflated at base; spermathecal gland extremely large, larger than width of reservoir. Males can be easily distinguished from all other species by the absence of projections from tVIII. Females can be of two forms, punctate and areolate, but both share the unique structure of the spermathecal complex: the relatively small, comma-shaped reservoir with very large spermathecal gland.

Description. *Male*. Total length: 0.97 mm; width across pronotum: 0.43 mm. COLORATION (Fig. 1.1). General color brown; costal cell of forewing darkened compared to the rest of corium; veins same color as membrane; apex of wing organ same color as the rest of wing organ. SURFACE AND VESTITURE. As in generic description. STRUCTURE. Submacropterous, with reduced membranous area posteriorly of the distal portion of 1AN (Fig. 1.12); veins (except for those forming costal cell) not

widened; wing organ almost equal in length to discal cell; wing organ with middle cavity, almost equal in length to wing organ; wing organ cavity with six pegs; wing organ pegs roughly as wide as long, blunt. ABDOMEN AND GENITALIA (Fig. 1.16). Sternite II+III on right side reaching the middle of sternite V; parasternite IV relatively small, with pouch and spine; parasternite V fused with parasternite IV; parasternite VI slightly shorter than length of sternite VI; tVIII without movable appendage on left side, without process on right side, half as long as tVII; vesica relatively short, two and a half coils; anophore tube-like, almost symmetrical; anophoric process relatively large, claw-shaped. *Female*. Total length: 0.88 mm; width across pronotum: 0.4 mm. COLORATION (Figs 1.1, 1.2, 1.5). General color dark brown to light brown; forewing dark brown to light brown, uniformly colored. SURFACE AND VESTITURE. Forewing weakly areolate or heavily punctate. STRUCTURE. Compound eye slightly wider than first antennal segment; apex of forewing rounded with slight incision; in areolate form apical round cell may be discerned. GENITALIA (Fig. 1.19). Spermathecal reservoir comma-shaped, with enlarged basal portion; spermathecal duct short, two to three length of reservoir, consists of two segments with small outbranching duct in between; proximal segment of spermathecal duct short, not coiled; spermathecal gland diameter larger than spermathecal reservoir width; spermathecal gland duct very short.

Etymology. Named after the absence of appendages or processes associated with tVIII, a condition unique amongst *Chinannus* species. An adjective derived from the Latin prefix “de-” and noun “forma”, meaning “departing from the correct shape”.

Distribution. Known from one locality in Pichincha, Ecuador.

Discussion. Two forms of females are known for the species, one with darker coloration and an areolate surface of the forewing, the other with lighter coloration and a punctate surface of the forewing. Only three female specimens from a single locality were studied, two of areolate and one of punctate form. Despite these differences, the structure of the spermathecal complex is similar in the two forms, and at the same time very different from all other studied *Chinannus* species. Based on this fact and considering that the three females were collected at the same locality, we treat the two forms as conspecific.

***Chinannus delapenae* sp. n.**

(Figs 1.2, 1.5, 1.12, 1.14H, 1.16, 1.19)

(urn:lsid:zoobank.org:act:0BDF3950-F9D2-44E5-B17C-CE35C08C7059)

HOLOTYPE: 1 ♂ ECUADOR, Napo, Limoncocha, 2.07472°S 79.92611°W, 250 m, 18-VI-76, S.B. Peck (UCR_ENT 00096974) (FMNH).

PARATYPES: 3 ♂(UCR_ENT 00096975-UCR_ENT 00096977) (FMNH), 1 ♂(UCR_ENT 00096978) (AMNH), 9 ♀(UCR_ENT 00096946-UCR_ENT 00096954) (FMNH), 1 ♀(UCR_ENT 00096955) (AMNH), ECUADOR, Napo, Limoncocha, 2.07472°S 79.92611°W, 250 m, 18-VI-76, S.B. Peck; 1 ♂ (UCR_ENT 00090464), 21-VI-76, S.B. Peck (FMNH).

Diagnosis. The species can be distinguished by the following combination of characters: forewing with well-developed membranous area posteriorly of the distal portion of 1AN; wing organ with middle cavity with 10 pegs; parasternite IV with pouch and long thin spine; appendage of tVIII straight, thin, and curved at apex; anophoric process claw-

shaped; female forewing strongly areolate, with pale band; spermathecal reservoir comma-shaped, inflated at base; spermathecal gland large, equal in width to reservoir. Males of this species can be easily distinguished from other species by the elongated parasternite IV with a long and thin spine. Females can be distinguished by the large spermathecal gland that is equal in diameter to the diameter of the spermathecal reservoir, and an extremely thick spermathecal gland duct.

Description. *Male*. Total length: 1.14 mm; width across pronotum: 0.51 mm. COLORATION (Fig. 1.2). General color brown; costal cell of forewing darkened compared to the rest of corium; veins same color as membrane; apex of wing organ same color as the rest of wing organ. SURFACE AND VESTITURE. As in generic description. STRUCTURE. Macropterous, with well-developed membranous area posteriorly of the distal portion of 1AN (Fig. 1.12); veins (except for those forming costal cell) not widened; wing organ almost equal in length to discal cell; wing organ with middle cavity, almost equal in length to wing organ; wing organ cavity with 10 pegs (Fig. 1.14H); wing organ pegs longer than wide. ABDOMEN AND GENITALIA (Fig. 1.16). Sternite II+III on right side reaching the middle of sternite VI; parasternite IV relatively large, with pouch and long thin spine; parasternite V very small, almost indistinct; parasternite VI slightly shorter than length of sternite VI; tVIII with movable appendage on left side, without process on right side, less than half as long as tVII; appendage of tVIII straight, thin, curved at apex; vesica relatively short, two and a half coils; anophore tube-like, almost symmetrical; anophoric process claw-shaped.

Female. Total length: 0.95 mm; width across pronotum: 0.46 mm. COLORATION (Figs 1.2, 5). General color brown; forewing brown with transverse pale band that strongly widens medially. SURFACE AND VESTITURE. Forewing strongly areolate. STRUCTURE. Compound eye slightly wider than first antennal segment; apex of forewing with prominent incision. GENITALIA (Fig. 1.19). Spermathecal reservoir comma-shaped, with enlarged basal portion; spermathecal duct short, two to three length of reservoir, consists of two segments with no outbranching ducts in between; proximal segment of spermathecal duct short, not coiled; spermathecal gland diameter larger than spermathecal reservoir width; spermathecal gland duct relatively short.

Etymology. Named after Robin Delapena who has sorted thousands of minute litter bugs from the bulk samples at the FMNH during the ARTS Dipsocoromorpha project. A noun in genitive case.

Distribution. Known from a single locality in Napo, Ecuador.

***Chinannus dissimilis* sp. n.**

(Figs 1.2, 1.5, 1.12, 1.14I, 1.16, 1.19)

(urn:lsid:zoobank.org:act:F7C56ED6-A70A-4326-8A3E-27DAA78F9DA8)

HOLOTYPE: 1 ♂ BOLIVIA, Cochabamba: Chapare Co., 5 km N Villa Tunari, 16.985°S 65.40472°W, 347 m, 22-XI-93, P. P. Parrillo and W. Rojas (UCR_ENT 00090926) (FMNH).

PARATYPES: 2 ♀(UCR_ENT 00090924, UCR_ENT 00090925), BOLIVIA,

Cochabamba, Chapare Co., 5 km N Villa Tunari, 16.985°S 65.40472°W, 347 m, 22-XI-93, P. P. Parrillo and W. Rojas (FMNH).

Diagnosis. The species can be distinguished by the following combination of characters: forewing with reduced membranous area posteriorly of the distal portion of 1AN; wing organ with middle cavity with five pegs, one peg situated in different plane from other four; parasternite IV with pouch and spine; appendage of tVIII with slight bend at proximal portion, thin at distal portion, curved at apex; anophoric process in shape of narrow lobe with rounded apex; female forewing weakly areolate, uniformly colored; spermathecal reservoir spherical; spermathecal gland diameter much smaller than width of reservoir.

Males of this species can be easily distinguished from all species except *C. loretensis* by wing organ with pegs situated not in one plane, and from *C. loretensis* by having five pegs in the wing organ, the presence of the appendage of tVIII, and the absence of the process of tVIII. Females of this species resemble *C. duopaxillatus* in general habitus and the structure of the genitalia, but differ in weakly areolate forewings.

Description. *Male*. Total length: 0.85 mm; width across pronotum: 0.45 mm. COLORATION (Fig. 1.2). General color brown; costal cell of forewing darkened compared to the rest of corium; veins same color as membrane; apex of wing organ same color as the rest of wing organ. SURFACE AND VESTITURE. As in generic description. STRUCTURE. Submacropterous, with reduced membranous area posteriorly of the distal portion of 1AN (Fig. 1.12); veins of forewing somewhat widened; wing organ almost equal in length to discal cell; wing organ with middle cavity, almost equal

in length to wing organ; wing organ cavity with five pegs, four aligned in one plane, fifth peg situated at different level (Fig. 1.14I); wing organ pegs longer than wide.

ABDOMEN AND GENITALIA (Fig. 1.16). Sternite II+III on right side reaching the middle of sternite V; parasternite IV relatively small, with pouch and spine; parasternite V fused with parasternite IV; parasternite VI roughly equal in length to sternite VI; tVIII with movable appendage on left side, without process on right side, half as long as tVII; appendage of tVIII with slight bend at proximal portion, thin at distal portion, curved at apex; vesica relatively short, three coils; anophore tube-like, almost symmetrical; anophoric process in shape of narrow lobe with rounded apex.

Female. Total length: 0.93 mm; width across pronotum: 0.44 mm. COLORATION (Figs 1.2, 5). General color brown; forewing brown, uniformly colored. SURFACE AND VESTITURE. Forewing weakly areolate. STRUCTURE. Compound eye slightly wider than first antennal segment; apex of forewing rounded. GENITALIA (Fig. 1.19). Spermathecal reservoir spherical; spermathecal duct long, more than three length of reservoir, consists of three segments with no outbranching ducts in between; proximal segment of spermathecal duct short, not coiled; spermathecal gland diameter much smaller than spermathecal reservoir width; spermathecal gland duct relatively long.

Etymology. Named for the non-uniform orientation of pegs in the wing organ. An adjective after Latin “dis-” and “similis” meaning “different”.

Distribution. Known from one locality from Cochabamba, Bolivia.

Chinannus duckensis sp. n.

(Figs 1.2, 1.12, 1.14J, 1.17)

(urn:lsid:zoobank.org:act:25443B91-3949-4611-A4BD-F48C6C96BAFE)

HOLOTYPE: 1 ♂ BRAZIL, Amazonas, Reserva Ducke, 25 km NNE Manaus, 2.9136°S 59.9464°W, 120 m, 24-VII-97, J. Heraty (UCR_ENT 00074571) (INPA).

Diagnosis. The species can be distinguished by the following combination of characters: forewing with well-developed membranous area posteriorly of the distal portion of 1AN; wing organ with middle cavity with seven pegs; parasternite IV with pouch and short blunt process; appendage of tVIII elbowed with twist, distal portion relatively short, barely reaching parasternite IV, and tapering at apex; anophoric process wide at base and strongly tapering at apex.

The species can be clearly distinguished by the combination of small size, the wing organ with seven pegs, and the short distal part of appendage of tVIII.

Description. *Male*. Total length: 0.88 mm; width across pronotum: 0.37 mm. COLORATION (Fig. 1.2). General color brown; costal cell of forewing darkened compared to the rest of corium; veins same color as membrane; apex of wing organ same color as the rest of wing organ. SURFACE AND VESTITURE. As in generic description. STRUCTURE. Macropterous, with well-developed membranous area posteriorly of the distal portion of 1AN (Fig. 1.12); veins (except for those forming costal cell) not widened; wing organ more than two thirds as long as discal cell; wing organ with middle cavity, almost equal in length to wing organ; wing organ cavity with seven pegs (Fig. 1.14J); wing organ pegs longer than wide. ABDOMEN AND GENITALIA

(Fig. 1.17). Sternite II+III on right side reaching the middle of sternite V; parasternite IV relatively small, with pouch and short blunt process; parasternite V half as long as sternite V; parasternite VI slightly shorter than length of sternite VI; tVIII with movable appendage on left side, without process on right side, half as long as tVII; appendage of tVIII elbowed with twist, distal portion relatively short, barely reaching parasternite IV, and tapering at apex; vesica short, two and a half coils; anophore tube-like, almost symmetrical; anophoric process wide at base and strongly tapering at apex.

Etymology. Name after the Reserva Florestal Adolpho Ducke, where a single specimen of this species was collected; an adjective.

Distribution. Known from one locality in Amazonas, Brazil.

***Chinannus duopaxillatus* sp. n.**

(Figs 1.2, 1.5, 1.10F-L, 1.12, 1.14K, 1.17, 1.19)

(urn:lsid:zoobank.org:act:DEF50A2A-DC3E-4B35-9774-BCB7B0E5F641)

HOLOTYPE: 1 ♂ FRENCH GUIANA, Cayenne, Regina Co., Pararé, Nouragues Nat. Res., 4.038°N 52.67286°W, 70 m, 16-IX-2010, C. Weirauch, L. Berniker, G. Zhang, Light Trap (UCR_ENT 00004808) (MNHN).

PARATYPES: 5 ♂ (UCR_ENT 00077869, UCR_ENT 00074579, UCR_ENT 00077891, UCR_ENT 00077871, UCR_ENT 00077852), 2 ♀(UCR_ENT 00077823, UCR_ENT 00074577), BRAZIL, Amazonas, Amazonas Reserva ZF2 off BR 174 ~50 km N of Manaus, 2.63333°S 60.15°W, 30-VII-97, J. Heraty (INPA); 1 ♂ (UCR_ENT 00004809), 2 ♂ (UCR_ENT 00004810, UCR_ENT 00082319), FRENCH GUIANA,

Cayenne, Regina Co., Pararé, Nouragues Nat. Res., 4.038°N 52.67286°W, 70 m, 16-IX-2010, C. Weirauch, L. Berniker, G. Zhang, Light Trap (MNHN); 2 ♂ (UCR_ENT 00011950, UCR_ENT 00011951), Guyane, 8 km W of Risquetout, 4.91828°N 52.55201°W, 45 m, 10 – 11-VI-2005, J. E. Eger (FSCA); 2 ♂ (UCR_ENT 00030204, UCR_ENT 00030203), PERU, Loreto, Maynas Co., Callicebus Res. Station Mishana, Rio Nanay, 25km SW Iquitos, 3.90888°S 73.41394°W, 120 m, 10 – 17-I-80, J. B. Heppner (USNM).

Diagnosis. This species can be distinguished by the following combination of characters: forewing with well-developed membranous area posteriorly of the distal portion of 1AN; wing organ with middle cavity with two pegs sitting in individual deep sockets; parasternite IV with pouch and spine; appendage of tVIII straight, thin, slightly curved at apex; vesica of medium length, four coils, with series of preapical projections; anophoric process hook-shaped, widened at base with rounded apex; female forewing weakly punctate, uniformly colored; spermathecal reservoir spherical; spermathecal gland diameter much smaller than width of reservoir.

Males of this species can be easily distinguished by having a wing organ with two pegs in deep sockets. Females of *C. duopaxillatus* resemble females of *C. dissimilis*, but have weakly punctate forewings.

Description. *Male*. Total length: 1.02 mm; width across pronotum: 0.51 mm. COLORATION (Fig. 1.2). General color brown to black; costal cell of forewing darkened compared to the rest of corium; veins same color as membrane; apex of wing organ same color as the rest of wing organ. SURFACE AND VESTITURE. As in generic

description. STRUCTURE. Macropterous, with well-developed membranous area posteriorly of the distal portion of 1AN (Fig. 1.12); veins (except for those forming costal cell) not widened; wing organ half as long as discal cell; wing organ with middle cavity, almost equal in length to wing organ; wing organ cavity with two pegs (Fig. 1.14K); wing organ pegs very slender, bent and tapering. ABDOMEN AND GENITALIA (Fig. 1.17). Sternite II+III on right side reaching posterior margin of sternite IV; parasternite IV relatively large, with pouch and spine; parasternite V fused with parasternite IV; parasternite VI slightly shorter than length of sternite VI; tVIII with movable appendage on left side, without process on right side, half as long as tVII; appendage of tVIII straight, thin, slightly curved at apex; vesica of medium length, four coils, with series of preapical projections; anophore tube-like, slightly asymmetrical with right side being little longer than left; anophoric process wide at base and strongly tapering at apex.

Female. Total length: 1.07 mm; width across pronotum: 0.46 mm. COLORATION (Figs 1.2, 1.5). General color brown; forewing brown, uniformly colored. SURFACE AND VESTITURE. Forewing weakly punctate. STRUCTURE. Compound eye slightly wider than first antennal segment; apex of forewing rounded. GENITALIA (Fig. 1.19). Spermathecal reservoir spherical; spermathecal duct long, more than three length of reservoir, consists of three segments with no outbranching ducts in between; proximal segment of spermathecal duct short, not coiled; spermathecal gland diameter much smaller than spermathecal reservoir width.

Etymology. Named after the wing organ with only two pegs. An adjective derived from the Latin prefix “duo-” and noun “paxillus”, meaning “bearing two pegs”.

Distribution. Known from French Guiana, Central Amazonia, and eastern Peru: this is the widest currently documented distribution range for any *Chinannus* species.

Discussion. We consider specimens from French Guiana, Amazonia, and Peru to be conspecific primarily based on the unique structure of the wing organ and the deep sockets from which the two pegs arise. The male genitalia of the specimens from all three regions look alike (Fig. 1.10I-L, Fig. 1.17) with slight variation in the curvature of the anophoric process and length of the spine of parasternite IV. However, the unique preapical projections of the vesica are present in specimens from all three geographic regions.

Chinannus grandis sp. n.

(Figs 1.2, 1.12, 1.14L, 1.17)

(urn:lsid:zoobank.org:act:8C42221A-E7DD-45E4-BA74-F7D341832A00)

HOLOTYPE: 1 ♂ PERU, Cusco, Wayqecha Research Center, 13.17527°S 71.58138°W, 2685 m, 3-XII-2011, C. Weirauch (UCR_ENT 00104908) (MUSM).

PARATYPES: 1 ♂ (UCR_ENT 00084387), PERU, Cusco, Wayqecha Research Center, 13.17527°S 71.58138°W, 2685 m, 4 – 6-XII-2011, C. Weirauch, J. Heraty (MUSM).

Diagnosis. The species can be distinguished by the following combination of characters: forewing with reduced membranous area posteriorly of the distal portion of 1AN; wing organ with middle cavity with six pegs; parasternite IV with pouch and spine; appendage of tVIII elbowed with twist, long and reaching base of abdomen; anophoric process claw-shaped.

This species is similar to *C. lewisi*, but has a wing organ with six pegs, darker coloration, and larger body size.

Description. *Male*. Total length: 1.24 mm; width across pronotum: 0.56 mm. COLORATION (Fig. 1.2). General color dark brown; costal cell of forewing darkened compared to the rest of corium; veins same color as membrane; apex of wing organ same color as the rest of wing organ. SURFACE AND VESTITURE. As in generic description. STRUCTURE. Submacropterous, with reduced membranous area posteriorly of the distal portion of 1AN (Fig. 1.12); veins (except for those forming costal cell) posteriorly of the fracture thickened, but not widened; wing organ around two thirds as long as discal cell; wing organ with middle cavity, shorter than length of wing organ; wing organ cavity with six pegs (Fig. 1.14L); wing organ pegs longer than wide. ABDOMEN AND GENITALIA (Fig. 1.17). Sternite II+III on right side reaching the middle of sternite V; parasternite IV relatively large, with pouch and spine; parasternite V half as long as sternite V; parasternite VI roughly equal in length to sternite VI; tVIII with movable appendage on left side, without process on right side, half as long as tVII; appendage of tVIII elbowed with twist, long and reaching base of abdomen, with tapering apex; vesica relatively short, two coils; anophore tube-like, almost symmetrical; anophoric process claw-shaped.

Female. Unknown.

Etymology. Named for the large size amongst congeners; an adjective.

Distribution. The species is known from one locality in Cusco, Peru.

***Chinannus inermis* sp. n.**

(Figs 1.2, 1.5, 1.12, 1.14M, 1.17, 1.19)

(urn:lsid:zoobank.org:act:55FBA38E-1F00-4F5C-906A-53DD3BD2D267)

HOLOTYPE: 1 ♂ PERU, Madre de Dios, Los Amigos Biol.Station trail 14, 12.57141°S 70.09538°W, 231 m, 23 – 24-XII-2010, J. Heraty (UCR_ENT 00058251) (MUSM).

PARATYPES: 2 ♂ (UCR_ENT 00096985, UCR_ENT 00096986), PERU, Madre de Dios, Tambopata Co., Lago Sandoval, 12.61056°S 69.03722°W, 285 m, 18-V-98, P.P. Parrillo (FMNH); 1 ♂(UCR_ENT 00091265), 18-V-98, P.P. Parrillo (FMNH); 1 ♀ (UCR_ENT 00091268), 19-V-98, P.P. Parrillo (FMNH); 1 ♂ (UCR_ENT 00078255), Los Amigos Biol.Station trail 10, 12.56233°S 70.09641°W, 300 m, 20 – 24-XII-2010, J. Heraty (MUSM); 1 ♂ (UCR_ENT 00077338), Los Amigos Biol.Station trail 14, 12.57141°S 70.09538°W, 231 m, 23 – 24-XII-2010, J. Heraty (MUSM).

Diagnosis. This species can be distinguished by the following combination of characters: forewing with reduced membranous area posteriorly of the distal portion of 1AN and thickened veins at apex; wing organ with middle cavity with six pegs; parasternite IV with slender elongated process, pouch and spine absent; appendage of tVIII elbowed with twist, distal portion straight and tapering at apex; anophoric process claw-shaped, keel with preapical spine; female forewing weakly punctate, uniformly colored; spermathecal reservoir C-shaped, greatly inflated at base; spermathecal gland diameter smaller than width of reservoir.

Males of this species can be easily distinguished from all species by the structure of parasternite IV with an elongated process. Females can be distinguished by a C-shaped spermathecal reservoir with enlarged basal portion.

Description. *Male*. Total length: 0.80 mm; width across pronotum: 0.39 mm. COLORATION (Fig. 1.2). General color brown; costal cell of forewing same color as veins at apex of wing; veins darker than membrane; apex of wing organ same color as the rest of wing organ. SURFACE AND VESTITURE. As in generic description. STRUCTURE. Submacropterous, with reduced membranous area posteriorly of the distal portion of 1AN (Fig. 1.12); veins of forewing clearly widened and fused at apex; wing organ almost equal in length to discal cell; wing organ with middle cavity, shorter than length of wing organ; wing organ cavity with six pegs (Fig. 1.14M); wing organ pegs longer than wide. ABDOMEN AND GENITALIA (Fig. 1.17). Sternite II+III on right side reaching posterior margin of sternite V; parasternite IV very small, with slender elongate process; parasternites V and VI membranous; tVIII with movable appendage on left side, without process on right side, less than half as long as tVII; appendage of tVIII elbowed with twist, distal portion straight and tapering at apex; vesica short, two and a half coils; anophore tube-like, almost symmetrical; anophoric process claw-shaped, keel with preapical spine.

Female. Total length: 0.85 mm; width across pronotum: 0.42 mm. COLORATION (Figs 1.2, 1.5). General color brown; forewing brown, uniformly colored. SURFACE AND VESTITURE. Forewing weakly punctate. STRUCTURE. Compound eye slightly wider than first antennal segment; apex of forewing rounded. GENITALIA (Fig. 1.19).

Spermathecal reservoir C-shaped with enlarged basal portion; spermathecal duct relatively short; spermathecal gland diameter smaller than largest width of reservoir.

Etymology. Named for the absence of the pouch and spine, a unique feature amongst congeners. The specific epithet is the Latin adjective "inermis" meaning "unarmed, toothless".

Distribution. Known from one locality from Madre de Dios, Peru.

Chinannus iquitosensis sp. n.

(Figs 1.2, 1.3, 1.5, 1.12, 1.14N, 1.17, 1.19)

(urn:lsid:zoobank.org:act:0C5D8DB3-52F6-403F-B131-D954D5FEFF25)

HOLOTYPE: 1 ♂ PERU, Loreto, 160km NE Iquitos, Explornapo Camp, Rio Sucusari 2 km from Rio Napo, 3.74367°S 73.25163°W, 27 – 31-VIII-92, P.E. Skelley (UCR_ENT 00011949) (FSCA).

PARATYPES: 1 ♀ (UCR_ENT 00012020), PERU, Loreto, 160km NE Iquitos, Explornapo Camp, Rio Sucusari 2 km from Rio Napo, 3.74367°S 73.25163°W, 27 – 31-VIII-92, P.E. Skelley (FSCA).

Diagnosis. This species can be distinguished by the following combination of characters: forewing with well-developed membranous area posteriorly of the distal portion of 1AN; wing organ with middle cavity with seven pegs; parasternite IV with pouch and spine; appendage of tVIII with slight bend at proximal portion, thin at distal portion, curved at apex; anophoric process in shape of narrow lobe with rounded and anteriorly curved apex; female forewing weakly punctate, uniformly colored; spermathecal reservoir

spherical; spermathecal duct wide, same width or wider than spermathecal gland; spermathecal gland diameter much smaller than width of reservoir.

This species resembles *C. dissimilis*: males are with respect to the shape of the genitalia, but differ in having a well-developed membranous area posteriorly of the distal portion of 1AN and seven pegs aligned in one plane in the wing organ; females are similar in the shape of the spermathecal reservoir, but are smaller, darker, and have larger eyes.

Description. *Male*. Total length: 1.01 mm; width across pronotum: 0.51 mm. COLORATION (Fig. 1.2). General color dark brown; costal cell of forewing darkened compared to the rest of corium; veins same color as membrane; apex of wing organ same color as the rest of wing organ. SURFACE AND VESTITURE. As in generic description. STRUCTURE. Macropterous, with well-developed membranous area posteriorly of the distal portion of 1AN (Fig. 1.12); veins (except for those forming costal cell) not widened; wing organ around two thirds as discal cell; wing organ with middle cavity, almost equal to length of wing organ; wing organ cavity with seven pegs (Fig. 1.14N); wing organ pegs roughly as long as wide, blunt. ABDOMEN AND GENITALIA (Fig. 1.17). Sternite II+III on right side reaching the middle of sternite V; parasternite IV relatively small, with pouch and spine; parasternite V fused with parasternite IV; parasternite VI roughly equal in length to sternite VI; tVIII with movable appendage on left side, without process on right side, half as long as tVII; appendage of tVIII with slight bend at proximal portion, thin at distal portion, curved at apex; vesica of medium length, three and a half coils; anophore tube-like, almost symmetrical; anophoric process in shape of narrow lobe with rounded and anteriorly curved apex.

Female. Total length: 0.86 mm; width across pronotum: 0.46 mm. COLORATION (Figs 1.3, 1.5). General color black; forewing black, uniformly colored. SURFACE AND VESTITURE. Forewing weakly punctate. STRUCTURE. Compound eye slightly wider than first antennal segment; apex of forewing rounded. GENITALIA (Fig. 1.19). Spermathecal reservoir spherical; spermathecal duct long and wide, more than three lengths of reservoir and same width or wider than spermathecal gland, consists of two segments with no outbranching ducts in between; proximal segment of spermathecal duct short, not coiled; spermathecal gland diameter much smaller than spermathecal reservoir width; spermathecal gland duct relatively long.

Etymology. Named for the nearest large city to the single known locality, Iquitos; an adjective.

Distribution. Known from one locality from Loreto, Peru.

Chinannus latus sp. n.

(Figs 1.3, 1.5, 1.12, 1.14O, 1.17, 1.19)

(urn:lsid:zoobank.org:act:4C85AF26-737E-4A5F-915D-C123D5367D94)

HOLOTYPE: 1 ♂ PANAMA, Bocas del Toro, Almirante, 9.3003°N 82.40214°W, 26-III-59, H. S. Dybas (UCR_ENT 00090712) (FMNH).

PARATYPES: 1 ♀ (UCR_ENT 00014567), COSTA RICA, Cartago, Turrialba. R.F. Rio Pacuare, P.N. Barbilla, Est. Barbilla, 9.97992°N 83.45232°W, 600 m, 20 – 24-X-2000, W. Arana. Tp. Mantillo (INBIO); 1 ♂ (UCR_ENT 00014568), 20 – 24-X-2000, W. Arana (INBIO); 1 ♂ (UCR_ENT 00014554), Limon, Estacion Hitoy Cerere, Sendero a

Espavel, 9.67484°N 83.01753°W, 19-IX-2002 – 5-X-2002, W. Arana (INBIO); 3 ♀ (UCR_ENT 00090705, UCR_ENT 00090706, UCR_ENT 00090711), PANAMA, Bocas del Toro, Almirante, 9.3003°N 82.40214°W, 26-III-59, H.S. Dybas (FMNH).

Diagnosis. This species can be distinguished by the following combination of characters: forewing with reduced membranous area posteriorly of the distal portion of 1AN; wing organ widened with middle cavity with 10 pegs; parasternite IV with pouch and spine; appendage of tVIII elbowed with twist, distal portion curved medially and tapering at apex; anophoric process claw-shaped; female forewing heavily punctate, with pale band; spermathecal reservoir comma-shaped, inflated at base.

This species is similar to *C. nicaraguensis* in dorsal habitus and structure of genitalia that are essentially the same, but males differ in having a wing organ with 10 pegs; females are difficult to distinguish from *C. nicaraguensis*, *C. bierigi*, *C. bispinosus*. See Discussion.

Description. *Male*. Total length: 0.98 mm; width across pronotum: 0.47 mm. COLORATION (Fig. 1.3). General color brown to black; costal cell of forewing same color as veins at apex of wing; veins same color as membrane; apex of wing organ same color as the rest of wing organ. SURFACE AND VESTITURE. As in generic description. STRUCTURE. Submacropterous, with reduced membranous area posteriorly of the distal portion of 1AN (Fig. 1.12); veins of forewing clearly widened and fused at apex; wing organ almost equal in length to discal cell; wing organ with widened, middle cavity, almost equal in length to wing organ; wing organ cavity with 10 pegs (Fig. 1.14O); wing organ pegs longer than wide. ABDOMEN AND GENITALIA (Fig. 1.17).

Sternite II+III on right side reaching the middle of sternite V; parasternite IV relatively small, with pouch and spine; parasternite V half as long as sternite V; parasternite VI slightly shorter than length of sternite VI; tVIII with movable appendage on left side, without process on right side, half as long as tVII; appendage of tVIII elbowed with twist, distal portion curved medially and tapering at apex; vesica relatively short, two and a half coils; anophore tube-like, almost symmetrical; anophoric process claw-shaped.

Female. Total length: 0.88 mm; width across pronotum: 0.49 mm. COLORATION (Figs 1.3, 1.5). General color black; forewing brown with transverse pale band that slightly widens medially. SURFACE AND VESTITURE. Forewing heavily punctate. STRUCTURE. Compound eye slightly wider than first antennal segment; apex of forewing rounded. GENITALIA (Fig. 1.19). Spermathecal reservoir comma-shaped, with enlarged basal portion; spermathecal duct short, two to three length of reservoir, consists of two segments with small outbranching duct in between; proximal segment of spermathecal duct short, not coiled; spermathecal gland diameter smaller than spermathecal reservoir width; spermathecal gland duct relatively short.

Etymology. Named for the widened wing organ. The specific epithet is the Latin adjective “latus” meaning “wide”.

Distribution. The species is known from several localities in eastern Costa Rica and western Panama.

Discussion. The species is most similar to *C. nicaraguensis* based on the general habitus and wing structure. The differences are only observed in males and associated with the fine structure of the wing organ. In both species the wing organ is widened, but *C. latus*

has 10 pegs that are parallel-sided, and *C. nicaraguensis* has eight pegs with pegs being slightly conical. Genitalic structures of two species are the same. In our phylogenetic analysis *C. latus* and *C. nicaraguensis* were supported as a monophyletic group. However due to absence of fresh material for *C. latus*, only the D3 region of 28S rDNA was sequenced for the species. Thus the monophyly of *C. latus* was not supported. Given that the specimens are well segregated between eastern Costa Rica and southern Nicaragua according to their wing organ structure, we consider *C. latus* and *C. nicaraguensis* as separate species.

***Chinannus lewisi* sp. n.**

(Figs 1.3, 1.5, 1.13, 1.14P, 1.17, 1.19)

(urn:lsid:zoobank.org:act:E4CA08DF-9AD9-4CF9-BE26-FF910B07DB14)

HOLOTYPE: 1 ♂ PERU, Cusco, Pillahuata, Manu Road km 128, 13.1333°S 71.4167°W, 20-IX-82, L.E. Watrous, G. Mazurek (UCR_ENT 00101415) (FMNH).

PARATYPES: 1 ♀ (UCR_ENT 00101097), PERU, Cusco, Consuelo, Manu Road km 165, 13.22387°S 72.01464°W, 1-X-82, L.E. Watrous, G. Mazurek (FMNH); 1 ♀ (UCR_ENT 00101373), Pillahuata, Manu Road km 128, 13.1333°S 71.4167°W, 16-IX-82, L.E. Watrous, G. Mazurek (FMNH); 1 ♂ (UCR_ENT 00101410), 19-IX-82, L.E. Watrous, G. Mazurek (AMNH); 4 ♀(UCR_ENT 00097837-UCR_ENT 00097841), 1 ♀(UCR_ENT 00097841) (AMNH), 20-IX-82, L.E. Watrous, G. Mazurek (FMNH); 1 ♂ (UCR_ENT 00101477), 1 ♀ (UCR_ENT 00101479), 26-IX-82, L.E. Watrous, G. Mazurek (FMNH).

Diagnosis. This species can be distinguished by the following combination of characters: forewing with reduced membranous area posteriorly of the distal portion of 1AN; wing organ with middle cavity with four pegs; parasternite IV with pouch and spine; appendage of tVIII elbowed with twist, long and reaching base of abdomen; anophoric process claw-shaped; female forewing weakly areolate, uniformly colored; apex of female forewing acute; spermathecal reservoir comma-shaped, inflated at base. Males are similar to *C. grandis*, but have a wing organ with four pegs, paler coloration, and smaller body size; females differ from other species in the combination of the uniformly colored forewings with acute apex and the large comma-shaped spermathecal reservoir.

Description. *Male*. Total length: 1.03 mm; width across pronotum: 0.56 mm. COLORATION (Fig. 1.3). General color brown; costal cell of forewing darkened compared to the rest of corium; veins same color as membrane; apex of wing organ same color as the rest of wing organ. SURFACE AND VESTITURE. As in generic description. STRUCTURE. Submacropterous, with reduced membranous area posteriorly of the distal portion of 1AN (Fig. 1.13); veins (except for those forming costal cell) posteriorly of the fracture thickened, but not widened; wing organ around two thirds as long as discal cell; wing organ with middle cavity, shorter than length of wing organ; wing organ cavity with four pegs (Fig. 1.14P); wing organ pegs longer than wide. ABDOMEN AND GENITALIA (Fig. 1.17). Sternite II+III on right side reaching the middle of sternite V; parasternite IV relatively large, with pouch and spine; parasternite V half as long as sternite V; parasternite VI roughly equal in length to sternite VI; tVIII

with movable appendage on left side, with short wide tapering process on right side, half as long as tVII; appendage of tVIII elbowed with twist, long and reaching base of abdomen, with tapering apex; vesica relatively short, two and a half coils; anophoric process claw-shaped.

Female. Total length: 1.01 mm; width across pronotum: 0.53 mm. COLORATION (Figs 1.3, 1.5). General color brown; forewing brown, uniformly colored. SURFACE AND VESTITURE. Forewing weakly areolate. STRUCTURE. Compound eye slightly wider than first antennal segment; apex of forewing acute. GENITALIA (Fig. 1.19). Spermathecal reservoir comma-shaped, with enlarged basal portion; spermathecal duct short, two to three length of reservoir, consists of two segments with no outbranching ducts in between; proximal segment of spermathecal duct short, not coiled; spermathecal gland diameter smaller than spermathecal reservoir width; spermathecal gland duct relatively short.

Etymology. Named after Jim Lewis (INBio), who facilitated specimen loans for Dipsocoromorpha and has spent many hours separating minute litter bugs from trap samples. A noun in genitive case.

Distribution. The species is known from one locality in Cusco, Peru.

***Chinannus loretensis* sp. n.**

(Figs 1.3, 1.13, 1.15A, 1.17)

(urn:lsid:zoobank.org:act:240E9E51-89EE-412F-9160-94A582E69291)

HOLOTYPE: 1 ♂ PERU, Amazonas, Pacaya–Samiria National Reserve, 5.2012°S 74.59319°W, 17-X-80, Vaucher (UCR_ENT 00089585) (MHNG).

PARATYPES: 1 ♂ (UCR_ENT 00089581), PERU, unknown locality (locality code PE-80/19), no date provided (MHNG).

Diagnosis. This species can be distinguished by the following combination of characters: forewing with well-developed membranous area posteriorly of the distal portion of 1AN; wing organ with middle curved cavity with three or four pegs, one peg situated in different plane from others; parasternite IV with pouch and short blunt process; tVIII with process on right side, movable appendage absent; anophoric process short and thin, directed laterally.

This species is similar to *C. paveli* in the shape of the genitalia but differs by the wing organ with pegs situated not in one plane and the wing organ cavity being slightly curved.

Description. *Male*. Total length: 0.88 mm; width across pronotum: 0.43 mm. COLORATION (Fig. 1.3). General color brown; costal cell of forewing darkened compared to the rest of corium; veins same color as membrane; apex of wing organ same color as the rest of wing organ. SURFACE AND VESTITURE. As in generic description. STRUCTURE. Macropterous, with well-developed membranous area posteriorly of the distal portion of 1AN (Fig. 1.13); veins (except for those forming costal cell) not widened; wing organ around two thirds as long as discal cell; wing organ with middle cavity; wing organ cavity curved, with three or four pegs total; two or three pegs aligned in one plane, one situated in different plane (Fig. 1.15A); wing organ pegs roughly as wide as long, tapering. ABDOMEN AND GENITALIA (Fig. 1.17). Sternite

II+III on right side reaching posterior margin of sternite IV; parasternite IV relatively large, with pouch and short blunt process; parasternite V fused with parasternite IV; parasternite VI roughly equal in length to sternite VI; tVIII without movable appendage on left side, with short narrow tapering process on right side, almost or more than half as long as tVII; vesica very short, one and a half coil; anophore tube-like, almost symmetrical; anophoric process short and thin, directed laterally.

Female. Unknown.

Etymology. Named after the Loreto region of Peru, where the specimen was collected.

Distribution. This species is known from one locality in Amazonas, Peru; an adjective.

Discussion. Despite the similarity to *C. paveli* in genitalic characters, the organization of the wing organ is quite different in *C. loretensis* where one peg is always situated aside from the others and the wing organ cavity is curved. This fact together with the relatively large distance between type localities (~1,135 km) suggests that the specimens from Peru and Bolivia belong to two different species.

***Chinannus monteverdensis* sp. n.**

(Figs 1.3, 1.5, 1.13, 1.15B, 1.17, 1.19)

(urn:lsid:zoobank.org:act:480EF95B-864F-4254-A908-53A6DD7AC031)

HOLOTYPE: 1 ♂ COSTA RICA, Guanacaste, Estacion Biologica Monteverde, S. Principal at station, 10.32056°N 84.81028°W, 1541 m, 29 – 30-IX-2014, C. Weirauch, S. Leon, A. Knyshov (UCR_ENT 00117259) (INBIO).

PARATYPES: 1 ♂ (UCR_ENT 00119030), COSTA RICA, Guanacaste, Estacion

Biologica Monteverde, S. Principal at station, 10.32056°N 84.81028°W, 1541 m, 30-IX-2014, C. Weirauch, S. Leon, A. Knyshov (AMNH); 1 ♂ (UCR_ENT 00120607), 1 ♀(UCR_ENT 00120606), 1 – 2-X-2014, C. Weirauch, S. Leon, A. Knyshov (INBIO); 1 ♂ (UCR_ENT 00116293), 5 ♀ (UCR_ENT 00116294-UCR_ENT 00116297, UCR_ENT 00110964) (UCR), 1 ♀ (UCR_ENT 00110965) (AMNH), 2-X-2014, C. Weirauch, S. Leon, A. Knyshov; 1 ♀ (UCR_ENT 00110963) (UCR), 1 ♀ (UCR_ENT 00110966) (INBIO), 4-X-2014, C. Weirauch, S. Leon, A. Knyshov.

Diagnosis. This species can be distinguished by the following combination of characters: forewing with well-developed membranous area posteriorly of the distal portion of 1AN; wing organ with middle cavity with nine pegs; parasternite IV with pouch and spine; appendage of tVIII elbowed with twist, distal portion curved medially and tapering at apex; anophoric process large, wide at base, narrow and hook-shaped at apex; female forewing heavily punctate, with pale band; apex of female forewing acute; spermathecal reservoir comma-shaped, inflated at base.

Similar to *C. bierigi* in general habitus, but larger, with males having different genitalia, and females having acute apex of the forewings.

Description. *Male*. Total length: 1.19 mm; width across pronotum: 0.47 mm. COLORATION (Fig. 1.3). General color black; costal cell of forewing darkened compared to the rest of corium; veins same color as membrane; apex of wing organ same color as the rest of wing organ. SURFACE AND VESTITURE. As in generic description. STRUCTURE. Macropterous, with well-developed membranous area posteriorly of the distal portion of 1AN (Fig. 1.13); veins (except for those forming costal

cell) not widened; wing organ almost equal in length to discal cell; wing organ with middle cavity, almost equal in length to wing organ; wing organ cavity with nine pegs; wing organ pegs longer than wide. ABDOMEN AND GENITALIA (Fig. 1.17). Sternite II+III on right side reaching posterior margin of sternite V; parasternite IV relatively large, with pouch and spine; parasternite V half as long as sternite V; parasternite VI slightly shorter than length of sternite VI; tVIII with movable appendage on left side, without process on right side, half as long as tVII; appendage of tVIII elbowed with twist, distal portion curved medially and tapering at apex; vesica relatively short, two and a half coils; anophore tube-like, almost symmetrical; anophoric process large, wide at base, narrow and hook-shaped at apex.

Female. Total length: 0.88 mm; width across pronotum: 0.49 mm. COLORATION (Figs 1.3, 5). General color black; forewing brown with transverse parallel-sided pale band. SURFACE AND VESTITURE. Forewing heavily punctate. STRUCTURE. Compound eye slightly wider than first antennal segment; apex of forewing acute. GENITALIA (Fig. 1.19). Spermathecal reservoir comma-shaped, with enlarged basal portion; spermathecal duct short, two to three lengths of reservoir, consists of two segments with no outbranching ducts in between; proximal segment of spermathecal duct short, not coiled; spermathecal gland diameter smaller than spermathecal reservoir width; spermathecal gland duct relatively short.

Etymology. Named after the Estacion Biologica Monteverde, where specimens of this species were collected; an adjective.

Distribution. The species is known from a single locality in Guanacaste, Costa Rica.

***Chinannus nicaraguensis* sp. n.**

(Figs 1.3, 1.5, 1.13, 1.15C, 1.18, 1.19)

(urn:lsid:zoobank.org:act:D3FF296E-1CB4-45FC-8ABC-7A62498A0199)

HOLOTYPE: 1 ♂ NICARAGUA, Region Autonoma del Atlantico Sur, 13km WNW Rama, 12.19472°N 84.33667°W, 190 m, 18-IV-2011, J. T. Longino (UCR_ENT 00098872) (FMNH).

PARATYPES: 4 ♂ (UCR_ENT 00096979-UCR_ENT 00096982) (FMNH), 6 ♂ (UCR_ENT 00096983-UCR_ENT 00096984) (AMNH), 3 ♀ (UCR_ENT 00098871, UCR_ENT 00097870, UCR_ENT 00097871) (FMNH), NICARAGUA, Chontales, 36km WNW Santo Tomas, 11.99278°N 84.77556°W, 480 m, 18-IV-2011, J. T. Longino; 1 ♂ (UCR_ENT 00098873), Region Autonoma del Atlantico Sur: 13km WNW Rama, 12.19472°N 84.33667°W, 190 m, 18-IV-2011, J. T. Longino (FMNH); 1 ♂ (UCR_ENT 00101300), 27km WSW Rama, 12.12278°N 84.46222°W, 50 m, 18-IV-2011, J. T. Longino (FMNH); 1 ♂ (UCR_ENT 00037001), Rio San Juan, Monte Cristo Resort, 3km SE Boca de Sabalos, 11.02444°N 84.45694°W, 50 m, 3-10-V-2005, S.L. Heydon (UCD).

Diagnosis. This species can be distinguished by the following combination of characters: forewing with reduced membranous area posteriorly of the distal portion of 1AN; wing organ widened with middle cavity with eight pegs; parasternite IV with pouch and spine; appendage of tVIII elbowed with twist, distal portion curved medially and tapering at apex; anophoric process claw-shaped; female forewing heavily punctate, with pale band; spermathecal reservoir comma-shaped, inflated at base.

This species is similar to *C. latus* in dorsal habitus and structure of genitalia, but males differ in having a wing organ with eight pegs (see also *C. latus* discussion); females are difficult to distinguish from *C. bierigi*, *C. bispinosus*, and *C. latus*.

Description. *Male*. Total length: 0.83 mm; width across pronotum: 0.47 mm. COLORATION (Fig. 1.3). General color black; costal cell of forewing same color as veins at apex of wing; veins same color as membrane; apex of wing organ same color as the rest of wing organ. SURFACE AND VESTITURE. As in generic description. STRUCTURE. Macropterous, with well-developed membranous area posteriorly of the distal portion of 1AN (Fig. 1.13); veins (except for those forming costal cell) not widened; wing organ almost equal in length to discal cell; wing organ with middle cavity, almost equal in length to wing organ; wing organ cavity with eight pegs (Fig. 1.15C); wing organ pegs longer than wide. ABDOMEN AND GENITALIA (Fig. 1.18). Sternite II+III on right side reaching the middle of sternite V; parasternite IV relatively small, with pouch and spine; parasternite V half as long as sternite V; parasternite VI slightly shorter than length of sternite VI; tVIII with movable appendage on left side, without process on right side, half as long as tVII; appendage of tVIII elbowed with twist, distal portion curved medially and tapering at apex; vesica very short, one and a half coil; anophore tube-like, almost symmetrical; anophoric process claw-shaped.

Female. Total length: 0.88 mm; width across pronotum: 0.49 mm. COLORATION (Figs 1.3, 1.5). General color black; forewing brown with transverse pale band that slightly widens medially. SURFACE AND VESTITURE. Forewing heavily punctate. STRUCTURE. Compound eye slightly wider than first antennal segment; apex of

forewing rounded. GENITALIA (Fig. 1.19). Spermathecal reservoir comma-shaped, with enlarged basal portion; spermathecal duct short, two to three lengths of reservoir, consists of two segments with small outbranching duct in between; proximal segment of spermathecal duct short, not coiled; spermathecal gland diameter smaller than spermathecal reservoir width; spermathecal gland duct relatively short.

Etymology. Named after the fact that all known specimen have been collected in Nicaragua; an adjective.

Distribution. The species is known from several localities in southeastern Nicaragua.

Chinannus parvioculatus sp. n.

(Figs 1.3, 1.5, 1.13, 1.15D, 1.18, 1.19)

(urn:lsid:zoobank.org:act:E1F46949-F9A0-4336-BAB7-262C02FD63E5)

HOLOTYPE: 1 ♂ VENEZUELA, Aragua, Rancho Grande, 15 km N Maracay, 9.16667°N 64.61667°W, 1000 m, 19 – 27-II-71, S. B. Peck (UCR_ENT 00097845) (FMNH).

PARATYPES: 1 ♂ (UCR_ENT 00095644), 2 ♀ (UCR_ENT 00095639, UCR_ENT 00095641), VENEZUELA, Aragua, Tiara, 50 km SW of Caracas, 10.13217°N 67.15624°W, 2000 m, 22-II-71, S. Peck (CUNI); 2 ♂ (UCR_ENT 00097842, UCR_ENT 00097846) (FMNH), 1 ♂ (UCR_ENT 00097847) (AMNH), 4 ♀ (UCR_ENT 00096939-UCR_ENT 00096942) (FMNH), Rancho Grande, 15 km N Maracay, 9.16667°N 64.61667°W, 1000 m, 19 – 27-II-71, S. B. Peck.

Diagnosis. This species can be distinguished by the following combination of characters: forewing with well-developed membranous area posteriorly of the distal portion of 1AN; wing organ with middle cavity with seven pegs; parasternite IV with pouch and spine; appendage of tVIII straight, thin at apex; anophoric process stick-shaped, without constriction, with apex not curved; female eyes very small, equal in width to first antennal segment; female forewing weakly areolate, uniformly colored, but lighter than head and pronotum; spermathecal reservoir C-shaped, inflated at base.

This species is similar to *C. schuhi* and *C. trinitatis* in the shape of the genitalia, but different in the number of pegs in the wing organ and straight stick-shaped anophoric process without constriction. The species was collected together with *C. advenus*, but males differ in the shape of the genitalia, females differ in coloration and in having smaller eyes.

Description. *Male*. Total length: 1.14 mm; width across pronotum: 0.56 mm. COLORATION (Fig. 1.3). General color brown; costal cell of forewing darkened compared to the rest of corium; veins same color as membrane; apex of wing organ same color as the rest of wing organ. SURFACE AND VESTITURE. As in generic description. STRUCTURE. Macropterous, with well-developed membranous area posteriorly of the distal portion of 1AN (Fig. 1.13); veins (except for those forming costal cell) not widened; wing organ two thirds as long as discal cell; wing organ with middle cavity, almost equal in length to wing organ; wing organ cavity with seven pegs (Fig. 1.15D); wing organ pegs longer than wide. ABDOMEN AND GENITALIA (Fig. 1.18). Sternite II+III on right side almost equal in length to left side; parasternite IV relatively

small, with pouch and rounded spine; parasternites V and VI roughly equal in length to corresponding sternites; tVIII with movable appendage on left side, without process on right side, half as long as tVII; appendage of tVIII straight, thin at apex; vesica relatively long, with approximately seven coils; anophore tube-like, strongly asymmetrical with right side being longer than left; anophoric process stick-shaped, without constriction, with apex not curved.

Female. Total length: 1.04 mm; width across pronotum: 0.51 mm. COLORATION (Figs 1.3, 1.5). General color brown; forewing pale brown, uniformly colored, but lighter than head and pronotum. SURFACE AND VESTITURE. Forewing weakly areolate. STRUCTURE. Compound eye very small, about same width as first antennal segment; apex of forewing abrupt. GENITALIA (Fig. 1.19). Spermathecal reservoir C-shaped, with inflated basal portion; spermathecal duct long, more than three length of reservoir, consists of two segments with small outbranching duct in between; proximal segment of spermathecal duct short, not coiled; spermathecal gland diameter smaller than spermathecal reservoir width; spermathecal gland duct relatively short.

Etymology. Named for the very small eyes in the females. An adjective combined from the Latin adjective “parvus” and noun “oculus”, meaning “having small eyes”.

Distribution. The species is known from a couple of localities in Aragua, Venezuela.

***Chinannus parvithecatus* sp. n.**

(Figs 1.4, 1.5, 1.13, 1.15E, 1.18, 1.19)

(urn:lsid:zoobank.org:act:C1BC6BF4-EEFB-406B-842B-54F53DAB6BC1)

HOLOTYPE: 1 ♂ BRAZIL, Para, Pirelli Plantation (triboca) nr. Belem, 1.45578°S 48.4902°W, VIII-62, W.L. Brown (UCR_ENT 00090632) (FMNH).

PARATYPES: 1 ♀ (UCR_ENT 00090631), BRAZIL, Para, Pirelli Plantation (triboca) nr. Belem, 1.45578°S 48.4902°W, VIII-62, W.L. Brown (FMNH).

Diagnosis. This species can be distinguished by the following combination of characters: forewing with reduced membranous area posteriorly of the distal portion of 1AN; wing organ with middle cavity with three pegs sitting in individual deep sockets; parasternite IV with pouch and spine; appendage of tVIII with slight bend at proximal portion, thin and straight at distal portion; anophoric process in shape of narrow lobe with rounded anteriorly curved apex; female forewing weakly areolate, uniformly colored; spermathecal reservoir spherical, very small; spermathecal gland diameter smaller than width of reservoir.

Males of this species are similar to *C. dissimilis* and *C. iquitosensis* in the shape of the genitalia, but differ in having a wing organ with three pegs in deep sockets. Females differ by the very small size of the spermathecal reservoir.

Description. *Male*. Total length: 0.85 mm; width across pronotum: 0.45 mm. COLORATION (Fig. 1.4). General color brown; costal cell of forewing darkened compared to the rest of corium; veins same color as membrane; apex of wing organ same color as the rest of wing organ. SURFACE AND VESTITURE. As in generic description. STRUCTURE. Submacropterous, with reduced membranous area posteriorly of the distal portion of 1AN (Fig. 1.13); veins (except for those forming costal cell) not widened; wing organ more than two thirds as long as discal cell; wing organ with middle

cavity, almost equal in length to wing organ; wing organ cavity with three pegs sitting in individual deep sockets (Fig. 1.15E); wing organ pegs very slender, straight and tapering. ABDOMEN AND GENITALIA (Fig. 1.18). Sternite II+III on right side reaching the middle of sternite V; parasternite IV relatively small, with pouch and spine; parasternite V fused with parasternite IV; parasternite VI roughly equal in length to sternite VI; tVIII with movable appendage on left side, without process on right side, less than half as long as tVII; appendage of tVIII with slight bend at proximal portion, thin and straight at distal portion; vesica of medium length, four and a half coils; anophore tube-like, almost symmetrical; anophoric process in shape of narrow lobe with rounded anteriorly curved apex.

Female. Total length: 0.93 mm; width across pronotum: 0.44 mm. COLORATION (Figs 1.4, 1.5). General color brown; forewing brown, uniformly colored. SURFACE AND VESTITURE. Forewing weakly areolate. STRUCTURE. Compound eye slightly wider than first antennal segment; apex of forewing abrupt. GENITALIA (Fig. 1.19). Spermathecal reservoir spherical, very small; spermathecal duct long, more than three length of reservoir, consists of three segments with no outbranching ducts in between; proximal segment of spermathecal duct short, not coiled; spermathecal gland diameter smaller than width of reservoir; spermathecal gland duct relatively long.

Etymology. Named for the very small size of the spermathecal reservoir. An adjective derived from the Latin adjective “parvus” and noun “theca”, meaning “having a small theca”.

Distribution. Known from one locality in Para, Brazil.

Chinannus paveli sp. n.

(Figs 1.4, 1.13, 1.15F, 1.18)

(urn:lsid:zoobank.org:act:72BAA10C-97FB-41D1-A1AC-DEE0FBA05A03)

HOLOTYPE: 1 ♂ BOLIVIA, El Beni, Vaca Diez Co., Tumichucua, Isla de Motacu, 11.14611°S 66.16528°W, 160 m, 31-X-1993 – 9-XI-1993, P. P. Parrillo and W. Rojas (UCR_ENT 00096957) (FMNH).

PARATYPES: 2 ♂ (UCR_ENT 00096962, UCR_ENT 00096963), BOLIVIA, El Beni, Vaca Diez Co., 2 km NW Tumichucua, 11.14611°S 66.16528°W, 160 m, 1 – 9-XI-93, P. P. Parrillo and W. Rojas (FMNH); 4 ♂ (UCR_ENT 00096956, UCR_ENT 00096958-UCR_ENT 00096960) (FMNH), 1 ♂ (UCR_ENT 00096961) (AMNH), Tumichucua, Isla de Motacu, 11.14611°S 66.16528°W, 160 m, 31-X-93 – 9-XI-93, P. P. Parrillo and W. Rojas (FMNH).

Diagnosis. This species can be distinguished by the following combination of characters: forewing with well-developed membranous area posteriorly of the distal portion of 1AN; wing organ with middle cavity with four pegs; parasternite IV with pouch and short blunt process; tVIII with process on right side, movable appendage absent; anophoric process short and thin, directed laterally.

Males of this species are similar to *C. loretensis* in the shape of the genitalia, but differ in that the wing organ pegs are situated in one plane (see also *C. loretensis* discussion).

Description. *Male*. Total length: 0.88 mm; width across pronotum: 0.43 mm.

COLORATION (Fig. 1.4). General color brown; costal cell of forewing darkened

compared to the rest of corium; veins same color as membrane; apex of wing organ same color as the rest of wing organ. SURFACE AND VESTITURE. As in generic description. STRUCTURE. Macropterous, with well-developed membranous area posteriorly of the distal portion of 1AN (Fig. 1.13); veins (except for those forming costal cell) not widened; wing organ more than four fifths as long as discal cell; wing organ with middle cavity, almost equal in length to wing organ; wing organ cavity with four pegs (Fig. 1.15F); wing organ pegs roughly as wide as long, rounded. ABDOMEN AND GENITALIA (Fig. 1.18). Sternite II+III on right side reaching posterior margin of sternite IV; parasternite IV relatively small, with pouch and short blunt process; parasternite V fused with parasternite IV; parasternite VI equal in length to sternite VI; tVIII without movable appendage on left side, with short narrow tapering process on right side, almost or more than half as long as tVII; vesica relatively short, two coils; anophore tube-like, almost symmetrical; anophoric process short and thin, directed laterally.

Female. Unknown.

Etymology. Named after Pavel Štys, a world-known specialist on Dipsocoromorpha. A noun in genitive case.

Distribution. The species is known from one locality in El Beni, Bolivia.

Chinannus pecki **sp. n.**

(Figs 1.4, 1.11F, 1.13, 1.15G, 1.18)

(urn:lsid:zoobank.org:act:5DA1274A-72EC-4907-89E8-E948AD3E10DD)

HOLOTYPE: 1 ♂ ECUADOR, Napo, Limoncocha, 2.07472°S 79.92611°W, 250 m, 21-VI-76, S. B. Peck (UCR_ENT 00090462) (FMNH).

Diagnosis. This species can be distinguished by the following combination of characters: forewing with well-developed membranous area posteriorly of the distal portion of 1AN; wing organ with middle cavity with three pegs; parasternite IV with pouch and flattened apex, spine absent; tVIII with process on right side, movable appendage absent; anophoric process long and thin, directed anteriorly.

This species is similar to *C. loretensis* and *C. parvithecatus* in having a wing organ with three pegs, however the position and shape of the pegs, as well as the structure of the genitalia are different. Somewhat similar to *C. caudalis* in the shape of the parasternite IV and the anophoric process, but differing in shape of the process of tVIII, wing organ cavity position, and number of wing organ pegs.

Description. *Male*. Total length: 0.88 mm; width across pronotum: 0.43 mm. COLORATION (Fig. 1.4). General color brown; costal cell of forewing darkened compared to the rest of corium; veins same color as membrane; apex of wing organ same color as the rest of wing organ. SURFACE AND VESTITURE. As in generic description. STRUCTURE. Macropterous, with well-developed membranous area posteriorly of the distal portion of 1AN (Fig. 1.13); veins (except for those forming costal cell) not widened; wing organ around two thirds as long as discal cell; wing organ with middle cavity, almost equal in length to wing organ; wing organ cavity with three pegs (Fig. 1.15G); wing organ pegs roughly as wide as long, blunt. ABDOMEN AND GENITALIA (Fig. 1.18). Sternite II+III on right side reaching posterior margin of

sternite IV; parasternite IV relatively large, with pouch and flattened process; parasternite V fused with parasternite IV; parasternite VI roughly equal in length to sternite VI; tVIII without movable appendage on left side, with short wide hook-shaped process on right side, almost half as long as tVII; vesica very short, one and a half coil; anophore tube-like, almost symmetrical; anophoric process long and thin, directed anteriorly.

Female. Unknown.

Etymology. Named after S.B. Peck who collected the type specimen as well as many other *Chinannus* specimens. A noun in genitive case.

Distribution. The species is known from one locality in Napo, Ecuador.

***Chinannus perplexus* sp. n.**

(Figs 1.4, 1.13, 1.18)

(urn:lsid:zoobank.org:act:30E9CE13-7C08-44D1-96FF-43FF874184E4)

HOLOTYPE: 1 ♂ COSTA RICA, Puntarenas, Osa Co. Co., Piedra Blanca, 8.7°N 83.261°W, 26-VII-77, E. A. Sugden (UCR_ENT 00037003) (UCD).

PARATYPES: 1 ♂ (UCR_ENT 00037002), COSTA RICA, Puntarenas, Osa Co. Co., Piedra Blanca, 8.7°N 83.261°W, 26-VII-77, E. A. Sugden (UCD).

Diagnosis. This species can be distinguished by the following combination of characters: forewing with reduced membranous area posteriorly of the distal portion of 1AN; wing organ absent; parasternite IV with pouch and spine; appendage of tVIII elbowed with twist, distal portion curved medially and tapering at apex; anophoric process claw-shaped, large, equal in length to width of pygophore.

This species differs from all other species by the absence of the wing organs.

Description. *Male*. Total length: 0.81 mm; width across pronotum: 0.42 mm. COLORATION (Fig. 1.4). General color black; costal cell of forewing same color as veins at apex of wing; veins darker than membrane. SURFACE AND VESTITURE. As in generic description. STRUCTURE. Submacropterous, with reduced membranous area posteriorly of the distal portion of 1AN (Fig. 1.13); veins of forewing clearly widened and thickened; M-vein of discal cell thick but without wing organ and peg-like structures. ABDOMEN AND GENITALIA (Fig. 1.18). Sternite II+III on right side reaching the posterior margin of sternite IV; parasternite IV relatively large, with pouch and spine; parasternite V half as long as sternite V; parasternite VI slightly shorter than length of sternite VI; tVIII with movable appendage on left side, without process on right side, less than half as long as tVII; appendage of tVIII elbowed with twist, distal portion curved medially and tapering at apex; vesica relatively short, two coils; anophore tube-like, almost symmetrical; anophoric anophoric process claw-shaped, large, equal in length to width of pygophore.

Etymology. Named for the absence of the wing organ. An adjective after Latin "perplexus" meaning "confused".

Distribution. Known from one locality from Puntarenas, Costa Rica.

Discussion. *C. perplexus* is the only known species of *Chinannus* that does not have a wing organ. However, the labium structure, wing venation, and organization of the genitalia clearly associates this species with other *Chinannus* species.

***Chinannus schuhi* sp. n.**

(Figs 1.4, 1.13, 1.15H, 1.18)

(urn:lsid:zoobank.org:act:D3129172-150C-4B6B-8A38-6816851F6BD8)

HOLOTYPE: 1 ♂ BRAZIL, Amapa, Serra do Navio, 0.9833°N 52.05°W, 6 – 7-V-73, R.T. Schuh (UCR_ENT 00096873) (AMNH).

Diagnosis. This species can be distinguished by the following combination of characters: forewing with well-developed membranous area posteriorly of the distal portion of 1AN; wing organ with middle cavity with six pegs; parasternite IV with pouch and spine; appendage of tVIII straight, thin, slightly curved at apex; anophoric process stick-shaped, without constriction, with apex curved caudally.

Similar to *C. parvioculatus* and *C. trinitatis* in the shape of the genitalia, but differs in the number of pegs.

Description. *Male*. Total length: 1.16 mm; width across pronotum: 0.56 mm.

COLORATION (Fig. 1.4). General color black; costal cell of forewing darkened compared to the rest of corium; veins same color as membrane; apex of wing organ same color as the rest of wing organ. SURFACE AND VESTITURE. As in generic description. STRUCTURE. Macropterous, with well-developed membranous area posteriorly of the distal portion of 1AN (Fig. 1.13); veins (except for those forming costal cell) not widened; wing organ around two thirds as long as discal cell, tilted in relation to rest of M-vein of discal cell; wing organ with middle cavity, shorter than length of wing organ; wing organ cavity with six pegs (Fig. 1.15H); wing organ pegs longer than wide. ABDOMEN AND GENITALIA (Fig. 1.18). Sternite II+III on right side almost equal in

length to left side; parasternite IV relatively small, with pouch and rounded spine; parasternites V and VI roughly equal in length to corresponding sternites; tVIII with movable appendage on left side, without process on right side, half as long as tVII; appendage of tVIII straight, thin, slightly curved at apex; vesica relatively long, with approximately seven coils; anophore tube-like, strongly asymmetrical with right side being longer than left; anophoric process stick-shaped, without constriction, with apex curved caudally.

Etymology. Named after R.T. Schuh (AMNH) who collected the only specimen of the species. A noun in genitive case.

Distribution. The species is known from one locality in Amara, Brazil.

Chinannus scudderi sp. n.

(Figs 1.4, 1.13, 1.15I, 1.18)

(urn:lsid:zoobank.org:act:7D6A6555-3B0E-4F95-84D6-7992171D4946)

HOLOTYPE: 1 ♂ ECUADOR: Orellana: Tiputini Biodiversity Station nr. Yasuni National Park, 0.63194°S 76.14417°W, 220 m, 5-II-99, T. L. Erwin et al. (UCR_ENT 00030667) (USNM).

PARATYPES: 2 ♂ (UCR_ENT 00094265-UCR_ENT 00094266), ECUADOR, Orellana, Estacion Cientifica Yasuni, 0.67111°S 76.4002°W, 200 m, 5-IX-99 – 10-IX-99, E. G. Riley (TAMU).

Diagnosis. This species can be distinguished by the following combination of characters: forewing with well-developed membranous area posteriorly of the distal portion of 1AN;

wing organ with middle cavity with 10 pegs; parasternite IV with pouch and spine; appendage of tVIII straight, thin, slightly curved at apex; anophoric process hook-shaped, widened at base with rounded apex.

Similar to *C. trinitatis* in the number of pegs but different in the shape of the wing organ cavity and anophoric process.

Description. *Male*. Total length: 1.14 mm; width across pronotum: 0.51 mm. COLORATION (Fig. 1.4). General color brown; costal cell of forewing darkened compared to the rest of corium; veins same color as membrane; apex of wing organ same color as the rest of wing organ. SURFACE AND VESTITURE. As in generic description. STRUCTURE. Macropterous, with well-developed membranous area posteriorly of the distal portion of 1AN (Fig. 1.13); veins (except for those forming costal cell) not widened; wing organ two thirds as long as discal cell; wing organ with middle cavity, almost equal in length to wing organ; wing organ cavity with 10 pegs (Fig. 1.15I); wing organ pegs longer than wide. ABDOMEN AND GENITALIA (Fig. 1.18). Sternite II+III on right side reaching posterior margin of sternite IV; parasternite IV relatively small, with pouch and rounded spine; parasternite V half as long as sternite V; parasternite VI roughly equal in length to sternite VI; tVIII with movable appendage on left side, without process on right side, half as long as TVII; appendage of tVIII straight, thin, slightly curved at apex; vesica of medium length, with four and a half coils; anophore tube-like, strongly asymmetrical with right side being longer than left; anophoric process hook-shaped, widened at base with rounded apex.

Female. Unknown.

Etymology. This species is named after G.G.E. Scudder, in recognition of his contribution to the study of *Chinannus* (see *C. advenus* discussion). A noun in genitive case.

Distribution. The species is known from one locality in Orellana, Ecuador.

***Chinannus translucidus* sp. n.**

(Figs 1.4, 1.13, 1.15J, 1.18)

(urn:lsid:zoobank.org:act:C6920385-7D6F-4A96-8675-3F16A56F64C2)

HOLOTYPE: 1 ♂ ECUADOR, Orellana, Yasuni Research Station, 0.67417°S 76.39741°W, 228 m, 1 – 5-XII-2009, D. Forero (UCR_ENT 00002824) (QCAZ).

PARATYPES: 1 ♂ (UCR_ENT 00090373), ECUADOR, Napo, 20 km SW Tena, 1.12162°S 77.94069°W, 600 m, 11-VII-76, S.B. Peck (FMNH); 1 ♂ (UCR_ENT 00078169), Orellana, Yasuni Research Station, 0.67417°S 76.39741°W, 228 m, 1 – 5-XII-2009, D. Forero (QCAZ).

Diagnosis. This species can be distinguished by the following combination of characters: forewing with reduced membranous area posteriorly of the distal portion of 1AN; wing organ with middle cavity with nine pegs and transparent patch at apex; parasternite IV with pouch and spine; appendage of tVIII elbowed with twist, distal portion straight and tapering at apex; anophoric process claw-shaped.

This species is most similar to *C. areolatus* in having a transparent patch on the wing organ and a similar shape of the spine of parasternite IV and appendage of tVIII. *C.*

translucidus can be distinguished from *C. areolatus* by the shorter wing organ with fewer pegs in it.

Description. *Male*. Total length: 0.76 mm; width across pronotum: 0.42 mm. COLORATION (Fig. 1.4). General color black; costal cell of forewing darkened compared to the rest of corium; veins same color as membrane; apex of wing organ with transparent patch at apex. SURFACE AND VESTITURE. As in generic description. STRUCTURE. Submacropterous, withreduced membranous area posteriorly of the distal portion of 1AN (Fig. 1.13); veins (except for those forming costal cell) not widened; wing organ more than four fifths as long as discal cell; wing organ with middle cavity, almost equal in length to wing organ; wing organ cavity with nine pegs (Fig. 1.15J); wing organ pegs longer than wide at apex of wing organ or roughly as wide as long, blunt at base of wing organ. ABDOMEN AND GENITALIA (Fig. 1.18). Sternite II+III on right side reaching posterior margin of sternite IV; parasternite IV relatively large, with large pouch and small spine; parasternite V half as long as sternite V; parasternite VI roughly equal in length to sternite VI; tVIII with movable appendage on left side, without process on right side, half as long as tVII; appendage of tVIII elbowed with twist, distal portion straight and tapering at apex; vesica relatively short, three coils; anophore tube-like, almost symmetrical; anophoric process claw-shaped.

Female. Unknown.

Etymology. Named for the transparent patch on the wing organ. The specific epithet is the Latin adjective “translucid” meaning transparent.

Distribution. This species is known from two localities in Napo and Orellana, Ecuador.

Chinannus trinitatis (China, 1946)

(Figs 1.4, 1.5, 1.7A-L, 1.8A-O, 1.9A-K, 1.11C, 1.13, 1.15K, 1.18, 1.19)

Ptenidiophyes trinitatis China, 1946: 148 (original description)

Chinannus trinitatis Wygodzinsky, 1948: 147 (revised generic placement)

HOLOTYPE: 1 ♀ TRINIDAD AND TOBAGO, Trinidad, Sangre Grande Regional Corporation Co., Sangre Grande, Brigand Hill, 10.48333°N 61.06667°W, 5-I-44, Strickland (UCR_ENT 00069186) (BMNH).

PARATYPES: 2 ♂ (UCR_ENT 00069184, UCR_ENT 00069185), TRINIDAD AND TOBAGO, Trinidad, Sangre Grande Regional Corporation Co., Sangre Grande, Marper, 10.50386°N 61.08683°W, 6-I-44, A.H. Strickland (BMNH).

Diagnosis. This species can be distinguished by the following combination of characters: forewing with well-developed membranous area posteriorly of the distal portion of 1AN; wing organ with middle curved cavity with 10 or 11 pegs; parasternite IV with pouch and spine; appendage of tVIII straight, thin at apex; anophoric process stick-shaped, medially constricted, with apex not curved; female forewing heavily punctate, uniformly colored; spermathecal reservoir T-shaped and large.

Males of this species resemble *C. schuhi* and *C. parvioculatus* in the shape of the genitalia, but differ in the number of pegs in the wing organ and medially constricted stick-shaped anophoric process. Females differ from other species by a large T-shaped spermathecal reservoir.

Redescription. *Male*. Total length: 1.17 mm; width across pronotum: 0.50 mm. COLORATION (Fig. 1.4). General color black; costal cell of forewing darkened compared to the rest of corium; veins same color as membrane; apex of wing organ same color as the rest of wing organ. SURFACE AND VESTITURE. As in generic description. STRUCTURE. Macropterous, with well-developed membranous area posteriorly of the distal portion of 1AN (Fig. 1.13); veins (except for those forming costal cell) not widened; wing organ two thirds as long as discal cell; wing organ with middle cavity, almost equal in length to wing organ; wing organ cavity curved, with 10 to 11 pegs (Fig. 1.15L); wing organ pegs longer than wide. ABDOMEN AND GENITALIA (Fig. 1.18). Sternite II+III on right side almost equal in length to left side; parasternite IV relatively small, with pouch and rounded spine; parasternites V and VI roughly equal in length to corresponding sternites; tVIII with movable appendage on left side, without process on right side, half as long as tVII; appendage of tVIII straight, thin at apex; vesica relatively long, eight to ten coils; anophore tube-like, strongly asymmetrical with right side being longer than left; anophoric process stick-shaped, medially constricted, with apex not curved.

Female. Total length: 0.82 mm; width across pronotum: 0.47 mm. COLORATION (Figs 1.4, 1.5). General color black; forewing black, uniformly colored. SURFACE AND VESTITURE. Forewing heavily punctate. STRUCTURE. Compound eye slightly wider than first antennal segment; apex of forewing abrupt. GENITALIA (Fig. 1.19). Spermathecal reservoir T-shaped, large; spermathecal duct relatively short, coiled;

spermathecal gland diameter much smaller than spermathecal reservoir width; spermathecal gland duct relatively long.

Distribution. The species is known from many localities in Trinidad and Tobago.

Other Specimens Examined. TRINIDAD AND TOBAGO: Tobago: 10 ♂ (UCR_ENT 00096964-UCR_ENT 00096972), 10 km NE Roxborough, Gilpin Trace, 11.28064°N 60.58597°W, 400 m, 26 – 30-VI-93, S. B. Peck, J. Kukalova-Peck (FMNH); Trinidad: Arima Co.: 40 ♂ (UCR_ENT 00091174), 8 km N Arima, Simla Research Station, 10.61667°N 61.26667°W, 240 m, 6 – 14-VI-93, S. B. Peck, J. Kukalova-Peck (FMNH); 14 ♂ (UCR_ENT 00091167, UCR_ENT 00096923-UCR_ENT 00096935), 6 – 10-VI-93, S. B. Peck, J. Kukalova-Peck (FMNH); 3 ♂ (UCR_ENT 00091125, UCR_ENT 00097850, UCR_ENT 00097851), 16 km N Arima, Andrews Trace, 10.71361°N 61.27417°W, 620 m, 7-VI-93, S.B. Peck and J. Kukalova-Peck (FMNH); 2 ♂ (UCR_ENT 00097859, UCR_ENT 00097860), 19 km N Arima, Lalaja Trace, 10.71361°N 61.27417°W, 650 m, 8-VI-93, S.B. Peck and J. Kukalova-Peck (FMNH); 2 ♂ (UCR_ENT 00097852, UCR_ENT 00097853), 4 ♀(UCR_ENT 00097854-UCR_ENT 00097857), 19 km N Arima, Lalaja Trace, 10.71361°N 61.27417°W, 620 m, 11-VI-93, S.B. Peck and J. Kukalova-Peck (FMNH); 2 ♀(UCR_ENT 00088070, UCR_ENT 00088071), Simla Research Station (e.g. William Beebe Tropical Research Station), 10.68727°N 61.2983°W, 22-VII-2013, C. Weirauch (UCR); 2 ♂ (UCR_ENT 00087478, UCR_ENT 00087655), 26 – 27-VII-2013, C. Weirauch (UCR); 3 ♂ (UCR_ENT 00084958, UCR_ENT 00084984, UCR_ENT 00100726), 1 ♀(UCR_ENT 00088673), 26-VII-2013, C. Weirauch (UCR); Couva-Tabaquite-Talparo Regional Corporation Co.:

1 ♀(UCR_ENT 00030674), Tortuga, 10.34169°N 61.38398°W, no date provided, E. McC. Callan (USNM); Saint George Co.: 6 ♂(UCR_ENT 00097864-UCR_ENT 00097869), Maracas Valley above Loango Village, 10.7085°N 61.41583°W, 600 m, 9 – 22-VI-93, S. B. Peck, J. Kukalova-Peck (FMNH); Tunapuna-Piarco Regional Corporation Co.: 1 ♀ (UCR_ENT 00102128), Brasso Seco Paria, 10.74917°N 61.26472°W, 148 m, 25-VII-2013, C. Weirauch (UCR); 1 ♂ (UCR_ENT 00091130), Mt. St. Benedict, 10.66154°N 61.39565°W, 240 m, 4-VI-93, S.B. Peck and J. Kukalova-Peck (FMNH); 1 ♀(UCR_ENT 00091142), 5-VI-93, S.B. Peck and J. Kukalova-Peck (FMNH); 3 ♂ (UCR_ENT 00097861-UCR_ENT 00097863), Mt. St. Benedict, 10.66154°N 61.39565°W, 230 m, 4 – 13-VI-93, S.B. Peck and J. Kukalova-Peck (FMNH); 1 ♂ (UCR_ENT 00087484), Tacarigua, Caura Royal Road, 10.68722°N 61.37°W, 104 m, 18 – 19-VII-2013, C. Weirauch, J. Heraty, A. Baker (UCR); 1 ♀(UCR_ENT 00086206), 18-VII-2013, C. Weirauch (UCR); 1 ♂ (UCR_ENT 00081798), Tacarigua, Maracas Falls Trail, 10.72083°N 61.40889°W, 155 m, 16-VII-2013, C. Weirauch (UCR); 1 ♂ (UCR_ENT 00086192), 16-VII-2013, J. Heraty (UCR); 1 ♀ (UCR_ENT 00088077), 18-VII-2013, C. Weirauch (UCR); Trinidad, unknown locality: 2 ♂ (UCR_ENT 00069187, UCR_ENT 00069188), 3 ♀ (UCR_ENT 00069189-UCR_ENT 00069191), 10.45852°N 61.2802°W, 1971, L.A. Mound (BMNH).

Chinannus sp. Peru

(Figs 1.4, 1.5)

Description. *Female*. Total length: 0.96 mm; width across pronotum: 0.46 mm. COLORATION (Fig. 1.4 *C.* sp. Peru, Fig. 1.5 *C.* sp. Peru). General color pale brown; forewing uniformly colored. SURFACE AND VESTITURE. Forewing heavily punctate. STRUCTURE. Compound eye slightly wider than first antennal segment; forewing with prominent spine on dorsal surface, as well as with apical spine. GENITALIA. Not studied.

Distribution. Known from a single specimen collected in Peru. The locality remains unknown, the locality code is AC/33 (W).

Specimens Examined. PERU: 1 ♀ (UCR_ENT 00089579), locality unknown (locality code AC/33 (W)) (MHNG).

Phylogenetic analysis

The best maximum likelihood tree (Fig. 1.20) shows *Chinannus* as monophyletic and "Ogeriinae" as paraphyletic, and provides some insights into relationships within *Chinannus*. Schizopteridae are well supported (100% bootstrap [bs]) as are the Hypselosomatinae (100% bs) and a clade containing Ogeriinae and Schizopterinae (98% bs). Relationships within this clade are much less well supported and we treat most of our subsequent results as tentative and requiring additional testing. Schizopterinae (here represented by species of *Schizoptera* Fieber, 1860, *Pinochius* Carayon, 1949, *Nannocoris* Reuter, 1891, and three representatives of the *Corixidea* group) are recovered

as monophyletic, although with low support (57% bs). Taxa that are currently classified as “Ogeriinae” (*Chinannus*, *Kaimon*, *Kokeshia*, and three undescribed “Ogeriinae”) are recovered as paraphyletic, with Ogeriinae sp 633 (from Colombia) + *Kokeshia* (from Southeast Asia) forming the sister group to the Schizopterinae. *Chinannus* is shown as the sister to Ogeriinae sp 2203 (from Africa) + *Kaimon* (from Australia) in Fig. 1.20, but this result is poorly supported.

Chinannus is recovered with 100% bootstrap support (Fig. 1.20), indicating that this genus is both morphologically and molecularly distinct. Our hypothesis further shows that *Chinannus* is subdivided into two major clades, one poorly supported clade (56% bs) comprising *C. caudalis* from Colombia, *C. duopaxillatus* from Peru and Brazil, and *C. trinitatis* from Trinidad, and the other containing the remaining taxa included in this analysis (71% bs). The latter clade is subdivided into two fairly well supported subclades consisting of taxa distributed along the rim of the Amazon basin, i.e. *C. inermis* (Southern Peru), *C. translucidus* (Ecuador), and *C. grandis* (Peru) (81% bs) and a second clade (88% bs) that contains all Central American taxa included in the analysis (*C. monteverdensis*, *C. bierigi*, *C. latus*, and *C. nicaraguensis* from Costa Rica and Nicaragua) and *C. communis* that is known from the Pacific coast and mid-elevation mountain ranges of the Eastern Cordillera in Colombia. Given that 16 species of *Chinannus* are missing from our phylogeny, we did not conduct a formal biogeographic analysis.

The clades recovered in our molecular phylogeny are also consistent with the distribution patterns of several morphological features. The Central American clade (*C. inermis*, *C.*

grandis, C. translucidus, C. monteverdensis, C. bierigi, *C. latus*, *C. nicaraguensis*, and *C. communis*) share a uniquely elbowed appendage of tVIII (Figs 1.16-18), a character that is not found elsewhere and may be a synapomorphy of this clade. In all species in this clade except *C. inermis*, females have a comma-shaped spermathecal reservoir with enlarged basal portion (Fig. 1.19) and a pale band on the forewings (Figs 1.1-5). Given our current phylogenetic hypothesis, these two characters may have been reduced in *C. inermis*. Finally, males in the clade *C. trinitatis* + *C. duopaxillatus* have a straight and thin appendage of tVIII not seen elsewhere and this character is like also a synapomorphy for this clade.

Male-female association

The material assembled by us revealed a total of 28 male-based morphospecies and 17 female-based morphospecies. For the male-based morphospecies we attempted to identify corresponding female morphospecies either by using comparison with type specimens (for *C. trinitatis* and *C. bierigi*), pairwise genetic distances of a portion of CO1 (for five species, see Table 1.4), or locality association (for the remaining species). CO1 distances provided support for the proposed species, with the highest intraspecific distance being 8.75% smaller than all interspecific distances (see Table 1.4). The relatively large distance between specimens of *C. bierigi* might be due to the low quality sequence of UCR_ENT 00004804. Males and females of *C. advenus* and *C. parvioculatus* were collected during the same collection event, but size and other morphological features were used for identification. The two nymphs found in the same locality with *C. advenus* and *C. parvioculatus* were not identified to species due to the lack of morphological

correlation with either species. One female was found in the material from an unknown locality in Peru. Considering that two species from Peru are being described based on males only, we refrain from describing the female here.

References

Carpintero, D.L. & Dellapé, P.M. (2006) *Williamsocoris*, a new genus of Schizopteridae (Heteroptera) from Argentina. *Zoological Science* 23, 653–655.

China, W.E. (1946) New Cryptostemmatidae (Hemiptera) from Trinidad, British West Indies. *Proceedings of the Royal Entomological Society of London (B)* 15, 148–154.

Emsley, M.G. (1969) The Schizopteridae (Hemiptera: Heteroptera) with the descriptions of new species from Trinidad. *Memoirs of the American Entomological* Society 25, 1–154.

Esaki, T. & Miyamoto, S. (1959) A new or little known *Hypselosoma* from Amami-Oshima and Japan, with the proposal of a new tribe for the genus (Hemiptera). *Sieboldia Fukuoka* 2, 109–120.

Fieber, F.X. (1860) Exegesen in Hemipteren. *Wiener Entomologische Monatschrift* 9, 257–272.

Folmer, O., Black, M., Hoeh, W., Lutz, R. & Vrijenhoek, R. (1994) DNA primers for amplification of mitochondrial cytochrome c oxidase subunit I from diverse metazoan invertebrates. *Molecular Marine Biology and Biotechnology* 3, 294–299.

Forero, D., Berniker, L. & Weirauch, C. (2013) Phylogeny and character evolution in the bee-assassins (Insecta: Heteroptera: Reduviidae). *Molecular Phylogenetics and Evolution* 66, 283–302.

Forthman, M., Chłond, D. & Weirauch C. (2015) Taxonomic monograph of the endemic millipede assassin bug fauna of Madagascar (Hemiptera: Reduviidae: Ectrichodiinae). *Bulletin of the American Museum of Natural History* 400, 1–152.

Giribet, G., Carranza, S., Baguñà, J., Riutort, M. & Ribera, C. (1996) First molecular evidence for the existence of a Tardigrada + Arthropoda clade. *Molecular Biology and Evolution* 13, 76–84.

Heymons, R. (1899) Beiträge zur Morphologie und Entwicklungsgeschichte der Rhynchoten. *Nova acta Leopoldina: Abhandlungen der Kaiserlich Leopoldinisch-Carolinisch Deutschen Akademie der Naturforscher* 74, 351–456.

Hill, L. (1980) Tasmanian Dipsocoroidea (Hemiptera: Heteroptera). *Australian Journal of Entomology* 19, 107–127.

Hill, L. (1987) First record of Dipsocoridae (Hemiptera) from Australia with the description of four new species of *Cryptostemma* Herrich-Schaeffer. *Australian Journal*

of Entomology 26, 129–139.

Hill, L. (1990) A revision of Australian *Pachyplagia* Gross (Heteroptera: Schizopteridae). *Invertebrate Systematics* 3, 605–617.

Hill, L. (2004) *Kaimon* (Heteroptera: Schizopteridae), a new, speciose genus from Australia. *Memoirs of the Queensland Museum* 49, 603–647.

Hill, L. (2013) A revision of *Hypselosoma* Reuter (Insecta: Heteroptera: Schizopteridae) from New Caledonia. *Memoirs of the Queensland Museum* 56, 407–455.

Hill, L. (2015) Three new genera of Schizopteridae from Australia with description of six new species (Hemiptera: Heteroptera: Schizopteridae). *Zootaxa* 3990, 73–96.

Kathirithamby, J., Hayward, A., Mcmahon, D., Ferreira, R., Andreazze, R., Almeida Andrade, H.T.D. & Fresneau, D. (2010) Conspecifics of a heterotrophic heteronomous species of Strepsiptera (Insecta) are matched by molecular characterization. *Systematic Entomology* 35, 234–242.

Li, M., Tian, Y., Zhao, Y. & Bu, W. (2012) Higher level phylogeny and the first divergence time estimation of Heteroptera (Insecta: Hemiptera) based on multiple genes. *PLoS one* 7, e32152.

Linnavuori, R. (1974) Hemiptera of the Sudan, with remarks on some species of the adjacent countries. *Annales Entomologici Fennici* 40, 116–138.

Makhan, M. (2013) *Soekhnandanius aschne* gen. et sp. nov., Schizopterinae (Hemiptera: Heteroptera: Schizopteridae) from Suriname. *Calodema* 291, 1–3.

McAtee, W.L. & Malloch, J.R. (1925) Revision of bugs of the family Cryptostemmatidae in the collection of the United States National Museum. *Proceedings of the United States National Museum* 67, 1–42.

Meier, R., Shiyang, K., Vaidya, G. & Ng, P. (2006) DNA Barcoding and Taxonomy in Diptera: A Tale of High Intraspecific Variability and Low Identification Success. *Systematic Biology* 55, 715–728.

Park, D.S., Foottit, R., Maw, E. & Hebert, P.D. (2011) Barcoding bugs: DNA-based identification of the true bugs (Insecta: Hemiptera: Heteroptera). *PloS one* 6, e18749.

Pilgrim, E.M. & Pitts, J.P. (2006) A molecular method for associating the dimorphic sexes of velvet ants (Hymenoptera: Mutillidae). *Journal of the Kansas Entomological Society* 79, 222–231.

Poinar, G. Jr & Brown, A. (2014) New genera and species of Jumping Ground Bugs (Hemiptera: Schizopteridae) in Dominican and Burmese amber, with a description of a meloid (Coleoptera: Meloidae) triungulin on a Burmese specimen. *Annales de la Société entomologique de France (N.S.): International Journal of Entomology* 50, 372–381.

Prendini, L., Weygoldt, P. & Wheeler, W.C. (2005) Systematics of the *Damon variegatus* group of African whip spiders (Chelicerata: Amblypygi): Evidence from behaviour, morphology and DNA. *Organisms Diversity & Evolution* 5, 203–236.

Rédei, D. (2007) A new species of the family Hypsipterygidae from Vietnam, with notes on the hypsipterygid fore wing venation (Heteroptera, Dipsocoromorpha). *Deutsche Entomologische Zeitschrift* 54, 43–50.

Rédei, D. (2008a) First record of *Pinochius* Carayon, 1949 from the Oriental Region, with description of a new species from Vietnam (Heteroptera: Schizopteridae). In: S. Grozeva and N. Simov (eds.), *Advances in Heteroptera research: festschrift in honor of 80th anniversary of Michail Josifov*. Pensoft Publishers, Sofia, Bulgaria, 327–337.

Rédei, D. (2008b) Two new species of *Kokeshia* from India and Thailand (Hemiptera: Heteroptera: Schizopteridae). *Acta Entomologica Musei Nationalis Pragae* 48, 241–250.

Rédei, D., Ren, S. & Bu, W. (2012) Two new species of *Kokeshia* from China (Hemiptera: Heteroptera: Schizopteridae). *Zootaxa* 3497, 29–36.

Reuter, O.M. (1882) Sur le genre *Schizoptera* Fieb. Revue d'entomologie 1, 162–164.

Reuter, O.M. (1891) Monographia Ceratocombidarum orbis terrestris. *Acta Societatis Scientiarum Fennica* 19, 1–28.

Reuter, O.M. (1910) Neue Beitrage zur Phylogenic und Systematik der Miriden nebst cinleitenden Bemerkungen uber die Phylogenic der Heteropteren-Familien. *Acta Societatis Scientiarum Fennica* 37: 1–169.

Schuh, R.T. & Slater, J.A. (1995) *True bugs of the world (Hemiptera: Heteroptera): classification and natural history.* Comstock Publishing Associates, Cornell University Press.

Schwendinger, P.J. & Giribet, G. (2005) The systematics of the south-east Asian genus *Fangensis* Rambla (Opiliones: Cyphophthalmi: Stylocellidae). *Invertebrate Systematics* 19: 297–323.

Scudder, G. (2010) The Schizopteridae (Hemiptera), a family new to Canada. *Journal of the Entomological Society of British Columbia* 107, 85–86.

Singh-Pruthi, H. (1925) The morphology of the male genitalia in Rhynchota. *Transactions of the Entomological Society of London* 1925, 127–267.

Stamatakis, A., Hoover, P. & Rougemont, J. (2008) A rapid bootstrap algorithm for the RAxML Web servers. *Systematic Biolology* 57, 758–771.

Štys, P. (1970) On the morphology and classification of the family Dipsocoridae s. lat., with particular reference to the genus *Hypsipteryx* Drake (Heteroptera). *Acta Entomologica Bohemoslovaca* 67, 21–46.

Štys, P. (1975) Redescription of *Ptenidiophyes mirabilis* Reuter (Heteroptera: Schizopteridae). *Věstník Československé Společnosti Zoologické* 39, 154–159.

Sweet, M.H. (1996) Comparative External Anatomy of the Pregenital Abdomen of the Hemiptera. In C. Schaeffer (ed.), *Studies on Hemipteran Phylogeny. Thomas Say Publications in Entomology: Proceedings.* Entomological Society of America, Lanham, MD, 119–158.

Uhler, P.R. (1904) List of Hemiptera-Heteroptera of Las Vegas hot springs, New Mexico, collected by Messrs E. A. Schwarz & Herbert S. Barber. *Proceedings of the United States National Museum* 27, 349–364.

Vaidya, G., Lohman, D.J. & Meier, R. (2011) SequenceMatrix: concatenation software for the fast assembly of multi-gene datasets with character set and codon information. *Cladistics* 27, 171–180.

Weirauch, C. (2012) *Voragocoris schuhi*, a new genus and species of Neotropical Schizopterinae (Hemiptera: Schizopteridae). *Entomologia Americana* 118, 285–294.

Weirauch, C. & Fernandes, J.A.M. (2015) Chapter 5: The minute litter bugs. In A. R. Panizzi and J. Gracia (eds.), *True Bugs (Heteroptera) of the Neotropics*. Springer, 99-109.

Weirauch, C. & Frankenberg, S. (2015) From “insect soup” to biodiversity discovery: taxonomic revision of *Peloridinannus* Wygodzinsky, 1951 (Hemiptera: Schizopteridae), with description of six new species. *Arthropod Systematics and Phylogenetics* 73(3), 457–475.

Weirauch, C. & Munro, J.B. (2009) Molecular phylogeny of the assassin bugs (Hemiptera: Reduviidae), based on mitochondrial and nuclear ribosomal genes. *Molecular Phylogenetics and Evolution* 53, 287–299.

Weirauch, C. & Štys, P. (2014) Litter bugs exposed: phylogenetic relationships of Dipsocoromorpha (Hemiptera: Heteroptera) based on molecular data. *Insect Systematics & Evolution* 45, 351–370.

Wheeler, W.C., Schuh, R.T. & Bang, R. (1993) Cladistic relationships among higher groups of Heteroptera: congruence between morphological and molecular data sets. *Entomologica Scandinavica* 24, 121–137.

Wygodzinsky, P. (1947) Sobre um novo genero e uma nova especie de Schizopterinae do Brasil (Cryptostemmatidae, Hemiptera). *Boletin de Entomologia Venezolana* 6, 25–35.

Wygodzinsky, P. (1948) On two new genera of Schizopterinae (Cryptostemmatidae) from the Neotropical region (Hemiptera). *Revista Brasileira de Biologia* 8, 143–155.

Wygodzinsky, P. (1950a) Contribution towards the knowledge of the family Cryptostemmatidae (Hemiptera). *Revista Brasileira de Biologia* 10, 377–392.

Wygodzinsky, P. (1950b) Schizopterinae from Angola (Cryptostemmatidae, Hemiptera). *Publicações Culturais da Companhia de Diamantes de Angola* 7, 9–48.

Wygodzinsky, P. (1951) Descripcion de generos y especies nuevos de la familia Cryptostemmatidae (Hemiptera). *Revista Brasileira de Biologia* 11, 259–270.

Wygodzinsky, P. (1960) Un nouvel *Hypeslosoma* de Madagascar, avec la description d'autre especes et des observations sur le genre (Schizopterinae, Dipsocoridae, Hemiptera). *Memoires de l'Institut Scientifique de Madagascar (E)* 11, 509–539.

Xie, Q., Tian, Y., Zheng, L. & Bu, W. (2008) 18S rRNA hyper-elongation and the phylogeny of Euhemiptera (Insecta: Hemiptera). *Molecular Phylogenetics and Evolution* 47, 463–471.

Zhang, G. & Weirauch, C. (2011) Matching dimorphic sexes and immature stages with adults: resolving the systematics of the *Bekilya* group of Malagasy assassin bugs (Hemiptera: Reduviidae: Peiratinae). Systematic Entomology 36, 115–138.

Table 1.1. Primers used in this study

Gene region	Primer name	Primer sequence (5′-3′)	Reference
18S	1f	TACCTGGTTGATCCTGCCAGTAG	Giribet *et al.* 1996
	5r	CTTGGCAAATGCTTTCGC	Giribet *et al.* 1996
	3f	GTTCGATTCCGGAGAGGGA	Giribet *et al.* 1996
	Bi	GAGTCTCGTTCGTTATCGGA	Giribet *et al.* 1996
28S D2	D2Fa	CGGGTTGCTTGAGAGTGC	Forero *et al.* 2013
	D2Ra	CTCCTTGGTCCGTGTTTC	Forero *et al.* 2013
28S D3-D5	D3Fa	TTGAAACACGGACCAAGGAG	Weirauch & Munro 2009
	D5Ra	CGCCAGTTCTGCTTACCA	Weirauch & Munro 2009
COI	LCO-S-1490	GGTCAACAAATCATAAAGATATTGG	Folmer *et al.* 1994
	HCOoutout	GTAAATATATGRTGDGCTC	Prendini *et al.* 2005; Schwendinger & Giribet 2005

Table 1.2. GenBank accession numbers for voucher specimens used in this study

Family	Taxon name in analysis	USI	18S rDNA	28S D2 rDNA	28S D3-D5 rDNA	COI
Ceratocombidae	*Ceratocombus* sp 125	UCR_ENT 00057546	KF781202	KF781233		N/A
Ceratocombidae	*Ceratocombus* sp 135	UCR_ENT 00057547	KF781200	KF781231		N/A
Dipsocoridae	*Cryptostemma* sp 249	UCR_ENT 00057528	KF781210	KF781247		N/A
Dipsocoridae	*Cryptostemma* sp 251	UCR_ENT 00057530	KF781211	KF781248		N/A
Schizopteridae	*Chinannus bierigi* 331	UCR_ENT 00077038	N/A	N/A	KT272729	KT272702
Schizopteridae	*Chinannus bierigi* 3360	UCR_ENT 00014790	N/A	N/A	KT272728	N/A
Schizopteridae	*Chinannus bierigi* 3361	UCR_ENT 00014792	N/A	N/A	KT272727	N/A
Schizopteridae	*Chinannus bierigi* 80	UCR_ENT 00004804	KF781208	KF781243		KT272701
Schizopteridae	*Chinannus caudalis* 539	UCR_ENT 00076331	N/A	N/A	KT272739	N/A
Schizopteridae	*Chinannus communis* 508	UCR_ENT 00076302	N/A	KT272719	KT272735	N/A
Schizopteridae	*Chinannus communis* 521	UCR_ENT 00074538	N/A	KT272718	KT272736	N/A
Schizopteridae	*Chinannus communis* 548	UCR_ENT 00076298	N/A	N/A	KT272741	N/A
Schizopteridae	*Chinannus communis* 652	UCR_ENT 00076272	N/A	KT272717	KT272742	N/A
Schizopteridae	*Chinannus duopaxillatus* 46	UCR_ENT 00004810	N/A	KF781244		KT272708
Schizopteridae	*Chinannus grandis* 372	UCR_ENT 00084387	N/A	KT272720	KT272740	KT272714
Schizopteridae	*Chinannus inermis* 168	UCR_ENT 00078255	N/A	N/A	KT272730	KT272709
Schizopteridae	*Chinannus latus* 5466	UCR_ENT 00090711	N/A	N/A	KT272731	N/A
Schizopteridae	*Chinannus latus* 5467	UCR_ENT 00090712	N/A	N/A	KT272732	N/A
Schizopteridae	*Chinannus monteverdensis* 4209	UCR_ENT 00110963	N/A	KT272722	KT272737	KT272711
Schizopteridae	*Chinannus monteverdensis* 4210	UCR_ENT 00110964	N/A	N/A	N/A	KT272710
Schizopteridae	*Chinannus monteverdensis* 4256	UCR_ENT 00116293	N/A	KT272721	KT272738	N/A
Schizopteridae	*Chinannus*	UCR_ENT	N/A	KT272725	KT272733	KT272713

	nicaraguensis 4208	00098871				
Schizopteridae	*Chinannus nicaraguensis* 6280	UCR_ENT 00101300	N/A	KT272724	KT272734	KT272712
Schizopteridae	*Chinannus translucidus* 127	UCR_ENT 00078169	KT272756	KT272723	N/A	KT272715
Schizopteridae	*Chinannus trinitatis* 1367	UCR_ENT 00086206	N/A	N/A	KT272743	KT272706
Schizopteridae	*Chinannus trinitatis* 1385	UCR_ENT 00086192	N/A	KT224608	KT272744	KT272705
Schizopteridae	*Chinannus trinitatis* 1915	UCR_ENT 00088673	KT272757	KT224609	KT272745	KT272707
Schizopteridae	*Chinannus trinitatis* 2409	UCR_ENT 00081798	N/A	KT224607	KT272746	KT272704
Schizopteridae	*Chinannus trinitatis* 2536	UCR_ENT 00088070	N/A	KT224606	N/A	KT272703
Schizopteridae	*Corixidea major* 3923	UCR_ENT 00012039	KT272758	KT224611	KT272747	N/A
Schizopteridae	*Dundonannus* sp 2637	UCR_ENT 00088110	N/A	KT224616	KT272748	N/A
Schizopteridae	*Hoplonannus craneae* 2213	UCR_ENT 00084981	KT272759	KT224610	KT272749	KT272716
Schizopteridae	*Kaimon* sp 443	UCR_ENT 00086064	N/A	N/A	KT272750	N/A
Schizopteridae	*Kokeshia* sp 1409	UCR_ENT 00063170	KT272760	KT224614	KT272751	N/A
Schizopteridae	*Kokeshia* sp 4627	UCR_ENT 00091486	KT272761	KT224615	KT272752	N/A
Schizopteridae	*Nannocoris* sp 93	UCR_ENT 00004800	KF781217	KF781253		N/A
Schizopteridae	Ogeriinae sp 2203	UCR_ENT 00087547	KT272763	KT224613	KT272754	N/A
Schizopteridae	Ogeriinae sp 2630	UCR_ENT 00088114	KT272764	KT224612	KT272755	N/A
Schizopteridae	Ogeriinae sp 633	UCR_ENT 00074536	KT272762	KT272726	KT272753	N/A
Schizopteridae	*Pateena polymitarior*	N/A	AY252302	AY252549		N/A
Schizopteridae	*Pinochius* sp 245	UCR_ENT 00057526	KF781222	KF781257		N/A
Schizopteridae	*Rectilamina* sp 12	UCR_ENT 00057525	KF781216	KF781252		N/A
Schizopteridae	*Schizoptera* sp 159	UCR_ENT 00057522	KF781226	KF781261		N/A
Schizopteridae	*Voragocoris schuhi* 254	UCR_ENT 00055624	KF781228	KF781263		N/A
Schizopteridae	*Williamsocoris* sp 171	UCR_ENT 00057523	KF781229	KF781264		N/A

Table 1.3. Specimen numbers per collecting method[1]

Method	At light	Berlese	FIT	Fogging	Hand col	LL	MT	Pan tr	Sweeping/ beating	Winkl
Males	7	41	76	1	-	8	65	25	2	17
Females	-	42	1	-	1	12	34	6	-	16
Nymphs	-	2	-	-	-	-	-	-	-	-
Total	7	85	77	1	1	20	99	31	2	25

[1] FIT – flight intercept trap; Hand col – hand collecting; LL – leaf litter sifting; MT – malaise trap; Pan tr – pan traps; Winkl – winkler funnel.

Table 1.4. Pairwise genetic distances between cytochrome c oxidase subunit I (CO1) across *Chinannus* species

Species	Intraspecific distance	Interspecific distance	Minimum gap between interspecific and intraspecific distances
C. bierigi	5.04%	13.78-19.89%	8.74%
C. duopaxillatus	N/A	17.08-24.01%	N/A
C. grandis	N/A	12.58-21.73%	N/A
C. inermis	N/A	12.60-18.83%	N/A
C. monteverdensis	<0.00%	12.08-20.95%	12.08%
C. nicaraguensis	<0.00%	12.08-20.40%	12.08%
C. translucidus	N/A	12.58-19.03%	N/A
C. trinitatis	0.39-2.52%	17.47-23.26%	14.95%

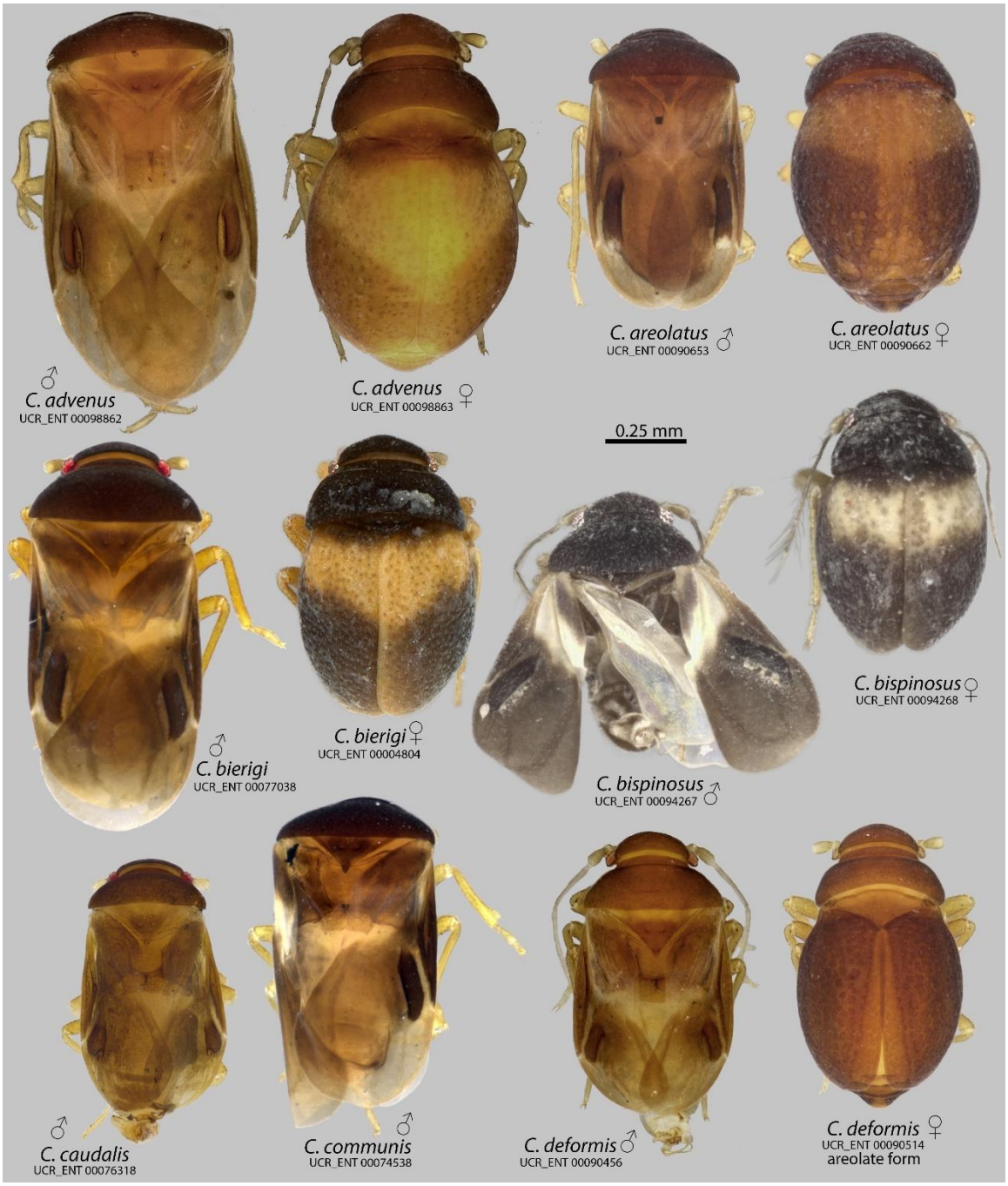

Figure 1.1. Dorsal habitus of *Chinannus* species.

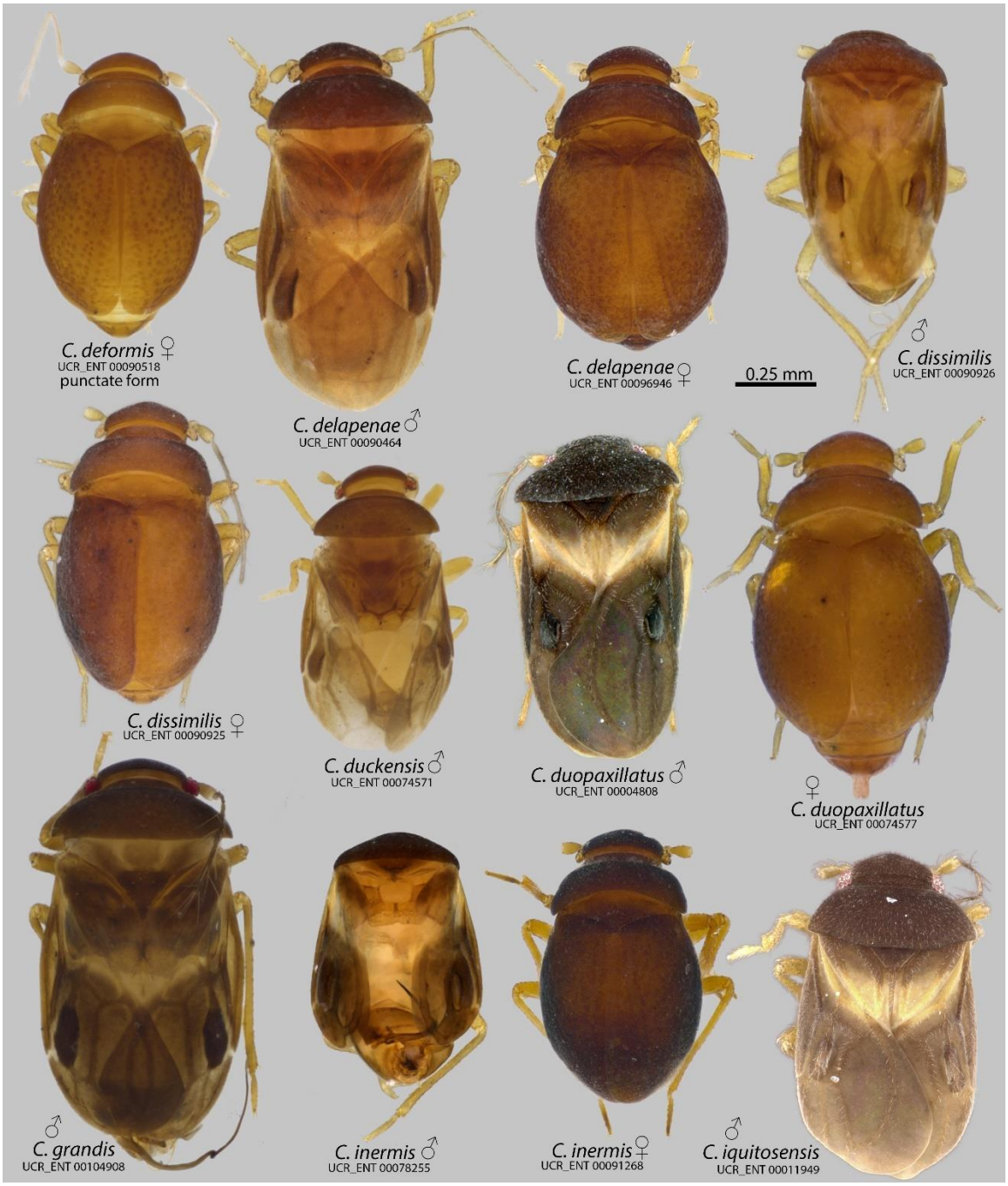

Figure 1.2. Dorsal habitus of *Chinannus* species.

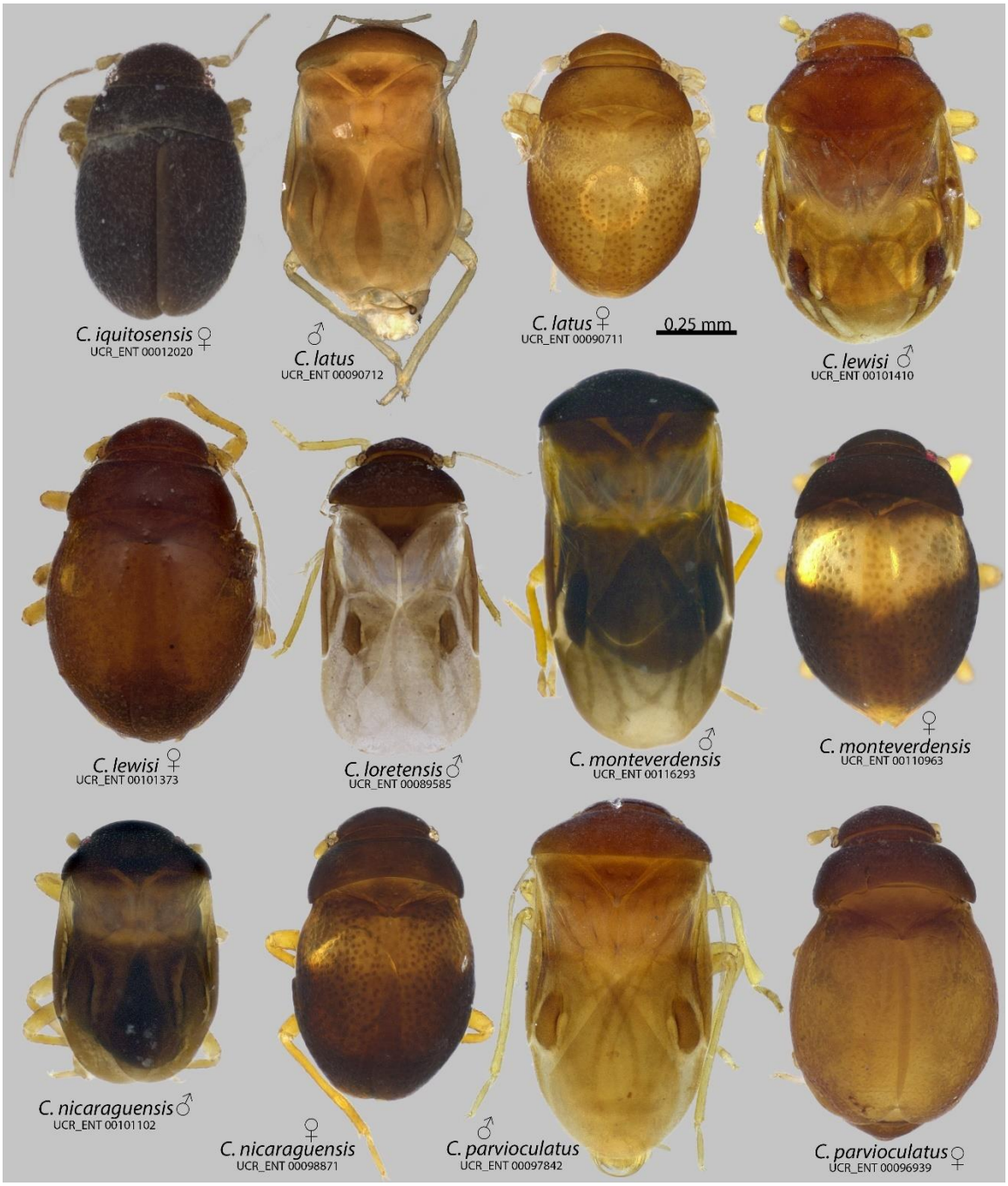

Figure 1.3. Dorsal habitus of *Chinannus* species.

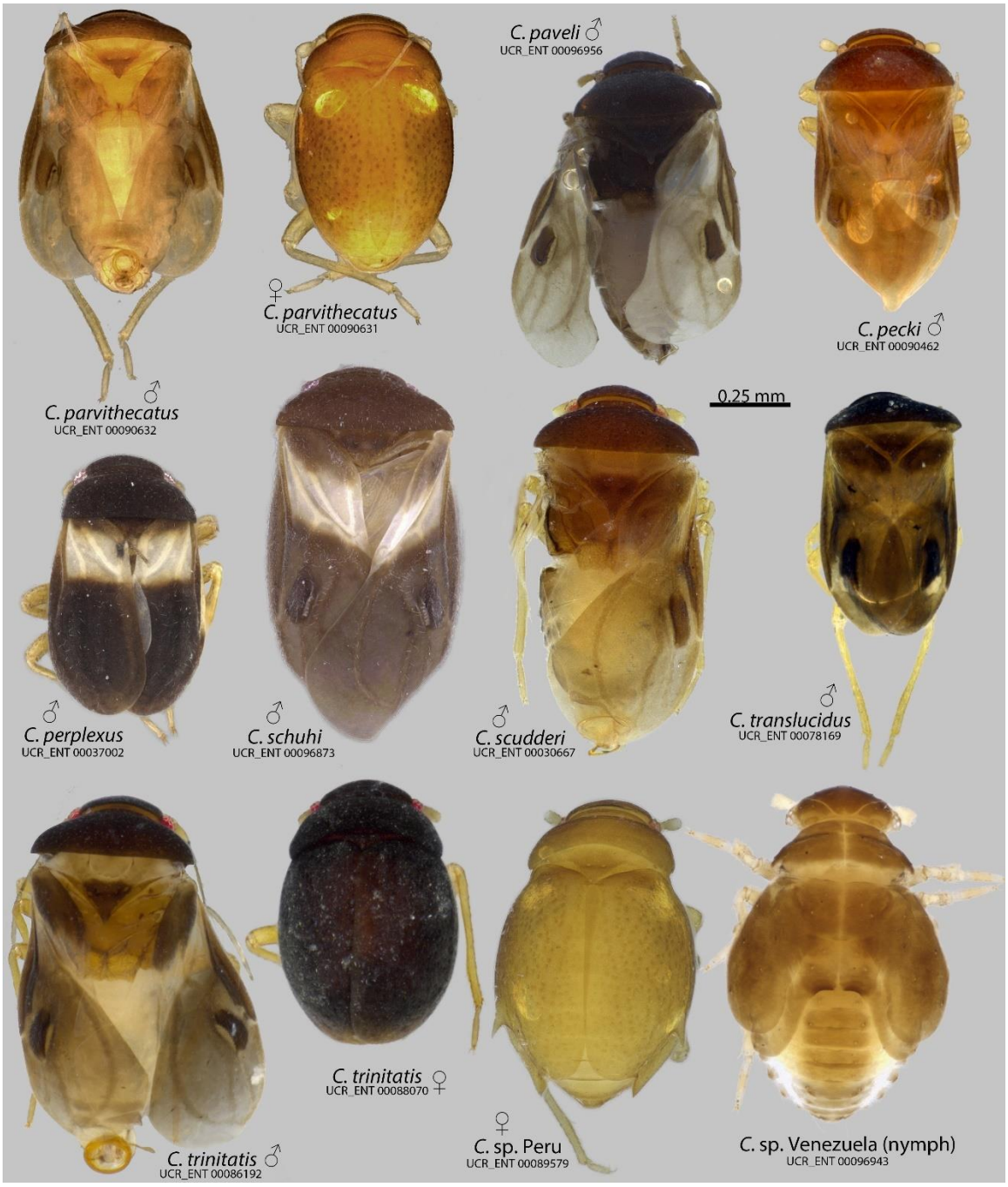

Figure 1.4. Dorsal habitus of *Chinannus* species.

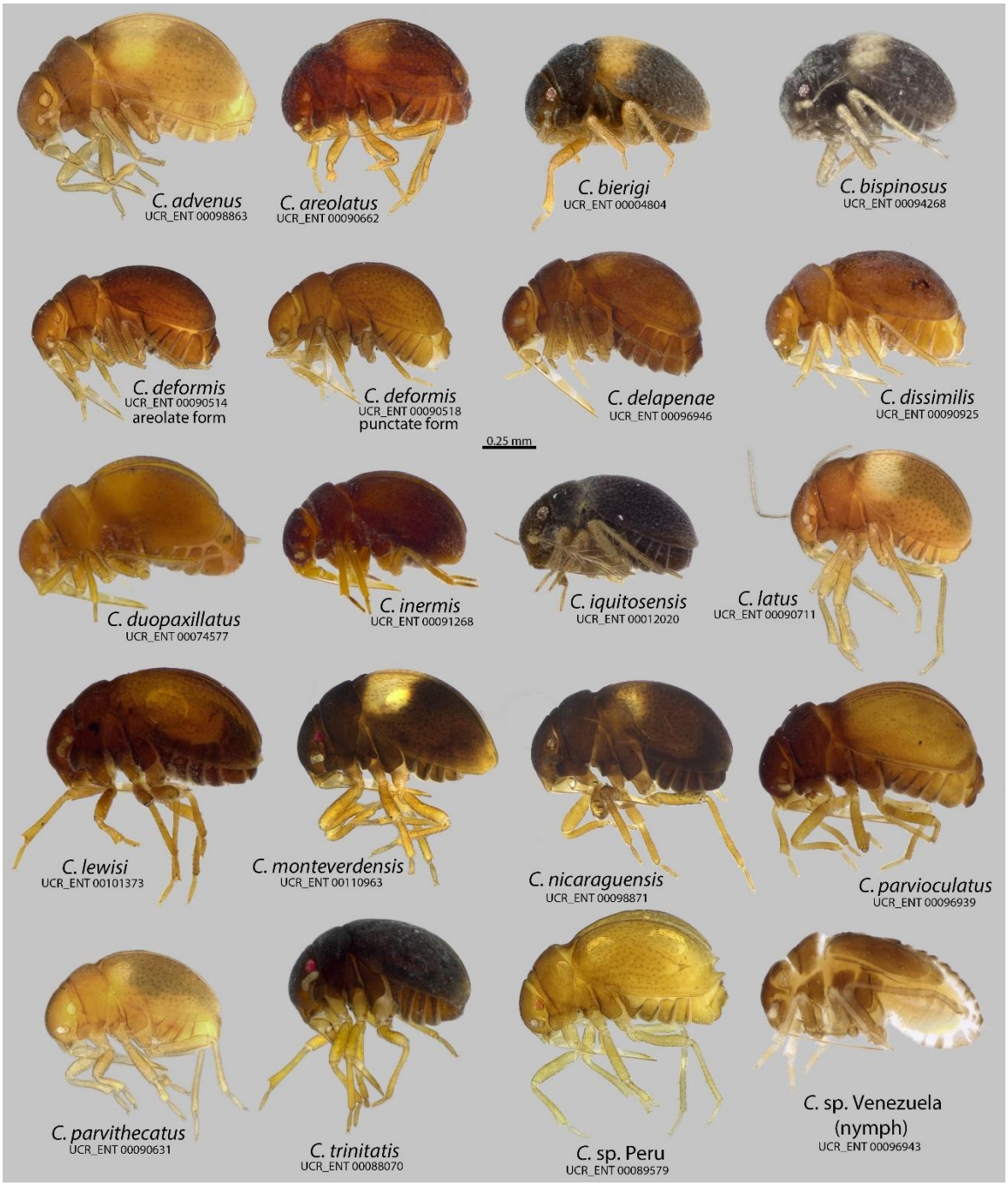

Figure 1.5. Lateral habitus of *Chinannus* females and a nymph.

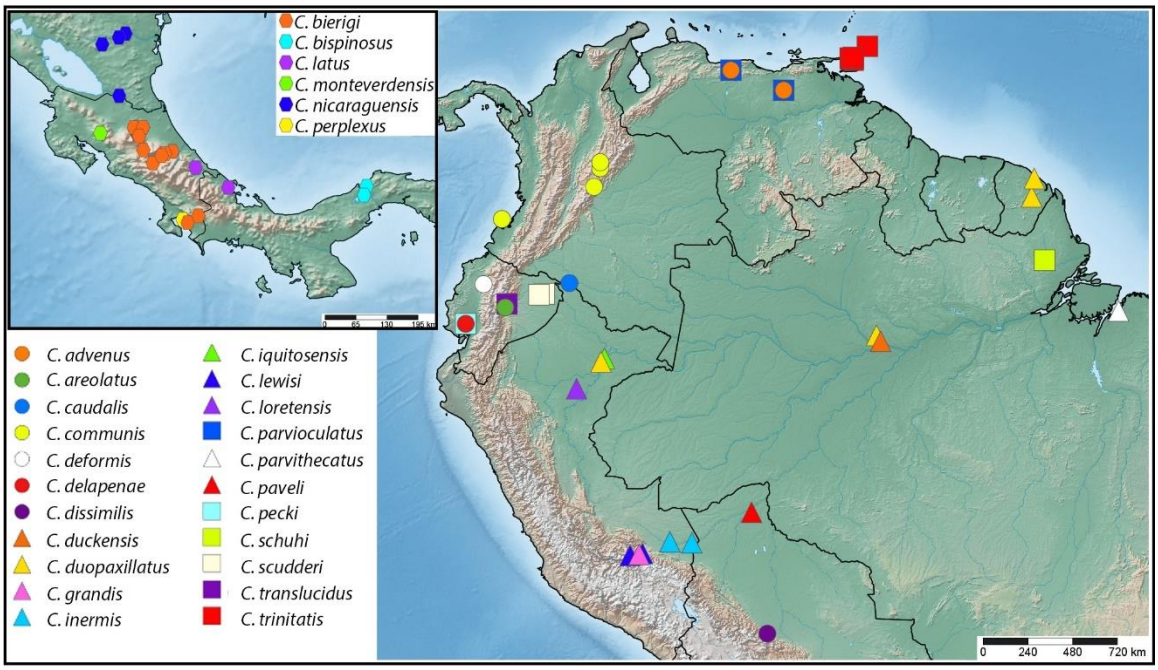

Figure 1.6. Distribution maps of *Chinannus* species.

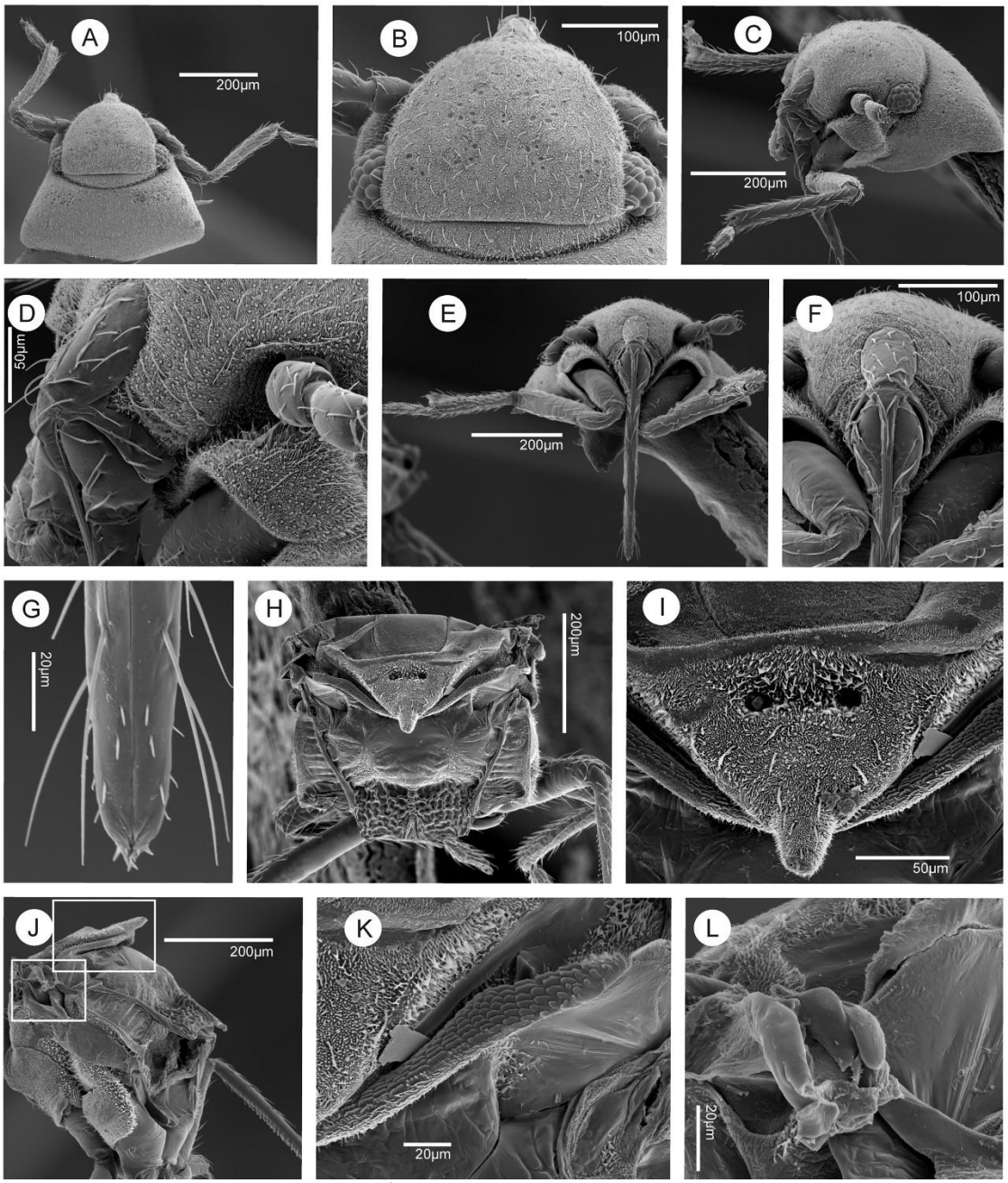

Figure 1.7. *Chinannus trinitatis*, ♂ UCR_ENT 00087478, scanning electron micrographs of male head and thorax. (A) Head and thorax, dorsal view. (B) Head, dorsal view. (C) Head and thorax, lateral view. (D) Head, close up, lateral view. (E) Head and thorax, frontal view. (F) Head, frontal view. (G) Apex of labium, dorsal. (H) Meso- and metathorax, dorsal view. (I) Scutellum, dorsal view. (J) Meso- and metathorax, lateral view, the white boxes indicate the position of the close-ups in K and L. (K) Frenulum, dorsolateral view. (L) Wing-coupling process with seemingly reduced microtrichia, lateral view.

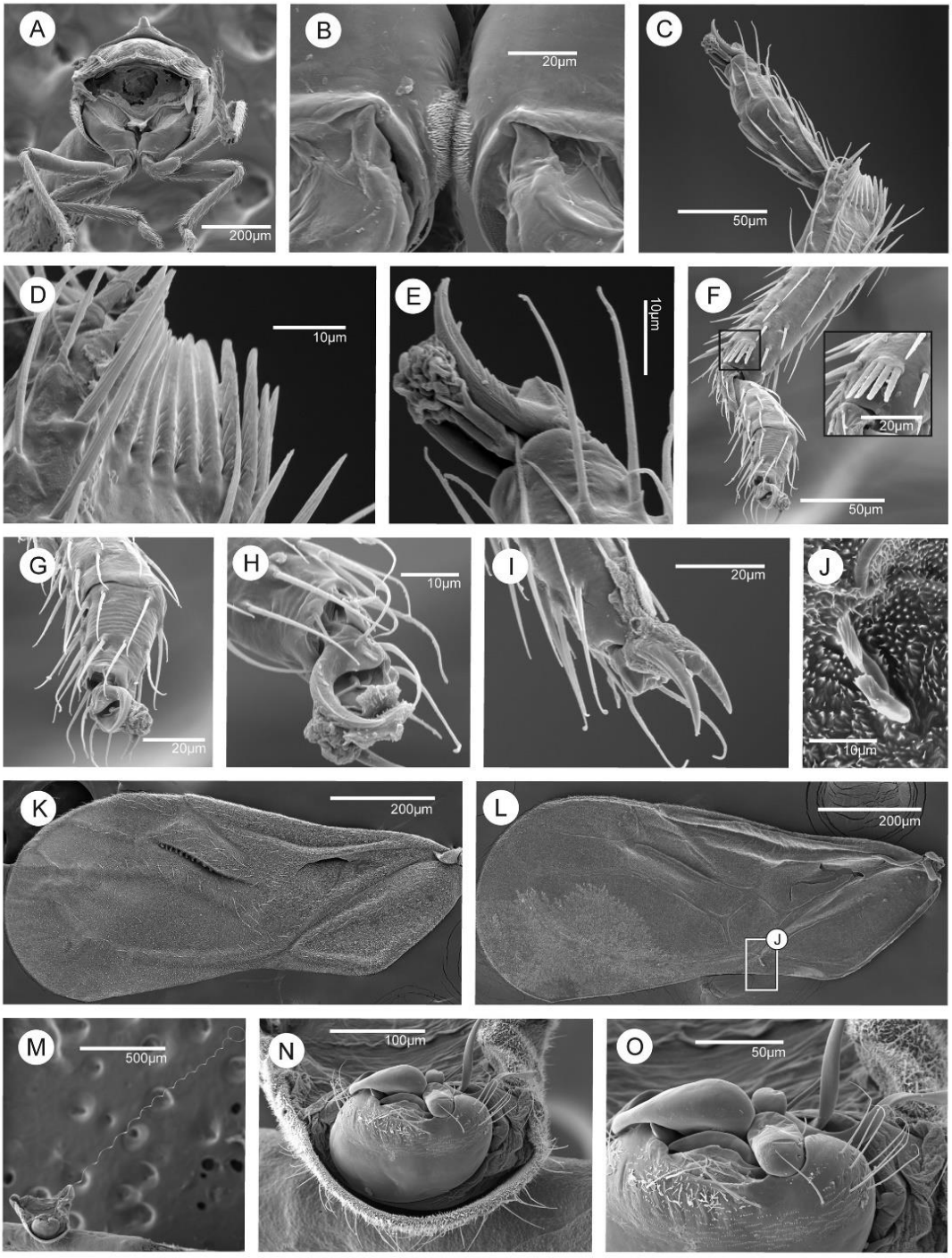
A
200µm
B
20µm
C
50µm
D
10µm
E
10µm
F
20µm
50µm
G
20µm
H
10µm
I
20µm
J
10µm
K
200µm
L
200µm
J
M
500µm
N
100µm
O
50µm

Figure 1.8. *Chinannus trinitatis*, ♂ UCR_ENT 00087478, scanning electron micrographs of male thorax and abdomen. (A) Metathorax, caudal view. (B) Coxal pads on metacoxae, caudal view. (C) Protibia and -tarsus, frontal view. (D) Protibial comb, close up, frontal view. (E) Protarsus and -pretarus, dorsal view. (F) Mesotibia, -tarsus, and -pretarsus, frontal view. (G) Mesotarsus and -pretarsus, frontal view. (H) Mesotarsus and -pretarsus, lateral view. (I) Metatarsus and -pretarsus, dorsolateral view. (J) Wing-to-wing clasping device on lateral surface of forewing, position indicated on L. (K) Forewing, dorsal view. (L) Forewing, ventral view, white box indicates position of wing-to-wing coupling device (close-up in J). (M) Abdomen and pygophore in caudal view with aedeagus extended. (N) Pygophore, caudal view. (O) Pygophore, close up, caudal view.

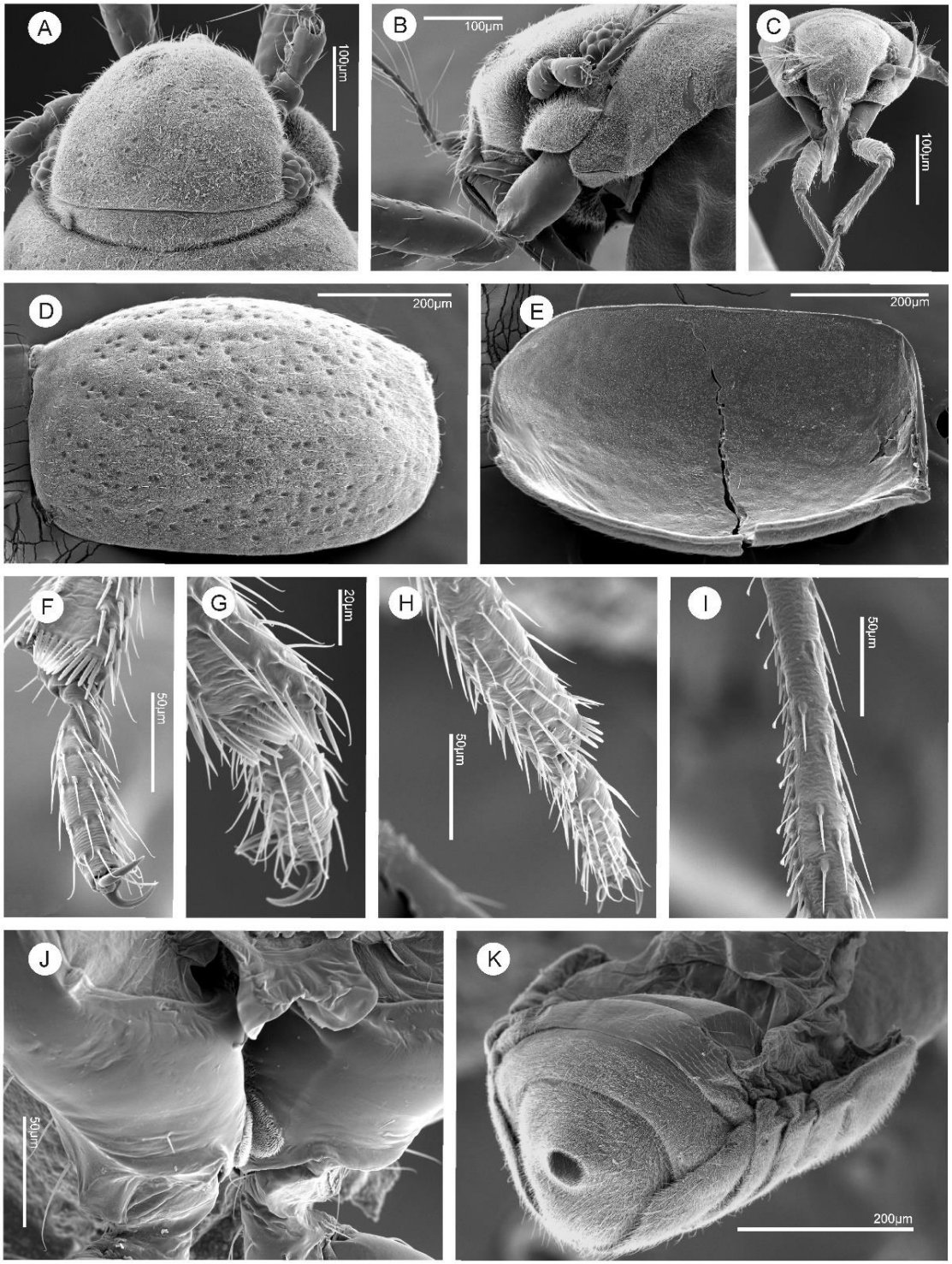
A
100µm
B
100µm
C
100µm
D
200µm
E
200µm
F
50µm
G
20µm
H
50µm
I
50µm
J
50µm
K
200µm

Figure 1.9. *Chinannus trinitatis*, ♀ UCR_ENT 00088077, scanning electron micrographs of female. (A) Head, dorsal view. (B) Head, lateral view. (C) Head and thorax, frontal view. (D) Forewing, dorsal view. (E) Forewing, ventral view. (F) Protibia, -tarsus, and -pretarsus, frontal view. (G) Protibia, -tarsus, and -pretarsus, frontal view. (H) Mesotibia and -tarsus, lateral view. (I) Metatibia with explanate setae, lateral view. (J) Coxal pads on metacoxae, caudal view. (K) Female abdomen, caudo-lateral view.

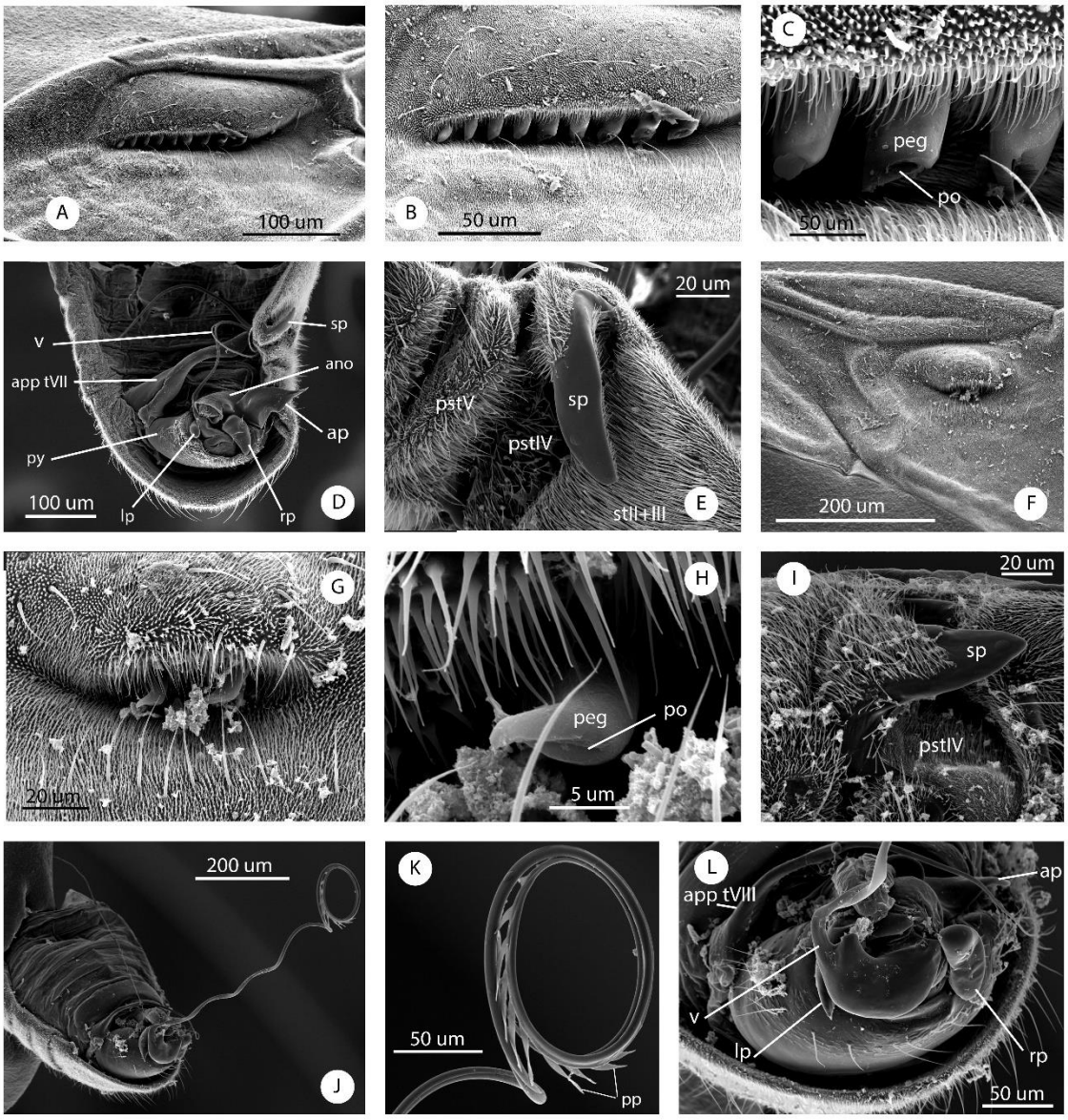

Figure 1.10. Scanning electron micrographs of selected male structures. (A-E) *Chinannus bierigi* UCR_ENT 00082335. (A) Forewing. (B) Wing organ. (C) Pegs of wing organ. (D) Abdomen, dorsal view. (E) Abdomen in lateral view, pouch and spine area. (F-L) *Chinannus duopaxillatus* UCR_ENT 00074579. (F) Forewing. (G) Wing organ. (H) Peg of wing organ. (I) Abdomen in lateral view, pouch and spine area. (J) Abdomen with aedeagus extended, dorsal view. (K) Tip of the vesica. (L) Close up of pygophore, caudal view.

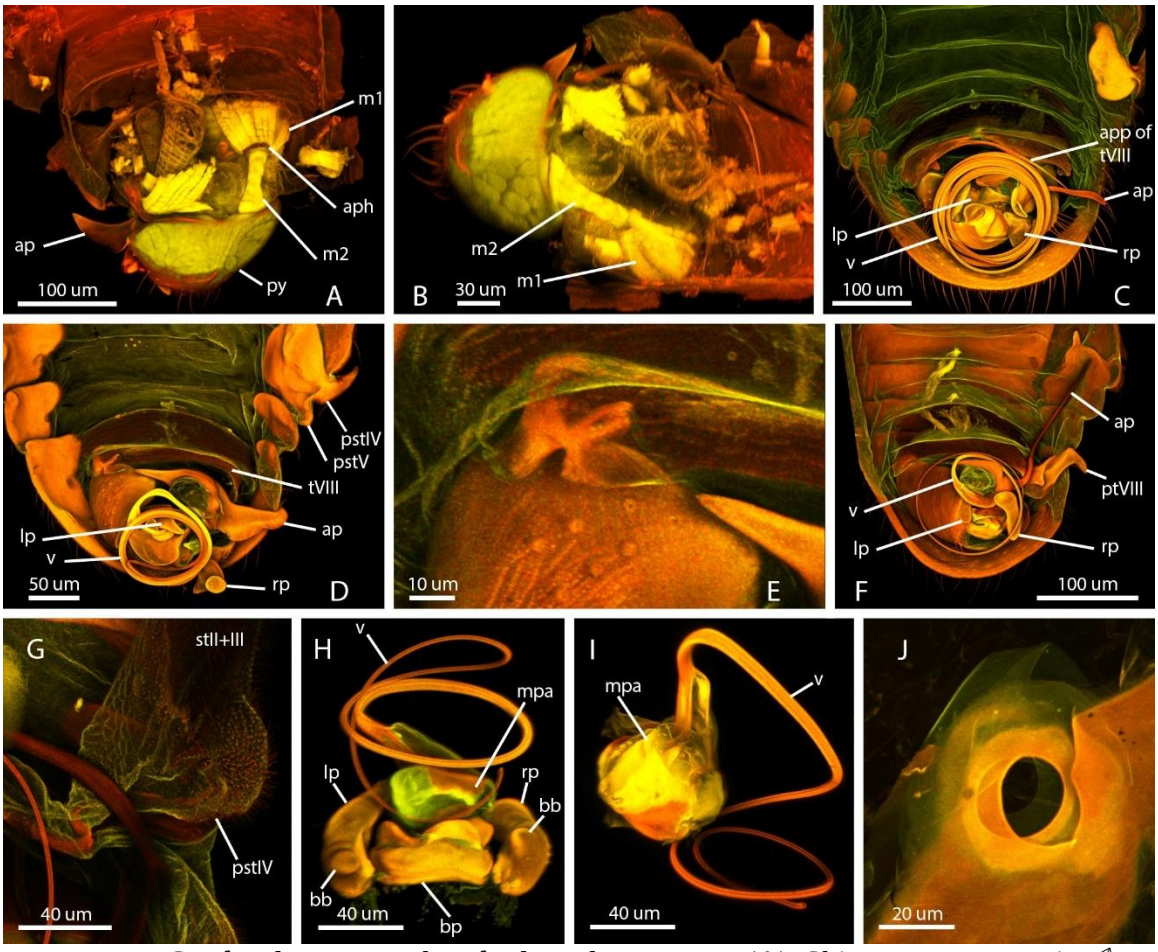

Figure 1.11. Confocal micrographs of selected structures. (A) *Chinannus communis*, ♂ UCR_ENT 00106844, abdomen in ventral view, sternites removed. (B) The same, in latero-ventral view. (C) *Chinannus trinitatis*, ♂ UCR_ENT 00081798, abdomen in dorsal view. (D) *Chinannus deformis*, ♂ UCR_ENT 00090456, abdomen in dorsal view. (E) The same, close up of tVIII structure. (F) *Chinannus pecki*, ♂ UCR_ENT 00090462, abdomen in dorsal view. (G) *Chinannus inermis*, ♂ UCR_ENT 00078255, abdomen in dorsal view, close up of pstIV. (H) *Chinannus communis*, ♂ UCR_ENT 00076302, aedeagus and parameres, viewed from caudal side of the specimen. (I) *Chinannus bierigi*, ♂ UCR_ENT 00088879, aedeagus. (J) *Chinannus bierigi*, ♀ UCR_ENT 00014792, place of connection of spermathecal duct to genital chamber.

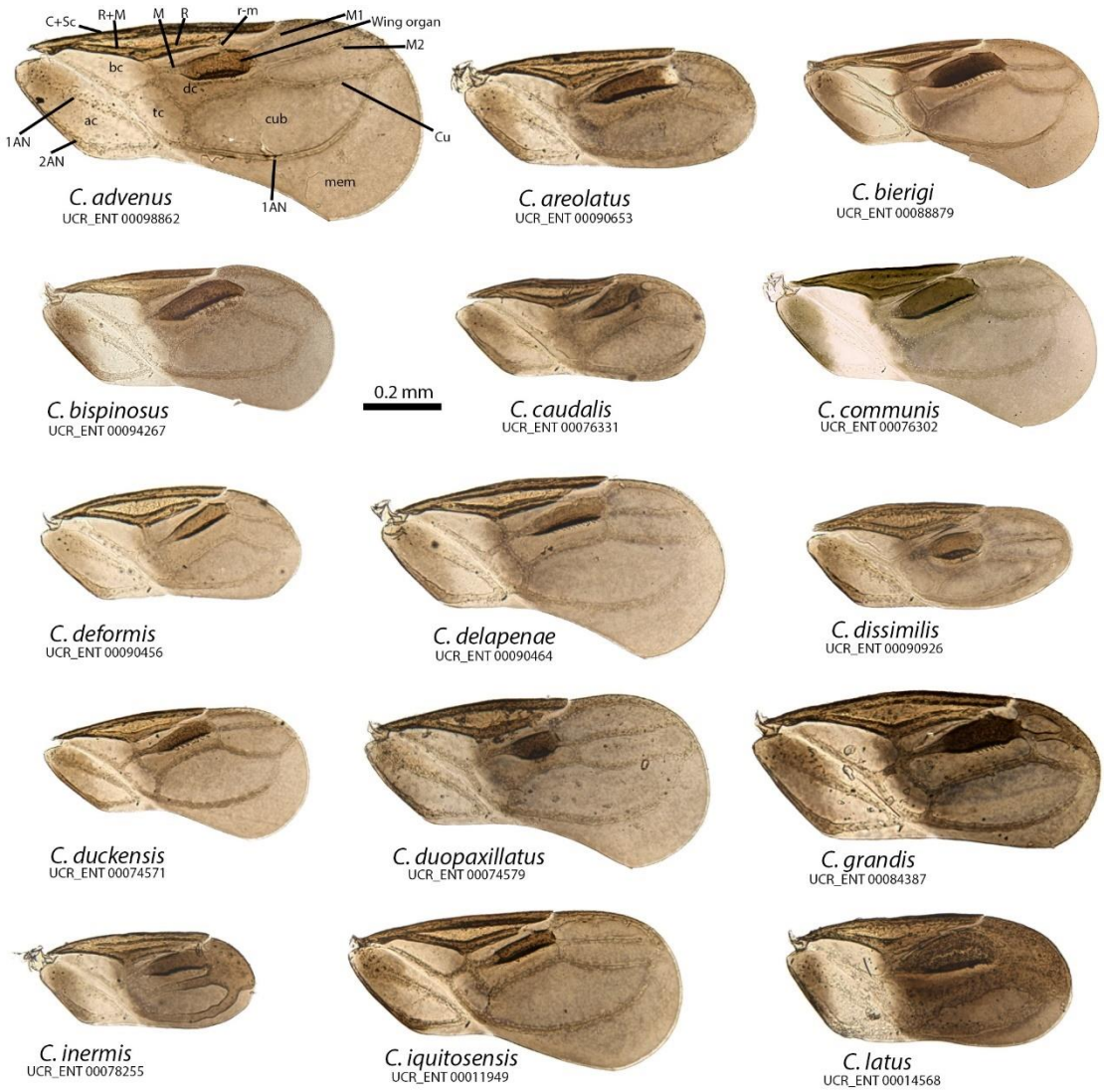

Figure 1.12. Forewings of male *Chinannus*.

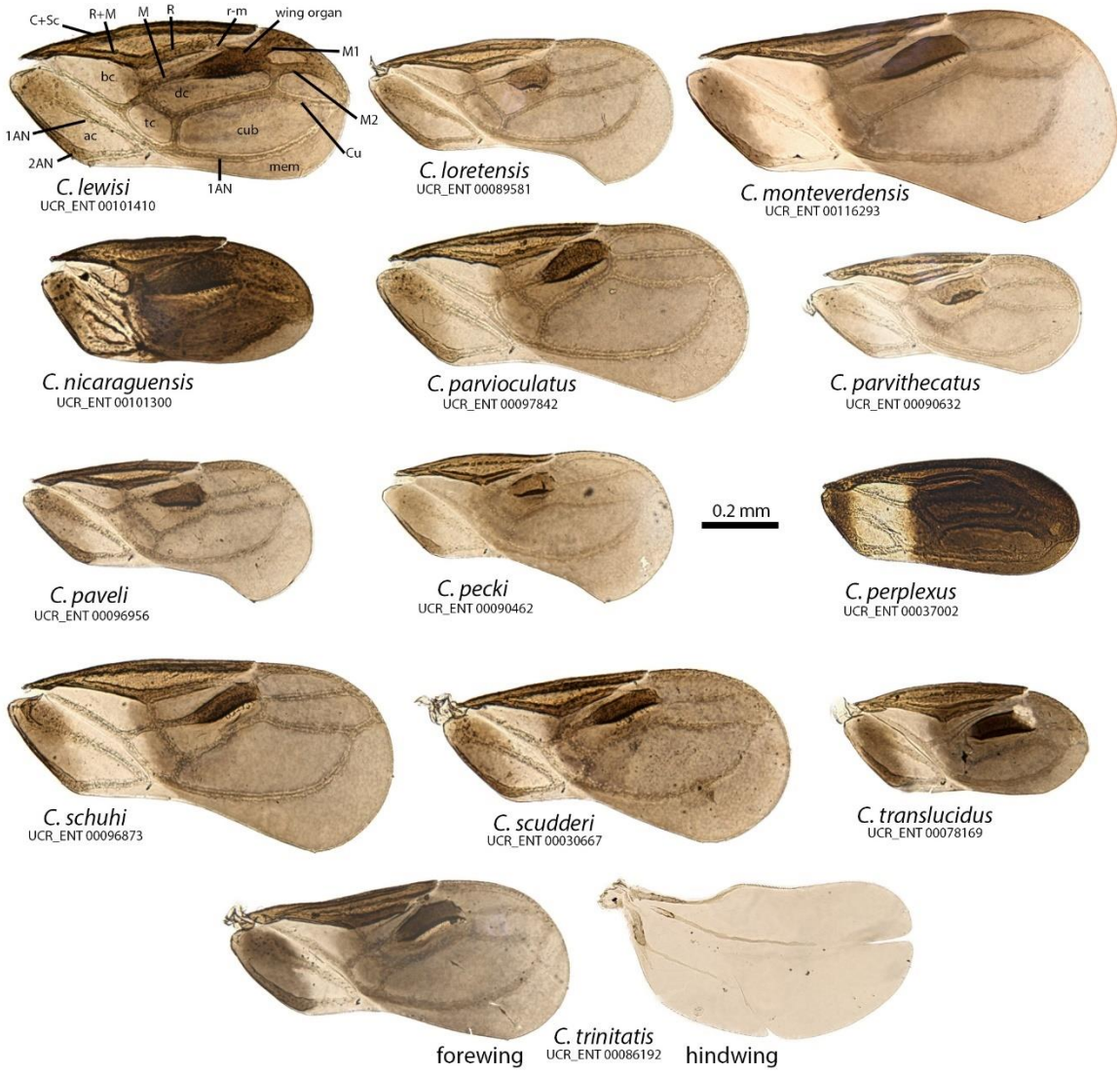

Figure 1.13. Forewings of male *Chinannus* and hindwing of *C. trinitatis*.

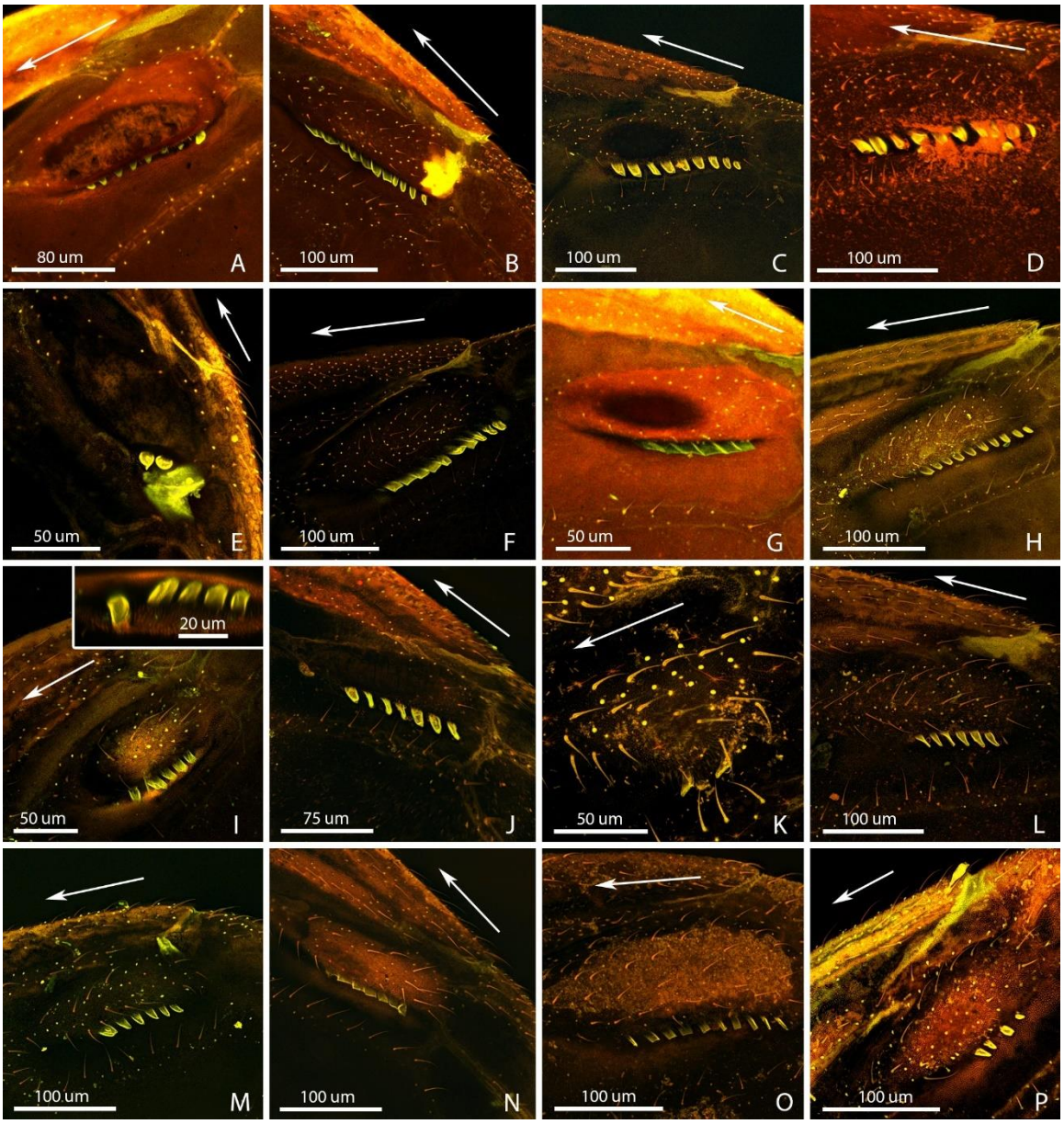

Figure 1.14. Confocal micrographs of male wing organ, arrows point to the base of the wing. (A) *Chinannus advenus*, UCR_ENT 00098862. (B) *Chinannus areolatus*, UCR_ENT 00090653. (C) *Chinannus bierigi*, UCR_ENT 00077038. (D) Chinannus *bispinosus* UCR_ENT 00094267. (E) *Chinannus caudalis*, UCR_ENT 00076331. (F) *Chinannus communis*, UCR_ENT 00076302. (G) *Chinannus deformis*, UCR_ENT 00090456. (H) *Chinannus delapenae*, UCR_ENT 00090464. (I) *Chinannus dissimilis*, UCR_ENT 00090926, with close up of the peg cavity. (J) *Chinannus duckensis*, UCR_ENT 00074571. (K) *Chinannus duopaxillatus*, UCR_ENT 00074579. (L) *Chinannus grandis*, UCR_ENT 00084387. (M) *Chinannus inermis*, UCR_ENT 00078255. (N) *Chinannus iquitosensis*, UCR_ENT 00011949. (O) *Chinannus latus*, UCR_ENT 00014568. (P) *Chinannus lewisi*, UCR_ENT 00101410.

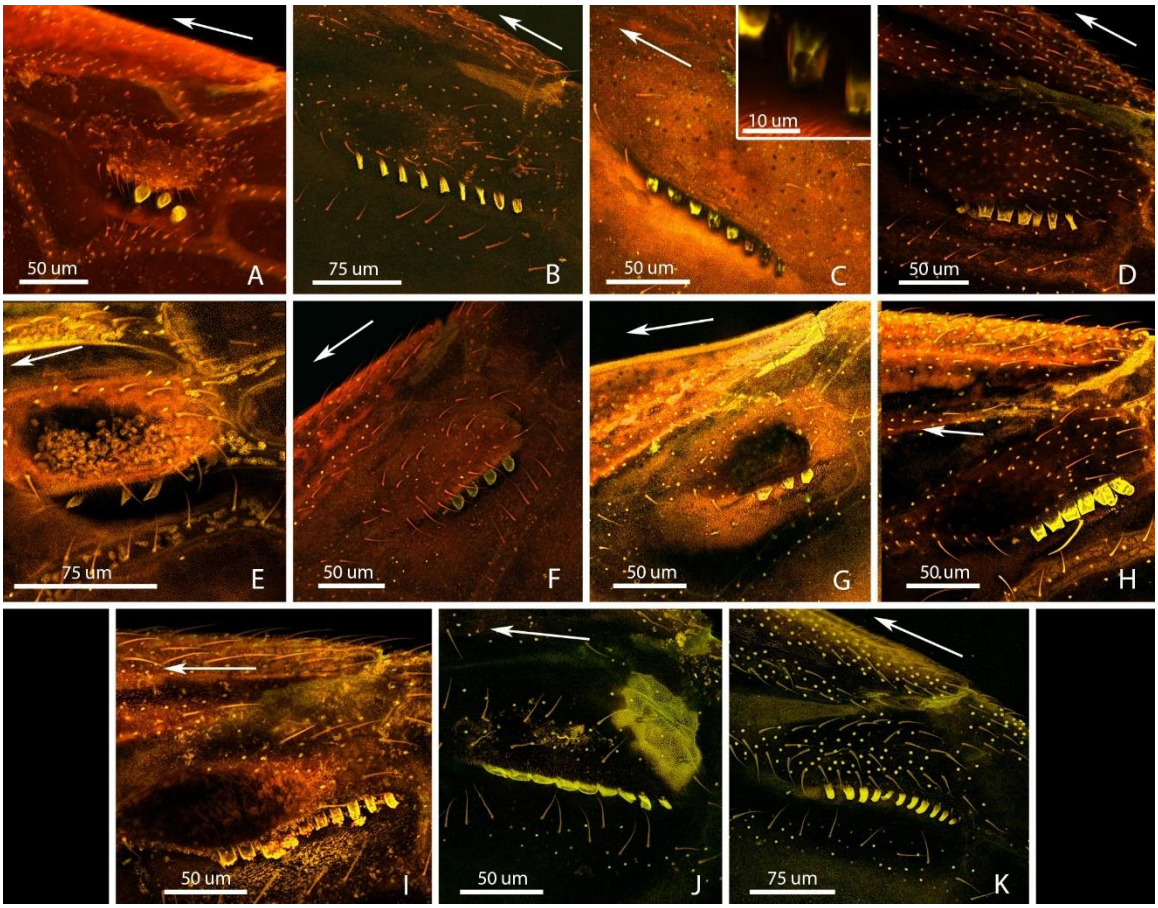

Figure 1.15. Confocal micrographs of male wing organ, arrows point to the base of the wing. (A) *Chinannus loretensis*, UCR_ENT 00089585. (B) *Chinannus monteverdensis*, UCR_ENT 00116293. (C) *Chinannus nicaraguensis*, UCR_ENT 00101300, with close up of a peg. (D) *Chinannus parvioculatus*, UCR_ENT 00097842. (E) *Chinannus parvithecatus*, UCR_ENT 00090632. (F) *Chinannus paveli*, UCR_ENT 00096956. (G) *Chinannus pecki*, UCR_ENT 00090462. (H) *Chinannus schuhi*, UCR_ENT 00096873. (I) *Chinannus scudderi*, UCR_ENT 00030667. (J) *Chinannus translucidus*, UCR_ENT 00078169. (K) *Chinannus trinitatis*, UCR_ENT 00086192.

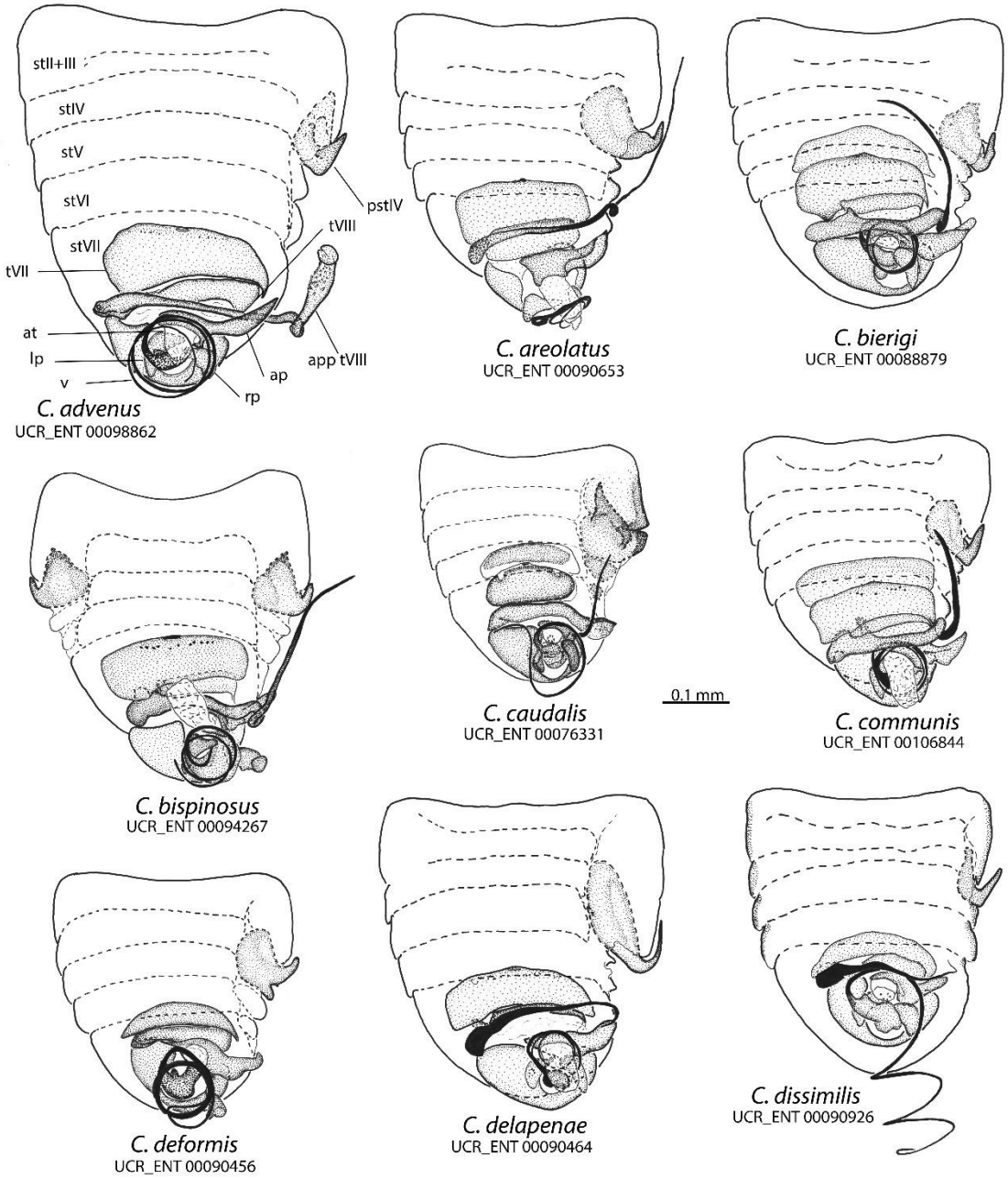

Figure 1.16. Male abdomen of *Chinannus*.

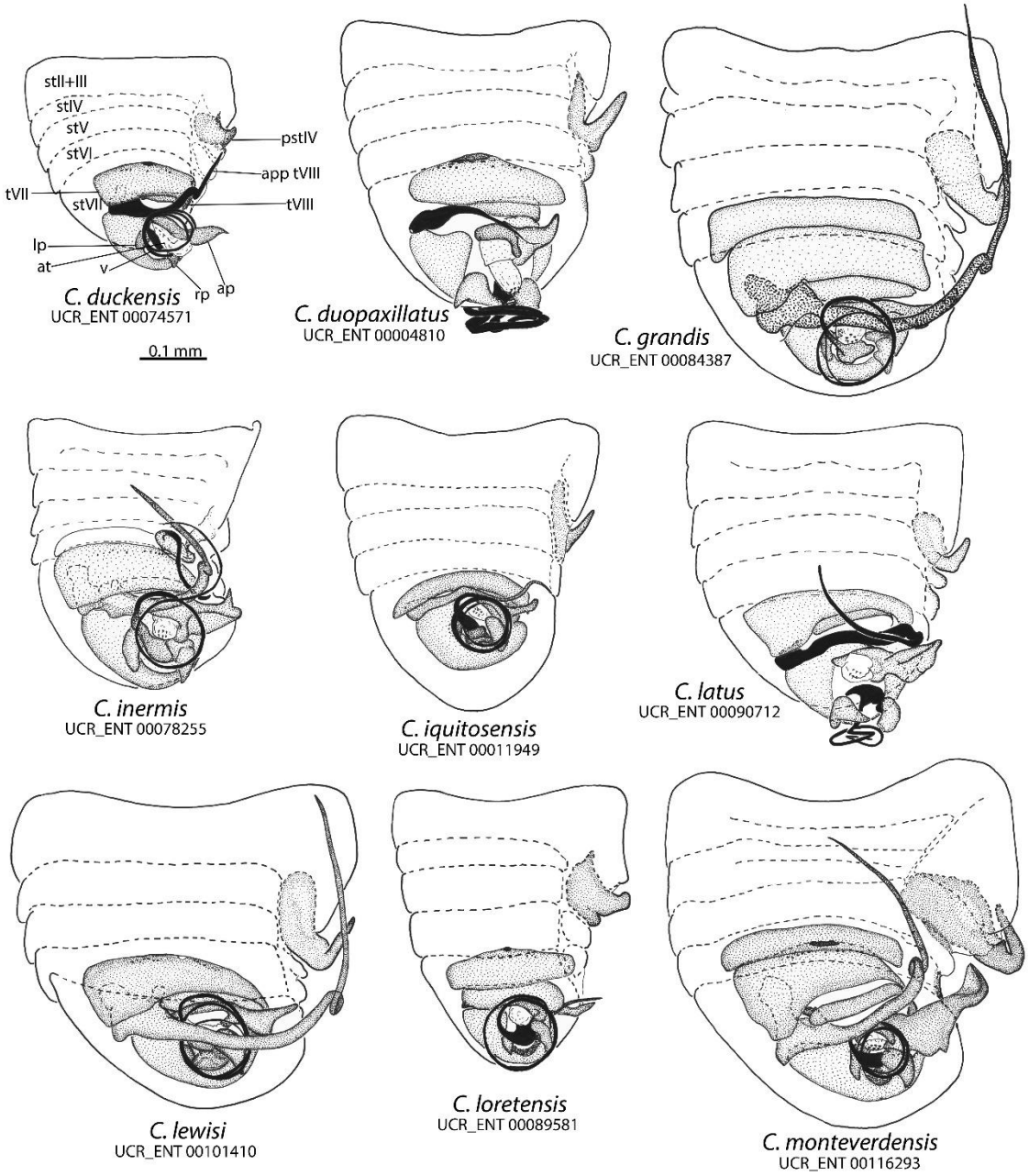

Figure 1.17. Male abdomen of *Chinannus*.

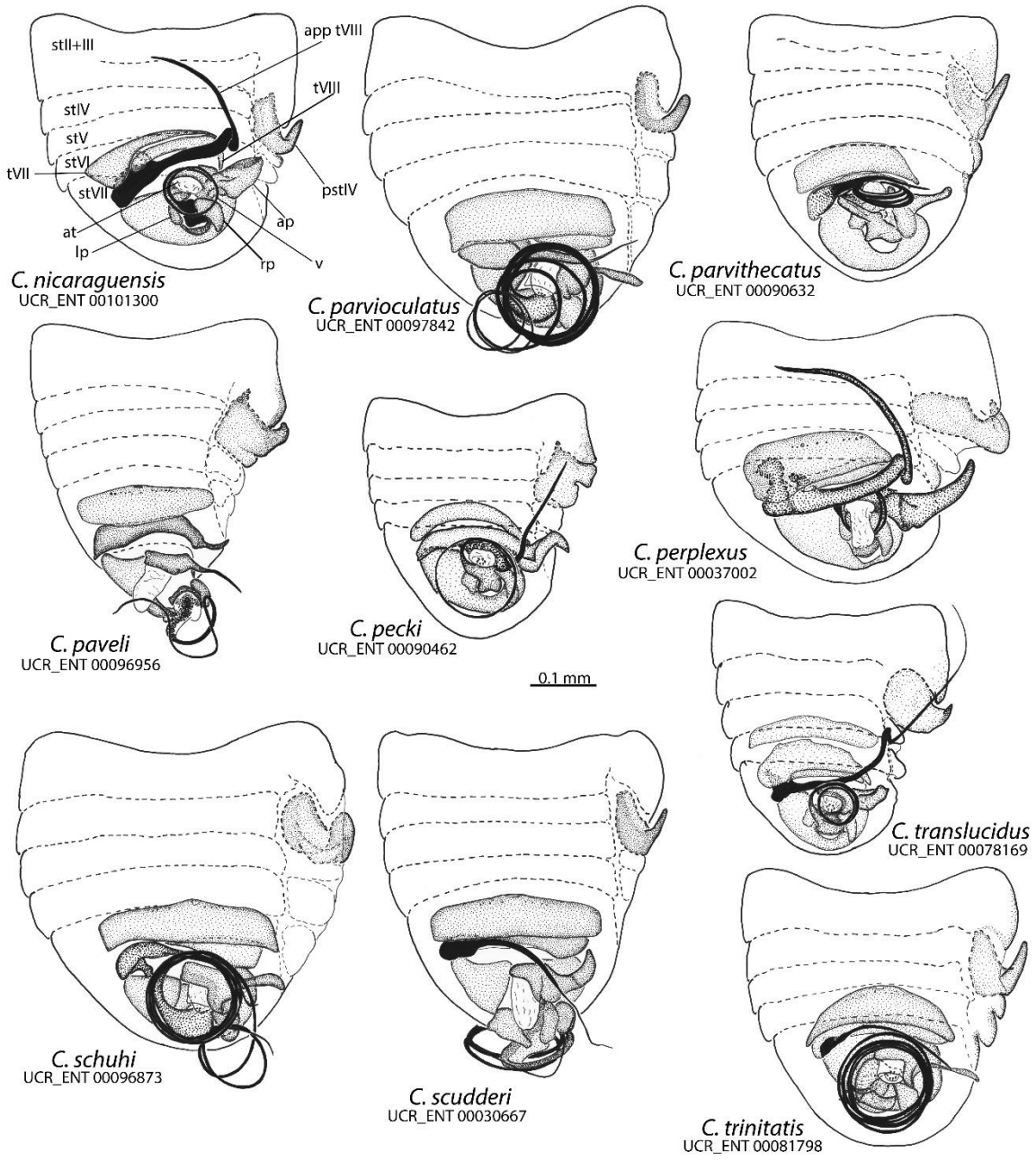

Figure 1.18. Male abdomen of *Chinannus*.

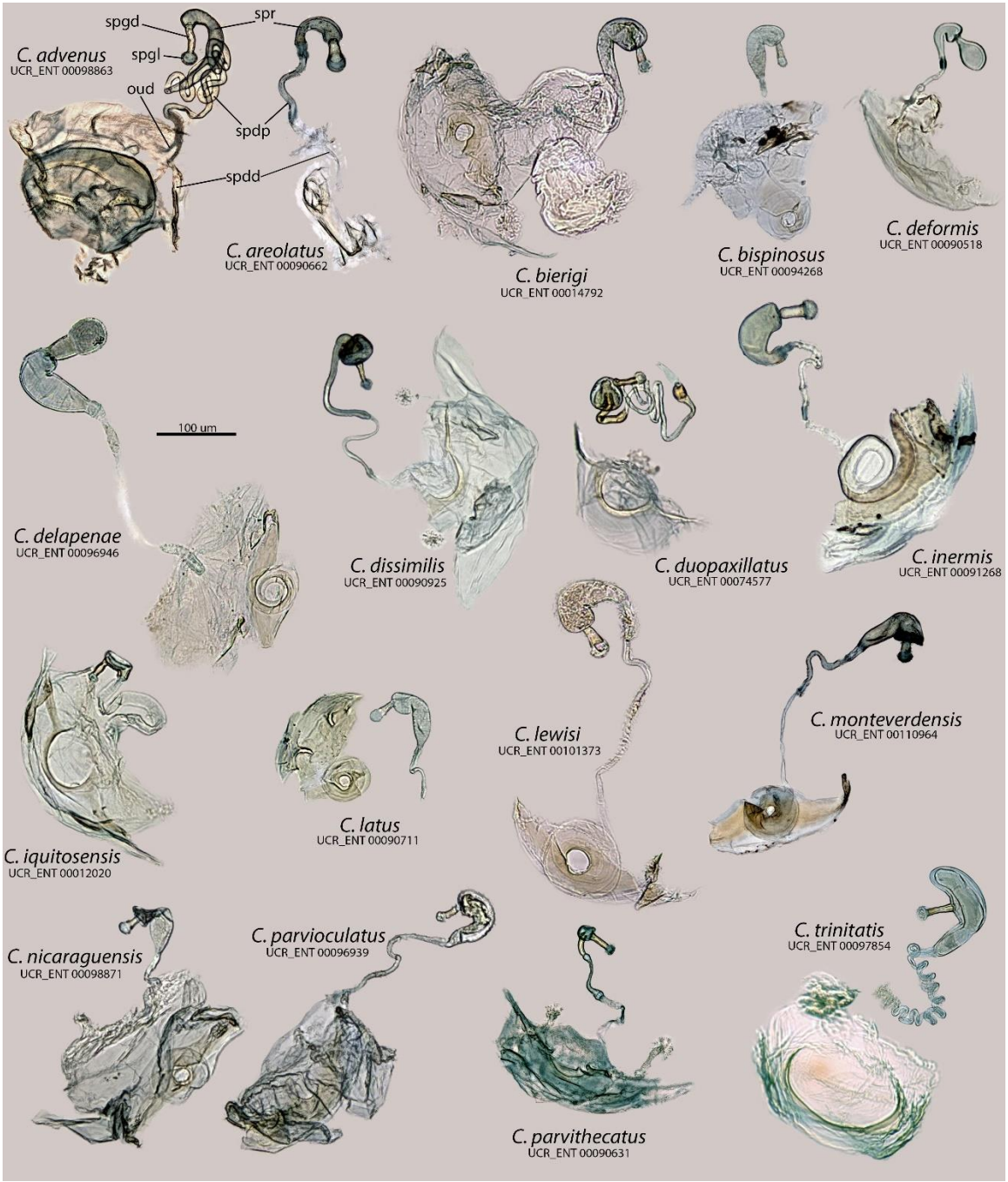

Figure 1.19. Internal female genitalia of *Chinannus*.

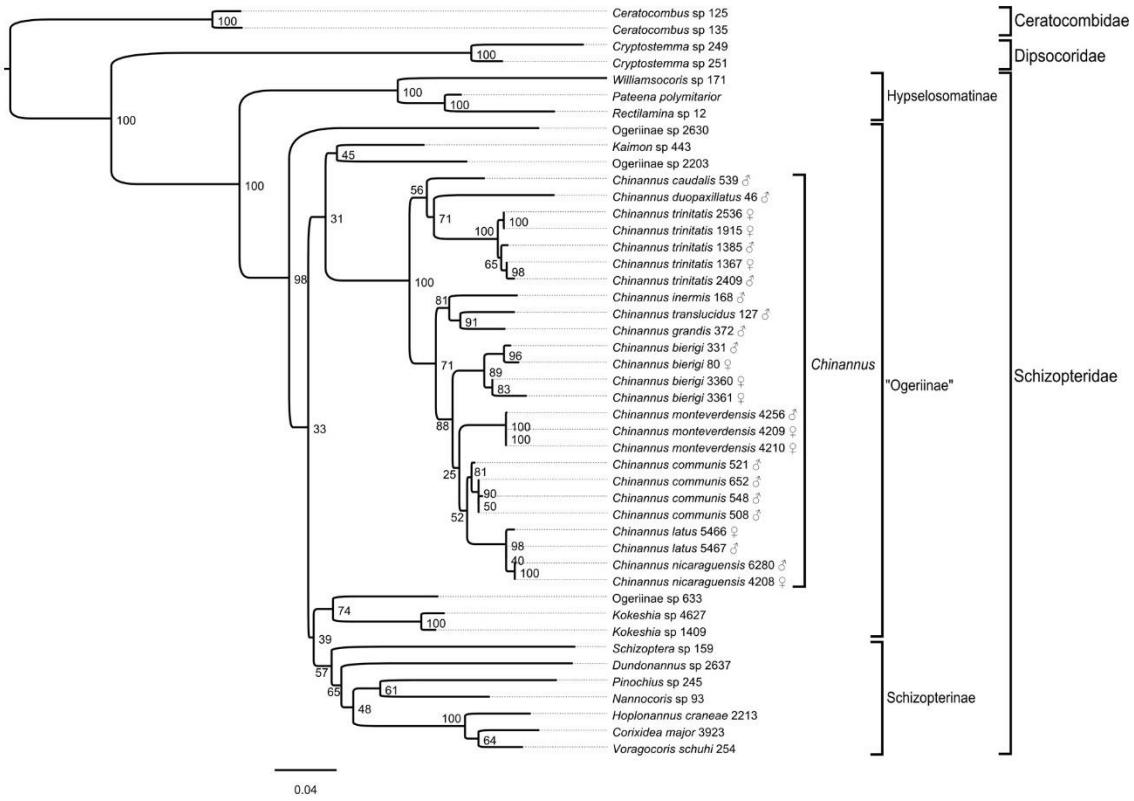

Figure 1.20. Best tree recovered from the RAxML analysis of the E-INS-I alignment of 18S and 28S rDNA and CO1. Numbers at nodes indicate bootstrap support values in per cent.

Chapter 2: Sequence capture using PCR-generated baits: a method for cost-efficient and data-rich phylogenies

Abstract

Gathering genetic data for rare species is one of the biggest remaining obstacles in modern phylogenetics, particularly for megadiverse groups such as arthropods. Next generation sequencing techniques allow for sequencing of short DNA fragments contained in preserved specimens >20 years old, but approaches such as whole genome sequencing are often too expensive for projects including many taxa. Several methods of reduced representation sequencing have been proposed that lower the cost of sequencing per specimen, but many remain costly because they involve synthesizing nucleotide probes and target hundreds of loci. These datasets are also frequently unique for each project and thus generally incompatible with other similar datasets.

Here, we explore utilization of in-house generated DNA baits to capture commonly utilized mitochondrial and ribosomal DNA loci from insect museum specimens of various age and preservation types without the a priori need to know the sequence of the target loci. Both within species and cross-species capture are explored, on preserved specimens ranging in age from one to 54 years old.

We found most samples produced sufficient amounts of data to assemble the nuclear ribosomal rRNA genes and near complete mitochondrial genomes and produce well-resolved phylogenies in line with expected results. The dataset obtained can be straightforwardly combined with the large cache of existing Sanger-sequencing-generated data built up over the past 30 years and targeted loci can be easily modified to those

commonly used in different taxa. Furthermore, the protocol we describe allows for inexpensive data generation (as low as ~$35/sample), of at least 20 kilobases per specimen, for specimens at least as old as ~1965, and can be easily conducted in most laboratories.

If widely applied, this technique will accelerate the accurate resolution of the Tree of Life especially on non-model organisms with limited existing genomic resources.

Introduction

Natural history museums host troves of biological material and sometimes the only known representatives of extinct or rare species (Coddington *et al.* 2009; Lim *et al.* 2011). In these cases, museum specimens represent the only accessible sources of genetic data for a given species and gathering data from such specimens in a cost-effective way is one of the primary obstacles yet to be overcome in modern phylogenetics. Specimens in museums may also allow for the inclusion of a temporal variable into analyses by comparing DNA sequence of individuals across different sampling dates and can even be used for the analysis of short-term evolutionary trends (Hartley *et al.* 2006; DiEuliis *et al.* 2016).

Preservation conditions of museum material can dramatically impact the viability of obtaining DNA sequence data. Traditional approaches used amplification of target regions of DNA followed by Sanger sequencing. This method is highly dependent on residual DNA fragment size and the proportion of endogenous DNA in the extract. While targeting shorter gene regions can mitigate the issue of DNA fragmentation, a low endogenous content is harder to overcome (Burrell *et al.* 2015), and even innovative new

PCR techniques are only capable of somewhat reliably amplifying fragments of less than 600 bp (Mitchell 2015). The development of next generation sequencing (NGS) has expanded the array of methods for DNA sequencing from museum specimens. For whole genome sequencing, an NGS library is prepared from the original DNA extract and this library is then combined with other samples for multiplex sequencing and allocated a certain proportion of reads on a sequencer, depending on desired sequencing depth and the total budget (Cridland *et al.* 2018; Kanda *et al.* 2015; Maddison & Cooper 2014). However, even low-coverage whole genome sequencing is currently still prohibitively expensive for all but very well-funded projects or studies focusing on relatively few samples.

As a way to decrease the cost per sample while still generating sufficient amounts of data for accurate phylogenetic placement, several methods of reduced representation sequencing have been proposed. Typically, these methods include selective hybrid capture of target loci, where the type and number of loci being captured depends on the scope and context of the study. During the past few years, utilization of commercially synthesized probes or microarray kits for the capture of conserved DNA regions has become popular for phylogenetic studies and can be applied to historical museum specimens (Bi *et al.* 2013; Blaimer *et al.* 2016; McCormack *et al.* 2015). These kits are designed based on existing reference genomes or transcriptomes and typically enrich many loci (~500-5000), thus a large amount of data is generated for each sample, but the cost per sample is relatively high. Other kits are designed to enrich mitochondrial genomes, including a kit specifically designed for mitochondrial DNA across insects (Liu

et al. 2016). However, all methods relying on commercially synthesized kits are relatively expensive and might not be feasible for low-budget projects. These kits are also limited by the original design and probe composition cannot be adjusted after synthesis. These limitations led us to explore an approach that uses in-house generated DNA baits for hybrid enrichment (Maricic *et al.* 2010). These baits can be produced from amplicons generated by PCR of short gene regions (Peñalba *et al.* 2014), or by long-range PCR of complete mitochondrial (Li *et al.* 2015; Maricic *et al.* 2010) or chloroplast genomes (Mariac *et al.* 2014), or even from ddRAD library fragments (Suchan *et al.* 2016). PCR-generated baits have so far only been applied to vertebrates and plants, and only in a few cases tested on archival specimens (Li *et al.* 2015). Appealing features of this approach include affordable synthesis of baits, independence from the need of a good quality reference, and flexibility of the synthesis workflow for low-cost modifications of the bait set (e.g., pooling different combinations of bait amplicons, using the same primers to obtain bait amplicons from different taxa, or generating additional baits with new sets of primers).

The diversity of arthropods is staggering, with estimates of about 80% of species still undescribed (Stork 2018) and an increasing number of species going extinct every day (Hallmann *et al.* 2017). While modern phylogenetic studies of vertebrates sometimes approach complete sampling of extant diversity, complete extant sampling of any large clade of arthropods is almost impossible due to the abundance of rare species, limited material, and the huge diversity of arthropods (Coddington *et al.* 2009; Lim *et al.* 2011). However, near-complete sampling is useful for many downstream analyses, including

unbiased estimation of lineage diversification rates (Cusimano & Renner 2010; Cusimano *et al.* 2012; Höhna *et al.* 2011). Scientists have just started to employ NGS to utilize the enormous resources of arthropod specimens deposited in natural history collections for gathering large DNA datasets (Stork *et al.* 2015; Stork 2018). We argue that insects in particular are an apt test case for the application of new NGS approaches to illuminating the dark areas in the Tree of Life, because most material in entomological collections is stored as dried and pinned or point-mounted specimens, which are often suitable for the retrieval of fragmented DNA. Previous applications of this approach on vertebrate and plant samples employed destructive extraction protocols to generate adequate amounts of DNA for capture. But DNA extraction can be performed without destroying external or genitalic morphological features and from individual and small specimens as in many insects. For a complete taxonomic sampling of large clades, already existing data should be compatible with character-rich new datasets generated at low costs.

Here, we test the efficiency of PCR-generated DNA baits (targeting the mitochondrial genome, nuclear ribosomal operon, and one nuclear protein-coding gene) to capture DNA sequences from museum-deposited insect specimens with different collection dates, preservation methods, and varying evolutionary relatedness, using phyline plant bugs (Insecta: Hemiptera: Miridae: Phylinae) as our test case. These loci were selected for optimal integration with existing, Sanger-based sequence data and to allow adequate coverage when multiplexing hundreds of libraries. Plant bugs are a group of >11,000 described species that include serious plant pests and beneficial insects (Cassis & Schuh 2012). Phylogenetic hypotheses for the entire group are in their infancy (Jung & Lee

2011), but studies targeting selected subfamilies including the Phylinae now provide testable hypotheses (Konstantinov & Knyshov 2015; Menard *et al.* 2014; Namyatova *et al.* 2015; Tatarnic & Cassis 2012). The taxonomic diversity of plant bugs in the Western U.S. is fairly well understood (Cassis & Schuh 2012; Weirauch *et al.* 2016), but few species have been incorporated into phylogenetic analyses, and some are only known from the type specimen(s). As the first test case, we selected a putatively monophyletic group of native oak-associated plant bugs, the so called "Orange Oak Bugs" (OOB) (Weirauch 2006a, 2006b), where some species may be monophagous on specific species of oaks, while at least two widespread and polymorphic species, *Phallospinophylus setosus* Weirauch and *Pygovepres vaccinicola* (Knight), feed on a variety of host plants (including Fagaceae, Rhamnaceae, and Rosaceae). We sampled specimens of these two species from a range of localities and host plants, together with several additional species of OOB that had not yet been included in phylogenetic analyses (Menard *et al.* 2014) to test the efficacy of capture across closely related samples and to investigate potential cryptic host plant races. As a second test case, we selected the genus *Tuxedo* Schuh with seven described species associated with host plants in several families (Schuh 2004); phylogenetic relationships within this genus are unknown. We aimed to sample several individuals from each of the seven species, including paratype specimens, to investigate capture efficiency at deeper phylogenetic levels and to explore host plant shifts within the genus. Both datasets were analyzed together with a Sanger-derived phylogenetic dataset of Phylinae (Menard *et al.* 2014), demonstrating the feasibility of combining existing and newly generated NGS data.

Material and methods

Taxon Sampling and Vouchering

See supplemental text S1 for details.

DNA Extraction

In most cases, only the abdomen (1-1.5 mm in length) was used for non-destructive DNA extraction, which was performed using a Qiagen DNeasy® Blood & Tissue kit (for relatively fresh ethanol specimens) or a combination of the previous kit with a Qiagen QIAquick® PCR purification kit (for dry specimens, see supplemental text S1), since the latter is commonly used for DNA extraction from degraded samples (Lee *et al.* 2010; Yang *et al.* 1998). Abdomens were soaked in the extraction buffer, such that cuticular structures remain undamaged, and mirrored standard genitalic dissection procedures for plant bug specimens. This approach allows for subsequent remounting of the abdominal cuticle and genitalia with the rest of the specimen, or in a genitalic vial.

General capture workflow

Bait Synthesis

The protocol was modified from Li *et al.* (2015). DNA extracts from freshly collected insects (bait donors) was subjected to several long range PCRs. We used Takara PrimeSTAR® GXL polymerase, a hot-start high-fidelity enzyme that is able to amplify long products. The PCR mix contained 10 µl PrimeSTAR® GXL buffer, 4 µl 2.5M dNTPs, 1 µl PrimeSTAR® GXL polymerase, 32 µl water, 1.5 µl of each primer (10 µM), and 1 µl of DNA template. The thermocycler program included initial denaturation at 98° for 3 min, 35 cycles of denaturation for 10 sec at 98°, followed by annealing at variable

temperatures for 15 sec, followed by elongation at 68° for a variable amount time, and with the final incubation at 68° for 15 min. Primer sequences and additional details on long-range PCR conditions are available in Table S2. Details on the primer design are available in supplemental text S1.

Here and elsewhere in this project we utilized custom Solid Phase Reversible Immobilization (SPRI) beads (Glenn *et al.* 2016; Rohland & Reich 2012) in the clean-up stages of the protocol. Long range PCR products were cleaned up and mixed, mixtures were diluted to the volume of 100 µl and sonicated on a Diagenode Bioruptor® UCD-200 with 30/30 cycles for 6 runs of 5 minutes. Sheared PCR products were end-repaired using a mix containing 2 µl 10× Tango buffer, 0.08 µl 25mM dNTPs, 0.2 µl 100mM ATP, 1 µl T4 PNK, and 0.4 µl T4 DNA polymerase. Samples were incubated at 25° for 15 min, at 12° for 5 min, and then cleaned up using SPRI beads. M13 adaptors were ligated to end-repaired fragments using a mixture containing 1 µl T4 DNA ligase, 4 µl 10× T4 DNA ligase buffer, 4 µl 50% PEG-4000, 2 µl 50µM M13 adaptor mix. The ligation reaction was carried at 22° for 30 min, after which a SPRI clean-up was performed. Then we conducted a fill-in reaction using a mixture containing 4 µl 10× ThermoPol buffer, 0.4 µl 25mM dNTPs, 1.5 µl Bst polymerase, large fragment. The reaction was carried at 37° for 20 min, followed by a SPRI clean up. We concluded the bait synthesis by simultaneously amplifying and biotinylating M13-adaptor-ligated bait libraries using the following master mix: 10 µl PrimeSTAR® GXL buffer, 4 µl 2.5M dNTPs, 1 µl PrimeSTAR® GXL polymerase, 32 µl water, 1.5 µl of each 5’ biotinylated M13 primer (10 µM), and 6 µl of template. The reaction was carried out in a thermocycler with the following settings:

initial denaturation at 98° for 3 min, ~18-30 cycles of denaturation for 10 sec at 98°, followed by annealing at 55° for 15 sec, followed by elongation at 68° for 30 sec, and with the final incubation at 68° for 15 min. Sequences for M13 adaptors and primers are given in Li *et al.* (2015), and these oligonucleotides and all others were ordered from Integrated DNA Technologies (IDT).

Target library preparation

We prepared Illumina®-compatible target libraries using a modified version of the protocol from Li *et al.* (2013). DNA extracts were run on a gel with Biotium GelRed® premixed loading buffer in ratios 1:2 to check average fragment size and determine if sonication was needed (i.e., for younger samples). These DNA extracts were quantified using Qubit™ fluorometer, and for more consistent sonication results approximately 70 ng of DNA (where possible, also see Table S1) were used for sonication. We modified end prep mix recipe to include *taq* polymerase that allowed to A-tail fragments and accommodate ligation of NEBNext® adaptors with T-overhang. The mix contained 2 µl 10× Tango buffer, 0.08 µl 25mM dNTPs, 0.2 µl 100mM ATP, 1 µl T4 PNK, 0.4 µl T4 DNA polymerase, and 10 µl 2× Takara EmeraldAmp® GT PCR mix, and samples were incubated at 25° for 15 min, at 12° for 5 min, and at 72° for 20 min. After end prep the reactions were cleaned up with SPRI beads, and we utilized a "with-bead" SPRI method as originally described in Fisher *et al.* (2011), carrying same SPRI beads through the library preparation steps. T-tailed loop adaptors from NEBNext® Multiplex Oligos for Illumina® kit E7600s were ligated to the DNA using a ligation mix consisting of 1 µl T4 DNA ligase, 4 µl 10× T4 DNA ligase buffer, 4 µl 50% PEG-4000, and 2.5 µl 15µM

NEBNext® adaptor. Ligation was carried at 22° for 30 min, followed by addition of 1.5 µl of NEBNext® USER enzyme, incubation at 37° for 15 min, and a SPRI clean up. The library preparation was concluded with a PCR using short IS7/IS8 primers (individual capture workflow, see Experiment 1 section) or indexing primers from the same NEBNext® kit (pooled capture workflow, see Experiment 2 section). PCR reaction contained 10 µl PrimeSTAR® GXL buffer, 4 µl 2.5M dNTPs, 1 µl PrimeSTAR® GXL polymerase, 32 µl water, 1.5 µl of each primer (10 µM), and 6 µl of template. PCR conditions were as follows: initial denaturation at 98° for 3 min, ~16-21 cycles (depending on the amount of starting material) of denaturation for 10 sec at 98°, followed by annealing at 60° for 15 sec, followed by elongation at 68° for 30 sec, and with the final incubation at 68° for 15 min. Sequences for IS7/IS8 primers are given in Meyer and Kircher (2010).

Target capture

Target captures were performed either individually for each sample (the protocol of Li *et al.* [2015]), or for a pool of samples (the protocol of Maricic *et al.* [2010]). The bait library was premixed with 2× BWT buffer and blocking oligos, denatured, and bound to Invitrogen Dynabeads® M-270 beads as in Li *et al.* (2015). Target libraries were premixed with blocking oligos, denatured at 95° for 5 min, cooled to 65°, mixed with the bait, and incubated for ~36 hours. We used only two blocking oligos as in Li *et al.* (2015) for the individual capture workflow, and eight blocking oligos as in Maricic *et al.* (2010) for the pooled capture workflow to block longer adaptor fragments. After incubation the mixture was carried through a series of washes using BWT, HW, and TET buffers (see Li

et al. (2015) for the details on wash protocol and contents of the buffers). Elution was conducted by incubating the beads with washed captured sample in 125mM NaOH (Maricic *et al.* 2010). We resubmitted the eluted captured libraries for a second round of hybridization repeating the above outlined workflow as suggested by Peñalba *et al.* (2014). After the second round of capture, the supernatant was cleaned up with SPRI beads and eluted in 50 µl of 10 mM Tris-HCl. Post-capture PCR followed the same PCR procedure as outlined above for preparation of target libraries, but either NEBNext® indexing primers (for individual capture protocol) or IS5/IS6 primers (for pooled capture protocol) were used, 20 µl of template were added, and variable number of cycles was performed (16-24). Sequences for IS5/IS6 primers are given in Meyer and Kircher (2010).

Amplified enriched libraries were cleaned and normalized with Just-a-Plate™ 96 PCR Purification and Normalization Kit. Subsequently libraries were run on a gel with GelRed® to check average fragment size, pooled together into several groups according to their size, which were then analyzed on a single Bioanalyzer chip to obtain more accurate fragment size distribution. Bioanalyzer results were used for final pooling.

Experiment 1 (individual capture experiment)

The bait DNA was produced from *Phallospinophylus setosus* sample ph32 and *Tuxedo drakei* Schuh sample ph47 for the OOB and *Tuxedo* subprojects, respectively. Target regions included the mitochondrial genome, nuclear ribosomal operon, and a fragment of the cytoplasmic dynein heavy chain gene. Baits were mixed in 1:1:5 molar proportion to increase dynein bait contents. Target libraries in the OOB subproject were prepared from

34 samples belonging to species in 10 genera, with majority of specimens being closely related to the bait donor, with the average CO1 pairwise distance to bait being 7.32% (ranging from 0% to 22.03%), age ranging from 1 to 40 years, with 14 specimens being dry point-mounted and 20 being ethanol-preserved (see Table S1). Target libraries in the *Tuxedo* subproject were prepared from 24 samples belonging to 11 species from four genera, with the majority of specimens being distantly related to the bait donor, with average CO1 pairwise distance to bait being 18.5% (ranging from 0.66% to 20.78%), age ranging from 1 to 54 years, with 15 specimens being dry point-mounted and nine being ethanol-preserved. Prior to enrichment the libraries were amplified using short IS7/IS8 primers without indexing. Target captures were conducted individually for each sample, 10 ng (most commonly) or 25 ng (only for samples ph29-ph31, ph33-ph35, ph55-ph60) of bait and 10 µl of Invitrogen Dynabeads® M-270 per reaction were used for each round of capture. DNA concentration of input target library was not quantified, and we used 6 µl of target library in each capture reaction. Indexing was done during the post-capture PCR. Samples have been sequenced on ~50% of Illumina® MiSeq® V3 2x300bp lane at the UCR IIGB Core Facility.

Experiment 2 (pooled capture experiment)

Only the *Tuxedo* subproject was used for this experiment. The bait was produced from *Tuxedo drakei* sample ph47. Target regions included the mitochondrial genome and nuclear ribosomal operon and all bait regions were mixed equimolarly. Target libraries were prepared from five samples belonging to four species from two genera, with average CO1 pairwise distance to probe 19.28% (ranging from 17.6% to 20.4%), age ranging

from 8 to 54 years, with four specimens being dry and one being ethanol-preserved. Prior to the enrichment libraries were amplified using NEBNext® indexing primers. An equimolar pool of five indexed libraries constituting about 450 ng of DNA was subjected to two rounds of capture. Approximately 500 ng of bait and 5 µl of Dynabeads® were used for each round. The post-capture PCR was done with IS5/IS6 to amplify already indexed captured libraries and was carried over in two aliquots, which were subsequently mixed. Samples were sequenced on ~5% of an Illumina® MiSeq® V3 2x300bp lane at the UCR IIGB Core Facility.

Unenriched target library sequencing

For six samples (three from each subproject) we sequenced unenriched libraries to assess the percent of reads on target. Briefly, the same adaptor-ligated fragments used to produce libraries for enrichment were subjected to indexing PCR with NEBNext® indexing primers, purified, and pooled for sequencing. Samples were sequenced on ~1% of an Illumina® HiSeq® X lane through NGXBio.

Bait Sample Sequencing

Since the DNA sequence of bait donors was of interest in this project, we also sequenced amplicons used for bait production. These LR PCR products were mixed in equimolar ratios and sonicated. Following sonication, end prep and adaptor ligation steps were performed as outlined in target library preparation section. Illumina®-compatible libraries were finalized in a PCR with NEBNext® indexing primers using PCR conditions outlined above. These bait amplicon libraries were sequenced on ~3% of an Illumina® MiSeq® V3 2x300bp lane at the UCR IIGB Core Facility.

Post-Sequencing Data Processing

Raw sequences were demultiplexed and adaptors were removed using bcl2fastq software (Illumina®) at the UCR IIGB Core Facility. Trimmomatic v0.36 (Bolger *et al.* 2014) was used to trim off low quality ends of the sequences as well as perform more thorough adaptor trimming. Reads were assembled into contigs with SPAdes (Bankevich *et al.* 2012). In cases where assembly did not yield complete target regions, we obtained them by mapping shorter contigs onto full length assemblies of other related samples. Assembled contigs were checked for misassembled regions and manually curated in Geneious v.10 (https://www.geneious.com, Kearse *et al.* 2012). We mapped reads on these contigs using BWA (Li & Durbin 2009) to assess the coverage depth (see Table S1), prior to average coverage calculations, reads were deduplicated using PRINSEQ (Schmieder & Edwards 2011).

To assess differences between enriched and unenriched samples, we mapped reads from both types of samples to contigs derived from enriched samples. The percentage of reads aligning to non-target regions was checked using histone 2A and histone 3 fragments, which are commonly sequenced for mirids. We used reference sequences available on GenBank to retrieve contigs from SPAdes assemblies, and then mapped reads of both enriched and unenriched samples onto these contigs (see Table S6).

We aligned all resulting 18S, 28S, and mitochondrial contigs using MAFFT v.7 (Katoh & Standley 2013) and manually inspected and trimmed alignments. Since accurate assembly of the mitochondrial control region with short reads without a close reference was problematic due to presence of repeats, we excluded it from the analysis. The

remainder of the mitochondrion was annotated by aligning it with the mitochondrial genome of a plant bug available on GenBank (NC_024641.1). We used a linear model to test the relationship between capture efficiency and distance to probe, and various statistical tests were used to assess the difference in capture efficiency between preservation methods, subprojects, experiments, and bait amount, as well as the difference between enriched and unenriched libraries. Statistical analyses were conducted in R v3.4.3.

Phylogenetic Analysis

See supplemental text S1 for details.

Results and Discussion

Expenses

Total expenses after bait and target library preparations, target capture, and sequencing and including all reagents and supplies came to about $54 per specimen or about $2.8 per 1 Kb of data in the first experiment, and about $39 per specimen or about $2.1 per 1 Kb of data in the second experiment (Table S3). Our estimates suggest that pooled capture together with using a higher throughput sequencer (e.g., a HiSeq® lane or a NextSeq® run) can generate the same amount of data for about half the price (up to $25 per specimen), however a greater number of samples (at least 360) need to be pooled together to efficiently utilize the sequencer. Our upper bound price of $54 per sample includes sequencing costs and is cheaper than the capture only costs of ~$68 per sample listed in Peñalba *et al.* (2014) who used a similar approach, although enriching for more targets. Both estimates are several times cheaper than phylogenomic scale target enrichment

solutions, or low coverage whole genome sequencing. Although recent studies did not provide detailed cost estimates, Blaimer *et al.* (2016) used on average 1,278,680 reads per sample and McCormack *et al.* (2015) 1,966,099, which is 7 to 11 times more than our average read allocation (166,971) per sample, and would result in increased cost per sample. Additionally, commercial probe kits ($3,000-$6,000) increase initial expenses and cost per sample as well ($210-$380 estimates in Peñalba *et al.* (2014), not including sequencing), although the metagenomic approach of Liu *et al.* (2016) for mitochondrial capture allows for extended usage of a single kit over many hundreds of specimens.

DNA extraction

The amount of DNA extracted greatly varied across samples (see Table S1). The minimum amount of DNA that was used for library preparation was 2.75 ng (sample 42), the average was 50 ng. This is vastly lower than the >1 µg in Maricic *et al.* (2010) and Peñalba *et al.* (2014), and could have impacted the capture results. The average fragment size for ethanol preserved material was large: we always detected a bright band larger than 10 Kb in size, with many extracts also with a smear of fragments spanning down to 300 bp. For dry point-mounted material we observed two types of fragmentation: extracts that had fragments of 500-700 bp on average in addition to long (~8Kb) fragments (dry specimens collected within past ten years), and extracts with only fragments shorter than 1000 bp (dry specimens collected more than ten years ago).

Sequencing and assembly

A total of 45% of an Illumina® MiSeq® V3 lane was used for the samples in the first experiment. The amount of reads obtained per sample is listed in Table S1 (average of

152,670, σ = 39,070). For bait samples, we obtained full bait contigs for the nuclear ribosomal operon, the dynein fragment, and the entire mitochondrial genome, although unambiguous assembly of the control region was problematic due to the lack of a close reference taxon and long read data. For other samples, we obtained full or partial mitochondrial contigs and nuclear ribosomal gene contigs for the majority of samples (see Table S1). Mitochondrial completeness is indicated on Fig. 2.2B and excludes the control region, and mitochondrial average coverage depth is indicated in Fig. 2.2C. We were able to obtain reliable ribosomal data for 48 taxa, but some sequences exhibited cross contamination of about 1% of reads by the bait taxon as detailed in supplemental text S1. In the second experiment, we observed a significantly higher percent of ribosomal operon reads on target (see capture efficiency section below) and both for recaptured libraries, as well as for the library prepared after the first experiment was complete (ph61), we have not detected contaminating reads. In both experiments, the amount of reads allocated and retrieved from the sequencer was considerably lower than ~400,000 reads per sample in Maricic *et al.* (2010) and 4,868,847 reads per sample in Li *et al.* (2015). This however did not have an adverse effect on coverage breadth of recovered target regions (Fig. 2.2B).

Capture efficiency

The percentage of reads on target varied from 0.61% to 33.95% and was on average 8.19% in the OOB subproject and 4.02% in *Tuxedo* subproject. The total percent of reads on target was significantly larger for samples that are close to bait specimens (p-value 0.000185, Figs 2.2A, 2.2E, Fig. 2.S4, Table 2.S5). However, only the percentage of reads

mapping to dynein significantly decreases with distance to bait (p-value 2.25e-08, Table 2.S5). The relationship between percent of reads mapping to the mitochondrial genome and the distance to bait was negative, but not significant, possibly due to the variation in total amount of target DNA submitted to capture reactions (equal volumes of target libraries were used in all reactions). The capture of dynein in the *Tuxedo* subproject performed worse (p-value 1e-06, Table 2.S5), which could be attributed to the higher average sequence divergence from the bait (Fig. 2.2D). Overall the average percent on target in the current study was comparable to ~16% in Maricic *et al.* (2010), but was considerably lower than ~50% in Li *et al.* (2015).

We also compared the percentage of on-target reads for some of the same specimens sequenced with and without enrichment and found a significant increase in enrichment (p-value 0.01563, see also Table 2.S5), ranging from 3 to 72 fold increase depending on the sample and target region, on average of 9.36 fold including all target regions or 15 fold with dynein results excluded (see below). However, the percentage of reads aligning to non-targeted regions (histone 2A and histone 3) was about the same or slightly less (Table 2.S6), suggesting that the libraries were otherwise comparable in quality.

Baits for a nuclear protein-coding gene (dynein) performed unsatisfactorily, even though they were five times more concentrated. Although we do not have a clear explanation as to why this bait performed suboptimally (see supplemental text 2.S1), the large middle intron may have been detrimental for bait efficacy. While the percentage of reads mapping to dynein is increased in captured samples compared to control samples (on

average 7.63 fold increase, p-value 0.01563), the increase is mostly attributed to reads mapping to the middle intron region, with exons being still insufficiently covered.

The average enrichment in the first experiment for ribosomal and mitochondrial regions compared to control specimens was ~15 fold (ranging from 2.68 to 56.75 fold), which we consider substantial given that ribosomal and mitochondrial baits constituted only 2/7 of the entire bait pool. Specifically, mitochondrial baits were only 14.3% of total bait pool, yet were able to enrich mitochondrial DNA 15 fold on average compared to controls. Some sequencing of non-enriched DNA libraries from insect museum specimens yielded from 0.002% to 0.08% of total reads mapping to the mitochondrial genome (Staats *et al.* 2013), although several metagenomic studies revealed a higher percentage of mitochondrial reads from 0.5% to 1.4% (Crampton-Platt *et al.* 2015; Tang *et al.* 2014). In our control samples the average percent of reads aligning to mitochondrion was 0.37%. While on the lower side, this value might be impacted by sample quality, for instance amount of starting DNA material, which was low in our case.

Suboptimal capture performance in our first experiment could be also attributed to the amount of bait. Overall, we observed a significant increase (p-value 0.00163) in the amount of reads on target in capture reactions where more bait was used (Table 2.S1, samples ph29-ph31, ph33-ph35, and ph55-ph60).

The second experiment tested five selected samples captured with a modified protocol where the amount of bait was increased, no dynein bait was used, and a more high throughput and less expensive pooled capture approach was used. As a result, we observed significantly higher percentage of reads on-target in this experiment (p-value

0.006003, see Table 2.S5) compared with the same samples in the first experiment. The average difference in capture efficiency between the first and second experiments was 5.23% (see Table 2.S1). We also noticed a larger variation of total amount of reads received for a given sample in the pool. This might be due to unequal divergence of samples in the pool with respect to the bait or difference in library quality due to the age of the specimens. Because of this, we recommend balancing sample pools prior to capture and performing individual captures for sensitive samples. Further adjustments of hybridization temperature and duration may further improve capture success, however these conditions may need to be modified on an individual basis.

Our results show no difference in capture efficiency as related to the age of the specimen (Fig. 2.2, specimens older than 20 years denoted with red asterisks) (p-values > 0.05, see Table 2.S6). We thus expect that even older specimens can be used (Blaimer *et al.* 2016), but for this pilot study the youngest available specimens were chosen. Similarly, we found no significant difference between dry and ethanol preserved samples as far as reads mapping to the target was concerned (p-values > 0.05, see Table 2.S6). The success rate in obtaining full sequences of the target region in this project is promising, as phylines are among the smallest mirids, are fragile soft-bodied insects, and are frequently killed using agents such as cyanide and ethyl acetate which are suboptimal for DNA preservation (http://research.amnh.org/pbi/description/collecting.html). Given these results, we speculate that other small soft-bodied insects may be successfully sequenced using such techniques. In contrast, large and/or hard-bodied insects such as many beetles may have different DNA degradation dynamics, because, e.g., abdominal tissue might

dry at a slower rate, thus increasing DNA degradation. Extractions from leg musculature, as was done for example in Blaimer *et al.* (2016), may be more appropriate for such specimens.

Phylogenetic analyses

Using the obtained data, we reconstructed a well-resolved phylogeny. Our phylogenetic analysis supports the monophyly of *Tuxedo* + *Pseudophylus*, the OOB clade, *Phallospinophylus setosus* and *Pygovepres vaccinicola* with the highest branch support (Fig. 2.2A, Fig. 2.S2). Our analysis did not find support for our hypothesis on the presence of host plant races within each of the widespread and polyphagous OOB species (Fig. 3). In contrast, the phylogenetic structure in *Phallospinophylus setosus* is more likely explained by geographic proximity between sampled localities.

Combined with the existing data of Menard *et al.* (2014), phylogenetic hypotheses inferred from our dataset are congruent with those presented in prior studies (Fig. 2.4, Fig. 2.S3). Deep level relationships within Oncotylina as well as the monophyly of the subtribe itself remain poorly supported based on this data set. As in Menard *et al.* (2014), "*Tuxedo"* + *Pseudophylus* are recovered as the sister group to Leucophoropterini, although with low support. Sampled species of Leucophoropterini were recovered in expected phylogenetic positions.

Conclusions

In conclusion, we were able to cost-efficiently ($2.8/sample/Kb) sequence long-range PCR products as well as perform hybrid enrichment using in-house generated baits and obtain DNA sequences (~20 Kb) from archival specimens (up to 54 years old) using a

minimal amount of DNA. This approach offers a much lower cost of bait production than other approaches, however, especially if LR PCR is chosen for amplicon generation, a high-quality sample of a related species is needed. While it is hard to scale up this method to produce baits for 500 targets, it is well suited to generate commonly used high-copy gene sequences for both archival and recently collected samples. It fits within a narrow 'Goldilocks' zone in terms of adequate data for accurately reconstructing phylogenies and relative cost effectiveness with the ability to multiplex at least ~120 individuals per MiSeq® run given the number of loci captured.

Finally, it is straightforward to combine such data with previously generated data using conventional Sanger sequencing. Commonly used primers for different genes for use in phylogenetic analysis of other groups are easy to add to our protocol. When applied to museum specimens, this approach is optimal for generating complete phylogenetic sampling for clades of interest and relatively cheaply contributing confidently resolved twigs to the Tree of Life.

References

Bankevich, A., Nurk, S., Antipov, D., Gurevich, A. A., Dvorkin, M., Kulikov, A. S., Lesin, V. M., Nikolenko, S. I., Pham, S., Prjibelski, A. D., Pyshkin, A. V., Sirotkin, A. V., Vyahhi, N., Tesler, G., Alekseyev, M. A. & Pevzner P. A. (2012) SPAdes: a new genome assembly algorithm and its applications to single-cell sequencing. *Journal of Computational Biology* 19(5), 455-477.

Bi, K., Linderoth, T., Vanderpool, D., Good, J. M., Nielsen, R. & Moritz, C. (2013) Unlocking the vault: next-generation museum population genomics. *Molecular Ecology* 22(24), 6018-6032.

Blaimer, B. B., Lloyd, M. W., Guillory, W. X. & Brady, S. G. (2016) Sequence capture and phylogenetic utility of genomic ultraconserved elements obtained from pinned insect specimens. *PloS One* 11(8), e0161531.

Bolger, A. M., Lohse, M. & Usadel, B. (2014) Trimmomatic: a flexible trimmer for Illumina sequence data. *Bioinformatics* 30(15), 2114-2120.

Burrell, A. S., Disotell, T. R. & Bergey, C. M. (2015) The use of museum specimens with high-throughput DNA sequencers. *Journal of Human Evolution* 79, 35-44.

Cassis, G. & Schuh, R. T. (2012) Systematics, biodiversity, biogeography, and host associations of the Miridae (Insecta: Hemiptera: Heteroptera: Cimicomorpha). *Annual Review of Entomology* 57, 377-404.

Coddington, J. A., Agnarsson, I., Miller, J. A., Kuntner, M. & Hormiga, G. (2009) Undersampling bias: the null hypothesis for singleton species in tropical arthropod surveys. *Journal of Animal Ecology* 78(3), 573-584.

Crampton-Platt, A., Timmermans, M. J., Gimmel, M. L., Kutty, S. N., Cockerill, T. D., Vun Khen, C. & Vogler, A. P. (2015) Soup to tree: the phylogeny of beetles inferred by mitochondrial metagenomics of a Bornean rainforest sample. *Molecular Biology and Evolution* 32(9), 2302-2316.

Cridland, J. M., Ramirez, S. R., Dean, C. A., Sciligo, A. & Tsutsui, N. D. (2018) Genome sequencing of museum specimens reveals rapid changes in the genetic composition of honey bees in California. *Genome Biology and Evolution* 10(2), 458-472.

Cusimano, N. & Renner, S. S. (2010) Slowdowns in diversification rates from real phylogenies may not be real. *Systematic Biology 59*(4), 458-464.

Cusimano, N., Stadler, T. & Renner, S. S. (2012) A new method for handling missing species in diversification analysis applicable to randomly or nonrandomly sampled phylogenies. *Systematic Biology* 61(5), 785-792.

DiEuliis, D., Johnson, K. R., Morse, S. S. & Schindel, D. E. (2016) Opinion: Specimen collections should have a much bigger role in infectious disease research and response. *Proceedings of the National Academy of Sciences* 113(1), 4-7.

Fisher, S., Barry, A., Abreu, J., Minie, B., Nolan, J., Delorey, T. M., Young, G., Fennell, T. J., Allen, A., Ambrogio, L., Berlin, A. M., Blumenstiel, B., Cibulskis, K., Friedrich, D., Johnson, R., Juhn, F., Reilly, B., Shammas, R., Stalker, J., Sykes, S. M., Thompson, J., Walsh, J., Zimmer, A., Zwirko, Z., Gabriel, S., Nicol, R. & Berlin, A. M. (2011) A scalable, fully automated process for construction of sequence-ready human exome targeted capture libraries. *Genome Biology* 12(1), R1.

Glenn, T. C., Nilsen, R., Kieran, T. J., Finger, J. W., Pierson, T. W., Bentley, K. E., Hoffberg, S., Louha, S., Garcia-De-Leon, F. J., Portilla, M. A. R., Reed, K., Anderson, J. L., Meece, J. K., Aggery, S., Rekaya, R., Alabady, M., Belanger, M., Winker, K. & Faircloth, B. C. (2016) Adapterama I: universal stubs and primers for thousands of dual-indexed Illumina libraries (iTru & iNext). *BioRxiv*, 049114.

Hallmann, C. A., Sorg, M., Jongejans, E., Siepel, H., Hofland, N., Schwan, H., Stenmans, W., Müller, A., Sumser, H., Hörren, T., Goulson, D. & de Kroon, H. (2017) More than 75 percent decline over 27 years in total flying insect biomass in protected areas. PloS One 12(10), e0185809.

Hartley, C. J., Newcomb, R. D., Russell, R. J., Yong, C. G., Stevens, J. R., Yeates, D. K., La Salle, J. & Oakeshott, J. G. (2006) Amplification of DNA from preserved specimens shows blowflies were preadapted for the rapid evolution of insecticide resistance. *Proceedings of the National Academy of Sciences* 103(23), 8757-8762.

Höhna, S., Stadler, T., Ronquist, F. & Britton, T. (2011) Inferring speciation and extinction rates under different sampling schemes. *Molecular Biology and Evolution* 28(9), 2577-2589.

Jung, S. & Lee, S. (2011) Molecular phylogeny of the plant bugs (Heteroptera: Miridae) and the evolution of feeding habits. *Cladistics* 28(1), 50-79.

Kanda, K., Pflug, J. M., Sproul, J. S., Dasenko, M. A. & Maddison, D. R. (2015) Successful recovery of nuclear protein-coding genes from small insects in museums using Illumina sequencing. *PLoS One* 10(12), e0143929.

Katoh, K. & Standley, D. M. (2013) MAFFT multiple sequence alignment software version 7: improvements in performance and usability. *Molecular Biology and Evolution* 30(4), 772-780.

Kearse, M., Moir, R., Wilson, A., Stones-Havas, S., Cheung, M., Sturrock, S., Buxton, S., Cooper, A., Markowitz, S., Duran, C., Thierer, T., Ashton, B., Meintjes, P. & Drummond A. (2012) Geneious Basic: an integrated and extendable desktop software platform for the organization and analysis of sequence data. *Bioinformatics* 28(12), 1647-1649.

Konstantinov, F. V. & Knyshov, A. A. (2015) The tribe Bryocorini (Insecta: Heteroptera: Miridae: Bryocorinae): phylogeny, description of a new genus, and adaptive radiation on ferns. *Zoological Journal of the Linnean Society* 175(3), 441-472.

Lee, H. Y., Park, M. J., Kim, N. Y., Sim, J. E., Yang, W. I. & Shin, K. J. (2010) Simple and highly effective DNA extraction methods from old skeletal remains using silica columns. *Forensic Science International: Genetics* 4(5), 275-280.

Li, C., Corrigan, S., Yang, L., Straube, N., Harris, M., Hofreiter, M., White, W. T. & Naylor, G. J. (2015) DNA capture reveals transoceanic gene flow in endangered river sharks. *Proceedings of the National Academy of Sciences* 112(43), 13302-13307.

Li, C., Hofreiter, M., Straube, N., Corrigan, S. & Naylor, G. J. (2013) Capturing protein-coding genes across highly divergent species. *Biotechniques* 54(6), 321-326.

Li, H. & Durbin, R. (2009) Fast and accurate short read alignment with Burrows–Wheeler transform. *Bioinformatics* 25(14), 1754-1760.

Lim, G. S., Balke, M. & Meier, R. (2011) Determining species boundaries in a world full of rarity: singletons, species delimitation methods. *Systematic Biology* 61(1), 165-169.

Liu, S., Wang, X., Xie, L., Tan, M., Li, Z., Su, X., Zhang, H., Misof, B., Kjer, K. M., Tang, M., Niehuis, O., Jiang, H. & Zhou, X. (2016) Mitochondrial capture enriches mito-DNA 100 fold, enabling PCR-free mitogenomics biodiversity analysis. *Molecular Ecology Resources* 16(2), 470-479.

Maddison, D. R. & Cooper, K. W. (2014) Species delimitation in the ground beetle subgenus *Liocosmius* (Coleoptera: Carabidae: Bembidion), including standard and next-generation sequencing of museum specimens. *Zoological Journal of the Linnean Society* 172(4), 741-770.

Mariac, C., Scarcelli, N., Pouzadou, J., Barnaud, A., Billot, C., Faye, A., Kougbeadjo, A., Maillol, V., Martin, G., Sabot, F., Santoni, S., Vigouroux, Y. & Couvreur, T. L. P. (2014) Cost-effective enrichment hybridization capture of chloroplast genomes at deep

multiplexing levels for population genetics and phylogeography studies. *Molecular Ecology Resources* 14(6), 1103-1113.

Maricic, T., Whitten, M. & Pääbo, S. (2010) Multiplexed DNA sequence capture of mitochondrial genomes using PCR products. *PloS One* 5(11), e14004.

McCormack, J. E., Tsai, W. L. & Faircloth, B. C. (2015) Sequence capture of ultraconserved elements from bird museum specimens. *Molecular Ecology Resources* 16(5), 1189-1203.

Menard, K. L., Schuh, R. T. & Woolley, J. B. (2014) Total-evidence phylogenetic analysis and reclassification of the Phylinae (Insecta: Heteroptera: Miridae), with the recognition of new tribes and subtribes and a redefinition of Phylini. *Cladistics* 30(4), 391-427.

Meyer, M. & Kircher, M. (2010) Illumina sequencing library preparation for highly multiplexed target capture and sequencing. *Cold Spring Harbor Protocols* 2010(6), pdb-prot5448.

Mitchell, A. (2015) Collecting in collections: a PCR strategy and primer set for DNA barcoding of decades-old dried museum specimens. *Molecular Ecology Resources* 15(5), 1102-1111.

Namyatova, A. A., Konstantinov, F. V. & Cassis, G. (2015) Phylogeny and systematics of the subfamily Bryocorinae with the emphasis on the tribe Dicyphini sensu Schuh, 1976 derived from morphological characters. *Systematic Entomology* 41, 3-40.

Peñalba, J. V., Smith, L. L., Tonione, M. A., Sass, C., Hykin, S. M., Skipwith, P. L., McGuire, J. A., Bowie, R. C. K. & Moritz, C. (2014) Sequence capture using PCR-generated probes: a cost-effective method of targeted high-throughput sequencing for nonmodel organisms. *Molecular Ecology Resources* 14(5), 1000-1010.

Rohland, N. & Reich, D. (2012) Cost-effective, high-throughput DNA sequencing libraries for multiplexed target capture. *Genome Research* 22(5), 939-946.

Schmieder, R. & Edwards, R. (2011) Quality control and preprocessing of metagenomic datasets. *Bioinformatics* 27(6), 863-864.

Schuh, R. T. (2004). Revision of *Tuxedo* Schuh (Hemiptera: Miridae: Phylinae). *American Museum Novitates* 3435, 1-26.

Staats, M., Erkens, R. H., van de Vossenberg, B., Wieringa, J. J., Kraaijeveld, K., Stielow, B., Geml, J., Richardson, J. E. & Bakker, F. T. (2013) Genomic treasure troves:

complete genome sequencing of herbarium and insect museum specimens. *PLoS One* 8(7), e69189.

Stork, N. E. (2018) How Many Species of Insects and Other Terrestrial Arthropods Are There on Earth? *Annual Review of Entomology* 63.

Stork, N. E., McBroom, J., Gely, C. & Hamilton, A. J. (2015) New approaches narrow global species estimates for beetles, insects, and terrestrial arthropods. *Proceedings of the National Academy of Sciences* 112(24), 7519-7523.

Suchan, T., Pitteloud, C., Gerasimova, N. S., Kostikova, A., Schmid, S., Arrigo, N., Pajkovic, M., Ronikier, M. & Alvarez, N. (2016) Hybridization capture using RAD probes (hyRAD), a new tool for performing genomic analyses on collection specimens. *PloS One*, 11(3), e0151651.

Tang, M., Tan, M., Meng, G., Yang, S., Su, X., Liu, S., Song, W., Li, Y., Wu, Q., Zhang, A. & Zhou, X. (2014) Multiplex sequencing of pooled mitochondrial genomes—a crucial step toward biodiversity analysis using mito-metagenomics. *Nucleic Acids Research* 42(22), e166-e166.

Tatarnic, N. J. & Cassis, G. (2012) The Halticini of the world (Insecta: Heteroptera: Miridae: Orthotylinae): generic reclassification, phylogeny, and host plant associations. *Zoological Journal of the Linnean Society* 164(3), 558-658.

Weirauch, C. (2006a) New genera, new species, and new combinations in western Nearctic Phylini (Heteroptera: Miridae: Phylinae). *American Museum Novitates* 3521, 1-41.

Weirauch, C. (2006b). New genera and species of oak-associated Phylini (Heteroptera: Miridae: Phylinae) from western North America. *American Museum Novitates* 3522, 1-54.

Weirauch, C., Seltmann, K. C., Schuh, R. T., Schwartz, M. D., Johnson, C., Feist, M. A. & Soltis, P. S. (2016) Areas of endemism in the Nearctic: a case study of 1339 species of Miridae (Insecta: Hemiptera) and their plant hosts. *Cladistics* 33(3), 279-294.

Yang, D. Y., Eng, B., Waye, J. S., Dudar, J. C. & Saunders, S. R. (1998) Improved DNA extraction from ancient bones using silica-based spin columns. *American journal of physical anthropology* 105(4), 539-543.

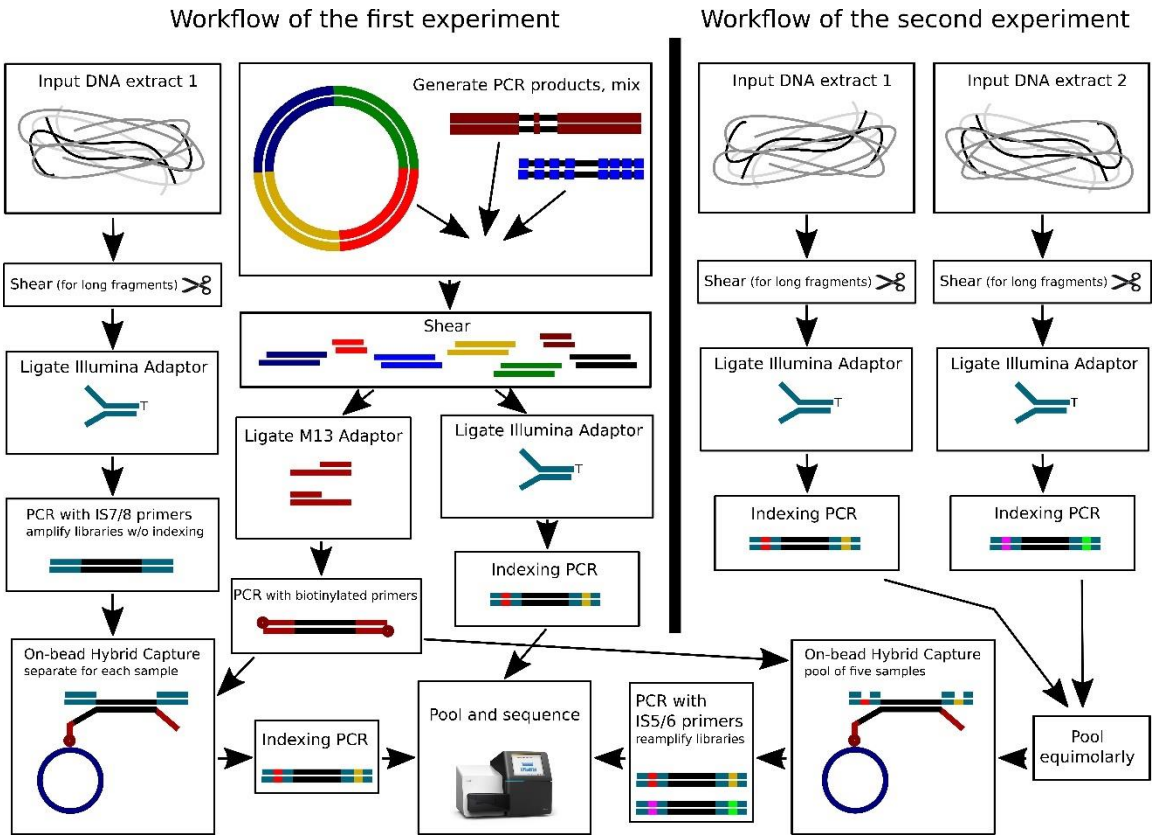

Figure 2.1. Procedure flowchart.

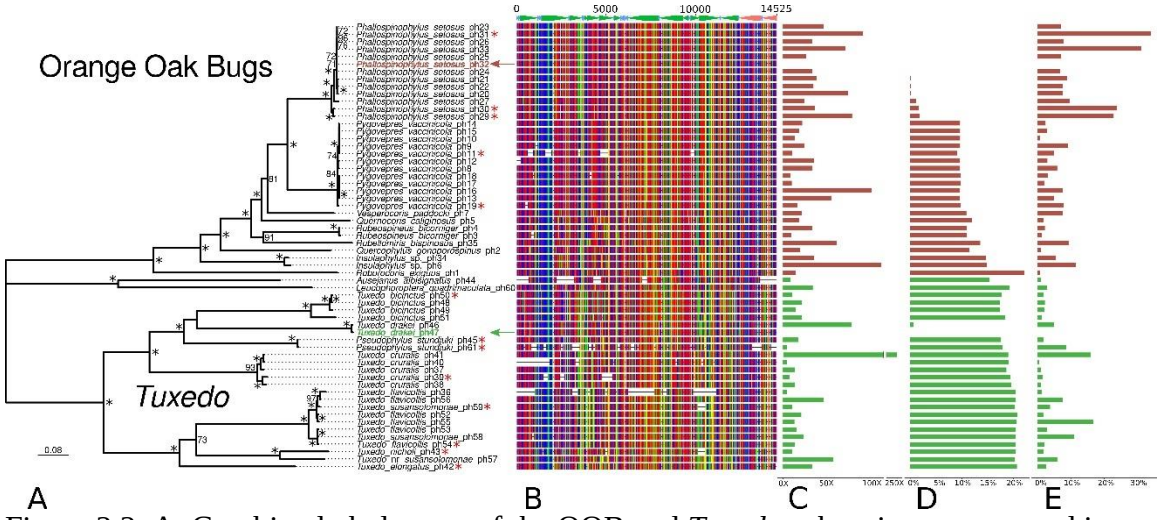

Figure 2.2. A. Combined phylogeny of the OOB and *Tuxedo* subprojects, generated in RAxML, values at nodes represent Rapid Bootstrap Support, values below 70 are not shown, asterisks indicate full support, arrows denote bait samples for the OOB (red) and *Tuxedo* (green) subprojects, red asterisks denote samples older than 20 years. B. Mitochondrial alignment completeness, control region excluded. C. Average coverage of mitochondrial contig(s), control region excluded. D. Pairwise COX1 distances between a bait and a captured sample. E. Total percent of reads mapping to target including mitochondrial genome, 18S, 28S, and dynein.

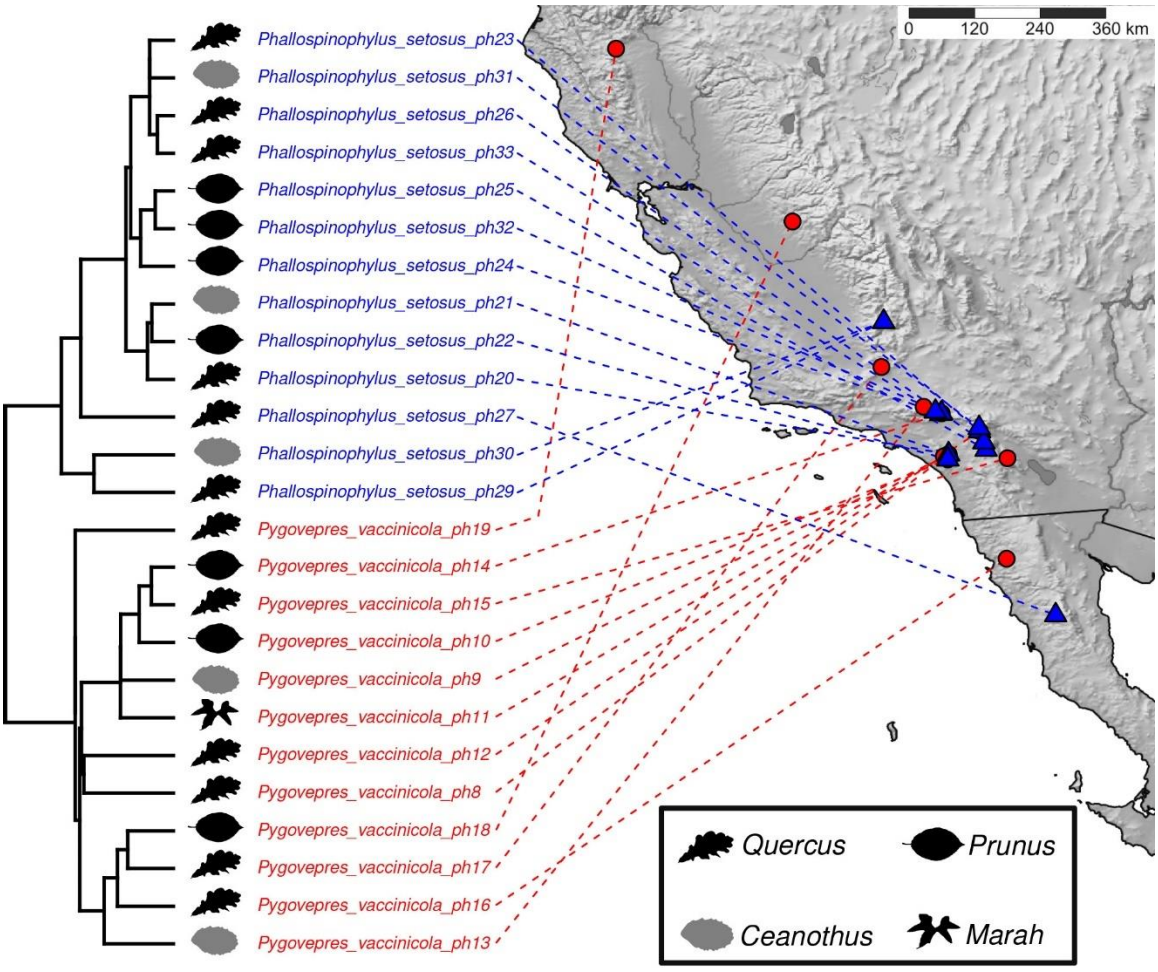

Figure 2.3. Host and distribution data for the Orange Oak Bug subproject, aligned with phylogeny (branches not to scale) and with host plant of specimens mapped using representative leaf shapes of plant genus.

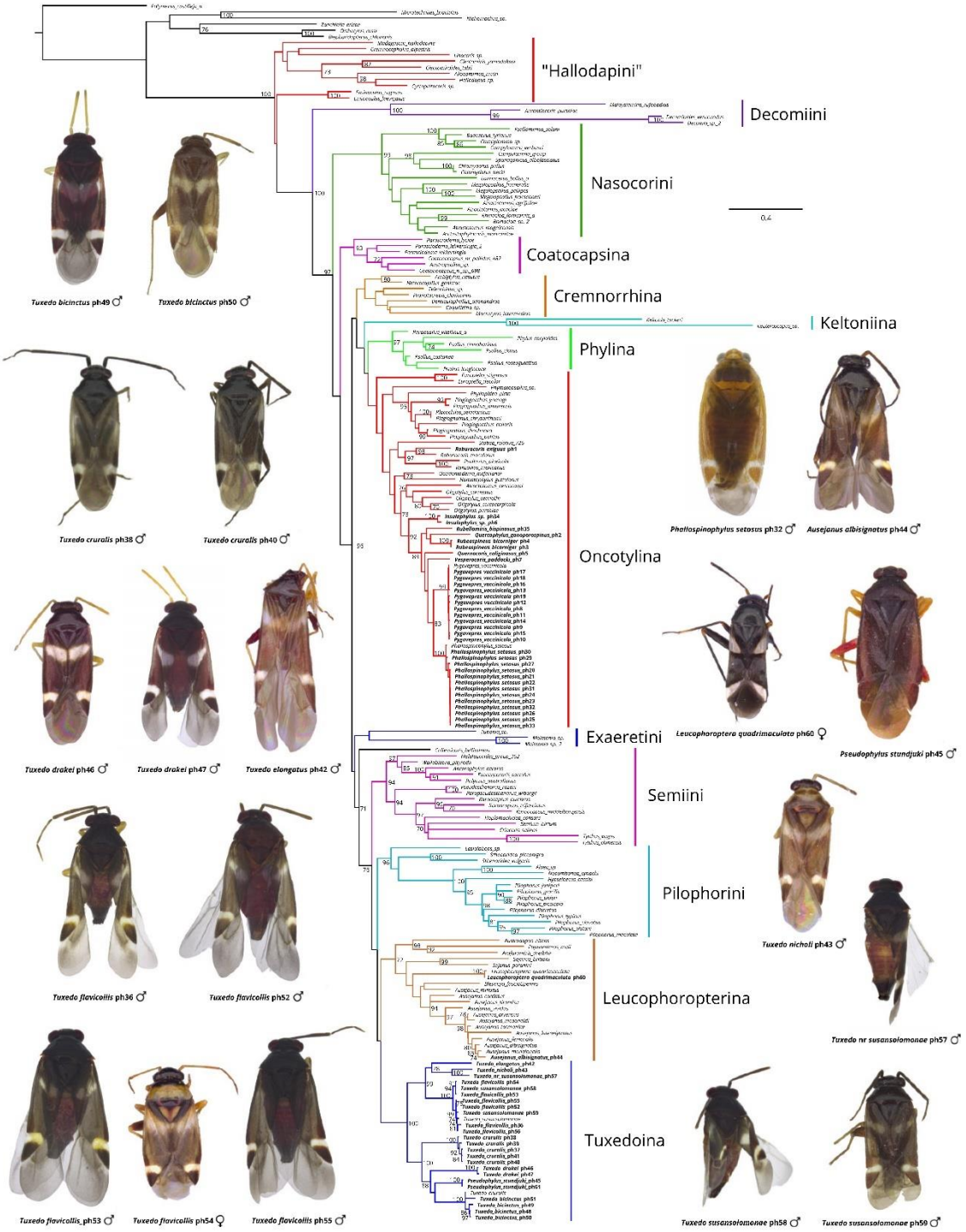

Figure 2.4. Phylogeny of Phylinae, generated in RAxML, with specimens for which new data was gathered in bold font, values at nodes represent Rapid Bootstrap Support, values below 70 not shown.

Supporting information

Supplemental text S1

Introduction

In an effort to encourage other researchers to try these techniques for the first time as we attempted, we present our methods, rationale, and results in greater detail, including some imperfections and ideas for improvements. As the best way to test a hybrid enrichment experiment is to actually sequence the captured libraries (which is a significant cost), we hope the following information will assist future practitioners of this method.

Methods

Specimens for this study were loaned from the American Museum of Natural History (AMNH), the Entomology Research Museum (UCRC), and the Zoological Institute, Russian Academy of Sciences (ZISP). A total of 61 specimens were used, 32 ethanol-preserved and 29 dry point- or card-mounted specimens (see Table S1 for detailed voucher information and sequencing results). Tentative voucher identifications were done based on habitus and host association data using Weirauch (2006a, 2006b) and Schuh (2004). The age of specimens at the moment of DNA extraction ranged from one to 54 years. Specimens of *Tuxedo*, *Leucophoroptera* Poppius, *Ausejanus* Menard and Schuh, and *Pseudophylus* Yasunaga were imaged using a Leica DFC 450 C imaging system. Image vouchers and specimen information are available through the Heteroptera Species Pages (http://research.amnh.org/pbi/heteropteraspeciespage/). After clearing abdominal soft tissue during the DNA extraction process, we examined male genitalic characters to confirm our tentative identifications. In cases where different diagnostic characters were

in conflict (e.g., in some *Tuxedo* spp., see results and discussion section in the main text), we based our identification on genitalic characters.

DNA extraction

When combining Qiagen DNeasy® Blood & Tissue kit with a Qiagen QIAquick® PCR purification, we initiated extractions and performed first centrifugation as per DNeasy® instructions, and then replaced washes using AW1 and AW2 buffers with washes using PE buffer from QIAquick® kit. We also used QIAquick® spin columns, and performed a final elution in 30 µl EB buffer. Due to low DNA concentration in the extract of one of the specimens (ph33), the extraction was repeated, involving the remaining body tissue.

Primer design and bait synthesis

As the mitochondrial genome sequence of donor specimens was unknown, mitochondrial amplicon primers were designed de novo using several mitochondrial genomes of plant bugs available on GenBank (NC_027143.1, NC_027144.1, NC_023796.1, KF679984.1, EU401991.2, HQ902161.1, NC_022677.1, NC_026669.1, NC_025299.1, NC_022922.1). After aligning these sequences, we searched for conserved regions and identified suitable priming sites that would generate four amplicons spanning the entire mitochondrion and should be applicable across the family Miridae.

For the nuclear ribosomal operon, we used a modified primer Ns1 and the original primer kb3 from Wang *et al.* (2015) that span an approximately 7.5 Kb region.

In order to design LR PCR primers for a nuclear protein-coding gene, we first utilized a recently published Hemiptera UCE probe set (Faircloth 2017), since many insect UCE loci are conserved exons (Bossert & Danforth 2018). We used BLAST to obtain UCE

locations on genome sequences of *Acyrthosiphon pisum*, *Cimex lecturarius*, and *Rhodnius prolixus.* We then applied filtering to retain only those genomic scaffolds that had two or more UCEs located not further than 20Kb apart (which would have conserved regions suitable for long-range PCR) and for which synteny was conserved across all three genomes (no exon rearrangements). We aligned fragments of filtered scaffolds containing UCE and examined them for presence of suitable priming site. In some cases, due to greater sequence similarity across all references, an adjacent exon was chosen for priming site instead of the UCE-containing exon. At the end we designed primers for three regions, out of which one performed the best in PCR tests across both subprojects. That region was annotated as a fragment of the cytoplasmic dynein heavy chain gene, contained nine exons and several introns including one large middle intron, and spanned from about 2.7 Kb (in *Tuxedo drakei*) to 4 Kb (in *Phallospinophylus setosus*). Biotinylated primers can contain dual biotin or have an extended spacer to improve binding efficiency, however these modifications come with a significant increase in price. We found that a single biotin connected to 5' end of the primer via a standard C6 spacer was sufficient for retaining bait molecules on beads.

Phylogenetic Analysis

For phylogenetic analysis, the dataset was concatenated and divided into 18 partitions with protein coding genes split further into codon positions. Substitution models and partitioning scheme were optimized using PartitionFinder 2.1.1 (Lanfear *et al.* 2016) or ModelFinder (Kalyaanamoorthy *et al.* 2017), which is an IQ-TREE built-in model and partition test. Phylogeny estimation was performed in RAxML v8.2.11 (Stamatakis 2014)

and IQ-TREE v1.5.4 (Nguyen *et al.* 2014). Branch support was calculated using Rapid Bootstrap (Stamatakis *et al.* 2008) which is shown on Fig. 2.2, Ultrafast Bootstrap (Minh *et al.* 2013), and SH-aLRT (Anisimova & Gascuel 2006), which are shown on Figs 2.S2 and 2.S3.

To test how well our data can be combined with previously generated data, we combined it with the dataset of Menard *et al.* (2014) which is the most comprehensive set of genetic data for related species. After downloading sequences from GenBank, we extracted 18S, 28S, 16S and COX1 sequences from our data and performed alignment and manual trimming. Alignments were then concatenated, optimized for model and partitioning scheme, and phylogenetically analyzed as above.

Illustrations for Figs 2.2, 2.3, and 2.S1 were drafted using R v3.4.3 and packages APE (Paradis *et al.* 2004), phytools (Revell 2012), ggtree (Yu *et al.* 2016) and ggbio (Yin *et al.* 2012). Relief image for Fig. 2.3 was taken from the SimpleMappr website (http://www.simplemappr.net/).

Results and Troubleshooting

Sample cross contamination

In many samples we observed the presence of some cross contamination by ribosomal operon amplicon DNA of the bait taxa (~1%). Since the ribosomal genes are very conserved across all plant bugs, we had to manually parse out contaminant reads for 18S and 28S and exclude several outgroup taxa where due to a low number of reads it was not possible to accurately decontaminate sequences. We suspected that contaminant ribosomal operon DNA came from our initial tests, where the operon PCR product was

used to produce Illumina® libraries. Our conclusion is based on few observations: 1) Contamination was limited to only ribosomal DNA; mitochondrial contigs on the contrary appeared to be devoid of contaminating reads even for the samples with the lowest coverage. 2) Since the bait library is prepared with the M13 adaptors, even if present in the final captured library, these molecules will not interfere with sequencing. 3) We found that some contaminating reads belonged to *Pygovepres vaccinicola*, which was not used for final bait set preparation, but was used in initial tests to prepare Illumina® libraries. 4) Sequenced bait samples also contained contaminant reads of other bait samples. 5) Initial tests included preparation of pre-indexed libraries, amplified only with short IS7/8 primers.

We thus recommend to prepare Illumina® libraries from bait amplicons (if desired) after target captures are completed and captured libraries are indexed. In the second sequencing run, we utilized the same bait preparation protocol, but were careful in preparing amplicon libraries after hybrid captures, as well as regularly replacing elution buffers, and observed no contaminant bait reads.

Nuclear protein-coding gene capture

Only in the OOB subproject did we observe noticeable numbers of reads mapping onto the dynein reference sequence (Table 2.1), however most reads mapped to a large intron in the middle of the bait region sequence (Fig. 2.S1). These reads were difficult to assemble since, apparently, they came from many unrelated fragments with similarity to this intron region (non-specific capture). Reads mapping to dynein exons and introns in between closely located exons was minimal in both subprojects (Fig. 2.S1), and the

obtained sequences were very conserved which rendered them uninformative for the project. We hoped to minimize costs by not purchasing COT-1 DNA to block repetitive elements in our first sequencing run. However, given our results, utilization of COT-1 DNA blocker should be considered as a potential way to improve capture efficiency when enriching for nuclear protein-coding genes.

As far as we know, this study is the first attempt to sequence LR PCR product of a nuclear protein coding gene for use as a capture bait. Long Range PCR can be utilized as an efficient method to obtain large genes of interest from high quality samples even when no close reference is available, since only primer regions need to be conserved.

While this approach may be utilized to a quick and economic way to obtain one or a small group of genes of interest from non-model organisms and indeed seems obvious, usage of such amplicons as baits should be approached with caution and tested before inclusion in a larger sequencing run.

Phylogenetic analyses

As part of the *Tuxedo* subproject, we sampled two specimens of *Pseudophylus stundjuki* (Kulik) since this species from Far East Asia rendered the Western Nearctic *Tuxedo* paraphyletic in a previous analysis (Menard *et al.* 2014). "*Tuxedo*" is here confirmed to be paraphyletic with respect to *Pseudophylus*, after thorough examination of our sequence data and comparison with data from Menard *et al.* (2014) and Jung and Lee (2011). All primarily Fagaceae-feeding species of "*Tuxedo*" form a well-supported monophyletic group. Species other than *Tuxedo flavicollis* (Knight) and *Tuxedo susansolomonae* Schuh were recovered as monophyletic and conform with genitalic-

based identifications. Phylogenetic analysis recovered two highly supported monophyletic groups within the *T. flavicollis/susansolomonae* species group, however the composition of each group is not congruent with either genitalic structure or coloration. One specimen (ph57) initially identified as *T. susansolomonae* is distantly related to the other members of the *T. flavicollis/susansolomonae* clade, is recovered instead as sister taxon to *T. nicholi* (Knight), and likely represents an undescribed species. Species within the OOB clade represented by multiple specimens are monophyletic with high support.

References

Anisimova, M. & Gascuel, O. (2006) Approximate likelihood-ratio test for branches: a fast, accurate, and powerful alternative. *Systematic Biology* 55(4), 539-552.

Bossert, S. & Danforth, B. N. (2018) On the universality of target enrichment baits for phylogenomic research. *Methods in Ecology and Evolution* 9(6), 1453-1460.

Faircloth, B. C. (2017) Identifying conserved genomic elements and designing universal bait sets to enrich them. *Methods in Ecology and Evolution* 8(9), 1103-1112.

Kalyaanamoorthy, S., Minh, B. Q., Wong, T. K., von Haeseler, A. & Jermiin, L. S. (2017) ModelFinder: fast model selection for accurate phylogenetic estimates. *Nature Methods* 14(6), 587.

Lanfear, R., Frandsen, P. B., Wright, A. M., Senfeld, T. & Calcott, B. (2016) PartitionFinder 2: new methods for selecting partitioned models of evolution for molecular and morphological phylogenetic analyses. *Molecular Biology and Evolution* 34(3), 772-773.

Minh, B. Q., Nguyen, M. A. T. & von Haeseler, A. (2013) Ultrafast approximation for phylogenetic bootstrap. *Molecular Biology and Evolution* 30(5), 1188-1195.

Nguyen, L. T., Schmidt, H. A., von Haeseler, A. & Minh, B. Q. (2014) IQ-TREE: a fast and effective stochastic algorithm for estimating maximum-likelihood phylogenies. *Molecular Biology and Evolution* 32(1), 268-274.

Paradis, E., Claude, J. & Strimmer, K. (2004) APE: analyses of phylogenetics and evolution in R language. *Bioinformatics* 20(2), 289-290.

Revell, L. J. (2012) phytools: an R package for phylogenetic comparative biology (and other things). *Methods in Ecology and Evolution* 3(2), 217-223.

Stamatakis, A. (2014) RAxML version 8: a tool for phylogenetic analysis and post-analysis of large phylogenies. *Bioinformatics* 30(9), 1312-1313.

Stamatakis, A., Hoover, P. & Rougemont, J. (2008) A rapid bootstrap algorithm for the RAxML web servers. *Systematic Biology* 57(5), 758-771.

Wang, Y. H., Cui, Y., Rédei, D., Baňař, P., Xie, Q., Štys, P., Damgaard, J., Chen, P., Yi, W., Wang, Y., Dang, K., Li, C. & Bu, W. (2016) Phylogenetic divergences of the true bugs (Insecta: Hemiptera: Heteroptera), with emphasis on the aquatic lineages: the last

piece of the aquatic insect jigsaw originated in the Late Permian/Early Triassic. *Cladistics* 32(4), 390-405.

Yin, T., Cook, D. & Lawrence, M. (2012) ggbio: an R package for extending the grammar of graphics for genomic data. *Genome Biology* 13(8), R77.

Yu, G., Smith, D. K., Zhu, H., Guan, Y. & Lam, T. T. Y. (2016) ggtree: an R package for visualization and annotation of phylogenetic trees with their covariates and other associated data. *Methods in Ecology and Evolution* 8(1), 28-36.

Table 2.S1. List of samples used in the project, voucher specimen information, and sequencing information.

ph#	USI	Species	Type status	Geographic region	Host plant	Preservation method	Collecting year	[dsDNA], ng/ul	DNA mass used for library prep (ng)	Amount of bait used, ng	PF Clusters	Filtered and merged reads	Filtered and merged reads (dedup)	Duplication rate	Mito: mapped reads	Mito: percent mapped	Mito: coverage depth	18S: mapped reads	18S: percent mapped	18S: coverage depth	28S: mapped reads	28S: percent mapped	28S: coverage depth	Dynein: mapped reads	Dynein: percent mapped	Total: reads mapped	Total: percent mapped	COX1 distance between a bait and a sample
Experiment 1																												
ph1	UCR_ENT 00127382	Roburocoris exiguus	none	Cleveland NF	Quercus	EtOH	2010	0.276	11.04	10	130078	128027	126880	0.90%	1041	0.81%	13.8616	30	0.02%	3.09044	43	0.03%	4.33417	2	0.00%	1116	0.87%	22.03%
ph2	UCR_ENT 00127369	Quercophylus gonoporospinus	none	Tehachapi	Quercus	dry	2009	6.52	78.24	10	153428	153550	152743	0.53%	1394	0.91%	19.0812	NA†	NA†	NA†	NA†	NA†	NA†	232	0.15%	1626	1.06%	11.51%
ph2_control																											0.23%	
ph3	UCR_ENT 00127383	Rubeospineus bicorniger	none	Los Angeles NF	Quercus	EtOH	2009	1.71	68.4	10	177774	177483	176589	0.50%	703	0.40%	9.27753	NA†	NA†	NA†	248	0.14%	21.7522	1438	0.81%	2389	1.35%	10.98%
ph4	UCR_ENT 00127370	Rubeospineus bicorniger	none	Baja	Quercus	dry	2009	0.616	9.24	10	204208	199266	195784	1.75%	2735	1.37%	32.9303	NA†	NA†	NA†	301	0.15%	20.4866	1459	0.73%	4495	2.26%	10.91%
ph5	UCR_ENT 00127371	Quernocoris caliginosus	none	Cleveland NF	Quercus	dry	2010	6.38	76.56	10	146948	145344	144916	0.29%	1372	0.94%	17.9123	NA†	NA†	NA†	227	0.16%	17.8322	1015	0.70%	2614	1.80%	11.92%
ph6	UCR_ENT 00127372	Insulaphylus sp.	none	Baja	Quercus	dry	2009	0.308	9.24	10	163679	157591	152074	3.50%	13537	8.59%	110.284	646	0.41%	44.917	738	0.47%	50.1585	3209	2.04%	18130	11.50%	14.82%
ph7	UCR_ENT 00127384	Vesperocoris paddocki	none	Los Padres	Quercus	EtOH	2007	2.52	75.6	10	142576	142125	141404	0.51%	1623	1.14%	20.869	NA†	NA†	NA†	918	0.65%	76.1237	8204	5.77%	10745	7.56%	10.87%
ph8	UCR_ENT 00127385	Pygovepres vaccinicola	none	Cleveland NF	Quercus	EtOH	2010	2.86	74.36	10	79353	80147	74500	7.05%	2470	3.08%	33.1782	61	0.08%	6.18787	98	0.12%	7.86628	2111	2.63%	4740	5.91%	9.65%
ph9	UCR_ENT 00127373	Pygovepres vaccinicola	none	Cleveland NF	Ceanothus	dry	2010	7.06	70.6	10	125133	123562	120335	2.61%	1889	1.53%	23.9774	987	0.80%	75.7632	1754	1.42%	114.08	6721	5.44%	11351	9.19%	9.66%
ph10	UCR_ENT 00127386	Pygovepres vaccinicola	none	Cleveland NF	Prunus	EtOH	2010	6.06	74.538	10	235524	236912	232620	1.81%	977	0.41%	13.0746	NA†	NA†	NA†	NA†	NA†	NA†	957	0.40%	1934	0.82%	9.66%
ph11	AMNH_PBI 00082512	Pygovepres vaccinicola	none	Cleveland NF	Marah	dry	1978	2.2	33	10	234450	227057	223678	1.49%	998	0.44%	10.1069	1107	0.49%	63.5918	1699	0.75%	92.6817	7713	3.40%	11517	5.07%	9.13%
ph12	UCR_ENT 00127387	Pygovepres vaccinicola	none	San Bernardino NF	Quercus	EtOH	2016	4.2	72.66	10	168633	167206	163864	2.00%	3200	1.91%	34.7008	30	0.02%	2.98168	48	0.03%	3.7232	1775	1.06%	5053	3.02%	9.65%
ph13	UCR_ENT 00127388	Pygovepres vaccinicola	none	Los Angeles NF	Ceanothus	EtOH	2016	0.76	38	10	159836	159278	158346	0.59%	4398	2.76%	53.8989	157	0.10%	14.6003	174	0.11%	14.7588	3153	1.98%	7882	4.95%	9.58%
ph14	UCR_ENT 00127389	Pygovepres vaccinicola	none	Los Angeles NF	Prunus	EtOH	2016	2.64	75.24	10	156298	154959	154104	0.55%	1611	1.04%	21.5415	155	0.10%	13.105	183	0.12%	14.1757	1903	1.23%	3852	2.49%	9.66%
ph15	UCR_ENT 00127390	Pygovepres vaccinicola	none	San Jacinto NF	Quercus	EtOH	2009	3.82	74.49	10	176319	178192	168409	5.49%	1459	0.82%	18.3962	93	0.05%	8.8446	117	0.07%	10.4295	3477	1.95%	5146	2.89%	9.66%
ph16	UCR_ENT 00127374	Pygovepres vaccinicola	none	Baja	Quercus	dry	2009	0.226	9.04	10	261616	254113	228454	10.10%	10191	4.01%	98.982	218	0.09%	13.355	265	0.10%	15.6146	8531	3.36%	19205	7.56%	9.58%
ph17	UCR_ENT 00127413	Pygovepres vaccinicola	none	Tehachapi	Quercus	EtOH	2009	4.32	75.6	10	161744	160556	158629	1.20%	786	0.49%	9.87092	116	0.07%	9.11229	132	0.08%	10.8353	2229	1.39%	3263	2.03%	9.74%
ph18	UCR_ENT 00127414	Pygovepres vaccinicola	none	Tehachapi	Prunus	EtOh	2009	3.18	74.73	10	140057	137063	136356	0.52%	716	0.52%	7.96659	221	0.16%	16.5306	224	0.16%	16.3917	3254	2.37%	4415	3.22%	9.82%
ph19	AMNH_PBI 00082518	Pygovepres vaccinicola	none	Shasta Co.	Quercus	dry	1984	7.72	77.2	10	195042	191489	167488	12.53%	1688	0.88%	15.8911	1151	0.60%	69.0346	2184	1.14%	110.787	10182	5.32%	15205	7.94%	9.74%
ph20	UCR_ENT 00127415	Phallospinophylus setosus	none	Cleveland NF	Quercus	EtOH	2010	3.56	71.2	10	248114	245729	214508	12.71%	7434	3.03%	72.8828	380	0.15%	26.3917	527	0.21%	38.7424	10354	4.21%	18695	7.61%	0.13%
ph21	UCR_ENT 00127375	Phallospinophylus setosus	none	Cleveland NF	Ceanothus	dry	2010	5.54	83.1	10	159940	157529	132835	15.68%	4094	2.60%	37.6226	359	0.23%	25.6961	508	0.32%	35.7781	8974	5.70%	13935	8.85%	0.07%
ph22	UCR_ENT 00127416	Phallospinophylus setosus	none	Cleveland NF	Prunus	EtOH	2010	1.87	74.8	10	182847	179982	173458	3.62%	3377	1.88%	34.178	301	0.17%	22.728	385	0.21%	27.5876	9703	5.39%	13766	7.65%	0.13%
ph23	UCR_ENT 00127395	Phallospinophylus setosus	none	San Bernardino NF	Quercus	EtOH	2016	3.5	70	10	175372	174075	161160	7.42%	4609	2.65%	45.4893	295	0.17%	23.5045	563	0.32%	40.8127	6932	3.98%	12399	7.12%	0.00%
ph24	UCR_ENT 00127396	Phallospinophylus setosus	none	Los Angeles NF	Prunus	EtOH	2009	2.92	73	10	158979	156929	149370	4.82%	3508	2.24%	32.5592	484	0.31%	39.8366	830	0.53%	66.1537	5936	3.78%	10758	6.86%	0.00%
ph25	UCR_ENT 00127376	Phallospinophylus setosus	none	San Jacinto NF	Prunus?	dry	2010	4.16	74.88	10	187491	183024	92752	49.32%	4265	2.33%	25.8512	389	0.21%	16.2267	565	0.31%	19.4696	7891	4.31%	13110	7.16%	0.00%
																											1.37%	
ph26	UCR_ENT 00127397	Phallospinophylus setosus	none	San Jacinto NF	Quercus	EtOH	2009	4.44	75.48	10	201740	198281	133357	32.74%	4106	2.07%	32.4041	306	0.15%	15.2422	461	0.23%	23.259	10519	5.31%	15392	7.76%	0.00%
ph27	UCR_ENT 00127398	Phallospinophylus setosus	none	Baja	Quercus	EtOH	2009	6.06	72.72	10	203169	199019	99699	49.90%	4010	2.01%	24.0353	682	0.34%	28.8785	1128	0.57%	35.8972	13222	6.64%	19042	9.57%	1.12%
ph28	UCR_ENT 00127399	Phallospinophylus setosus	none	Tehachapi	Quercus	EtOH	2009	4.26	72.42	10	243084	236322	65515	72.28%	NA†	NA†	NA†	NA†	NA†	NA†	NA†	NA†	NA†	NA†	NA†	NA†	NA†	NA†
ph29	AMNH_PBI 00082453	Phallospinophylus setosus	none	Tulare Co.	Quercus	dry	1978	3.44	51.6	25	174628	164972	155883	5.51%	9744	5.91%	77.2913	1059	0.64%	57.5104	1626	0.99%	83.4698	25175	15.26%	37604	22.79%	1.79%
ph30	AMNH_PBI 00082567	Phallospinophylus setosus	none	Tulare Co.	Ceanothus	dry	1978	2.52	37.8	25	231106	215919	194434	9.95%	4413	2.04%	36.0177	3048	1.41%	124.559	3756	1.74%	140.556	39847	18.45%	51064	23.65%	1.66%
ph31	AMNH_PBI 00082575	Phallospinophylus setosus	none	San Bernardino NF	Ceanothus	dry	1977	0.674	10.11	25	137771	129184	115784	10.37%	11023	8.53%	89.2148	1973	1.53%	97.604	3688	2.85%	150.804	27180	21.04%	43864	33.95%	0.00%
																											1.22%	
ph32‡	UCR_ENT 00127400	Phallospinophylus setosus	none	Los Angeles NF	Prunus	EtOH	2016	2.26			477874	488748	188234	61.49%														
ph33	UCR_ENT 00061245	Phallospinophylus setosus	none	Los Angeles NF	Quercus	dry	2009	4.3	64.5	25	117627	115080	108265	5.92%	8019	6.97%	69.6609	1096	0.95%	72.8249	1913	1.66%	107.528	24564	21.35%	35592	30.93%	0.00%
ph34	UCR_ENT 00127401	Insulaphylus sp.	none	Los Angeles NF	Quercus	EtOH	2016	4.38	74.46	25	158420	157638	155235	1.52%	2556	1.62%	34.8036	NA†	NA†	NA†	3038	1.93%	221.822	3229	2.05%	8823	5.60%	14.64%
ph35	UCR_ENT 00127402	Rubellomiris bispinosus	none	San Jacinto NF	Quercus	EtOH	2009	1.83	73.2	25	113379	115573	112310	2.82%	3755	3.25%	60.1884	NA†	NA†	NA†	2166	1.87%	141.893	4834	4.18%	10755	9.31%	13.55%
ph36	UCR_ENT 00127403	Tuxedo flavicollis	none	San Gabriels	Ceanothus	EtOH	2016	0.902	36.08	10	92094	91688	90313	1.50%	221	0.24%	4.17547	461	0.50%	35.7073	533	0.58%	41.2995	31	0.03%	1246	1.36%	20.38%
ph37	UCR_ENT 00127404	Tuxedo cruralis	none	Baja	Ceanothus	EtOH	2009	2.2	74.8	10	152070	150714	147489	2.14%	1022	0.68%	12.9058	289	0.19%	23.1464	240	0.16%	18.2607	12	0.01%	1563	1.04%	18.62%
ph38	UCRC ENT 277960	Tuxedo cruralis	none	Santa Catalina	Cercocarpus	dry	2008	1.55	62	10	189047	187115	184503	1.40%	996	0.53%	13.0652	550	0.29%	42.5184	609	0.33%	42.9142	22	0.01%	2177	1.16%	19.51%
ph39	UCR_ENT 00061761	Tuxedo cruralis	none	Los Padres	Ceanothus	dry	1977	1.4	21	10	121381	117839	115773	1.75%	660	0.56%	7.66924	558	0.47%	37.8137	673	0.57%	42.8548	20	0.02%	1911	1.62%	19.39%
ph40	UCR_ENT 00127377	Tuxedo cruralis	none	Cleveland	Cercocarpus	dry	2010	1.12	44.8	10	166127	156472	154217	1.44%	380	0.24%	4.38708	240	0.15%	17.3591	321	0.21%	19.2929	15	0.01%	956	0.61%	19.08%
ph41	UCR_ENT 00127378	Tuxedo cruralis	none	Los Padres	Quercus	dry	2007	0.106	4.24	10	199572	193698	176738	8.76%	30296	15.64%	258.987	231	0.12%	16.5828	249	0.13%	17.012	8	0.00%	30784	15.89%	18.97%
ph42	UCR_ENT 00124208	Tuxedo elongatus	paratype	Siskiyou	Chrysolepis	dry	1985	0.11	2.75	10	154837	149029	136729	8.25%	3401	2.28%	32.7475	295	0.20%	23.6585	305	0.20%	28.5825	5	0.00%	4006	2.69%	20.65%
																											0.92%	
ph43	UCR_ENT 00124209	Tuxedo nicholi	none	Arizona	Quercus	dry	1983	0.566	14.15	10	128082	124762	122707	1.65%	988	0.79%	10.5853	580	0.46%	37.5604	607	0.49%	38.2207	50	0.04%	2225	1.78%	20.46%
ph44	AMNH_PBI 00271922	Ausejanus albisignatus	none	Australia		dry	1999	0.142	5.68	10	122419	118609	117116	1.26%	933	0.79%	8.41977	213	0.18%	15.193	210	0.18%	14.3961	1	0.00%	1357	1.14%	15.31%
ph45	AMNH_PBI 00234761	Pseudophylus stundjuki	none	Russia	Pyrus domestica	dry	1963	0.618	15.45	10	128411	124971	122725	1.80%	1764	1.41%	17.2437	174	0.14%	11.8394	382	0.31%	12.1518	10	0.01%	2330	1.86%	17.60%
ph46	AMNH_PBI 00322474	Tuxedo drakei	none	Kern Co.	Fremontodendron	dry	2004	3.16	72.68	10	217404	212868	200164	5.97%	8941	4.20%	76.7723	689	0.32%	50.1347	828	0.39%	55.9677	324	0.15%	10782	5.07%	0.66%
																											0.39%	
ph47‡	UCR_ENT 00127405	Tuxedo drakei	none	San Gabriels	Fremontodendron	EtOH	2016	3.1			437390	415926	175841	57.72%														
ph48	UCR_ENT 00127379	Tuxedo bicinctus	none	San Gabriels	Cercocarpus	dry	2009	0.234	9.36	10	218974	211310	206211	2.41%	1966	0.93%	21.359	1226	0.58%	74.2586	1482	0.70%	79.4659	101	0.05%	4775	2.26%	17.31%
ph49	UCR_ENT 00127406	Tuxedo bicinctus	none	San Bernardino	Cercocarpus	EtOH	2016	1.21	48.4	10	167268	165486	161883	2.18%	1146	0.69%	14.2143	1065	0.64%	78.7786	1187	0.72%	84.441	88	0.05%	3486	2.11%	17.37%
ph50	UCR_ENT 00127380	Tuxedo bicinctus	none	~Cleveland	Ceanothus	dry	1979	1.53	22.95	10	247749	242705	235526	2.96%	1048	0.43%	10.2613	1753	0.72%	103.295	1879	0.77%	103.383	64	0.03%	4744	1.95%	17.65%
ph51	AMNH_PBI 00303164	Tuxedo bicinctus	none	Kern Co.	Cercocarpus	dry	2004	1.51	60.4	10	199541	197218	194672	1.29%	1937	0.98%	20.821	308	0.16%	23.9846	363	0.18%	26.5047	52	0.03%	2660	1.35%	18.35%
ph52	UCR_ENT 00127407	Tuxedo flavicollis	none	San Gabriels	Quercus	EtOH	2011	0.936	37.44	10	151620	151613	150329	0.85%	1751	1.15%	20.5295	606	0.40%	51.3449	285	0.19%	21.7794	10	0.01%	2652	1.75%	20.78%
																											0.65%	
ph53	UCR_ENT 00127417	Tuxedo flavicollis	none	Baja	Quercus	EtOH	2009	1.09	43.6	10	100264	99989	98713	1.28%	1231	1.23%	15.3749	842	0.84%	72.2523	872	0.87%	70.0371	14	0.01%	2959	2.96%	20.35%
ph54	UCR_ENT 00124210	Tuxedo flavicollis	none	San Luis Obispo	Quercus	dry	1985	4.52	67.8	10	169211	164906	163348	0.94%	1463	0.89%	13.5354	1039	0.63%	64.6738	943	0.57%	57.8907	22	0.01%	3467	2.10%	20.40%
ph55	UCR_ENT 00127418	Tuxedo flavicollis	none	Tehachapi	Quercus	EtOH	2009	0.846	33.84	21	150306	149362	129184	13.51%	996	0.67%	12.804	10655	7.13%	562.762	13241	8.87%	609.559	67	0.04%	24959	16.71%	20.60%
ph56	UCR_ENT 00127419	Tuxedo flavicollis	none	Los Padres	Quercus	EtOH	2007	1.21	48.4	21	119391	120440	116373	3.38%	2946	2.45%	45.1772	2757	2.29%	233.799	3444	2.86%	251.834	77	0.06%	9224	7.66%	20.42%
ph57	UCR_ENT 00127420	Tuxedo nr susansolomonae	none	Baja	Quercus	EtOH	2009	0.914	36.56	21	180677	182114	175173	3.81%	4351	2.39%	56.4749	2828	1.55%	222.789	3531	1.94%	250.415	69	0.04%	10779	5.92%	20.30%
ph58	UCR_ENT 00127412	Tuxedo susansolomonae	none	San Gabriels	Quercus	EtOH	2016	0.696	27.84	21	147887	147486	137036	7.09%	1576	1.07%	22.7188	8088	5.48%	513.552	6378	4.32%	367.853	69	0.05%	16111	10.92%	20.35%
ph59	UCR_ENT 00127381	Tuxedo susansolomonae	paratype	San Jacinto	Quercus	dry	1976	0.772	19.3	21	183084	176924	173139	2.14%	951	0.54%	10.0994	2635	1.49%	159.152	3126	1.77%	166.138	26	0.01%	6738	3.81%	20.26%
ph60	AMNH_PBI 00272096	Leucophoroptera quadrimaculata	none	Australia		dry	2004	2.96	74	21	225540	218222	203023	6.96%	3206	1.47%	33.3436	3008	1.38%	159.906	NA†	NA†	NA†	17	0.01%	6231	2.86%	19.16%
Experiment 2																												
ph61	AMNH_PBI 00234872	Pseudophylus stundjuki	none	Russia		dry	1985	8.03	40.15		120233	118580	57411	51.58%	809	0.68%	4.23413	3442	2.90%	96.6703	5987	5.05%	87.6388	NA	NA	10238	8.63%	17.83%
ph45	AMNH_PBI 00234761	Pseudophylus stundjuki	none	Russia	Pyrus domestica	dry	1963	0.618	15.45		229282	226703	112806	50.24%	5330	2.35%	23.4212	2543	1.12%	70.8435	5503	2.43%	76.2825	NA	NA	13376	5.90%	17.60%
ph59	UCR_ENT 00127381	Tuxedo susansolomonae	paratype	San Jacinto	Quercus	dry	1976	0.772	19.3	500	111690	110430	52175	52.75%	500	0.45%	3.17897	6064	5.49%	163.543	6205	5.62%	157.164	NA	NA	12769	11.56%	20.26%
ph54	UCR_ENT 00124210	Tuxedo flavicollis	none	San Luis Obispo	Quercus	dry	1985	4.52	67.8		150714	149727	64773	56.74%	1320	0.88%	5.81821	5143	3.43%	148.684	5103	3.41%	139.368	NA	NA	11566	7.72%	20.40%
ph57	UCR_ENT 00127420	Tuxedo nr susansolomonae	none	Baja	Quercus	EtOH	2009	0.914	36.56		248967	255061	103903	59.26%	5654	2.22%	36.255	9152	3.59%	434.985	9206	3.61%	407.608	NA	NA	24012	9.41%	20.30%

† Excluded from calculations and analyses due to sample cross contamination

‡ For samples ph32 and ph47 amplicons used for bait synthesis were sequenced

Table 2.S2. Primers and conditions for LR PCR.

Amplicon	Primers	Reference	Annealing temp	Elongation time	Amplicon size
Mitochondrion set 1	GGTYTKAACTCAGATCATGTAAA	This study	46°	10 min	~ 4700 - 4900 bp
	WTAACTTTGAAGGTTAWWAGTTT	This study			
Mitochondrion set 2	ACTAWTAACCTTCAAAGTTAW	This study	44°	6 min	4710 - 4713 bp
	THTTAGGTCGAAACTAAHWG	This study			
Mitochondrion set 3	WTACWHTTAGTTTCGACCTAADA	This study	44°	6 min	4416 - 4418 bp
	GABCCRAARTTTCATCATA	This study			
Mitochondrion set 4	DTCWTTAATCYCCAAAATTAAYATTT	This study	44°	6 min	2994 - 2996 bp
	TAAGTTACCTTAGGGATAACAGC	This study			
Nuclear ribosomal operon	AGTCATATGCTTGTCTCAAAGCTTAAG	This study	55°	10 min	7372 – 7662 bp
	AGCGTGGCAACTGCTCT	Wang *et al.* (2015)			
Dynein fragment	GACCARTCRCCGAACCAATT	This study	53°	5 min	2899 – 4132 bp
	TACACYTGGCTBGCTGAACAT	This study			

Table 2.S3. Estimated cost of the project.

Product	Total for 1 MiSeq run, 120 samples, individual captures	Extra costs for 2 MiSeq runs, 240 samples, pooled captures	Extra costs for 3 MiSeq runs, 360 samples, pooled captures	Total for 1 NextSeq run, 360 samples, pooled captures
PCR polymerase				
PrimeSTAR GXL	$250	$250	$250	$750
Bait PCR reagents				
Primers	$300			$300
Sonication	$2			$2
SPRI beads (custom made)				
SeraMag Speadbeads	$400			$400
PEG-8000	$25			$25
EDTA	$25			$25
Tris-HCl	$25			$25
NaCl	$42			$42
DNA ladder	$50			$50
End prep reagents				
Tango	$15			$15
dNTP mixture	$130			$130
ATP	$40			$40
T4 kinase	$194	$194	$194	$582
T4 polymerase	$191	$191	$191	$573
EmeraldAMP / Taq (For A-tailing)	$57			$57
Ligation reagents				
T4 ligase	$203	$203	$203	$609
Bst polymerase	$70			$70
M13 adaptors	$40			$40
Library PCR primers				
Biotinylated primers	$80			$80
NEBNext E7600s	$460			$460
Additional indexing oligos	$385			$385
Capture reagents				
Agilent Hybridization	$500			$500

Buffers kit				
Dynabeads M-270	$400			$400
Blocking oligos (not purified)	$350			$350
IS7/8 or IS5/6 primers	$100			$100
Miscellaneous				
Normalization kit	$98	$98	$98	$294
Bioanalyzer run	$55	$55	$55	$165
Qubit	$160	$160	$160	$480
Pipette tips	$200	$200	$200	$600
Sequencing				
Sequencing	$1,636	$1,636	$1,636	$2,022
Totals				
Total expenses	$6,483	$9,469.60	$12,456.60	$9,571
Cost per sample	$54.02	$39.46	$34.60	$26.59
Cost per 1 Kb of sequence data	$2.84	$2.08	$1.82	$1.40

Table 2.S4. Accession numbers for raw reads and final sequences

Sample	Raw reads (Experiment 1)	Raw reads (Experiment 2)	Raw reads (control sequencing)	Mitochondrial genome	18s	28s
ph1	SRR6869657	N/A	N/A			
ph2	SRR6869656	N/A	SRR7890471			
ph3	SRR6869659	N/A	N/A			
ph4	SRR6869658	N/A	N/A			
ph5	SRR6869653	N/A	N/A			
ph6	SRR6869652	N/A	N/A			
ph7	SRR6869655	N/A	N/A			
ph8	SRR6869654	N/A	N/A			
ph9	SRR6869649	N/A	N/A			
ph10	SRR6869661	N/A	N/A			
ph11	SRR6869646	N/A	N/A			
ph12	SRR6869645	N/A	N/A			
ph13	SRR6869644	N/A	N/A			
ph14	SRR6869643	N/A	N/A			
ph15	SRR6869642	N/A	N/A			
ph16	SRR6869641	N/A	N/A			
ph17	SRR6869640	N/A	N/A			
ph18	SRR6869639	N/A	N/A			
ph19	SRR6869648	N/A	N/A			
ph20	SRR6869647	N/A	N/A			
ph21	SRR6869677	N/A	N/A			
ph22	SRR6869678	N/A	N/A			
ph23	SRR6869675	N/A	N/A			
ph24	SRR6869676	N/A	N/A			
ph25	SRR6869673	N/A	SRR7890470			
ph26	SRR6869674	N/A	N/A			
ph27	SRR6869671	N/A	N/A			
ph29	SRR6869672	N/A	N/A			
ph30	SRR6869669	N/A	N/A			
ph31	SRR6869670	N/A	SRR7890469			
ph32	SRR6869700	N/A	N/A			
ph33	SRR6869699	N/A	N/A			
ph34	SRR6869702	N/A	N/A			
ph35	SRR6869701	N/A	N/A			
ph36	SRR6869696	N/A	N/A			
ph37	SRR6869695	N/A	N/A			
ph38	SRR6869698	N/A	N/A			
ph39	SRR6869697	N/A	N/A			

ph40	SRR6869694	N/A	N/A			
ph41	SRR6869693	N/A	N/A			
ph42	SRR6869667	N/A	SRR7890468			
ph43	SRR6869668	N/A	N/A			
ph44	SRR6869679	N/A	N/A			
ph45	SRR6869681	SRR6869689	N/A			
ph46	SRR6869663	N/A	SRR7890467			
ph47	SRR6869664	N/A	N/A			
ph48	SRR6869665	N/A	N/A			
ph49	SRR6869666	N/A	N/A			
ph50	SRR6869690	N/A	N/A			
ph51	SRR6869691	N/A	N/A			
ph52	SRR6869687	N/A	SRR7890466			
ph53	SRR6869686	N/A	N/A			
ph54	SRR6869684	SRR6869683	N/A			
ph55	SRR6869682	N/A	N/A			
ph56	SRR6869650	N/A	N/A			
ph57	SRR6869651	SRR6869662	N/A			
ph58	SRR6869680	N/A	N/A			
ph59	SRR6869685	SRR6869660	N/A			
ph60	SRR6869692	N/A	N/A			
ph61	N/A	SRR6869688	N/A			

Table 2.S5. Results of statistical tests of difference between different datasets

Dataset	Test	Alternative	Result, p-value	Sample size
Total % on target ~ % CO1 distance	Linear model		Negative relationship, 0.000185*	57
% on mito ~ % CO1 distance	Linear model		Negative relationship, 0.0668	57
% on 18S ~ % CO1 distance	Linear model		Positive relationship, 0.0778	49
% on 28S ~ % CO1 distance	Linear model		Positive relationship, 0.206	54
% on dynein ~ % CO1 distance	Linear model		Negative relationship, 2.25e-08*	57
Total % on target ~ age	Linear model		Positive relationship, 0.143435	57
% on mito ~ age	Linear model		Positive relationship, 0.875825	57
% on 18S ~ age	Linear model		Positive relationship, 0.92212	49
% on 28S ~ age	Linear model		Positive relationship, 0.76092	54
% on dynein ~ age	Linear model		Positive relationship, 0.062	57
Total % on target between preservation methods	Approximative 2-Sample Permutation Test (two sided)	EtOH ≠ dry	0.8165	45
% on mito on target between preservation methods	Approximative 2-Sample Permutation Test (two sided)	EtOH ≠ dry	0.3461	45
% on 18S between preservation method	Approximative 2-Sample Permutation Test (two sided)	EtOH ≠ dry	0.0929	39
% on 28S between preservation method	Approximative 2-Sample Permutation Test (two sided)	EtOH ≠ dry	0.1241	43
% on dyn between preservation method	Approximative 2-Sample Permutation Test (two sided)	EtOH ≠ dry	0.1944	45
Total % on target between OOB and *Tuxedo*	Approximative 2-Sample Permutation Test (one sided)	OOB > *Tuxedo*	0.0083*	57
% on mito between OOB and *Tuxedo* (OOB>*Tuxedo*)	Approximative 2-Sample Permutation Test (one sided)	OOB > *Tuxedo*	0.1974	57
% on 18S between OOB and *Tuxedo*	Approximative 2-Sample Permutation Test (one sided)	OOB < *Tuxedo*	0.0096*	49
% on 28S between OOB and *Tuxedo*	Approximative 2-Sample Permutation Test (one sided)	OOB < *Tuxedo*	0.0833	54
% on dynein between OOB and *Tuxedo*	Approximative 2-Sample Permutation Test (one sided)	OOB > *Tuxedo*	1e-06*	57
Total % on target between 10 ng bait and 21/25 ng bait	2-Sample bootstrap Welch t-test (one sided)	21/25ng > 10ng	0.00163*	57
% on mito between 10 ng bait and 21/25 ng bait	Approximative 2-Sample Permutation Test (one sided)	21/25ng > 10ng	0.1005	57
% on 18S between 10 ng bait and 21/25 ng bait	2-Sample bootstrap Welch t-test (one sided)	21/25ng > 10ng	0.00059*	49
% on 28S between 10 ng bait and 21/25 ng bait	2-Sample bootstrap Welch t-test (one sided)	21/25ng > 10ng	8e-06*	54
% on dynein between 10 ng bait and 21/25 ng bait	2-Sample bootstrap Welch t-test (one sided)	21/25ng > 10ng	0.023225*	57
Total % on target between enriched and	Wilcoxon Signed Rank test (one sided)	enriched > not enriched	0.01563*	6

not enriched				
Total % on target (dynein excluded) between enriched and not enriched	Wilcoxon Signed Rank test (one sided)	enriched > not enriched	0.01563*	6
% on mito between enriched and not enriched	Wilcoxon Signed Rank test (one sided)	enriched > not enriched	0.03149*	6
% on 18S between enriched and not enriched	Wilcoxon Signed Rank test (one sided)	enriched > not enriched	0.03125*	5
% on 28S between enriched and not enriched	Wilcoxon Signed Rank test (one sided)	enriched > not enriched	0.03125*	5
% on dynein between enriched and not enriched	Wilcoxon Signed Rank test (one sided)	enriched > not enriched	0.01563*	6
% on histone 2A between enriched and not enriched	Wilcoxon Signed Rank test (two sided)	enriched ≠ not enriched	0.3125	6
% on histone 3 between enriched and not enriched	Wilcoxon Signed Rank test (two sided)	enriched ≠ not enriched	0.1107	6
Total % on target between experiment 1 and 2	Paired t-test (one sided)	Exp2 > Exp1	0.006003*	4
% on mito between experiment 1 and 2	Paired t-test (one sided)	Exp2 > Exp1	0.6875	4
% on 18S between experiment 1 and 2	Paired t-test (one sided)	Exp2 > Exp1	0.01537*	4
% on 28S between experiment 1 and 2	Paired t-test (one sided)	Exp2 > Exp1	0.005887*	4

Table 2.S6. Percentage of reads mapping to histone 2A and histone 3

Sample	Histone 2A			Histone 3		
	Enriched (% mapped)	Non-enriched (% mapped)	Enriched / non-enriched	Enriched (% mapped)	Non-enriched (% mapped)	Enriched / non-enriched
ph2	0.01584	0.01349	1.17	0.00765	0.01349	0.57
ph25	0.00326	0.00444	0.73	0.00326	0.00536	0.61
ph31	0.00387	0.01593	0.24	0.00697	0.01795	0.39
ph42	0	0.00020	0	0	0.00020	0
ph46	0	0.00071	0	0	0.00053	0
ph52	0.00066	0.00074	0.89	0	0.00062	0

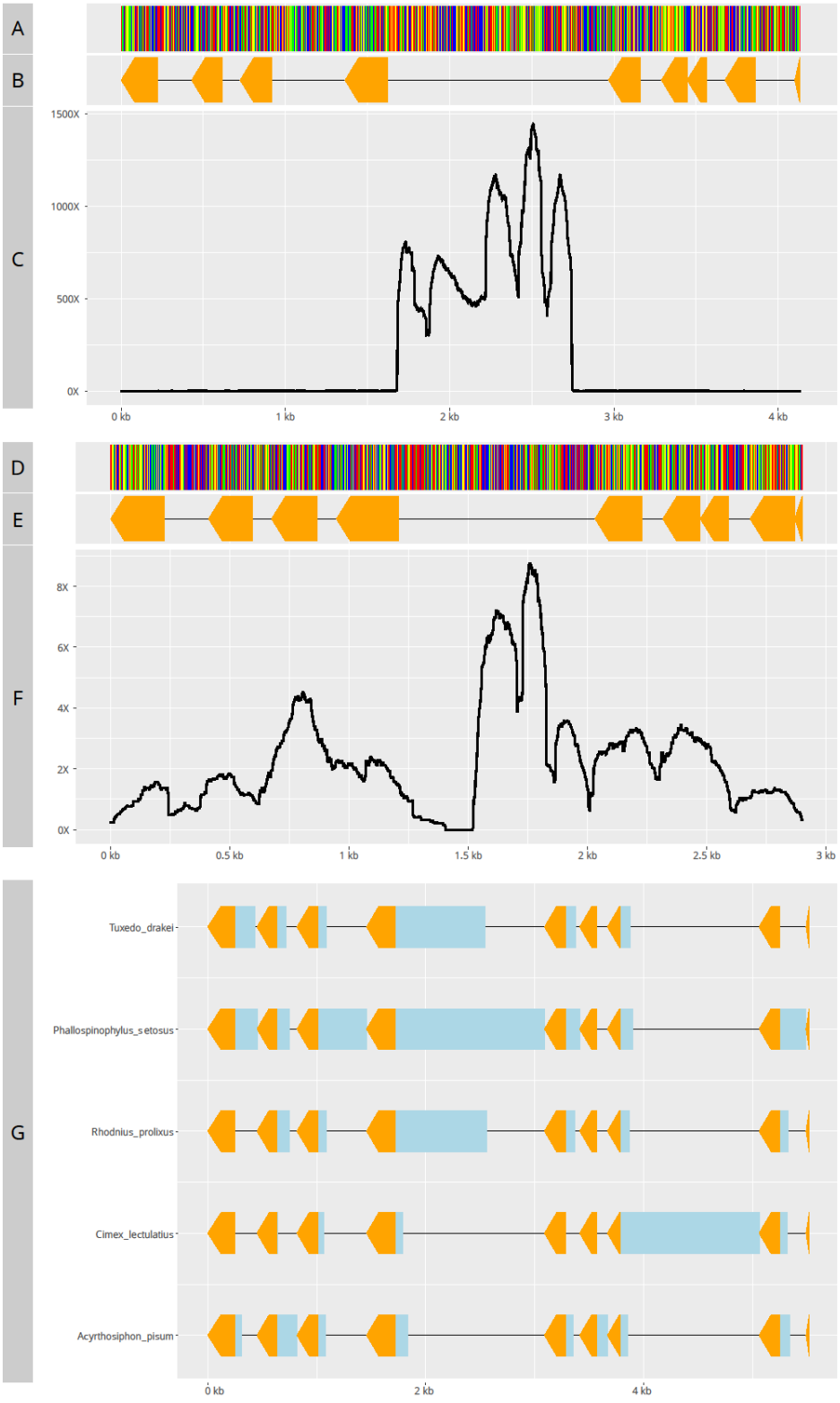
A
B
C
1500X
1000X
500X
0X
0 kb
1 kb
2 kb
3 kb
4 kb
D
E
F
8X
6X
4X
2X
0X
0 kb
0.5 kb
1 kb
1.5 kb
2 kb
2.5 kb
3 kb
G
Tuxedo_drakei
Phallospinophylus_setosus
Rhodnius_prolixus
Cimex_lectulatius
Acyrthosiphon_pisum
0 kb
2 kb
4 kb

Figure 2.S1. Dynein capture results. A, B, C – the OOB subproject: A. *Phallospinophylus setosus* bait sequence. B. Locations of exons (orange). C. Average coverage in captured samples. D, E, F – the *Tuxedo* subproject: D. *Tuxedo drakei* bait sequence. E. Locations of exons (orange). F. Average coverage in captured samples. G. Comparison of sizes of introns (blue) between genomes, used for bait design, and actual baits for the OOB and *Tuxedo* subprojects; sequences are aligned using exons (orange).

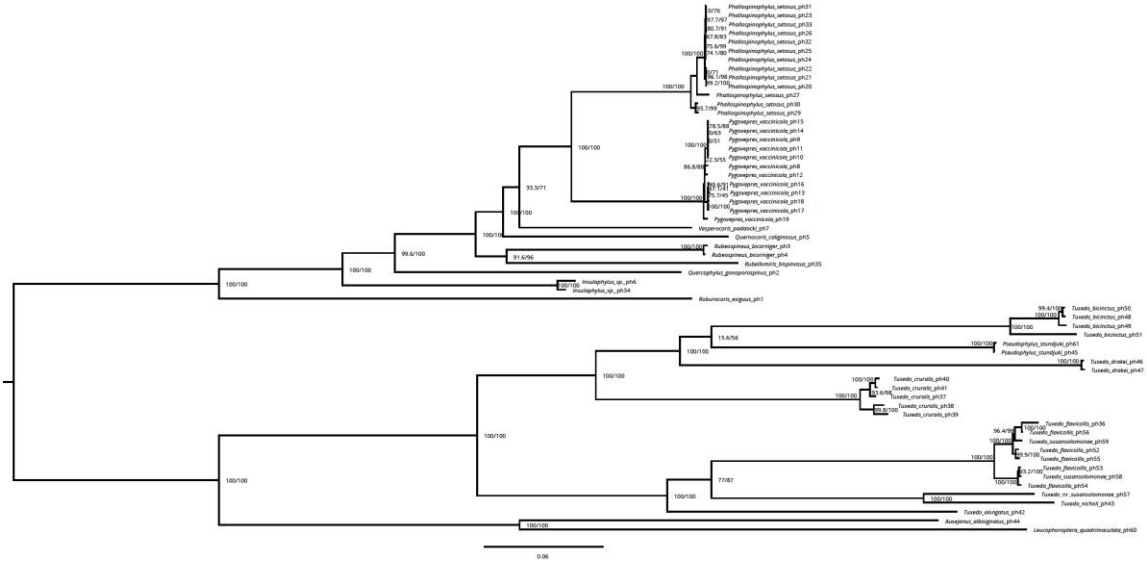

Figure 2.S2. Combined phylogeny of the OOB and *Tuxedo* subprojects, generated in IQ-TREE, values at nodes represent SH-aLRT and UFBoot support respectively.

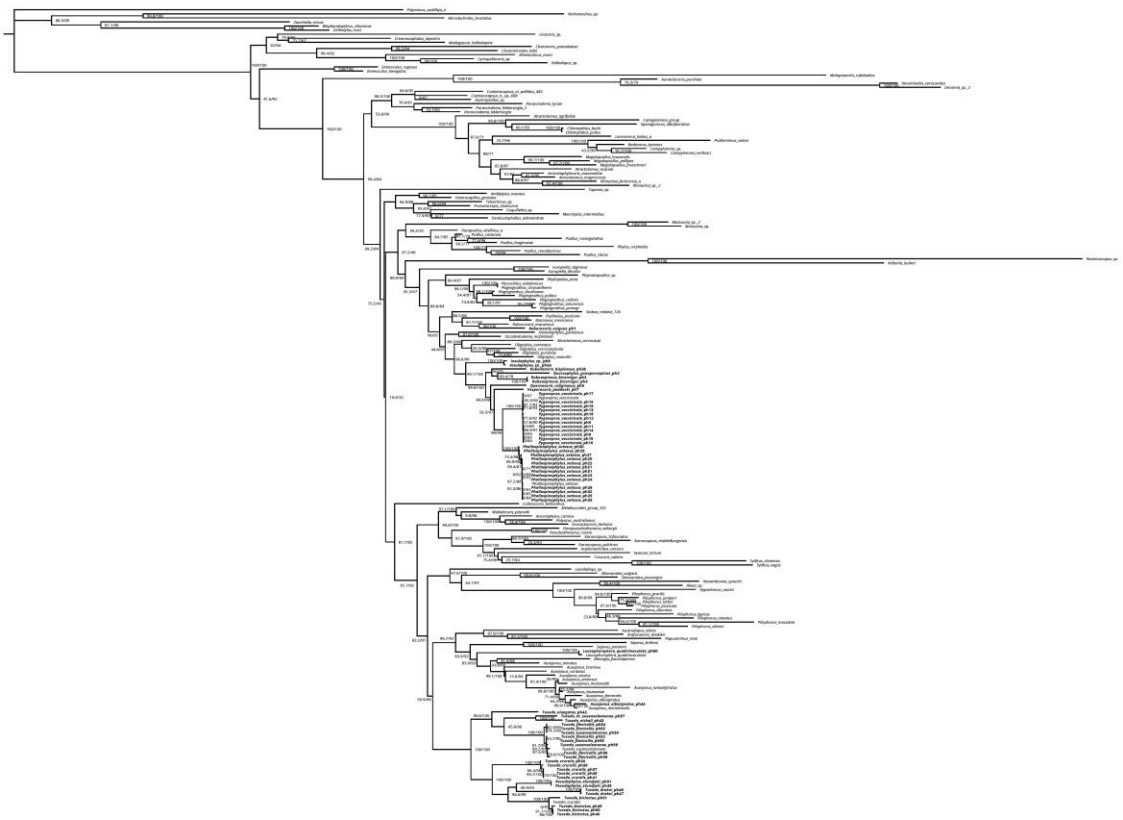

Figure 2.S3. Phylogeny of Phylinae, generated in IQ-TREE, specimens for which new data was gathered in bold font, values at nodes represent SH-aLRT and UFBoot support respectively.

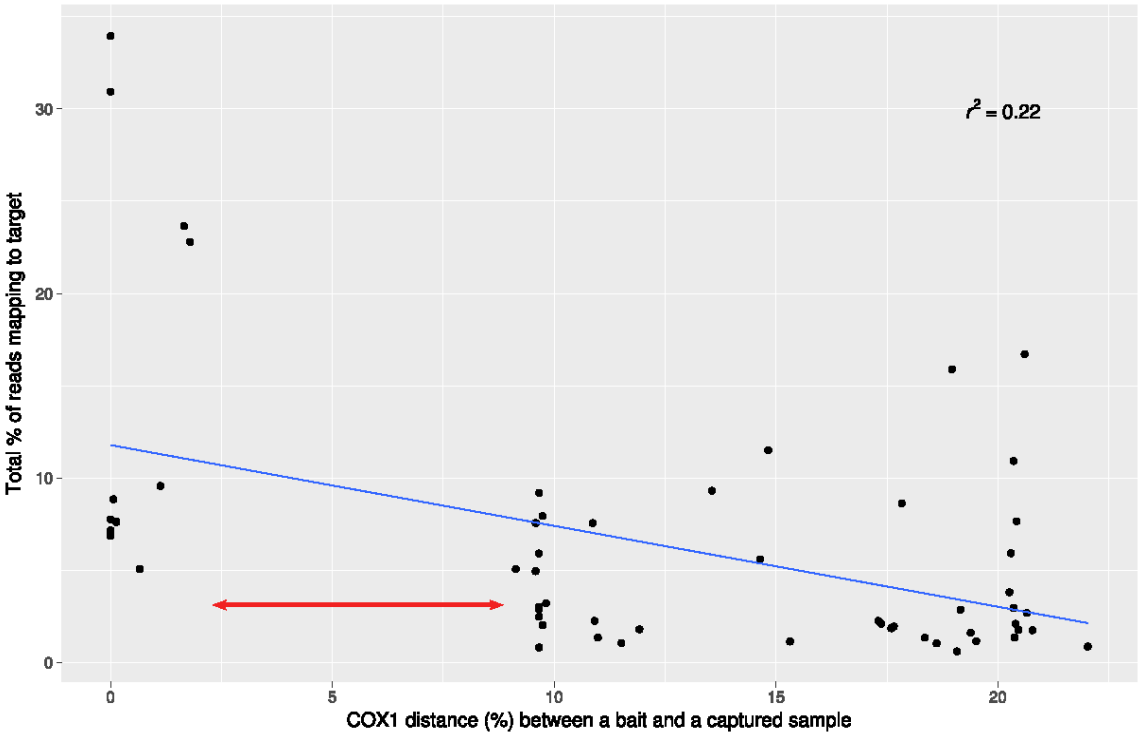

Figure 2.S4. Scatter plot showing relation between COX1 distance to bait and total percentage of reads on target. Red arrow indicates the gap between intra- and interspecific distances.

Chapter 3: Phylogenetic analysis of the *Corixidea* Reuter genus group

Abstract

While being a valuable source of specimens, insect natural history collections continue to be underutilized in molecular systematics, mostly due to difficulties in obtaining DNA sequences. Old specimens or specimens stored under suboptimal conditions are intractable for traditional Sanger sequencing. Phylogenomic next generation sequencing (NGS) methods are still expensive, however, coupling enrichment of DNA extracts for only few gene regions with NGS can decrease costs to those comparable with traditional Sanger sequencing. We here use an inexpensive hybrid capture with in-house generated baits to retrieve commonly utilized ribosomal and mitochondrial loci from old museum specimens and combine them with a Sanger generated dataset comprised of recently collected material. We focus on the *Corixidea* genus group (Schizopteridae), which comprises rarely collected, small (1-2mm), and primarily tropical insects of which only about 10-20% of the species have been described. A molecular phylogeny is needed to resolve relationships and revise the genus-level classification to correctly place the ~150 yet to be described species. The majority of specimens, however, were collected in the mid-20th century and are point-mounted or stored in 70% ethanol. Our dataset contains 101 taxa, 11 of which were preserved in low percentage ethanol, 48 are dry and point-mounted, and 40 are older than 20 years at DNA extraction. The hybrid capture generated dataset proved sufficient for reconstructing a well-supported phylogeny, and for the oldest successfully sequenced specimen (95 years) to be unambiguously placed in that phylogeny. We successfully sequenced several specimens with unquantifiable DNA in

the extract, as well as specimens visibly contaminated with fungus. Combination of this dataset with Sanger sequenced taxa produced a well-sampled phylogeny, with about 50% of the predicted diversity being represented. Ancestral character states of selected morphological features were inferred and used to reexamine homology hypotheses and inform an upcoming taxonomic revision.

Introduction

Molecular data have revolutionized systematic research during the past decades and, although lagging behind their ubiquity in vertebrate systematics, now also dominate the area of arthropod phylogenetics. PCR- and Sanger sequencing-based DNA sampling has primarily relied on freshly collected and appropriately stored individuals that can be expected to result in high-quality sequence data, in contrast to museum specimens that are often old and of poor quality (Burrell *et al.* 2015). However, many species of insects and other arthropods are only known from few archived individuals and rarely if ever recollected after initial description (Coddington *et al.* 2009; Lim *et al.* 2011). Museum specimens are therefore crucial when building densely sampled phylogenies of megadiverse lineages such as many groups of arthropods. While pinned and dry specimens may be intractable for PCR and Sanger sequencing approaches because of age or contamination with fungi, mites or pollen, liquid-preserved specimens pose their own set of challenges. For most of the past century, arthropods have been collected in bulk using passive collecting methods including Malaise traps, yellow pan traps, or leaf litter and soil extractions. Historical trap residues have often been preserved in lower percent ethanol, making specimens unsuitable for traditional molecular approaches. Nevertheless,

these trap residues have been accumulated in natural history collections around the world for decades, representing a massive, virtually untapped resource that has the potential to uncover biodiversity on a global scale. Next generation sequencing (NGS) methods now allow for the generation of DNA sequences from suboptimally preserved specimens, including subfossil remains (e.g., Gamba *et al.* 2015), old pinned specimens, and trap residues (Sproul & Maddison 2017).

A persistent problem with NGS approaches is that per-sample costs of phylogenomic scale applications is still too high for many research projects in arthropod systematics, where often a very large number of samples need to be incorporated into analyses. Whole genome sequencing approaches require substantial numbers of reads per sample even for low coverage assemblies and are typically used to resolve deeper level phylogenetic relationships or place selected critical taxa into an existing phylogeny (Kanda *et al.* 2015; Maddison & Cooper 2014). Target capture approaches, that enrich for 100s–1000s of loci, decrease the per sample sequencing costs, but require existing genomic and transcriptomic references for efficient bait design and include considerable expense for commercial probe synthesis (Bi *et al.* 2013; Blaimer *et al.* 2016; McCormack *et al.* 2015). Recently shown to be applicable to low quality ethanol-preserved arthropod samples (Wood *et al.* 2018), enrichment and sequencing of thousands of loci remains financially inaccessible in the context of taxonomic revisions in species rich groups where it may be critical to sequence 100 or more taxa. The majority of published taxonomic studies at the generic or tribal levels are therefore still only informed by morphology or by a Sanger-generated molecular dataset consisting of a small subsample

of species (Knyshov *et al.* 2016; Leon & Weirauch 2017). We aimed at mitigating these issues and advancing cost-efficient ways to sample molecular data from poorly preserved museum specimens for large integrative taxonomic projects and modified and tested on insects (Knyshov *et al.* in review) a previously developed hybrid capture approach (Maricic *et al.* 2010). The approach targets only selected commonly utilized loci, uses cheap in-house generated baits, and does not require genomic or transcriptomic resources for probe design. This allows for greater cost efficiency and a price per sample that is comparable to that of traditional Sanger sequencing.

The scope of the present study is the Neotropical *Corixidea* genus group – a putative clade currently consisting of six genera in one of the least studied families of hemipteran insects – Schizopteridae (Insecta: Hemiptera: Heteroptera). Despite comprising only ~350 described species (Weirauch *et al.* 2018), it is the largest family of the heteropteran infraorder Dipsocoromorpha, and several hundred species remain to be described. Schizopteridae are minute (1-2 mm total length) and typically dwell in leaf litter and other cryptic tropical forest microhabitats. Considered as "rare" in most natural history museums, they in fact remain uncurated in residues of bulk samples from leaf litter extraction, Malaise traps, yellow pan traps, or other passive collecting methods. Targeted residue-sample sorting led by us over a 3-year period has resulted in >17,000 specimens of Schizopteridae from all biogeographic regions, including ~8,000 from the New World, and with ~2,500 specimens belonging to the *Corixidea* genus group alone.

The *Corixidea* genus group was outlined by Emsley (1969), who included five genera of Neotropical schizopterids – *Corixidea* Reuter, *Hoplonannus* McAtee & Malloch,

Membracioides McAtee & Malloch, *Oncerodes* Uhler, and *Voccoroda* Wygodzinsky – with the sixth genus, *Voragocoris* Weirauch, added later (Weirauch 2012). Only 18 species are currently described in the genus group, but at least ~150 await description given our examination of available specimens. The group as a whole is well defined as monophyletic based on morphology (Emsley 1969; Weirauch 2012), but current generic concepts do not unambiguously accommodate many of the undescribed species. Among the genus-level diagnostic characters for *Corixidea* group genera and some other Schizopteridae are the presence, location, and structure of so-called male-specific organs (MSOs), which include prominent modifications on the head, thorax, and forewing that appear to be associated with glands (Hill 1990, 2004, 2013; Knyshov *et al.* 2016; Frankenberg *et al.* 2018; Weirauch 2012). Due to their conspicuous structure, MSOs are used to diagnose all or some species in three out of six genera of the *Corixidea* genus group (Emsley 1969; Weirauch 2012). The function of these structures is unknown, but given that they are absent in females and likely glandular, a role in the context of mate attraction and recognition or courtship and mating would seem plausible. MSOs also occur in eight genera outside the *Corixidea* genus group (Frankenberg *et al.* 2018; Hill 2004; Knyshov *et al.* 2016), but homology hypotheses have so far not been explored in a phylogenetic framework. The *Corixidea* genus group is a good system for such a study as only a single MSO may occur in a given species, suggesting that these structures may be homologous, despite differences in position on either head, prothorax, or forewing. Based on a densely sampled phylogeny, we will be able to test if MSOs in the *Corixidea* genus group are homologous, and if not, how many times and where they evolved.

We here use a densely sampled, robust molecular phylogeny and ancestral state reconstructions (ASRs) of putative genus-level diagnostic features to inform a taxonomic revision of the *Corixidea* genus group, attempting to set an example for revisionary systematic projects in other species rich clades. To produce a molecular dataset, we combined existing Sanger data from recently collected specimens with data generated from older, primarily point-mounted or residue-derived specimens using hybrid enrichment approaches. Voucher specimens are important for downstream assessment of morphological features, and we therefore utilized whole-body "non-destructive" DNA extraction for these fragile and tiny insects preserving diagnostic cuticular structures. Specifically, we aimed to 1) using hybrid enrichment approaches obtain sequence data for low-quality samples not accessible to traditional Sanger sequencing and sample ~50% of the estimated species-level diversity; 2) include specimens of different quality to determine robustness of the method on old age, low input DNA, contamination, and other factors; and 3) use ASR of several putatively genus-diagnostic features, including MSOs, to test homology hypotheses and shape the genus-level classification of the group for an upcoming taxonomic revisions.

Materials and Methods

Specimen Sampling and Vouchers

Sanger and Illumina datasets

For the Sanger dataset, a total of 73 specimens, representing 50 putative species, were selected for extraction, 42 of which were preserved in 95% ethanol, five point-mounted, and 18 preserved in 70% ethanol or ethanol of unknown quality. Specimen age at DNA extraction for the Sanger dataset ranged from 2 to 22 years (i.e. collected between 1995 and 2015). The Illumina dataset comprised 61 specimens, representing 60 putative species, of which 47 were point-mounted, three preserved in 95% ethanol, and 11 preserved in 70% ethanol or ethanol of unknown quality. DNA extracts from three specimens from the Sanger dataset (ED6683, ED5868, and ED4221) were used in the Illumina dataset for comparative purposes. Specimen age at DNA extraction for the Illumina dataset ranged from 9 to 106 years (collected between 1911 and 2008).

Voucher information

Specimens were collected during field trips conducted by the Weirauch and Heraty labs or loaned from various institutions (Tables 3.1, 3.2). The majority of ethanol preserved specimens were separated from bulk or residue samples. Prior to extraction, specimens were imaged in two or three views on a Leica DFC 450 C Microsystems imaging system with Planapo 1.0x or 2.0x objectives and stacked using Leica Application Suite V4.3. Label information was entered in the PBI instance of the Arthropod Easy Capture database, georeferenced, and made available through the http://research.amnh.org/pbi/heteropteraspeciespage/ website.

DNA Preparation and Sequencing Procedures

Sanger dataset

The abdomen was separated from the thorax to expose tissue in both tagmata, and specimens were incubated overnight in Qiagen ATL buffer and Proteinase K. The extractions were finalized following Qiagen DNeasy kit instructions and reagents. PCR for one 18S rDNA, two 28S rDNA, one COX1 and one 16S rDNA gene regions was conducted using EmeraldAMP GT mastermix (supplementary text 3.S1). For samples where we failed to recover the two 28S amplicons, we split the 28S regions further to a total of four reactions and attempted to amplify shorter fragments (supplementary text 3.S1). Generated amplicons were purified using SureClean or custom made SPRI beads mixture (Glenn *et al.* 2016; Rohland & Reich 2012). Amplicons were sequenced on an Applied Biosystems 3730xl DNA Sequencer at the Institute for Integrative Genome Biology (University of California Riverside; UCR) or at Macrogen USA. Sequences are uploaded to NCBI GenBank, accession numbers are indicated in Supplementary Table 3.1 (will be indicated in the final version of the paper).

Illumina dataset

PCR-generated baits for ribosomal and mitochondrial genes were prepared as in Knyshov *et al.* (in review) using the same 5'blocked primers. To reduce costs, we relied on long range PCR to amplify the ribosomal operon and mitochondrion in the lowest possible number of reactions. Since no ingroup sample of sufficient quality was available, a recently collected (2016) specimen (scpp77) of the closely related genus *Schizoptera* was used to produce amplicons for all target regions, with the *Corixidea* group sample

ED4276 used to generate additional mitochondrial baits. DNA extraction was initiated as for the Sanger dataset, however more thorough precautions (i.e. bleaching, blank controls) were utilized. Extractions were finalized using a QIAquick kit following kit instructions and reagents, following Knyshov *et al.* in review. Libraries were prepared without shearing, otherwise following Knyshov *et al.* (in review). Hybrid captures followed a pooled design from Knyshov *et al.* (in review), where individual libraries were pooled by 8 to 12 per capture reaction. Enriched pools were mixed with bait amplicons and two unenriched benchmarking libraries (for samples scpp7 and scpp54) and sequenced on ~50% of a MiSeq V3 lane at the Institute for Integrative Genome Biology (UCR). Raw reads are uploaded to the NCBI SRA, assembled sequences are uploaded to NCBI GenBank, accession numbers are indicated in Supplementary Table 3.S2 (will be indicated in the final version of the paper).

Sequence Data Processing

Sanger reads were processed using Sequencher V4.8 (http://www.genecodes.com) or Geneious 10 (Kearse *et al.* 2012). Illumina reads were first processed in Trimmomatic v0.36 (Bolger *et al.* 2014), then assembled using SPAdes 3.10.1 (Bankevich *et al.* 2012), with smaller contigs scaffolded across larger contigs of different samples or bait samples. BBmap (Bushnell 2014) was used to map reads to Illumina dataset assemblies to assess their quality and percent on target, and for common contaminants to assess contamination proportion. Individual genes were aligned in MAFFT v.7.271 (Katoh & Standley 2013) and gene trees generated using RAxML v. 8.2.10 (Stamatakis 2014) under GTRGAMMA model. Gene trees were inspected for presence of long branches as a proxy for

contamination, and using both read mapping and branch length information, original sequences were revisited to remove contaminant regions and mis-assemblies.

Phylogenetic Analyses

For the Sanger-only dataset, we minimize missing data by excluding taxa that had only a single gene region successfully sequenced and were morphologically similar to or conspecific with other taxa in the dataset. The Maximum Likelihood phylogenetic analyses were performed in IQ-TREE (Nguyen *et al.* 2014), and built-in ModelFinder (Kalyaanamoorthy *et al.* 2017) was used to determine the partitioning scheme and perform a model test. Branch support values were calculated using Ultrafast Bootstrap (Minh *et al.* 2013) and SH-aLRT (Anisimova & Gascuel 2006). This maximum likelihood analysis was repeated 10 times to assure convergence. Additionally, we ran a Bayesian analysis in MrBayes (Ronquist & Huelsenbeck 2003) with model parameters set to those obtained by IQ-TREE and branch support assessed using posterior probability values. The Illumina-only dataset was processed in the same way except that only genes with a low proportion of missing data (38 or more out of 60 taxa present) were selected for the final analysis. For a combined Sanger-Illumina analysis, the two datasets were merged by locus, aligned, and manually trimmed to adjust the gene size between the two datasets (the hybrid capture output spanned larger gene regions than the Sanger sequenced regions). Data matrices and resulting phylograms are uploaded to TreeBASE (accession numbers will be indicated in the final version of the paper).

Morphological Matrix and ASR

Voucher specimens were placed in glycerin after DNA extraction and morphological features were coded as outlined below. Schematic illustrations of character states were generated from light microscopical observations of voucher specimens and are shown on Figure 3.2.

1. Second costal cell: 0 – trapezoidal; 1 – rectangular.
2. Process of mediotergite 7: 0 – absent; 1 – present.
3. Medial process of mediotergite 8: 0 – absent; 1 – posteriorly directed; 2 – anteriorly directed; 3 – laterally directed.
4. Right side process of mediotergite 8: 0 – absent; 1 – present.
5. Denticulate area on mediotergite 8: 0 – absent; 1 – present.
6. Anophoric process: 0 – absent; 1 – present.
7. Conjunctival appendages: 0 – absent; 1 – present.
8. Posterior margin of pygophore: 0 – symmetrical; 1 – asymmetrical.
9. Anterior right-side process of pygophore: 0 – absent; 1 – present.
10. Ventral cavity of pygophore: 0 – absent; 1 – present.
11. Right paramere direction: 0 – left; 1 – anterior.

More details on character selection and description are provided in the Supplementary Text 3.S2. A joint maximum likelihood ASR was performed in R (R Core Team 2017) using the APE package (Paradis *et al.* 2004). Branch lengths may have an impact on the ASR (Cusimano & Renner 2014), and non-random missing data distribution in our combined dataset have led to some terminal branches being very short, or of length zero

(Fig. 3.S4). This has affected ASR of some internal nodes (data not shown), and in order to mitigate these effects, prior to the final reconstruction, the phylogeny was transformed to ultrametric using penalized likelihood (Sanderson 2002). Additionally, outgroup taxa (10 terminals) and female specimens (7 terminals) were removed from the phylogeny, as primarily male characters were used.

We observed only one type of MSO in each individual and species, and despite different positions on the head or thorax and a range of cuticular modifications associated with the organ, the underlying gland or glandular trichomes are similar. We therefore tested if MSOs across the *Corixidea* group may be homologous by coding the differently positioned organs as different states of the same character in our ASR. The seven states representing topological categories were coded as follows, with colors in parentheses corresponding to of pie charts in Figure 3.3: absent (grey); frons (blue); posterior vertex to anterior pronotum (yellow); posterior pronotum (purple); scutellum (green); clavus of the forewing (red); corium of the forewing (orange). Character states were illustrated using scanning electron micrographs (SEM) taken on a FEI XL30-FEG microscope. ASR was carried out as above. Illustrations were generated using the R packages APE (Paradis *et al.* 2004) and ggtree (Yu *et al.* 2016).

Results

DNA Extraction and Sequencing Results

Sanger dataset

Out of 73 extracted specimens 62 produced at least one successfully sequenced PCR product (Supplementary Table S1). Most of the dry or 70% ethanol preserved specimens

failed, with the oldest successfully Sanger-sequenced specimen having been collected in 1995 and preserved in 70% ethanol, although only two small fragments of 28S were recovered.

Illumina dataset

The quality of DNA extracts for the Illumina dataset is shown in Supplementary Table 3.S2. Extraction of 11 of the 61 samples resulted in unquantifiable DNA. On average 12.4 ng was used to produce libraries. As a result of pooling and sequencing 111,016 PE clusters were produced on average per sample (Table 3.2). Significant contamination was observed in some samples, with the most abundant contaminants being *Aspergillus* sp. and *Homo sapiens*. The highest proportion of fungus reads was detected in specimens severely overgrown with fungus (Fig. 3.1). Two samples (scpp52 and scpp54; collected in 1932 and 1911, respectively) produced only contaminant reads, most of which mapped to *Aspergillus* sp. Thus, the oldest successfully sequenced dry point-mounted specimen was collected in 1922, the oldest sequenced 70%-ethanol preserved specimen in 1975.

Capture efficiency

The percent on target varied from 0.8% to 40%, and averaged at 12% (Table 3.2). One of the two samples tested in both enriched and unenriched conditions (sample scpp7, 1994 year of collection) yielded 0.07% on target without capture vs 4.8% after capture (68-fold increase). The other tested sample (scpp54, 1911 year of collection) yielded only contaminant reads in both enriched and unenriched conditions, however the percent of reads mapping to *Aspergillus* sp. ribosomal operon increased from 0.26% before capture to 8.9% after capture (34-fold increase). On average, 82% of nuclear ribosomal operon

genes and 27% of the mitochondrial genome were recovered per sample. The relationship between collection year, preservation type, percent of target recovered, and contamination proportion is shown in Figure 3.1.

Sequencing Comparison between Sanger and Illumina Datasets

Samples used for both Sanger and Illumina datasets produced better results after enrichment: sample ED5868 (70% ethanol), for which only short fragments of 28S had been amplified using Sanger sequencing, yielded near complete ribosomal and partial mitochondrial sequence after capture, while sample ED4221 (70% ethanol) for Sanger sequencing failed entirely, produced a near complete ribosomal sequence after capture (Fig. 3.1). Despite lower success rate in retrieving mitochondrial genes in the Illumina dataset, its missing data proportion is comparable to that of the Sanger dataset for mitochondrial regions of interest: 47% (Sanger) vs 60% (Illumina) for cytochrome oxidase 1 and 33% (Sanger) vs 38% (Illumina) for 16S rDNA.

Cost Comparison between Sanger and Illumina Datasets

Sample processing for the Sanger dataset ranged between $26.50-40.50 ($2.6-4.0 per reaction x 2 directions x 5 gene regions + $0.3 PCR cost + $0.25 cleaning), excluding DNA extraction costs. Approximately 3600 bp were generated at about $7.36-$11.25 per 1 Kb of data. Costs associated with the Illumina dataset are similar to results reported in Knyshov *et al.* (in review) and are approximately $40 per sample excluding DNA extraction cost, consisting of $25 for preparation reagents and $13.6 for sequencing. Approximately 10Kb were generated at about $4 per 1 Kb of data. Given the amount of reads on target in unenriched libraries, we estimate that about 50 times more reads (5

million) per sample would be required for a low coverage whole genome sequencing strategy to obtain the same data. Only the use of the new generation of sequencers such as Illumina HiSeq X or NovaSeq would therefore result in a comparable cost per sample.

Phylogenetic Analyses

The final Sanger dataset consisted of 4 genes and 3,575 bp with 42 ingroup taxa and nine outgroup taxa. The proportion of missing data was 37.63%. We generated several Illumina datasets depending on number of genes included, with the largest comprising 10 genes, 14,508 bp, and a proportion of missing data of 40.73%. The final Illumina dataset that we considered to be optimal in terms of phylogenetic resolution and amount of missing data (29.13%) consisted of 6 genes and 9,656 bp. We used the sequenced bait donor specimen of *Schizoptera* sp. (scpp77) as an outgroup.

The maximum likelihood phylogeny based on this Illumina dataset using IQ-TREE is shown in Figure 3.1, with the results of the MrBayes analysis is in Supplementary Figure 3.S1. The phylogeny reconstructed from the Sanger dataset is shown in Supplementary Figures 3.S2 and 3.S3. The results of the combined Sanger and Illumina likelihood analysis are shown as Figures 3.2 and 3.3, with outgroups and female specimens removed. Results of the unpruned combined analyses are available as Supplementary Figures 3.S4 and 3.S5.

Separate phylogenetic analyses of the Sanger and Illumina datasets recovered mostly congruent topologies, with all numbered focal clades recovered in both analyses, and with absolute or near absolute support in the Illumina-derived analysis (compare Figs 3.1 and 3.S2). Deeper level support was higher in the Illumina dataset, but nevertheless

support between some of the focal clades has remained low (e.g., the branch leading to clade 1 + (clade 2 + clade 3)). Among the focal clades, clade 7 corresponds to the genus *Hoplonannus* (based on sampled described species, see Figs 3.S2-S5), clade 1 to *Membracioides* (based on sampled species being morphologically similar to described species), and clade 3 to *Voragocoris* (based on sampled described species, see Figs 3.S2-S5), confirming their monophyly. Sampled species of *Corixidea* that included the described species *C. crassa* McAtee & Malloch, *C. major* McAtee & Malloch, and *C. doddsi* Van Duzee (see Figs 3.1, 3.S2-S5), fell into two distinct clades (5 and 6), suggesting that the genus is paraphyletic. Based on the presence of diagnostic and synapomorphic morphological features, clade 6 also includes *C. beebei* Emsley, *C. julieae* Emsley, and *C. underwoodi* Emsley, while *C. major* and *C. doddsi*, as well as several undescribed species, belong to clade 5. Clades 3, 4, 8, and 9 do not align with any of the described genera, and will likely be described as new genera, should ASR of diagnostic features find them to be diagnosable (see below).

Reconstruction of diagnostic features, including MSOs

Results of the ASR of morphological features are summarized on Figure 3.2 as bar plots with probabilities of character states for focal nodes. Based on this reconstruction (Fig. 3.2), clades are recognized by the following combination of characters: *Membracioides* (clade 1) by a posteriorly directed process of tergum 8 (character 3: state 1) and the presence of conjunctival appendages (7: 1); *Voragocoris* (clade 2) by a posteriorly directed process of tergum 8 (3: 1) and the presence of a ventral cavity on the pygophore (10: 1); the *Corixidea major* group (clade 5) by a laterally directed process on tergum 8

(3: 3) and the presence of a serrated area on tergum 8 (5: 1); the *Corixidea crassa* group (clade 6) with one sub-clade characterized by the anteriorly directed process of tergum 8 (3: 2), and the other by the combination of a laterally directed process of tergum 8 (3: 3) and the presence of an anophoric process (6: 1); and *Hoplonannus* (clade 7) by the presence of an anophoric process (6: 1). Although no species of *Voccoroda* were sampled, *Voccoroda carioca* Wygodzinsky is likely to fall into clade 5 based on presence of the laterally directed process of tergum 8 and lack of an anophoric process. The monotypic genus *Oncerodes*, known only from the coleopteroid female holotype, cannot be placed in the current phylogenetic framework; coleopteroidy evolved at least four times independently in the *Corixidea* genus group, and females lack other genus-level diagnostic features.

Our test of homology of MSOs and reconstruction of their ancestral location on the body indicate that the most recent common ancestor of the *Corixidea* genus group did not possess a MSO and that these structures evolved eight times independently in seven of the nine recognized clades (Fig. 3.3). The most recent common ancestors of clades 1, 2, and 6 featured MSOs posteriorly on the pronotum, frons, and clavus, respectively. All examined species of *Voragocoris* (clade 2) have a similarly structured and positioned frontal MSO. In contrast, only certain species of *Membracioides* (clade 1) carry the MSO-associated pronotal extension, while MSOs in other species are located on the anterior margin of the pronotum or the forewing, or are lost. Similarly, even though a claval MSO is the most likely reconstruction for the most recent common ancestor of clade 6, one species within the group has lost this MSO and it is located on the anterior

margin of the pronotum in other species. Our reconstructions show that MSOs on the posterior margin of the vertex or anterior part of the pronotum evolved nine times independently in five of the genus-level clades (yellow in Fig. 3.3), making this character unsuitable as a genus-level diagnostic feature.

Discussion

We here show that custom-generated bait capture and Illumina sequencing procedures allow for inexpensive collection of DNA sequence data from both pinned and low-percentage ethanol archival insect specimens, as a complement to traditional Sanger sequencing datasets. This set of approaches has the potential to transform integrative taxonomy of species rich arthropod groups by generating robust phylogenetic frameworks based on a large number of terminals. Importantly, it can capitalize on the hidden biodiversity resources formed by suboptimally preserved, historical passive trap residues. Employing the same bait synthesis reagents and primers as Knyshov *et al.* (in review) used for plant bugs (Hemiptera: Miridae), we highlight the universality and low cost of modification of this toolkit to the distantly related true bug family Schizopteridae. We obtained near complete 18S and 28S sequences as well as partial mitochondrial sequences for most specimens, including for extracts with low or unquantifiable DNA concentrations and specimens up to 95 years old. Sequencing was also successful for low-quality ethanol preserved specimens from residue samples, as well as for specimens visibly contaminated with fungi. Since baits spanned complete ribosomal and mitochondrial sequences, on average 3-fold more data was recovered compared to our Sanger dataset, yielding a better resolved and supported topology. Mitochondrial captures

performed on average worse than ribosomal, potentially due to the fairly large phylogenetic distances between baits and samples compared to the design of Knyshov *et al.* (in review). Nevertheless, the proportion of missing data for targeted mitochondrial markers was comparable between the Illumina and Sanger datasets. Overall, our results suggest a broad applicability of the utilized techniques to other groups of neglected, small, and/or species rich arthropods.

Our findings highlight the importance of the DNA-based phylogenies for descriptive taxonomy. We were able to detect several well-supported clades within the sampled *Corixidea* genus group specimens. ASR of selected morphological characters showed that while only few characters are uniquely synapomorphic and many others are homoplastic, the clades can be unambiguously identified by a combination of several characters. Thus, the produced phylogenetic hypotheses, which also include several representatives of previously described genera, can be easily translated into a new classification of the group. Four or five new genera would be described to accommodate newly detected clades. Additionally, the genus *Corixidea* was recovered as paraphyletic and should be split into two genera.

While MSOs have been widely used as diagnostic characters in schizopterid taxonomy, we showed that these organs are highly homoplastic within the *Corixidea* genus group and often not suitable as diagnostic features, although they are group-defining for certain clades. A notable exception is *Voragocoris*, where the frontal MSO was present in the most recent common ancestor of this clade, and is retained in all descendants. Our reconstructions show that MSOs evolved convergently multiple times, with only two of

the nine clades lacking MSOs in all species. Intriguingly, MSOs can differ dramatically between closely related species, and based on our likelihood reconstructions we detected two instances where the MSO position appears to have switched between the pronotum and the forewing, essentially questioning if the positional homology criterion applies to these structures. Assuming that all MSOs exude glandular secretions, potentially used during mate attraction or mating, sexual selection may be involved in shaping and diversifying these organs. Closer examination of the MSO ultrastructure, analysis of the chemical composition of the associated glands and molecular mechanisms underlying their function, as well as behavioral experiments could further shed light on the evolution and function of this intriguing system.

References

Anisimova, M. & Gascuel, O. (2006) Approximate likelihood-ratio test for branches: a fast, accurate, and powerful alternative. *Systematic Biology* 55(4), 539–552.

Bankevich, A., Nurk, S., Antipov, D., Gurevich, A. A., Dvorkin, M., Kulikov, A. S., Lesin, V. M., Nikolenko, S. I., Pham, S., Prjibelski, A. D., Pyshkin, A. V., Sirotkin, A. V., Vyahhi, N., Tesler, G., Alekseyev, M. A. & Pevzner P. A. (2012) SPAdes: a new genome assembly algorithm and its applications to single-cell sequencing. *Journal of Computational Biology* 19(5), 455-477.

Bi, K., Linderoth, T., Vanderpool, D., Good, J. M., Nielsen, R. & Moritz, C. (2013) Unlocking the vault: next-generation museum population genomics. *Molecular Ecology* 22(24), 6018-6032.

Blaimer, B. B., Lloyd, M. W., Guillory, W. X. & Brady, S. G. (2016) Sequence capture and phylogenetic utility of genomic ultraconserved elements obtained from pinned insect specimens. *PloS One* 11(8), e0161531.

Bolger, A. M., Lohse, M. & Usadel, B. (2014) Trimmomatic: a flexible trimmer for Illumina sequence data. *Bioinformatics* 30(15), 2114-2120.

Burrell, A. S., Disotell, T. R. & Bergey, C. M. (2015) The use of museum specimens with high-throughput DNA sequencers. *Journal of Human Evolution* 79, 35-44.

Bushnell B. (2014) BBMap: a fast, accurate, splice-aware aligner.

Coddington, J. A., Agnarsson, I., Miller, J. A., Kuntner, M. & Hormiga, G. (2009) Undersampling bias: the null hypothesis for singleton species in tropical arthropod surveys. *Journal of Animal Ecology* 78(3), 573-584.

Cusimano, N. & Renner, S.S. (2014) Ultrametric trees or phylograms for ancestral state reconstruction: does it matter. *Taxon* 63(4), 721–726.

Emsley, M.G. (1969) The Schizopteridae (Hemiptera: Heteroptera) with the descriptions of new species from Trinidad. *Memoirs of the American Entomological Society* 25, 1–154.

Frankenberg, S., Hoong, C., Knyshov, A. & Weirauch, C. (2018) Heads up: evolution of exaggerated head length in the minute litter bug genus *Nannocoris* Reuter (Hemiptera: Schizopteridae). *Organisms Diversity & Evolution* 18(2), 211–224.

Gamba, C., Hanghøj, K., Gaunitz, C., Alfarhan, A.H., Alquraishi, S.A., Al-Rasheid, K.A., Bradley, D.G. & Orlando, L. (2016) Comparing the performance of three ancient

DNA extraction methods for high-throughput sequencing. *Molecular Ecology Resources* 16(2), 459–469.

Glenn, T. C., Nilsen, R., Kieran, T. J., Finger, J. W., Pierson, T. W., Bentley, K. E., Hoffberg, S., Louha, S., Garcia-De-Leon, F. J., Portilla, M. A. R., Reed, K., Anderson, J. L., Meece, J. K., Aggery, S., Rekaya, R., Alabady, M., Belanger, M., Winker, K. & Faircloth, B. C. (2016) Adapterama I: universal stubs and primers for thousands of dual-indexed Illumina libraries (iTru & iNext). *BioRxiv*, 049114.

Hill, L. (1990) Australian *Ogeria* Distant (Heteroptera: Schizopteridae). *Invertebrate Systematics* 4(4), 697–720.

Hill, L. (2004) *Kaimon* (Heteroptera: Schizopteridae), a new, speciose genus from Australia. *Memoirs of the Queensland Museum* 49(2), 603–647.

Hill, L. (2013) A revision of *Hypselosoma* Reuter (Insecta: Heteroptera: Schizopteridae) from New Caledonia. *Memoirs of the Queensland Museum* 56(2), 407–455.

Kalyaanamoorthy, S., Minh, B. Q., Wong, T. K., von Haeseler, A. & Jermiin, L. S. (2017) ModelFinder: fast model selection for accurate phylogenetic estimates. *Nature Methods* 14(6), 587.

Kanda, K., Pflug, J. M., Sproul, J. S., Dasenko, M. A. & Maddison, D. R. (2015) Successful recovery of nuclear protein-coding genes from small insects in museums using Illumina sequencing. *PLoS One* 10(12), e0143929.

Katoh, K. & Standley, D. M. (2013) MAFFT multiple sequence alignment software version 7: improvements in performance and usability. *Molecular Biology and Evolution* 30(4), 772-780.

Kearse, M., Moir, R., Wilson, A., Stones-Havas, S., Cheung, M., Sturrock, S., Buxton, S., Cooper, A., Markowitz, S., Duran, C., Thierer, T., Ashton, B., Meintjes, P. & Drummond A. (2012) Geneious Basic: an integrated and extendable desktop software platform for the organization and analysis of sequence data. *Bioinformatics* 28(12), 1647-1649.

Knyshov, A., Leon, S., Hoey-Chamberlain, R. & Weirauch, C. (2016) *Pegs, pouches, and spines: systematics and comparative morphology of the New World litter bug genus Chinannus Wygodzinsky, 1948*. Entomological Society of America, Annapolis, MD.

Leon, S. & Weirauch, C. (2017) Molecular phylogeny informs generic and subgeneric concepts in the *Schizoptera* Fieber genus group (Heteroptera: Schizopteridae) and reveals multiple origins of female-specific elytra. *Invertebrate Systematics* 31, 191–207.

Lim, G. S., Balke, M. & Meier, R. (2011) Determining species boundaries in a world full of rarity: singletons, species delimitation methods. *Systematic Biology* 61(1), 165-169.

Maddison, D. R. & Cooper, K. W. (2014) Species delimitation in the ground beetle subgenus *Liocosmius* (Coleoptera: Carabidae: Bembidion), including standard and next-generation sequencing of museum specimens. *Zoological Journal of the Linnean Society* 172(4), 741-770.

Maricic, T., Whitten, M. & Pääbo, S. (2010) Multiplexed DNA sequence capture of mitochondrial genomes using PCR products. *PloS One* 5(11), e14004.

McCormack, J. E., Tsai, W. L. & Faircloth, B. C. (2015) Sequence capture of ultraconserved elements from bird museum specimens. *Molecular Ecology Resources* 16(5), 1189-1203.

Minh, B. Q., Nguyen, M. A. T. & von Haeseler, A. (2013) Ultrafast approximation for phylogenetic bootstrap. *Molecular Biology and Evolution* 30(5), 1188-1195.

Nguyen, L. T., Schmidt, H. A., von Haeseler, A. & Minh, B. Q. (2014) IQ-TREE: a fast and effective stochastic algorithm for estimating maximum-likelihood phylogenies. *Molecular Biology and Evolution* 32(1), 268-274.

Paradis, E., Claude, J. & Strimmer, K. (2004) APE: analyses of phylogenetics and evolution in R language. *Bioinformatics* 20(2), 289-290.

Rohland, N. & Reich, D. (2012) Cost-effective, high-throughput DNA sequencing libraries for multiplexed target capture. *Genome Research* 22(5), 939-946.

Ronquist F. & Huelsenbeck J.P. (2003) MrBayes 3: Bayesian phylogenetic inference under mixed models. *Bioinformatics* 19(12), 1572–1574.

Sanderson, M.J. (2002) Estimating absolute rates of molecular evolution and divergence times: a penalized likelihood approach. *Molecular Biology and Evolution* 19(1), 101–109.

Sproul, J.S. & Maddison, D.R. (2017) Sequencing historical specimens: successful preparation of small specimens with low amounts of degraded DNA. *Molecular Ecology Resources* 17(6), 1183–1201.

Stamatakis, A. (2014) RAxML version 8: a tool for phylogenetic analysis and post-analysis of large phylogenies. *Bioinformatics* 30(9), 1312-1313.

Weirauch, C. (2012) *Voragocoris schuhi*, a new genus and species of Neotropical Schizopterinae (Hemiptera: Schizopteridae). *Entomologia Americana* 118, 285–294.

Weirauch, C., Whorrall, K., Knyshov, A. & Hoey-Chamberlain, R. (2018) Giant among dwarfs: *Meganannus lewisi*, gen. n. and sp. n., a new genus and species of minute litter bugs from Costa Rica (Hemiptera: Schizopteridae). *Zootaxa* 4370, 156–170.

Wood, H.M., González, V.L., Lloyd, M., Coddington, J. & Scharff, N. (2018) Next-generation museum genomics: Phylogenetic relationships among palpimanoid spiders using sequence capture techniques (Araneae: Palpimanoidea). *Molecular Phylogenetics and Evolution* 127, 907–918.

Yu, G., Smith, D. K., Zhu, H., Guan, Y. & Lam, T. T. Y. (2016) ggtree: an R package for visualization and annotation of phylogenetic trees with their covariates and other associated data. *Methods in Ecology and Evolution* 8(1), 28-36.

Table 3.1. Information on the vouchers used in the final Sanger dataset analyses

sample code	year	preservation	deposition	clade (genus)	species
ED4	2010	EtOH 95%	UCRC	1 (*Membracioides*)	
ED82	2010	EtOH 95%	UCRC	7 (*Hoplonannus*)	
ED86	2010	EtOH 95%	UCRC	6 (*Corixidea*)	*C. crassa*
ED206	2010	EtOH 95%	UCRC	2 (*Voragocoris*)	
ED207	2010	EtOH 95%	UCRC	1 (*Membracioides*)	
ED253	?	EtOH 95%	UCRC	5 (*Corixidea*)	
ED254	2011	EtOH 95%	UCRC	2 (*Voragocoris*)	*V. schuhi*
ED261	2010	EtOH 95%	UCRC	6 (*Corixidea*)	
ED293	2010	EtOH 95%	UCRC	6 (*Corixidea*)	
ED363	2010	EtOH 95%	UCRC	7 (*Hoplonannus*)	
ED371	2010	EtOH 95%	UCRC	7 (*Hoplonannus*)	
ED377	2010	EtOH 95%	UCRC	1 (*Membracioides*)	
ED394	2011	EtOH ?%	UCRC	1 (*Membracioides*)	
ED478	2000	EtOH ?%	IAvH	1 (*Membracioides*)	
ED479	2000	EtOH ?%	IAvH	7 (*Hoplonannus*)	
ED528	2000	EtOH ?%	IAvH	1 (*Membracioides*)	
ED939	2000	EtOH ?%	IAvH	1 (*Membracioides*)	
ED1010	?	EtOH ?%	UCRC	7 (*Hoplonannus*)	
ED1012	?	EtOH ?%	UCRC	6 (*Corixidea*)	
ED1019	?	EtOH ?%	UCRC	8	
ED1112	2000	EtOH ?%	UCRC	6 (*Corixidea*)	
ED1113	2000	EtOH ?%	UCRC	7 (*Hoplonannus*)	
ED1217	2013	EtOH 95%	UCRC	7 (*Hoplonannus*)	
ED1218	2013	EtOH 95%	UCRC	7 (*Hoplonannus*)	
ED2213	2013	EtOH 95%	UCRC	7 (*Hoplonannus*)	*H. craneae*
ED2662	2013	EtOH 95%	UCRC	7 (*Hoplonannus*)	*H. craneae*
ED3001	2001	EtOH ?%	IAvH	9	
ED3466	2013	EtOH 95%	UCRC	7 (*Hoplonannus*)	*H. paenebrunneus*
ED3787	2001	EtOH ?%	IAvH	6 (*Corixidea*)	
ED3886	2011	EtOH 95%	UCRC	1 (*Membracioides*)	
ED3923	2014	EtOH 70%	FSCA	5 (*Corixidea*)	*C. major*
ED4214	2011	EtOH 95%	FMNH	1 (*Membracioides*)	
ED4219	2008	EtOH 95%	FMNH	1 (*Membracioides*)	
ED4276	2014	EtOH 95%	UCRC	1 (*Membracioides*)	
ED6507	2010	EtOH 95%	UCRC	1 (*Membracioides*)	
ED6635	2010	EtOH ?%	UCRC	1 (*Membracioides*)	

ED6797	2015	EtOH 95%	UCRC	7 (*Hoplonannus*)	
ED7200	2015	EtOH 95%	MTEC	7 (*Hoplonannus*)	
ED7232	2011	EtOH 95%	UCRC	1 (*Membracioides*)	
ED7234	2014	dry	WSU	5 (*Corixidea*)	
ED7236	2013	dry	WSU	6 (*Corixidea*)	
ED9220	2012	dry	INBIO	7 (*Hoplonannus*)	

Table 3.2. Information on the vouchers used in the Illumina dataset

sample code	year	preservation	deposition	raw clusters	Total % on target	18S & 28S completeness	Mitochondrion completeness	clade (genus)	species
scpp1	1994	dry	FSCA	102401	16.848	0.93	0.18	7 (*Hoplonannus*)	
scpp2	1992	dry	FSCA	28251	11.039	0.70	0.00	4	
scpp3	1992	dry	FSCA	24227	4.721	0.53	0.00	6 (*Corixidea*)	
scpp4	1992	dry	FSCA	27573	9.010	0.55	0.00	6 (*Corixidea*)	
scpp5	1998	dry	UCRC	191004	15.348	0.95	0.24	5 (*Corixidea*)	
scpp6	1999	dry	TAMU	155352	17.959	0.95	0.00	6 (*Corixidea*)	
scpp7	1994	dry	USNM	173379	4.833	0.94	0.71	1 (*Membracioides*)	
scpp8	1994	dry	USNM	163840	16.474	0.95	0.45	1 (*Membracioides*)	
scpp9	1996	dry	USNM	110026	0.811	0.60	0.11	3 (*Voragocoris*)	
scpp10	1997	dry	TAMU	163875	7.601	0.92	0.00	2	
scpp11	1998	dry	UCRC	74587	9.192	0.81	0.19	2	
scpp12	1997	dry	TAMU	285132	40.115	0.95	0.54	1 (*Membracioides*)	
scpp13	1997	dry	TAMU	188520	3.524	0.94	0.69	8	
scpp14	1968	dry	BMNH	62435	9.894	0.92	0.00	6 (*Corixidea*)	
scpp15	1963	dry	AMNH	52953	15.164	0.87	0.00	6 (*Corixidea*)	
scpp16	1963	dry	AMNH	82713	10.123	0.93	0.00	1 (*Membracioides*)	
scpp17	1963	dry	AMNH	27531	12.119	0.75	0.00	6 (*Corixidea*)	
scpp18	1991	dry	UCD	36206	6.741	0.71	0.00	1 (*Membracioides*)	
scpp19	1996	dry	FSCA	48760	11.390	0.68	0.13	4	
scpp20	1972	dry	AMNH	78792	4.448	0.85	0.17	7 (*Hoplonannus*)	
scpp21	1963	dry	AMNH	50463	6.005	0.89	0.15	3 (*Voragocoris*)	
scpp22	1963	dry	AMNH	60932	11.972	0.65	0.00	3 (*Voragocoris*)	
scpp23	1973	dry	AMNH	62657	8.388	0.93	0.44	6 (*Corixidea*)	
scpp24	1972	dry	AMNH	132980	4.044	0.92	0.31	6 (*Corixidea*)	
scpp25	1953	dry	AMNH	40850	11.513	0.95	0.53	5 (*Corixidea*)	
scpp26	1981	dry	UCD	82353	8.157	0.95	0.57	7 (*Hoplonannus*)	
scpp27	1967	dry	USNM	55416	10.762	0.95	0.24	7 (*Hoplonannus*)	
scpp28	1999	dry	TAMU	212556	34.143	0.95	0.57	1 (*Membracioides*)	
scpp29	1952	dry	USNM	119503	27.798	0.56	0.36	6 (*Corixidea*)	
scpp30	1971	dry	AMNH	178563	5.176	0.95	0.22	1 (*Membracioides*)	
scpp31	1994	dry	USNM	46741	1.351	0.44	0.00	8	
scpp32	1972	dry	AMNH	159271	13.493	0.95	0.60	3 (*Voragocoris*)	
scpp33	1987	dry	USNM	270567	7.982	0.95	0.44	6 (*Corixidea*)	
scpp34	1964	dry	AMNH	86641	7.530	0.91	0.30	5 (*Corixidea*)	
scpp35	1984	dry	USNM	140942	3.444	0.95	0.82	4	
scpp36	1986	dry	TAMU	34837	1.151	0.40	0.05	6 (*Corixidea*)	
scpp37	2002	70% EtOH	FMNH	82363	0.895	0.75	0.01	5 (*Corixidea*)	
scpp38	1995	70% EtOH	FMNH	85697	5.098	0.95	0.51	2	
scpp39	2008	95% EtOH	MTEC	94588	8.920	0.95	0.81	2	
scpp40	2003	?% EtOH	UCRC	112939	23.529	0.81	0.40	4	
scpp41	1993	70% EtOH	FMNH	131573	5.089	0.91	0.41	9	
scpp42	1975	70% EtOH	FMNH	67107	6.319	0.93	0.24	2	
scpp43	1996	70% EtOH	USNM	30322	4.406	0.89	0.32	8	
scpp44	1999	95%	UCRC	88273	14.044	0.94	0.29	7 (*Hoplonannus*)	

		EtOH							
scpp45	1997	95% EtOH	UCRC	532156	1.122	0.93	0.50	7 (*Hoplonannus*)	
scpp46	2001	70% EtOH	IAvH	68078	31.301	0.95	0.38	1 (*Membracioides*)	
scpp47	2001	70% EtOH	IAvH	62202	6.256	0.95	0.10	9	
scpp48	2000	70% EtOH	IAvH	51980	13.241	0.95	0.52	1 (*Membracioides*)	
scpp49	2001	?% EtOH	LACM	111706	13.638	0.93	0.18	7 (*Hoplonannus*)	
scpp50	1995	?% EtOH	LACM	74057	2.013	0.95	0.08	1 (*Membracioides*)	
scpp51	2001	dry	TAMU	353231	36.916	0.95	0.21	8	
scpp52	1932	dry	AMNH	37974	11.091	0.00	0.00	Uknown	
scpp53	1997	dry	TAMU	170352	40.205	0.97	0.00		
scpp54	1911	dry	USNM	35269	8.932	0.00	0.00	3 (*Voragocoris*)	
scpp55	1963	dry	USNM	151826	9.006	0.95	0.66	1 (*Membracioides*)	
scpp56	1985	dry	TAMU	194792	9.688	0.95	0.25	1 (*Membracioides*)	
scpp57	1966	dry	AMNH	219543	2.088	0.93	0.69	1 (*Membracioides*)	
scpp58	1981	dry	UCD	51034	5.800	0.84	0.30	3 (*Voragocoris*)	
scpp59	1999	dry	TAMU	103479	15.877	0.93	0.57	1 (*Membracioides*)	
scpp60	1945	dry	USNM	29366	17.721	0.43	0.00	5 (*Corixidea*)	
scpp61	1922	dry	CAS	19281	23.343	0.83	0.16	5 (*Corixidea*)	*C. doddsi*
Average				111017	11.587	0.82	0.27		

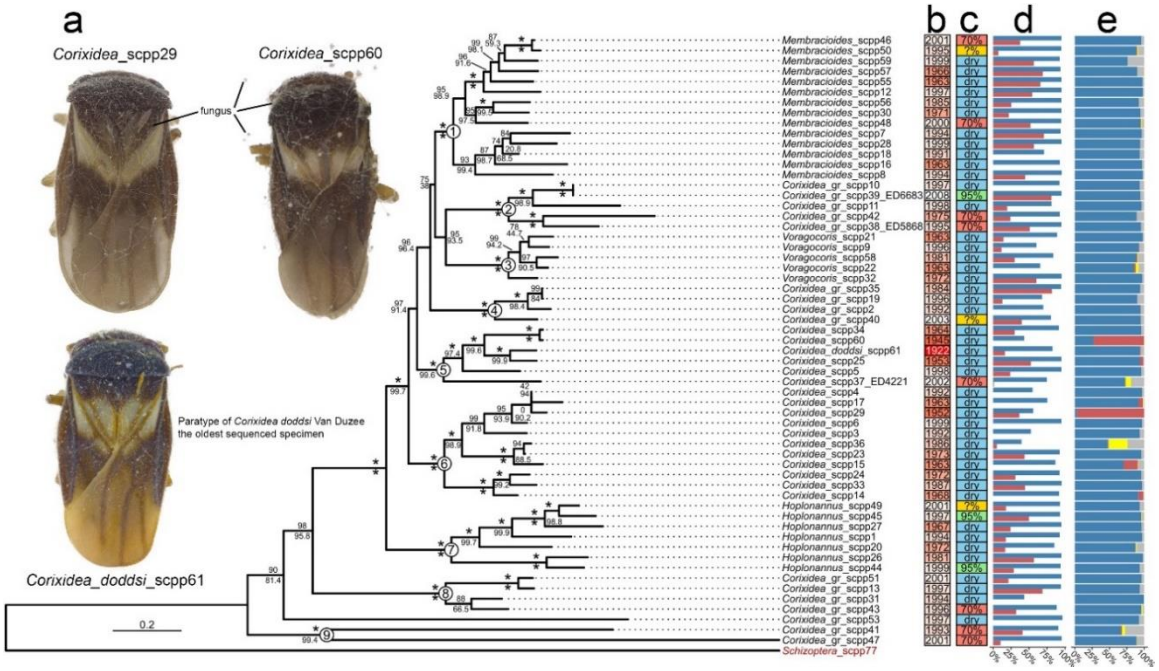

Figure 3.1. a. Phylogenetic reconstruction based on the Illumina dataset and using IQ-TREE. Taxa names with ED suffix represent samples that were also attempted to be sequenced for the Sanger dataset. Circled numbers at nodes indicate focal clades. Numbers above branches indicate Ultrafast Bootstrap support, below branches – SH-aLRT support. Asterisks denote absolute support (100%). Images show two successfully sequenced specimens that were severely contaminated with fungus, as well as the oldest sequenced specimen. b. Year of collection. c. Preservation method. d. Fraction of the target regions that was successfully recovered. Blue bars represent nuclear ribosomal genes, red bars the mitochondrial genome. e. Fraction of target region reads mapping to: blue – *Corixidea* (target), red – *Aspergillus* sp., yellow – human, grey – other contaminant.

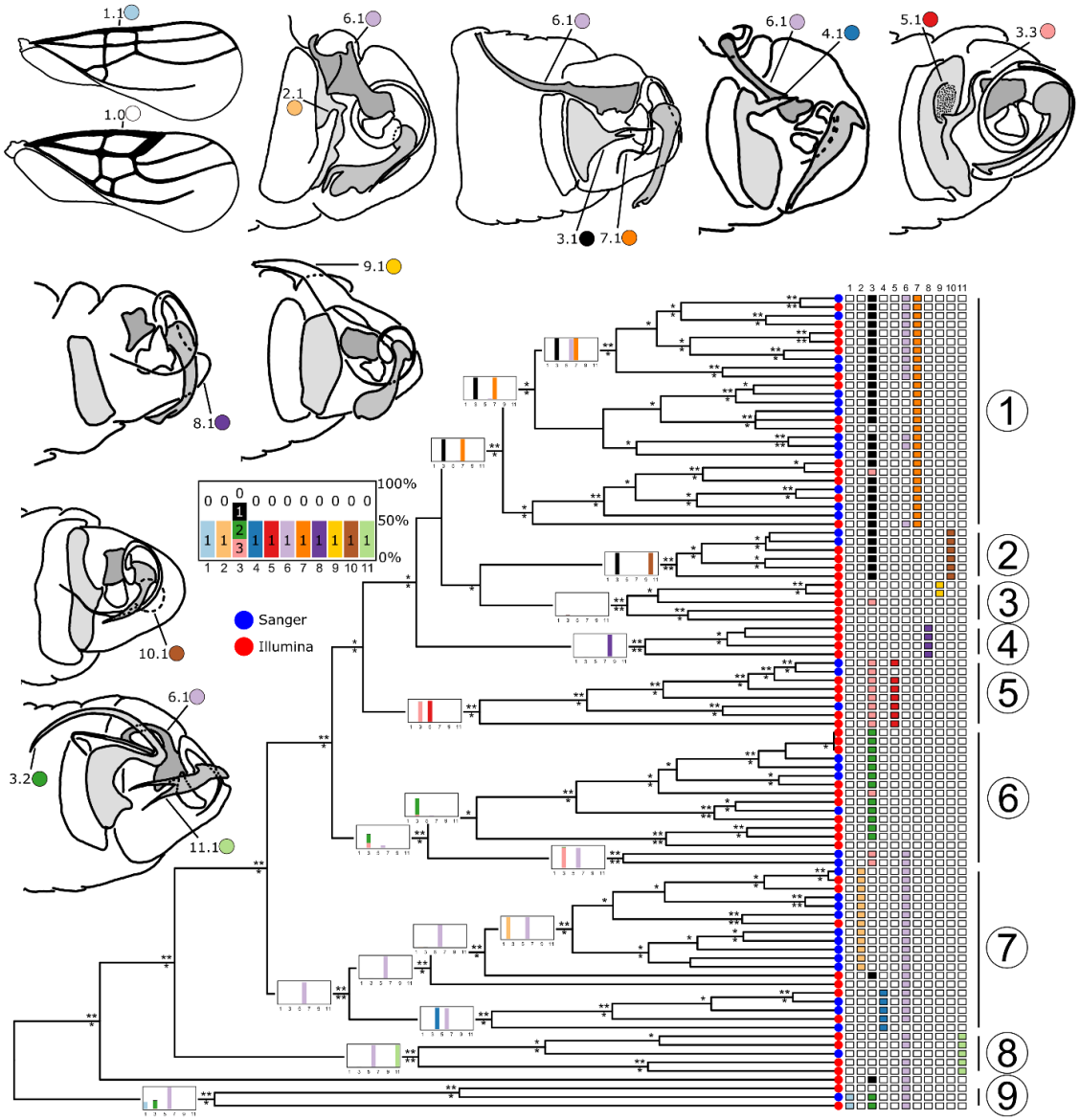

Figure 3.2. Phylogenetic reconstruction based on the combined dataset and using IQ-TREE, outgroups and female specimens removed. Asterisks above branches indicate Rapid Bootstrap support, below branches – SH-aLRT support, two asterisks denote full support (100%), one asterisk denotes 80-99% support, not shown for support lower than 80%. Bar plots indicate probabilities of character states for 11 characters, see the large annotated bar plot legend. Filled circles at tips represent Sanger sequenced specimens (blue) or Illumina sequenced specimens (red). Table on the right shows how all terminal taxa were coded for 11 focal characters, colors correspond with bar plots. Circled numbers indicate focal clades. Illustrations on top left show different states of the focal characters.

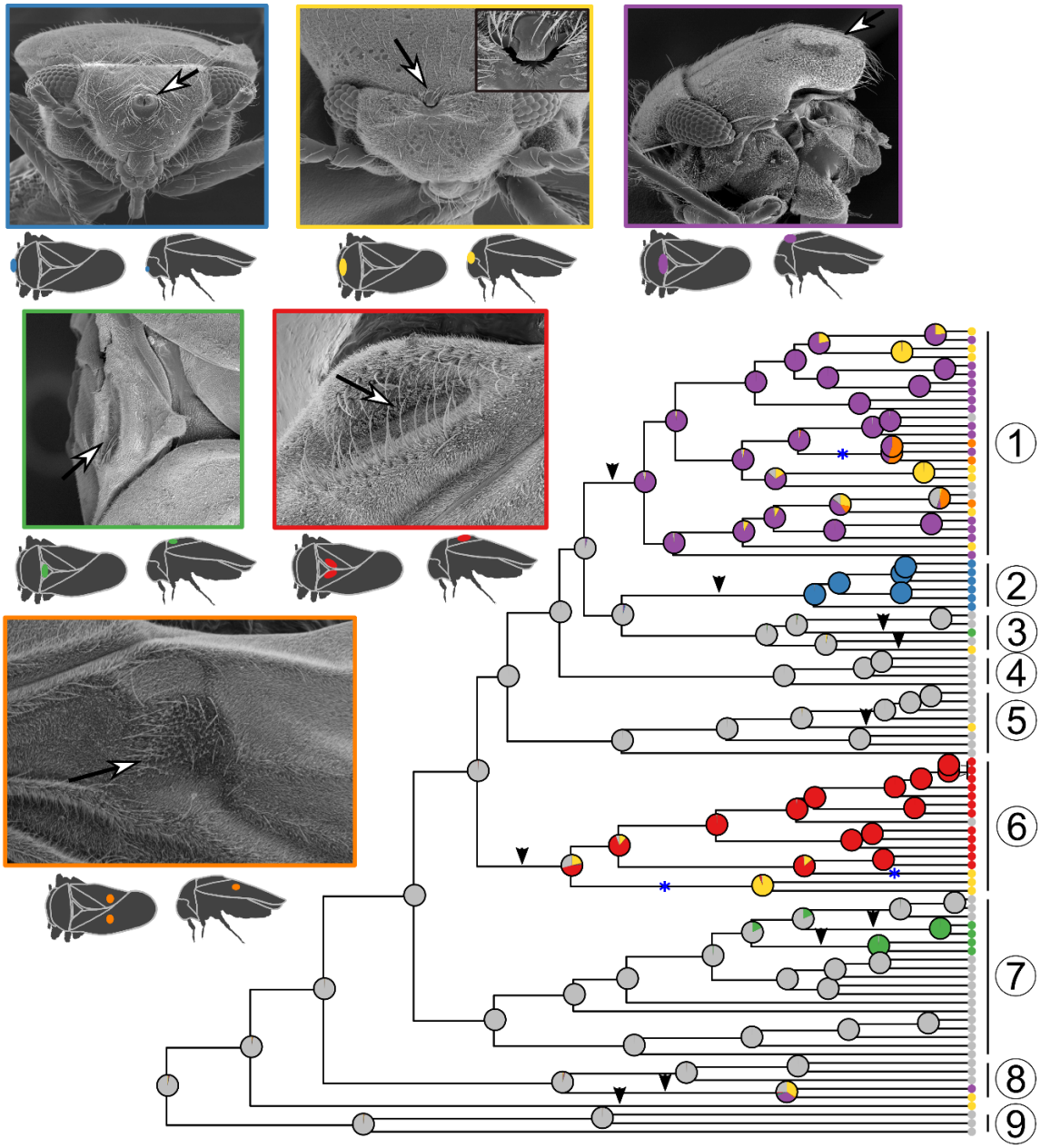

Figure 3.3. Phylogenetic reconstruction based on the combined dataset and using IQ-TREE, outgroups and female specimens removed. Pie charts indicate probabilities of MSO state, illustrations on top left show SEM documentation of different states, silhouettes highlight relative position of the organ on the body, colors correspond with pie charts. Grey represent lacking / undetected MSO. Black arrows indicate branches with reconstructed independent origins of MSO. Blue asterisks denote branches where MSO shifts between body and wing.

Supporting information

Table 3.S1. Information on the vouchers used in the final Sanger dataset analyses.

sample code	year	preservation	deposition	USI	country	sex	18S	D2	D3	COI	16S	final dataset	clade (genus)	species
ED4	2010	EtOH 95%	UCRC	UCR_ENT 00078206	Costa Rica	M	X	X	+	+	+	yes	1 (Membracioides)	ED4
ED65	2010	EtOH 95%	UCRC	UCR_ENT 00078193	Costa Rica	F	-	-	-	+	+		1 (Membracioides)	ED65
ED82	2010	EtOH 95%	UCRC	UCR_ENT 00004790	Costa Rica	F	+	+	+	+	+	yes	7 (Hoplonannus)	ED82
ED86	2010	EtOH 95%	UCRC	UCR_ENT 00078140	Costa Rica	M	+	+	+	+	+	yes	6 (Corixidea)	ED86
ED206	2010	EtOH 95%	UCRC	UCR_ENT 00082340	Peru	M	+	+	+	+	+	yes	2 (Voragocoris)	ED206
ED207	2010	EtOH 95%	UCRC	UCR_ENT 00077334	Peru	F	+	+	+	-	+	yes	1 (Membracioides)	ED207
ED253	?	EtOH 95%	UCRC	UCR_ENT 00057532	Peru	M	+	+	+	X	+	yes	5 (Corixidea)	ED253
ED254	2011	EtOH 95%	UCRC	UCR_ENT 00055624	Peru	M	+	+	+	-	-	yes	2 (Voragocoris)	ED254
ED261	2010	EtOH 95%	UCRC	UCR_ENT 00077381	French Guiana	M	+	+	+	-	+	yes	6 (Corixidea)	ED261
ED293	2010	EtOH 95%	UCRC	UCR_ENT 00082161	French Guiana	F	+	+	+	+	+	yes	6 (Corixidea)	ED293
ED363	2010	EtOH 95%	UCRC	UCR_ENT 00084410	Costa Rica	M	+	X	+	+	+	yes	7 (Hoplonannus)	ED363
ED371	2010	EtOH 95%	UCRC	UCR_ENT 00084376	Peru	M	-	-	+	X	-	yes	7 (Hoplonannus)	ED371
ED377	2010	EtOH 95%	UCRC	UCR_ENT 00084401	Peru	M	+	+	+	+	+	yes	1 (Membracioides)	ED377
ED380	2010	EtOH 95%	UCRC	UCR_ENT 00084415	Peru	M	X	+	+	X	-		1 (Membracioides)	ED380
ED394	2011	EtOH ?%	UCRC	UCR_ENT 00086057	Colombia	M	+	X	+	+	+	yes	1 (Membracioides)	ED394
ED478	2000	EtOH ?%	IAvH	UCR_ENT 00076304	Colombia	M	+	+	+	+	+	yes	1 (Membracioides)	ED478
ED479	2000	EtOH ?%	IAvH	UCR_ENT 00076295	Colombia	M	+	X	+	-	+	yes	7 (Hoplonannus)	ED479
ED528	2000	EtOH ?%	IAvH	UCR_ENT 00076278	Colombia	M	+	+	+	X	+	yes	1 (Membracioides)	ED528
ED547	2001	EtOH ?%	IAvH	UCR_ENT 00076328	Colombia	M	X	X	X	X	-		1 (Membracioides)	ED547
ED583	2000	EtOH ?%	IAvH	UCR_ENT 00076326	Colombia	M	X	X	X	X	-		1 (Membracioides)	ED583
ED939	2000	EtOH ?%	IAvH	UCR_ENT 00081387	Colombia	M	+	+	+	+	+	yes	1 (Membracioides)	ED939
ED1010	?	EtOH ?%	UCRC	UCR_ENT 00081277	Guyana	M	+	+	+	X	+	yes	7 (Hoplonannus)	ED1010
ED1012	?	EtOH ?%	UCRC	UCR_ENT 00081303	Guyana	M	+	+	+	X	+	yes	6 (Corixidea)	ED1012
ED1019	?	EtOH ?%	UCRC	UCR_ENT 00081314	Guyana	M	+	X	+	X	+	yes	8	ED1019
ED1112	2000	EtOH ?%	UCRC	UCR_ENT 00082388	Argentina	M	X	+	+	+	X	yes	6 (Corixidea)	ED1112
ED1113	2000	EtOH ?%	UCRC	UCR_ENT 00082376	Argentina	M	+	+	+	X	+	yes	7 (Hoplonannus)	ED1113
ED1217	2013	EtOH 95%	UCRC	UCR_ENT 00081677	Honduras	M	+	X	+	+	+	yes	7 (Hoplonannus)	ED1217
ED1218	2013	EtOH 95%	UCRC	UCR_ENT 00081695	Honduras	F	+	+	+	+	-	yes	7 (Hoplonannus)	ED1218
ED2160	2003	EtOH 95%	UCD	UCR_ENT 00043562	Costa Rica	M	X	X	X	X	-		1 (Membracioides)	ED2160
ED2213	2013	EtOH 95%	UCRC	UCR_ENT 00084981	Trinidad	M	+	+	+	+	+	yes	7 (Hoplonannus)	ED2213
ED2662	2013	EtOH 95%	UCRC	UCR_ENT 00088133	Trinidad	M	+	+	+	+	X	yes	7 (Hoplonannus)	ED2662
ED2663	2013	EtOH 95%	UCRC	UCR_ENT 00088134	Trinidad	F	-	+	+	+	X		7 (Hoplonannus)	ED2663
ED2773	2013	EtOH 95%	UCRC	UCR_ENT 00087476	Trinidad	M	-	-	X	-	-		7 (Hoplonannus)	ED2773
ED3001	2001	EtOH ?%	IAvH	UCR_ENT 00093183	Colombia	M	+	+	+	+	+	yes	9	ED3001
ED3028	?	EtOH 70%	UCRC	UCR_ENT 00026583	Ecuador	M	X	+	+	-	-		8	ED3028
ED3230	2014	EtOH 70%	FSCA	UCR_ENT 00011864	USA-FL	M	-	-	-	+	-		5 (Corixidea)	ED3230
ED3436	2013	EtOH 95%	UCRC	UCR_ENT 00102125	Trinidad	M	-	-	X	-	-		7 (Hoplonannus)	ED3436
ED3437	2013	EtOH 95%	UCRC	UCR_ENT 00102126	Trinidad	F	-	-	X	-	-		7 (Hoplonannus)	ED3437
ED3466	2013	EtOH 95%	UCRC	UCR_ENT 00100834	Trinidad	M	+	+	+	+	+	yes	7 (Hoplonannus)	ED3466
ED3470	2013	EtOH 95%	UCRC	UCR_ENT 00100836	Trinidad	F	-	-	-	+	-		7 (Hoplonannus)	ED3470
ED3787	2001	EtOH ?%	IAvH	UCR_ENT 00076269	Colombia	M	+	+	+	X	+	yes	6 (Corixidea)	ED3787
ED3886	2011	EtOH 95%	UCRC	UCR_ENT 00104906	Peru	M	+	X	+	+	+	yes	1 (Membracioides)	ED3886

Table 3.S2. Information on the vouchers used in the Illumina dataset.

sample code	year	preservation	deposition	USI	country	sex	extracted [ng/ul]	starting amount of DNA (ng)	capture pool	raw clusters	trimmed and merged reads	Corixidea	Aspergillus	Homo	Other	Corixidea_mito	Total % on target	% mito on target	18S & 28S completeness	Mitochondrion completeness	clade (genus)
scpp1	1994	dry	FSCA	UCR_ENT 00011947	Peru	M	0.602	9.03	1	102401	99297	15992	0	0	454	284	16.84844457	0.286010655	0.927895798	0.177937709	7 (Hoplonannus)
scpp2	1992	dry	FSCA	UCR_ENT 00011939	Peru	M	0.15	2.25	1	28251	27114	2837	16	0	140	0	11.038577862	0	0.697782602	0	4
scpp3	1992	dry	FSCA	UCR_ENT 00011937	Peru	M	0.266	3.99	1	24227	22748	1005	0	0	69	0	4.72129418	0	0.527213521	0	6 (Corixidea)
scpp4	1992	dry	FSCA	UCR_ENT 00011945	Peru	M	0.136	2.04	1	27573	25284	2213	8	0	57	0	9.009650372	0	0.550628004	0	6 (Corixidea)
scpp5	1998	dry	UCRC	UCRC_ENT 00069688	Ecuador	M	2.36	35.4	1	191004	190333	27430	0	0	1150	633	15.34836313	0.332575013	0.949759653	0.237639553	5 (Corixidea)
scpp6	1999	dry	TAMU	UCR_ENT 00094168	Ecuador	M	2.28	34.2	1	155352	154259	26897	0	0	807	0	17.95940593	0	0.950069778	0	6 (Corixidea)
scpp7	1994	dry	USNM	UCR_ENT 00026719	Ecuador	M	2.42	36.3	1	173379	174338	6191	0	0	210	2024	4.832566623	1.160963186	0.937509691	0.707093822	1 (Membracioides)
scpp8	1994	dry	USNM	UCR_ENT 00026717	Ecuador	M	1.9	28.5	1	163840	162524	23551	0	0	465	2759	16.47448992	1.697595432	0.954101411	0.446346008	1 (Membracioides)
scpp9	1996	dry	USNM	UCR_ENT 00026700	Ecuador	F	4.4	44	1	110026	109340	744	4	0	57	82	0.811231022	0.074995427	0.604279733	0.114622869	3 (Voragocoris)
scpp10	1997	dry	TAMU	UCR_ENT 00094138	Mexico	M	2.04	30.6	1	163875	163544	11682	0	0	749	0	7.601012572	0	0.923088851	0	2
scpp11	1998	dry	UCRC	UCRC_ENT 00038404	Mexico	M	1.05	15.75	1	74587	72661	6109	0	0	226	344	9.192001211	0.473431414	0.81175376	0.193361397	2
scpp12	1997	dry	TAMU	UCR_ENT 00094136	Mexico	M	4.02	40.2	1	285132	283452	103324	0	0	1932	8451	40.11508121	2.981457178	0.952705846	0.544337865	1 (Membracioides)
scpp13	1997	dry	TAMU	UCR_ENT 00094147	Mexico	M	0.438	6.57	3	188520	186311	3639	8	0	246	2673	3.524214888	1.434697898	0.943247015	0.686357049	8
scpp14	1968	dry	BMNH	BMNH-E-1496367	Brazil	M	0.223	3.345	6	62435	61259	5560	433	0	68	0	9.894056384	0	0.918747093	0	6 (Corixidea)
scpp15	1963	dry	AMNH	UCR_ENT 00096836	Brazil	M	<0.05	<1.25	4	52953	37154	3962	1161	41	470	0	15.16391236	0	0.86602574	0	6 (Corixidea)
scpp16	1963	dry	AMNH	UCR_ENT 00096775	Brazil	M	0.137	3.425	6	82713	80879	7966	1	12	208	0	10.12252872	0	0.930376803	0	1 (Membracioides)
scpp17	1963	dry	AMNH	UCR_ENT 00096768	Brazil	M	0.059	1.475	5	27531	24235	2706	187	16	28	0	12.11883639	0	0.753915336	0	6 (Corixidea)
scpp18	1991	dry	UCD	UCR_ENT 00036597	Brazil	M	0.505	7.575	2	36206	35557	2254	0	0	143	0	6.741288635	0	0.70817181	0	1 (Membracioides)
scpp19	1996	dry	FSCA	UCR_ENT 00011938	Brazil	M	0.583	8.745	2	48760	48507	4786	0	0	513	226	11.39010864	0.465912136	0.683516824	0.128355531	4
scpp20	1972	dry	AMNH	UCR_ENT 00096840	Brazil	M	<0.05	<1.25	4	78792	76793	2618	20	41	314	423	4.448322113	0.550831456	0.853310591	0.168863432	7 (Hoplonannus)
scpp21	1963	dry	AMNH	UCR_ENT 00096783	Brazil	M	0.105	2.625	5	50463	47614	2718	0	0	56	85	6.004536481	0.178518923	0.889440223	0.145055218	3 (Voragocoris)
scpp22	1963	dry	AMNH	UCR_ENT 00096795	Brazil	M	<0.05	<1.25	4	60932	55899	5727	138	281	546	0	11.97159162	0	0.652969453	0	3 (Voragocoris)
scpp23	1973	dry	AMNH	UCR_ENT 00096833	Brazil	M	0.299	4.485	3	62657	61519	4124	0	0	171	865	8.387652595	1.40606967	0.926190107	0.437995998	6 (Corixidea)
scpp24	1972	dry	AMNH	UCR_ENT 00096829	Brazil	M	0.499	7.485	3	132980	131688	4492	0	0	187	646	4.043648624	0.490553429	0.924174291	0.307501208	6 (Corixidea)
scpp25	1953	dry	AMNH	UCR_ENT 00096822	Brazil	M	0.058	1.45	5	40850	38313	3366	160	1	43	841	11.51306345	2.195077389	0.950069778	0.526533711	5 (Corixidea)
scpp26	1981	dry	UCD	UCR_ENT 00036586	Panama	M	0.097	2.425	5	82353	79706	5042	1	1	90	1368	8.157478734	1.71630743	0.949294464	0.570837071	7 (Hoplonannus)
scpp27	1967	dry	USNM	UCR_ENT 00026655	Panama	M	0.096	2.4	5	55416	52703	5307	12	2	189	162	10.7621957	0.307382881	0.94851915	0.244358567	7 (Hoplonannus)
scpp28	1999	dry	TAMU	UCR_ENT 00093407	Panama	M	0.641	9.615	2	212556	215786	57562	0	0	3469	12645	34.14308621	5.85997238	0.952550783	0.569801946	1 (Membracioides)
scpp29	1952	dry	USNM	UCR_ENT 00026665	Panama	M	<0.05	<1.25	4	119503	115239	1029	30018	6	0	981	27.79788093	0.851274308	0.55869127	0.364019046	6 (Corixidea)
scpp30	1971	dry	AMNH	UCR_ENT 00096868	Nicaragua	M	<0.05	<1.25	4	178563	177478	8086	5	3	440	652	5.175852782	0.367369477	0.950534967	0.217859361	1 (Membracioides)
scpp31	1994	dry	USNM	UCR_ENT 00026714	Ecuador	M	0.972	14.58	2	46741	46542	624	0	0	5	0	1.351467492	0	0.435261281	0	8
scpp32	1972	dry	AMNH	UCR_ENT 00096830	Peru	M	0.251	3.765	3	159271	157581	16150	1	0	405	4707	13.49337801	2.987035239	0.95348116	0.602166862	3 (Voragocoris)
scpp33	1987	dry	USNM	UCR_ENT 00026646	Bolivia	M	1.69	25.35	3	270567	269885	19638	0	0	608	1297	7.982288753	0.48057506	0.953636223	0.441791457	6 (Corixidea)
scpp34	1964	dry	AMNH	UCR_ENT 00096820	Bolivia	F	0.258	3.87	3	86641	84984	5596	12	0	226	565	7.52965264	0.664831027	0.913164832	0.299565247	5 (Corixidea)
scpp35	1984	dry	USNM	UCR_ENT 00026642	Venezuela	M	0.15	3.75	5	140942	139295	2488	1	0	150	2158	3.443770415	1.549230051	0.945262831	0.819267131	4
scpp36	1986	dry	TAMU	UCR_ENT 00093415	Venezuela	F	<0.05	<1.25	4	34837	30942	151	3	87	75	40	1.150539719	0.129274126	0.395100016	0.054349175	6 (Corixidea)
scpp37	2002	70% EtOH	FMNH	UCR_ENT 00097836	Uruguay	M	<0.05	<1.25	4	82363	80296	520	4	56	135	4	0.895436884	0.004981568	0.748178012	0.011291724	5 (Corixidea)
scpp38	1995	70% EtOH	FMNH	UCR_ENT 00091113	Cuba	M	0.307	4.605	3	85697	85490	3561	0	0	167	630	5.097672242	0.736928296	0.949294464	0.508936581	2
scpp39	2008	95% EtOH	MTEC	UCR_ENT 00120065	Mexico	M	0.242	3.63	3	94588	94848	6063	5	6	331	2055	8.919534413	2.166624494	0.952860909	0.810572079	2
scpp40	2003	?% EtOH	UCRC	UCR_ENT 00082216	Argentina	M	1.51	22.65	2	112939	116675	7001	2	0	337	20113	23.52946218	17.23848297	0.80508606	0.39817818	4
scpp41	1993	70% EtOH	FMNH	UCR_ENT 00125481	Bolivia	M	<0.05	<1.25	4	131573	129755	4068	77	285	1684	489	5.08882124	0.37686409	0.909288262	0.409081499	9
scpp42	1975	70% EtOH	FMNH	UCR_ENT 00090599	Jamaica	M	0.381	5.715	3	67107	67245	3427	2	0	399	421	6.318685404	0.626068853	0.929601489	0.239804016	2
scpp43	1996	70% EtOH	USNM	UCR_ENT 00027857	Ecuador	M	0.269	4.035	3	30322	30115	963	6	16	21	321	4.406441972	1.065913996	0.885253528	0.320198744	8
scpp44	1999	95% EtOH	UCRC	UCR_ENT 00084245	Guyana	M	1.15	17.25	2	88273	89336	7741	20	11	520	4254	14.04361064	4.761798155	0.935959063	0.286315644	7 (Hoplonannus)
scpp45	1997	95% EtOH	UCRC	UCR_ENT 00074573	Brazil	M	0.178	4.45	6	532156	534090	4765	20	37	159	1010	1.121721058	0.189106705	0.932237556	0.496515078	7 (Hoplonannus)
scpp46	2001	70% EtOH	IAvH	UCR_ENT 00074802	Colombia	M	1.2	18	2	68078	70706	17264	0	0	699	4169	31.30144542	5.896246429	0.950845092	0.376923608	1 (Membracioides)
scpp47	2001	70% EtOH	IAvH	UCR_ENT 00074804	Colombia	M	0.308	4.62	3	62202	61317	3391	5	15	386	39	6.25601383	0.063603895	0.953791285	0.102121851	9
scpp48	2000	70% EtOH	IAvH	UCR_ENT 00077492	Colombia	M	0.131	3.275	6	51980	50614	4613	38	72	147	1832	13.24139566	3.619551903	0.946193208	0.518528742	1 (Membracioides)
scpp49	2001	?% EtOH	LACM	UCR_ENT 00086682	Peru	M	1.79	26.85	2	111706	112992	13464	0	0	904	1042	13.63813367	0.922189182	0.931772368	0.179283693	7 (Hoplonannus)
scpp50	1995	?% EtOH	LACM	UCR_ENT 00086538	Costa Rica	M	0.195	4.875	5	74057	73514	1253	8	24	120	75	2.013221971	0.102021384	0.946813459	0.076599269	1 (Membracioides)
scpp51	2001	dry	TAMU	UCR_ENT 00094178	Panama	M	1.63	24.45	2	353231	360657	126649	0	0	4648	1843	36.9159617	0.511011848	0.951930532	0.213373818	8
scpp52	1932	dry	AMNH	UCR_ENT 00096849	Cuba	M	<0.05	<1.25	6	37974	36516	0	3605	4	441	0	11.09102859	0	0	0	uknown

scpp53	1997	dry	TAMU	UCR_ENT 00094167	Dominic Rep	M	1.28	19.2	2	170352	167684	62555	0	0	4862	0	40.20478996	0	0.96511087	0	
scpp54	1911	dry	USNM	UCR_ENT 00026652	Trinidad	M	<0.05	<1.25	6	35269	34203	0	2248	44	763	0	8.931965032	0	0	0	3 (Voragocoris)
scpp55	1963	dry	USNM	UCR_ENT 00026602	Colombia	M	0.188	4.7	5	151826	144211	10325	1	0	234	2427	9.005554361	1.682950676	0.950845092	0.657649576	1 (Membracioides)
scpp56	1985	dry	TAMU	UCR_ENT 00094195	Mexico	M	1.52	22.8	2	194792	197943	15554	1	0	1261	2361	9.688142546	1.192767615	0.94851915	0.252432544	1 (Membracioides)
scpp57	1966	dry	AMNH	UCR_ENT 00096689	Mexico	M	0.606	9.09	3	219543	218217	2138	0	3	231	2184	2.087830004	1.000838615	0.934563498	0.690704575	1 (Membracioides)
scpp58	1981	dry	UCD	UCR_ENT 00036589	Panama	M	<0.05	<1.25	6	51034	50069	2224	23	29	214	414	5.799996006	0.826858935	0.836718871	0.299910289	3 (Voragocoris)
scpp59	1999	dry	TAMU	UCR_ENT 00094197	Panama	M	1.48	22.2	2	103479	104861	3265	0	0	1040	12344	15.87720888	11.77177406	0.92634517	0.565937478	1 (Membracioides)
scpp60	1945	dry	USNM	UCR_ENT 00026657	USA-FL	M	0.062	1.55	6	29366	28074	1362	3608	5	0	0	17.72102301	0	0.434175841	0	5 (Corixidea)
scpp61	1922	dry	CAS	UCR_ENT 00099073	Mexico	M	0.064	1.6	6	19281	18211	3750	49	2	192	258	23.34303443	1.416726155	0.826019538	0.164446898	5 (Corixidea)

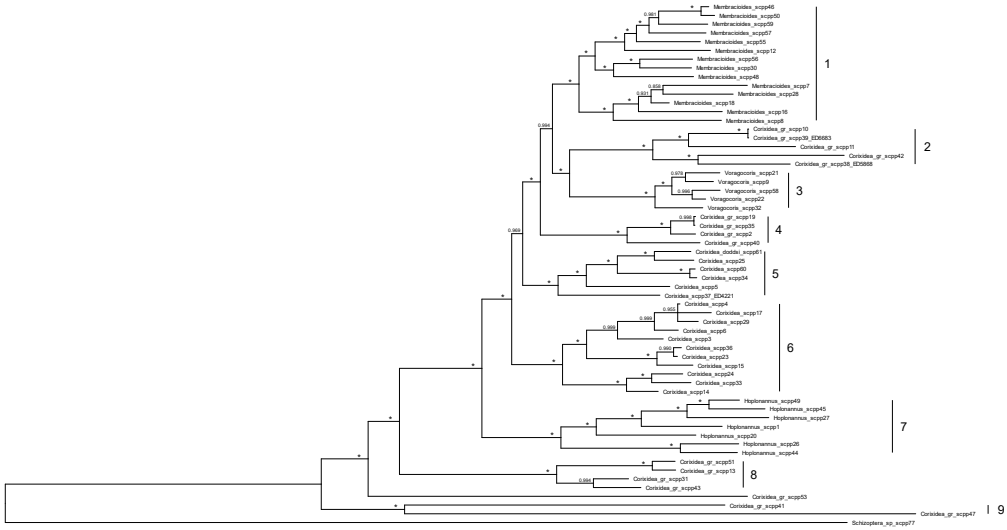

Figure 3.S1. Phylogenetic reconstruction based on the Illumina dataset and using MrBayes. Posterior probability of 1.0 is denoted with asterisk. Numbers on the right denote the focal clades.

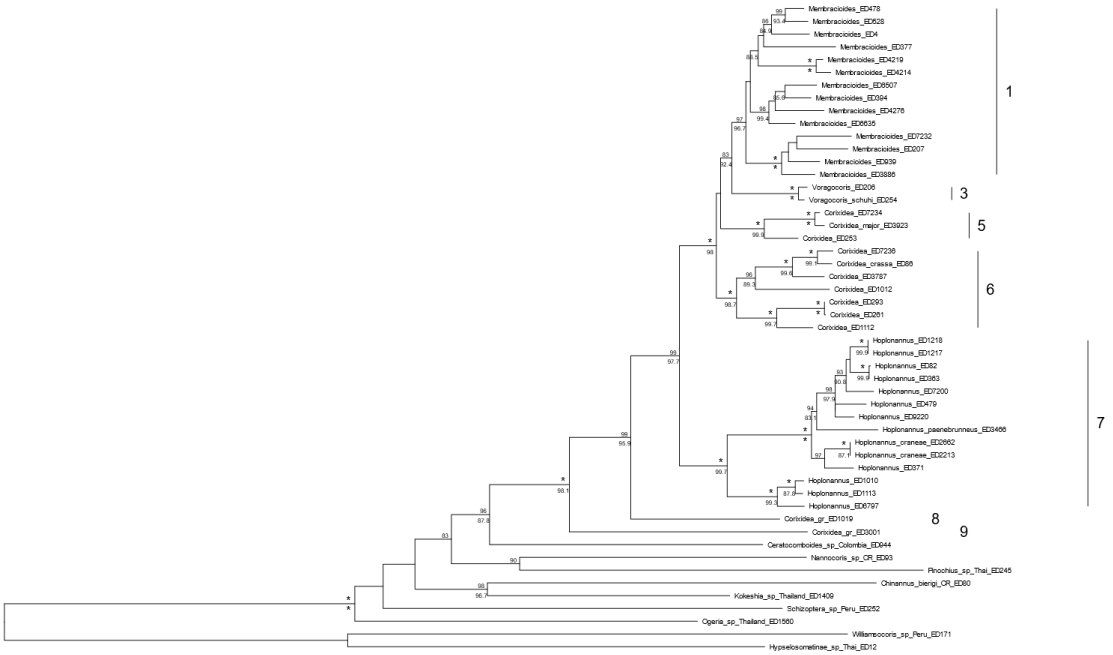

Figure 3.S2. Phylogenetic reconstruction based on the Sanger dataset and using IQ-TREE. Numbers above branches indicate Rapid Bootstrap support, below branches – SH-aLRT support, not shown for support lower than 80%. Asterisks denote absolute support (100%). Numbers on the right denote the focal clades.

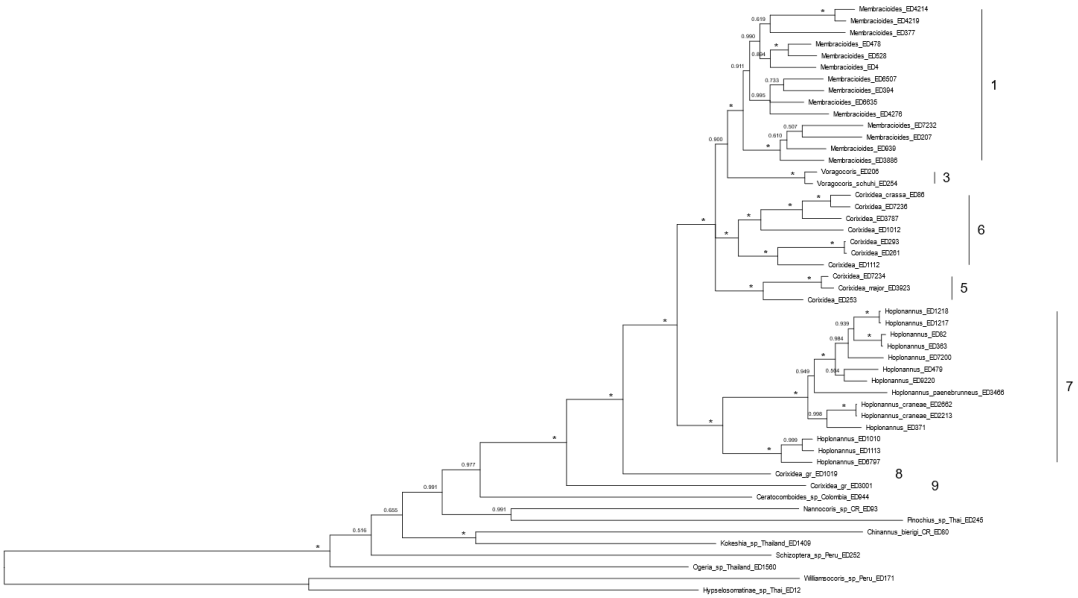

Figure 3.S3. Phylogenetic reconstruction based on the Sanger dataset and using MrBayes. Posterior probability of 1.0 is denoted with asterisk. Numbers on the right denote the focal clades.

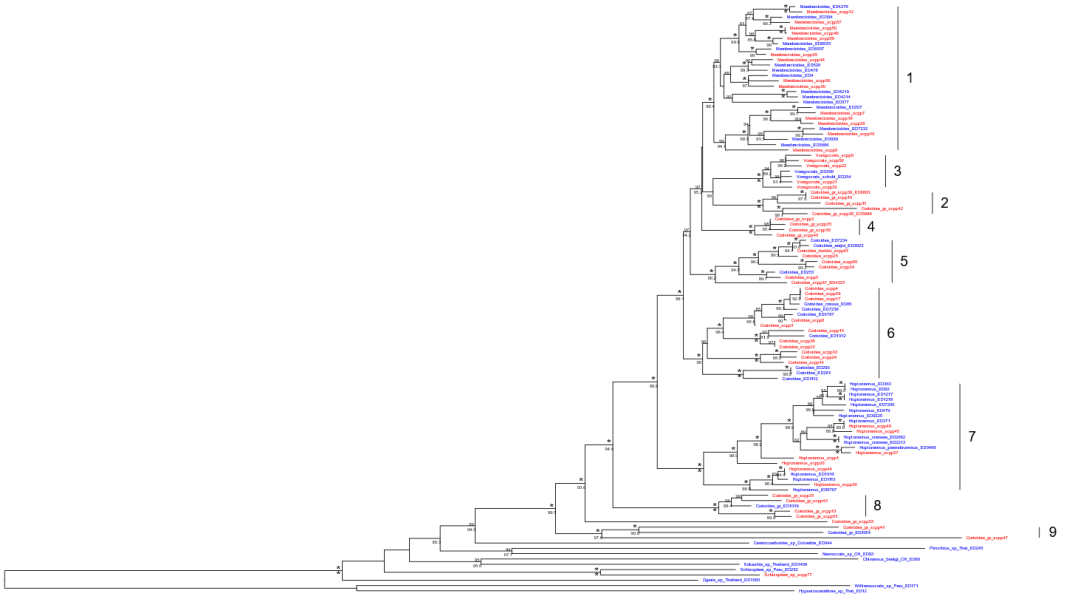

Figure 3.S4. Phylogenetic reconstruction based on the combined dataset and using IQ-TREE. Numbers above branches indicate Rapid Bootstrap support, below branches – SH-aLRT support, not shown for support lower than 80%. Asterisks denote absolute support (100%). Numbers on the right denote the focal clades. Terminal taxa from the Illumina dataset are in red, from the Sanger dataset are in blue.

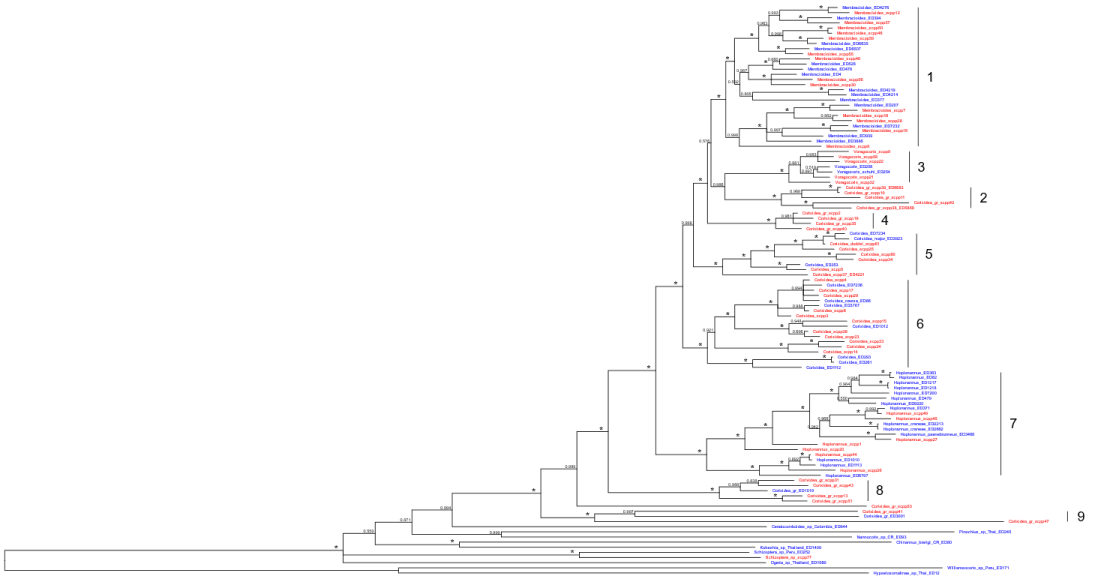

Figure 3.S5. Phylogenetic reconstruction based on the Sanger dataset and using MrBayes. Posterior probability of 1.0 is denoted with asterisk. Numbers on the right denote the focal clades. Terminal taxa from the Illumina dataset are in red, from the Sanger dataset are in blue.

Chapter 4: Taxonomic revision of the genus *Voragocoris* Weirauch

Abstract

The New World schizopterid genus *Voragocoris* is revised. Diagnoses, descriptions, and a key to species are provided. Photographs of overall habitus and selected morphological features, including genitalia, are given.

Introduction

The dipsocoromorphan family Schizopteridae is the most diverse, both in terms of morphology and species numbers, in the infraorder and contains about 350 species (Weirauch *et al.* 2018). About 100 of these species have been described during the past 10 years (Azar & Nel 2010; Costas *et al.* 2015; Hill 2013, 2014, 2015; Knyshov *et al.* 2016; Leon & Weirauch 2016b; a; Makhan 2013a; b; Poinar & Brown 2014; Rédei 2008b; a; Weirauch 2012; Weirauch *et al.* 2017, 2018; Weirauch & Frankenberg 2015), and the examination of curated, but especially also of uncurated bulk samples in natural history collections indicates that many more species remain to be described. One of the most commonly encountered taxa in samples from the New World is the *Corixidea* genus group, originally proposed by Emsley (1969). The group originally included the genera *Corixidea* Reuter, *Voccoroda* Wygodzinsky, *Hoplonannus* McAtee & Malloch, *Membracioides* McAtee & Malloch, and *Oncerodes* Uhler, and was diagnosed by the truncate labium, a feature that is unique among Schizopteridae, similar wing venation with two triangular marginal cells, absence of a pronotal collar, and presence of so called hyperpleural lobes (Emsley 1969). Weirauch (2012) added to this group the genus *Voragocoris* Weirauch, which shares the above diagnostic features, but in addition has a

unique modification of the frontal region of the head in males. The restriction to males and distinctive species-diagnostic differences of this structure that are documented below are reminiscent of male-specific organs that are now discovered in various groups of Schizopteridae (Frankenberg *et al.* 2018; Hill 1990, 2004, 2013; Knyshov *et al.* 2016; Knyshov *et al.* in prep.).

A phylogenetic analysis focused on the *Corixidea* genus group (Knyshov *et al.* in prep.) supported the monophyly of *Voragocoris* and revealed several undescribed species based on DNA data. In the present study we examined molecular vouchers from Knyshov *et al.* (in prep.) and additional specimens of this genus, and discovered seven undescribed species that are described and documented below. Results of this revision significantly extend both, our knowledge of the distribution ranges and variation of male-specific morphology.

Material and methods

A total of ~2,500 specimens of the *Corixidea* genus group were sorted and examined. Of these, and based on the distinctive head morphology of males, 47 specimens belong to *Voragocoris* and were incorporated into the present revision. Specimens are deposited in the following institutions: Florida State Collection of Arthropods (FSCA), American Museum of Natural History (AMNH), National Museum of Natural History (USNM), Instituto Nacional de Biodiversidad (INBio), Field Museum of Natural History (FMNH), University of California Davis (UCD), University of California Riverside (UCRC), Instituto de Investigación de Recursos Biológicos Alexander von Humboldt (IAvH), Museo de Historia Natural, Universidad Nacional Mayor de San Marcos (MUSM).

Habitus images were taken with a Leica DFC 450 C Microsystems imaging system with Planapo 1.0x or 2.0x objectives and stacked using Leica Application Suite V4.3. Specimens were DNA extracted (Knyshov *et al.* in prep.) or incubated for 10 min in hot 10% KOH solution to clear internal tissues. Cleared specimens were dissected and imaged. Dorsal and lateral images of the head and prothorax were taken with a Leica DFC 450 C, frontal images of the head and prothorax and all abdomen images were taken on a Zeiss Axioskop 2 compound microscope. Measurements (Table 4.1) were done using the habitus images. Total length was measured from the anterior tip of the head to the tip of the apex of forewing.

Label information was entered in the PBI instance of the Arthropod Easy Capture (AEC) database, georeferenced, and made available through the http://research.amnh.org/pbi/heteropteraspeciespage/ website. Distribution map was prepared using SimpleMappr (http://www.simplemappr.net/) and data exported from the PBI database.

Terminology generally follows Weirauch (2012), with terms for genitalic features after Knyshov *et al.* (2018). The following abbreviations are used: a – anophore, aap – anterior anophoric process, DAG – dorsal obdominal gland, hpl – hypopleural lobe; lp – left paramere, mt – mediotergite, mt8p – mediotergite 8 process, mso – male-specific organ, pap – posterior anophoric process, phs – patch of hairlike sensilla, py – pygophore, pyc – pygophore cavity, rp – right paramere, sp – spiracle, st – sternum, ts – tibial spines, v – vesica.

Results and Discussion

Voragocoris Weirauch, 2012

Type species: *Voragocoris schuhi* Weirauch, 2012 (original designation).

Diagnosis. Distinguished from other Schizopteridae by the truncate three-segmented labium (Figs 4.2-5); the forewing with two marginal cells heavily sclerotized and rest of forewing membranous (Fig. 4.1); absence of a pronotal collar (Fig. 4.4); presence of distinct hypopleural lobes (Fig. 4.1); male frons with a male-specific organ, frequently covered by dense pale setae (Figs 4.1-4); ventral side of the pygophore with a pygophore cavity (Fig. 4.3). Based on male specimens, this genus can be distinguished from other genera of the *Corixidea* genus group by the presence of a frontal male-specific organ and a pygophore cavity. Females are indistinct from other *Corixidea* genus group taxa.

Redescription. *Male*. Body size 0.86-1.14 mm, elongate oval, macropterous (Figs 4.1-3). COLORATION. Brown to black, appendages yellow to pale brown, forewing with white fascia on corium and clavus. SURFACE AND VESTITURE. Body, except appendages and abdominal terga, with dense cover of microtrichia; head, pronotum and wing veins with short to medium-length light brown setae, abdomen densely covered with elongate, light brown setae; location of male-specific organ may be overgrown with long dense light setae; sterna 4 and 5 each with patches of hairlike sensilla (Fig. 4.6). STRUCTURE. Head with frontal margin slightly to strongly rounded, eyes large, about 1/3 to 1/2 width of synthlipsis, ocelli roughly equal in size to one ommatidium, located close to anterior-ventral margin of compound eye (Fig. 4.5); frons with male-specific organ, with orifice of varying structure (Fig. 4.4); labium three-segmented, terminal segment blunt;

pronotum trapezoidal, lateral margin apically concave, posterior margin medially convex; pronotal collar absent; scutellum triangular, with protruded rounded tip; metepisternum with posterior margin rounded; median mesosternal and metasternal processes absent; metendosternite with concave widened apex; adhesive pad on hind coxa well-developed; tarsal formula 3-3-3; pretarsus with setiform parempodia; bladder-like arolia present on fore- and mid leg; abdomen symmetrical, with six visible sterna corresponding to segments 2+3, 4, 5, 6, 7, and pygophore (Fig. 4.7); sternum 2+3 slightly longer than preceding sterna; terga of pregenital abdomen weakly sclerotized, mediotergite 7 rectangular, mediotergite 8 roughly rectangular, short, with medial hook-shaped process (Figs 4.7-8). GENITALIA (Figs 4.7-8). Pygophore weakly asymmetrical, with symmetrical outline, narrower than pregenital abdomen, very lightly dorsoventrally flattened; plane of parameres rotated almost at 90 degrees with respect to longitudinal body axis; right paramere long, slightly curved, gradually tapering at apex; left paramere much smaller than right, roughly as long as wide; aedeagus devoid of visible conjunctival appendages, vesica forming about one coil, more or less flattened from base to about 2/3 of length, then abruptly narrowed and tube-like, sometimes with short process at point of width change; anophore well sclerotized and sometimes with very small laterally directed anterior anophoric process; posterior anophoric process normally developed, rounded, ridge-like.

Female. Body length 0.97 mm, elongate oval, macropterous (Figs 4.1G, 4.2G). COLORATION and SURFACE AND VESTITURE. As in male, except without dense setation on frons and without patches of hairlike setae on abdominal sterna 4 and 5 (Fig.

4.9A). STRUCTURE. As in male, but without male-specific organ on frons; tarsal formula 2-2-3, arolia absent; abdomen with five visible sterna corresponding to segments 2+3, 4, 5, 6, and 7; sternum 7 much longer than preceding sterna, symmetrical (Fig. 4.9A). GENITALIA. Ovipositor vestigial, spermathecal reservoir bean-shaped, narrower at base and wider at apex, spermathecal duct relatively short and straight (Fig. 4.9B).

Distribution. From Belize in Central America to southern Peru and eastern Brazil in the south-east of South America.

Discussion. The genus was originally diagnosed based on the presence of a bilobed projection on the frons, here referred to as a frontal male-specific organ. Although this frontal male-specific organ was indeed found in all species studied for the present revisions, it is not necessarily present as a bilobed projection in all species, but shows considerable variation (see Figs 4 and 5). Additionally, the ventral cavity of the pygophore is very small and inconspicuous in some species, while prominent in others. The patches of hairlike sensilla on abdominal sterna 4 and 5 on the other hand are always present, even in species with small frontal modifications and small pygophore cavity. Interestingly, the variation in male genitalia between species is minor compared to other genera of the *Corixidea* genus group, and is limited to slight differences in the size of the mediotergite 8 process and presence and shape of the minute anterior anophoric process.

Key to species of *Voragocoris* (based on male specimens):

1. Pygophore with a small ventral depression, pygophore cavity small or indistinct (Figs 4.3A-C,E,G) 2

- Pygophore with a deep depression, pygophore cavity large (Figs 4.3D, 4.3F, 4.3H, 4.3I).....4

2. Male-specific organ obscure, small, and located very close to clypeus (Fig. 4.4G) ....*V. obscurus* n. sp.

- Male-specific organ prominent, removed from clypeus.....3

3. Frons bulging, male-specific organ orifice small, heavily sclerotized, vertex depressed (Figs 4.1L, 4.4E, 4.5E), tergite 8 process large (Figs 4.7E, 4.8E)...*V. convexifrons* n. sp.

- Frons not bulging, male-specific organ orifice with ventral margin V-shaped, vertex not depressed (Figs 4.1K, 4.4A-C, 4.5A-C), tergite 8 process small (Figs 4.7A-C, 4.8A-C) .....*V. brevicavus* n. sp.

4. Male-specific organ orifice with a prominent dorso-anteriorly directed spine on ventral margin (Figs 4.2J, 4.3I, 4.4I, 4.4J, 4.5I) ..... *V. unicornis* n. sp.

- Male-specific organ orifice without a prominent spine on ventral margin.....5

5. Frons with large, tapering in lateral view, anterior projection around male-specific organ (Fig. 4.2I, 4.5H), foretibia with row of prominent black spines (Fig. 4.4H)..... ..... *V. rostralis* n. sp.

- Frons without large, tapering in lateral view, anterior projection, foretibia without a row of prominent black spines.....6

6. Male-specific organ orifice with prominent ventro-anteriorly directed dorsal spine (Fig. 4.5D).....*V. cavifrons* n. sp.

- Male-specific organ orifice without prominent ventro-anteriorly directed spine on dorsal margin 7

7. Male-specific organ orifice with crescent-shaped pattern (Fig. 4.4F), pygophore cavity noticeably shifted to left side (Fig. 4.7F) ..... *V. crescentus* n. sp.
- Male-specific organ orifice with straight rounded bilobed projection, pygophore cavity in center 8
8. Vesica with one small process, paramere wider ..... *V. schuhi* Weirauch
- Vesica with several processes, paramere narrower ..... *V. amrishi* Makhan

Voragocoris amrishi Makhan, 2013

Discussion. The original description of this species from Suriname is lacking information on some crucial features. According to the photographs provided, the specimens are very similar to *V. schuhi* based on shape of the male-specific organ on the frons (prominent projecting bilobed process with rounded apex), large slightly elongate pygophore cavity, and presence of vesical processes. The only substantial difference is in the number of vesical processes; however, the vesica documented in Makhan (2013) was damaged, and thus additional processes could be artifacts of the dissection procedures. The difference in paramere shape reported by Makhan (2013) is difficult to evaluate, but is surprising, as according to our investigations, paramere variation in the genus is minimal. Thus, *V. amrishi* is potentially a synonym of *V. schuhi* from southeastern Peru, despite the very distant type localities of these two taxa. We here refrain from synonymizing the two species until additional material from across the Amazon basin becomes available.

Voragocoris brevicavus new species

Holotype: **PANAMA: Canal Zone:** Isla Pantera, 9.23694°N 79.91083°W, 24 Aug 1981, R. B. Kimsey, 1♂ (UCR_ENT 00036589) (UCD).

Paratypes: **BELIZE: Cayo:** British Honduras: Cayo Dist Mile 66, Western Highway, 17.20228°N 88.64395°W, 07 Jul 1969, 1♂ (UCR_ENT 00091561) (FSCA). **BRAZIL: Para:** Marituba, Mun. Ananindeua, 1.36038°S 48.34249°W, Nov 1963, Oliveira & Wygodzinsky, 2♂ (UCR_ENT 00096793, UCR_ENT 00096795) (AMNH). **COSTA RICA: Guanacaste:** Nicoya, Humedal Mata Redonda, Cerrito, 10.14444°N 85.45278°W, 8 m, 04 Jul 2005 - 07 Jul 2005, J. Azofeifa, B. Gamboa, J. Gutiérrez, M. Moraga, Y. Cardenas, 1♂ (UCR_ENT 00094421) (INBIO). **PANAMA: Canal Zone:** Barro Colorado Island, 04 Jul 1941 - 11 Jul 1941, J. Zetek, 1♂ (UCR_ENT 00026697) (USNM). Canal Zone Penitentiary, 9.1°N 79.68333°W, 12 Jan 1946 - 13 Jan 1946, A. O. Meyer, 3♂ (UCR_ENT 00090869) (FMNH); 15 Jan 1946 - 16 Jan 1946, A. O. Meyer, Light Trap, 1♂ (UCR_ENT 00090811) (FMNH). Lion Hill Island, 9.21667°N 79.86667°E, 27 Sep 1981, R. B. Kimsey, 1♂ (UCR_ENT 00036588) (UCD). Loma Boracho, 23 Oct 1951, F. S. Blanton, Light Trap, 1♂ (UCR_ENT 00026688) (USNM). Madden Dam, 9.21667°N 79.61667°W, 15 Jun 1946, A. O. Meyer, 2♂ (UCR_ENT 00090874, UCR_ENT 00097162) (FMNH). Pantera Island, 9.23667°N 79.91111°W, 24 Aug 1981, R. B. Kimsey, 1♂ (UCR_ENT 00036590) (UCD). Puma Island, 9.25°N 79.9°E, 05 Sep 1981, R. B. Kimsey, 1♂ (UCR_ENT 00037081) (UCD); 21 Sep 1981, R. B. Kimsey, 2♂ (UCR_ENT 00036587, UCR_ENT 00036591) (UCD); 26 Oct 1981, R. B. Kimsey, Light Trap, 1♂ (UCR_ENT 00036603) (UCD). Tabernilla, 13 May 1907, A.

Busck, 1♂ (UCR_ENT 00026696) (USNM). 17 Apr 1952, F. S. Blanton, 1♂ (UCR_ENT 00026669) (USNM). **Panama:** ***Tocumen Co.:*** Panama: Prov. Of Panama, Tocumen, 9.06749°N 79.36908°W, 03 Aug 1970 - 07 Aug 1970, 1♂ (UCR_ENT 00091925) (FSCA); 17 Aug 1970 - 21 Aug 1970, 1♂ (UCR_ENT 00091868) (FSCA).

Diagnosis. This species can be recognized by the following combination of characters: small, dorso-ventrally elongated male-specific organ orifice, with V-shaped carina ventrally delimiting the orifice (Figs 4.4A-C); relatively flat frons and vertex (Figs 4.5A-C); foretibia without black spines; unequal in size patches of hairlike sensilla on sterna 4-5 (Figs 4.6A-C); small mediotergite 8 process (Figs 4.7A-C); triangular, slightly constricted from sides pygophore; small pygophore cavity; absence of anterior anophoric process (Figs 4.8A-C). Most similar to *V. convexifrons*, but distinguished by the flat vertex and frons, larger frontal organ orifice, and smaller mediotergite 8 process.

Description. *Male* (Figs 4.1A-C, 4.2A-C, 4.3A-C). Body length 0.86-1.03 mm. COLORATION. Brown to dark brown. SURFACE AND VESTITURE. As in generic description, patches of hairlike sensilla on sterna 4-5 unequal in size, patch on sternum 4 small and round, patch on sternum 5 large and transverse. STRUCTURE. Head with frons lightly curved in lateral view, with small depression corresponding to male-specific organ; male-specific organ orifice relatively small, dorso-ventrally elongated, with ventral V-shaped carina (Figs 4.4A-C); vertex flat, without furrow; thorax and pregenital abdomen as in generic description. GENITALIA (Figs 4.8A-C). Mediotergite 8 with small hook-like process curved dorsally; pygophore triangular, lightly constricted from sides, apex narrowly rounded; pygophore cavity small, round, located close to posterior

margin of pygophore; vesica without noticeable processes; anterior anophoric process absent.

Female. Unknown.

Etymology. Named for the small pygophore cavity ("brevis" – small, "cavus" – cavity).

Distribution. The species is known from Belize to Para, Brazil.

Discussion. The majority of examined specimens of this species were collected in a relatively small geographic area, encompassing Costa Rica and Panama, however three additional specimens, one from Belize, and two from eastern Brazil were tentatively assigned to this species (Figs 4.1B-C, 4.10). We carefully inspected morphological features of the geographical outliers, especially the specimens from Brazil, and failed to find any firm delimiting features. Few minor differences were observed in the shape of the male-specific organ orifice, and in the case of the Brazil specimens, in smaller body size and a larger patch of the hairlike sensilla on sternum 4. The range from Belize to eastern Brazil would seem quite extraordinary given that the known ranges of other schizopterid species tend to be considerably smaller. However, in absence of strongly diverging characters, we feel that it would be premature to describe the specimens from Brazil as separate species, especially given how few specimens in total were studied.

Voragocoris cavifrons new species

Holotype: **BRAZIL: Para:** Marituba, Mun. Ananindeua, 1.36038°S 48.34249°W, Nov 1963, Oliveira & Wygodzinsky, 1♂ (UCR_ENT 00096783) (AMNH).

Paratypes: **BRAZIL: Para:** Marituba, Município Ananindeua, Nov 1963, Oliveira & Wygodzinsky, 1♂ (UCR_ENT 00096779) (AMNH).

Diagnosis. This species can be recognized by the following combination of characters: large round male-specific organ orifice with dorsal spine (Figs 4.4D, 4.5D); relatively flat frons except dorsal convex portion with male-specific organ (Fig 4.5D); foretibia without black spines (Fig 4.4D); unequal in size patches of hairlike sensilla on sterna 4-5 (Fig 4.6D); small mediotergite 8 process (Fig 4.7D); posteriorly rounded pygophore; large pygophore cavity; presence of anterior anophoric process (Fig 4.8D). Drastically differs from other species in shape of the male-specific organ orifice.

Description. *Male* (Figs 4.1D, 4.2D, 4.3D). Body length 1.05 mm. COLORATION. Brown to dark brown. SURFACE AND VESTITURE. As in generic description, patches of hairlike sensilla on sterna 4-5 unequal in size, patch on sternum 4 small and slightly oval, patch on sternum 5 large and transverse. STRUCTURE. Head with frons flat in lateral view, apical portion bulging, with large round depression corresponding to male-specific organ orifice, and large dorsal spine (Figs 4.4D, 4.5D); male-specific organ with deep cylindrical cavity (Fig 4.4D); vertex flat, without furrow (Fig 4.4D); thorax and pregenital abdomen as in generic description. GENITALIA (Figs 4.8A-C). Mediotergite 8 with small hook-like process curved dorsally; pygophore rounded, apex broadly rounded; pygophore cavity large, slightly elongate; vesica without noticeable processes; anterior anophoric process present, slender and tapering (Fig 4.8D).

Female. Unknown.

Etymology. Named for the pronounced cavity of the frontal male-specific organ.

Distribution. The species is known from a single locality in Para, Brazil.

Voragocoris convexifrons new species

Holotype: **PANAMA: Darien:** El Real, 8.11028°N 77.73444°W, 08 Aug 1952, F. S. Blanton, 1♂ (UCR_ENT 00026661) (USNM).

Paratypes: **COSTA RICA: Puntarenas:** ***Osa Co.:*** Quebrada Seca, 8.99332°N 83.56924°W, 18 Aug 2005, M. Moraga, 2♂ (UCR_ENT 00094422, UCR_ENT 00094423) (INBIO). **PANAMA: Darien:** El Real, 8.11028°N 77.73444°W, 08 Aug 1952, F. S. Blanton, 3♂ (UCR_ENT 00026662-UCR_ENT 00026664) (USNM).

Diagnosis. This species can be recognized by the following combination of characters: small, dorso-ventrally elongated male-specific organ orifice without V-shaped carina ventrally delimiting the orifice (Fig 4.4E); very convex frons and depressed vertex (Fig 4.1L, 4.5E); foretibia without black spines; unequal in size patches of hairlike sensilla on sterna 4-5 (Fig 4.6E); large mediotergite 8 process (Figs 4.7E, 4.8E); triangular, slightly constricted from sides pygophore; small pygophore cavity; absence of anterior anophoric process (Fig 4.8E). Most similar to V. *brevicavus*, but distinguished by the depressed vertex and convex frons, male-specific organ orifice without ventral V-shaped carina, and larger mediotergite 8 process.

Description. *Male* (Figs 4.1E, 4.1L, 4.2E, 4.3E). Body length 1.05 mm. COLORATION. Dark brown to black. SURFACE AND VESTITURE. As in generic description, patches of hairlike sensilla on sterna 4-5 unequal in size, patch on sternum 4 small and slightly

oval, patch on sternum 5 large and transverse. STRUCTURE. Head with frons broadly convex in lateral view, with relatively small round depression corresponding to male-specific organ (Figs 4.4E, 4.5E); male-specific organ orifice very small, dorso-ventrally elongated, without ventral V-shaped carina (Figs 4.4E); vertex medially depressed, with furrow running from top of vertex to about 1/2 of distance from top of head to male-specific organ orifice (Fig 4.4E); thorax and pregenital abdomen as in generic description. GENITALIA (Figs 4.7E, 4.8E). Mediotergite 8 with large hook-like process curved dorsally; pygophore triangular, lightly constricted from sides, apex narrowly rounded; pygophore cavity small, round, located close to posterior margin of pygophore; vesica without noticeable processes; anterior anophoric process absent.

Etymology. Named for the very convex frons.

Distribution. This species is known from two localities, in Costa Rica and Panama, respectively.

Voragocoris crescentus new species

Holotype: **ECUADOR: Orellana:** ***Tiputini Biodiversity Station Co.:*** nr Yasuni National Park Erwin Transect - T/4, 0.63194°N 76.14417°W, 220 m, 24 Oct 1998, T.L. Erwin, 1♂ (UCR_ENT 00026581) (USNM).

Paratypes: **ECUADOR: Napo:** Res. Ethnica Waorani, 1 km S. Onkone Gare Camp, 0.65278°N 76.43333°W, 220 m, 21 Jun 1994, T. L. Erwin et al., 1♀ (UCR_ENT 00026700) (USNM). Res. Ethnica Waorani, 1km S. Onkone Gare Camp, 0.63333°N 76.6°E, 220 m, 25 Jun 1944, T.L. Erwin, 1♀ (UCR_ENT 00026702) (USNM); 18 Jan

1994, T.L. Erwin, 1♂ (UCR_ENT 00026706) (USNM); 21 Jun 1994, T. L. Erwin et al., 1♂ (UCR_ENT 00026705) (USNM); 25 Jun 1994, T. L. Erwin et al., 1♂ (UCR_ENT 00026704) (USNM); 29 Jun 1994, T. L. Erwin et al., 1♀ (UCR_ENT 00026703) (USNM); 03 Jul 1994, T. L. Erwin et al., 1♀ (UCR_ENT 00026701) (USNM). **Orellana:** Tiputini Biodiversity Station nr Yasuni National Park Erwin Transect - T/10, 0.63194°N 76.14417°W, 220 m, 05 Feb 1999, T.L. Erwin, 1♂ (UCR_ENT 00028010) (USNM). Transect Ent. 1 km S. Onkone Gare Camp, Reserva Etnica Waorani, Onkone Gare Camp, 0.65714°N 76.453°W, 216 m, 02 Oct 1996, T. L. Erwin et al., 1♂ (UCR_ENT 00027858) (USNM); 03 Oct 1996, T. L. Erwin et al., 4♂ (UCR_ENT 00028069, UCR_ENT 00028070) (USNM). **Sucumbios:** 38 km S of Pompeya, 0.65278°N 76.43333°E, 220 m, 02 Feb 2996 - 14 Feb 2996, T. J. Henry, 1♀ (UCR_ENT 00026638), 1♀ (UCR_ENT 00026639) (USNM).

Diagnosis. This species can be recognized by the following combination of characters: small, crescent-shaped male-specific organ orifice (Fig 4.4F); relatively flat frons and vertex (Fig 4.5F); foretibia without black spines; unequal in size patches of hairlike sensilla on sterna 4-5 (Fig 4.6F); small mediotergite 8 process (Fig 4.7F); posteriorly rounded pygophore with larger right side extension; large pygophore cavity; presence of anterior anophoric process (Fig 4.8F). Most similar to *V. brevicavus*, but distinguished by the large pygophore cavity, and to *Voragocoris* species with large pygophore cavity, from which it is distinguished by the small crescent-shaped male-specific organ orifice.

Description. *Male* (Figs 4.1F, 4.2F, 4.3F). Body length 1.14 mm. COLORATION. Brown to dark brown. SURFACE AND VESTITURE. As in generic description, patches

of hairlike sensilla on sterna 4-5 unequal in size, patch on sternum 4 smaller than on sternum 5, both transverse (Fig 4.6F). STRUCTURE. Head with frons lightly curved in lateral view, with small depression corresponding to male-specific organ (Fig 4.5F); male-specific organ orifice relatively small, dorso-ventrally elongated, with ventral V-shaped carina; vertex flat, without furrow (Fig 4.4F); thorax and pregenital abdomen as in generic description. GENITALIA (Figs 4.7F, 4.8F). Mediotergite 8 with small hook-like process curved dorsally; pygophore rounded, with larger right side extension, apex broadly rounded; pygophore cavity large, round; vesica without noticeable processes; anterior anophoric process present, slender and tapering (Fig 4.8F).

Female (Figs 4.1G, 4.2G, 4.9): body length 0.97 mm, elongate oval, macropterous. Other features as in generic description.

Etymology. Named for the crescent-shaped orifice of the male-specific organ.

Distribution. This species is known from multiple localities in northern Ecuador.

Voragocoris obscurus new species

Holotype: **PERU: Junin:** San Ramon de Pangoa, 40 km SE Satipo, 11.48333°S 74.4°W, 750 m, 28 Feb 1972, R.T. and J.C. Schuh, 1♂ (UCR_ENT 00096830) (AMNH).

Diagnosis. This species can be recognized by the following combination of characters: very small, inconspicuous male-specific organ orifice, located very close to clypeus (Fig 4.4G); relatively flat frons and vertex (Fig 4.5G); foretibia without black spines; equal in size patches of hairlike sensilla on sterna 4-5 (Fig 4.6G); small mediotergite 8 process (Fig 4.7G, 4.8G); triangular, slightly constricted from sides pygophore; indistinct, only

lightly depressed pygophore cavity; presence of anterior anophoric process (Fig 4.8G). Most similar to V. *brevicavus*, from which could be distinguished by inconspicuous male-specific organ orifice, very reduced pygophore cavity, and presence of anterior anophoric process.

Description. *Male* (Figs 4.1H, 4.2H, 4.3G). Body length 1.02 mm. COLORATION. Brown to dark brown. SURFACE AND VESTITURE. As in generic description, patches of hairlike sensilla on sterna 4-5 equal in size, both round (Fig 4.6). STRUCTURE. Head with frons lightly curved in lateral view, with very small depression corresponding to male-specific organ (Fig 4.5G); male-specific organ orifice very small, very close to clypeus (Figs 4.4G); vertex flat, without furrow; thorax and pregenital abdomen as in generic description. GENITALIA (Figs 4.7G, 4.8G). Mediotergite 8 with small hook-like process curved dorsally; pygophore triangular, lightly constricted from sides, apex narrowly rounded; pygophore cavity indistinct, only lightly depressed; vesica without noticeable processes; anterior anophoric process present, flat and lobe-like (Fig 4.8G). *Female*. Unknown.

Etymology. Named for having a very small and inconspicuous male-specific organ and pygophore cavity.

Distribution. This species is known from a single specimen from Peru.

Voragocoris rostralis new species

Holotype: **PERU: Madre de Dios:** Los Amigos Biol.Sta. trail 10, 12.56233°S 70.09641°W, 300 m, 25 Dec 2010, C. Weirauch, 1♂ (UCR_ENT 00082340) (UCR).

Paratypes: **PERU: Madre de Dios:** Los Amigos Biol.Sta. trail 10, 12.56233°S 70.09641°W, 300 m, 25 Dec 2010, C. Weirauch, 1♂ (UCR_ENT 00077337) (UCR).

Diagnosis. This species can be recognized by the following combination of characters: large male-specific organ orifice, located on a prominent tapering bilobed frontal projection (Fig 4.5H); flat vertex, tapering bilobed projection on frons; foretibia conspicuous with black spines (Figs 4.4H, 4.5H); unequal in size patches of hairlike sensilla on sterna 4-5 (Fig 4.6H); small mediotergite 8 process (Fig 4.7H); posteriorly rounded pygophore; large pygophore cavity; presence of anterior anophoric process (Fig 4.8H). Most similar to V. *schuhi*, but distinguished by the tapering bilobed projection on frons, surrounding the frontal organ orifice.

Description. *Male* (Figs 4.1I, 4.2I, 4.3H). Body length 1.06 mm. COLORATION. Dark brown to black. SURFACE AND VESTITURE. As in generic description, patches of hairlike sensilla on sterna 4-5 unequal in size, patch on sternum 4 slightly smaller and slightly oval, patch on sternum 5 large and oval. STRUCTURE. Head with frons flat in lateral view, with large tapering bilobed projection (Figs 4.2I, 4.5H); male-specific organ at apex of prominent frontal projection (Fig 4.4H); vertex flat, with furrow running from top of vertex to about 1/2 of distance from top of head to male-specific organ orifice (Fig 4.4H); thorax and pregenital abdomen as in generic description. GENITALIA (Figs 4.7H, 4.8H). Mediotergite 8 with small hook-like process curved dorsally; pygophore rounded, apex broadly rounded; pygophore cavity large, round; vesica without noticeable processes; anterior anophoric process present, slender and tapering (Fig 4.8H).

Female. Unknown.

Etymology. Named for the pronounced tapering frontal projection of the male-specific organ, resembling a rostrum.

Distribution. This species is known from a single locality in Peru.

Voragocoris schuhi Weirauch, 2012

Diagnosis. This species can be recognized by the following combination of characters: large male-specific organ orifice, located on a prominent rounded bilobed frontal projection; relatively flat vertex and frons; foretibia without black spines; unequal in size patches of hairlike sensilla on sterna 4-5; small mediotergite 8 process; posteriorly rounded pygophore; large pygophore cavity; absense of anterior anophoric process. Most similar to *V. rostralis*, but distinguished by the rounded bilobed projection on frons, surrounding the male-specific organ orifice; and to *V. amrishi*, but distinguished by having only single vesical process. See diagnosis and discussion sections of *V. amrishi* for additional information.

Description. See Weirauch (2012).

Voragocoris unicornis new species

Holotype: **COLOMBIA: Amazonas:** Mata Mata, Amacayacu, 3.82111°S 70.26111°W, 29 Aug 1997 - 03 Sep 1997, M. Sharkey, 1♂ (UCR_ENT 00081313) (UCR).

Diagnosis. This species can be recognized by the following combination of characters: large male-specific organ orifice, located on a prominent bilobed frontal projection, with dorsally directed medial spine (Fig 4.4J, 4.5I); flat vertex, tapering bilobed projection on

frons; foretibia without black spines; almost equal in size patches of hairlike sensilla on sterna 4-5 (Fig 4.6I); small mediotergite 8 process (Figs 4.7I, 4.8I); posteriorly rounded pygophore; large pygophore cavity; presence of anterior anophoric process (Fig 4.8I). Most similar to *V. schuhi* and *V. rostralis*, but distinguished by the presence of dorsally directed medial spine on frons.

Description. *Male* (Figs 4.1J, 4.2J, 4.3I). Body length 1.11 mm. COLORATION. Brown to dark brown. SURFACE AND VESTITURE. As in generic description, patches of hairlike sensilla on sterna 4-5 almost equal in size, patch on sternum 4 round, patch on sternum 5 oval. STRUCTURE. Head with frons flat in lateral view, with prominent bilobed projection and dorsally directed medial spine (Figs 4.4I, 4.5I, 4.5J); male-specific organ at apex of prominent frontal projection (Fig 4.4I); vertex flat, with furrow running from top of vertex to about 1/3 of distance from top of head to male-specific organ orifice (Fig 4.4I); thorax and pregenital abdomen as in generic description. GENITALIA (Figs 4.7I, 4.8I). mediotergite 8 with small hook-like process curved dorsally; pygophore rounded, apex broadly rounded; pygophore cavity large, elongate oval; vesica without noticeable processes; anterior anophoric process present, slender and tapering (Fig 4.8I). *Female*. Unknown.

Etymology. Named for having a single large spine originating on a frontal projection (“uno” – one, “cornis” – horn).

Distribution. The species is known from a single specimen from Colombia.

References

Azar, D. & Nel, A. (2010) The earliest fossil schizopterid bug (Insecta: Heteroptera) in the Lower Cretaceous amber of Lebanon. *Annales de la Société entomologique de France* 46, 193–197.

Costas, M., Lopez, T. & Vazquez, M.A. (2015) Parque Nacional de la Isla de Coiba, Panamá. *Heteropterus Revista de Entomologia* 15, 101–109.

Emsley, M.G. (1969) The Schizopteridae (Hemiptera: Heteroptera) with the descriptions of new species from Trinidad. *Memoirs of the American Entomological Society* 25, 1–154.

Frankenberg, S., Hoong, C., Knyshov, A. & Weirauch, C. (2018) Heads up: evolution of exaggerated head length in the minute litter bug genus *Nannocoris* Reuter (Hemiptera: Schizopteridae). *Organisms Diversity & Evolution* 18, 211–224.

Hill, L. (1990) Australian *Ogeria* Distant (Heteroptera: Schizopteridae). *Invertebrate Systematics* 4, 697–720.

Hill, L. (2004) *Kaimon* (Heteroptera: Schizopteridae), a new, speciose genus from Australia. *Memoirs of the Queensland Museum* 49, 603–647.

Hill, L. (2013) A revision of *Hypselosoma* Reuter (Insecta: Heteroptera: Schizopteridae) from New Caledonia. *Memoirs of the Queensland Museum* 56, 407–455.

Hill, L. (2014) Revision of *Silhouettanus* with description of nine new species (Hemiptera: Heteroptera: Schizopteridae). *Zootaxa* 3815, 353–385.

Hill, L. (2015) Three new genera of Schizopteridae from Australia with description of six new species (Hemiptera: Heteroptera: Schizopteridae). *Zootaxa* 3990, 73–96.

Knyshov, A., Hoey-Chamberlain, R. & Weirauch, C. (2018) Comparative morphology of male genitalic structures in the minute litter bugs Dipsocoromorpha (Insecta: Hemiptera: Heteroptera). *Journal of Morphology* 279, 1480–1517.

Knyshov, A., Leon, S., Hoey-Chamberlain, R. & Weirauch, C. (2016) *Pegs, pouches, and spines: systematics and comparative morphology of the New World litter bug genus Chinannus Wygodzinsky, 1948*. Entomological Society of America, Annapolis, MD.

Leon, S. & Weirauch, C. (2016a) Scratching the surface? Taxonomic revision of the subgenus *Schizoptera* (*Odontorhagus*) reveals vast undocumented biodiversity in the largest litter bug genus *Schizoptera* Fieber (Hemiptera: Dipsocoromorpha). *Zootaxa* 4184, 255–284.

Leon, S. & Weirauch, C. (2016b) Small Bugs, Big Changes: Taxonomic Revision of *Orthorhagus* McAtee & Malloch. *Neotropical Entomology* 45(5), 559–572.

Makhan, D. (2013a) *Voragocoris amrishi* sp. nov., a new Schizopterinae (Hemiptera: Heteroptera: Schizopteridae) from Suriname. *Calodema* 293, 1–4.

Makhan, M. (2013b) *Soekhnandanius aschne* gen. et sp. nov., Schizopterinae (Hemiptera: Heteroptera: Schizopteridae) from Suriname. *Calodema* 291, 1–3.

Poinar, G.J. & Brown, A. (2014) New genera and species of Jumping Ground Bugs (Hemiptera: Schizopteridae) in Dominican and Burmese amber, with a description of a meloid (Coleoptera: Meloidae) triungulin on a Burmese specimen. *Annales de la Société entomologique de France (N.S.): International Journal of Entomology* 50, 372–381.

Rédei, D. (2008a) First record of *Pinochius* Carayon, 1949 from the Oriental Region, with description of a new species from Vietnam (Heteroptera: Schizopteridae). In: S. Grozeva and N. Simov (Eds), *Advances in Heteroptera research: festschrift in honor of 80th anniversary of Michail Josifov. [Pensoft Series Faunistica No 82.]*. Pensoft Publishers, pp. 327–337.

Rédei, D. (2008b) Two new species of *Kokeshia* from India and Thailand (Hemiptera: Heteroptera: Schizopteridae). *Acta Entomologica Musei Nationalis Pragae, 48*(2), 241–250.

Weirauch, C. (2012) *Voragocoris schuhi*, a new genus and species of Neotropical Schizopterinae (Hemiptera: Schizopteridae). *Entomologia Americana* 118, 285–294.

Weirauch, C. & Frankenberg, S. (2015) From "insect soup" to biodiversity discovery: taxonomic revision of *Peloridinannus* Wygodzinsky, 1951 (Hemiptera: Schizopteridae), with description of six new species. *Arthropod Systematics and Phylogenetics* 73, 457–471.

Weirauch, C., Knyshov, A. & Hoey-Chamberlain, R. (2017) *Machadonannus brailovskyi*, n. sp., a new species of Schizopteridae from the Afrotropical region. *Dugesiana* 24, 279–286.

Weirauch, C., Whorrall, K., Knyshov, A. & Hoey-Chamberlain, R. (2018) Giant among dwarfs: *Meganannus lewisi*, gen. n. and sp. n., a new genus and species of minute litter bugs from Costa Rica (Hemiptera: Schizopteridae). *Zootaxa* 4370, 156–170.

Table 4.1. Measurements (in mm) of selected specimens of *Voragocoris*.

Species	Total length	Head across eyes	Synthlipsis	Pronotal width
V. brevicavus Panama	0.98	0.47	0.27	0.53
V. brevicavus Belize	1.03	0.44	0.25	0.46
V. brevicavus Brazil	0.86	0.48	0.27	0.53
V. cavifrons	1.05	0.53	0.29	0.56
V. convexifrons	1.05	0.43	0.23	0.53
V. crescentus male	1.14	0.53	0.30	0.55
V. crescentus female	0.97	0.40	0.22	0.45
V. obscurus	1.02	0.48	0.27	0.53
V. rostralis	1.06	0.50	0.25	0.51
V. unicornis	1.11	0.49	0.27	0.54

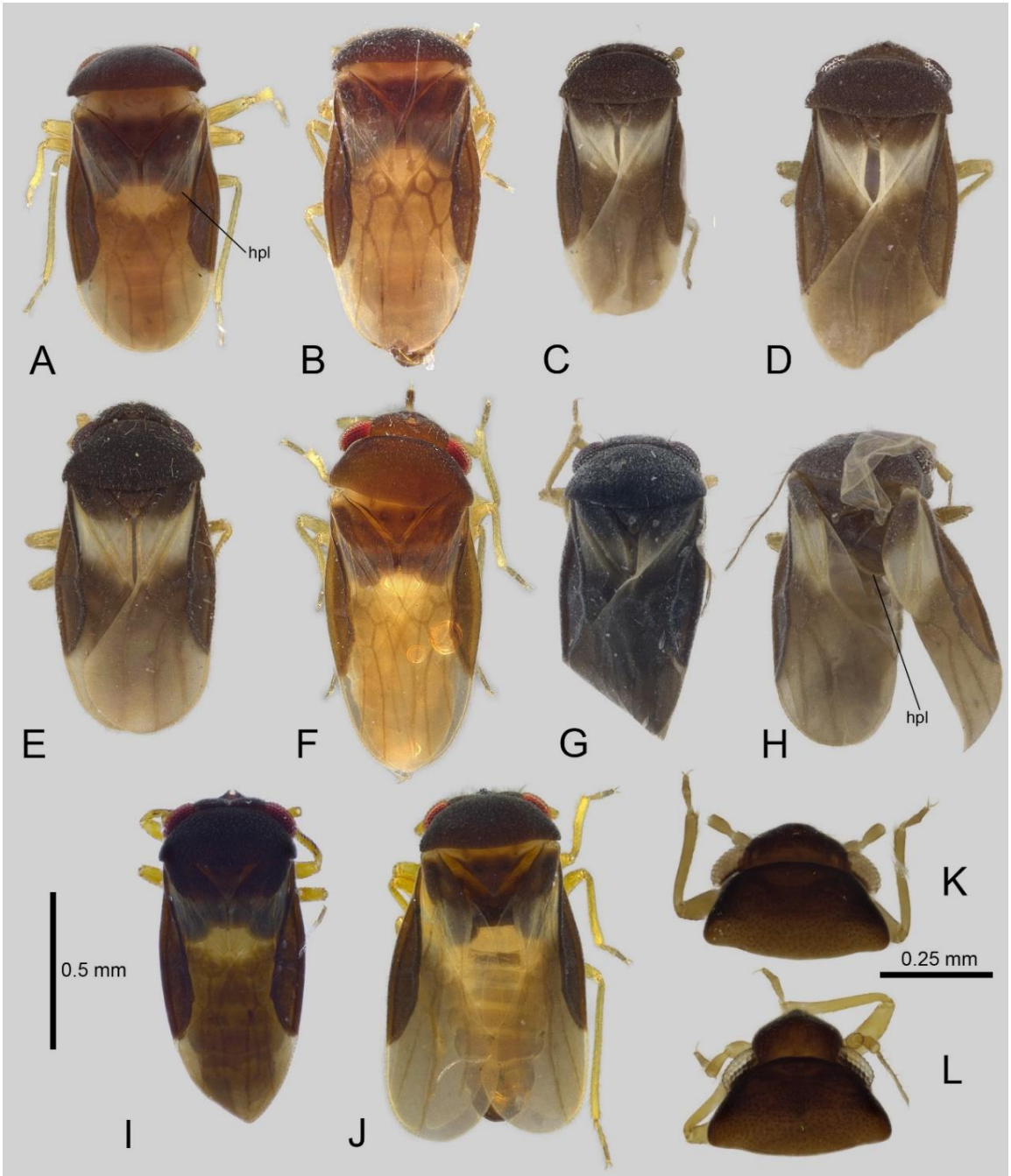

Figure 4.1. Habitus of *Voragocoris*, dorsal view. A. *V. brevicavus*, male, Panama. B. *V. brevicavus*, male, Belize. C. *V. brevicavus*, male, Brazil. D. *V. cavifrons*, male. E. *V. convexifrons*, male. F. *V. crescentus*, male. G. *V. crescentus*, female. H. *V. obscurus*, male. I. *V. rostralis*, male. J. *V. unicornis*, male. K. *V. brevicavus*, dorsal view on frons. L. *V. convexifrons*, dorsal view on frons. Scale bar of 0.5 mm is for figures A-J, scale bar of 0.25 mm is for figures K-L.

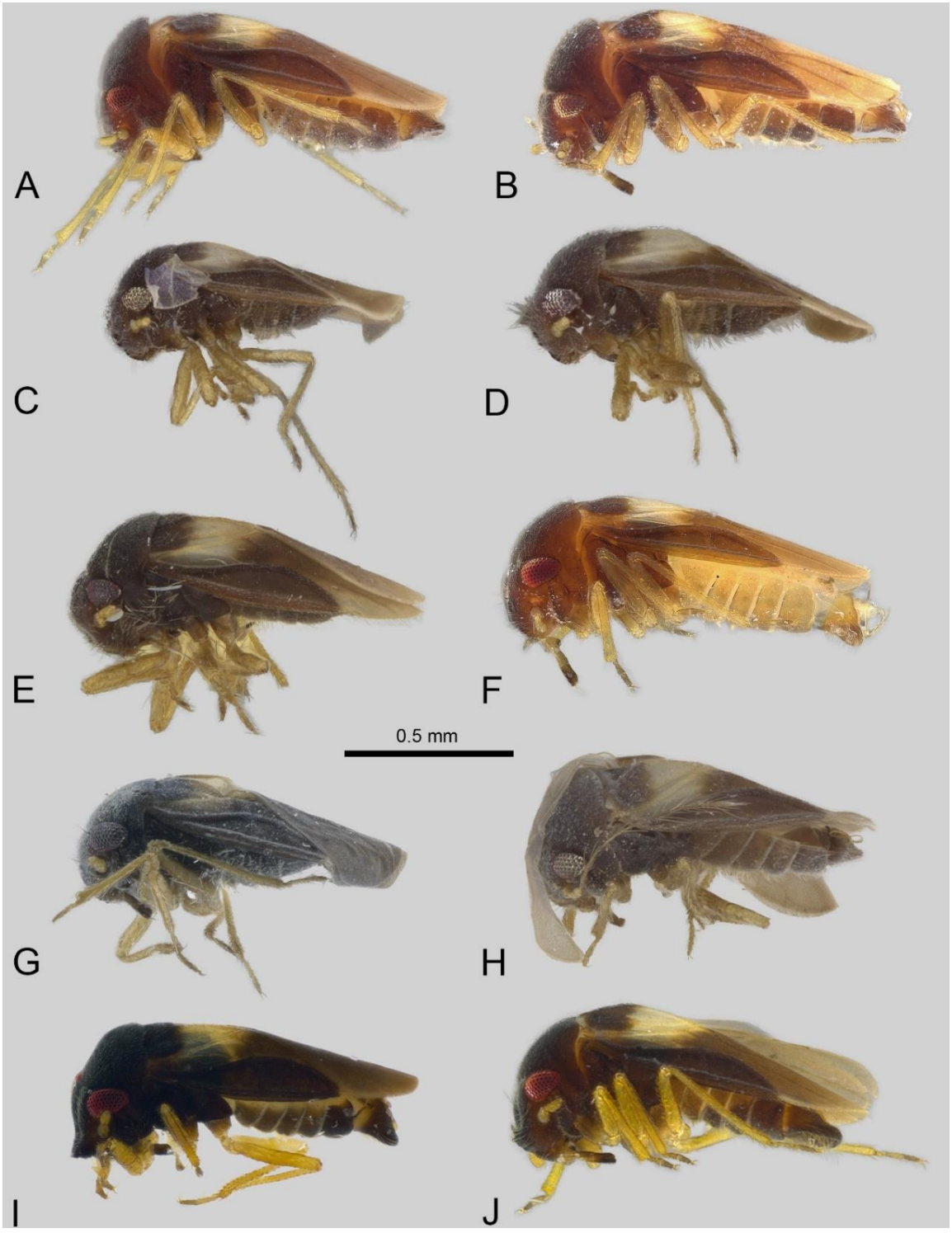
A
B
C
D
E
F
0.5 mm
G
H
I
J

Figure 4.2. Habitus of *Voragocoris*, lateral view. A. *V. brevicavus*, male, Panama. B. *V. brevicavus*, male, Belize. C. *V. brevicavus*, male, Brazil. D. *V. cavifrons*, male. E. *V. convexifrons*, male. F. *V. crescentus*, male. G. *V. crescentus*, female. H. *V. obscurus*, male. I. *V. rostralis*, male. J. *V. unicornis*, male.

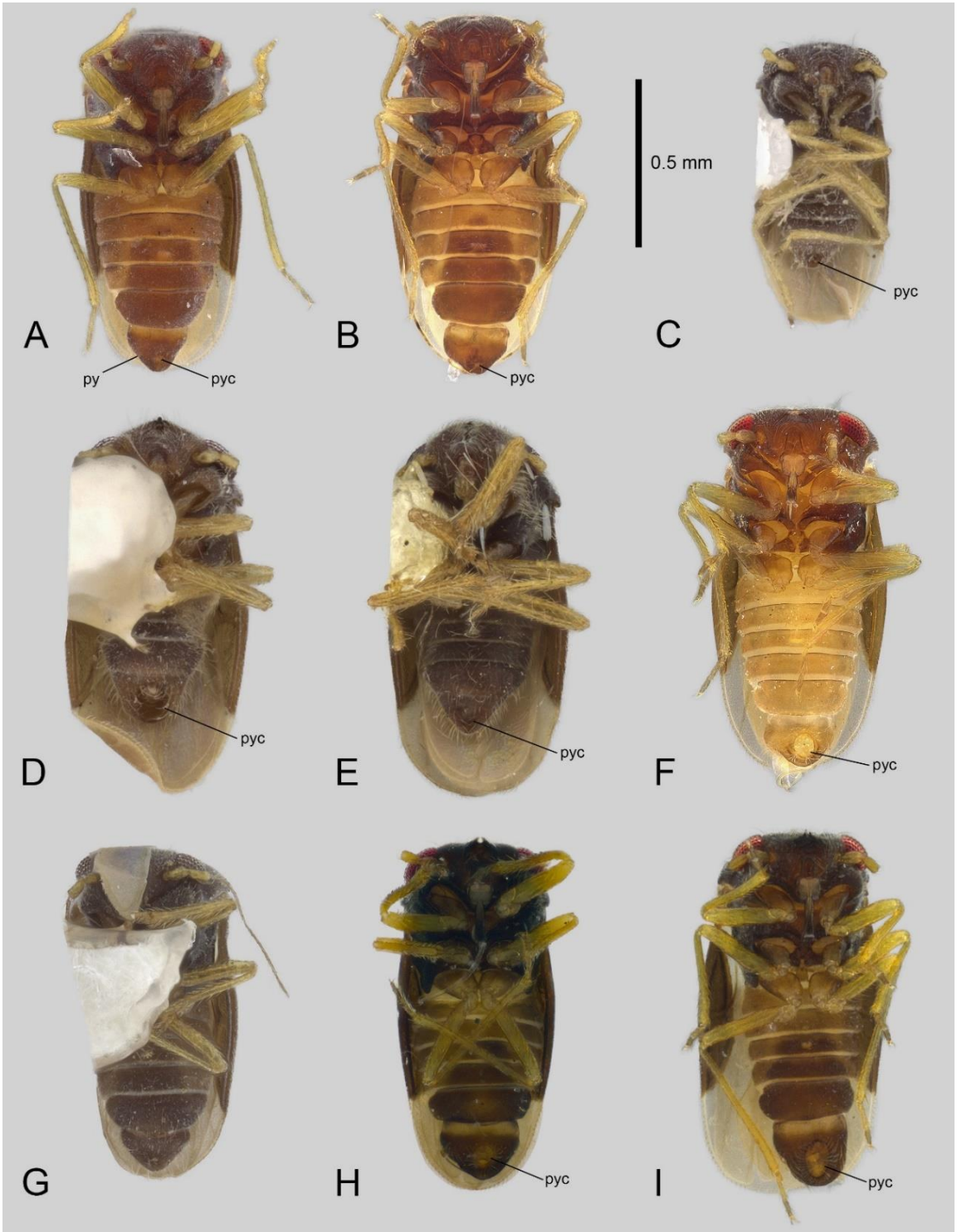

Figure 4.3. Habitus of *Voragocoris* male specimens, ventral view. A. *V. brevicavus*, Panama. B. *V. brevicavus*, Belize. C. *V. brevicavus*, Brazil. D. *V. cavifrons*. E. *V. convexifrons*. F. *V. crescentus*. G. *V. obscurus*. H. *V. rostralis*. I. *V. unicornis*.

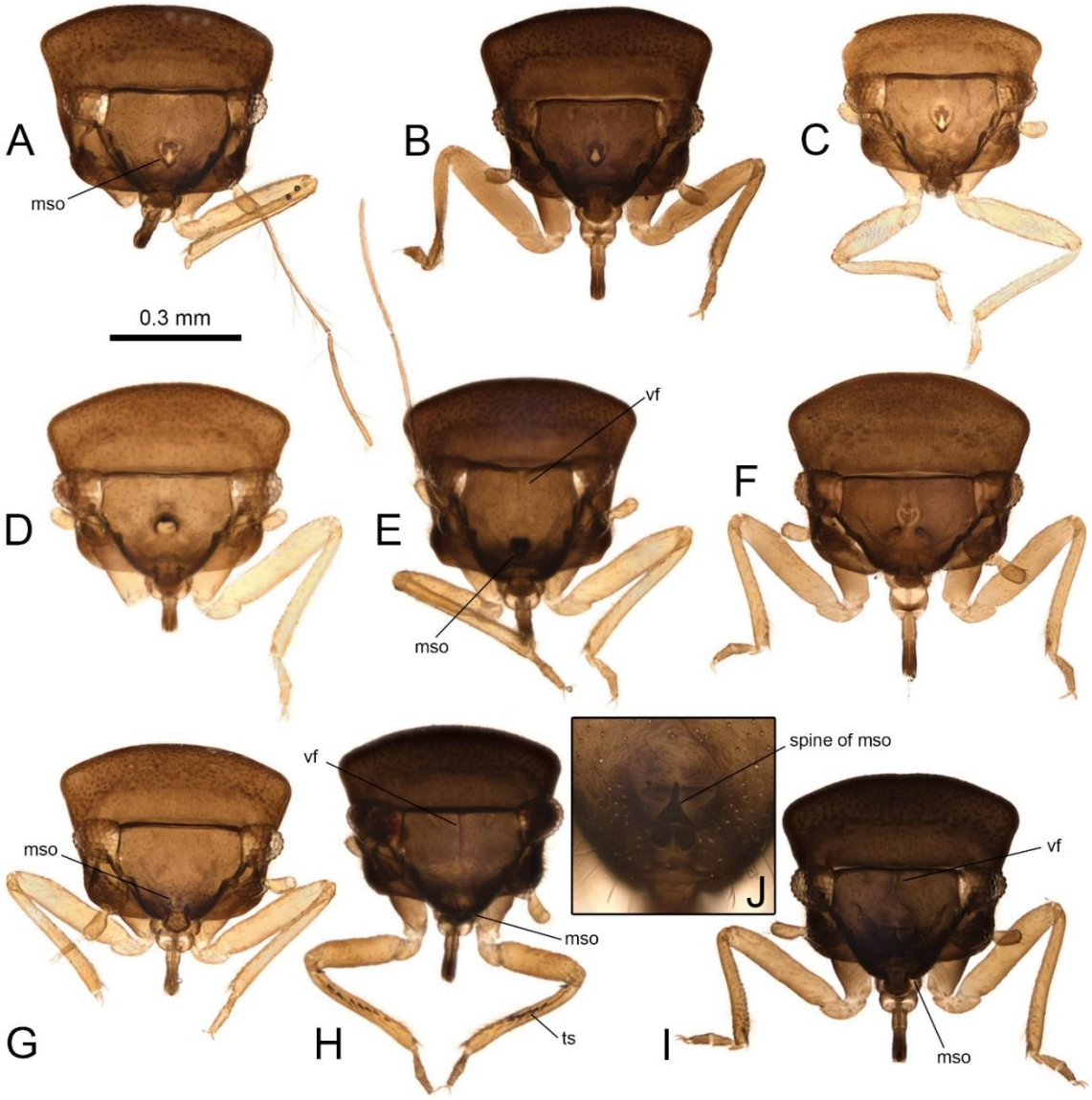

Figure 4.4. Frontal view of head and prothorax of *Voragocoris* male specimens. A. *V. brevicavus*, Panama. B. *V. brevicavus*, Belize. C. *V. brevicavus*, Brazil. D. *V. cavifrons*. E. *V. convexifrons*. F. *V. crescentus*. G. *V. obscurus*. H. *V. rostralis*. I. *V. unicornis*. J. *V. unicornis*, frontal male-specific organ close-up.

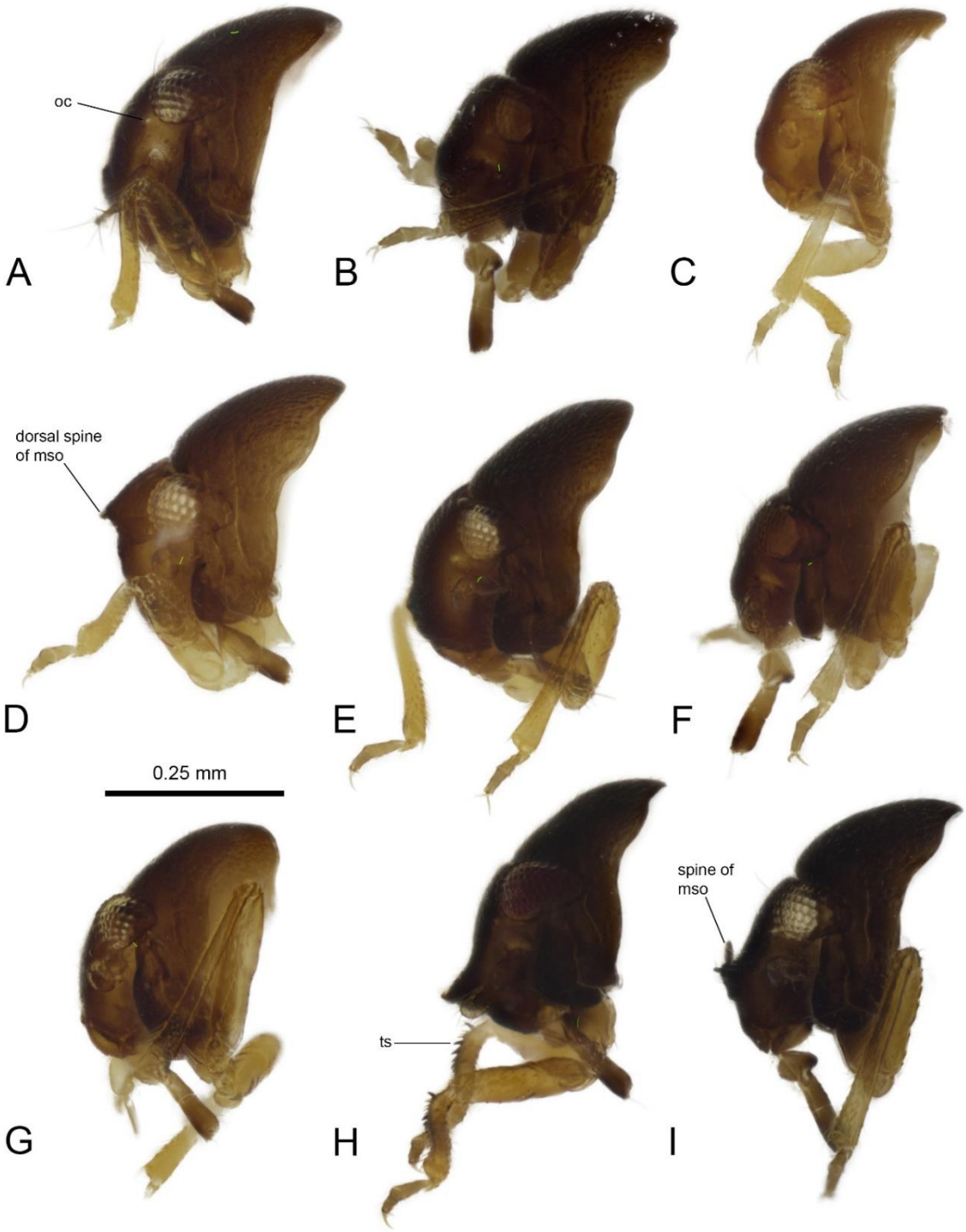

Figure 4.5. Lateral view of head and prothorax of *Voragocoris* male specimens. A. *V. brevicavus*, Panama. B. *V. brevicavus*, Belize. C. *V. brevicavus*, Brazil. D. *V. cavifrons*. E. *V. convexifrons*. F. *V. crescentus*. G. *V. obscurus*. H. *V. rostralis*. I. *V. unicornis*.

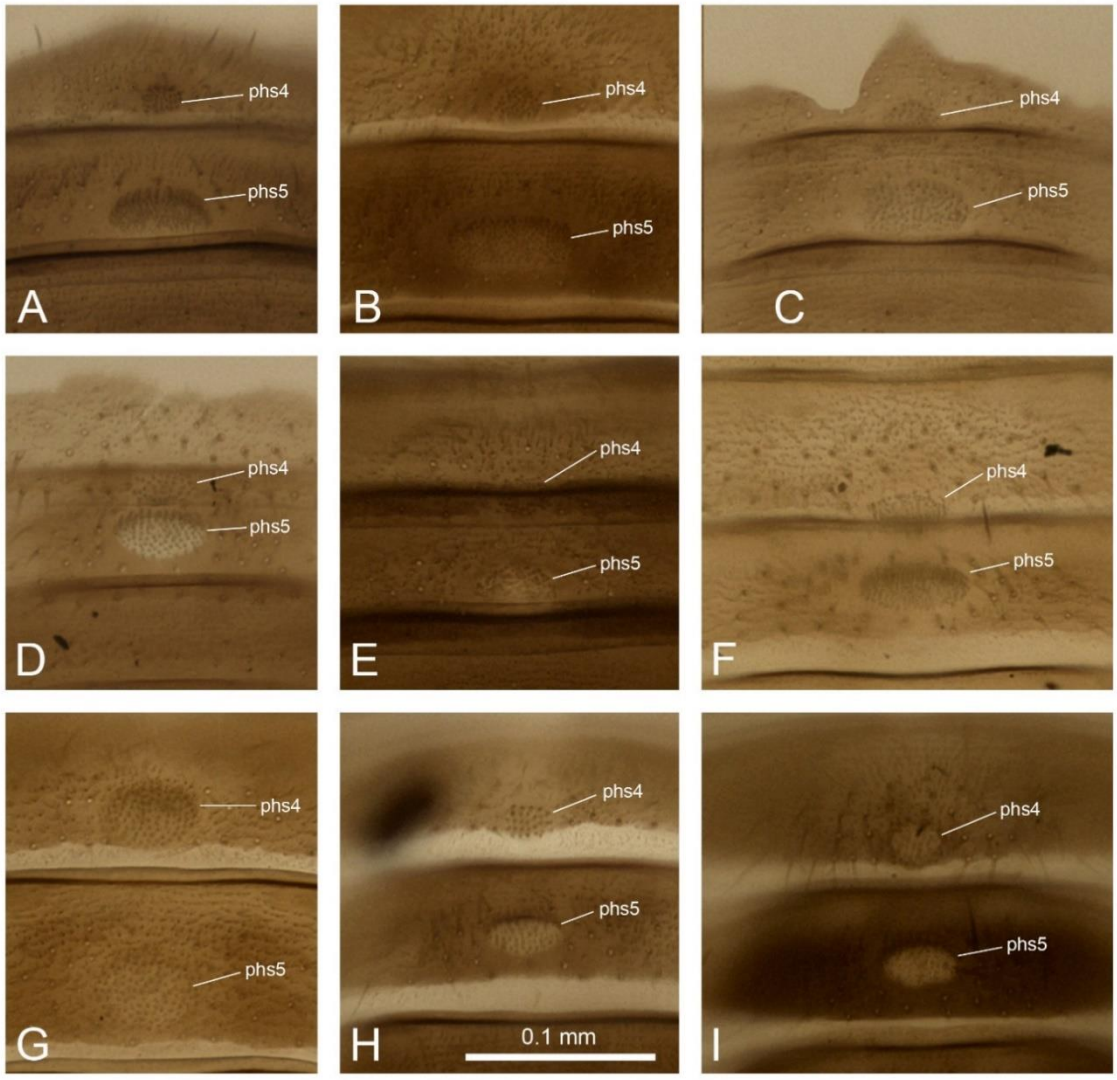

Figure 4.6. Ventral view of male abdomen of *Voragocoris*, showing patches of hairlike sensilla. A. *V. brevicavus*, Panama. B. *V. brevicavus*, Belize. C. *V. brevicavus*, Brazil. D. *V. cavifrons*. E. *V. convexifrons*. F. *V. crescentus*. G. *V. obscurus*. H. *V. rostralis*. I. *V. unicornis*. All images are scaled equally.

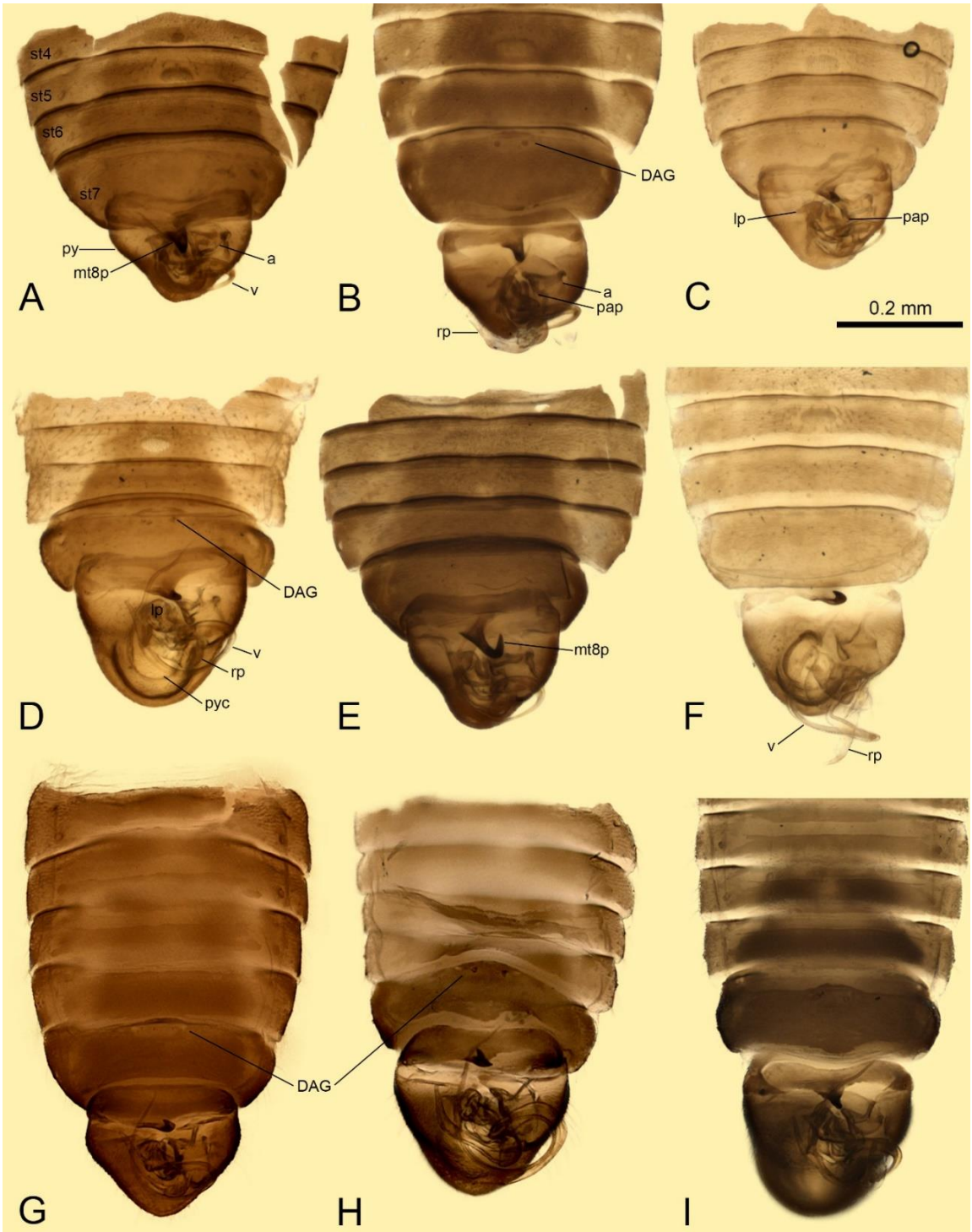

Figure 4.7. Overview of male abdomen of *Voragocoris*. A. *V. brevicavus*, Panama. B. *V. brevicavus*, Belize. C. *V. brevicavus*, Brazil. D. *V. cavifrons*. E. *V. convexifrons*. F. *V. crescentus*. G. *V. obscurus*. H. *V. rostralis*. I. *V. unicornis*.

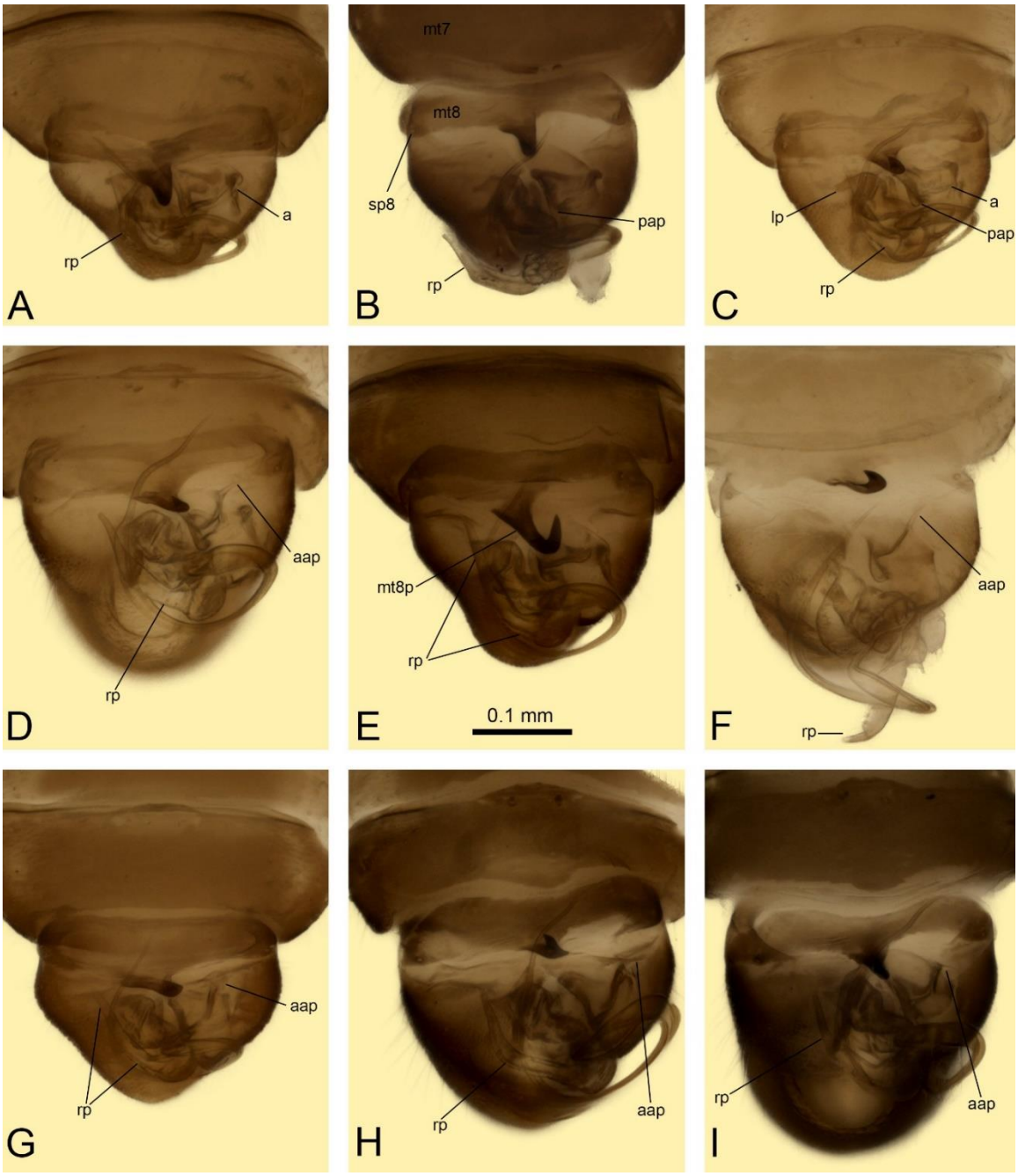

Figure 4.8. Close-up of male genitalia of *Voragocoris*. A. *V. brevicavus*, Panama. B. *V. brevicavus*, Belize. C. *V. brevicavus*, Brazil. D. *V. cavifrons*. E. *V. convexifrons*. F. *V. crescentus*. G. *V. obscurus*. H. *V. rostralis*. I. *V. unicornis*. All images are scaled equally.

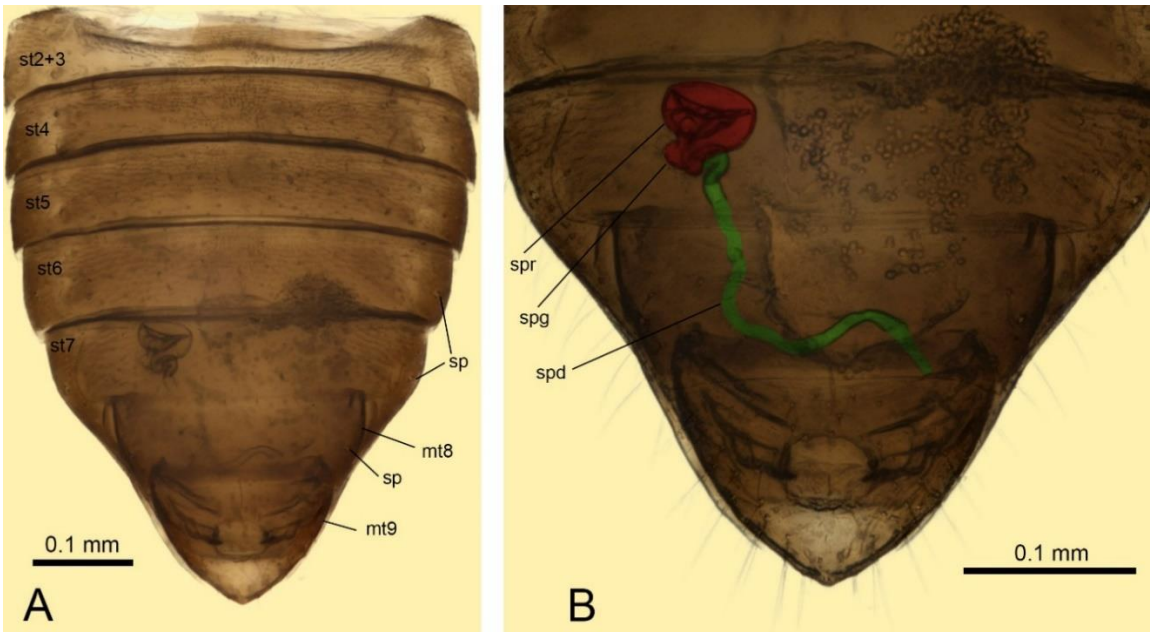

Figure 4.9. Female abdomen and genitalia of *Voragocoris crescentus*. A. Overview of abdomen. B. Close-up of the tip of the abdomen with spermathecal complex colored.

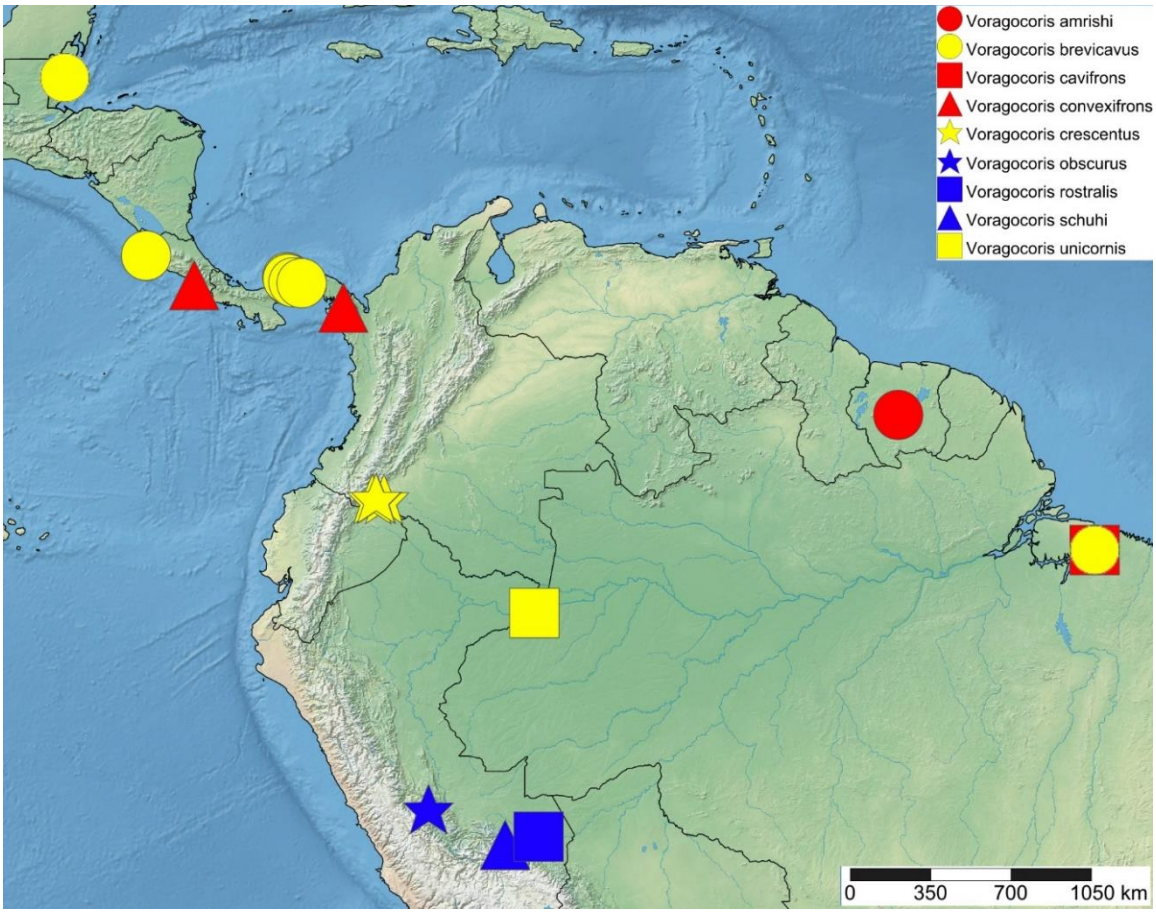

Figure 4.10. Distribution map of *Voragocoris* species.

Chapter 5: Comparative morphology of male genitalic structures across Dipsocoromorpha

Abstract

Insect male genitalia are among the most evolutionarily plastic morphological features that have proven to be valuable for both species identifications and phylogenetic analyses at higher taxonomic levels. Accurate usage of genitalic characters in taxonomic descriptions and phylogenetic analyses depends on consistency of terminology and validity of homology hypotheses. Both areas are underdeveloped in many insect groups. We here document morphology and advance homology hypotheses of male genitalic features for the hemipteran infraorder Dipsocoromorpha, the minute litter bugs. Genitalic structures and the pregenital abdomen in Dipsocoromorpha are strikingly modified and diverse compared to other Heteroptera. In addition to variation in the shape of phallic structures (parameres and aedeagus), minute litter bug genitalia vary in the direction and degree of asymmetry and feature a plethora of processes derived from various abdominal segments with significant variation at low taxonomic levels. Here, male genitalic structures for an extensive taxonomic sample (32 genera and 71 specimens) are documented using scanning electron and confocal microscopy, and a universal terminology for genitalic structures across minute litter bugs is established that will facilitate species discovery and evolutionary research. We conclude by proposing primary homology hypotheses across the infraorder that now can be tested in a phylogenetic framework.

Introduction

Typically differing even between closely related species, insect male genitalia are among the most evolutionarily plastic morphological features (Eberhard 1985). Their apparently fast rate of morphological change has been hypothesized to be due to sexual selection (e.g., Simmons 2014) and provides systematists with diagnostic features at various taxonomic levels (Schuh & Slater 1995; Singh-Pruthi 1925). While often used as species diagnostic characters, especially where other somatic differences are subtle or variable, genitalic features can also be part of the diagnoses for groups at higher taxonomic levels, as e.g., in the Miridae (plant bugs), where species are classified into subfamilies based on the shape of the pygophore and parameres, and the structure of the aedeagus (Schuh & Slater 1995). Male genitalia often also provide important character systems for morphology-based phylogenetic analyses (Yoshizawa & Johnson 2006). However, accurate usage of genitalic characters in classifications and phylogenetic frameworks depends on the consistency of terminology and validity of homology hypotheses. Historically, genitalic terminology in different insect orders has developed at least partially in isolation, resulting in incompatible and sometimes misleading terminology when applied outside of that group. On one hand, a plethora of terms has been suggested for homologous genitalic structures even within Heteroptera, making descriptions and diagnoses unnecessarily complicated. On the other hand, structures that based on the outcomes of phylogenetic analyses are shown to be convergently evolved in different groups are frequently still denoted by the same terms, implying homology where likely

none exists. To overcome these problems, comparative morphological studies are critical to assess primary homology hypotheses and revise terminology.

Dipsocoromorpha (minute litter bugs) is a small, relatively poorly studied monophyletic group within the Heteroptera (true bugs) that currently encompasses only ~430 described species (Weirauch *et al.* 2018) yet exhibits an astounding diversity of male genitalic structures. Structural variation across the infraorder and the five currently recognized families includes various types and degrees of asymmetry of the genitalia, modifications of the pregenital abdominal segments, and the length of the intromittent organ that ranges from being shorter than the pygophore to 20 times the insect's body length (Frankenberg & Weirauch in review; Štys 1970). This situation greatly contrasts with those in the closely related infraorders Enicocephalomorpha and Gerromorpha (Wang *et al.* 2017) that lack pregenital modifications and show modest levels of genitalic variation. Even more strikingly, and not typically encountered in other insect groups to the same extent (but see Bowsher *et al.* 2013), is the abundance of taxon-specific processes and appendages on various segments that have been discussed in the framework of accessory genitalia (Štys 1974). Both symmetry-asymmetry shifts and presence-absence of accessory structures could be associated with one or more factors related to sexual selection and causing change in mating position (Huber 2010; Huber *et al.* 2007). Although the functional morphology of the aedeagus and parameres has been described for some dipsocoromorphan taxa (e.g., Hill 1987a; Melber & Köhler 1992), direct observations of mating behavior that could shed light on the functional aspects of other bizarre abdominal modifications are virtually non-existent (Štys 1974), likely due to the

small size, cryptic habitats, and primarily tropical distribution (Emsley 1969) of species in this group. Interestingly, female genitalia in minute litter bugs are nearly or perfectly symmetrical, the ovipositor is reduced in the majority of species, and structural variation is typically limited to the shape of the spermathecal reservoir and length of the spermathecal duct that approximates the length of the male vesica (Emsley 1969; Knyshov *et al.* 2016; Pluot-Sigwalt & Péricart 2003; Weirauch & Frankenberg 2015). This study therefore focuses on documentation and discussion of the diverse male genitalic structures.

The astounding diversity of genitalic structures of minute litter bugs has received very little attention outside of the small group of taxonomists who began illustrating male genitalia of Dipsocoromorpha around the middle of the 20th century as part of their taxonomic descriptions and evaluations of evolutionary relationships across the group (e.g., Wygodzinsky 1948a, 1948b). Most publications reviewing male genitalic morphology of insects (Dupius 1970; Matsuda 1976; Scudder 1971) or true bugs (Singh-Pruthi 1925; Yang & Chang 2000) omitted Dipsocoromorpha or only included observations on few species. However, the abundance of appendages and processes that are unique to a particular species or genus made it difficult to recognize homologous features and establish a standardized terminology. Multiple terms have been used for the same structures (see Table 5.2), and homology hypotheses between them have never been proposed and tested. Only two papers from the late 60s (Emsley 1969; Štys 1970) provided more synthetic synopses of dipsocoromorphan genitalic features. However, Emsley (1969) limited his study to only one of the dipsocoromorphan families and Štys

(1970) largely based his review on literature data. Terminology in many cases is incompatible between the two studies and homology hypotheses for certain abdominal structures differ (see Table 5.2).

As part of a United States National Science Foundation (NSF) funded Advancing Revisionary Taxonomy and Systematics (ARTS) project, we assembled the largest worldwide collection of minute litter bugs and described several new genera (Hoey-Chamberlain & Weirauch 2016; Weirauch *et al.* 2018) and many new species (Knyshov *et al.* 2016; Leon & Weirauch 2016a, 2016b; Weirauch & Frankenberg 2015; Weirauch *et al.* 2017). This collection contains species that represent 28 relatively common and species-rich genera of Dipsocoromorpha in the three species-rich families and representatives of four currently undescribed genera. This material therefore has provided us with the opportunity to conduct the most comprehensive comparative morphological study of male genitalic structures of Dipsocoromorpha to date. Here we aim not only to document genitalia in the realm of species discovery, but also to establish a universal terminology for genitalic structures across the group and propose primary homology hypotheses that can subsequently be tested in a phylogenetic framework.

Material and Methods

Material

Material used in the present study comprises 71 specimens belonging to 32 genera, four of which are currently undescribed. Taxon sampling was somewhat limited by availability, but overall achieved the aim of studying at least one species per genus with examination of multiple species when possible, resulting in a taxonomic sample (see

Table 5.1) that fairly comprehensively represents the phylogenetic diversity of the group (Knyshov *et al.* in prep.). Hypsipterygidae and Stemmocryptidae, for which specimens for comparative genitalic examination remained unavailable to us, are reviewed in the discussion section based on the excellent documentations of Štys (1970, 1983b). Examined specimens were assigned a unique specimen identifier number (USI) and associated information can be retrieved from the Heteroptera Species Pages website (http://research.amnh.org/pbi/heteropteraspeciespage/).

Methods

Selected specimens were first habitus imaged using a Leica DFC 450 C imaging system. They were then cleared with either KOH or proteinase K (for specimens subsequently subjected to DNA extraction, Knyshov *et al.* in prep.). Abdomens were then separated and imaged using a Zeiss Axioskop 2 compound microscope and a Leica SP5 Inverted confocal microscope. The male aedeagus was dissected out of the genital capsule and imaged separately using confocal microscopy. Additional specimens were visualized using scanning electron microscopy using a FEI XL30-FEG electron microscope. For confocal microscopy, 488 and 543 nm lasers were used to excite the cuticle, detectors were set to the diapasons of 500-535 nm (green in figures), and 555-700nm (red in figures); these colors are retained in Figs 5.17-21 and in plates documenting the pregenital abdomen in Figs 5.11-16. To facilitate comparision between structures across different taxa and to emphasize our homology hypotheses, genitalic features in Figs 5.7-16 were color coded as follows: light blue – tergum 7, pink – tergum 8, green – left paramere, blue – right paramere, orange – aedeagus, red – segments 10+11.

Terminology

A terminological vocabulary was assembled after review of pertinent taxonomic and comparative papers on Dipsocoromorpha, with preferred terms as well as synonyms indicated in Table 5.2.

Terminology for lateral abdominal sclerites in Dipsocoromorpha

A number of different abdominal appendages in minute litter bugs have frequently been treated as modified laterotergites implying that these structures are serial homologs to lateral sclerites of the pregenital abdomen (e.g., Štys 1970). Whenever not appendage-like, the lateral sclerites of the abdominal terga can be located in dorsal or ventral positions, or be separated into dorsal and ventral sclerites (see results and discussion). Possibly because of this variation, several terms have been used to refer to these structures: laterotergite (Hill 1980; Štys 1970, 1985), paratergite (Emsley 1969), and/or parasternite (Emsley 1969; Wygodzinsky 1948b, 1958). As an attempt to address this problem in Hemiptera in general, Sweet (1996) argued, based on musculature attachment and spiracle position, that these sclerites that had long been considered to be part of the tergum or the sternum instead belong to the pleurum. He proposed the terms epipleurite and hypopleurite for these sclerites. Klug and Klass (2007) on the contrary concluded that dorso-ventral musculature and spiracle positions are not reliable in demarcating tergal, pleural, and sternal borders, which was also admitted by Sweet (1996). Cassis and Schuh (2010) examined Sweet's (1996) hypothesis in a cladistic framework, reviewed the relevant iterature, and concluded that at present the origin of the connexival region in Heteroptera remains unclear. The terms epi- and hypopleurite have not become adopted

in the hemipteran literature, and we are unaware of any further studies shedding light on the origin of the connexival sclerites. Here, we use the term laterotergite (or dorsal and ventral laterotergites), which is the most frequently used term for lateral abdominal sclerites in Dipsocoromorpha and the term used for these sclerites in a recent textbook on insect morphology (Beutel *et al.* 2014). We also conclude that despite the single term, homology of these sclerites even across Dipsocoromorpha is doubtful (see discussion), and researchers should exercise care in using this data for phylogenetic purposes.

Terminology for male intromittent organ and its components

The heteropteran male intromittent organ, here referred to as aedeagus after Singh-Pruthi (1925) and others, has also been called phallus (Snodgrass 1936, 1957) or penis (Matsuda 1976). The aedeagus is typically comprised of basal plates (single or multiple sclerites at the base), phallosoma or phallotheca (typically more or less sclerotized portion), and endosoma (that can be sclerotized or membranous, and typically retracts into the phallosoma) (Singh-Pruthi 1925). Snodgrass (1936, 1957) used the term aedeagus for phallosoma and endosoma together, and the term phallus for all of the components including the basal plates. However, since the terms aedeagus and phallus have been used interchangeably in the literature, we do not follow this somewhat confusing terminology. The endosoma may be differentiated into proximal conjunctiva that may have sclerotized appendages, and the distal vesica (Singh-Pruthi 1925). See the discussion on how and why we use this terminology for Dipsocoromorpha.

Results

Each description starts with an overview of the pregenital abdomen (segments 1-7), sclerotization patterns, presence or absence of lateral subdivisions of terga or sterna (dorsal or ventral laterotergites), spiracle positions, and dorsal abdominal gland (DAG) scars locations. Following this section is the review of modifications of the pregenital abdomen, which occur on the anterior area of the abdomen, the entire abdomen, or are restricted to segment 7. We suspect that most modifications of segment 7 are related to genitalic functions; however, we here follow the traditional subdivision of pregenital and genital abdomen at the border of segments 7 and 8. The documentation of genitalic structures begins with segment 8 and its modifications, followed by the pygophore (segment 9), parameres, and aedeagus. For the conjunctiva we focus on characterizing elongated, supposedly eversible, sclerites (conjunctival appendages). Segments 10-11 are reviewed at the end. Figure plates are organized in the following sequence: Figs 5.1-2 show dorsal habitus images of selected genera of Dipsocoromorpha, Figs 5.3-6 show an overview of the abdomen of selected genera, Figs 5.7-16 show apical pregenital abdomen and genitalia of all examined genera, and finally Figs 5.17-21 show the aedeagus of most of the studied genera.

Ceratocombidae Dohrn, 1859

Ceratocombinae Dohrn, 1859

Ceratocombini Dohrn, 1859

Ceratocombus Signoret, 1852

Vouchers: *Ceratocombus* sp. (N/A, UCR_ENT 00045174, UCR_ENT 00074810)

Figs 5.1A, 5.7A, 5.11A, 5.17A

Description. **Pregenital abdomen.** Symmetrical, not curved laterally, dorsum less sclerotized than ventrum. Segment 8 and pygophore more sclerotized than segments 1-7. Dorsal surface smooth. Pregenital laterotergites distinct. Six pairs of spiracles present (segments 3-8), located on laterotergites. Scars of DAG orifices present on anterior margin of mediotergites 4, 5, 6, and 7, inconspicuous on first three and distinct on last. **Pregenital abdomen modifications.** Mediotergite 7 symmetrical, short, medially split by membrane into two sclerites. Laterotergites 7 distinct, symmetrical, flat and short. Sternum 7 symmetrical, short. **Genitalia.** Pronounced lateral directionality absent. Mediotergite 8 symmetrical, short or long. Laterotergites 8 distinct, symmetrical, elongated. Sternum 8 symmetrical, long. Pygophore symmetrical, oval, closed dorsally, dorsal surface of pygophore with ridges. Laterotergites 9 distinct, symmetrical, equal in size, elongated. Parameres symmetrical, left equal in size to right. Both parameres elongated, basal process short and rounded, apical process elongated and tapering. Basal plates symmetrical. Phallosoma frame-like, composed of dorsal V-shaped sclerite, attached to basal plates with closed end, without ornamentation, and ventral U-shaped sclerite, attached to basal plates with open end. Conjunctiva heavily sclerotized, composed of two large lateral sclerites, attached to opened end of V-shaped dorsal sclerite, and one medial sclerite, covering vesica from beneath. Vesica with narrow base and straight thin short distal region, folded onto phallosoma in repose. Anophore indistinct, fused with pygophore. Anal tube membranous.

Variation. Genitalic differences among different species of *Ceratocombus* are surprisingly subtle compared to other ceratocombid genera (Štys 1982).

Notes. As opposed to Štys (1977), we treat the dorsal wall of the pygophore as primarily consisting of mediotergite 9, not the anophore (or proctiger), based on its close association with laterotergites 9 in other Ceratocombinae.

Leptonannus Reuter, 1891

Vouchers: *Leptonannus* sp. (UCR_ENT 00036781, UCR_ENT 00125845)

Figs 5.1B, 5.3A, 5.7B, 5.11B, 5.17B

Description. **Pregenital abdomen.** Symmetrical, not curved laterally, dorsum and ventrum equally sclerotized. Segment 8 and pygophore more sclerotized than segments 1-7. Dorsal surface smooth. Pregenital laterotergites distinct except for segment 7. Six pairs of spiracles present (segments 3-8), located on laterotergites. Scars of DAG orifices present on anterior margin of mediotergites 4, 5, and 6. **Pregenital abdomen modifications.** Sterna 2-6 with medial membranous area. Mediotergite 7 symmetrical, short. Laterotergites 7 indistinct. Sternum 7 entire. **Genitalia.** Pronounced lateral directionality absent. Mediotergite 8 symmetrical, short. Laterotergites 8 distinct, symmetrical, elongated. Sternum 8 symmetrical, long. Pygophore symmetrical, oval, closed dorsally, dorsal surface of pygophore with ridges, posterior margin of pygophore may have two elongated rounded processes. Laterotergites 9 distinct, symmetrical, equal in size, elongated. Parameres symmetrical, left equal in size to right. Both parameres elongated, basal process short and rounded, apical process elongated and rounded. Basal

plates symmetrical. Phallosoma frame-like, composed of dorsal V-shaped sclerite, attached to basal plates with closed end, without ornamentation, and ventral U-shaped sclerite, attached to basal plates with open end. Conjunctiva heavily sclerotized, composed of two small proximal lateral sclerites, attached to opened end of V-shaped dorsal sclerite, two large distal lateral sclerites attached to small sclerites, and one medial sclerite, covering vesica from beneath. Vesica with wide base with folding mechanism and thin long distal region, folded onto pahllosoma in repose. Anophore symmetrical, without processes, tightly associated with dorsal sclerite of pygophore. Anal tube ventrally sclerotized.

Notes. The examined specimen from Thailand was identified as *Leptonannus* based on non-genitalic characters. Its genitalic features however significantly differ from the examined specimen that we identified as belonging to this genus from Cameroon as well as *L. biguttulus* Reuter, 1891 (Wygodzinsky 1953): the laterotergites 8 are not appendage-like and processes on the posterior margin of the pygophore are absent.

Issidomimini Štys, 1970

Kvamula Štys, 1982

Vouchers: *Kvamula* sp. (UCR_ENT 00036927, UCR_ENT 00045529)

Figs 5.7C, 5.11C, 5.17C

Description. **Pregenital abdomen.** Symmetrical, not curved laterally, both dorsum and ventrum extremely weakly sclerotized. Segment 8 and pygophore more sclerotized than segments 1-7. Dorsal surface smooth. Pregenital laterotergites hard to discern due to

weak pregenital abdomen sclerotization. Six pairs of spiracles present (segments 3-8), located on laterotergites, those on segment 8 completely fused with tergum and sternum, recognized as small tubercles. Scars of DAG orifices present on anterior margin of mediotergites 4, 5, and 6. **Pregenital abdomen modifications.** Mediotergite 7 symmetrical, short. Sternum 7 symmetrical, short. **Genitalia.** Pronounced lateral directionality absent. Segment 8 symmetrical, ring-like, with tergum and sternum completely merged and without laterotergal appendages. Pygophore symmetrical, oval, closed dorsally, dorsal surface of pygophore with ridges. Laterotergites 9 distinct, symmetrical, equal in size, elongated. Parameres symmetrical, left equal in size to right. Both parameres elongated, basal process short to elongated and rounded or hook-shaped, apical process elongated, L-shaped or straight, tapering. Basal plates symmetrical. Phallosoma frame-like, composed of dorsal V-shaped sclerite, attached to basal plates with closed end, denticulate, and ventral U-shaped sclerite, attached to basal plates with open end. Conjunctiva heavily sclerotized, composed of two large lateral sclerites, attached to opened end of V-shaped dorsal sclerite, and one medial sclerite, covering vesica from beneath. Vesica with narrow base and straight thin short distal region and curved apex, folded onto phallosoma in repose. Anophore indistinct, possibly fused with pygophore. Anal tube membranous.

Variation. The shape of laterotergites 9 and parameres, but also the degree of pregenital abdomen sclerotization vary distinctly between species in this genus (Štys 1982).

Muatianvuaia Wygodzinsky, 1953

Vouchers: *Muatianvuaia* sp. (UCR_ENT 00036812, UCR_ENT 00036957, UCR_ENT 00086455)

Figs 5.1C, 5.3B, 5.11D, 5.11E, 5.17D

Description. **Pregenital abdomen.** Symmetrical, not curved laterally, dorsum and ventrum equally sclerotized. Segment 8 and pygophore more sclerotized than segments 1-7. Dorsal surface smooth. Pregenital laterotergites distinct. Six pairs of spiracles present (segments 3-8), located on laterotergites. Scars of DAG orifices indistinct. **Pregenital abdomen modifications.** Mediotergite 7 symmetrical, short, medially split by membrane into two sclerites. Laterotergites 7 distinct, symmetrical, flat and short. Sternum 7 symmetrical, short. **Genitalia.** Pronounced lateral directionality absent. Mediotergite 8 symmetrical, short or long. Laterotergites 8 distinct, symmetrical, short or elongated. Sternum 8 symmetrical, long. Pygophore symmetrical, oval, closed dorsally, dorsal surface of pygophore with ridges. Laterotergites 9 distinct, symmetrical, equal in size, elongated. Parameres symmetrical, left equal in size to right. Both parameres elongated, basal process short to elongated and rounded or hook-shaped, apical process elongated, L-shaped and folded, or straight, tapering; additional basal process present in specimen UCR_ENT 00086455. Basal plates symmetrical.

Phallosoma frame-like, composed of dorsal V-shaped sclerite, attached to basal plates with closed end, denticulate, and ventral U-shaped sclerite, attached to basal plates with open end. Conjunctiva heavily sclerotized, composed of two large lateral sclerites, attached to opened end of V-shaped dorsal sclerite, and distally paired medial sclerite,

converging to vesica from beneath. Vesica with narrow base and straight thin short distal region and straight apex, folded onto phallosome in repose. Anophore indistinct, possibly fused with pygophore. Anal tube membranous.

Variation. Shape of parameres and shape and size of laterotergites 8 vary distinctly between species of this genus (Wygodzinsky 1953).

Trichotonanninae Štys, 1970

Trichotonannus Reuter, 1891

Vouchers: *Trichotonannus* sp. (UCR_ENT 00120713, UCR_ENT 00125043)

Figs 5.1D, 5.3C, 5.7D, 5.11F, 5.17E

Description. **Pregenital abdomen.** Strongly asymmetrical, dextrally curved, dorsum and ventrum equally sclerotized. All abdominal segments equally sclerotized. Dorsal surface smooth. Pregenital laterotergites distinct. Seven pairs of spiracles present (segments 2-8), located on laterotergites. Scars of DAG orifices indistinct. **Pregenital abdomen modifications.** Mediotergites 3-6 with median membranous area and two lateral membranous areas (in addition to membranes between mediotergite and laterotergites). Mediotergite 7 asymmetrical, short. Laterotergites 7 distinct, asymmetrical, appendage-like. Sternum 7 symmetrical. **Genitalia.** Dextrally directed. Mediotergite 8 asymmetrical, short. Laterotergites 8 distinct, asymmetrical, appendage-like. Three additional projections situated medially to laterotergites 8, here termed middle mediotergal process, right mediotergal process, and left mediotergal appendage. Sternum 8 asymmetrical, long. Pygophore asymmetrical, elongate, closed dorsally, dorsal surface smooth and

weakly sclerotized. Laterotergites 9 indistinct. Parameres asymmetrical, left larger than right. Left paramere elongated, basal process short and rounded, apical process elongated and tapering. Right paramere short, basal process short and rounded, apical process short and rounded. Basal plates strongly asymmetrical, with the largest medial region observed among Dipsocoromorpha. Basal plates joined to circular sclerite of complicated phallosomal complex, which additionally includes two lateral sclerites and main sclerite that envelopes endosoma from beneath. Conjunctiva largely membranous, irregularly shaped, with one long appendage. Vesica with wide base and coiled thin extremely long distal region. Anophore asymmetrical, with ridges and processes. Anal tube membranous.

Variation. Shape of tergum 8 and parameres is the most variable among species of this genus (Carvalho 1989; Wygodzinsky 1953).

Notes. *Trichotonannus* is the only genus of Ceratocombidae with two or three additional processes on mediotergite 8. Moreover, the left process of the mediotergite in the specimen UCR_ENT 00120713 appears to be movable. Since the pygophore is closed dorsally and separated by a membrane from the apparent mediotergite 8, treating its processes and appendages as laterotergites 9 is problematic, and their nature is thus unclear.

Dipsocoridae Dohrn, 1859

Cryptostemma Herrich-Schaeffer, 1835

Vouchers: *Cryptostemma* sp. (N/A, UCR_ENT 00061211, UCR_ENT 00091400)

Figs 5.1E, 5.3D, 5.7E, 5.12A, 5.17F, 5.17G

Description. **Pregenital abdomen.** Strongly asymmetrical, sinistrally curved, dorsum and ventrum equally sclerotized. All abdominal segments equally sclerotized. Dorsal surface smooth. Pregenital laterotergites distinct, two sclerites (dorsal and ventral laterotergites) present on right side. Five pairs of spiracles present (segments 4-8), located on laterotergites or on membranes between dorsal and ventral laterotergites. Scars of DAG orifices present on anterior margin of mediotergites 4, 5, and 6. **Pregenital abdomen modifications.** Mediotergite 7 asymmetrical, short, fused with mediotergite 8 and demarcated by evident suture, with brush on right side. Laterotergites 7 distinct, asymmetrical, left oval, not appendage-like, right partially fused with mediotergite. Additional process of mediotergite present on right side, roughly equal in size to left laterotergite 8, elongated and curved. Sternum 7 asymmetrical, short, with brush on left side. **Genitalia.** Sinistrally directed. Mediotergite 8 asymmetrical, very short, fused with mediotergite 7 (see above). Laterotergites 8 distinct, asymmetrical, left elongated, appendage-like and curved, right short, with brush. Sternum 8 asymmetrical, long. Pygophore asymmetrical, oval, closed dorsally, dorsal surface of pygophore with ridges and processes. Laterotergites 9 indistinct. Parameres asymmetrical, left equal in size to right. Left paramere elongated, basal process short and rounded, apical process elongated and tapering. Right paramere short, basal process bifurcated and rounded, apical process elongated and rounded. Basal plates weakly asymmetrical. Phallosoma represented by U-sclerite. Conjunctiva heavily sclerotized, irregularly shaped, its sclerites with short rounded processes. Vesica with wide base and coiled thin long distal region. Anophore indistinct. Anal tube membranous.

Variation. Species of this genus exhibit large variation in modifications of the pregenital abdomen, where laterotergite 3 and/or 6 may bear processes or be appendage-like (Streito & Pericart 2005; Wygodzinsky 1948a, 1952).

Notes. After observing the right-hand appendage of segment 7 we came to the same conclusion as Wygodzinsky (1948a, 1962): this appendage is not of laterotergal origin because a laterotergite 7 (similar to the laterotergites on preceding segments) is present on the right side, and the right spiracle of segment 7 is located on this laterotergite and not on the secondary appendage. We consider this appendage to be an appendage of mediotergite 7. This appendage may be absent in some species (Hill 1987a).

Schizopteridae Reuter, 1891

Hypselosomatinae Esaki & Miyamoto, 1959

Hypselosoma Reuter, 1891

Vouchers: *Hypselosoma* sp. (UCR_ENT 00045351, UCR_ENT 00091321), *H. haplacanthatum* Hill, 2013 (UCR_ENT 00090357)

Figs 5.1F, 5.7F, 5.12B, 5.12C, 5.18A

Description. **Pregenital abdomen.** Symmetrical to weakly asymmetrical, not laterally curved, dorsum slightly more sclerotized than ventrum. All abdominal segments equally sclerotized. Dorsal surface smooth. Pregenital laterotergites indistinct. Three pairs of spiracles present (segments 6-8), located on lateral margins of sterna (segments 6-7), or on lateral margins of mediotergite (segment 8). Scars of DAG orifices present along anterior margin of mediotergite 7. **Pregenital abdomen modifications.** Sternum 4 with

short hooked process on left side (in UCR_ENT 00045351). Sternum 3 with medial oval pit-like structure (in UCR_ENT 00090357). Mediotergite 7 symmetrical, short. Laterotergites 7 indistinct. Sternum 7 symmetrical, short. **Genitalia.** No pronounced lateral directionality. Mediotergite 8 symmetrical, short. Laterotergites 8 indistinct. Sternum 8 long. Pygophore slightly asymmetrical, transverse, open dorsally. Mediotergite 9 distinct. Laterotergites 9 distinct, asymmetrical, equal in size, elongated, with hooked apices. Parameres asymmetrical, left equal in size to right, or left larger than right. Left paramere elongated, basal process short and rounded, apical process elongated and tapering. Right paramere short to elongated, basal process short to elongated, rounded, apical process elongated and rounded or tapering. Basal plates weakly asymmetrical. Phallosoma represented by Y-sclerite. Conjunctiva heavily sclerotized, irregularly shaped, with one apparently free elongated spinous appendage. Vesica with wide base and coiled thin long distal region and may have curved slender processes originating from its base. Anophore symmetrical, without processes, weakly sclerotized or indistinct. Anal tube membranous.

Variation. Shape and size of laterotergites 9, parameres, and structure and number of conjunctival appendages and development of vesical processes vary distinctly among species of this genus (Hill 1987b, 2013).

Rectilamina Hill, 1984

Vouchers: *Rectilamina* sp. (UCR_ENT 00084928, UCR_ENT 00084929, UCR_ENT 00088314)

Figs 5.1G, 5.8A, 5.12D, 5.18B

Description. **Pregenital abdomen.** Weakly asymmetrical, not laterally curved, dorsum and ventrum equally sclerotized. All abdominal segments equally sclerotized. Dorsal surface smooth. Pregenital laterotergites indistinct. Seven pairs of spiracles present (segments 2-8), located on sides of sterna (segments 2-7), or on processes of mediotergite (segment 8). Scars of DAG orifices present along anterior margin of mediotergite 7. **Pregenital abdomen modifications.** Mediotergite 7 slightly asymmetrical, long. Laterotergites 7 indistinct. Sternum 7 asymmetrical, long. **Genitalia.** Sinistrally directed. Mediotergite 8 asymmetrical, short, with asymmetric processes at sides. Laterotergites 8 indistinct. Sternum 8 asymmetrical, long, with large process on left side. Pygophore asymmetrical, elongate, open dorsally, with large process on posterior margin, mediotergite 9 indistinct. Laterotergites 9 indistinct. Parameres asymmetrical, left smaller than right. Left paramere short, basal process short and rounded, apical process elongated and rounded. Right paramere elongated, basal process indistinct, apical process elongated, club-shaped, with patch of long stout setae at apex. Basal plates strongly asymmetrical. Phallosoma represented by circular sclerite. Conjunctiva largely membranous, with one or two elongated rounded appendages, and sheath forming sclerite oriented along axis of vesica. Vesica with narrow base and coiled thin long distal region. Anophore asymmetrical, with short thick rounded process. Anal tube sclerotized.

Variation. Shape and size of processes of tergum 8 vary distinctly between species of this genus.

Williamsocoris Carpintero & Dellape, 2006

Vouchers: *Williamsocoris* sp. (UCR_ENT 00057523)

Figs 5.1H, 5.12E, 5.18C

Description. **Pregenital abdomen.** Weakly asymmetrical, not laterally curved, dorsum slightly less sclerotized than ventrum. Segment 8 and pygophore more sclerotized than segments 1-7. Dorsal surface smooth. Pregenital laterotergites indistinct. Seven pairs of spiracles present (segments 2-8), located on sides of sterna (segments 2-7), or on processes of mediotergite (segment 8). Scars of DAG orifices present along anterior margin of mediotergite 7. **Pregenital abdomen modifications.** Mediotergite 7 symmetrical, short. Laterotergites 7 indistinct. Sternum 7 asymmetrical, long. **Genitalia.** Sinistrally directed. Mediotergite 8 asymmetrical, short, with asymmetric processes at sides. Laterotergites 8 indistinct. Sternum 8 asymmetrical, short. Pygophore asymmetrical, oval, open dorsally, with large process on posterior margin, mediotergite 9 indistinct. Laterotergites 9 indistinct. Parameres asymmetrical, left smaller than right. Left paramere short, basal process short and rounded, apical process elongated and rounded. Right paramere elongated, basal process short and rounded, apical process elongated, club-shaped, with patch of long stout setae at apex. Basal plates strongly asymmetrical. Phallosoma represented by circular sclerite. Conjunctiva largely membranous, with one or two elongated rounded appendages. Vesica with narrow base and coiled thin long distal region, with additional sclerites forming sheath. Anophore asymmetrical, with long thick curved laterally directed process. Anal tube sclerotized at apex.

Schizopteridae incertae sedis (Ogeriinae or Schizopterinae)

Guapinannus Wygodzinsky, 1951

Vouchers: *Guapinannus* sp. (UCR_ENT 00090715, UCR_ENT 00090717)

Figs 5.1I, 5.8B, 5.12F, 5.18D

Description. **Pregenital abdomen.** Symmetrical, not laterally curved, dorsum and ventrum equally sclerotized. All abdominal segments equally sclerotized. Dorsal surface smooth. Pregenital laterotergites indistinct. Three pairs of spiracles present (segments 6-8), located on lateral margins of sterna (segments 6-7), or on lateral margins of mediotergite (segment 8). Scars of DAG orifices present medially along anterior margin of mediotergite 7. **Pregenital abdomen modifications.** Mediotergites 7 symmetrical, short. Laterotergites 7 indistinct. Sternum 7 symmetrical, modified into subgenital plate. **Genitalia.** Dextrally directed. Mediotergite 8 symmetrical, long. Laterotergites 8 indistinct. Sternum 8 indistinct. Pygophore symmetrical, oval, open dorsally, mediotergite 9 indistinct. Laterotergites 9 indistinct. Parameres asymmetrical, left equal in size to right. Both parameres elongated, basal process short and rounded, apical process elongated and rounded. Basal plates weakly asymmetrical. Phallosoma reduced. Conjunctiva heavily sclerotized, irregularly shaped, without appendages. Vesica with wide base and coiled thick short distal region. Anophore slightly asymmetrical, with short thin straight posteriorly directed process. Anal tube membranous.

Notes. This is the first description of male abdominal features in this genus.

Peloridinannus Wygodzinsky, 1951

Vouchers: *Peloridinannus sinefenestra* Weirauch & Frankenberg, 2015 (UCR_ENT 00090782), *P. moe* Weirauch & Frankenberg, 2015 (UCR_ENT 00098861)

Figs 5.1J, 5.8C, 5.13A, 5.18E

Description. **Pregenital abdomen.** Symmetrical, not laterally curved, dorsum slightly less sclerotized than ventrum. All abdominal segments equally sclerotized. Dorsal surface smooth. Pregenital laterotergites indistinct, although line of weakness on sides of sterna present. Three pairs of spiracles present (segments 6-8), located on lateral margins of sterna (segments 6-7), or on lateral margins of mediotergite (segment 8). Scars of DAG orifices indistinct. **Pregenital abdomen modifications.** Mediotergite 7 symmetrical, short. Laterotergites 7 indistinct. Sternum 7 asymmetrical, modified into subgenital plate. **Genitalia.** Dextrally directed. Mediotergite 8 slightly asymmetrical, long. Laterotergites 8 indistinct. Sternum 8 indistinct. Pygophore slightly asymmetrical, oval, open dorsally, mediotergite 9 indistinct. Laterotergite 9 distinct on right side, elongated. Parameres asymmetrical, left smaller than right. Left paramere elongated, basal process short and rounded, apical process elongated, curved, and tapering. Right paramere elongated, basal process short and tapering, apical process elongated, bifurcated or not, and tapering. Basal plates strongly asymmetrical. Phallosoma reduced. Conjunctiva membranous, irregularly shaped, with one elongated rounded L-shaped appendage. Vesica with wide base and coiled thin short to long distal region. Anophore asymmetrical, without processes. Anal tube membranous.

Variation. Segment 7 may be without a process; the shape of laterotergite 9 and length of vesica vary distinctly among species of this genus.

Ogeriinae Emsley, 1969

Chinannus Wygodzinsky, 1948

Vouchers: *Chinannus bierigi* Wygodzinsky, 1948 (UCR_ENT 00082335), *C. trinitatis* (China, 1946) (UCR_ENT 00081798, UCR_ENT 00086192), *C. communis* Knyshov et al., 2016 (UCR_ENT 00076302)

Figs 5.1K, 5.8D, 5.13B, 5.18F

Description. **Pregenital abdomen.** Strongly asymmetrical, dextrally curved, dorsum slightly less sclerotized than ventrum. All abdominal segments equally sclerotized. Dorsal surface smooth. Pregenital laterotergites distinct on right side of segments 4-7. Three pairs of spiracles present (segments 6-8), located on lateral margins of sterna (left side of segments 6-7), on laterotergites (right side of segments 6-7), or on lateral margins of mediotergite (segment 8). Scars of DAG orifices present along anterior margin of mediotergite 7. **Pregenital abdomen modifications.** Laterotergite 4 with pouch and spine. Mediotergite 7 slightly asymmetrical, short. Laterotergite 7 distinct on right side, small. Sternum 7 slightly asymmetrical, modified into subgenital plate. **Genitalia.** Dextrally directed. Mediotergite 8 slightly asymmetrical. Laterotergite 8 distinct on left side, appendage-like. Sternum 8 indistinct. Pygophore slightly asymmetrical, oval, open dorsally, mediotergite 9 indistinct. Laterotergites 9 indistinct. Parameres asymmetrical, left equal in size to right. Both parameres short, basal process short and rounded, apical

process short or elongated, rounded. Basal plates strongly asymmetrical. Phallosoma reduced. Conjunctiva largely mnembranous, irregularly shaped, without appendages. Vesica with wide base and coiled thin long to extremely long distal region. Anophore asymmetrical, with long thin or thick straight or curved anterior process and small rounded posterior process on right side. Anal tube membranous.

Variation. The shape of the pregenital abdominal processes and vesical length vary distinctly among species of this genus (Knyshov *et al.* 2016). Mediotergite 8 may have a process on the right side.

Notes. See discussion section for remarks on laterotergites.

Kaimon Hill, 2004

Vouchers: *Kaimon* sp. (UCR_ENT 00091319, UCR_ENT 00096999)

Figs 5.1L, 5.4A, 5.8E, 5.13C, 5.19A

Description. **Pregenital abdomen.** Symmetrical, not laterally curved, dorsum and ventrum equally sclerotized. All abdominal segments equally sclerotized. Dorsal surface carinulated. Pregenital laterotergites indistinct. Three pairs of spiracles present (segments 6-8), located on lateral margins of sterna (segments 6-7), or on lateral margins of mediotergite (segment 8). Scars of DAG orifices present along anterior margin of mediotergite 7, inconspicuous. **Pregenital abdomen modifications.** Mediotergite 7 slightly asymmetrical, short. Laterotergites 7 indistinct. Sternum 7 slightly asymmetrical, modified into subgenital plate. **Genitalia.** Dextrally directed. Mediotergite 8 asymmetrical, short. Laterotergites 8 indistinct. Sternum 8 indistinct. Pygophore

asymmetrical, elongate, open dorsally, mediotergite 9 indistinct. Laterotergites 9 indistinct. Parameres asymmetrical, left larger than right. Left paramere elongated, basal process short and rounded, apical process elongated and tapering. Right paramere short, basal process short and rounded, apical process short and rounded. Basal plates weakly asymmetrical. Phallosoma reduced. Conjunctiva heavily sclerotized, irregularly shaped, without appendages. Vesica with wide base and coiled thick short distal region with preapical thick process. Anophore slightly asymmetrical, without processes. Anal tube membranous.

Variation. The shape of the left paramere and structure of the aedeagus vary distinctly among species of this genus (Hill 2004). The preapical process of the vesica is absent in some species.

Notes. In contrast to the conclusions by Hill (2004), sternum 8 is indistinct as it is in other Ogeriinae, although the thickened posterior lateral areas might represent vestiges of sternum 8 that are largely fused with sternum 7.

Kokeshia Miyamoto, 1960

Vouchers: *Kokeshia* sp. (UCR_ENT 00063170, UCR_ENT 00081331, UCR_ENT 00088975)

Figs 5.8F, 5.13D, 5.19B

Description. **Pregenital abdomen.** Symmetrical, not laterally curved, dorsum and ventrum equally sclerotized. All abdominal segments equally sclerotized. Dorsal surface smooth. Pregenital laterotergites distinct. Spiracles indistinct in males (although in

females three pairs of spiracles present). Scars of DAG orifices present along anterior margin of mediotergite 7. **Pregenital abdomen modifications.** Mediotergite 7 slightly asymmetrical, short. Laterotergite 7 distinct on right side. Sternum 7 symmetrical, modified into subgenital plate. **Genitalia.** No pronounced lateral directionality. Mediotergite 8 asymmetrical, short, with median constriction forming two hemitergites with processes or brushes. Laterotergites 8 indistinct. Sternum 8 indistinct. Pygophore symmetrical, oval, open dorsally, mediotergite 9 indistinct. Laterotergites 9 indistinct. Parameres asymmetrical, left equal in size to right. Left paramere elongated, basal process elongated and rounded, apical process elongated and rounded. Right paramere elongated, basal process short and rounded, apical process elongated and rounded. Basal plates strongly asymmetrical. Phallosoma reduced. Conjunctiva heavily sclerotized, irregularly shaped, with one broad and rounded appendage. Vesica with wide base and coiled thin long distal region. Anophore slightly asymmetrical, without processes. Anal tube membranous.

Variation. Most variation among species of this genus is seen in the shape of mediotergite 8 and its processes, the shape of the parameres and the length of the vesica (Miyamoto 1960; Rédei 2008b; Rédei *et al.* 2012; Štys 1985).

Meganannus Weirauch *et al.*, 2018

Vouchers: *Meganannus lewisi* Weirauch *et al.*, 2018 (UCR_ENT 00014802)

Figs 5.1M, 5.13E, 5.19C

Description. **Pregenital abdomen.** Strongly asymmetrical, not curved laterally, dorsum slightly less sclerotized than ventrum. All abdominal segments equally sclerotized. Dorsal surface smooth. Pregenital laterotergites indistinct. Three pairs of spiracles present (segments 6-8), located on lateral margins of sterna (segments 6-7), or on lateral margins of mediotergite (segment 8), on sclerotized stalk-like projections. Scars of DAG orifices present along anterior margin of mediotergite 7. **Pregenital abdomen modifications.** Sternum 4 with pouch on right side. Mediotergite 7 asymmetrical, short. Laterotergites 7 indistinct. Sternum 7 asymmetrical, modified into subgenital plate. **Genitalia.** Dextrally curved. Mediotergite 8 asymmetrical, short, with long curved appendage on left side. Laterotergites 8 indistinct. Sternum 8 indistinct. Pygophore slightly asymmetrical, oval, open dorsally, mediotergite 9 indistinct. Laterotergites 9 indistinct. Parameres asymmetrical, left smaller than right. Both parameres elongated, basal process short and rounded, apical process elongated and rounded. Basal plates strongly asymmetrical. Phallosoma reduced. Conjunctiva membranous, irregularly shaped, large and complicated, with many sclerites and one large but short curved spinous appendage. Vesica with wide base and coiled thin extremely long distal region. Anophore asymmetrical, with long thick straight anteriorly directed process. Anal tube membranous.

Ogeria Distant, 1913

Vouchers: *Ogeria* sp. (UCR_ENT 00086442)

Figs 5.1N, 5.4B, 5.13F, 5.19D

Description. **Pregenital abdomen.** Symmetrical, not laterally curved, dorsum and ventrum equally sclerotized. All abdominal segments equally sclerotized. Dorsal surface carinulated. Pregenital laterotergites indistinct. Three pairs of spiracles present (segments 6-8), located on lateral margins of sterna (segments 6-7), or on lateral margins of mediotergite (segment 8). Scars of DAG orifices present along anterior margin of mediotergite 7. **Pregenital abdomen modifications.** Mediotergite 7 symmetrical, short. Laterotergites 7 indistinct. Sternum 7 symmetrical, modified into subgenital plate. **Genitalia.** Pronounced lateral directionality absent. Mediotergite 8 slightly asymmetrical, short. Laterotergites 8 indistinct. Sternum 8 indistinct. Pygophore slightly asymmetrical, oval, open dorsally, mediotergite 9 indistinct. Laterotergites 9 indistinct. Parameres asymmetrical, left equal in size to right. Left paramere short, basal process short and rounded, apical process short and rounded. Right paramere elongated, basal process short and rounded, apical process elongated and curved, tapering. Basal plates weakly asymmetrical. Phallosoma reduced. Conjunctiva heavily sclerotized, irregularly shaped, with one short rounded appendage. Vesica with wide base and coiled thin long distal region. Anophore slightly asymmetrical, without processes. Anal tube membranous. **Variation**. Left paramere is sometimes smaller than right, vesical process may be present, and vesica itself may be denticulate (Hill 1990).

Undescribed genus 1

Vouchers: UCR_ENT 00090562, UCR_ENT 00098868

Figs 5.4C, 5.9A, 5.14A

Description. **Pregenital abdomen.** Symmetrical, not laterally curved, dorsum and ventrum equally sclerotized. All abdominal segments equally sclerotized. Dorsal surface smooth. Pregenital laterotergites distinct except for segment 7. Three pairs of spiracles present (segments 6-8), located on lateral margins of sterna (segments 6-7), or on lateral margins of mediotergite (segment 8). Scars of DAG orifices present medially along anterior margin of mediotergite 7. **Pregenital abdomen modifications.** Mediotergite 7 symmetrical, short. Laterotergites 7 indistinct. Sternum 7 slightly asymmetrical, modified into subgenital plate. **Genitalia.** Pronounced lateral directionality absent. Mediotergite 8 asymmetrical, short. Laterotergites 8 indistinct. Sternum 8 indistinct. Pygophore symmetrical, oval, open dorsally, mediotergite 9 indistinct. Laterotergites 9 indistinct. Parameres asymmetrical, left equal in size to right. Left paramere elongated, basal process elongated and rounded, apical process elongated and rounded. Right paramere elongated, basal process short and rounded, apical process elongated and rounded. Basal plates strongly asymmetrical. Phallosoma reduced. Conjunctiva sclerotized, irregularly shaped, with one short curved spinous appendage. Vesica with wide base and coiled thin long distal region. Anophore slightly asymmetrical, without processes. Anal tube membranous.

Undescribed genus 2

Vouchers: UCR_ENT 00014811

Figs 5.1O, 5.4D, 5.13B, 5.19E

Description. **Pregenital abdomen.** Symmetrical, not laterally curved, dorsum and ventrum equally sclerotized. All abdominal segments equally sclerotized. Dorsal surface smooth. Pregenital laterotergites indistinct. Two pairs of spiracles present (segments 7-8), located on lateral margins of sternum (segment 7), or on lateral margins of mediotergite (segment 8). Scars of DAG orifices present medially along anterior margin of mediotergite 7. **Pregenital abdomen modifications.** Mediotergite 7 symmetrical, short. Laterotergites indistinct. Sternum 7 symmetrical, long. **Genitalia.** Sinistrally directed. Mediotergite 8 symmetrical, short. Laterotergites 8 indistinct. Sternum 8 indistinct. Pygophore symmetrical, oval, open dorsally, mediotergite 9 indistinct. Laterotergites 9 distinct, nearly symmetrical, elongated. Parameres asymmetrical, left larger than right. Left paramere elongated, basal process elongated and rounded, apical process elongated and rounded. Right paramere elongated, basal process short and rounded, apical process elongated and rounded. Basal plates weakly asymmetrical. Phallosoma reduced. Conjunctiva heavily sclerotized, represented by large quadrate sclerite and one short rounded appendage. Vesica with narrow base and coiled thick short distal region, expanding around apex into funnel. Anophore symmetrical, without processes. Anal tube membranous.

Schizopterinae Reuter, 1891

Ceratocomboides McAtee & Malloch, 1925

Vouchers: *Ceratocomboides* sp. (UCR_ENT 00077448, UCR_ENT 00099292)

Figs 5.1P, 5.5A, 5.14C, 5.19F

Description. **Pregenital abdomen.** Symmetrical, not laterally curved, dorsum less sclerotized than ventrum. All abdominal segments equally sclerotized. Dorsal surface smooth. Pregenital laterotergites distinct, both large ventral and small dorsal (see notes). Three pairs of spiracles present (segments 6-8), located on lateral margins of sterna (segments 6-7), or on lateral margins of mediotergite (segment 8). Scars of DAG orifices present medially along anterior margin of mediotergite 7. **Pregenital abdomen modifications.** Mediotergite 7 symmetrical, short. Laterotergites 7 distinct, symmetrical, flat and short. Sternum 7 symmetrical, modified into subgenital plate. **Genitalia.** Dextrally directed. Mediotergite 8 asymmetrical, short. Laterotergites 8 indistinct. Sternum 8 indistinct. Pygophore asymmetrical, oval, titled to the right, open dorsally, mediotergite 9 indistinct. Laterotergites 9 indistinct. Parameres asymmetrical, left smaller than right. Left paramere short, basal process short and rounded, apical process short and rounded. Right paramere elongated, basal process short and rounded, apical process elongated and rounded. Basal plates strongly asymmetrical. Phallosoma reduced. Conjunctiva largely membranous, irregularly-shaped, with at least one appendage. Vesica with wide base and coiled thin long distal region. Anophore asymmetrical, with small rounded posterior anophoric process. Anal tube membranous.

Variation. Variation among species of this genus is subtle. Mediotergite 8 may have a process on the right side (Wygodzinsky 1950b).

Notes. The dorsal and ventral laterotergites drastically differ in shape and size. The dorsal sclerites are oval, shorter than mediotergites and separated by vast membranous areas, whereas the ventral sclerites are rectangular and of the same length as the sterna

and separated from the latter by small membranous areas. It is possible that either of these two types of sclerites is not homologous to the laterotergites in other taxa. See discussion.

Corixidea Reuter, 1891

Vouchers: *Corixidea major* McAtee & Malloch, 1925 (UCR_ENT 00093506, UCR_ENT 00012039)

Figs 5.1Q, 5.5B, 5.14D

Description. **Pregenital abdomen.** Weakly asymmetrical, not laterally curved, dorsum less sclerotized than ventrum. All abdominal segments equally sclerotized. Dorsal surface smooth. Pregenital laterotergites indistinct. Three pairs of spiracles present (segments 6-8), located on lateral margins of sterna (segments 6-7), or on lateral margins of mediotergite (segment 8). Scars of DAG orifices present medially along anterior margin of mediotergite 7. **Pregenital abdomen modifications.** Mediotergite 7 symmetrical, short. Laterotergites 7 indistinct. Sternum 7 asymmetrical, long. **Genitalia.** Dextrally directed. Mediotergite 8 asymmetrical, with process on right side. Laterotergites 8 indistinct. Sternum 8 indistinct. Pygophore slightly asymmetrical, oval, open dorsally, mediotergite 9 indistinct. Laterotergites 9 indistinct. Parameres asymmetrical, left smaller than right. Left paramere short, basal process short and rounded, apical process short and rounded. Right paramere elongated, basal process short and rounded, apical process elongated, with hooked apex. Basal plates weakly asymmetrical. Phallosoma reduced. Conjunctiva sclerotized, irregularly shaped, without appendages. Vesica with wide base

and coiled thin long distal region with spinous process. Anophore slightly asymmetrical, with small rounded posterior anophoric process. Anal tube membranous.

Variation. The greatest differences among species of this genus are found in the structure of the mediotergite 8 and the shape and direction of its process (Emsley 1969). Other species of *Corixidea* do not have a vesical process.

Dundonannus Wygodzinsky, 1950

Vouchers: *Dundonannus* sp. (UCR_ENT 00081642, UCR_ENT 00087529, UCR_ENT 00089713)

Figs 5.2A, 5.9B, 5.14E, 5.14F

Description. **Pregenital abdomen.** Strongly asymmetrical, dextrally curved, dorsum less sclerotized than ventrum. All abdominal segments equally sclerotized. Dorsal surface smooth. Pregenital laterotergites distinct on segments 5, 6, and 7: small ventral sclerite on segment V located next to opening on right side of sternum, ventral sclerite located on segment VI, and downward directed curved dorsal sclerite on segment VII. Three pairs of spiracles present (segments 6-8), located on lateral margins of sterna (segments 6-7), or on left margin of mediotergite and right membranous or sclerotized stalk-like projection (segment 8). Scars of DAG orifices present along anterior margin of mediotergite 7. **Pregenital abdomen modifications.** Sternum 5 with an opening on right side. Mediotergite 7 asymmetrical, short. Laterotergite 7 distinct on right side, elongated, concave, forming a cavity. Sternum 7 asymmetrical, long. **Genitalia.** Dextrally directed. Mediotergite 8 asymmetrical, short, with complex structure on right side, large bulbous

structure of which (cymbium) fits in cavity between sternum 7 and laterotergite 7. Laterotergites 8 indistinct. Sternum 8 indistinct. Pygophore asymmetrical, oval, titled to the right, open dorsally, mediotergite 9 indistinct. Laterotergites 9 indistinct. Parameres asymmetrical, left smaller than right. Left paramere short or elongated, basal process short and rounded, apical process short or elongated, rounded. Left paramere elongated, basal process short and rounded, apical process elongated, with hooked apex. Basal plates strongly asymmetrical. Phallosoma reduced. Conjunctiva sclerotized, irregularly shaped, with one elongated spinous appendage and one short rounded sclerite. Vesica with wide base and coiled thin short distal region. Anophore slightly asymmetrical, with small rounded posterior anophoric process. Anal tube membranous.

Variation. The structure of tergum 8 with complicated membranous areas and sclerites varies more than other structures among species of this genus (Southwood 1961; Wygodzinsky 1950b). See Štys (1974) for terms suggested for these specialized structures.

Notes. We consider the specimen from Thailand as belonging to *Dundonannus*, as its structure of segment 8 is more similar to described *Dundonannus* species than to *Semangananus* Štys, 1974.

Hoplonannus McAtee & Malloch, 1925

Vouchers: *Hoplonannus* sp. (UCR_ENT 00081393)

Figs 5.9C, 5.20A

Description. **Pregenital abdomen.** Weakly asymmetrical, not laterally curved, dorsum less sclerotized than ventrum. All abdominal segments equally sclerotized. Dorsal surface smooth. Pregenital laterotergites indistinct. Three pairs of spiracles present (segments 6-8), located on lateral margins of sterna (segments 6-7), or on lateral margins of mediotergite (segment 8). Scars of DAG orifices present medially along anterior margin of mediotergite 7. **Pregenital abdomen modifications.** Sterna 3-6 with medial membranous area. Sternum 6 with short process on right side. Mediotergite 7 asymmetrical, short. Laterotergites 7 indistinct. Sternum 7 slightly asymmetrical, long, with rounded process on right side. **Genitalia.** Dextrally directed. Mediotergite 8 slightly asymmetrical, short, with posteriorly directed curved process. Laterotergites 8 indistinct. Sternum 8 indistinct. Pygophore asymmetrical, oval, open dorsally, with lobe-like expansion on right side, mediotergite 9 indistinct. Laterotergites 9 indistinct. Parameres asymmetrical, left smaller than right. Left paramere short, basal process short and rounded, apical process short and rounded. Right paramere elongated, basal process short and rounded, apical process elongated, with serrated apex. Basal plates strongly asymmetrical. Phallosoma reduced. Conjunctiva heavily sclerotized, irregularly shaped, without appendages. Vesica with wide base and coiled thin short distal region. Anophore asymmetrical, with long straight anteriorly directed anterior anophoric process and small rounded posterior anophoric process. Anal tube membranous.

Variation. Considerable variation across species is seen in the shape of the right paramere and anterior anophoric process (Emsley 1969). The curved process of the mediotergite 8 that occurs in other species is absent in the documented species.

Machadonannus Wygodzinsky, 1950

Vouchers: *Machadonannus brailovskyi* Weirauch *et al.*, 2017 (UCR_ENT 00125913)

Figs 5.2B, 5.5C, 5.15A, 5.20B

Description. **Pregenital abdomen.** Strongly asymmetrical, dextrally curved, dorsum less sclerotized than ventrum. All abdominal segments equally sclerotized. Dorsal surface smooth. Pregenital laterotergites distinct on segments 4 and 6. Three pairs of spiracles present (segments 6-8), located on lateral margins of sterna (segments 6-7), or on left margin of mediotergite and right sclerotized stalk-like projection (segment 8). Scars of DAG orifices present along anterior margin of mediotergite 7, inconspicuous. **Pregenital abdomen modifications.** Sternum 4 with posteriorly located ventral laterotergite. Sternum 5 with anteriorly directed process. Sternum 6 with laterally located ventral laterotergite. Mediotergite 7 asymmetrical, short, anterior margin strongly sclerotized and serrated on right side. Laterotergites 7 indistinct. Sternum 7 asymmetrical, long. **Genitalia.** Dextrally directed. Mediotergite 8 asymmetrical, short. Laterotergites 8 indistinct. Sternum 8 indistinct. Pygophore asymmetrical, oval, open dorsally, mediotergite 9 indistinct. Laterotergites 9 indistinct. Parameres asymmetrical, left smaller than right. Left paramere short, basal process short and tapering, apical process elongated and rounded. Right paramere elongated, basal process short and rounded, apical process elongated and tapering. Basal plates strongly asymmetrical. Phallosoma reduced. Conjunctiva heavily sclerotized, irregularly shaped, without appendages. Vesica with wide base and coiled thin long distal region. Anophore asymmetrical, with long thick

twisted and antero-laterally directed anterior process and small rounded posterior anophoric process; anterior anophoric process consists of hollow outer process and slender vesica-like inner process. Anal tube membranous.

Membracioides McAtee & Malloch, 1925

Vouchers: *Membracioides* sp. (UCR_ENT 00084401, UCR_ENT 00084415)

Figs 5.2C, 5.15B, 5.20C

Description. **Pregenital abdomen.** Weakly asymmetrical, not laterally curved, dorsum less sclerotized than ventrum. All abdominal segments equally sclerotized. Dorsal surface smooth. Pregenital laterotergites indistinct. Three pairs of spiracles present (segments 6-8), located on lateral margins of sterna (segments 6-7), or on lateral margins of mediotergite (segment 8). Scars of DAG orifices present medially along anterior margin of mediotergite 7. **Pregenital abdomen modifications.** Mediotergite 7 symmetrical, short. Laterotergites 7 indistinct. Sternum 7 asymmetric, long, with short serrated process on right side. **Genitalia.** Dextrally directed. Mediotergite 8 asymmetrical, short, with elongated process on posterior margin that curved anteriorly. Laterotergites 8 indistinct. Sternum 8 indistinct. Pygophore slightly asymmetrical, oval, open dorsally, mediotergite 9 indistinct. Laterotergites 9 indistinct. Parameres asymmetrical, left smaller than right. Left paramere short, basal process short and rounded, apical process short and tapering. Right paramere elongated, basal process short and rounded, apical process elongated, with hooked apex. Basal plates weakly asymmetrical. Phallosoma reduced. Conjunctiva sclerotized, irregularly shaped, with one elongated spinous appendage. Vesica with wide

base and coiled thin short distal region. Anophore slightly asymmetrical, with small rounded posterior anophoric process. Anal tube membranous.

Variation. In previously described species an elongated anterior anophoric process is present and the shape of the mediotergite 8 process is different (Emsley 1969).

Nannocoris Reuter, 1891

Vouchers: *Nannocoris* sp. (UCR_ENT 00081615, UCR_ENT 00088078, UCR_ENT 00097001)

Figs 5.2D, 5.9D, 5.15C, 5.15D, 5.20D

Description. **Pregenital abdomen.** Weakly asymmetrical, not laterally curved, dorsum less sclerotized than ventrum. All abdominal segments equally sclerotized. Dorsal surface smooth. Pregenital laterotergites indistinct. Three pairs of spiracles present (segments 6-8), located on lateral margins of sterna (segments 6-7), or on lateral margins of mediotergite (segments 8), right sometimes on stalk-like processes. Scars of DAG orifices present medially along anterior margin of mediotergite 7. **Pregenital abdomen modifications.** Mediotergite 7 asymmetrical, short. Laterotergites 7 indistinct. Sternum 7 asymmetrical, long. **Genitalia.** Dextrally directed. Mediotergite 8 asymmetrical, short, with median constriction. Laterotergites 8 indistinct. Sternum 8 indistinct. Pygophore asymmetrical, oval, open dorsally, mediotergite 9 indistinct. Laterotergites 9 distinct, asymmetrical, elongated. Parameres asymmetrical, left equal in size to right, or left smaller than right. Left paramere elongated, basal process short and rounded, apical process elongated and rounded. Right paramere elongated, basal process small and

rounded, apical process elongated, with cleft apex. Basal plates strongly asymmetrical. Phallosoma reduced. Conjunctiva largely membranous, irregularly shaped, without appendages. Vesica with wide base and coiled thin short to extremely long distal region. Anophore asymmetrical, with extremely complicated long anteriorly directed anterior processes and small rounded posterior process. Anal tube membranous.

Variation. The shape of tergum 8 and parameres and vesical length vary distinctly among species of this genus (Emsley 1969).

Pinochius Carayon, 1949

Vouchers: *Pinochius* sp. (UCR_ENT 00036917, UCR_ENT 00081616)

Figs 5.2E, 5.9E, 5.15E, 5.20E

Description. **Pregenital abdomen.** Weakly asymmetrical, not laterally curved, dorsal sclerotization weak. All abdominal segments equally sclerotized. Dorsal surface smooth. Pregenital laterotergites indistinct. Three pairs of spiracles present (segments 6-8), located on lateral margins of sterna (segments 6-7), or on lateral margins of mediotergite (segment 8), right sometimes on stalk-like processes. Scars of DAG orifices indistinct. **Pregenital abdomen modifications.** Mediotergite 7 asymmetrical, short. Laterotergites 7 indistinct. Sternum 7 asymmetrical, long. **Genitalia.** Dextrally directed. Mediotergite 8 asymmetrical, short, with process on right side. Laterotergites 8 indistinct. Sternum 8 indistinct. Pygophore asymmetrical, oval, open dorsally, mediotergite 9 indistinct. Laterotergites 9 indistinct. Parameres asymmetrical, left equal in size to right. Left paramere short, basal process short and rounded, apical process short and rounded. Right

paramere elongated, basal process short and rounded, apical process elongated and tapering, with preapical process. Basal plates strongly asymmetrical. Phallosoma reduced. Conjunctiva sclerotized, irregularly shaped, without appendages. Vesica with wide base and coiled thin long distal region. Anophore asymmetrical, with long thin multifurcated laterally directed anterior process and small rounded posterior process. Anal tube membranous.

Variation. The right side process of mediotergite 8 is absent in some species (Rédei 2008a).

Ptenidiophyes Reuter, 1891

Vouchers: *Ptenidiophyes* sp. (UCR_ENT 00014874, UCR_ENT 00116306)

Figs 5.2F, 5.5D, 5.15F, 5.20F

Description. **Pregenital abdomen.** Weakly asymmetrical, not laterally curved, dorsum less sclerotized than ventrum. All abdominal segments equally sclerotized. Dorsal surface smooth. Pregenital laterotergites indistinct. Three pairs of spiracles present (segments 6-8), located on lateral margins of sterna (segments 6-7), or on lateral margins of mediotergite (segment 8). Scars of DAG orifices present medially along anterior margin of mediotergite 7. **Pregenital abdomen modifications.** Mediotergite 7 slightly asymmetrical, short. Laterotergites 7 indistinct. Sternum 7 asymmetrical, modified into subgenital plate. **Genitalia.** Dextrally directed. Mediotergite 8 asymmetrical, short. Laterotergites 8 indistinct. Sternum 8 indistinct. Pygophore asymmetrical, oval, titled to the right, open dorsally, mediotergite 9 indistinct. Laterotergites 9 indistinct. Parameres

asymmetrical, left smaller than right. Left paramere short, basal process short and rounded, apical process elongated and rounded. Right paramere elongated, basal process short and rounded, apical process elongated and rounded. Basal plates weakly asymmetrical. Phallosoma reduced. Conjunctiva largely membranous, irregularly shaped, without appendages. Vesica with wide base and coiled thin short distal region. Anophore asymmetrical, with small rounded posterior anophoric process. Anal tube membranous.

Notes. This is the first description of male abdominal features for this genus.

Schizoptera Fieber, 1860

Vouchers: *Schizoptera* (*Odontorhagus*) sp. (UCR_ENT 00081350, UCR_ENT 00086114), *S.* (*Cantharocoris*) sp. (UCR_ENT 00082350, UCR_ENT 00028650, UCR_ENT 00100817), *S.* (*Schizoptera*) sp. (UCR_ENT 00077905, UCR_ENT 00077331).

Figs 5.2Q, 5.9F, 5.16A, 5.16B, 5.21A, 5.21B, 5.21C, 5.21D, 5.21E

Description. **Pregenital abdomen.** Weakly asymmetrical, not laterally curved, dorsum less sclerotized than ventrum. All abdominal segments equally sclerotized. Dorsal surface smooth. Pregenital laterotergites indistinct. Three pairs of spiracles present (segments 6-8), located on lateral margins of sterna (segments 6-7), or on lateral margins of mediotergite (segment 8). Scars of DAG orifices present medially along anterior margin of mediotergite 7. **Pregenital abdomen modifications.** Mediotergite 7 slightly asymmetrical, short. Laterotergites 7 indistinct. Sternum 7 asymmetrical, modified into subgenital plate. **Genitalia.** Dextrally directed. Mediotergite 8 asymmetrical, short.

Laterotergites 8 indistinct. Sternum 8 indistinct. Pygophore asymmetrical, oval, titled to the right, open dorsally, mediotergite 9 indistinct. Laterotergites 9 indistinct. Parameres asymmetrical, left typically smaller than right. Left paramere short, basal process short and rounded, apical process short and rounded. Right paramere elongated, basal process short and rounded, apical process elongated and rounded or tapering. Basal plates strongly asymmetrical. Phallosoma reduced. Conjunctiva largely membranous, irregularly shaped, typically with one elongated and one short spinous appendage. Vesica with wide base and coiled thin long to extremely long distal region. Anophore slightly asymmetrical, with small rounded posterior anophoric process. Anal tube membranous. **Variation**. The shape and size of parameres, the shape of conjunctival appendages and the length of the vesica vary among species of this genus (Emsley 1969; Leon & Weirauch 2016a).

Vilhenannus Wygodzinsky, 1950

Vouchers: *Vilhenannus* sp. (UCR_ENT 00126002)

Figs 5.2H, 5.6A, 5.16C, 5.21F

Description. **Pregenital abdomen.** Strongly asymmetrical, dextrally curved, dorsum less sclerotized than ventrum. All abdominal segments equally sclerotized. Dorsal surface smooth. Pregenital laterotergite distinct on segment 4. Three pairs of spiracles present (segments 6-8), located on lateral margins of sterna (segments 6-7) except for right segment 6 spiracle that located on sternal process, or on left margin of mediotergite and right sclerotized stalk-like projection (segment 8). Scars of DAG indistinct. **Pregenital**

abdomen modifications. Sternum 4 with posteriorly located ventral laterotergite. Sternum 5 with laterally directed process. Sternum 6 with laterally directed process. Mediotergite 7 asymmetrical, short. Laterotergites 7 indistinct. Sternum 7 asymmetrical, long. **Genitalia.** Dextrally directed. Mediotergite 8 asymmetrical, short. Laterotergites 8 indistinct. Sternum 8 indistinct. Pygophore asymmetrical, oval, open dorsally, mediotergite 9 indistinct. Laterotergites 9 indistinct. Parameres asymmetrical, left smaller than right. Left paramere short, basal process short and rounded, apical process short and rounded. Right paramere elongated, basal process short and rounded, apical process elongated and tapering, with preapical process. Basal plates strongly asymmetrical. Phallosoma reduced. Conjunctiva largely membranous, irregularly shaped, without appendages. Vesica with wide base and coiled thin short distal region. Anophore asymmetrical, with thick twisted and antero-laterally directed anterior process and small rounded posterior anophoric process; anterior anophoric process consists of hollow outer process and slender vesica-like inner process. Anal tube membranous.

Voragocoris Weirauch, 2012

Vouchers: *Voragocoris schuhi* Weirauch, 2012 (UCR_ENT 00055625)

Fig. 5.10A

Description. **Pregenital abdomen.** Weakly asymmetrical, not laterally curved, dorsum less sclerotized than ventrum. All abdominal segments equally sclerotized. Dorsal surface smooth. Pregenital laterotergites indistinct. Three pairs of spiracles present (segments 6-8), located on lateral margins of sterna (segments 6-7), or on lateral margins of

mediotergite (segment 8). Scars of DAG orifices present medially along anterior margin of mediotergite 7. **Pregenital abdomen modifications.** Sterna 4 and 5 with oval areas with setae. Mediotergite 7 slightly asymmetrical, short. Laterotergites 7 indistinct. Sternum 7 slightly asymmetrical, long. **Genitalia.** Dextrally directed. Mediotergite 8 asymmetrical, short, with short process on posterior margin. Laterotergites 8 indistinct. Sternum 8 indistinct. Pygophore slightly asymmetrical, oval, open dorsally, mediotergite 9 indistinct. Laterotergites 9 indistinct. Parameres asymmetrical, left smaller than right. Left paramere short, basal process short and rounded, apical process short and rounded. Right paramere elongated, basal process short and rounded, apical process elongated, with hooked apex. Basal plates strongly asymmetrical. Phallosoma reduced. Conjunctiva irregularly shaped, without appendages. Vesica with wide base and coiled thin long distal region with short spinous process. Anophore slightly asymmetrical, with small rounded posterior anophoric process. Anal tube membranous.

Undescribed genus 3

Vouchers: UCR_ENT 00082360, UCR_ENT 00086175

Figs 5.2I, 5.6B, 5.10B

Description. **Pregenital abdomen.** Symmetrical, not laterally curved, dorsum less sclerotized than ventrum. All abdominal segments equally sclerotized. Dorsal surface smooth. Pregenital laterotergites distinct. Three pairs of spiracles present (segments 6-8), located on lateral margins of sterna (segments 6-7), or on lateral margins of mediotergite (segment 8). Scars of DAG orifices present along anterior margin of mediotergite 7.

Pregenital abdomen modifications. Mediotergite 7 symmetrical, short. Laterotergites 7 indistinct. Sternum 7 slightly asymmetrical, long. **Genitalia.** Dextrally directed. Mediotergite 8 asymmetrical, long. Laterotergites 8 indistinct. Sternum 8 indistinct. Pygophore asymmetrical, oval, open dorsally, with spinous processes on right side, mediotergite 9 distinct. Laterotergites 9 distinct, asymmetrical, elongated. Parameres asymmetrical, left smaller than right. Left paramere short, basal process elongated and tapering, apical process short and rounded. Right paramere elongated, basal process elongated and rounded, apical process elongated, with hooked apex. Basal plates weakly asymmetrical. Phallosoma reduced. Conjunctiva largely membranous, irregularly shaped, with one elongated spinous appendage and one short rounded appendage. Vesica with wide base and coiled thin short distal region. Anophore slightly asymmetrical, with small rounded posterior anophoric process. Anal tube membranous.

Undescribed genus 4

Vouchers: UCR_ENT 00106838

Figs 5.2J, 5.16D

Description. **Pregenital abdomen.** Symmetrical, not laterally curved, dorsum less sclerotized than ventrum. All abdominal segments equally sclerotized. Dorsal surface smooth. Pregenital laterotergites indistinct. Three pairs of spiracles present (segments 6-8), located on lateral, margins of sterna (segments 6-7), or on lateral margins of mediotergite (segment 8). Scars of DAG orifices present medially along anterior margin of mediotergite 7. **Pregenital abdomen modifications.** Mediotergite 7 slightly

asymmetrical, short. Laterotergites 7 indistinct. Sternum 7 symmetrical, long. **Genitalia.** Dextrally directed. Mediotergite 8 slightly asymmetrical, short. Laterotergites 8 indistinct. Sternum 8 indistinct. Pygophore symmetrical, oval, open dorsally, mediotergite 9 indistinct. Laterotergites 9 indistinct. Parameres asymmetrical, left equal in size to right. Left paramere elongated, basal process short and rounded, apical process elongated and rounded. Right paramere elongated, basal process short and rounded, apical process elongated and rounded. Basal plates weakly asymmetrical. Phallosoma reduced. Conjunctiva largely membranous, irregularly shaped, without appendages. Vesica with wide base and coiled thin short distal region. Anophore slightly asymmetrical, with long thin slightly curved and laterally directed anterior process and small rounded posterior anophoric process. Anal tube membranous.

Discussion

Pregenital abdomen (segments 1-7)

Overview

The male pregenital abdomen of Dipsocoromorpha consists of segments 1-7, where a sclerotized segment 1 is only represented by a mediotergite that is fused with mediotergite 2 (Figs 5.3-6). In Ceratocombidae, the dorsum and ventrum are generally equally weakly sclerotized, whereas in Dipsocoridae and Schizopteridae the dorsum and ventrum are either equally strongly sclerotized (Figs 5.3D, 5.4), or the dorsum is less sclerotized than the ventrum (Figs 5.5-6). Laterotergites are present in Ceratocombidae, Dipsocoridae, Hypsipterygidae, Stemmocryptidae and some Schizopteridae, although

homology of these sclerites among families, and within Schizopteridae is unlikely. Only Dipsocoridae and *Trichotonannus* have both dorsal and ventral laterotergites (Figs 5.3C-D), while in other taxa of Dipsocoromorpha only one sclerite (either dorsally or ventrally located) is present per side. A maximum of seven pairs of spiracles is present in Dipsocoromorpha, located on segments 2-7. As indicated by Štys (1970), the number of spiracles varies within Ceratocombidae and Dipsocoridae, but is rather stable within Hypsipterygidae and Schizopteridae. Our observations are congruent with previous reports (Hill 1984), but oppose Hill (2013) on different spiracle formulae of *Hypselosoma* (three pairs) and other Hypselosomatinae (seven pairs), as well as confirm the claims that male *Kokeshia* specimens have aspiraculate abdomens (Miyamoto 1960; Štys 1985). The position and quantity of DAG orifices varies in Ceratocombidae and Dipsocoridae, but is stable within Schizopteridae (Figs 5.8-10, congruent with observations of Štys (1959); DAG orifices are indistinct in Hypsipterygidae and Stemmocryptidae.

While the asymmetry of genitalic structures is characteristic for most Dipsocoromorpha, the pregenital abdomen varies from being completely symmetrical (in Ceratocombinae (Figs 5.3A-B), Hypsipterygidae, Stemmocryptidae, and some Schizopteridae (Figs 5.4, 5.5A, 5.5D)) to strongly asymmetrical (in Dipsocoridae, *Trichotonannus*, and many Schizopteridae (Figs 5.3C-D, 5.5C, 5.6A)).

Formation of subgenital plate

The subgenital plate is the greatly enlarged sternum of the segment preceding the pygophore that covers the pygophore from beneath (either formed by sternum 8, or when reduced, by sternum 7). In Dipsocoromorpha, a subgenital plate is developed in two

groups of Schizopteridae, the schizopterine genera *Ptenidiophyes* and *Schizoptera* (Figs 5.5D, 5.9F, 5.15F) and the ogerines *Chinannus, Kaimon, Kokeshia,* and *Ogeria* (Figs 5.8D, 5.8F, 5.13B, 5.13C, 5.13F, 5.14A), and is represented by sternum 7. While in Ogeriinae it is usually symmetrical and apically rounded, it is always asymmetrical and frequently bears processes in *Schizoptera*. In other minute litter bugs the last visible pre-pygophoral sternum (either segment 7 or 8) is elongated, but does not cover the pygophore completely.

Modifications of pregenital abdominal segments

Modifications of the pregenital abdomen are typically restricted to specific areas, outlined in Emsley (1969) with focus on Schizopteridae: 1) the side of the abdomen, either left (Dipsocoridae (Fig. 5.3D), some *Hypselosoma* species) or right (many Schizopteridae (Figs 5.3C-D, 5.5C, 5.6A)); 2) segment 7, which may be treated as a genitalic modification (Dipsocoridae, *Trichotonannus*, several genera of Schizopteridae (Figs 5.7D, 5.7E, 5.11F, 5.12A, 5.15A, 5.16C); and 3) the modification of sternum 7 into a subgenital plate (see section above).

Another modification of the pregenital abdomen not previously discussed in the literature is the presence of a longitudinal membranous fold on the ventral or ventro-lateral areas of the pregenital abdomen (in few cases paired folds on each side). These folds effectively subdivide sterna into two or three unequal sclerites and may in theory allow terminal abdominal segments to be rotated or twisted along the longitudinal body axis. Depending on how close the longitudinal folds are located to the side of the sterna, the subdivided smaller sclerites have been referred to as “ventral laterotergites” or “parasternites” in the

literature. We have utilized the same terminology here (see for example, *Chinannus*, *Ceratocomboides*). However, variation in the position of these folds and their number hint to a possible non-tergal nature of the subdivided ventral sclerites; the ventral sclerites are therefore likely non-homologous with dorsally located laterotergites.

Genital segments and genitalia

8th segment

Sternum 8 is distinct in Ceratocombidae, Dipsocoridae, Hypsipterygidae, Stemmocryptidae, and Hypselosomatinae (Figs 5.3, 5.7, 5.8A, 5.12C-D), but reduced in other Schizopteridae. Both laterotergites 8 are distinct in Dipsocoridae and some Ceratocombidae, and are frequently appendage-like (Figs 5.7A-E, 5.11, 5.12A, except *Kvamula*). Some Schizopteridae have appendages associated with tergum 8, typically only on one side (Figs 5.8D, 5.13E). Whenever a spiracle is associated with such an appendage, we consider it to be a laterotergite. Mediotergite 8 can also have immobile processes originating from posterior or lateral sides (Stemmocryptidae, *Trichotonannus* and various genera of Schizopteridae). Muscles are attached to the appendage of tergum 8 in *Chinannus* suggesting that it is a movable structure (Knyshov *et al.* 2016). Although the musculature of laterotergites 8 was not studied in the present paper, the similar cuticular structure suggests mobility of these appendages in other Schizopteridae as well.

Pygophore

The pygophore is completely closed dorsally in Ceratocombidae and Dipsocoridae, with the mediotergite, laterotergites, and sternum fused with each other (Figs 5.7A-E, 5.11, 5.12A). In Stemmocryptidae and *Hypselosoma*, mediotergite 9, laterotergites 9, and

sternum 9 are connected by membranes (Fig. 5.7F). In Hypsipterygidae and Schizopteridae except *Hypselosoma*, mediotergite 9 is indistinct, and laterotergites 9 are mostly indistinct with few exceptions (*Peloridinannus, Nannocoris*, and two of the undescribed genera, Figs 5.8C, 5.10B, 5.13A, 5.14B, 5.15C). In all examined taxa, whenever distinct, laterotergites 9 are appendage-like.

Parameres

Parameres are symmetrical in Ceratocombini and Issidomimini except *Issidomimus*. In other Dipsocoromorpha, the parameres are weakly to strongly asymmetrical. In Schizopteridae, one of the parameres is frequently smaller than the other (either left or right), but sometimes the parameres are of roughly similar size. In almost all examined specimens at least one of the parameres has a posteriorly directed basal process, which is frequently very small and rounded, but may become more prominent. In some species of *Muatianvuaia*, an additional anteriorly directed basal process may be present (Fig. 5.11D). The overall variation of paramere shape across Dipsocoromorpha is substantial and hard to capture in simple descriptions.

Aedeagus

In Dipsocoromorpha, the aedeagus deviates from the typical heteropteran structure: it is typically devoid of retractable parts (except in Ceratocombinae and Stemmocryptidae), its distal portion (vesica) is typically exposed at rest, and the middle portion of the aedeagus is very compact. This last feature blurs the distinction between phallosoma and endosoma (see methods for section on male intromittent organ terminology). While structures attributable to the phallosoma can be recognized in Ceratocombidae,

Dipsocoridae, Hypsipterygidae, Stemmocryptidae, and Hypselosomatinae (sclerites in between conjunctiva and basal plates, Figs 5.17, 5.18A-C), in Schizopteridae except Hypselosomatinae the phallosoma is indistinct (Figs 5.18D-F, 5.19-21). Although it is possible that the compact middle portion of the aedeagus in the latter case is formed by both the phallosoma and conjunctiva, this scenario renders the homology between the "conjunctiva" in non-hypselosomatine Schizopteridae and the conjunctiva in other Dipsocoromorpha questionable, requiring the use of different terms. A detailed study of the minute aedeagus of Schizopteridae was beyond the scope of the present study and data to decisively support this hypothesis are therefore currently unavailable. We therefore propose a different hypothesis, building on Hill's works (Hill 1987a, 2013): the phallosoma is the region of the aedeagus distal to the basal plates and is represented by two sclerites in Ceratocombinae (here termed dorsal and ventral sclerites of the phallosoma, Figs 5.17A-D), several complicated sclerites in *Trichotonannus* (Fig. 5.17E), a U-shaped sclerite (Fig. 5.17F-G) or two elongated sclerites in Dipsocoridae, a U-shaped sclerite in Hypsipterygidae, irregularly shaped sclerites in Stemmocryptidae, a Y-shaped sclerite in *Hypselosoma* (Fig. 5.18A), a U-sclerite or circular sclerite (Figs 5.18B-C) in other Hypselosomatinae, and reduced in other Schizopteridae. We suggest new terms for the phallosomal sclerites of Ceratocombinae as they are characteristic and easily comparable among genera. We define as conjunctiva the region of the aedeagus that is distal to the phallosoma (Figs 5.17-21) and is represented by one or several sclerites (Ceratocombidae, Dipsocoridae, and Hypsipterygidae) or a combination of sclerites and appendages (Stemmocryptidae and Schizopteridae). Finally, we define the vesica as the

distal most region of the aedeagus that is represented by a short or long, coiled or straight tubular process, sometimes with additional outbranching processes (Figs 5.17-21).

Anophore and anophoric processes

The anophore (sclerite of segment 10) is present in most Dipsocoromorpha (Figs 5.7-16), but indistinct in Ceratocombinae, Dipsocoridae, and Stemmocryptidae, possibly because of a fusion with mediotergite 9. In these groups it is difficult to determine if tergum 9 is completely reduced or just fused with the anophore in taxa where the pygophore is dorsally opened and an anophore is present. In Schizopteridae, the anophore frequently bears a variously shaped and sized process, typically originating from the anterior portion of the anophore (Figs 5.8B, 5.8D, 5.9C-E, 5.12E-F, 5.13B, 5.13E, 5.15A, 5.15C-E, 5.16C-D). In a few taxa, e.g., *Machadonannus*, *Nannocoris*, and *Vilhenannus*, several processes may be present (Figs 5.9D, 5.15A, 5.15C-D, 5.16C). Contrary to Wygodzinsky's (1950b) interpretation, we did not find evidence for the association of the caudal processes in *Vilhenannus* with segments 7 or 9. Interestingly, in the same paper he treated similar processes in *Machadonannus* as belonging to the anophore. We here hypothesize that both the outer and inner processes belong to the anophore. In Schizopterinae, the anophore also bears a posterior anophoric process that is small and rounded (Figs 5.9B-E, 5.10B, 5.14C-F, 5.15-16).

Towards a phylogenetic interpretation of dipsocoromoprhan pregenital and genital structures

While a formal phylogenetic analysis is beyond the scope of the present study, several primary homology hypotheses can be outlined, so that they can be tested in the future. In this sense, we hypotheseize that the:

- carinulation of the pregenital abdomen is homologous in *Kaimon, Ogeria,* and *Pachyplagia*;
- pregenital laterotergites of *Kokeshia* are homologous to those of the undescribed genus 1;
- the indistinct sternum 8 is homologous across Schizopteridae (except Hypselosomatinae, where it is distinct);
- apical and basal processes of the parameres are homologous across Dipsocoromorpha;
- the shape of the pygophore, parameres and laterotergites 9, and structure of the aedeagus are homologous across Ceratocombinae;
- phallosomal sclerites of Ceratocombinae (dorsal and ventral sclerites) are homologous to the single U-sclerite or the two elongated sclerites of Dipsocoridae, to the U-shaped sclerite of Hypsipterygidae, to the irregularly shaped phallosomal sclerites of Stemmocryptidae, to the Y-shaped phallosomal sclerite of *Hypselosoma*, and the U-shaped or circular sclerite of other Hypselosomatinae;
- the posterior anophoric process is homologous across Schizopterinae;

- modifications of the pregenital abdomen and structure of the anterior anophoric process are homologous between *Machadonannus* and *Vilhenannus*.

Conclusions

The data presented show astounding diversity of abdominal structures in a relatively small group of insects, the Dipsocoromorpha. We speculate that this diversity will continue to grow as more taxa are being discovered and described. Several regions of the abdomen (lateral sclerites, middle portion of aedeagus, and some unique abdominal structures) still pose problems for discerning homology and proposing adequate terminology, and more in depth morphological studies are needed to address these problems. Finally, given that diversity in genitalic structures is likely generated by sexual selection (Huber 2010; Huber *et al.* 2007), Dipsocoromorpha may be an interesting group for further investigations of the evolution of complex male genitalia.

References

Azar, D., Nel, A., Coty, D. & Garrouste, R. (2010) The second fossil ceratocombid bug from the Miocene amber of Chiapas (Mexico) (Hemiptera: Ceratocombidae). *Annales de la Société entomologique de France* 46(1-2), 100–102.

Beutel, R. G., Friedrich, F., Yang, X.-K. & Ge, S.-Q. (2014) *Insect morphology and phylogeny: a textbook for students of entomology*. Berlin: Walter de Gruyter.

Bowsher, J. H., Ang, Y., Ferderer, T. & Meier, R. (2013) Deciphering the evolutionary history and developmental mechanisms of a complex sexual ornament: the abdominal appendages of Sepsidae (Diptera). *Evolution* 67(4), 1069–1080.

Carpintero, D. L. & Dellapé, P. M. (2006) *Williamsocoris*, a new genus of Schizopteridae (Heteroptera) from Argentina. *Zoological Science* 23(7), 653–655.

Carvalho, J. C. M. (1989) On a curious new species of Dipsocoridae from Sulawesi (Hemiptera). *Bulletin de l'Institut Royal Des Sciences Naturelles de Belgique Entomologie* 58, 185–188.

Cassis, G. & Schuh, R. T. (2010) Systematic methods, fossils, and relationships within Heteroptera (Insecta). *Cladistics* 26(3), 262–280.

China, W. E. (1946) New Cryptostemmatidae (Hemiptera) from Trinidad, British West Indies. *Proceedings of the Royal Entomological Society of London (B)* 15, 148–154.

Drake, C. J. (1961) A new subfamily, genus and two new species of Dipsocoridae (Hemiptera). *Publicacoes Culturais Da Companhia de Diamantes de Angola* 52, 77–80.

Dupius, C. (1970) Heteroptera. In S.L. Tuxen (Ed.), *Taxonomist's glossary of genitalia in insects* (pp. 190–209). Copenhagen: Munksgaard.

Eberhard, W. G. (1985) *Sexual selection and animal genitalia* (Vol. 244). Cambridge, MA: Harvard University Press.

Emsley, M. G. (1969) The Schizopteridae (Hemiptera: Heteroptera) with the descriptions of new species from Trinidad. *Memoirs of the American Entomological Society* 25, 1–154.

Esaki, T. & Miyamoto, S. (1959) A new or little known *Hypselosoma* from Amami-Oshima and Japan, with the proposal of a new tribe for the genus (Hemiptera). *Sieboldia Fukuoka* 2, 109–120.

Frankenberg, S. & Weirauch, C. Correlated evolution of genitalic structures in animals with exaggerated male and female genitalia. *The Biological Journal of the Linnean Society*, in review.

Gross, G. F. (1951) On three new genera and species of Schizopterinae (Heteroptera-Cryptostemmatidae) from Australia. *Records of the South Australian Museum* 9, 535–544.

Hill, L. (1980) Tasmanian Dipsocoroidea (Hemiptera: Heteroptera). *Australian Journal of Entomology* 19(2), 107–127.

Hill, L. (1984) New genera of Hypselosomatinae (Heteroptera: Schizopteridae) from Australia. *Australia Journal of Zoology, Supplementary Series* 103, 1–55.

Hill, L. (1987a) 1st Record of Dipsocoridae (Hemiptera) from Australia with the Description of 4 New Species of *Cryptostemma* Herrich-Schaeffer. *Journal of the Australian Entomological Society* 26, 129–139.

Hill, L. (1987b) Four new Australian species of *Hypselosoma* Reuter (Heteroptera: Schizopteridae). *Australian Journal of Entomology* 26(3), 265–278.

Hill, L. (1990) Australian *Ogeria* Distant (Heteroptera: Schizopteridae). *Invertebrate Systematics* 4(4), 697–720.

Hill, L. (2004) *Kaimon* (Heteroptera: Schizopteridae), a new, speciose genus from Australia. *Memoirs of the Queensland Museum* 49(2), 603–647.

Hill, L. (2013) A revision of *Hypselosoma* Reuter (Insecta: Heteroptera: Schizopteridae) from New Caledonia. *Memoirs of the Queensland Museum* 56(2), 407–455.

Hoey-Chamberlain, R. & Weirauch, C. (2016) Two new genera of big-eyed minute litter bugs (Hemiptera, Schizopteridae, Hypselosomatinae) from Brazil and the Caribbean. *ZooKeys* 640, 79–102.

Huber, B. A. (2010) Mating positions and the evolution of asymmetric insect genitalia. *Genetica* 138(1), 19-25.

Huber, B. A., Sinclair, B. J. & Schmitt, M. (2007) The evolution of asymmetric genitalia in spiders and insects. *Biological Reviews* 82(4), 647-698.

Kellen, W. R. (1961) A new species of *Ogeria* from the South Pacific (Hemiptera: Cryptostemmatidae). *Proceedings of the Entomological Society of Washington* 63, 17–20.

Klug, R. & Klass, K.-D. (2007) The potential value of the mid-abdominal musculature and nervous system in the reconstruction of interordinal relationships in lower Neoptera. *Arthropod Systematics & Phylogeny* 65(1), 100.

Knyshov et al., in preparation. Evolutionary history of minute litter bugs (Hemiptera: Dipsocoromorpha) based on morphological and molecular data.

Knyshov, A., Leon, S., Hoey-Chamberlain, R. & Weirauch, C. (2016) *Pegs, pouches, and spines: systematics and comparative morphology of the New World litter bug genus Chinannus Wygodzinsky, 1948*. Entomological Society of America, Annapolis, MD.

Leon, S. & Weirauch, C. (2016a) Scratching the surface? Taxonomic revision of the subgenus *Schizoptera* (*Odontorhagus*) reveals vast undocumented biodiversity in the largest litter bug genus *Schizoptera* Fieber (Hemiptera: Dipsocoromorpha). *Zootaxa* 4184(2), 255–284.

Leon, S. & Weirauch, C. (2016b) Small Bugs, Big Changes: Taxonomic Revision of *Orthorhagus* McAtee & Malloch. *Neotropical Entomology* 45(3), 1–14.

Linnavuori, R. (1974) Hemiptera of the Sudan, with remarks on some species of the adjacent countries. Families Cryptostemmatidae, Cimicidae, Polyctenidae, Joppeicidae, Reduviidae, Pachynomidae, Nabidaea, Leptopodidae, Saldidae, Henicocephalidae and Berytidae. *Annales Entomologici Fennici* 40(3), 116–138.

Matsuda, R. (1976). *Morphology and evolution of the insect abdomen. With special reference to developmental patterns and their bearings upon systematics*. Oxford: Pergamon press.

McAtee, W. L. & Malloch, J. R. (1925) Revision of bugs of the family Cryptostemmatidae in the collection of the United States National Museum. *Proceedings of the United States National Museum* 67(2585), 1–42.

Melber, A. & Köhler, R. (1992) Die Gattung *Ceratocombus* Signoret, 1852 in Nordwestdeutschland (Heteroptera, Ceratocombidae). *Bonner Zoologische Beitrage* 43, 229–246.

Miyamoto, S. (1960) A new genus of Schizopterinae from Japan (Heteroptera, Dipsocoridae). *Sieboldia Fukuoka* 2, 163–170.

Miyamoto, S. (1964) A new species of *Cryptostemma* from Japan (Hemiptera, Dipsocoridae). *Kontyu Tokyo* 32, 517–519.

Pericart, J. & Matocq, A. (2003) Two species of Dipsocoridae new for Algeria, one new for science (Heteroptera, Dipsocoromorpha). *Nouvelle Revue d'Entomologie* 20(3), 255–257.

Pluot-Sigwalt, D. & Péricart, J. (2003) The spermatheca of the Dipsocoridae with special reference to the strange "loculus capsulae" in *Harpago* species (Heteroptera, Dipsocoromorpha). *Annales de la Société entomologique de France* 39(2), 129–138.

Rédei, D. (2007). A new species of the family Hypsipterygidae from Vietnam, with notes on the hypsipterygid fore wing venation (Heteroptera, Dipsocoromorpha). *Deutsche Entomologische Zeitschrift* 54(1), 43–50.

Rédei, D. (2008a) First record of *Pinochius* Carayon, 1949 from the Oriental Region, with description of a new species from Vietnam (Heteroptera: Schizopteridae). In S. Grozeva & N. Simov (Eds.), *Advances in Heteroptera research: festschrift in honor of 80th anniversary of Michail Josifov. [Pensoft Series Faunistica No 82.]* (pp. 327–337). Sofia: Pensoft Publishers.

Rédei, D. (2008b) Two new species of *Kokeshia* from India and Thailand (Hemiptera: Heteroptera: Schizopteridae). *Acta Entomologica Musei Nationalis Pragae* 48(2), 241–250.

Rédei, D., Ren, S. & Bu, W. (2012) Two new species of *Kokeshia* from China (Hemiptera: Heteroptera: Schizopteridae). *Zootaxa* 3497, 29–36.

Schuh, R. T. & Slater, J. A. (1995) *True bugs of the world (Hemiptera: Heteroptera): classification and natural history*. Ithaca: Comstock Publishing Associates, Cornell University Press.

Scudder, G. (1971) Comparative morphology of insect genitalia. *Annual Review of Entomology* 16(1), 379–406.

Simmons, L. W. (2014) Sexual selection and genital evolution. *Austral Entomology*, *53*(1), 1–17.

Singh-Pruthi, H. (1925) The morphology of the male genitalia in Rhynchota. *Transactions of the Entomological Society of London* 1925, 127–267.

Snodgrass, R. E. (1936) Morphology of the Insect abdomen. Part III. The male genitalia (including arthropods other than Insects). *Smithsonian Miscellaneous Collections* 95(14), 1–96.

Snodgrass, R. E. (1957) A revised interpretation of the external reproductive organs of male Insects. *Smithsonian Miscellaneous Collections* 135(6), 1–60.

Southwood, T. R. E. (1961) Two new Schizopteridae (Hem.) collected by the Imperial College 1957 Ghana expedition. *Entomologist's Monthly Magazine* 97, 89–92.

Streito, J.-C. & Pericart, J. (2005) Revision of the genus *Harpago* Linnavuori, 1951 and interesting capture of Dipsocoridae in Europe (Heteroptera, Dipsocoridae). *Nouvelle Revue d'Entomologie* 22(1), 63–72.

Štys, P. (1958) *Ceratocombus* (*Xylonannus*) *kunsti* n. sp.- a new species of Dipsocoridae from Czechoslovakia (Heteroptera). *Acta Societatis Entomologicae Cechoslovenicae* 55, 372–379.

Štys, P. (1959) The 5th stage nymph of *Ceratocombus* (*Ceratocombus*) *coleoptratus* (Zetterstedt, 1819) and notes on the morphology and systematics of Dipsocoridae (Heteroptera). *Acta Entomologica Musei Nationalis Pragae* 33, 377–388.

Štys, P. (1970) On the morphology and classification of the family Dipsocoridae s. lat., with particular reference to the genus *Hypsipteryx* Drake (Heteroptera). *Acta Entomologica Bohemoslovaca* 67, 21–46.

Štys, P. (1974) *Semangananus mirus* gen. n., sp. n. from Celebes - a bug with accessory male genitalia (Heteroptera, Schizopheridae). *Acta Entomologica Bohemoslovaca* 71(6), 382–397.

Štys, P. (1977) First records of Dipsocoridae and Ceratocombidge from Madagascar (Heteroptera). *Acta Entomologica Bohemoslovaca* 74(5), 295-315.

Štys, P. (1982) A new Oriental genus of Ceratocombidae and higher classification of the family (Heteroptera). *Acta Entomologica Bohemoslovaca* 79, 354–376.

Štys, P. (1983a) A new coleopteriform genus and species of Ceratocombidae from Zaire (Heteroptera, Dipsocoromorpha). *Věstník Československé Zoologické Společnosti* 42, 221–230.

Štys, P. (1983b) A new family of Heteroptera with dipsocoromorphan affinities from Papua New Guinea. *Acta Entomologica Bohemoslovaca* 80(4), 256–292.

Štys, P. (1985) Two new species of *Kokeshia* (Heteroptera, Schizopteridae) from Nepal and appraisal of alleged synapomorphies of Paraneoptera. *Acta Entomologica Bohemoslovaca* 82(3), 187–205.

Sweet, M. H. (1996) Comparative External Anatomy of the Pregenital Abdomen of the Hemiptera. In Schaefer, C. W. (Ed.), *Studies on Hemipteran Phylogeny* (pp. 119–158). Lanham, Maryland: Entomological Society of America.

Wang, Y.H., Wu, H.Y., Rédei, D., Xie, Q., Chen, Y., Chen, P.P., Dong, Z.E., Dang, K., Damgaard, J., Štys, P. & Wu, Y.Z. (2017) When did the ancestor of true bugs become stinky? Disentangling the phylogenomics of Hemiptera–Heteroptera. *Cladistics* 2017, 1–25.

Weirauch, C., Knyshov, A. & Hoey-Chamberlain, R. (2017) *Machadonannus brailovskyi*, n. sp., a new species of Schizopteridae from the Afrotropical region. *Dugesiana* 24(2), 279–286.

Weirauch, C. & Frankenberg, S. (2015) From "insect soup" to biodiversity discovery: taxonomic revision of *Peloridinannus* Wygodzinsky, 1951 (Hemiptera: Schizopteridae), with description of six new species. *Arthropod Systematics and Phylogenetics* 73(3), 457–475.

Weirauch, C., Whorrall, K., Knyshov, A. & Hoey-Chamberlain, R. (2018) Giant among dwarfs: *Meganannus lewisi*, gen. n. and sp. n., a new genus and species of minute litter bugs from Costa Rica (Hemiptera: Schizopteridae). *Zootaxa* 4370(2), 156–170.

Wygodzinsky, P. (1948a) Contributions towards the knowledge of the genus *Cryptostemma* Herrich-Schaeffer, 1835 (Cryptostemmatidae, Hemiptera). *Revista de Entomologia* 19, 283–294.

Wygodzinsky, P. (1948b) On two new genera of Schizopterinae (Cryptostemmatidae) from the Neotropical region (Hemiptera). *Revista Brasileira de Biologia* 8, 143–155.

Wygodzinsky, P. (1950a) Contribution towards the knowledge of the family Cryptostemmatidae (Hemiptera). *Revista Brasileira de Biologia* 10, 377–392.

Wygodzinsky, P. (1950b) Schizopterinae from Angola (Cryptostemmatidae, Hemiptera). *Publicacoes Culturais Mus Dundo Companhia Diamantes Angola Lisbon* 7, 9–47.

Wygodzinsky, P. (1952) Sobre algunos Cryptostemmatidae, principalmente de la Argentina (Hemiptera). *Acta Zoologica Lilloana* 10, 51–74.

Wygodzinsky, P. (1953) Cryptostemmatinae from Angola (Cryptostemmatidae, Hemiptera). *Publicaçoes Culturais Da Companhia de Diamantes de Angola* 16, 29–47.

Wygodzinsky, P. (1958) Hemiptera (Heteroptera): Dipsocoridae. In *South African Animal Life Vol. V.* (pp. 109–111). Hanstrom, Brinck & Rudebeck.

Wygodzinsky, P. (1960) Un nouvel *Hypeslosoma* de Madagascar, avec la description d'autre especes et des observations sur le genre (Schizopterinae, Dipsocoridae, Hemiptera). *Memoires de l'Institut Scientifique de Madagascar (E)* 11(1959), 509–539.

Wygodzinsky, P. (1962). Studies on the fauna of Curaçao and other Caribbean Islands: No. 53. The Heteroptera of the Netherlands Antilles-IV. Dipsocoridae. *Natuurwet Stud Suriname 1960* 22, 62–66.

Yang, C.-T. & Chang, T.-Y. (2000) *The external male genitalia of Hemiptera (Homoptera-Heteroptera)*. Taichung: Shih Way Publishers.

Yoshizawa, K. & Johnson, K. P. (2006) Morphology of male genitalia in lice and their relatives and phylogenetic implications. *Systematic Entomology* 31(2), 350–361.

Table 5.1. Voucher specimens used in the present study

Family	Subfamily	Tribe	Genus	Species	Unique specimen indentifier	Figures
Ceratocombidae	Ceratocombinae	Ceratocombini	*Ceratocombus*	sp.	N/A	7A
Ceratocombidae	Ceratocombinae	Ceratocombini	*Ceratocombus*	sp.	UCR_ENT 00045174	1A, 11A
Ceratocombidae	Ceratocombinae	Ceratocombini	*Ceratocombus*	sp.	UCR_ENT 00074810	17A
Ceratocombidae	Ceratocombinae	Ceratocombini	*Leptonannus*	sp.	UCR_ENT 00036781	7B
Ceratocombidae	Ceratocombinae	Ceratocombini	*Leptonannus*	sp.	UCR_ENT 00125845	1B, 3A, 11B, 17B
Ceratocombidae	Ceratocombinae	Issidomimini	*Kvamula*	sp.	UCR_ENT 00036927	7C
Ceratocombidae	Ceratocombinae	Issidomimini	*Kvamula*	sp.	UCR_ENT 00045529	11C, 17C
Ceratocombidae	Ceratocombinae	Issidomimini	*Muatianvuaia*	sp.	UCR_ENT 00086455	11D, 17D
Ceratocombidae	Ceratocombinae	Issidomimini	*Muatianvuaia*	sp.	UCR_ENT 00036812	1C
Ceratocombidae	Ceratocombinae	Issidomimini	*Muatianvuaia*	sp.	UCR_ENT 00036957	3B, 11E
Ceratocombidae	Trichotonanninae		*Trichotonannus*	sp.	UCR_ENT 00120713	1D, 3C, 11F, 17E
Ceratocombidae	Trichotonanninae		*Trichotonannus*	sp.	UCR_ENT 00125043	7D
Dipsocoridae			*Cryptostemma*	sp.	N/A	7E
Dipsocoridae			*Cryptostemma*	sp.	UCR_ENT 00061211	1E, 3D, 12A, 17F
Dipsocoridae			*Cryptostemma*	sp.	UCR_ENT 00091400	17G
Schizopteridae	Hypselosomatinae		*Hypselosoma*	sp.	UCR_ENT 00091321	7F
Schizopteridae	Hypselosomatinae		*Hypselosoma*	sp.	UCR_ENT 00045351	1F, 12B, 18A
Schizopteridae	Hypselosomatinae		*Hypselosoma*	*haplacanthatum*	UCR_ENT 00090357	12C
Schizopteridae	Hypselosomatinae		*Rectilamina*	sp.	UCR_ENT 00084929	8A
Schizopteridae	Hypselosomatinae		*Rectilamina*	sp.	UCR_ENT 00084928	12D, 18B
Schizopteridae	Hypselosomatinae		*Rectilamina*	sp.	UCR_ENT 00088314	1G
Schizopteridae	Hypselosomatinae		*Williamsocoris*	sp.	UCR_ENT 00057523	1H, 12E, 18C
Schizopteridae			*Guapinannus*	sp.	UCR_ENT 00090715	8B
Schizopteridae			*Guapinannus*	sp.	UCR_ENT 00090717	1I, 12F, 18D
Schizopteridae			*Peloridinannus*	*sinefenestra*	UCR_ENT 00090782	8C
Schizopteridae			*Peloridinannus*	*moe*	UCR_ENT 00098861	1J, 13A, 18E
Schizopteridae	Ogeriinae		*Chinannus*	*bierigi*	UCR_ENT 00082335	8D
Schizopteridae	Ogeriinae		*Chinannus*	*trinitatis*	UCR_ENT 00081798	13B
Schizopteridae	Ogeriinae		*Chinannus*	*trinitatis*	UCR_ENT 00086192	1K

Schizopteridae	Ogeriinae		*Chinannus*	*communis*	UCR_ENT 00076302	18F
Schizopteridae	Ogeriinae		*Kaimon*	sp.	UCR_ENT 00096999	1L, 8E
Schizopteridae	Ogeriinae		*Kaimon*	sp.	UCR_ENT 00091319	4A, 13C, 19A
Schizopteridae	Ogeriinae		*Kokeshia*	sp.	UCR_ENT 00081331	8F
Schizopteridae	Ogeriinae		*Kokeshia*	sp.	UCR_ENT 00063170	13D
Schizopteridae	Ogeriinae		*Kokeshia*	sp.	UCR_ENT 00088975	19B
Schizopteridae	Ogeriinae		*Meganannus*	*lewisi*	UCR_ENT 00014802	1M, 13E, 19C
Schizopteridae	Ogeriinae		*Ogeria*	sp.	UCR_ENT 00086442	1N, 4B, 13F, 19D
Schizopteridae	Ogeriinae		Undescribed genus 1	sp.	UCR_ENT 00098868	9A
Schizopteridae	Ogeriinae		Undescribed genus 1	sp.	UCR_ENT 00090562	4C, 13A
Schizopteridae	Ogeriinae		Undescribed genus 2	sp.	UCR_ENT 00014811	1O, 4D, 13B, 19E
Schizopteridae	Schizopterinae		*Ceratocomboides*	sp.	UCR_ENT 00099292	1P, 5A, 14C
Schizopteridae	Schizopterinae		*Ceratocomboides*	sp.	UCR_ENT 00077448	19F
Schizopteridae	Schizopterinae		*Corixidea*	*major*	UCR_ENT 00012039	5B, 14D
Schizopteridae	Schizopterinae		*Corixidea*	*major*	UCR_ENT 00093506	1Q
Schizopteridae	Schizopterinae		*Dundonannus*	sp.	UCR_ENT 00089713	9B
Schizopteridae	Schizopterinae		*Dundonannus*	sp.	UCR_ENT 00081642	14E
Schizopteridae	Schizopterinae		*Dundonannus*	sp.	UCR_ENT 00087529	2A, 14F
Schizopteridae	Schizopterinae		*Hoplonannus*	sp.	UCR_ENT 00081393	9C, 20A
Schizopteridae	Schizopterinae		*Machadonannus*	*brailovskyi*	UCR_ENT 00125913	2B, 5C, 15A, 20B
Schizopteridae	Schizopterinae		*Membracioides*	sp.	UCR_ENT 00084415	15B, 20C
Schizopteridae	Schizopterinae		*Membracioides*	sp.	UCR_ENT 00084401	2C
Schizopteridae	Schizopterinae		*Nannocoris*	sp.	UCR_ENT 00097001	9D
Schizopteridae	Schizopterinae		*Nannocoris*	sp.	UCR_ENT 00081615	2D, 15C, 20D
Schizopteridae	Schizopterinae		*Nannocoris*	sp.	UCR_ENT 00088078	15D
Schizopteridae	Schizopterinae		*Pinochius*	sp.	UCR_ENT 00036917	9E
Schizopteridae	Schizopterinae		*Pinochius*	sp.	UCR_ENT 00081616	2E, 15E, 20E
Schizopteridae	Schizopterinae		*Ptenidiophyes*	sp.	UCR_ENT 00014874	2F
Schizopteridae	Schizopterinae		*Ptenidiophyes*	sp.	UCR_ENT 00116306	5D, 15F, 20F
Schizopteridae	Schizopterinae		*Schizoptera*	sp.	UCR_ENT 00081350	16A
Schizopteridae	Schizopterinae		*Schizoptera*	sp.	UCR_ENT	16B, 21A

					00082350	
Schizopteridae	Schizopterinae		*Schizoptera*	sp.	UCR_ENT 00100817	2G
Schizopteridae	Schizopterinae		*Schizoptera*	sp.	UCR_ENT 00077905	21E, 21D
Schizopteridae	Schizopterinae		*Schizoptera*	sp.	UCR_ENT 00086114	21B
Schizopteridae	Schizopterinae		*Schizoptera*	sp.	UCR_ENT 00077331	21E
Schizopteridae	Schizopterinae		*Schizoptera*	sp.	UCR_ENT 00028650	9F
Schizopteridae	Schizopterinae		*Vilhenannus*	sp.	UCR_ENT 00126002	2H, 6A, 16C, 21F
Schizopteridae	Schizopterinae		*Voragocoris*	*schuhi*	UCR_ENT 00055625	10A
Schizopteridae	Schizopterinae		Undescribed genus 3	sp.	UCR_ENT 00082360	6B
Schizopteridae	Schizopterinae		Undescribed genus 3	sp.	UCR_ENT 00086175	2I, 10B
Schizopteridae	Schizopterinae		Undescribed genus 4	sp.	UCR_ENT 00106838	2J, 16D

Table 5.2. Terminology used in the present study with synonyms from the literature

Preferred term	Abbreviation	Definition	Previously used terms	References
Aedeagus	aed	Male intromittent organ (including basal plates - bp)	Aedeagus	China (1946) w/o bp, Emsley (1969) w/o bp, Esaki and Miyamoto (1959, 1960), Hill (1987a, 1987b), Hill (1984, 2004) w/o bp, Wygodzinsky (1948a, 1948b, 1950a, 1950b, 1953)
			Penis	Carvalho (1989), Linnavuori (1974)
			Phallus	Drake (1961), Rédei (2007, 2008a, 2008b), Rédei *et al.* (2012), Štys (1970, 1974, 1977, 1982, 1983a, 1983b, 1985), Wygodzinsky (1960, 1962)
Anal tube	at	Tubular structure composed of membranous portion of segment 10 and entire segment 11	Anal tube	Carpintero and Dellapé (2006), China (1946), Emsley (1969), Hill (1980, 1984, 1987b)
			Anal cone	Wygodzinsky (1948b)
Anophore	ano	Sclerite (typically tubular) of segment 10	Anophore	Emsley (1969), Gross (1951), Hill (1980, 1987a, 1987b, 2004, 2013), Hill (1984) as t9?, Štys (1970), Wygodzinsky (1950a, 1950b, 1953, 1960)
			Proctiger	Rédei (2008a), Rédei (2008b) as s10+11, Štys (1974, 1977, 1982, 1983a, 1983b, 1985)
Anophoric process	anop	(Anterior) process of anophore	Anophoric process	Hill (1984), Knyshov *et al.* (2016)
			Anophoric appendage	Emsley (1969), Hill (1980, 1984)
			Paraproctal appendage	Carpintero and Dellapé (2006)

Apical process of paramere	app	Main dorsally or laterally directed process of paramere	Apical process	Rédei (2007)
			Apical appendage	Štys (1970)
			Distal lobe	Hill (2013)
			Hypophysis	Rédei (2008b), Štys (1983a, 1983b)
Appendage of mediotergite #	mt#ap			
Basal plates	bp	Basal part of aedeagus that is in Dipsocoromorpha also tightly associated with parameres	Basal plate(s)	Emsley (1969), Hill (1980, 1984, 1987a, 1987b, 2004, 2013), Rédei (2008b), Štys (1970), Wygodzinsky (1948a, 1948b)
			Articulatory apparatus	Wygodzinsky (1960)
			Basal apparatus	Štys (1983a, 1983b)
Basal process of paramere	bpp	Posteriorly directed basal process of paramere	Apophysis	Štys (1983b)
			Basal bump	Knyshov *et al.* (2016)
			Basal / posterior extension	Rédei (2008b)
			Proximal lobe	Hill (2013)
Conjunctiva	con	Portion of aedeagus with sclerites and appendages, located between phallosoma and vesica	Conjunctiva / conjunctive	Emsley (1969), Gross (1951), Hill (2004, 2013), Štys (1982, 1985), Wygodzinsky (1960)
			Phallobase	Emsley (1969) (?), Rédei (2008b)
			Phallosoma	Gross (1951), Wygodzinsky (1948a, 1948b, 1950a)
			Phallotheca	Štys (1982)
Conjunctival appendage	capp	Elongated sclerites of conjunctiva	Conjunctival appendage	Emsley (1969), Gross (1951), Wygodzinsky (1948b)
			Conjunctival process	Rédei (2008b), Štys (1985)
			Process of conjunctival sclerite	Hill (1980, 1987b, 2004, 2013)
			Process of phallus	Rédei (2008b)
Conjunctival sclerite	cs	Sclerite of conjunctiva, not forming an appendage	Conjunctival sclerite	Hill (1980, 1987b, 2004, 2013)
Dorsal abdominal gland scars	DAG	Scars of scent gland orifices	Dorsal abdominal gland orifice scars	Knyshov *et al.*, (2016) and elsewhere

Dorsal sclerite of phallosoma	dph			
Hemitergite	hmt	Part of mediotergite whenever it is not entire	Hemitergite	Rédei (2008b), Rédei *et al.* (2012), Štys (1985)
Laterotergite, dorsal laterotergite, ventral laterotergite	lt, dlt, vlt	Lateral sclerite of tergum, see discussion in text	Laterotergite	Azar, Nel, Coty, and Garrouste (2010), Hill (1980, 1987a, 2013), Melber and Köhler (1992), Pericart and Matocq (2003), Štys (1958, 1970, 1974, 1977, 1982, 1983a, 1983b)
			Parasternite	Emsley (1969), Linnavuori (1974), Wygodzinsky (1948a, 1948b, 1953, 1960)
			Paratergite	Emsley (1969)
Mediotergite	mt			
Paramere	lp, rp		Paramere	Carpintero and Dellapé (2006), Carvalho (1989), China (1946), Drake (1961), Emsley (1969), Esaki and Miyamoto (1959), Hill (1980, 1984, 1987a, 1987b, 2004, 2013), Melber and Köhler (1992), Miyamoto (1960, 1964), Pericart and Matocq (2003), Rédei (2007, 2008b, 2008a), Rédei *et al.* (2012), Štys (1970, 1974, 1977, 1982, 1983a, 1983b, 1985), Wygodzinsky (1953, 1960, 1962)
			Clasper	Gross (1951), Kellen (1961), Wygodzinsky (1948a, 1950a, 1950b, 1953)
			Stylus	Linnavuori (1974)
Phallosoma	phsm	Middle portion of	Basal struts	Hill (1987a)

		aedeagus between basal plates and endosoma (conjunctiva and vesica)	Phallotheca	Wygodzinsky (1960)
			U-sclerite	Hill (2013)
			Y-sclerite	Hill (1987b, 2013)
Posterior anophoric process	panop	Typically small and rounded process on posterior anophore		
Pregenital abdomen		Abdominal segments 1-7	Pregenital abdomen	Rédei *et al.* (2012), Štys (1970, 1983a)
			Pregenital segments	Carpintero and Dellapé (2006), Emsley (1969), Hill (1984)
Process of mediotergite #	mt#p			
Pygophore	pyg	Abdominal segment 9	Pygopgore	Carpintero and Dellapé (2006), Carvalho (1989), China (1946), Gross (1951), Linnavuori (1974), Rédei (2008b, 2008a), Štys (1970, 1974, 1982, 1983a, 1983b, 1985), Wygodzinsky (1962)
			Genital capsule	China (1946), Emsley (1969), Esaki & Miyamoto (1959), Hill (1980, 1984, 1987b, 2004, 2013), Miyamoto (1964), Rédei (2007), Rédei *et al.* (2012), Wygodzinsky (1948b, 1960)
			Hypopygium	Linnavuori (1974), McAtee and Malloch (1925), Wygodzinsky (1948a, 1948a, 1953, 1960)
Sclerite of phallosoma	sph			
Segment	s			
Sternum	st		Sternum	Emsley (1969), Hill (1980, 1984), Štys (1985)
			Sternite	China (1946),

				Wygodzinsky (1948b, 1950a, 1950b, 1962) and elsewhere
			Ventrite	China (1946), Štys (1974, 1977, 1982, 1983a, 1983b)
			Zygosternum	Carpintero and Dellapé (2006), Štys (1958, 1959, 1970)
Subgenital plate	st7	Enlarged sternum 7	Subgenital plate	Štys (1958, 1970, 1985)
			Seventh sternite	Wygodzinsky (1948b, 1960)
			Seventh ventrite	China (1946)
			Sternum 7	Štys (1985)
Ventral sclerite of phallosoma	vph			
Vesica	v	Apical portion of aedeagus	Vesica	Carpintero and Dellapé (2006), Carvalho (1989), China (1946), Emsley (1969), Gross (1951), Hill (1980, 1984, 1987a, 1987b, 2004, 2013), Rédei (2008a), Wygodzinsky (1948a, 1948b, 1950a, 1950b, 1953, 1960)
			Penis	Esaki and Miyamoto (1959), Miyamoto (1960)
			Processus gonopori	Carpintero and Dellapé (2006), Rédei (2007), Štys (1970, 1974, 1977, 1982, 1983a, 1983b, 1985)
Vesical process	vp	Cuticular outgrowth on the side of vesica	Vesical process	Hill (1987b, 2013)
			Vesical branch	Hill (2004)

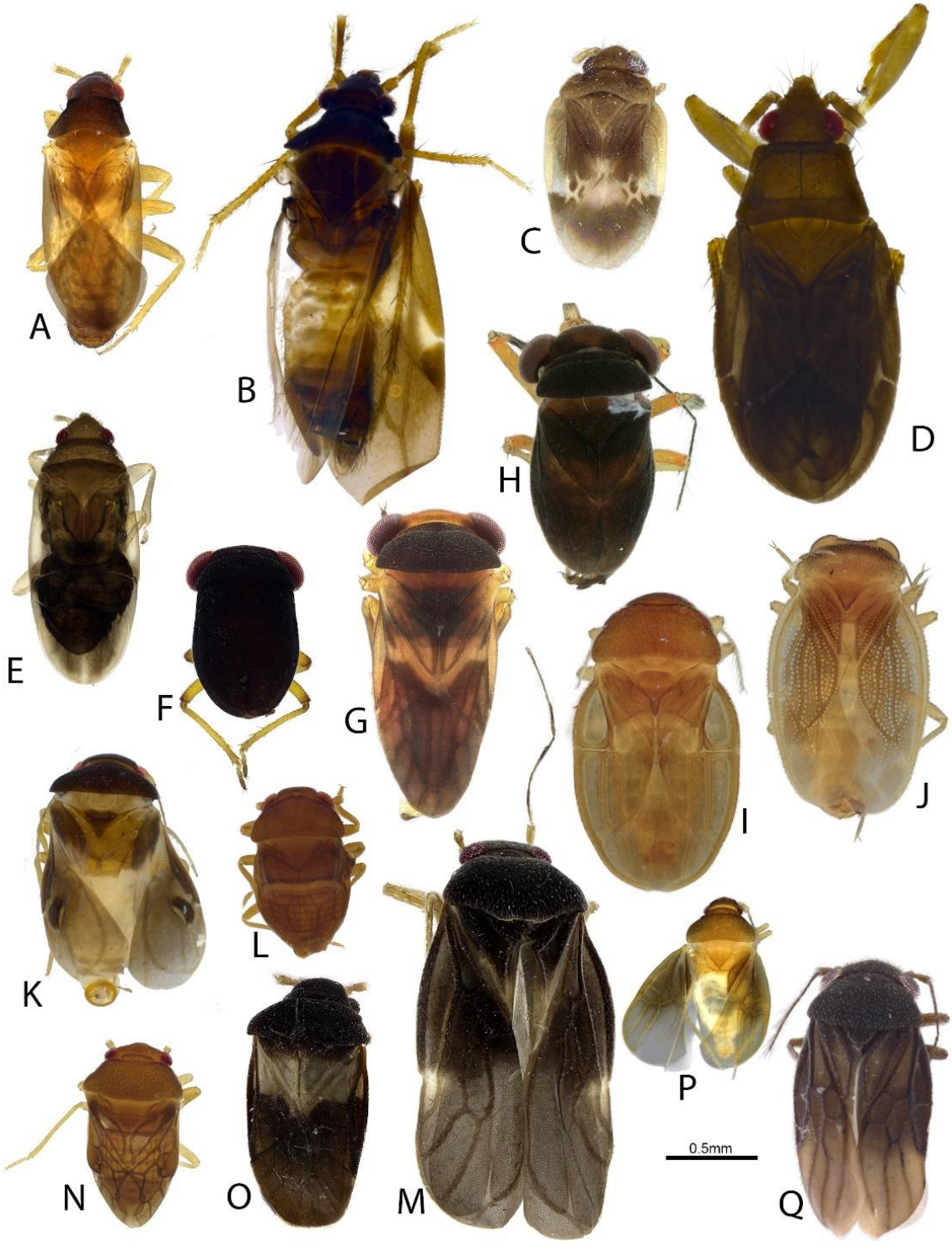
A
B
C
D
E
F
G
H
I
J
K
L
M
N
O
P
Q
0.5mm

Figure 5.1. Dorsal habitus of representatives of genera included in this study. A-D. Ceratocombidae. A. *Ceratocombus* sp. B. *Leptonannus* sp. C. *Muatianvuaia* sp. D. *Trichotonannus* sp. E. Dipsocoridae, *Cryptostemma* sp. F-H. Schizopteridae: Hypselosomatinae. F. *Hypselosoma* sp. G. *Rectilamina* sp. H. *Williamsocoris* sp. I-J. Schizopteridae incertae sedis. I. *Guapinannus* sp. J. *Peloridinannus moe*. K-O. Schizopteridae: Ogeriinae. K. *Chinannus trinitatis*. L. *Kaimon* sp. M. *Meganannus lewisi*. N. *Ogeria* sp. O. Undescribed genus 2. P-Q. Schizopteridae: Schizopterinae. P. *Ceratocomboides* sp. Q. *Corixidea major*.

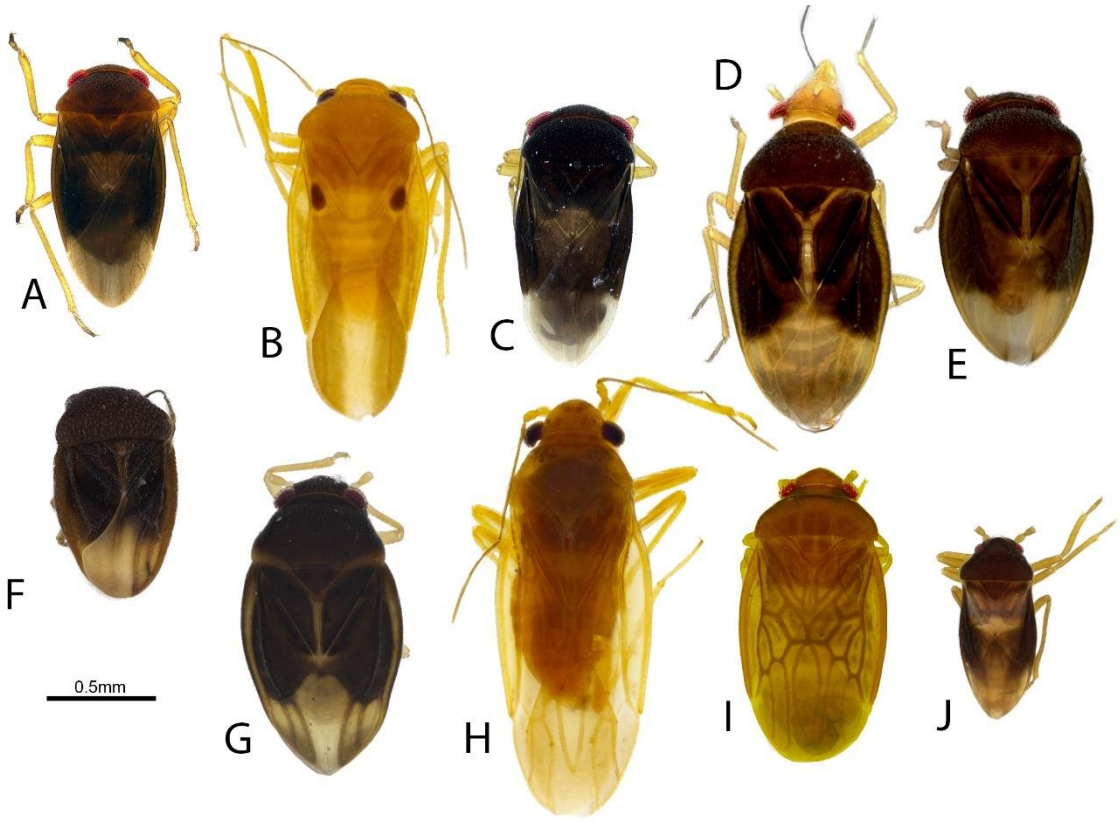

Figure 5.2. Dorsal habitus of representatives of genera included in this study (Schizopteridae: Schizopterinae). A. *Dundonannus*. B. *Machadonannus brailovskyi*. C. *Membracioides* sp. D. *Nannocoris* sp. E. *Pinochius* sp. F. *Ptenidiophyes* sp. G. *Schizoptera* sp. H. *Vilhenannus* sp. I. Undescribed genus 3. J. Undescribed genus 4.

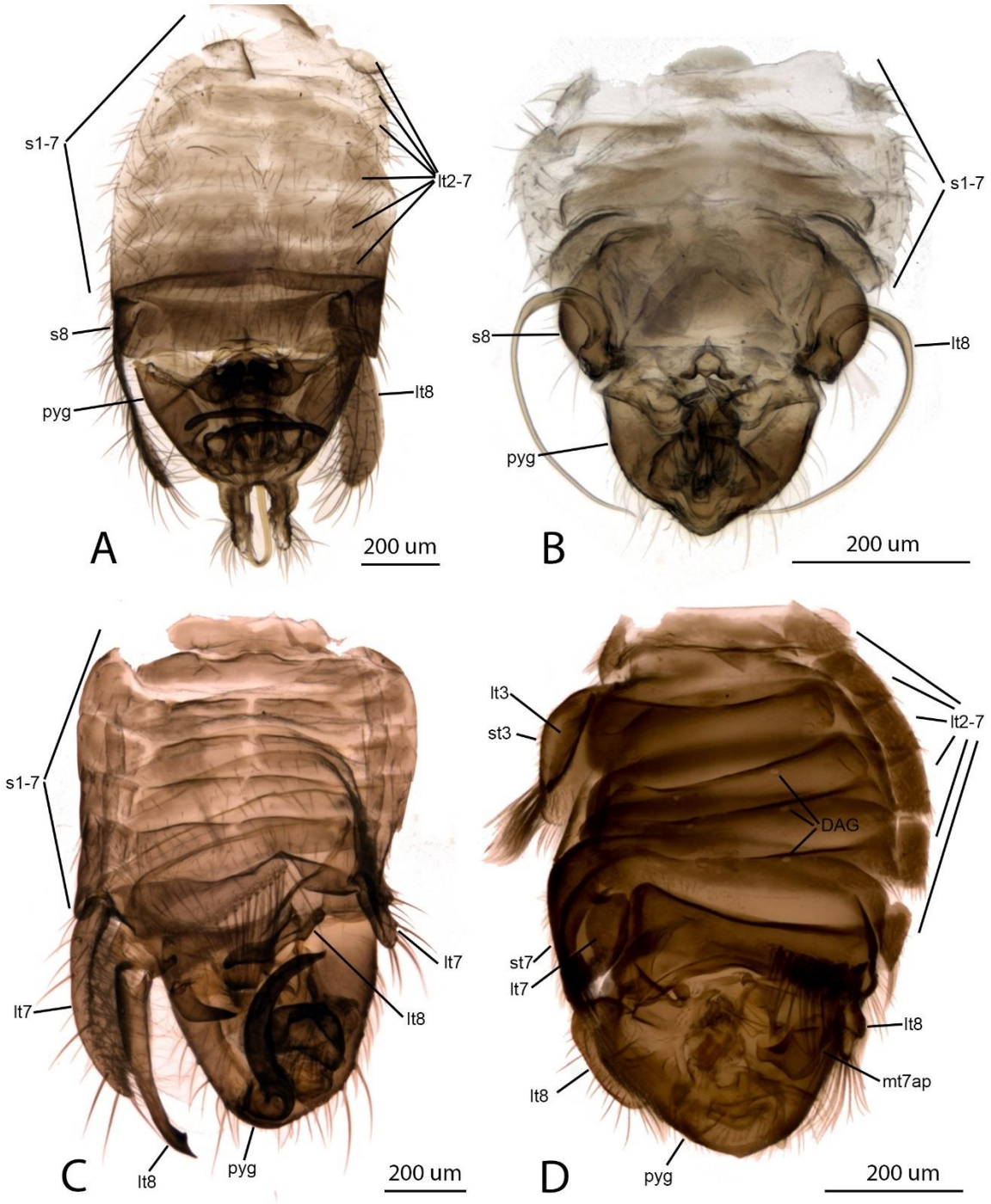

Figure 5.3. Dorsal habitus of male abdomen. A-C. Ceratocombidae. A. *Leptonannus* sp. B. *Muatianvuaia* sp. C. *Trichotonannus* sp. D. Dipsocoridae, *Cryptostemma* sp. Abbreviations: DAG – dorsal abdominal gland orifices, lt – laterotergite, mt7ap – appendage of mediotergite 7, pyg – pygophore, s – segment, st – sternum.

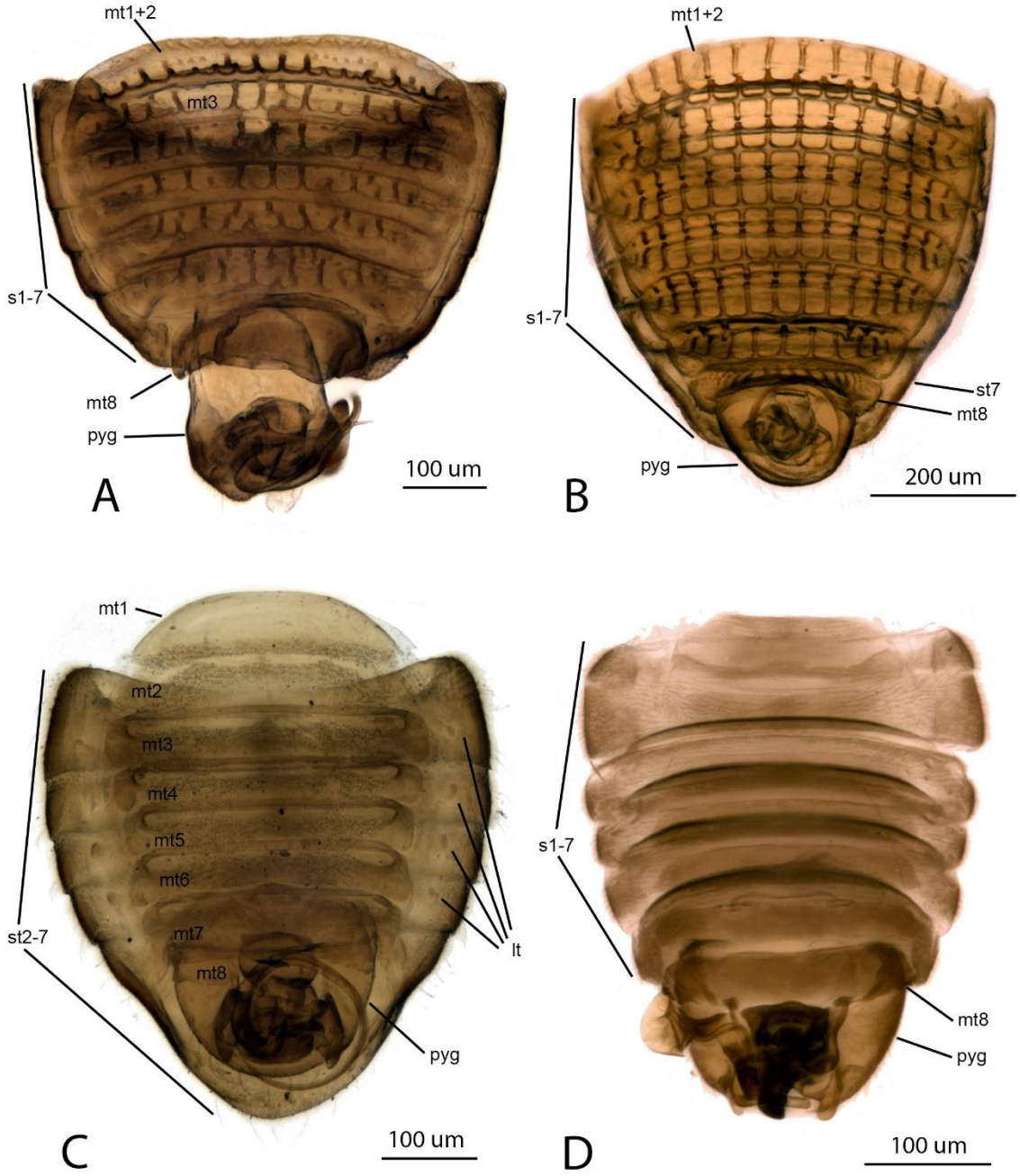

Figure 5.4. Dorsal habitus of male abdomen (Schizopteridae: Ogeriinae). A. *Kaimon* sp. B. *Ogeria* sp. C. Undescribed genus 1. D. Undescribed genus 2. Abbreviations: lt – laterotergite, mt – mediotergite, pyg – pygophore, s – segment, st – sternum.

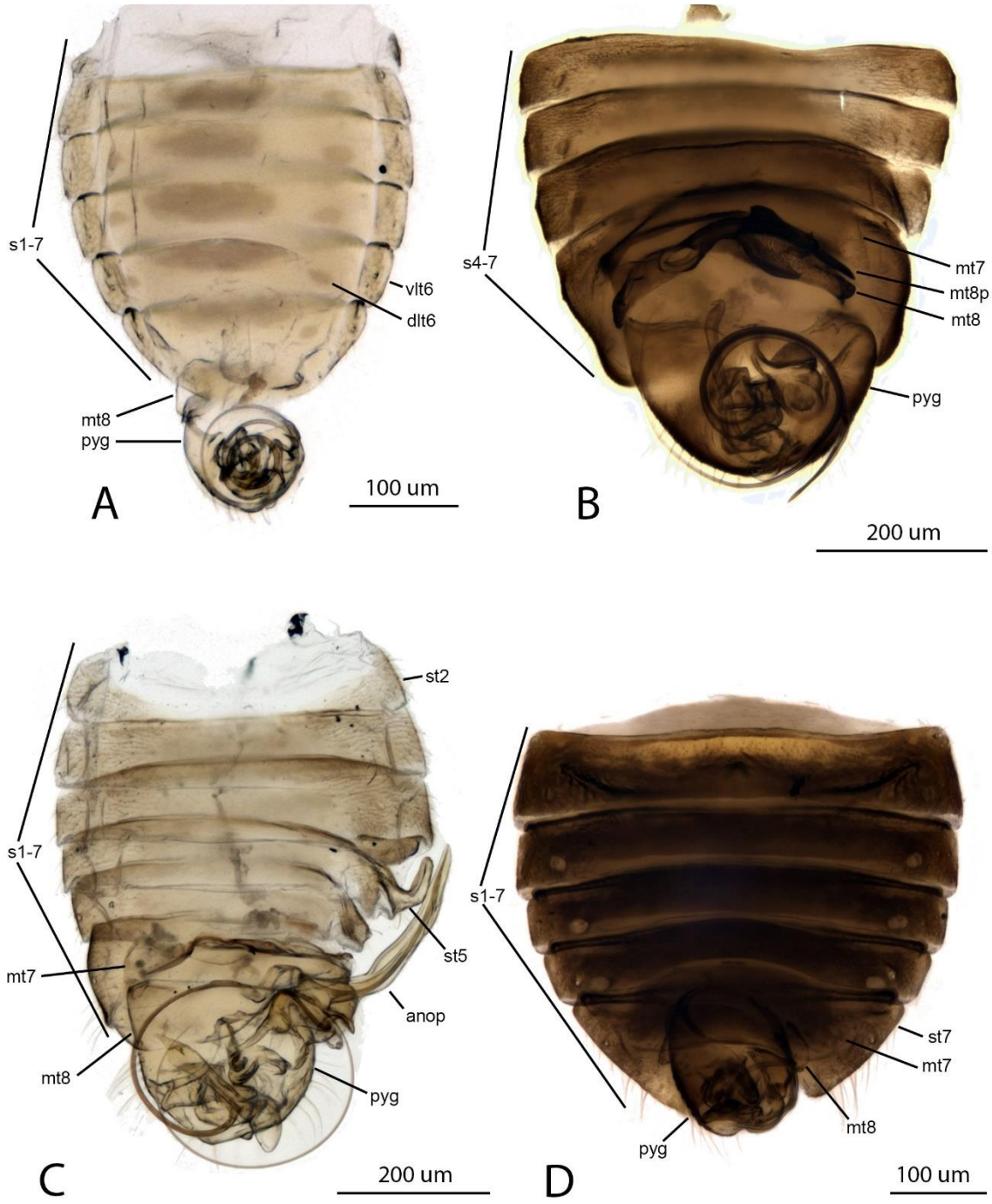

Figure 5.5. Dorsal habitus of male abdomen (Schizopteridae: Schizopterinae). A. *Ceratocomboides* sp. B. *Corixidea major*. C. *Machadonannus brailovskyi*. D. *Ptenidiophyes* sp. Abbreviations: anop – anophoric process, dlt – dorsal laterotergite, mt – mediotergite, mt8p – process of mediotergite 8, pyg – pygophore, s – segment, st – sternum, vlt – ventral laterotergite.

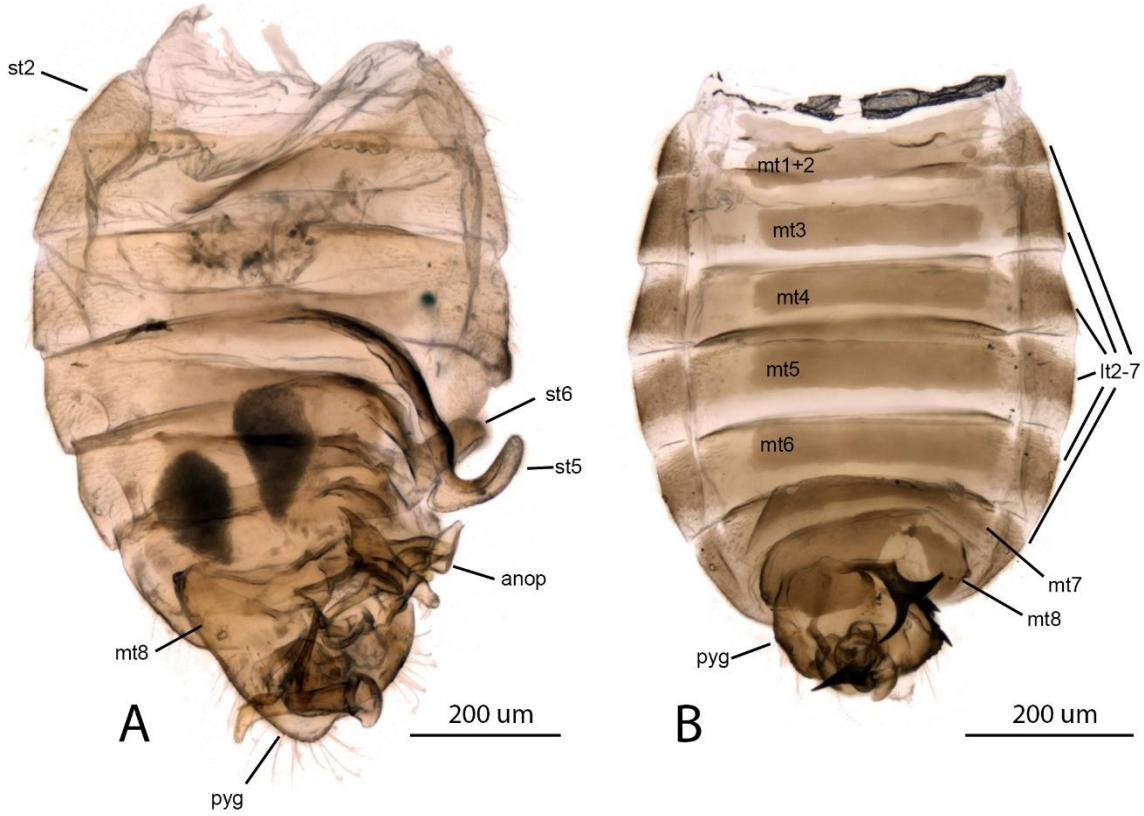

Figure 5.6. Dorsal habitus of male abdomen (Schizopteridae: Schizopterinae) A. *Vilhenannus* sp. B. Undescribed genus 3. Abbreviations: anop – anophoric process, lt – laterotergite, mt – mediotergite, pyg – pygophore, st – sternum.

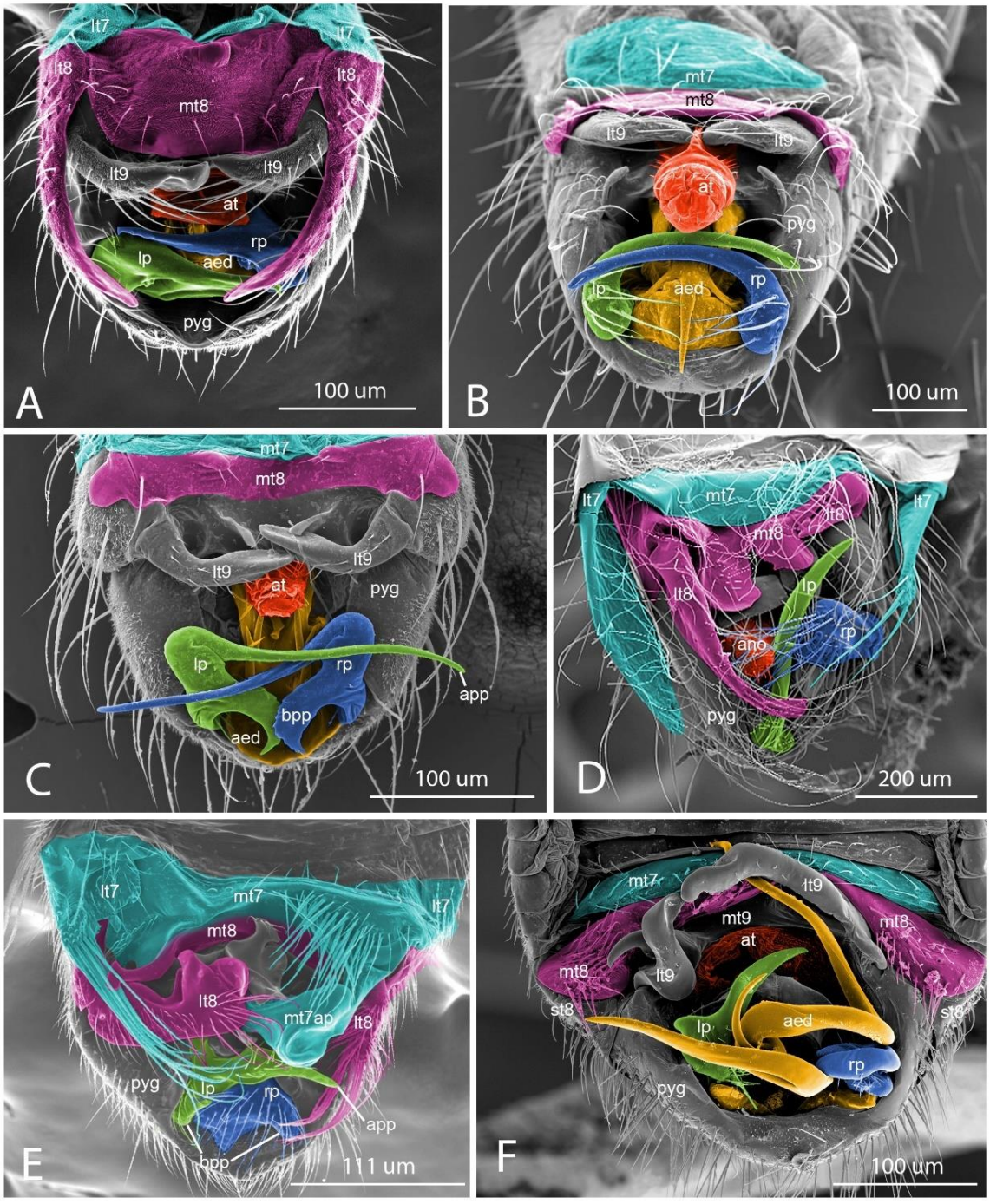
lt7
lt8
mt8
lt9
at
rp
lp
aed
pyg
100 um
A
B
mt7
ano
app
bpp
200 um
C
D
mt9
st8
111 um
E
F

Figure 5.7. Scanning electron micrographs of genitalia. A-D. Ceratocombidae. A. *Ceratocombus* sp. B. *Leptonannus* sp. C. *Kvamula* sp. D. *Trichotonannus* sp. E. Dipsocoridae, *Cryptostemma* sp. F. Schizopteridae: Hypselosomatinae, *Hypselosoma* sp. Abbreviations: aed – aedeagus, ano – anophore, app – apical process of paramere, at – anal tube, bpp – basal process of paramere, lp – left paramere, lt – laterotergite, mt – mediotergite, mt7ap – appendage of mediotergite 7, pyg – pygophore, rp – right paramere, st – sternum.

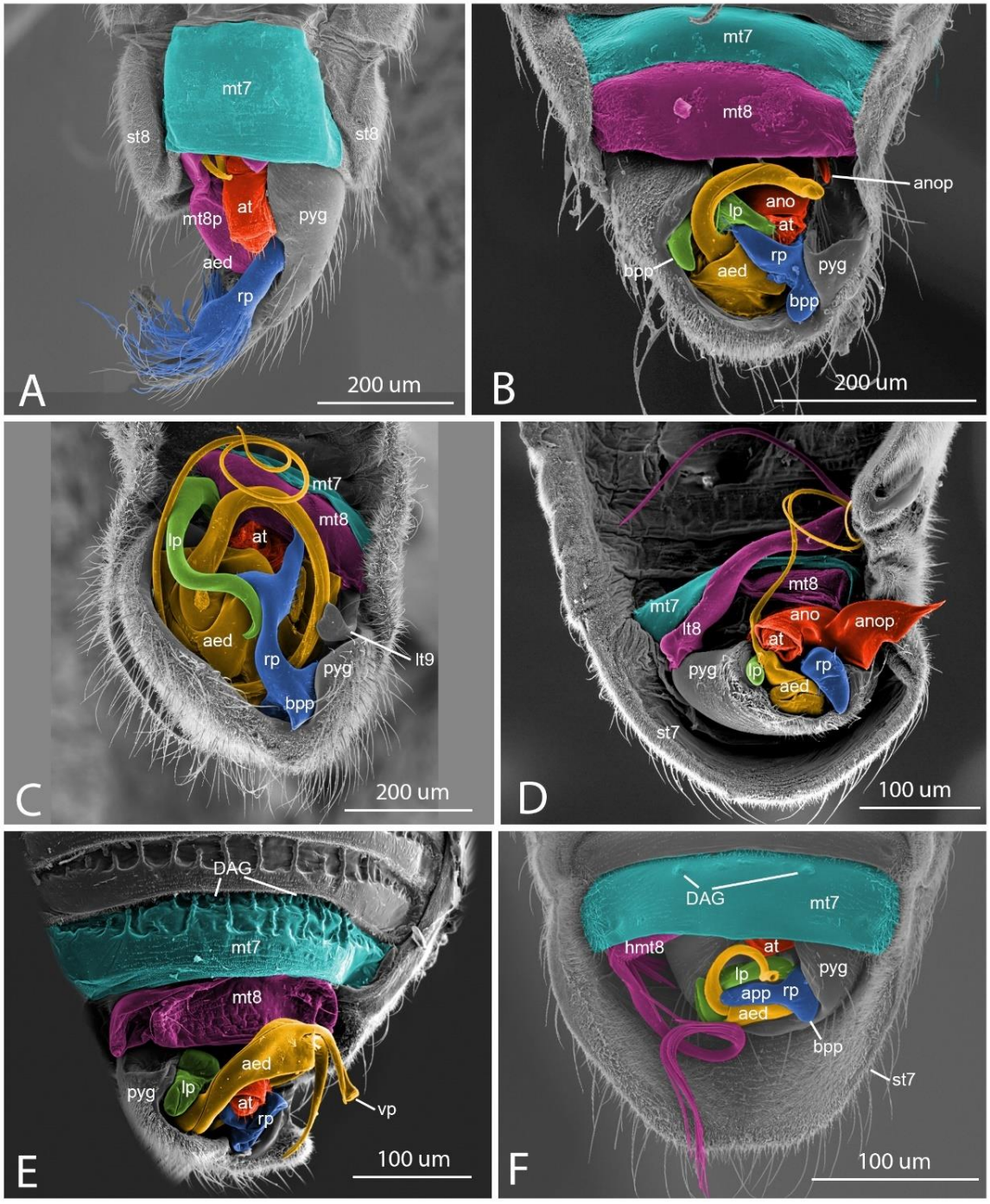
mt7
st8
st8
at
mt8p
pyg
aed
rp
A
200 um
mt7
mt8
anop
ano
lp
at
rp
bpp
aed
pyg
bpp
B
200 um
mt7
mt8
lp
at
aed
rp
pyg
lt9
bpp
C
200 um
mt8
mt7
lt8
ano
anop
at
pyg
lp
rp
aed
st7
D
100 um
DAG
mt7
mt7
mt8
aed
pyg
lp
at
rp
vp
E
100 um
DAG
mt7
hmt8
at
lp
pyg
app
rp
aed
bpp
st7
F
100 um

Figure 5.8. Scanning electron micrographs of genitalia (Schizopteridae). A. Hypselosomatinae, *Rectilamina* sp. B-C. Schizopteridae incertae sedis. B. *Guapinannus* sp. C. *Peloridinannus sinefenestra*. D-F. Ogeriinae. D. *Chinannus bierigi*. E. *Kaimon* sp. F. *Kokeshia* sp. Abbreviations: aed – aedeagus, ano – anophore, anop – anophoric process, app – apical process of paramere, at – anal tube, bpp – basal process of paramere, DAG – dorsal abdominal gland orifices, hmt – hemitergite, lp – left paramere, lt – laterotergite, mt – mediotergite, mt8p – process of mediotergite 8, pyg – pygophore, rp – right paramere, st – sternum, vp – vesical process.

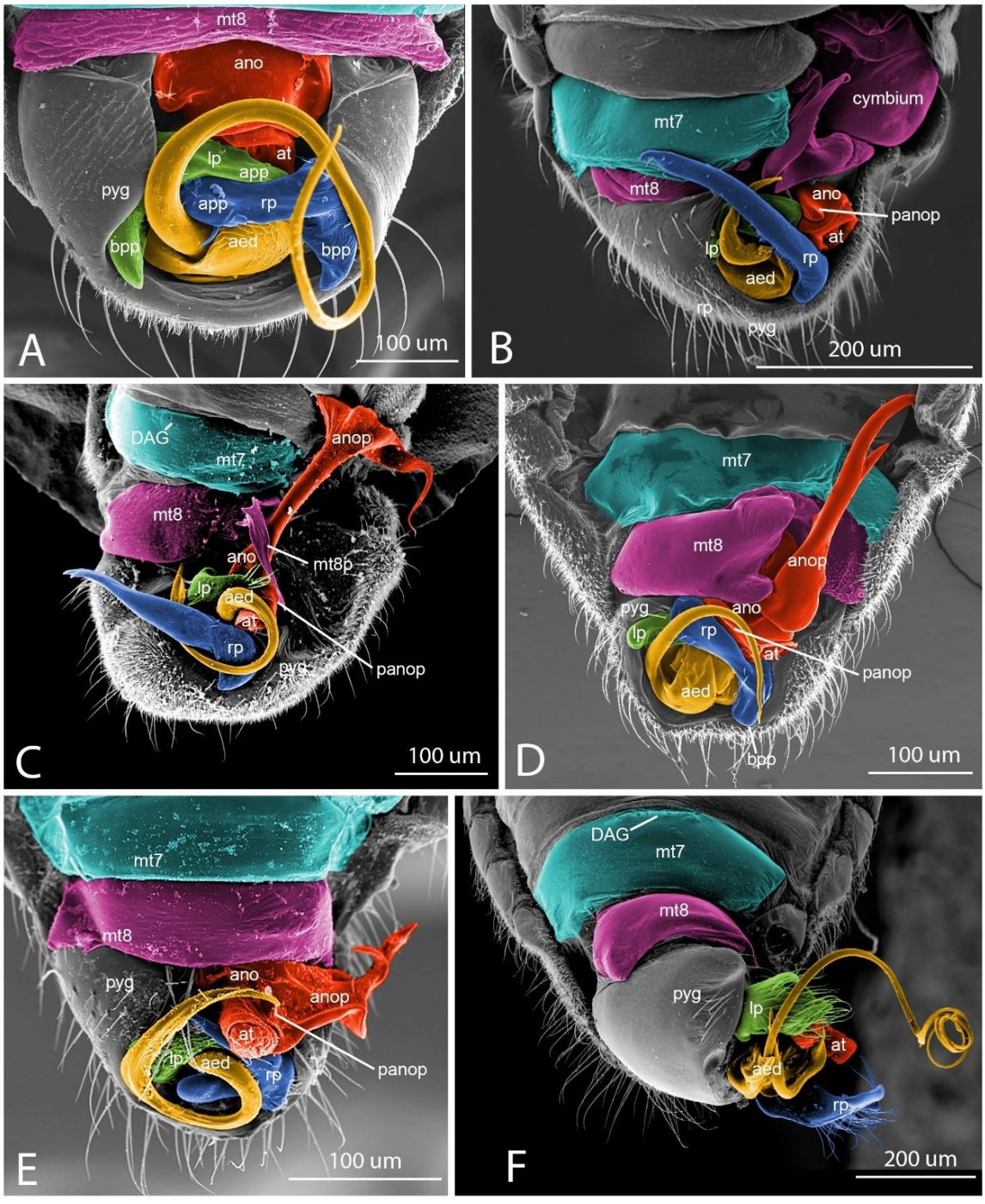
mt8
ano
lp
at
app
pyg
app
rp
bpp
aed
bpp
A
100 um
mt7
cymbium
mt8
ano
panop
at
lp
rp
aed
rp
pyg
B
200 um
DAG
mt7
anop
mt8
ano
mt8p
lp
aed
at
rp
pyg
panop
C
100 um
mt7
mt8
anop
pyg
ano
lp
rp
at
panop
aed
bpp
D
100 um
mt7
mt8
pyg
ano
anop
at
lp
aed
rp
panop
E
100 um
DAG
mt7
mt8
pyg
lp
at
aed
rp
F
200 um

Figure 5.9. Scanning electron micrographs of genitalia (Schizopteridae). A. Ogeriinae, Undescribed genus 1. B-F. Schizopterinae. B. *Dundonannus* sp. C. *Hoplonannus* sp. D. *Nannocoris* sp. E. *Pinochius* sp. F. *Schizoptera* (*Cantharocoris*) sp. Abbreviations: aed – aedeagus, ano – anophore, anop – anophoric process, app – apical process of paramere, at – anal tube, bpp – basal process of paramere, DAG – dorsal abdominal gland orifices, lp – left paramere, mt – mediotergite, mt8p – process of mediotergite 8, panop – posterior anophoric process, pyg – pygophore, rp – right paramere, vp – vesical process.

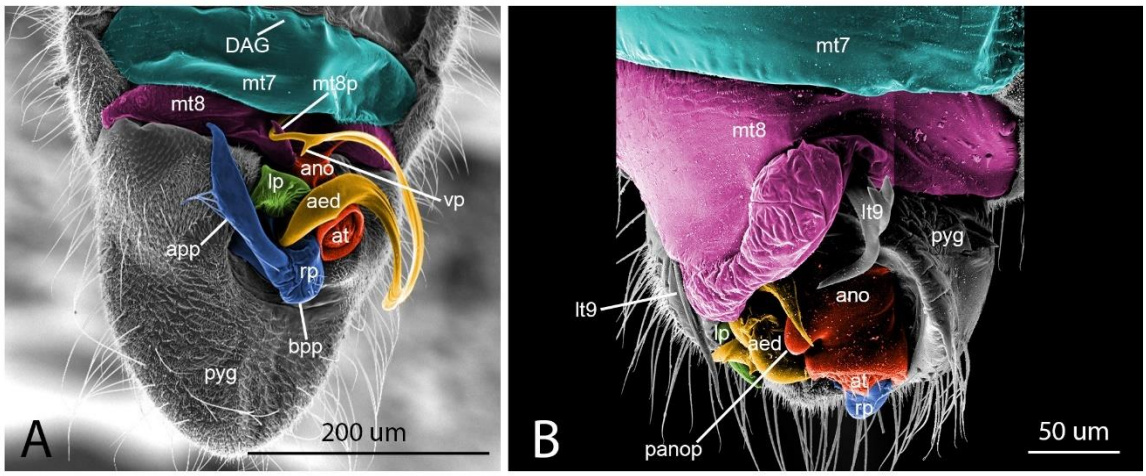

Figure 5.10. Scanning electron micrographs of genitalia (Schizopteridae: Schizopterinae). A. *Voragocoris schuhi*. B. Undescribed genus 3. Abbreviations: aed – aedeagus, ano – anophore, app – apical process of paramere, at – anal tube, bpp – basal process of paramere, DAG – dorsal abdominal gland orifices, lp – left paramere, lt – laterotergite, mt – mediotergite, mt8p – process of mediotergite 8, panop – posterior anophoric process, pyg – pygophore, rp – right paramere, vp – vesical process.

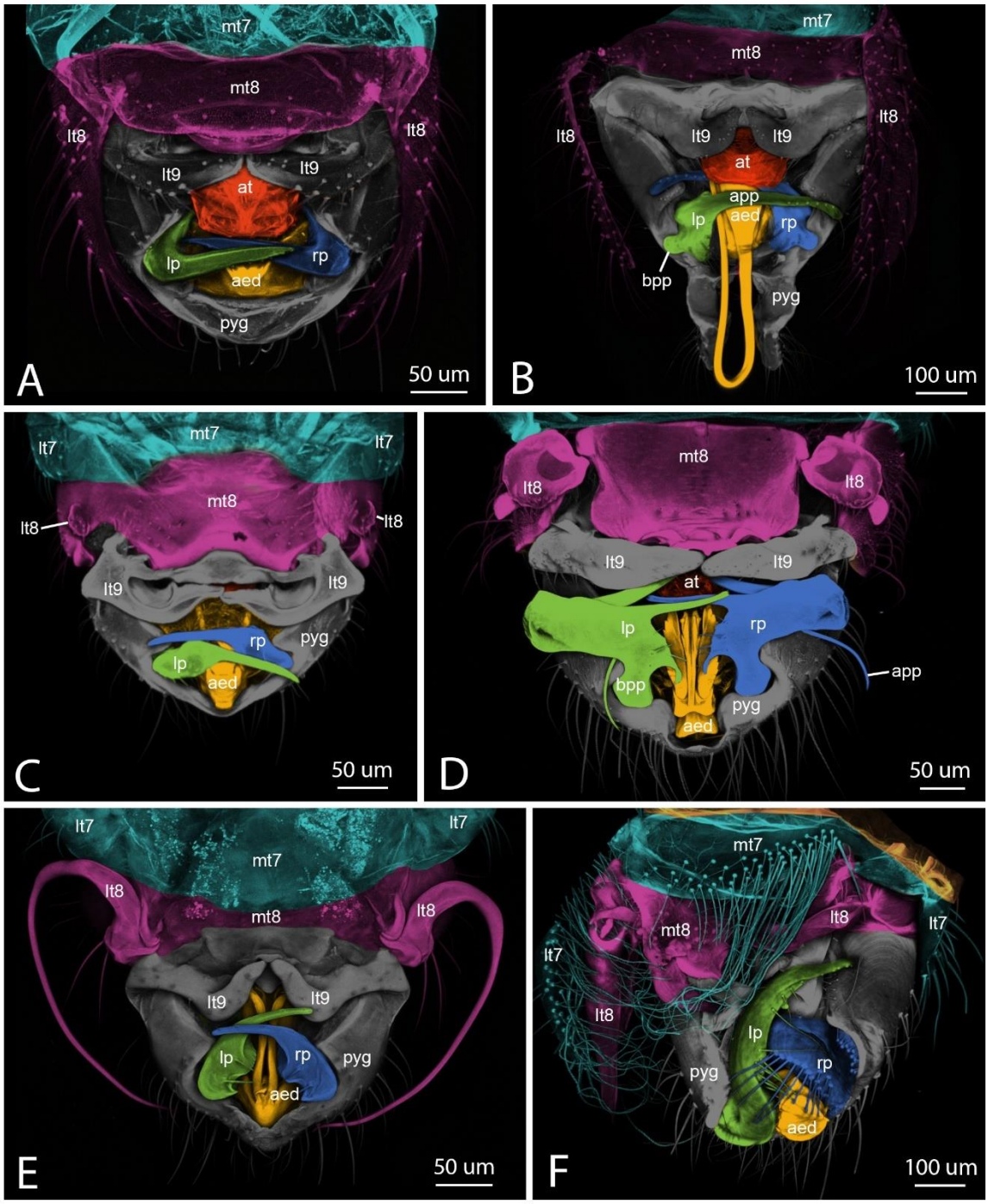

Figure 5.11. Confocal micrographs of genitalia (Ceratocombidae). A. *Ceratocombus* sp. B. *Leptonannus* sp. C. *Kvamula* sp. D-E. *Muatianvuaia* sp. F. *Trichotonannus* sp. Abbreviations: aed – aedeagus, app – apical process of paramere, at – anal tube, bpp – basal process of paramere, lp – left paramere, lt – laterotergite, mt – mediotergite, pyg – pygophore, rp – right paramere, st – sternum.

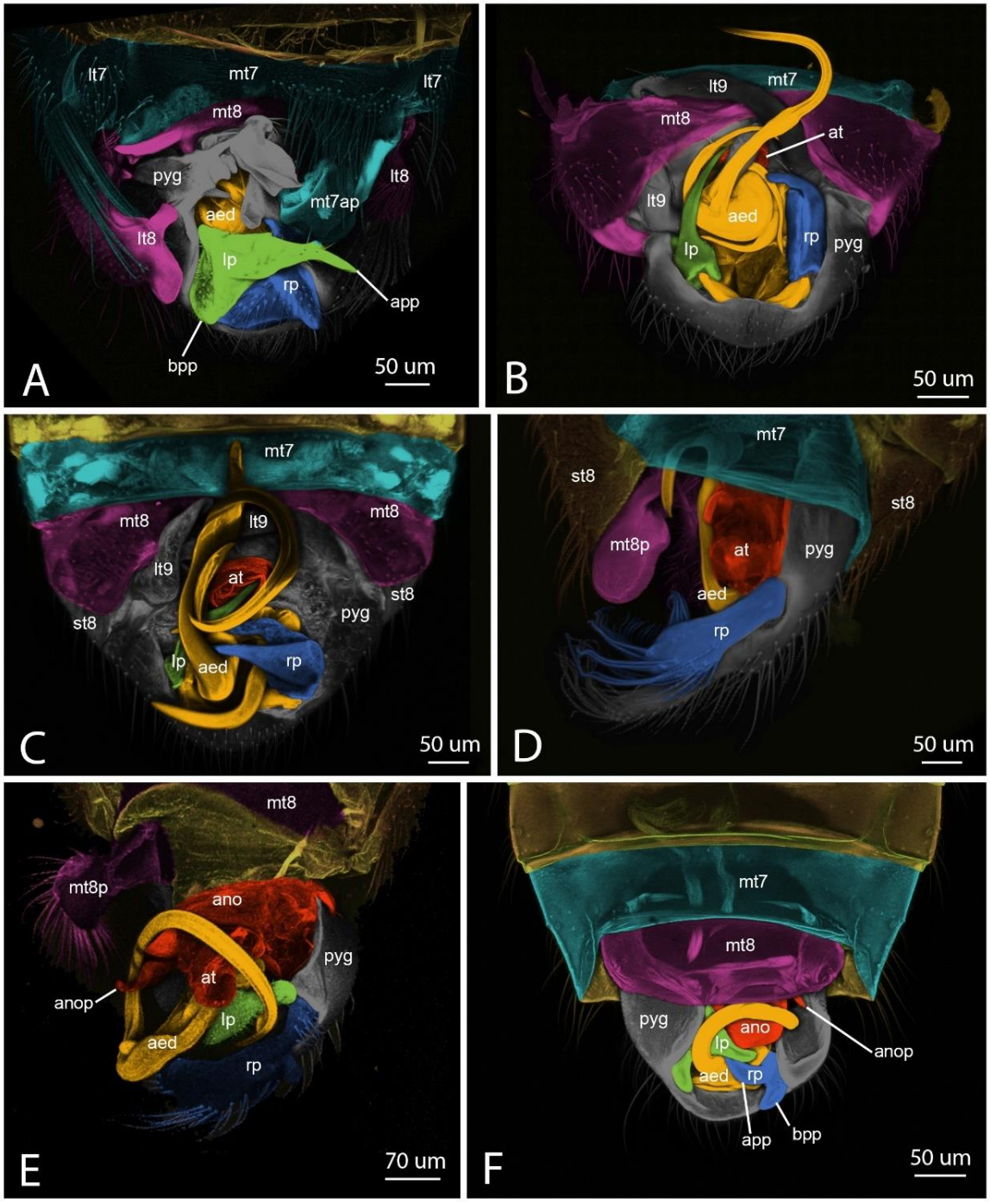
lt7
mt7
lt7
mt8
pyg
lt8
mt7ap
aed
lt8
lp
rp
app
bpp
A
50 um
lt9
mt7
mt8
at
lt9
aed
rp
pyg
lp
B
50 um
mt7
mt8
lt9
mt8
lt9
at
st8
st8
pyg
lp
aed
rp
C
50 um
mt7
st8
st8
mt8p
at
pyg
aed
rp
D
50 um
mt8
mt8p
ano
pyg
at
anop
lp
aed
rp
E
70 um
mt7
mt8
pyg
ano
lp
anop
aed
rp
app
bpp
F
50 um

Figure 5.12. Confocal micrographs of genitalia. A. Dipsocoridae, *Cryptostemma* sp. B-E. Schizopteridae: Hypselosomatinae. B. *Hypselosoma* sp. C. *Hypselosoma haplacanthatum*. D. *Rectilamina* sp. E. *Williamsocoris* sp. F. Schizopteridae incertae sedis, *Guapinannus* sp. Abbreviations: aed – aedeagus, ano – anophore, anop – anophoric process, app – apical process of paramere, at – anal tube, bpp – basal process of paramere, lp – left paramere, lt – laterotergite, mt – mediotergite, mt7ap – appendage of mediotergite 7, mt8p – process of mediotergite 8, pyg – pygophore, rp – right paramere, st – sternum.

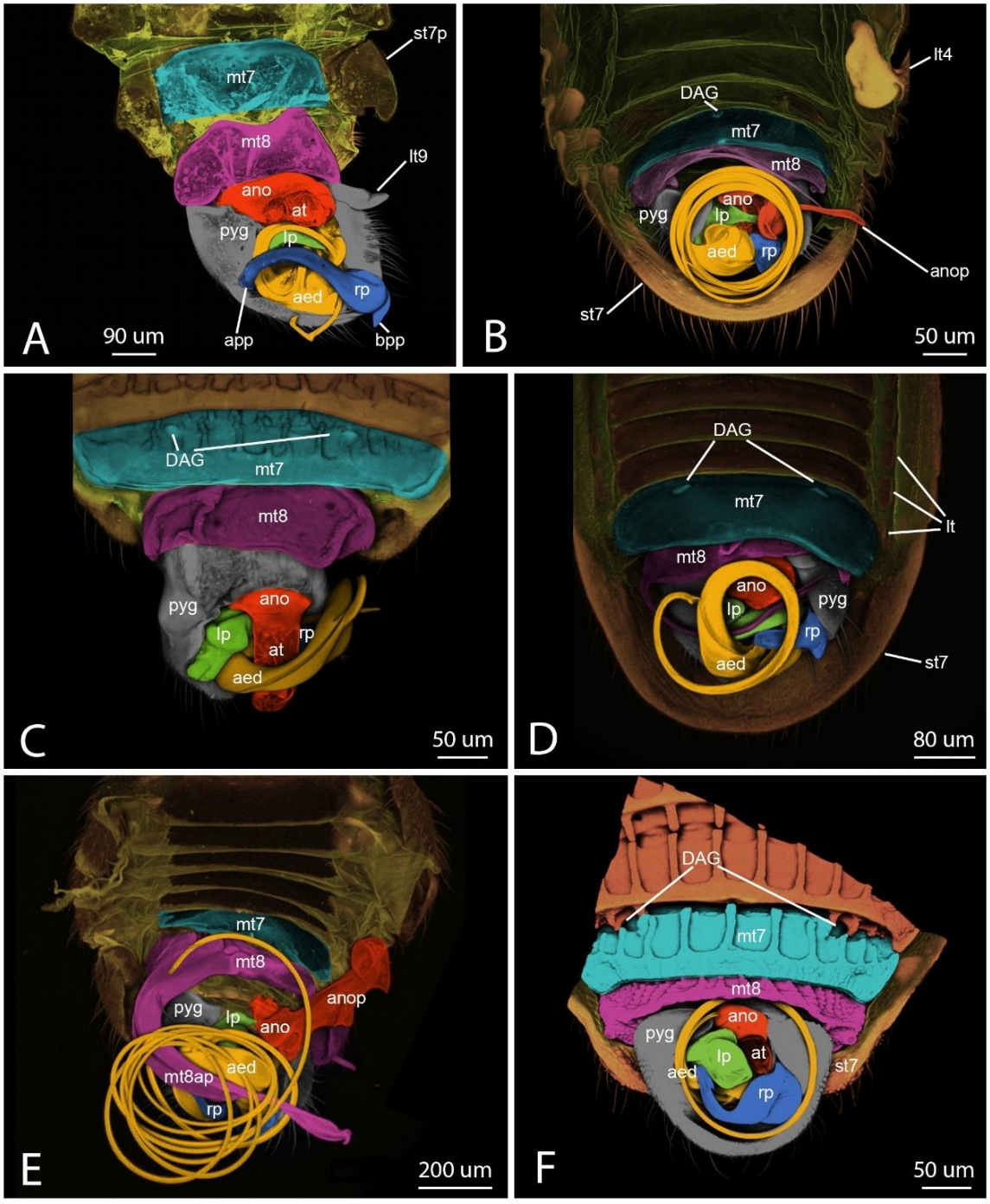
st7p
mt7
mt8
lt9
ano
at
pyg
lp
aed
rp
app
bpp
A
90 um
lt4
DAG
mt7
mt8
ano
lp
pyg
aed
rp
anop
st7
B
50 um
DAG
mt7
mt8
pyg
ano
lp
rp
at
aed
C
50 um
DAG
mt7
lt
mt8
ano
lp
pyg
rp
aed
st7
D
80 um
mt7
mt8
anop
pyg
lp
ano
mt8ap
aed
rp
E
200 um
DAG
mt7
mt8
ano
pyg
lp
at
aed
st7
rp
F
50 um

Figure 5.13. Confocal micrographs of genitalia (Schizopteridae). A. Schizopteridae incertae sedis, *Peloridinannus moe*. B-F. Ogeriinae. B. *Chinannus trinitatis*. C. *Kaimon* sp. D. *Kokeshia* sp. E. *Meganannus lewisi*. F. *Ogeria* sp. Abbreviations: aed – aedeagus, ano – anophore, anop – anophoric process, app – apical process of paramere, at – anal tube, bpp – basal process of paramere, DAG – dorsal abdominal gland orifices, lp – left paramere, lt – laterotergite, mt – mediotergite, mt8ap – appendage of mediotergite 8, pyg – pygophore, rp – right paramere, st – sternum, st7p – process of sternum 7.

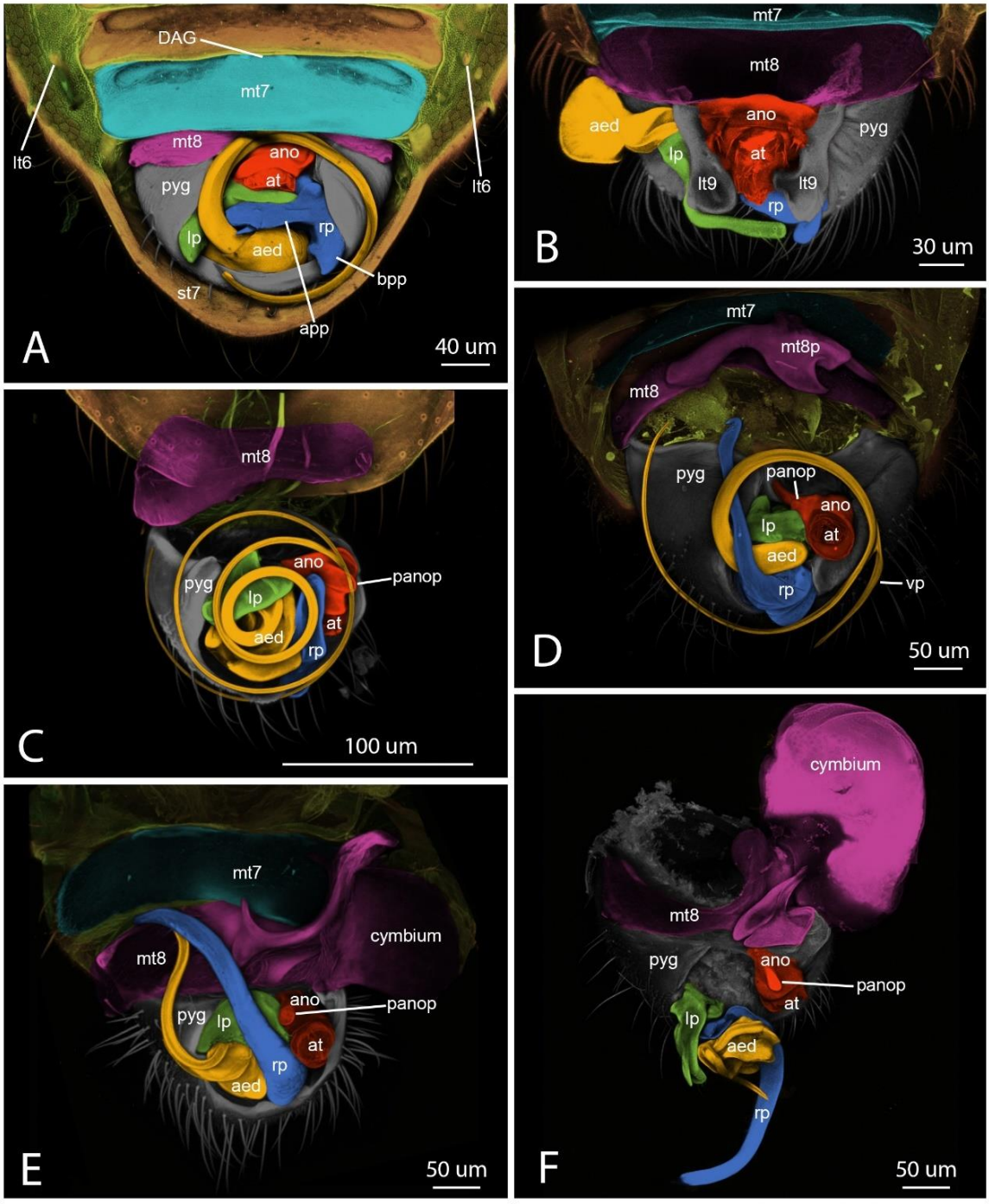
DAG
mt7
lt6
lt6
mt8
ano
at
pyg
lp
rp
aed
bpp
st7
app
A
40 um
mt7
mt8
aed
ano
pyg
lp
at
lt9
lt9
rp
B
30 um
mt8
ano
panop
pyg
lp
at
aed
rp
C
100 um
mt7
mt8p
mt8
pyg
panop
ano
lp
at
aed
rp
vp
D
50 um
mt7
cymbium
mt8
pyg
ano
panop
lp
at
aed
rp
E
50 um
cymbium
mt8
pyg
ano
panop
at
lp
aed
rp
F
50 um

Figure 5.14. Confocal micrographs of genitalia (Schizopteridae). A-B. Ogeriinae. A. Undescribed genus 1. B. Undescribed genus 2. C-F. Schizopterinae. C. *Ceratocomboides* sp. D. *Corixidea major*. E-F. *Dundonannus* sp. Abbreviations: aed – aedeagus, ano – anophore, app – apical process of paramere, at – anal tube, bpp – basal process of paramere, DAG – dorsal abdominal gland orifices, lp – left paramere, lt – laterotergite, mt – mediotergite, mt8p – process of mediotergite 8, panop – posterior anophoric process, pyg – pygophore, rp – right paramere, st – sternum, vp – vesical process.

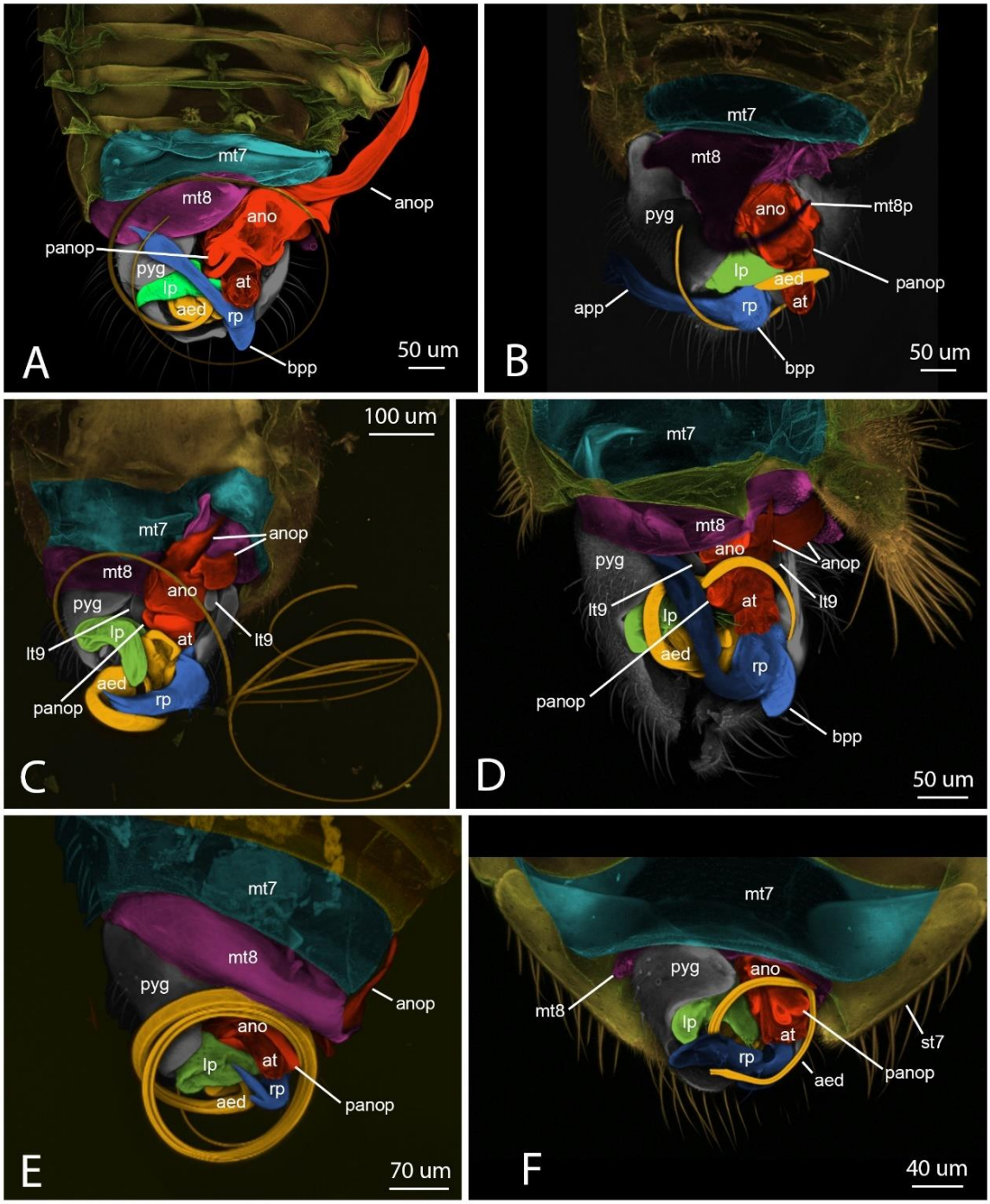
A
mt7
mt8
ano
anop
panop
pyg
lp
at
aed
rp
bpp
50 um
B
mt7
mt8
pyg
ano
mt8p
lp
aed
panop
app
rp
at
bpp
50 um
C
100 um
mt7
anop
mt8
ano
pyg
lp
at
lt9
lt9
aed
panop
rp
D
mt7
mt8
ano
anop
pyg
lt9
at
lt9
lp
aed
rp
panop
bpp
50 um
E
mt7
mt8
pyg
anop
ano
lp
at
rp
aed
panop
70 um
F
mt7
pyg
ano
mt8
lp
at
st7
rp
aed
panop
40 um

Figure 5.15. Confocal micrographs of genitalia (Schizopteridae: Schizopterinae). A. *Machadonannus brailovskyi*. B. *Membracioides* sp. C-D. *Nannocoris* sp. E. *Pinochius* sp. F. *Ptenidiophyes* sp. Abbreviations: aed – aedeagus, ano – anophore, anop – (anterior) anophoric process, app – apical process of paramere, at – anal tube, bpp – basal process of paramere, lp – left paramere, lt – laterotergite, mt – mediotergite, mt8p – process of mediotergite 8, panop – posterior anophoric process, pyg – pygophore, rp – right paramere, st – sternum, vp – vesical process.

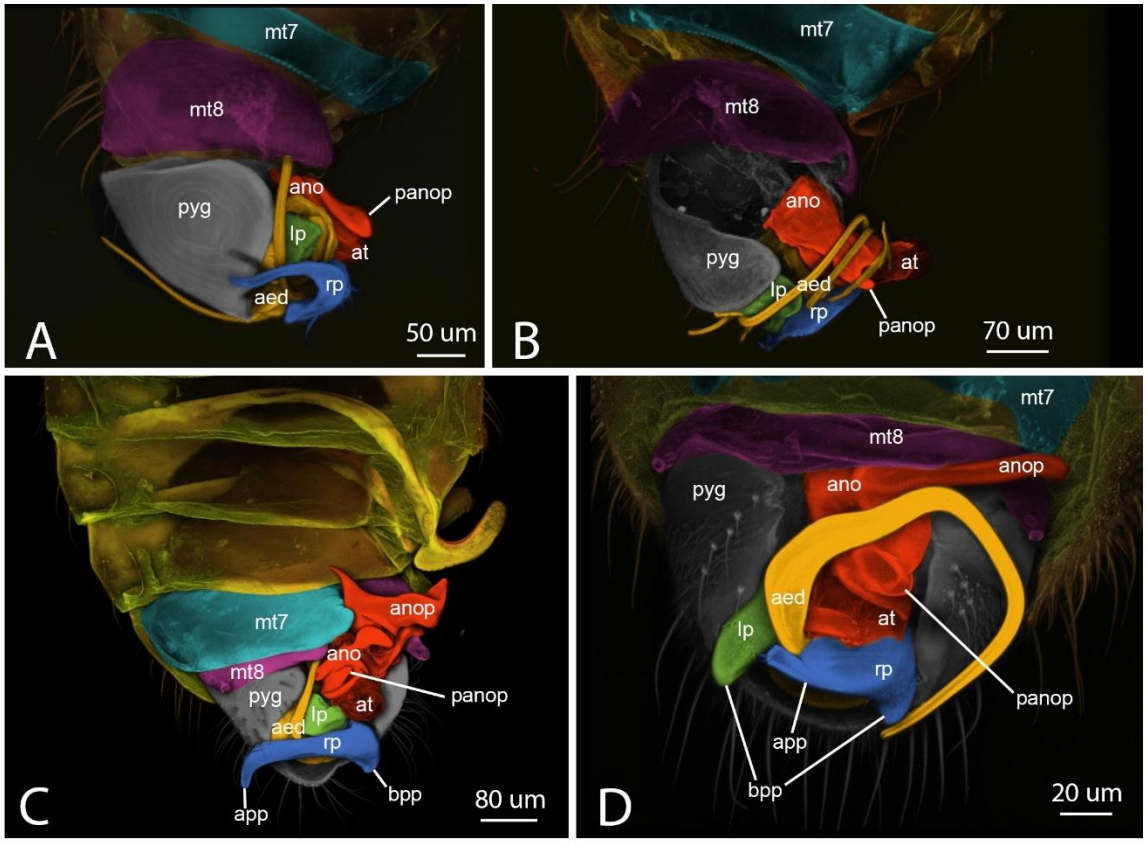

Figure 5.16. Confocal micrographs of genitalia (Schizopteridae: Schizopterinae). A. *Schizoptera* (*Odontorhagus*) sp. B. *Schizoptera* (*Schizoptera*) sp. C. *Vilhenannus* sp. D. Undescribed genus 4. Abbreviations: aed – aedeagus, ano – anophore, anop – (anterior) anophoric process, app – apical process of paramere, at – anal tube, bpp – basal process of paramere, lp – left paramere, mt – mediotergite, panop – posterior anophoric process, pyg – pygophore, rp – right paramere.

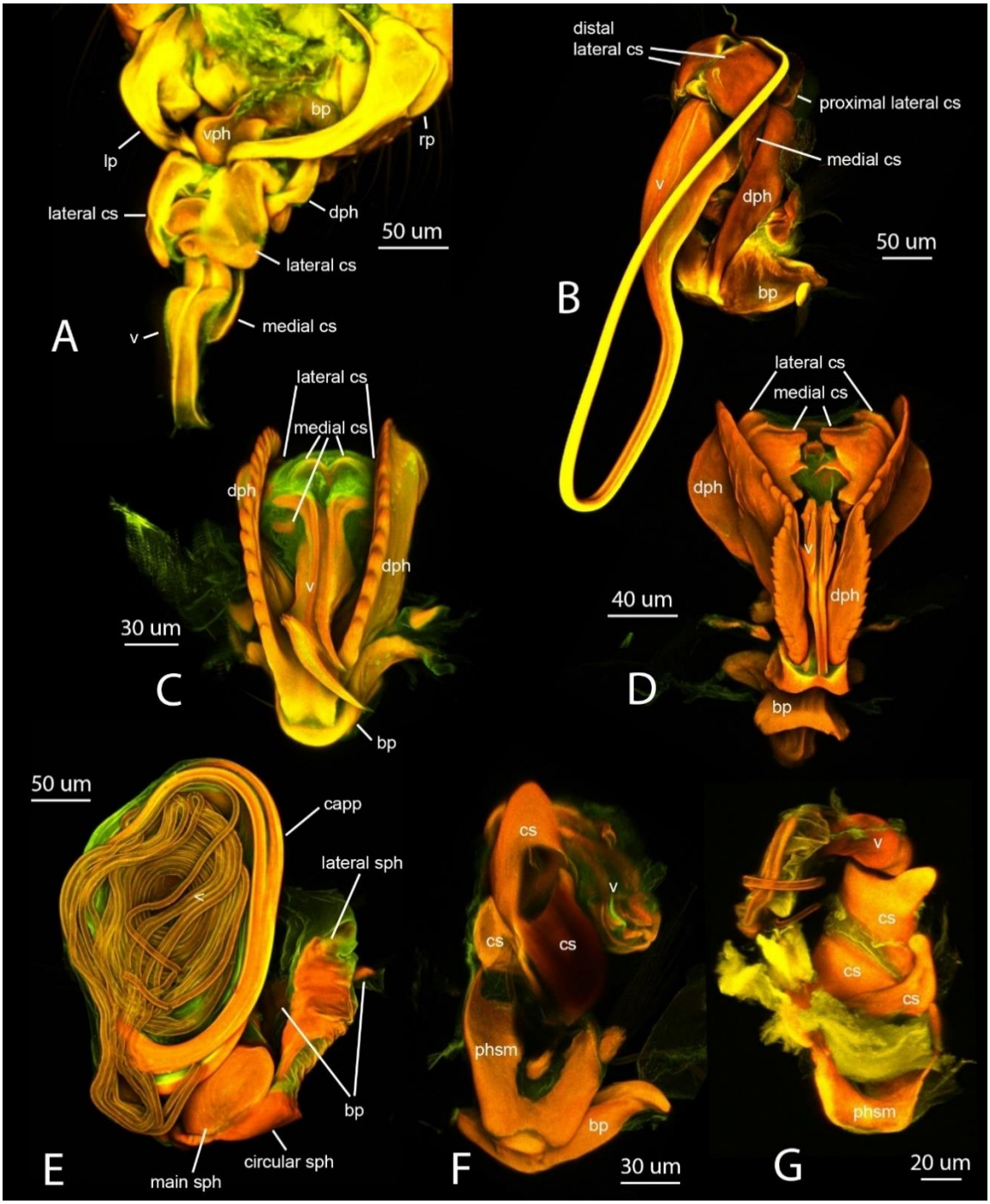

Figure 5.17. Confocal micrographs of aedeagus, dorsal view. A-E. Ceratocombidae. A. *Ceratocombus* sp. B. *Leptonannus* sp. C. *Kvamula* sp. D. *Muatianvuaia* sp. E. *Trichotonannus* sp. F-G. Dipsocoridae, *Cryptostemma* sp. Abbreviations: bp – basal plates, capp – conjunctival appendage, cs – conjunctival sclerite, dph – dorsal sclerite of phallosoma, lp – left paramere, phsm – phallosoma, rp – right paramere, sph – sclerite of phallosoma, v – vesica, vph – ventral sclerite of phallosoma.

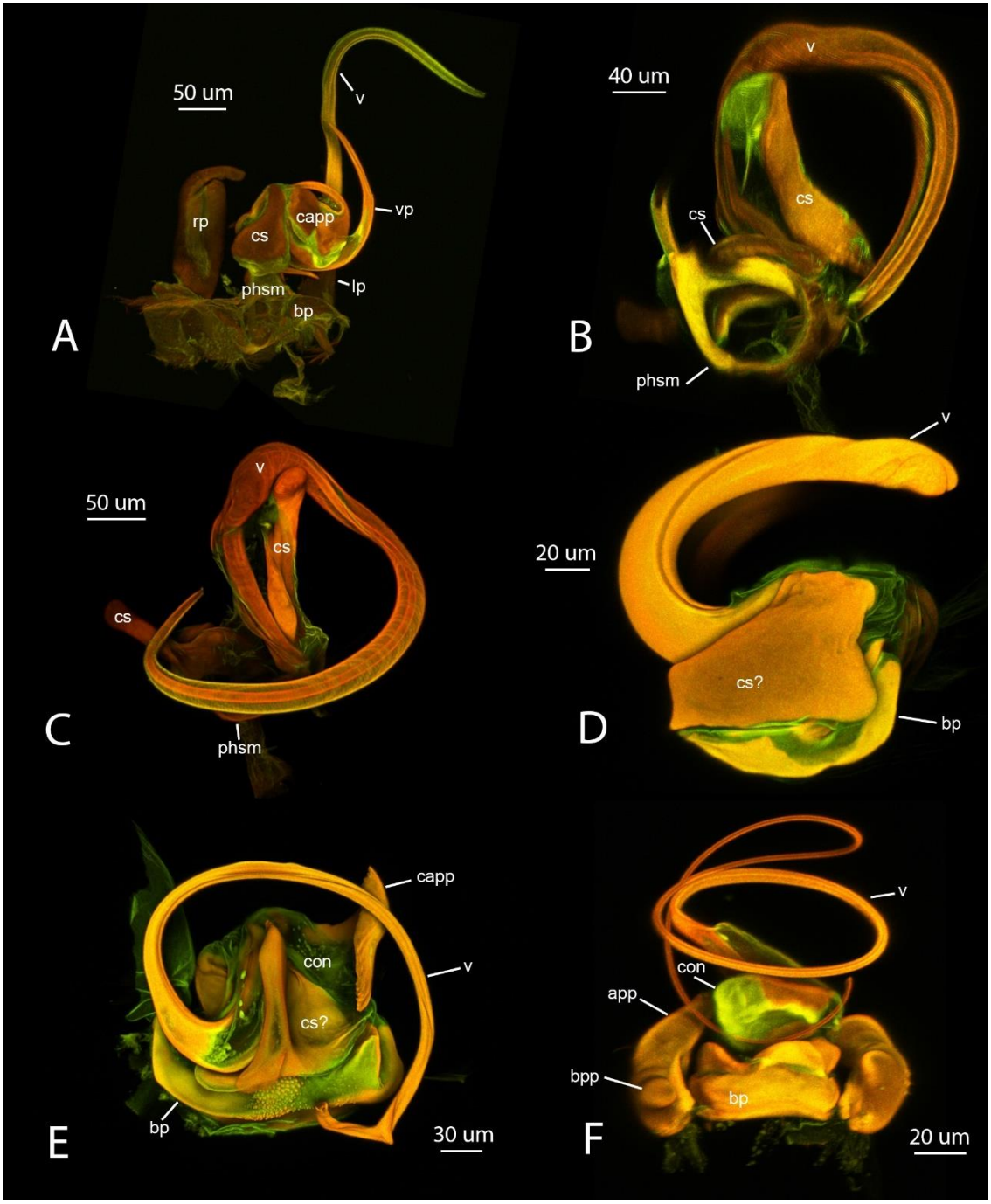
A
50 um
v
vp
capp
rp
cs
phsm
lp
bp
B
40 um
v
cs
cs
phsm
C
50 um
v
cs
cs
phsm
D
20 um
v
cs?
bp
E
capp
v
con
cs?
bp
30 um
F
v
con
app
bpp
bp
20 um

Figure 5.18. Confocal micrographs of aedeagus (Schizopteridae). A-C. Hypselosomatinae. A. *Hypselosoma* sp., ventral view. B. *Rectilamina* sp., ventral view. C. *Williamsocoris* sp., ventral view. D-E. Schizopteridae incertae sedis. D. *Guapinannus* sp., dorsal view. E. *Peloridinannus moe*, dorsal view. F. Ogeriinae, *Chinannus communis*, caudal view. Abbreviations: app – apical process of paramere, bp – basal plates, bpp – basal process of paramere, capp – conjunctival appendage, con – conjunctiva, cs – conjunctival sclerite, lp – left paramere, phsm – phallosoma, rp – right paramere, v – vesica, vp – vesical process.

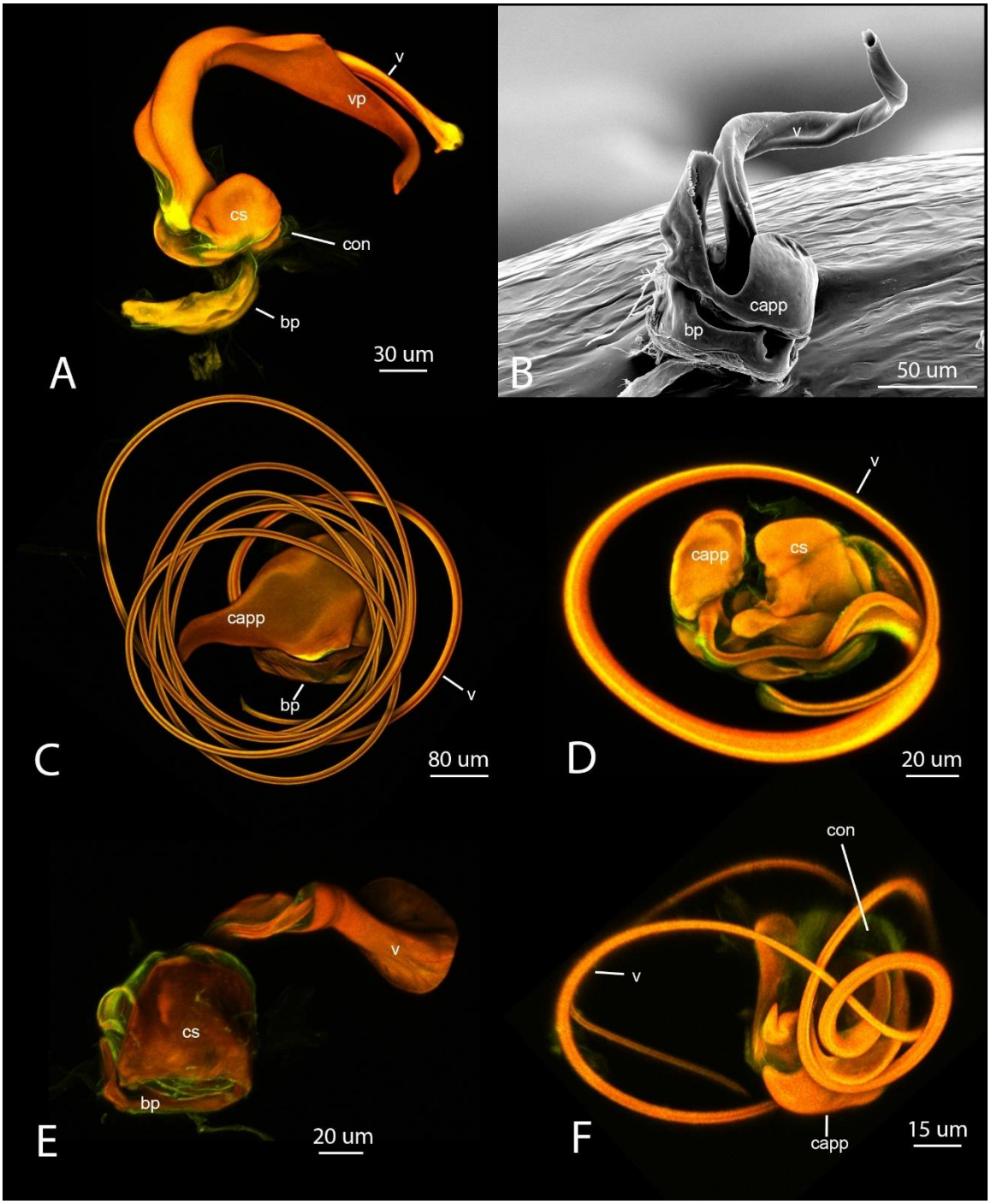

Figure 5.19. Confocal or scanning electron micrographs of aedeagus (Schizopteridae). A-E. Ogeriinae. A. *Kaimon* sp., ventral view. B. *Kokeshia* sp., caudal view. C. *Meganannus lewisi*, dorsal view. D. *Ogeria* sp., dorsal view, basal plates removed. E. Undescribed genus 2, anterior view. F. Schizopterinae, *Ceratocomboides* sp., dorsal view, basal plates removed. Abbreviations: bp – basal plates, capp – conjunctival appendage, con – conjunctiva, cs – conjunctival sclerite, v – vesica, vp – vesical process.

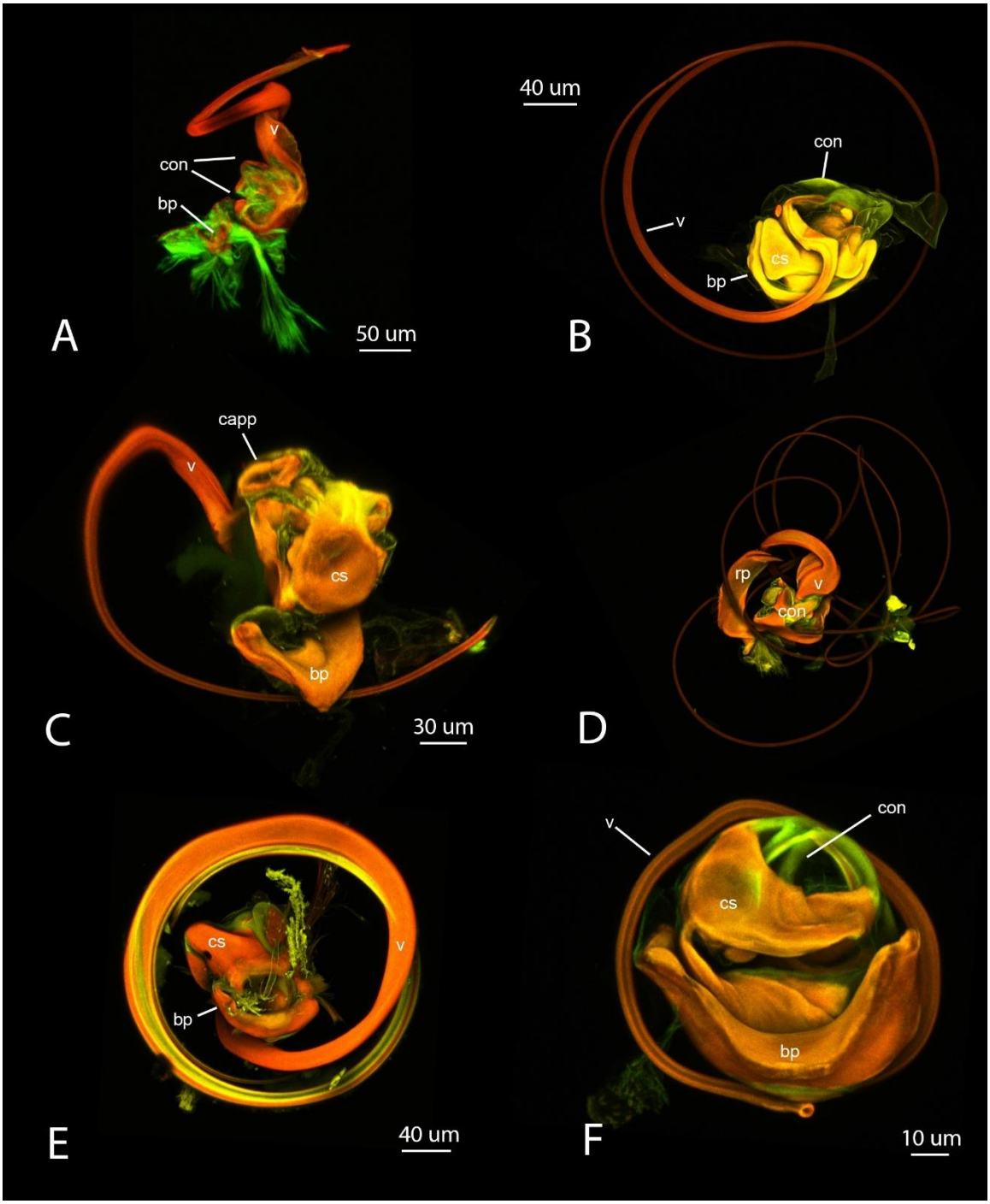

Figure 5.20. Confocal micrographs of aedeagus (Schizopteridae: Schizopterinae). A. *Hoplonannus* sp., lateral view. B. *Machadonannus brailovskyi*, dorsal view. C. *Membracioides* sp., ventral view. D. *Nannocoris* sp., anterior view. E. *Pinochius* sp., ventral view. F. *Ptenidiophyes* sp., ventral view. Abbreviations: bp – basal plates, capp – conjunctival appendage, con – conjunctiva, cs – conjunctival sclerite, rp – right paramere, v – vesica.

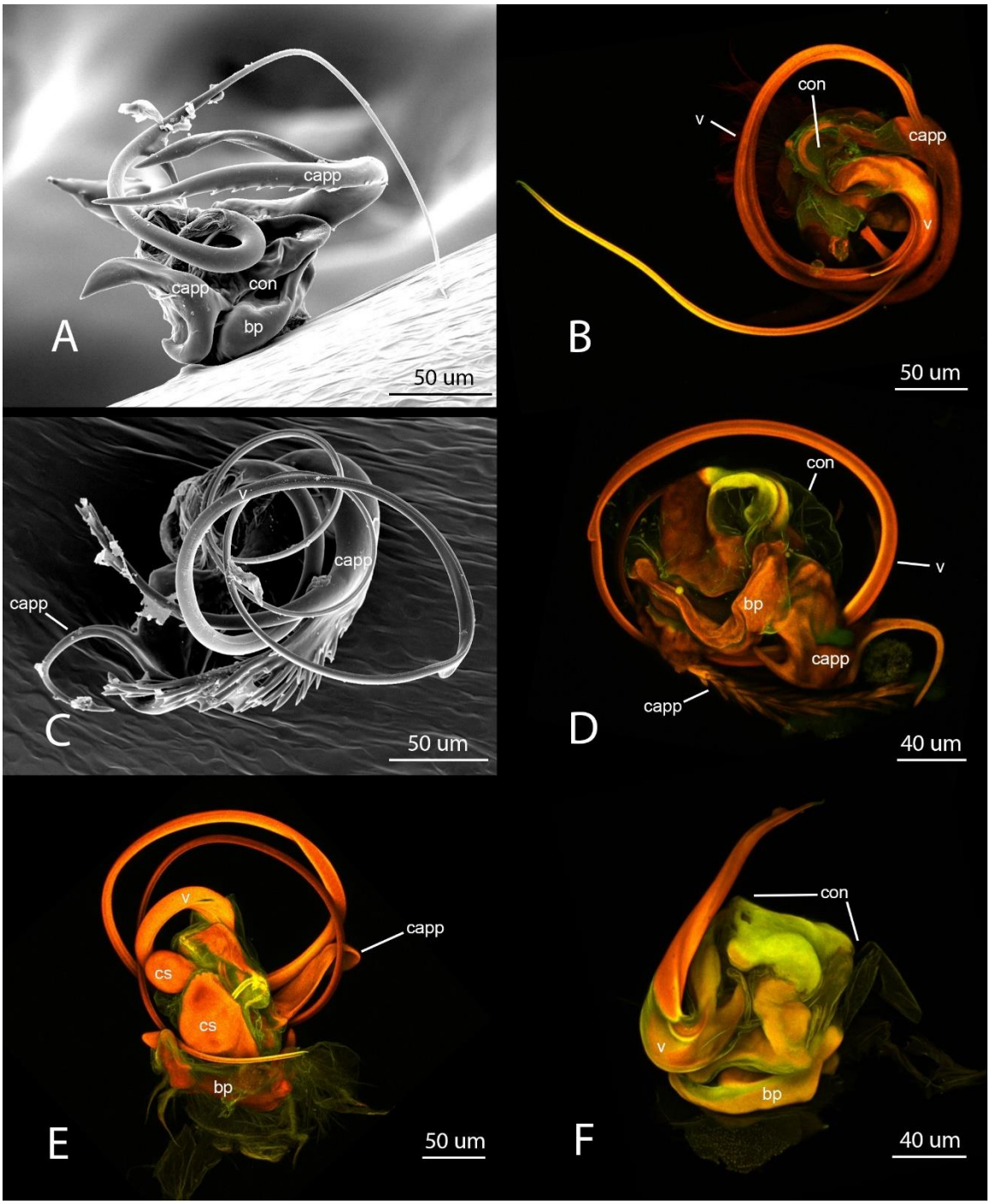

Figure 5.21. Confocal or scanning electron micrographs of aedeagus (Schizopteridae: Schizopterinae). A. *Schizoptera* (*Cantharocoris*) sp., caudal view. B. *Schizoptera* (*Odontorhagus*) sp., dorsal view. C-E. *Schizoptera* (*Schizoptera*) sp. C. Dorsal view. D. Ventral view. E. Ventral view. F. *Vilhenannus* sp., dorsal view. Abbreviations: bp – basal plates, capp – conjunctival appendage, con – conjunctiva, cs – conjunctival sclerite, v – vesica.

Chapter 6: Phylogenetic analysis of Dipsocoromorpha with emphasis on the family Schizopteridae

Abstract

Currently comprising only about 430 species, Dipsocoromorpha or minute litter bugs are one of the small infraorders of Heteroptera. They comprise five morphologically distinct families, Ceratocombidae, Dipsocoridae, Hypsipterygidae, Schizopteridae, and Stemmocryptidae, but relationships between and within these families are poorly understood due to the lack of comprehensive phylogenetic studies. A phylogenetic hypothesis based on a combination of molecular and morphological data is important to both evaluate and revise the higher-level classification and to explore the evolutionary history of unusual morphological features such as beetle-like forewings, jumping devices, and the highly modified and diverse male genitalia. We here use a dataset combing Sanger-derived (~4500 bp; 108 taxa) and Illumina-generated (~7500 bp; 24 taxa) sequence data with a morphological matrix (159 characters) and taxon sampling that comprises all currently recognized family-, subfamily- and tribal-level taxa and comprehensive genus-level sampling to investigate phylogenetic relationships within litter bugs. Our results support the monophyly of Dipsocoromorpha, Schizopteridae, and Dipsocoridae, while Ceratocombidae and the schizopterine subfamily Ogeriinae are paraphyletic. A new classification is proposed that recognizes six families, including Trichotonannidae, n. stat., and two subfamilies each within the two larger families Ceratocombidae and Schizopteridae. Ancestral state reconstructions outline the complex

evolutionary history of many morphological characters, including 16 independent origins of coleopteroidy, and at least five shifts in the degree of genitalic asymmetry.

Introduction

Dipsocoromorpha, the minute litter bugs, are one of the two least species-rich infraorders of the hemipteran suborder Heteroptera, comprising only about 430 described species. As their common name implies, Dipsocoromorpha occur in leaf litter, but other microhabitats including bark, rotten wood, low vegetation, the tree canopy, banks of streams and even mangroves are also utilized by different taxa. Although not difficult to collect using passive trapping techniques, litter bugs are small (0.5-3mm), mostly restricted to undersampled wet tropical and subtropical environments around the world, and few specialists have focused on the group, resulting in few curated specimens in natural history collections. The taxonomic history of Dipsocoromorpha started in the late 19th century (Sahlberg 1875; Reuter 1894; Uhler 1904), then collectively referred to as Cryptostemmatidae. Monographs of the New World fauna (McAtee & Malloch 1925) and of Schizopteridae with emphasis on Trinidad (Emsley 1969) remained for a long time the two taxonomically most comprehensive treatments. Descriptive work with excellent morphological documentation using light microscopical techniques started in the mid-20th century, spearheaded by P. Wygodzinsky (e.g., Wygodzinsky 1947, 1948, 1953, 1960) and later P. Štys (e.g., Štys 1958, 1970, 1985). Almost half of the around 70 valid genera were described as monotypic, suggesting that the group is morphologically diverse. A recent surge in revisionary taxonomic research has started to document the vast undescribed diversity at the species level, while also discovering and describing new

genera (Weirauch & Frankenberg 2015; Knyshov *et al.* 2016; Leon & Weirauch 2016a, 2016b; Weirauch *et al.* 2018c).

Substantial comparative morphological research on the group had accumulated by the 1970s, mostly due to publications by Wygodzinsky, Štys, and Emsley, and Štys (1970) and Štys and Kerzhner (1975) proposed the currently accepted classification. Dipsocoromorpha consist of five families that range from the monotypic Stemmocryptidae that are only known from the type series of *Stemmocrypta antenna* Štys from Indonesia to Schizopteridae that show substantial morphological and species-level diversity. Ceratocombidae comprise seven genera and ~50 species and are subdivided into the Old World Trichotonanninae, characterized by strongly asymmetrical male genitalia, and Ceratocombinae with symmetrical genitalic structures and worldwide distribution. The latter subfamily is further subdivided into Issidomimini with three genera, all from the Old World and some with elytriform wings, and the cosmopolitan Ceratocombini. Dipsocoridae, recognized by the very long costal fracture and sinistral genitalic asymmetry, currently consist of three genera (sometimes treated as one or two genera due to small morphological differences) and ~30 species distributed worldwide. The family-level taxon Hypsipterygidae was created to accommodate the single genus *Hypsipteryx* Drake with 4 extant species from Africa and South East Asia that share unique wing venation and other features that set them apart from the remaining Dipsocoromorpha. Schizopteridae is the largest family comprising three subfamilies (Hypselosomatinae, Ogeriinae, and Schizopterinae) and about 350 species distributed in all biogeographic regions with highest diversity in the tropics. The infraorder also

includes several fossil species, including two Ceratocombidae, one each of Dipsocoridae and Hypsipterygidae, and eight Schizopteridae (Wygodzinsky 1959; Bechly & Wittmann 2000; Perrichot *et al.* 2007; Azar & Nel 2010; Azar *et al.* 2010; Poinar & Brown 2014; Hartung *et al.* 2017). Interestingly, the oldest known fossils in the group date to the Early Cretaceous and were classified within the schizopterid subfamily Hypselosomatinae, suggesting that major divergences within Dipsocoromorpha happened prior to about 120 mya.

Phylogenetic studies focusing on Dipsocoromorpha have remained rare. Although the monophyly of Dipsocoromorpha now appears to be well supported (e.g., Weirauch & Schuh 2011; Weirauch and Štys 2014) and phylogenetic hypotheses for specific genera or genus groups have started to appear (e.g., Knyshov *et al.* 2016; Frankenberg *et al.* 2018), Dipsocoromorpha as a whole have not been subjected to phylogenetic analyses using explicit algorithms. However, several morphology-derived hypotheses on relationships were proposed during the second half of the 20th century, and present testable hypotheses. Among those are the tree-like scenario put forward by Emsley (1969) with emphasis on Schizopteridae, in which he recognized the subfamilies Hypselosomatinae and Schizopterinae, as well as several genus groups within Schizopterinae, but left a number of schizopterid genera unplaced. Štys (1970, 1982) focused on relationships across Dipsocoromorpha, culminating in the current hypothesis of relationships outlined in Štys (1983): Hypsipterygidae and Schizopteridae were hypothesized to be closely related, while Ceratocombidae, Dipsocoridae, Stemmocryptidae were thought to form the "lower Dipsocoromorpha" with uncertain relationships among the families (Štys 1983). Štys

(1982) also used Hennigian argumentation to reconstruct a phylogeny of Ceratocombidae. The use of molecular data to infer phylogenetic relationships of Dipsocoromorpha is still in its infancy. The first phylogenetic analysis of Dipsocoromorpha by Weirauch and Štys (2014) used molecular markers (parts of 18S and 28S rDNA, ~3,500bp), but was based on limited taxon sampling of Schizopteridae (15 genera; three subfamilies) as well as Ceratocombidae and Dipsocoridae (both represented by only the type genus of each respective family). Dipsocoromorpha were recovered as monophyletic with high support, as were the three sampled families. All subfamilies of Schizopteridae were monophyletic with moderate to strong support. Molecular data for the rarely collected and species-poor taxa Hypsipterygidae and Stemmocryptidae have not been collected to date, and relationships between these families and the three larger families are unknown. Several smaller phylogenetic analyses focused on subordinate taxa within Schizopteridae, utilizing the same set of molecular markers (Knyshov *et al.* 2016; Leon & Weirauch 2017; Frankenberg *et al.* 2018). With increased taxon sampling, Ogeriinae were shown to be paraphyletic (Knyshov *et al.* 2016; Frankenberg *et al.* 2018), while Hypselosomatinae and Schizopterinae were consistently recovered as monophyletic (Knyshov *et al.* 2016; Leon & Weirauch 2017; Frankenberg *et al.* 2018), although with varying support. Relationships among genera within Schizopteridae have largely remained unresolved, although several taxonomically focused studies are in progress (e.g., Hoey-Chamberlain *et al*. in prep.). A phylogenetic hypothesis based on a combination of molecular and morphological data, sampling of a

significant portion of the described genus-level diversity, and explicit phylogenetic procedures is clearly overdue.

Dipsocoromorpha possess an array of morphological features that are unusual or unique among Heteroptera. Their forewing venation is prominent and contains a large number of veins compared to other Heteroptera, and was traditionally viewed as plesiomorphic. In addition, different groups of Dipsocoromorpha contain macropterous as well as submacropterous and brachypterous species and the texture of the forewing ranges from almost uniformly membranous (i.e. no clear distinction between corium and membrane) to elytriform (i.e. entire forewing forming a shell of variable degrees of uniform sclerotization). Forewings can also be sexually dimorphic and/or polymorphic within species. The ancestral state reconstruction of Leon and Weirauch (2017), although primarily focused on the genus *Schizoptera* and thus with limited taxon sampling of non-*Schizoptera* genus group taxa, concluded that elytriform forewings in females evolved at least seven times independently within Schizopteridae, and three times within the genus *Schizoptera*. Otherwise only seen in the leptopodomorphan family Omaniidae, the hind legs of many dipsocoromorphan taxa have coxal adhesive pads that are thought to be involved in synchronizing the hind legs during jumping behaviors. Unique among Heteroptera, the tarsal formula of minute litter bugs varies dramatically between taxa and sexes. Males, but not females, in many taxa have a unique bladder-like arolium on the fore- and middle leg pretarsi. So called male-specific organs (MSOs) comprise variously shaped cavities and protuberances on the head, thorax, or wings that often, and possibly always, are associated with glandular units. These structures that are restricted to males

and in some species recognizably distort the habitus of a specimen are unknown in other Heteroptera, but occur in a substantial number of schizopterid species (Hill 1990, 2004, 2013; Weirauch 2012; Knyshov *et al.* 2016; Frankenberg *et al.* 2018). Finally, male genitalic features of Dipsocoromorpha demonstrate enormous structural diversity and variation in the degree of asymmetry (Knyshov *et al.* 2018). The functional morphology of the above mentioned features has remained unexplored, and due to the small size and largely circumtropical distribution of most dipsocoromorphan species, behavioral data may continue to be difficult to obtain. Similarly, the macroevolutionary patterns of these features are unknown. However, using a well-sampled and well-supported phylogeny, the evolutionary history of these features can be investigated with respect to number and direction of transitions and correlation with other traits, potentially providing insights into some of the selection pressures that have led to diversification in this group.

Here we present the most comprehensive phylogenetic analysis of Dipsocoromorpha to date. We attempt to mitigate limitations of previous analyses by including drastically improved taxon sampling, expanded molecular datasets, and – for the first time in the framework of a phylogenetic analysis of this group – a morphological dataset. The material assembled during this US National Science Foundation funded project allowed us to generate molecular data for four out of seven genera of Ceratocombidae, rare Hypsipterygidae, and about 30 genera of Schizopteridae that represent all major currently known genus groups. Although, we utilize the same gene regions as in Weirauch and Štys (2014) for the majority of taxa, we generated expanded dataset of ~7.5 Kb for a subset of 26 taxa sampled across the phylogeny in an attempt to improve support for deep

divergences and the backbone of Schizopteridae. The coding of morphological characters allowed us to include the exceptionally rare Stemmocryptidae, enables future inclusion of fossil taxa, and makes the results of the combined morphological and molecular phylogenetic reconstructions translatable into a revised classification.

Our study aims to: 1) assemble the largest molecular and morphological dataset for Dipsocoromorpha with comprehensive genus-level taxon sampling to generate a robust phylogenetic hypothesis for relationships within the group; 2) highlight the potential of integrating in-house generated bait capture procedures for including rare and suboptimally preserved, yet phylogenetically critical taxa, into combined analyses; 3) use the best-supported topology and reconstructed morphological synapomorphies to revise the classification of the group; 4) explore the evolution of selected morphological characters, including wing type transitions, male genitalic asymmetry, and MSOs.

Material and Methods

Voucher information

A total of 144 specimens were included in this study, aiming for comprehensive sampling of Dipsocoromorpha at the genus-level and above. Several speciose genera of Schizopteridae and Ceratocombidae that are the focus of targeted recent or ongoing studies (e.g., Knyshov *et al.* 2016; Leon & Weirauch 2017; Frankenberg *et al.* 2018) are represented by only a few species. Molecular and morphological data for 133 of these taxa were generated by us from voucher specimens and for 11 were taken from NCBI (DNA sequence data) and publications (morphological data). Species of Nepomorpha,

Gerromorpha, and Enicocephalomorpha were used as outgroups. Specimens were loaned from multiple institutions as listed in Table 6.1. Specimen information (locality and collection event, identification, sex, etc.) was digitized and is available through the http://research.amnh.org/pbi/heteropteraspeciespage/ website. Specimens were imaged in two or three views using a Leica DFC 450 C Microsystems system with Planapo 1.0x or 2.0x objectives and stacked using Leica Application Suite V4.3 (Figure 6.1). Slide-mounted specimens were imaged on a Zeiss Axioskop 2 compound microscope using Archimed V5.4.1 and stacked using Zerene Stacker V1.02.

DNA Extraction, PCR, and Sanger sequencing

We extracted DNA nondestructively from whole specimens using a Qiagen DNeasy Blood and Tissue Kit. We amplified one or two regions of 18S rDNA and two or three regions of 28S rDNA (see accession numbers in Table 6.1). All PCR reactions were done using Takara EmeraldAmp GT PCR Master Mix, using primers from Forero *et al.* (2013), Giribet *et al.* (1996), Menard *et al.* (2014), and Weirauch and Munro (2009). Each reaction contained 12.5 µl of the master mix, 9.5 µl of water, 0.5 µl of each primer and 2 µl of the DNA template. The thermocycler program included initial denaturation at 94°C for 5 min, 35 cycles of denaturation at 94°C for 30 sec, annealing at 48°C for 30 sec, elongation at 72°C for 45 sec, final elongation at 72°C for 7 min. Total of 108 specimens were sequenced (Table 6.1, "Sanger"), sequences for five additional taxa were obtained from GenBank.

Hybrid capture and Illumina sequencing

We used the protocol of Knyshov *et al.* (in review) to obtain substantially larger molecular datasets for a subset of taxa. Using the primers listed in Knyshov *et al.* (under review), we selected eight specimens with good DNA quality (1 dipsocorid, 1 ceratocombid, 2 Ogeriinae and 2 Schizopterinae) and used long range PCR to amplify the nuclear ribosomal operon and the mitochondrion. PCR products were turned into Illumina libraries and sequenced on 5% of a MiSeq V3 lane at IIGB UCR. For hybrid capture following the pooled protocol of Knyshov *et al.* (in review), the amplicons were also turned into biotinylated bait to enrich DNA of 18 crucial taxa for which only extracts of suboptimal quality were available. Two pools with 9 libraries each were enriched for the fragments of interest and subsequently sequenced on 13% of a MiSeq V3 lane at IIGB UCR. Total of 24 specimens were sequenced (Table 6.1, "Illumina" and "Illumina, PROBE"), sequences for six additional taxa were obtained from GenBank.

Morphological character documentation and coding

A total of 159 morphological characters were scored for 144 taxa. Among these are more than 30 characters derived from head structures, 24 from the thorax excluding appendages, 28 from the forewing, 19 from leg morphology, and the remaining characters encode morphology of the abdomen including male and to a much lesser degree female genitalic structures. Scanning electron micrographs for Figures 6.2 and 6.3 were taken on a FEI XL30-FEG electron microscope using specimens prepared on a Cressington 108 auto sputter coater. Forewing images for Figure 6.4 were taken using a Zeiss Axioskop 2 compound microscope with a digital camera.

Many of the morphological features here coded as phylogenetic characters have previously been used to describe and diagnose dipsocoromorphan taxa, e.g., the number of labial segments or absence or presence of metacoxal pads. Others are derived from our own comparative morphological investigations, e.g., the shape, size, and vestiture of mandibular and maxillary plates on the head. The terminology and primary homology hypotheses for male genitalic features are taken from Knyshov *et al.* (2018). Another important source of character information is the forewing venation. This character system is critically important for the integration of fossil taxa in phylogenetic hypotheses, because wings are frequently well preserved in fossil species. Although vein homology in closely related taxa of minute litter bugs is often intuitive, formulating a framework across Dipsocoromorpha has proven to be a challenge. Emsley (1969) was one of the first to provide a comprehensive analysis of venation in Schizopteridae, however, his hypothesis lacked consistency even between closely related taxa (compare *Pinochius* on Fig. 32 and *Nannocoris* on Fig. 33). Subsequently, Hill (1984, 1987) used Emsley's terminology for Hypselosomatinae and Dipsocoridae. Rédei (2007) examined *Hypsipteryx* which exhibits a venation pattern that differs dramatically from all other Dipsocoromorpha and provided a different venation hypothesis. Hill (2013) adopted Rédei's (2007) new hypothesis for *Hypselosoma*, which was followed by Hoey-Chamberlain and Weirauch (2016). *Peloridinannus*, which also deviates from the more typical schizopterid venation, was investigated by Wygodzinsky (1951) and Weirauch and Frankenberg (2015). Wing venation hypotheses for Ogeriinae were optimized by Knyshov *et al.* (2016), and later used by Weirauch *et al.* (2018c). Schizopterinae wing

venation hypotheses of Emsley (1969) were evaluated and modified by Rédei (2008) and then adopted by Leon and Weirauch (2016a, 2016b). The above mentioned groups of venation hypotheses were incompatible, mainly disagreeing on the interpretation of costal and anal veins, and corresponding cells. We recently proposed the core of a set of new homology hypotheses for Dipsocoromorpha wing venation (Weirauch *et al.* 2018a). That study only included representatives of Hypselosomatinae and Schizopterinae (Schizopteridae). We here expand it to non-schizopterid Dipsocoromorpha, taxa currently classified as Ogeriinae (Schizopteridae), and fossil taxa (Du *et al.*, unpublished), many of which show highly divergent wing venation patterns. Our framework of hypotheses is primarily based on recognition of similar vein and cell patterns, and not on the direct light microscopical observation of tracheae within a given longitudinal vein that proved to be difficult due to the small size and preservation of specimens. This new hypothesis is reflected in the forewings of 18 taxa shown on Figure 6.4, and is mostly consistent with Knyshov *et al.* (2016) and Weirauch *et al.* (2018a, 2018c). In short, we propose that the anterior costal margin in Dipsocoromorpha comprises C+Sc, distally followed by R with between one and three branches reaching the costal margin; we treat the distalmost veins reaching the wing margin as M and Cu. The two veins in the clavus are here treated as An1 and An2 veins, with An1 traversing the claval suture and either ending freely in the distal part of the forewing (membrane) or merging with Cu to form a closed cub cell.

Phylogenetic Analyses

Sanger sequences were assembled and edited in Sequencher V4.8 or Geneious 10. Next-generation sequencing (NGS) raw reads were processed in Trimmomatic (Bolger *et al.*

2014) to remove adaptors and low quality regions, and assembled in SPAdes (Bankevich *et al.* 2012). Geneious 10 was used to search for target contigs in assemblies and to map reads onto them for assembly quality check. We combined assembled sequences by gene and aligned in MAFFT (Katoh & Standley 2013) using the E-INS-i algorithm. Alignments were manually corrected and trimmed using SeaView (Gouy *et al.* 2009). The DNA alignments were concatenated together and with morphological matrix using a custom python script (available at https://github.com/AlexKnyshov/main_repo/blob/master/concat.py).

Initial analyses were performed on several subsets of the dataset: only taxa sequenced on the Illumina platform, with ribosomal and mitochondrial data analyzed separately and in combination, Sanger sequenced taxa, morphological partition, and all sets combined. Results of our initial analyses showed an overall topological congruence between the small Sanger sequenced dataset (partial 18S and 28S rDNA) and near complete sampling of the same ribosomal genes using Illumina sequencing, but the support along the backbone of the phylogeny was dramatically lower in the small data set. In contrast, inclusion of mitochondrial data in the analyses did not positively impact support values, and resulted in a few spurious relationships. Thus the final analyses and results presented here consisted of ribosomal (Sanger + Illumina datasets) and morphological data.

Maximum likelihood (ML) phylogenetic reconstruction was done in RAxML 8.2.10 (Stamatakis 2014) with three partitions (18S, 28S, and morphology). Molecular partitions were analyzed under GTRGAMMA, while the morphological partition was analyzed under the multistate GAMMA model. Branch support was assessed with Rapid Bootstrap

(Stamatakis *et al.* 2008). The resulting phylogeny was visualized using R (R Core Team 2018) and packages APE (Paradis *et al.* 2004) and ggtree (Yu *et al.* 2017) (Fig. 5). A phylogenetic reconstruction using parsimony (MP) was done in TNT 1.5 (Goloboff & Catalano 2016). Gaps and question marks were treated as missing data, as the missing data distribution was biased, and overall proportion of missing data high (62.82%). "New Technology Search" was conducted with default sectorial search, drift, and tree fusing. Driven search was run until the best tree was found 20 times, initial addseq was set to 20. The resulted trees were used to produce the strict consensus topology, the branch support was calculated using bootstrap resampling (Fig. 6.S1).

Ancestral State Reconstruction

Both ML and MP ancestral state reconstructions were performed on the ML phylogeny in R, using functions ace and MPR from the package APE and custom made utility scripts. During the ML reconstructions, for characters with missing data taxa, reconstruction was performed on a pruned tree with such taxa removed, results were associated with the corresponding nodes of the original phylogeny using custom made R scripts and visualized using package ggtree. The evolutionary history of "MSO" character was traced by recoding all MSO features as a single character with absent and present states (Fig. 6.6).

Results

Phylogenetic analysis

Both ML (Fig. 6.5) and MP (Fig. 6.S1) analyses reconstructed Dipsocoromorpha as monophyletic with full support. Relationships at the root of Dipsocoromorpha were unresolved, as various topologies were recovered in different analyses, all with low support. Importantly, the family Ceratocombidae was never recovered as monophyletic, with the ceratocombid genus *Trichotonannus* being separated from the remaining Ceratocombidae. The latter group consists of Ceratocombini and Issidomimini and was recovered in all analyses with >90% bootstrap support [BS]. The sister group relationship between Hypsipterygidae and Schizopteridae received high support (>=99% BS) in both ML and MP analyses. Within Schizopteridae, the subfamily Hypselosomatinae is sister to the remainder of Schizopteridae in the ML topology, while being nested within other Schizopteridae according to the MP topology. The subfamily Schizopterinae was recovered as monophyletic, but Ogeriinae together with several early diverging currently unplaced genera are paraphyletic with respect to Schizopterinae (both ML and MP analyses), or also with respect to Hypselosomatinae (MP analysis). Within Schizopteridae, several genus group-level clades are well supported, among them *Guapinannus* Wygodzinsky, *Kokeshia* Miyamoto, *Luachimonannus* Wygodzinsky, and an undescribed genus from the New World (but poorly supported in MP); and a clade of the *Ogeria* genus group, comprising *Kaimon* Hill, *Ogeria* Distant, and *Pachyplagia* Gross. Within Schizopterinae, *Silhouettanus* Emsley is the sister to the remaining genera, which form two large clades. One includes *Nannocoris* Reuter, *Pinochius* Carayon, the

Corixidea genus group sensu Emsley (1969), two undescribed genera from the New World, and is well supported in ML analysis. The other clade that is well supported in both analyses includes the *Dundonannus* group sensu Emsley (1969), and the *Schizoptera* group sensu Leon and Weirauch (2017).

Ancestral state reconstruction of morphological characters

Both maximum likelihood (ML) and parsimony (MP) ancestral state reconstructions were considered for the report below. Few cases of disagreement are highlighted, most recent common ancestor is abbreviated as MRCA, taxon names follow the old classification. Figures 6.1-4 illustrate many of the morphological characters and states that have remained poorly documented in the recent literature.

0. Overall body shape: (0) oval; (1) suboval; (2) elongate ovoid. Dipsocoromorpha generally have suboval body shape, with Stemmocryptidae being very elongate.

1. Head, shape in frontal view: (0) wider than high; (1) higher than wide. Head with width considerably larger than height is a synapomorphy of Schizopteridae.

2. Head, vestiture: (0) without dense cover of microtrichia; (1) with dense cover of microtrichia. According to the reconstruction, dense cover of microtrichia has independently originated in Issidomimini, Dipsocoridae, and Schizopteridae.

3. Male-specific organ on frons: (0) absent; (1) present. Presence of the frontal male-specific organ is a synapomorphy of the genus *Voragocoris* (Weirauch 2012).

4. Frons/vertex, muscle scars: (0) indistinct; (1) distinct. Distinct muscle scars are synapomorphic in two groups, Issidomimini and Schizopteridae.

5. Frons/vertex, pattern of muscle scars: (0) posterior scars arranged in submedian longitudinal lines; (1) anterior and posterior groups of scars; (2) x-shaped arrangement; (3) pair of parallel submedian line. The x-shaped pattern is a synapomorphy of Dipsocoromorpha, with transition to having anterior and posterior groups of scars in the MRCA of Schizopterinae+"Ogeriinae". Within Schizopterinae+"Ogeriinae" changes to states 0, 2, and back to 1 are inferred.

6. Frons, pit-like structures ventrad of ocelli: (0) absent; (1) present. A synapomorphy of Hypselosomatinae.

7. Eyes in frontal view, size: (0) about 1/3 of synthlispis; (1) 1/2 of synthlipsis; (2) smaller than 1/3 of synthlipsis. Medium sized eyes are a plesiomorphy of Dipsocoromorpha. Very large eyes are a synapomorphy of Hypselosomatinae, while transitions to very small eyes happen multiple times within Schizopteridae.

8. Ocelli in male: (0) absent; (1) present. Absence of ocelli in a macropterous male is a unique feature of *Hypsipteryx* (Štys 1970).

9. Position of ocelli: (0) adjacent to eye; (1) removed from eye; (2) on bulbous posterior lobe of head. Ocelli adjacent to eyes are a synapomorphy of Dipsocorormorpha (or of Dipsocoromorpha and Enicocephalomorpha under ML), with transitions to being removed from the eye in schizopterid MRCA and several deeply nested lineages.

10. Ocelli in female: (0) absent; (1) present. Presence of ocelli in female is a plesiomorphy of Dipsocoromorha. Around 17 losses and six gains of ocelli are inferred under ML.

11. Md plate: (0) present; (1) obsolete. Obsolete mandibular plate is a synapomorphy of Schizopterinae+"Ogeriinae", with reversal to present within Schizopterinae.

12. Md plate, size: (0) small; (1) large. Large mandibular plate is plesiomorphic for Dipsocoromorpha. Small mandibular plate is a synapomorphy of Schizopteridae.

13. Md plate, vestiture: (0) glabrous; (1) with microtrichia. Mandibular plate with microtrichia is a synapomorphy of Schizopterinae+"Ogeriinae", with a reversal to glabrous inferred within this clade.

14. Mx plate, size: (0) small, triangular; (1) very large; (2) small, elongate; (3) large elongate; (4) large trapezoidal; (5) very small and narrow. Large maxillary plate is plesiomorphic for Dipsocoromorpha, with multiple transitions to other sizes inferred.

15. Mx plate, stout ventrolateral seta: (0) absent; (1) present. Stout ventrolateral seta is a synapomorphy of Schizopterinae except *Silhouettanus*.

16. Buccula, shape (lateral view): (0) slender; (1) laterally inflated. Laterally inflated bucculae are synapomorphic for Schizopteridae.

17. Clypeus, shape: (0) wider dorsally than ventrally; (1) narrower dorsally than ventrally; (2) same width throughout. Ventrally widened clypeus is reconstructed to be a synapomorphy of Schizopteridae, with dorsally widened clypeus being synapomorphic to Hypselosomatinae and few other schizopterid lineages.

18. Clypeus, macrosetae (male): (0) absent; (1) 5 setae (4 dorsal 1 ventral); (2) 3 setae; (3) 5 setae (2 dorsal 3 ventral). Presence and number of clypeal macrosetae is diagnostic for genera of Hypselosomatinae (e.g., Hill 1984, 2013).

19. Labrum, shape: (0) short triangular; (1) long triangular; (2) elongate. Elongate labrum is a synapomorphy of Dipsocoromorpha.

20. Labium segmentation: (0) 4-segmented; (1) 3-segmented. Labium with 3 segments is a synapomorphy of Schizopterinae except *Silhouettanus*.

21. Labium, shape: (0) straight; (1) apical segment curved. Apically curved labial segment evolved independently in *Nannocoris* and *Silhouettanus*.

22. Labium, relative length: (0) reaching mesocoxa; (1) surpassing mesocoxa; (2) surpassing metacoxa; (3) not reaching mesocoxa. Medium-sized labium is characteristic for majority of Dipsocoromorpha, although ML and MP reconstructions disagree on exact placement of the change from ancestrally short labium. Within Dipsocoromorpha, very long labium evolved in *Chinannus*, *Nannocoris*, and *Silhouettanus*.

23. Labium, width (segment 3 or 3/4): (0) slender; (1) broad. Broad 3rd labial segment is a synapomorphy of Schizopteridae, with multiple reversals to slender within the group.

24. Labium, length of segment 2: (0) short; (1) moderately long; (2) long. Elongation of second labial segments was inferred four times within different genera of Schizopterinae+"Ogeriinae" clade.

25. Labium, length of segment 3: (0) short; (1) long; (2) very long. Very long third labial segment is inferred to be synapomorphic for Dipsocoromorpha, with change to short in Schizopteridae, and reversals to long in two "Ogeriinae" genera.

26. Labium, length of segment 4: (0) very short; (1) short; (2) moderately long; (3) long. Long fourth labial segment is inferred to be synapomorphic for Dipsocoromorpha,

with change to moderately long in or within Schizopteridae (depending on the reconstruction mode). Short fourth segment is a synapomorphy of Hypselosomatinae.

27. Labial segment 3/4: (0) short; (1) moderately long. For schizopterids with only three labial segments, short terminal segment is synapomorphic, with transition to long in *Pinochius*.

28. Labium, segment 1: (0) not bulbous; (1) bulbous. Bulbous first labial segment in males is a synapomorphy of *Williamsocoris* (Carpintero & Dellapé 2006).

29. Labium, shape of tip: (0) tapering; (1) blunt. Blunt labium is a synapomorphy of the *Corixidea* genus group (Emsley 1969; Weirauch 2012).

30. Antenna, relative length of segments: (0) with scape and pedicel very short and flagellomeres much longer; (1) pedicel longer than scape, of similar length to flagellomeres. Very short scape and pedicel is one of the most easily recognizable synapomorphies of Dipsocoromorpha (e.g., Štys 1983).

31. Antenna, relative length of scape and pedicel: (0) same length; (1) pedicel about twice as long as scape. Plesiomorphic for Dipsocoromorpha condition of longer pedicel is found in early diverging families, while scape and pedicel of equal length is a synapomorphy of Hypsipterygidae and Schizopteridae.

32. Antenna, relative thickness of segments: (0) scape and pedicel much stouter than flagellomeres; (1) scape and pedicel not much stouter than flagellomere. Thick scape and pedicel and thin flagellomeres is another prominent synapomorphy of Dipsocoromorpha (e.g., Štys 1983).

33. Male-specific organ as pit dorsally on head: (0) absent; (1) present. Dorsally located pit on the head is a synapomorphy of *Nannocoris* (Frankenberg *et al*. 2018).

34. Male-specific organ between posterior margin of head and anterior margin of pronotum: (0) absent; (1) present. Vertex organ is a synapomorphy of *Kaimon* (Hill, 2004), and independently an apomorphy of some *Membracioides* species (Knyshov *et al.* in prep).

35. Pronotum, shape: (0) wider than long; (1) trapezoidal (about as wide as long). Trapezoidal pronotum is plesiomorphic for Dipsocoromorpha, with transitions to transversal in Issidomimini (diagnostic), Hypsipterigydae, and Hypselosomatinae.

36. Anterior and posterior pronotal lobes: (0) well-delimited; (1) not clearly delimited. No clear delimitation between pronotal lobes is synapomorphic for Dipsocoromorpha.

37. Lateral margin of pronotum: (0) convex; (1) almost straight; (2) slightly concave. Straight margins of pronotum are characteristic for early diverging Dipsocoromorpha, although according to our reconstructions, character change took place in the MRCA of Dipsocoromorpha and Enicocephalomorpha. Convex lateral margins are synapomorphic for Hypsipterygidae and Schizopteridae.

38. Pronotal collar: (0) absent; (1) present. Pronotal collar is plesiomorphic feature of Dipsocoromorpha, that gets reduced independently in Stemmocryptidae, Issidomimini, the *Corixidea* genus group, and *Ptenidiophyes*.

39. Pronotal collar, separation from remainder of pronotum: (0) entirely separated; (1) separated only laterally. Only laterally separated collar is a synapomorphy of Dipsocoridae.

40. Male-specific organ consisting of complex gland and opening on anterior margin of anterior pronotal lobe: (0) absent; (1) present. This type of male-specific organ is synapomorphic for some species of an undescribed genus of Schizopterinae.

41. Pronotal male specific organ: (0) absent; (1) present. Posterior pronotal organ is synapomorphic for some species of *Membracioides* (Emsley 1969; Knyshov *et al*. in prep).

42. Scutellum, shape: (0) triangular with straight or convex lateral margins; (1) triangular with slightly concave lateral margin; (2) triangular with tip; (3) rounded. Triangular scutellum with slightly concave lateral margins is synapomorphic for Dipsocoromorpha. Rounded scutellum is apomorphic for Hypsipterygidae, triangular with straight or convex lateral margins may be a synapomorphy of Hypselosomatinae depending on the reconstruction mode. Shape of scutellum in Schizopterinae+"Ogeriinae" varies, but is frequently triangular with tip.

43. Scutellum, size: (0) small; (1) large. Large scutellum is plesiomorphic for Dipsocoromorpha, with small scutellum independently derived in Hypsipterygidae and part of Schizopterinae.

44. Pronotum and proepimeron suture or fold: (0) absent; (1) present. The suture originated independently in three lineages of Schizopterinae: *Nannocoris*, *Ptenidiophyes*, and part of *Schizoptera*.

45. Blunt tooth on propleuron: (0) absent; (1) present. Blunt tooth on propleuron is a synapomorphy of *Schizoptera* (*Odontorhagus*) (Leon & Weirauch 2016b, 2017).

46. Proepisternum: (0) not inflated; (1) inflated. Inflated proepisternum is one of the most diagnostic synapomorphies of Schizopteridae (Emsley 1969; Štys 1970).

47. Proepimeron: (0) not enlarged; (1) enlarged. Enlarged proepimeron is characteristic for Ceratocombidae, Dipsocoridae, and Hypsipterygidae, and according to our reconstructions is a synapomorphy for Dipsocoromorpha except Stemmocryptidae, and gets reverted to not enlarged in Schizopteridae.

48. Mesepisternal and mesepimeral lobes covering base of coxa: (0) absent; (1) present. Absent lobes are plesiomorphic for Dipsocoromorpha, with transition to present being a synapomorphy of Schizopteridae.

49. Posterolateral spine on metepisternum: (0) absent; (1) well developed. Metepisternal spine is one of the diagnostic synapomorphies of the *Kophaegis+Ptenidiophyes+Schizoptera* clade.

50. Metepimeron: (0) well-developed; (1) reduced or absent. Reduced metepimeron is a synapomorphy of Hypsipterygidae+Schizopteridae.

51. Metathoracic gland, evaporatory structure: (0) absent; (1) groove along margin of coxal lobe; (2) long process; (3) metasternum and precoxae as evaporatorium; (4) evaporatory area with mushroom bodies. Evaporatory structures of the scent gland are ancestrally absent in Dipsocoromorpha, with three different types of these structures evolving independently in Dipsocoridae, Stemmocryptidae, the *Dundonannus* group, and the *Schizoptera* group.

52. Metepisternal groove area: (0) with groove only; (1) with glabrous area at ventral margin; (2) glabrous area extending dorsad. Small glabrous area is synapomorphic for

Kophaegis and *Schizoptera*, with enlarged area being synapomorphic for *Schizoptera* (*Cantharocoris*) (Leon & Weirauch 2017).

53. Mesosternum, lateral protuberances: (0) absent; (1) present. Lateral protuberances inferred to have evolved four times independently within Schizopteridae.

54. Median mesosternal spine: (0) absent; (1) present. According to our reconstructions, a prominent mesosternal spine is limited to Schizopteridae and have evolved five times independently, with transitions back to being absent four times.

55. Median metasternal spine: (0) absent; (1) present. As is the mesosternal spine, metasternal spine have independently evolved two times and lost five times, all within Schizopteridae.

56. Metasternal spine, shape: (0) simple, not bifurcating; (1) bifurcating. Not bifurcating spine is ancestral for Schizopteridae, with two transitions to bifurcating in two undescribed genera.

57. Metendosternite: (0) absent; (1) present. Metendosternite is a synapomorphy of Schizopteridae (Emsley 1969; Hill 2015).

58. Metendosternite, shape: (0) bifurcating; (1) not bifurcating; (2) blunt with lateral lobes; (3) short and broad. Metendosternite is ancestrally bifurcating in Schizopteridae, with a single transition to blunt, and four reversals to state (0) again. Not bifurcating metendosternite is synapomorphy of *Guapinannus*, while short and broad process is synapomorphic for *Kophaegis+Schizoptera*.

59. Wing-to-thorax coupling, druckknopf: (0) absent; (1) small; (2) well developed. Frequent transitions between states of this character were inferred, and condition in the

MRCA of Dipsocoromorpha is small. The coupling mechanism is well developed in Schizopteridae, although nine independent reductions are estimated.

60. Forewing type (male): (0) macropterous; (1) brachypterous. Ancestrally macropterous males of Dipsocoromorpha were estimated to undergo 12 independent transitions to brachyptery within the infraorder.

61. Forewing type (female): (0) macropterous; (1) brachypterous; (2) micropterous; (3) absent. As with males, ancestral condition of female forewings is macropterous, however 21 transitions to brachyptery, 1 to microptery, and 3 reversals to macroptery are inferred within Dipsocoromorpha.

62. Forewing elytriform (in at least one sex): (0) absent; (1) present. Our reconstructions suggest 16 independent transitions to elytriform forewings within Dipsocoromorpha.

63. Elytriform forewing: (0) without vein traces; (1) with vein traces. As coleopteroidy occur independently, characteristics of the forewings are likely to be independent between different groups. On the other hand, within groups with elytriform forewings, presence or absence of vein traces is inferred to be stable.

64. Elytriform forewing (pits): (0) smooth; (1) with pits; (2) areoles. Areoles are uniquely characteristic for *Hypsohapsis*. Other states have similar distributions across the phylogeny, see the discussion on character 63.

65. Forewing, distinct costal fracture: (0) absent; (1) present. Costal fracture is inferred to be a synapomorphy of Dipsocoromorpha+Enicocephalomorpha. The character is homoplastic, the fracture is reduced in Issidomimini and MRCA of

Hypsipterygidae+Schizopteridae, with two gains and four reductions within Schizopteridae.

66. Costal fracture, length: (0) short; (1) long; (2) as line of weakness in anterior wing margin. According to our reconstruction, ancestrally short fracture changes to long independently in Dipsocoridae and Stemmocryptidae. Line of weakness in the costal margin of the wing is synapomorphic for Schizopteridae.

67. scc more heavily sclerotized than remaining cells: (0) absent; (1) present. Within Schizopteridae this character is homoplastic. Notably, two states of this character differentiate *Glyptocombus+Williamsocoris* clade (absent, synapomorphy) and the rest of Hypselosomatinae (present, plesiomorphic).

68. R distally with: (0) 1 branch; (1) 2 branches; (2) 3 branches. Three branches of R are synapomorphic for Schizopteridae, although multiple reversals to 2 and 1 branch conditions are inferred within the family.

69. R1: (0) merging with Sc in middle or proximal part of forewing; (1) merging with Sc in distal part of forewing. Character state 1 is independently derived in genera *Nannocoris*, *Silhouettanus*, and the *Dundonannus* genus group.

70. R2: (0) joining Sc at oblique angle; (1) joining Sc at right angle. Joining of R2 with Sc at right angle arose in Hypsypterygidae and three times independently within Schizopteridae: in *Guapinannus*, *Peloridinannus*, and the *Schizoptera* genus group.

71. rc: (0) absent; (1) present. rc cell is ancestrally present in Dipsocoromorpha, and independently lost in the MRCA of Ceratocombinae and Stemmocryptidae, and in Schizopterinae except *Silhouettanus*.

72. rc (split): (0) absent; (1) present. Splitting of rc into rca and rcb occurred independently in Hypsipterygidae and *Peloridinannus*.

73. bc: (0) absent; (1) present. Presence of bc is a synapomorphy of Dipsocoromorpha.

74. bc, shape: (0) shorter than tc; (1) about same length as tc; (2) longer than tc. The cell shape is ancestrally long with multiple transitions to being shorter within Dipsocoromorpha.

75. dc: (0) absent; (1) present. Presence of dc is a synapomorphy of Dipsocoromorpha.

76. dc, dimension: (0) much longer than wide; (1) about as long. Roughly equally long and wide dc was inferred to originate three times independently.

77. dc, shape: (0) elongate; (1) trapezoidal; (2) pentagonal; (3) hexagonal. Elongate dc is a synapomorphy of Schizopteridae, modified to other types within the family. Trapezoidal dc is a synapomorphy of Schizopterinae, and is encountered in two groups of "Ogeriinae". Pentagonal dc is independently derived and is a synapomorphy of the *Schizoptera* group and the *Corixidea* group.

78. M and Cu proximal to dc1: (0) not connected; (1) connected via m-cu crossvein; (2) merged together. M merged with Cu was inferred as ancestral for Dipsocoromorpha. In the MRCA of Hypsipterygidae+Schizopteridae two veins are reconstructed to be connected via a crossvein.

79. dc1: (0) present; (1) collapsed. Collapsed dc1 due to distal merging of M and Cu ocurred independently in *Leptonannus* and an undescribed genus of Schizopteridae.

80. M and trapezoidal cell: (0) not connected; (1) connected though crossvein; (2) connected directly. Direct connection of M and tc is inferred to be ancestral for

Dipsocoromorpha, with a single shift to absence of connection in Ceratocombinae, and four shifts to crossvein connection within Schizopteridae.

81. tc: (0) open; (1) closed. Closed tc is ancestral for Dipsocoromorpha, with independent shifts to open in the MRCA of Stemmocryptidae and Dipsocoridae, and in an undescribed genus of Schizopteridae.

82. tc, shape: (0) short; (1) elongate. Elongate trapezoidal cell is plesiomorphic for Schizopteridae and transitioned to being short in MRCA of Schizopterinae. Within Schizopterinae, a reversal to elongate condition is inferred to be a synapomorphy of the *Dundonannus* group.

83. Distal part of Cu: (0) parallel or subparallel with M; (1) curved, not parallel or subparallel with M. Distal part of Cu curved is a plesiomorphic state for Dipsocoromorpha, with two or three independent transitions to parallel state (depending on the reconstruction mode).

84. Wing organ formed by M, with row of processes: (0) absent; (1) present. Wing organ on M vein is a diagnostic synapomorphy of the genus *Chinannus* (Knyshov *et al.* 2016).

85. Wing organ consisting of sclerotized area between wing margin and dc, with cavity and trichomes [?]: (0) absent; (1) present. Wing organ between costal margin and dc evolved two times independently, in the genus *Ogeria* and an undescribed genus from the New World (see Fig. 4).

86. cub: (0) closed cell; (1) open. Open cub cell is a synapomorphy of Schizopterinae except *Silhouettanus*, and according to our reconstructions, independently evolved in the genus *Kaimon*.

87. cub, closed: (0) removed from wing margin; (1) reaching wing margin. Within Dipsocoromorpha, cub reaching wing margin is limited to the genus *Meganannus*.

88. Veins, sculpture: (0) not traced by areoles; (1) traced by areoles. Wing veins traced by areoles are limited to the genus *Peloridinannus*.

89. Forecoxa, shape and size: (0) large, elongate; (1) small, less elongate. Large elongate forecoxae are reconstructed to be synapomorphic for Dipsocoromorpha. Within the infraorder, small forecoxa are a synapomorphy of Hypsipterygidae+Schizopteridae.

90. Metacoxa, adhesive pads: (0) absent; (1) present. Presence / absence of adhesive pads varies within Dipsocoromorpha, and reconstructions of character transitions differ depending on the method. According to our ML reconstruction, the pads are synapomorphic for Dipsocoromorpha, and get reduced two times independently in Ceratocombini and Dipsocoridae.

91. Metacoxa, adhesive pads extension: (0) small and area bearing microtrichia not raised; (1) larger, area bearing microtrichia raised. Large adhesive pads extension is reconstructed to be a synapomorphy of Hypsipterygidae+Schizopteridae.

92. Trochanter, subdivision: (0) not subdivided; (1) subdivided. Subdivided trochanter is a striking yet overlooked synapomorphy of Dipsocoromorpha.

93. Protibia distal expansion: (0) absent; (1) present; (2) extreme. Reconstructions of this character transitions differ depending on the method, but according to our ML

reconstruction, protibial expansion was ancestrally absent in Dipsocoromorpha and was independently acquired in Stemmocryptidae, Ceratocombinae, and Schizopteridae.

94. Mesotibial comb: (0) absent; (1) present. Mesotibial comb is inferred to be ancestral for Dipsocoromorpha, and reduced three times independently in Ceratocombinae, *Hypselosoma*, and a clade within Schizopterinae+"Ogeriinae".

95. Metatibial comb: (0) absent; (1) present. Metatibial comb is reconstructed to be a synapomorphy of Dipsocoromorpha, and underwent five transitions between states within the infraorder, however reconstructions of transition placements differ depending on the method.

96. Hind tibia longitudinal comb: (0) absent; (1) well-developed; (2) short and/or less differentiated. According to our reconstructions, well-developed longitudinal comb is a synapomorphy of Schizopterinae+"Ogeriinae", and within this clade four transitions to absent and three transitions to short comb were inferred.

97. Hind tibia, row of slender setae: (0) absent; (1) capitate, moderately elongate; (2) slender apex, very long. Capitate setae on hind tibia are reconstructed to be a synapomorphy of Schizopterinae+"Ogeriinae", with four reversals to ancestral for Dipsocoromorpha state 0, as well as one transition to having long setae with slender apex.

98. Protarsus, segmentation in male: (0) 3-segmented; (1) 2-segmented; (2) 1-segmented. Male protarsus was inferred to be ancestrally 3-segmented, with nine transitions to 2-segmented.

99. Mesotarsus, segmentation in male: (0) 3-segmented; (1) 2-segmented; (2) 1-segmented. Male mesotarsus was inferred to be ancestrally 3-segmented, with seven transitions to 2-segmented.

100. Metatarsus, segmentation in male: (0) 3-segmented; (1) 2-segmented; (2) 1-segmented. Male metatarsus was inferred to be ancestrally 3-segmented, with six transitions to 2-segmented.

101. Protarsus, segmentation in female: (0) 3-segmented; (1) 2-segmented; (2) 1-segmented. Female protarsus was inferred to be ancestrally 2-segmented, with a single transition to 3-segmented which is synapomorphic for the *Ogeria* group (*Kaimon+Ogeria+Pachyplagia*).

102. Mesotarsus, segmentation in female: (0) 3-segmented; (1) 2-segmented; (2) 1-segmented. Female mesotarsus was inferred to be ancestrally 2-segmented, with a single transition to 3-segmented which is synapomorphic for the *Ogeria* group.

103. Metatarsus, segmentation in female: (0) 3-segmented; (1) 2-segmented; (2) 1-segmented. Reconstructions of this character transitions differ depending on the method, but according to our ML analysis, 3-segmented metatarsus was ancestral for Dipsocoromorpha and seven times transitioned to 2-segmented state.

104. Protarsus much stouter than metatarsus in male: (0) absent; (1) present. Apparent evolutionary history of this character is complex, and according to our ML reconstruction having protarsus enlarged is a synapomoprhy of Dipsocoromorpha, with 10 reversals within the group.

105. Mesotarsus much stouter than metatarsus in male: (0) absent; (1) present. Evolutionary history of this character is similar to 104, except that both *Trichotonannus* and Stemmocryptidae lack mesotarsal expansion.

106. Claws, sculpture: (0) smooth; (1) ventral surface with serration. Serrated claws are limited to the genus *Meganannus*.

107. Claws, symmetry: (0) symmetrical; (1) asymmetrical. Within Dipsocoromorpha, asymmetric claws are a synapomorphy for some species of an undescribed genus of Schizopterinae.

108. Bladder-like arolia on fore- and midlegs in males: (0) absent; (1) present. Reconstructions of this character are ambiguous with respect to the number of origins. From 4 to 7 independent origins (synapomorphies of smaller groups) and 2-4 reversals within Dipsocoromorpha were inferred.

109. Bladder-like arolia: (0) always everted; (1) inflatable. Inflatable arolia are a synapomorphy of Hypselosomatinae.

110. Bladder-like arolia structure: (0) with dorsal sclerite and ventral membranous lobe; (1) only consisting of membranous lobe. Having dorsal sclerite was inferred to a be an independent synapomorphy for Issidomimini, and for a clade within Schizopteridae.

111. Parempodia: (0) setiform; (1) explanate. Setiform parempodia are ancestral for Dipsocoromorpha, and explanate parempodia evolve two or three times independently within Schizopterinae.

112. Abdominal tergites, texture: (0) smooth; (1) with reticulate pattern. Reticulate pattern on the abdominal tergites is a diagnostic synapomorphy of the *Ogeria* group (Hill 2004).

113. S1+2 spiracles: (0) absent; (1) present. S1+2 spiracles were inferred to be plesiomorphic for Dipsocoromorpha, with transition to absent occuring in MRCA of the clade comprised of Ceratocombinae, Dipsocoridae, Hypsipterygidae, and Schizopteridae. Subsequent reversal to present occurred in Hypsipterygidae and Hypselosomatinae except *Hypselosoma*.

114. S3 spiracles: (0) absent; (1) present. S3 spiracles were inferred to be plesiomorphic for Dipsocoromorpha, with one of the transitions to absent being synapomorphic for Dipsocoridae. Reconstruction of the other transitions vary between methods, as these spiracles are absent in *Hypselosoma* and Schizopterinae+"Ogeriinae". According to the ML reconstruction, absent spiracles III are synapomorphic for Schizopterinae, with reversal to present occurring within Hypselosomatinae.

115. S4 spiracles: (0) absent; (1) present. Evolutionary history of this character is similar to character 114.

116. S5 spiracles: (0) absent; (1) present. Evolutionary history of this character is similar to character 114.

117. S6 spiracles: (0) absent; (1) present. Present S6 spiracles are inferred to be ancestral for Dipsocoromorpha, with transition to absent being synapomorphic for the genus *Kokeshia* (Miyamoto 1960; Štys 1985).

118. S7 spiracles: (0) absent; (1) present. Evolutionary history of this character is similar to character 117.

119. S8 spiracles: (0) absent; (1) present. Evolutionary history of this character is similar to character 117.

120. DAG scars 4: (0) absent; (1) present. Absent DAG scars on segment 4 are plesiomorphic for Dipsocoromorpha, with scars being present in some Issidomimini and being an independent synapomorphy of Dipsocoridae.

121. DAG scars 5: (0) absent; (1) present. Evolutionary history of this character is similar to character 120.

122. DAG scars 6: (0) absent; (1) present. Absent DAG scars on segment 6 are plesiomorphic for Dipsocoromorpha, with present scars inferred for the MRCAs of Dipsocoridae and Ceratocombinae.

123. DAG scars 7: (0) absent; (1) present. Absent DAG scars on segment 7 are plesiomorphic for Dipsocoromorpha, and two independent gains were inferred, one is a synapomorphy of *Ceratocombus*, another is a synapomorphy of Schizopteridae.

124. Asymmetry of the pregenital abdomen: (0) none; (1) dextral; (2) sinistral. No pregenital asymmetry was inferred to be plesiomorphic for Dipsocoromorpha. Dextral pregenital asymmetry evolved five times independently, while sinistral pregenital asymmetry is a unique synapomorphy of Dipsocoridae.

125. Male pregenital laterotergites: (0) absent; (1) present. Pregenital laterotergites were inferred to be ancestrally present in Dipsocoromorpha, and became absent in

MRCA of Schizopteridae. Two subsequent reversals to present (in *Silhouettanus* and *Ceratocomboides*) were reconstructed within Schizopterinae.

126. Male, ventrally located spinous laterotergite 4: (0) absent; (1) present. Spinous laterotergite V is a synapomorphy of the genus *Chinannus* (Knyshov *et al.* 2016).

127. Male, process on right side of sternite 5: (0) absent; (1) present. Process of sternite V is a synapomorphy of the clade *Machadonannus*+*Vilhenannus*.

128. Male sternum 7: (0) not covering pygophore; (1) largely or completely covers pygophore. State 1, which is sometimes referred to as subgenital plate, was reconstructed to be ancestrally absent in Dipsocoromorpha and have evolved four times independently in "Ogeriinae" and single time in Schizopterinae (synapomorphy of the clade *Kophaegis*+*Ptenidiophyes*+*Schizoptera*).

129. Processes of male sternum 7: (0) absent; (1) present. Processes on male sternum 7 are a diagnostic synapomorphy of the genus *Schizoptera* (Leon & Weirauch 2017).

130. Pronounced genitalic directionality: (0) none; (1) dextral; (2) sinistral. As was shown in Knyshov *et al.* (2018), male genitalic directionality dramatically varies within Dipsocoromorpha, and placement of character transitions varies depending on the method of reconstruction. According to our ML reconstruction, no directionality is ancestral for Dipsocoromorpha, with shifts to dextral being synapomorphic for Trichotonanninae, and independently for Hypsipterygidae+Schizopteridae. Within Schizopteridae, sinistral directionality is synapomorphic for Hypselosomatinae except *Hypselosoma*, as well as for the earliest diverging "Ogeriinae" species. Transitions to absence of genitalic directionality inferred to have occurred in the MRCA of *Hypselosoma*, and three times

within “Ogeriinae”. Outside of Schizopteridae, sinistral directionality is synapomorphic for Dipsocoridae.

131. Male sternum 8: (0) well developed; (1) indistinct. Reduction of male sternum 8 is a diagnostic synapomorphy of Schizopterinae+”Ogeriinae”.

132. Male, cavity in segment 8: (0) absent; (1) present. Cavity in male segment 8 is a diagnostic synapomorphy for the genera *Dundonannus* and *Semangananus* (Wygodzinsky 1950; Štys 1974).

133. Left male laterotergite 8: (0) not appendage-like; (1) appendage-like. Appendage-like laterotergites 8 were inferred to be a synapomorphy of Dipsocoromorpha, as they are characteristic for three early diverging families. Not appendage-like laterotergites are reconstructed to be synapomorphic for Hypsipterygidae+Schizopteridae, with a reversal to appendage-like in the genus *Chinannus*.

134. Right male laterotergite 8: (0) not appendage-like; (1) appendage-like. With the exception of being absent in *Chinannus*, evolutionary history of the character is same as in character 133.

135. Pygophore, dorsal wall: (0) sclerotized; (1) membranous. Sclerotized dorsal wall of pygophore is reconstructed to be synapomorphic for Dipsocoromorpha, with transitions to membranous in Stemmocryptidae and MRCA of Hypsipterygidae+Schizopteridae.

136. Pygophore, tilt in respect to pregenital abdomen: (0) not tilted; (1) tilted to the side. Not tilted pygophore was reconstructed as a synapomorphy of Dipsocoromorpha, with tilted pygophore being a synapomorphy of the *Schizoptera* genus group (Leon & Weirauch 2017).

137. Left male laterotergite 9: (0) indistinct; (1) distinct. Reconstructions of this character transitions differ depending on the mode, but according to our ML analysis indistinct laterotergite is ancestral for Dipsocoromorpha, and transitions to distinct occurred independently in Stemmocryptidae and in MRCA of the clade comprised of Ceratocombinae, Dipsocoridae, Hypsipterygidae, and Schizopteridae. Subsequent reversals to indistinct laterotergites are synapomorphic for Dipsocoridae, Hypselosomatinae except *Hypselosoma*, and a large clade within Schizopterinae+"Ogeriinae". Within Schizopterinae, laterotergites reappeared two time independently in genera *Silhouettanus* and *Nannocoris*.

138. Right male laterotergite 9: (0) indistinct; (1) distinct. Evolutionary history of this character is similar to character 137, however, distinct right male laterotergite also independently transitioned to being distinct in the genus *Peloridinannus* (Weirauch & Frankenberg 2015).

139. Left paramere: (0) longer than wide; (1) roughly as long as wide. Left paramere was reconstructed to be ancestrally longer than wide and undergo five transitions to being as wide as long and four reversals to longer than wide within Dipsocoromorpha.

140. Right paramere: (0) longer than wide; (1) roughly as long as wide. Right paramere was reconstructed to be ancestrally longer than wide and undergo five transitions to being as wide as long within Dipsocoromorpha. Interestingly, as opposed to left paramere, no reversals to longer than wide state have been inferred.

141. Parameres, symmetry: (0) symmetrical; (1) asymmetrical. Asymmetrical parameres were reconstructed to be a synapomorphy of Dipsocoromorpha, with symmetrical parameres being a synapomorphy of Ceratocombinae.

142. Plane of parameres in respect to longitudinal body axis: (0) perpendicular; (1) deviated. Ancestrally perpendicular in Dipsocoromorpha, plane of parameres deviated six times independently and reverted to perpendicular three times.

143. Male genitalia, support system around anophore = proctiger: (0) absent; (1) present. The support system around anophore is a synapomorphy of Enicocephalomorpha.

144. Middle portion of aedeagus = phallosoma: (0) present; (1) reduced. Presence of phallosoma was reconstructed to be ancestral for Dipsocoromorpha, with a single reduction event synapomorphic for Schizopterinae+"Ogeriinae".

145. Conjunctival appendages: (0) absent; (1) present. Conjunctival appendages were reconstructed to be a synapomorphy of Dipsocoromorpha, with 10 reductions and one reversal occurring within the infraorder.

146. Vesica, length: (0) short, less than 10 times as long as wide; (1) long, more than 10 times as long as wide. Long vesica was reconstructed to be plesiomorphic for Dipsocoromorpha, with shifts to short vesica in Stemmocryptidae, Issidomimini, *Ceratocombus*, and four times within Schizopteridae.

147. Vesica, shape: (0) coiled; (1) not coiled. Coiled vesica was reconstructed to be synapomorphic for Dipsocoromorpha. Within this clade the transition to not coiled

condition is a synapomorphy of Ceratocombinae, and occurred independently in Stemmocryptidae.

148. Vesical processes: (0) absent; (1) present. Vesical processes are relatively rare within Dipsocoromorpha and evolved four times independently within Schizopterinae+"Ogeriinae" clade.

149. Anophore: (0) membranous = absent; (1) sclerotized = present. Sclerotized anophore was reconstructed to be ancestral for Dipsocoromorpha, with independent transitions to membranous in Ceratocombinae (one shift according to MP and two according to ML), and in *Hypselosoma*.

150. Anterior anophoric process: (0) absent; (1) present. Anterior anophoric process is limited to Schizopteridae and was inferred to have evolved eight times independently.

151. Posterior anophoric process: (0) absent; (1) present. Posterior anophoric process was reconstructed to be a synapomorphy of Schizopterinae.

152. Ovipositor: (0) formed by interlocking gonapophyses; (1) with gonapophyses free, not interlocking. Dipsocoromopha were inferred to have ancestrally interlocking gonapophyses, that became free in Stemmocryptidae, Hypsipterygidae, and a clade within Schizopteridae.

153. Gonapophyses, length: (0) short; (1) elongate. Elongate gonapophyses were reconstructed to be ancestral for Dipsocoromorpha and transition to short in the MRCA of Stemmocryptidae and Dipsocoridae, in Hypsipterygidae, and a clade within Schizopteridae.

154. Gonapophyses, armature: (0) without strong teeth; (1) with many strong teeth; (2) with 2-3 strong teeth; (3) with 4 strong teeth; (4) with multiple setigerous tubercles. According to our reconstructions, having many strong teeth is ancestral for Dipsocoromorpha, with multiple transitions to other character states.

155. Spermatheca, sclerotization: (0) heavily sclerotized; (1) weakly sclerotized. Spermatheca was inferred to be ancestrally sclerotized in Dipsocoromorpha with eight transitions to being weakly sclerotized.

156. Spermatheca, structure: (0) without spermathecal gland duct; (1) subdivided into spermathecal duct, reservoir, spermathecal gland duct, and spermathecal gland; (2) gynatrial complex. Spermatheca subdivided into spermathecal duct, reservoir, spermathecal gland duct, and spermathecal gland was reconstructed to be a synapomorphy of Dipsocoromorpha.

157. Spermatheca, reservoir, shape: (0) straight; (1) bent. Shape of spermathecal reservoir was reconstructed to be ancestrally bent and transitioned to straight in the MRCA of Dipsocoridae and Stemmocryptidae, in *Leptonannus*, in Hypsipterygidae, and three times within Schizopteridae.

158. Spermatheca, reservoir, diameter of distal and proximal parts: (0) equal; (1) unequal. Unequal diameter was reconstructed to be ancestral for Dipsocoromorpha and transitioned to equal in Stemmocryptidae, Leptonannus, and a clade within Schizopteridae.

Discussion

Phylogenetic results and revised classification

The monophyly of the infraorder and sister-group relationship with Enicocephalomorpha recovered in our analyses are in accordance with previously published, sparsely sampled analyses (Weirauch & Štys 2014) and analyses across Heteroptera (Wang *et al.* 2017; Weirauch *et al.* 2018b). Our sampling of Dipsocoridae was limited to *Cryptostemma*, which was recovered as monophyletic in our analyses. However, given that three genera of Dipsocoridae differ only in subtle morphological features, the entire family is likely to be monophyletic. The family Ceratocombidae was rendered paraphyletic with respect to Dipsocoridae, Hypsipterygidae, and Schizopteridae, although branch support of the early splitting events is low. Nevertheless, Ceratocombinae and Trichotonanninae were never recovered as sister taxa, and we therefore propose to elevate both Ceratocombinae and Trichotonanninae to family level. The two large clades within Ceratocombidae that were previously treated at the tribal level, Ceratocombini and Issidomimini, are here elevated to subfamily level, i.e. Ceratocombinae and Issidomiminae. According to our phylogenetic inferences, the schizopterid subfamily Ogeriinae is paraphyletic with respect to Schizopterinae, which was supported to be monophyletic. Bootstrap support for some of the early diverging clades of "Ogeriinae" was low, and we therefore refrain from creating several subfamily-level taxa to accommodate these lineages. Instead, we here synonymize "Ogeriinae" with Schizopterinae, thus reducing the number of schizopterid subfamilies to two, Hypselosomatinae and Schizopterinae. The revised higher-level classification of Dipsocoromorpha therefore is as follows:

1. family Stemmocryptidae (single genus *Stemmocrypta*)
2. family Trichotonannidae (single genus *Trichotonannus*)
3. family Dipsocoridae
4. family Ceratocombidae
    a. subfamily Ceratocombinae
    b. subfamily Issidomiminae
5. family Hypsipterygidae (single genus *Hypsipteryx*)
6. family Schizopteridae
    a. subfamily Hypselosomatinae
    b. subfamily Schizopterinae

Major synapomorphic and diagnostic features of the taxa proposed in the revised classification

Infraorder Dipsocoromorpha:

- Antenna with scape and pedicel very short and long flagellomeres, scape and pedicel much stouter than flagellomeres (30-0 and 32-0)
- Metacoxal adhesive pads present (90-1)
- Subdivided trochanters (92-1)
- Bladder-like arolia in males present (104-1)
- Parameres asymmetrical (141-1)
- Spermatheca subdivided into spermathecal duct, reservoir, and spermathecal gland (156-1)

Family Stemmocryptidae:

- Small eyes (7-2)
- Pronotal collar absent (38-0)
- Metathoracic gland with metasternum and precoxale as evaporatorium (51-3)
- Protibia with distal expansion (93-1)

Family Trichotonannidae:

- Dextral asymmetry of pregenital abdomen (124-1) and dextral genitalic directionality (130-1)
- Plane of parameres in respect to longitudinal body axis not perpendicular (142-1)
- Weakly sclerotized spermatheca (155-1)

Family Dipsocoridae

- Metathoracic gland, evaporatory area with mushroom bodies (51-4)
- Metacoxal adhesive pads absent (90-0)
- Mesotarsus much stouter than metatarsus in male (105-1)
- DAG scars on segment 4 (120-1) and 6 (122-1) present
- Sinistral asymmetry of pregenital abdomen (124-2) and sinistral genitalic directionality (130-2)
- Plane of parameres in respect to longitudinal body axis not perpendicular (142-1)

Family Ceratocombidae

- Protibia with distal expansion present (94-1)
- Parameres symmetrical (141-0)
- Vesica short (146-0)
- Vesica not coiled (147-1)

Subfamily Ceratocombinae

- Metacoxal adhesive pads absent (90-0)
- Protarsus not much stouter than metatarsus in male (104-0)

Subfamily Issidomiminae

- Vertex/frons scars distinct (4-1)
- Pronotum wider than long (35-0)
- Pronotal collar absent (38-0)
- Metatarsus 3-segmented in male (100-1)
- Mesotarsus much stouter than metatarsus in male (105-1)
- Bladder-like arolia on fore- and mid legs in male present (108-1)

Family Hypsipterygidae

- Ocelli in male absent (8-0)
- Scutellum small (43-0)
- All male legs 2-segmented (98-1, 99-1, 100-1)

- Protarsus similar to metatarsus in male (104-0)
- Ovipositor with gonapophyses free, not interlocking (152-1)

Family Schizopteridae

- Head wider than high (1-0)
- Frons/vertex muscle scars distinct (4-1)
- 3rd labial segment short (25-0)
- Proepisternum inflated (46-1)
- Metendosternite present (57-1)
- Male pregenital laterotergites absent (125-0)

Subfamily Hypselosomatinae

- Frons with pit-like structures ventrad of ocelli (6-1)
- Eyes in frontal view ½ of synthlipsis (7-1)
- Bladder-like arolia on male fore- and mid legs present (108-1)
- Bladder-like arolia apparently inflatable (109-1)

Subfamily Schizopterinae

- Anterior and posterior groups of scars on frons/vertex (5-1)
- Hind tibia longitudinal comb well developed (96-1)
- Hind tibia row of slender setae with capitate and moderately elongate setae (97-1)

- Male sternum VIII indistinct (131-1)
- Middle portion of aedeagus = Phallosoma reduced (144-1)

Potential of integrating legacy and NGS data

We successfully integrated traditional Sanger sequencing data with cost effective Next Generation Sequencing approaches. Our results show that approximately doubled amount of sequence data for ~20% of taxa, belonging to all major lineages, can improve the robustness of the reconstruction. The method of utilizing a mixture of PCR generated baits from across the infraorder proved effective to enrich for relatively conserved ribosomal genes across a selection of very divergent taxa. On the other hand, obtaining mitochondrial data was less successful, and phylogenetic signal of mitochondrial genes appeared to be ineffective for reconstructing deeper level relationships, or signal was obscured by the large proportion of missing data.

Evolutionary history of selected morphological characters

We reconstructed the evolutionary history of selected features that are characteristic for and variable within the infraorder (Fig. 6.6). The first set of characters (60-62) represent changes in wing type in both sexes, as these changes are known to be dimorphic, as well as in presence and absence of beetle-like, or elytriform, forewings. Our results show congruence with genus level insights of Leon and Weirauch (2017) on a much larger scale. Transitions to submacropterous conditions in males (60-1) are inferred to having occurred 12 times, while similar transitions in females (61-1) occurred 22 times, including one shift to microptery (61-2). Beetle-like forewings in either females or both

sexes originated 16 times (62-1) across Dipsocoromorpha, with the majority of transitions occurring within Schizopteridae, but also two in Ceratocombidae and once in Dipsocoridae.

The bladder-like arolium on the pretarsus of Dipsocoromorpha is unique among Heteroptera, and when present, is limited to the fore and mid legs of males, while females never possess this structure. Although no direct observations have been made that provide insights into the function of these structures, their occurrence in males only and on the two pairs of legs that may be most critical for holding onto the female during mating, may suggest a role in the context of mating behaviors. Our reconstructions show the origin of these bladder-like arolia in the MRCA of Dipsocoromorpha, with a series of subsequent losses and gains throughout the infraorder. The fine structure of arolia in Hypselosomatinae differs considerably from those in other Dipsocoromorpha (109-1) and Schizopteridae and Issidomiminae possess a sclerite dorsally on the arolium (110-0), potentially supporting the notion of independently derived arolia within the infraorder.

Dipsocoromorpha are also among the few groups of Heteroptera that are capable of moving by jumping considerable distances. We inferred jumping behaviors by observing the presence or absence of coxal pads (90-1) that are thought to be involved in jumping behaviors. Our inference suggests a single origin of these structures in the MRCA of Dipsocoromorpha and two independent losses in Ceratocombidae and Dipsocoridae, respectively.

Finally, and as documented in Knyshov *et al.* (2018), the diversity of male genitalic structures in Dipsocoromorpha is astounding. We reconstructed the evolutionary history

of male pregenital asymmetry (124) as an indicator of strong genitalic modifications, and male genitalic directionality (130) as a potentially more homoplastic character system. Our results indicate that the pregenital abdomen was ancestrally symmetrical without prominent genitalic directionality, as it is in most other Heteroptera. Genitalic directionality independently shifted twice from symmetrical to dextral asymmetry (in Trichotonannidae and in the clade of Hypsipterygidae + Schizopteridae), and three times to sinistral asymmetry (in Dipsocoridae, Hypselosomatinae except *Hypselosoma*, and in an undescribed genus of Schizopterinae). More dramatic pregenital asymmetry has evolved six times independently, with five shifts being to dextral and one to sinistral asymmetry. These patterns likely suggest a range of different mating positions (Huber *et al.* 2007; Huber 2011) and could represent an intriguing system to study the functional morphology and evolution of genitalic structures in a closely related group of organisms.

References

Azar, D. & Nel, A. (2010) The earliest fossil schizopterid bug (Insecta: Heteroptera) in the Lower Cretaceous amber of Lebanon. *Annales de la Société entomologique de France* 46, 193–197.

Azar, D., Nel, A., Coty, D. & Garrouste, R. (2010) The second fossil ceratocombid bug from the Miocene amber of Chiapas (Mexico) (Hemiptera: Ceratocombidae). *Annales de la Société entomologique de France* 46(1-2), 100–102.

Bankevich, A., Nurk, S., Antipov, D., Gurevich, A. A., Dvorkin, M., Kulikov, A. S., Lesin, V. M., Nikolenko, S. I., Pham, S., Prjibelski, A. D., Pyshkin, A. V., Sirotkin, A. V., Vyahhi, N., Tesler, G., Alekseyev, M. A. & Pevzner P. A. (2012) SPAdes: a new genome assembly algorithm and its applications to single-cell sequencing. *Journal of Computational Biology* 19(5), 455-477.

Bechly, G. & Wittmann, M. (2000) Two new tropical bugs (Insecta: Heteroptera: Thaumastocoridae - Xylastodorinae and Hypsipterygidae) from Baltic amber. *Stuttgarter Beiträge zur Naturkunde: Serie B (Geologie und Paläontologie)* 289, 1–11.

Bolger, A. M., Lohse, M. & Usadel, B. (2014) Trimmomatic: a flexible trimmer for Illumina sequence data. *Bioinformatics* 30(15), 2114-2120.

Carpintero, D. L. & Dellapé, P. M. (2006) *Williamsocoris*, a new genus of Schizopteridae (Heteroptera) from Argentina. *Zoological Science* 23(7), 653–655.

Emsley, M. G. (1969) The Schizopteridae (Hemiptera: Heteroptera) with the descriptions of new species from Trinidad. *Memoirs of the American Entomological Society* 25, 1–154.

Forero, D., Berniker, L. & Weirauch, C. (2013) Phylogeny and character evolution in the bee-assassins (Insecta: Heteroptera: Reduviidae). *Molecular Phylogenetics and Evolution* 66, 283–302.

Frankenberg, S., Hoong, C., Knyshov, A. & Weirauch, C. (2018) Heads up: evolution of exaggerated head length in the minute litter bug genus *Nannocoris* Reuter (Hemiptera: Schizopteridae). *Organisms Diversity & Evolution* 18, 211–224.

Giribet, G., Carranza, S., Baguñà, J., Riutort, M. & Ribera, C. (1996) First molecular evidence for the existence of a Tardigrada + Arthropoda clade. *Molecular Biology and Evolution* 13, 76–84.

Goloboff, P.A. & Catalano, S.A. (2016) TNT version 1.5, including a full implementation of phylogenetic morphometrics. *Cladistics* 32, 221–238.

Gouy, M., Guindon, S. & Gascuel, O. (2009) SeaView version 4: a multiplatform graphical user interface for sequence alignment and phylogenetic tree building. *Molecular Biology and Evolution* 27, 221–224.

Hartung, V., Garrouste, R. & Nel, A. (2017) The first fossil Dipsocoridae found in the early Eocene amber of France (Hemiptera: Heteroptera). *Comptes Rendus Palevol* 16, 715–720.

Hill, L. (2015) Three new genera of Schizopteridae from Australia with description of six new species (Hemiptera: Heteroptera: Schizopteridae). *Zootaxa* 3990, 73–96.

Hill, L. (2013) A revision of *Hypselosoma* Reuter (Insecta: Heteroptera: Schizopteridae) from New Caledonia. *Memoirs of the Queensland Museum* 56, 407–455.

Hill, L. (2004) *Kaimon* (Heteroptera: Schizopteridae), a new, speciose genus from Australia. *Memoirs of the Queensland Museum* 49, 603–647.

Hill, L. (1990) Australian *Ogeria* Distant (Heteroptera: Schizopteridae). *Invertebrate Systematics* 4, 697–720.

Hill, L. (1987) Four new Australian species of *Hypselosoma* Reuter (Heteroptera: Schizopteridae). *Australian Journal of Entomology* 26(3), 265–278.

Hill, L. (1984) New genera of Hypselosomatinae (Heteroptera: Schizopteridae) from Australia. *Australia Journal of Zoology, Supplementary Series* 103, 1–55.

Hoey-Chamberlain, R. & Weirauch, C. (2016) Two new genera of big-eyed minute litter bugs (Hemiptera, Schizopteridae, Hypselosomatinae) from Brazil and the Caribbean. *ZooKeys* 640, 79–102.

Huber, B. A. (2010) Mating positions and the evolution of asymmetric insect genitalia. *Genetica* 138(1), 19-25.

Huber, B. A., Sinclair, B. J. & Schmitt, M. (2007) The evolution of asymmetric genitalia in spiders and insects. *Biological Reviews* 82(4), 647-698.

Katoh, K. & Standley, D. M. (2013) MAFFT multiple sequence alignment software version 7: improvements in performance and usability. *Molecular Biology and Evolution* 30(4), 772-780.

Knyshov, A., Gordon, E. & Weirauch, C. Cost-efficient high throughput capture of museum arthropod specimen DNA using PCR-generated baits. Methods in Ecology and Evolution, in review.

Knyshov, A., Hoey-Chamberlain, R. & Weirauch, C. (2018) Comparative morphology of male genitalic structures in the minute litter bugs Dipsocoromorpha (Insecta: Hemiptera: Heteroptera). *Journal of Morphology* 279, 1480–1517.

Knyshov, A., Leon, S., Hoey-Chamberlain, R. & Weirauch, C. (2016) *Pegs, pouches, and spines: systematics and comparative morphology of the New World litter bug genus Chinannus Wygodzinsky, 1948*. Entomological Society of America, Annapolis, MD.

Leon, S. & Weirauch, C. (2017) Molecular phylogeny informs generic and subgeneric concepts in the *Schizoptera* Fieber genus group (Heteroptera: Schizopteridae) and reveals multiple origins of female-specific elytra. *Invertebrate Systematics* 31, 191–207.

Leon, S. & Weirauch, C. (2016a) Small Bugs, Big Changes: Taxonomic Revision of *Orthorhagus* McAtee & Malloch. *Neotropical Entomology*, 1–14.

Leon, S. & Weirauch, C. (2016b) Scratching the surface? Taxonomic revision of the subgenus *Schizoptera* (*Odontorhagus*) reveals vast undocumented biodiversity in the largest litter bug genus *Schizoptera* Fieber (Hemiptera: Dipsocoromorpha). *Zootaxa* 4184, 30.

McAtee, W.L. & Malloch, J.R. (1925) Revision of bugs of the family Cryptostemmatidae in the collection of the United States National Museum. *Proceedings of the United States National Museum* 67, 1–42.

Menard, K. L., Schuh, R. T. & Woolley, J. B. (2014) Total-evidence phylogenetic analysis and reclassification of the Phylinae (Insecta: Heteroptera: Miridae), with the recognition of new tribes and subtribes and a redefinition of Phylini. *Cladistics* 30(4), 391-427.

Miyamoto, S. (1960) A new genus of Schizopterinae from Japan (Heteroptera, Dipsocoridae). *Sieboldia Fukuoka* 2, 163–170.

Paradis, E., Claude, J. & Strimmer, K. (2004) APE: analyses of phylogenetics and evolution in R language. *Bioinformatics* 20(2), 289-290.

Perrichot, V., Nel, A.E. & Neraudeau, D. (2007) Schizopterid bugs (Insecta: Heteroptera) in mid-Cretaceous ambers from France and Myanmar (Burma). *Palaeontology* 50, 1367–1374.

Poinar, G. Jr & Brown, A. (2014) New genera and species of Jumping Ground Bugs (Hemiptera: Schizopteridae) in Dominican and Burmese amber, with a description of a meloid (Coleoptera: Meloidae) triungulin on a Burmese specimen. *Annales de la Société entomologique de France (N.S.): International Journal of Entomology* 50, 372–381.

Rédei, D. (2008) First record of *Pinochius* Carayon, 1949 from the Oriental Region, with description of a new species from Vietnam (Heteroptera: Schizopteridae). In: S. Grozeva and N. Simov (eds.), *Advances in Heteroptera research: festschrift in honor of 80th anniversary of Michail Josifov*. Pensoft Publishers, Sofia, Bulgaria, 327–337.

Rédei, D. (2007) A new species of the family Hypsipterygidae from Vietnam, with notes on the hypsipterygid fore wing venation (Heteroptera, Dipsocoromorpha). *Deutsche Entomologische Zeitschrift* 54, 43–50.

Reuter, O.M. (1894) Monographia Ceratocombidarum orbis terrestris. *Acta Societatis Scientiarum Fennica* 6, 1–28.

Sahlberg, J. (1875) Synopsis Armphibicorisarum et Hydrocorisarum Fenniae. *Notiser ur Sällskapets pro Fauna et Flora Fennica förhandlingar* 9, 241–301.

Stamatakis, A. (2014) RAxML version 8: a tool for phylogenetic analysis and post-analysis of large phylogenies. *Bioinformatics* 30(9), 1312-1313.

Stamatakis, A., Hoover, P. & Rougemont, J. (2008) A rapid bootstrap algorithm for the RAxML web servers. *Systematic Biology* 57(5), 758-771.

Štys, P. (1985) Two new species of *Kokeshia* (Heteroptera, Schizopteridae) from Nepal and appraisal of alleged synapomorphies of Paraneoptera. *Acta Entomologica Bohemoslovaca* 82, 187–205.

Štys, P. (1983) A new family of Heteroptera with dipsocoromorphan affinities from Papua New Guinea. *Acta Entomologica Bohemoslovaca* 80, 256–292.

Štys, P. (1982) A new genus and species of Schizopteridae with porrect head from Papua New Guinea (Heteroptera). *Acta Entomologica Bohemoslovaca* 79, 450–456.

Štys, P. (1974) *Semangananus mirus* gen. n., sp. n. from Celebes - a bug with accessory male genitalia (Heteroptera, Schizopheridae). *Acta Entomologica Bohemoslovaca* 71(6), 382–397.

Štys, P. (1970) On the morphology and classification of the family Dipsocoridae s. lat., with particular reference to the genus *Hypsipteryx* Drake (Heteroptera). *Acta Entomologica Bohemoslovaca* 67, 21–46.

Štys, P. (1958) *Ceratocombus* (*Xylonannus*) *kunsti* n. sp.- a new species of Dipsocoridae from Czechoslovakia (Heteroptera). *Acta Societatis Entomologicae Cechoslovenicae* 55, 372–379.

Štys, P., Kerzhner, I. 1975. Rank and nomenclature of higher taxa in recent Heteroptera. *Acta Entomologica Bohemoslovaca* 72, 65–79.

Uhler, P.R. (1904) List of Hemiptera-Heteroptera of Las Vegas hot springs, New Mexico, collected by Messrs E. A. Schwarz & Herbert S. Barber. *Proceedings of the United States National Museum* 27, 349–364.

Wang, Y.-H., Wu, H.-Y., Rédei, D., Xie, Q., Chen, Y., Chen, P.-P., Dong, Z.-E., Dang, K., Damgaard, J., Štys, P., Wu, Y.-Z., Luo, J.-Y., Sun, X.-Y., Hartung, V., Kuechler, S.M., Liu, Y., Liu, H.-X. & Bu, W.-J. (2017) When did the ancestor of true bugs become stinky? Disentangling the phylogenomics of Hemiptera–Heteroptera. *Cladistics* 2017, 1–25.

Weirauch, C. (2012) *Voragocoris schuhi*, a new genus and species of Neotropical Schizopterinae (Hemiptera: Schizopteridae). *Entomologia Americana* 118, 285–294.

Weirauch, C. & Frankenberg, S. (2015) From "insect soup" to biodiversity discovery: taxonomic revision of *Peloridinannus* Wygodzinsky, 1951 (Hemiptera: Schizopteridae), with description of six new species. *Arthropod Systematics and Phylogenetics* 73(3), 457–475.

Weirauch, C., Hoey-Chamberlain, R. & Knyshov, A. (2018a) Synopsis of Schizopteridae (Hemiptera, Heteroptera, Dipsocoromorpha) from the United States, with description of seven new species from the US and Mexico. *ZooKeys* 796, 49–82.

Weirauch, C. & Munro, J.B. (2009) Molecular phylogeny of the assassin bugs (Hemiptera: Reduviidae), based on mitochondrial and nuclear ribosomal genes. *Molecular Phylogenetics and Evolution* 53, 287–299.

Weirauch, C. & Schuh, R.T. (2011) Systematics and evolution of Heteroptera: 25 Years of Progress. *Annual Review of Entomology* 56, 487–510.

Weirauch, C., Schuh, R.T., Cassis, G. & Wheeler, W.C. (2018b) Revisiting habitat and lifestyle transitions in Heteroptera (Insecta: Hemiptera): insights from a combined morphological and molecular phylogeny. *Cladistics* 2018, 1–39.

Weirauch, C. & Štys, P. (2014) Litter bugs exposed: phylogenetic relationships of Dipsocoromorpha (Hemiptera: Heteroptera) based on molecular data. *Insect Systematics & Evolution* 45, 351–370.

Weirauch, C., Whorrall, K., Knyshov, A. & Hoey-Chamberlain, R. (2018) Giant among dwarfs: *Meganannus lewisi*, gen. n. and sp. n., a new genus and species of minute litter bugs from Costa Rica (Hemiptera: Schizopteridae). *Zootaxa* 4370(2), 156–170.

Wygodzinsky, P. (1960) Un nouvel *Hypeslosoma* de Madagascar, avec la description d'autre especes et des observations sur le genre (Schizopterinae, Dipsocoridae, Hemiptera). *Memoires de l'Institut Scientifique de Madagascar (E)* 11(1959), 509–539.

Wygodzinsky, P. (1959) A new hemipteran (Dipsocoridae) from the Miocene amber of Chiapas, Mexico. *Journal of Paleontology* 33, 853–854.

Wygodzinsky, P. (1953) Cryptostemmatinae from Angola (Cryptostemmatidae, Hemiptera). *Publicaçoes Culturais Da Companhia de Diamantes de Angola* 16, 29–47.

Wygodzinsky, P. (1951) Descripcion de generos y especies nuevos de la familia Cryptostemmatidae (Hemiptera). *Revista Brasileira de Biologia* 11, 259–270.

Wygodzinsky, P. (1950) Schizopterinae from Angola (Cryptostemmatidae, Hemiptera). *Publicacoes Culturais Mus Dundo Companhia Diamantes Angola Lisbon* 7, 9–47.

Wygodzinsky, P. (1948) Contributions towards the knowledge of the genus *Cryptostemma* Herrich-Schaeffer, 1835 (Cryptostemmatidae, Hemiptera). *Revista de Entomologia* 19, 283–294.

Wygodzinsky, P. (1947) Sobre um novo genero e uma nova especie de Schizopterinae do Brasil (Cryptostemmatidae, Hemiptera). *Boletin de Entomologia Venezolana* 6, 25–35.

Yu, G., Smith, D. K., Zhu, H., Guan, Y. & Lam, T. T. Y. (2016) ggtree: an R package for visualization and annotation of phylogenetic trees with their covariates and other associated data. *Methods in Ecology and Evolution* 8(1), 28-36.

Table 6.1. Information on specimens, used in this study.

Name in analysis	Infraorder	Family	Subfamily	Tribe / genus group	USI	Depository	Source	18S	28S 5'	28S 3'
Ochterus_marginatus_GB	Nepomorpha				N/A	N/A	Genbank	KJ461251	KJ461315	
Ranatra_chinensis_GB	Nepomorpha				N/A	N/A	Genbank	KJ461186		
Macrovelia_hornii	Gerromorpha				N/A	N/A	Genbank	AY252196	AY252450	
Ptilomera_tigrina_GB	Gerromorpha				N/A	N/A	Genbank	KJ461233	JF719825	
Mesovelia_mulsanti	Gerromorpha				N/A	N/A	Genbank	AY252123	EU871213	
Enicocephalus_cubanus_GB	Enicocephalomorpha				N/A	N/A	Genbank	KJ461314	KJ461254	
Enicoceph_FG_79	Enicocephalomorpha				UCR_ENT 00078137	UCR	Sanger		TBA	
Enicocephalinae_Thai_133	Enicocephalomorpha				UCR_ENT 00077019	TIGER	Sanger	KF781214	TBA	
Enicocephalinae_sp_Ecu_150	Enicocephalomorpha				UCR_ENT 00057554	UCR	Sanger	KF781212	KF781249	
Enicoceph_Thai_128	Enicocephalomorpha				UCR_ENT 00057552	TIGER	Sanger		TBA	
Enicocephalinae_sp_Nig_137	Enicocephalomorpha				UCR_ENT 00057553	UCR	Sanger	KF781213	KF781250	
Cryptostemma_sp_Peru_251	Dipsocoromorpha	Dipsocoridae			UCR_ENT 00057530	UCR	Sanger	KF781211	KF781248	
Cryptostemma_sp_Peru_4993	Dipsocoromorpha	Dipsocoridae			UCR_ENT 00120572	UCR	Illumina, PROBE	TBA	TBA	
Cryptostemma_sp_Peru_249	Dipsocoromorpha	Dipsocoridae			UCR_ENT 00057528	UCR	Sanger	KF781210	KF781210	
Cryptostemma_wygodzinskyi_GB	Dipsocoromorpha	Dipsocoridae			N/A	N/A	Genbank	KJ461279	KJ461206	
Cryptostemma_alienum	Dipsocoromorpha	Dipsocoridae			N/A	N/A	Genbank	KX822001	KX822002	
Cryptostemma_sp_WCW2003	Dipsocoromorpha	Dipsocoridae			N/A	N/A	Genbank	AY252301		
Leptonannus_sp_Borneo_00036782	Dipsocoromorpha	Ceratocombidae	Ceratocombinae	Ceratocombini	UCR_ENT 00036782	UCD	Illumina	TBA	TBA	
Ceratocombus_Thai_97	Dipsocoromorpha	Ceratocombidae	Ceratocombinae	Ceratocombini	UCR_ENT 00067655	TIGER	Sanger		TBA	
Ceratocombus_Xylonannus_sp_Ecu_152	Dipsocoromorpha	Ceratocombidae	Ceratocombinae	Ceratocombini	UCR_ENT 00057550	UCR	Sanger		KF781201	
Ceratocombus_Ceratocombus_sp_Thai_107	Dipsocoromorpha	Ceratocombidae	Ceratocombinae	Ceratocombini	UCR_ENT 00057538	TIGER	Sanger	KF781205	KF781237	
Ceratocombus_Ceratocombus_sp_Thai_105	Dipsocoromorpha	Ceratocombidae	Ceratocombinae	Ceratocombini	UCR_ENT 00057537	TIGER	Sanger	KF781203	KF781235	
Ceratocombus_Ceratocombus_sp_Thai_113	Dipsocoromorpha	Ceratocombidae	Ceratocombinae	Ceratocombini	UCR_ENT 00057542	TIGER	Sanger		KF781239	
Ceratocombus_vagans_247	Dipsocoromorpha	Ceratocombidae	Ceratocombinae	Ceratocombini	UCR_ENT 00057521	UCR	Sanger	KF781242	KF781207	
Ceratocombus_sp_GB	Dipsocoromorpha	Ceratocombidae	Ceratocombinae	Ceratocombini	N/A	N/A	Genbank	KJ461176	KJ461241	
Ceratocombus_Xylonannus_sp_Bru_135	Dipsocoromorpha	Ceratocombidae	Ceratocombinae	Ceratocombini	UCR_ENT 00057547	UCR	Sanger	KF781200	KF781231	
Ceratocombus_Xylonannus_sp_Ecu_125	Dipsocoromorpha	Ceratocombidae	Ceratocombinae	Ceratocombini	UCR_ENT 00057546	UCR	Sanger	KF781202	KF781233	
Ceratocombus_Xylonannus_sp_Thai_116	Dipsocoromorpha	Ceratocombidae	Ceratocombinae	Ceratocombini	UCR_ENT 00057544	TIGER	Sanger	KF781206	KF781240	
Ceratocombus_sp_Thai_102	Dipsocoromorpha	Ceratocombidae	Ceratocombinae	Ceratocombini	UCR_ENT 00057536	TIGER	Sanger	KF781204	KF781236	
Ceratocombus_Xylonannus_sp_Bru_139	Dipsocoromorpha	Ceratocombidae	Ceratocombinae	Ceratocombini	UCR_ENT 00057548	UCR	Sanger	KF781201	KF781232	
Ceratocombus_Xylonannus_sp_Thai_76	Dipsocoromorpha	Ceratocombidae	Ceratocombinae	Ceratocombini	UCR_ENT 00057535	TIGER	Sanger		KF781241	
Ceratocombus_Ceratocombus_sp_Thai_109	Dipsocoromorpha	Ceratocombidae	Ceratocombinae	Ceratocombini	UCR_ENT 00057540	TIGER	Sanger		KF781238	
Issidomimini_sp_Malaysia_6813	Dipsocoromorpha	Ceratocombidae	Ceratocombinae	Issidomimini	UCR_ENT 00120040	CDFA	Sanger		TBA	
Issidomimini_Cambodia_2364	Dipsocoromorpha	Ceratocombidae	Ceratocombinae	Issidomimini	UCR_ENT 00088926	MHNG	Sanger		TBA	
Kvamula_sp_Madagascar_2043	Dipsocoromorpha	Ceratocombidae	Ceratocombinae	Issidomimini	UCR_ENT 00045585	CAS	Sanger		MK087702	

Issidomimini_sp_Thailand_7196	Dipsocoromorpha	Ceratocombidae	Ceratocombinae	Issidomimini	UCR_ENT 00099070	TIGER	Sanger		TBA
Issidomimini_Cameroon_4361	Dipsocoromorpha	Ceratocombidae	Ceratocombinae	Issidomimini	UCR_ENT 00118997	UCR	Sanger	TBA	TBA
Issidomimini_Cameroon_2838	Dipsocoromorpha	Ceratocombidae	Ceratocombinae	Issidomimini	UCR_ENT 00086455	UCR	Sanger	TBA	TBA
Hypselosoma_sp_Madagascar_1942	Dipsocoromorpha	Schizopteridae	Hypselosomatinae		UCR_ENT 00079083	CAS	Sanger	TBA	TBA
Hypselosoma_sp_Madagascar_1949	Dipsocoromorpha	Schizopteridae	Hypselosomatinae		UCR_ENT 00079090	CAS	Sanger		TBA
Hypselosoma_pauliani_Madagascar_2037	Dipsocoromorpha	Schizopteridae	Hypselosomatinae		UCR_ENT 00044861	CAS	Illumina	TBA	TBA
Hypselosoma_sp_Thailand_3024	Dipsocoromorpha	Schizopteridae	Hypselosomatinae		UCR_ENT 00084969	UCR	Sanger	TBA	TBA
Hypselosoma_sp_Vietnam_4594	Dipsocoromorpha	Schizopteridae	Hypselosomatinae		UCR_ENT 00091524	FSCA	Sanger		TBA
Hypselosoma_sp_India_2396	Dipsocoromorpha	Schizopteridae	Hypselosomatinae		UCR_ENT 00088949	MHNG	Sanger		TBA
Hypselosomatinae_sp_Brazil_3677	Dipsocoromorpha	Schizopteridae	Hypselosomatinae		UCR_ENT 00111639	UFRJ	Sanger	TBA	TBA
Rectilamina_sp_Thai_12	Dipsocoromorpha	Schizopteridae	Hypselosomatinae		UCR_ENT 00057525	TIGER	Sanger	KF781216	KF781252
Rectilamina_sp1_Thailand_1450	Dipsocoromorpha	Schizopteridae	Hypselosomatinae		UCR_ENT 00084928	TIGER	Sanger	TBA	TBA
Rectilamina_spinosisura_Australia_1005	Dipsocoromorpha	Schizopteridae	Hypselosomatinae		UCR_ENT 00081325	UCRC	Sanger	TBA	TBA
Rectilamina_australis_Australia_449	Dipsocoromorpha	Schizopteridae	Hypselosomatinae		UCR_ENT 00086089	UCR	Sanger	TBA	TBA
Hyselosomatinae_sp4_Cuba_5870	Dipsocoromorpha	Schizopteridae	Hypselosomatinae		UCR_ENT 00091115	FMNH	Sanger	MF661998	MF662020 MF662059
Hypselosomatinae_sp_FG_361	Dipsocoromorpha	Schizopteridae	Hypselosomatinae		UCR_ENT 00084398	UCR	Sanger	TBA	TBA
Williamsocoris_sp_Trinidad_2643	Dipsocoromorpha	Schizopteridae	Hypselosomatinae		UCR_ENT 00088667	UCR	Sanger	MF662014	MF662052 MF662090
Ommatides_sp11_Peru_412	Dipsocoromorpha	Schizopteridae	Hypselosomatinae		UCR_ENT 00086134	UCR	Sanger	TBA	TBA
Ommatides_sp2_Trinidad_2659	Dipsocoromorpha	Schizopteridae	Hypselosomatinae		UCR_ENT 00088130	UCR	Sanger	KU315259	KX810857 KU315296
Williamsocoris_sp_Peru_171	Dipsocoromorpha	Schizopteridae	Hypselosomatinae		UCR_ENT 00057523	UCR	Sanger	KF781229	KF781264
Hypselosomatinae_sp_Colombia_819	Dipsocoromorpha	Schizopteridae	Hypselosomatinae		UCR_ENT 00077426	SHARKEY	Sanger		TBA
Glyptocombus_sp_FL_4274	Dipsocoromorpha	Schizopteridae	Hypselosomatinae		UCR_ENT 00012051	FSCA	Sanger	TBA	TBA
Glyptocombus_saltator_4203	Dipsocoromorpha	Schizopteridae	Hypselosomatinae		UCR_ENT 00094273	TAMU	Sanger	MF661996	KX810856 KU315295
Meganannus_CostaRica_3365	Dipsocoromorpha	Schizopteridae	Ogeriinae		UCR_ENT 00014802	INBio	Illumina	TBA	TBA
Guapinannus_sp_9144	Dipsocoromorpha	Schizopteridae	Ogeriinae		N/A	N/A	Illumina	TBA	TBA
Guapinannus_sp_Nicaragua_6083	Dipsocoromorpha	Schizopteridae	Ogeriinae		UCR_ENT 00101103	FMNH	Sanger		MF662018 MF662057
Kokeshia_Vietnam_4627	Dipsocoromorpha	Schizopteridae	Ogeriinae		UCR_ENT 00091486	FSCA	Sanger	KT272761	KT224615 KT272752
Kokeshia_sp_Thailand_1692	Dipsocoromorpha	Schizopteridae	Ogeriinae		UCR_ENT 00086185	TIGER	Illumina, PROBE	TBA	TBA
Kokeshia_sp_Thailand_1409	Dipsocoromorpha	Schizopteridae	Ogeriinae		UCR_ENT 00063170	TIGER	Sanger	KT272760	KT224614 KT272751
Kokeshia_xiei_GB	Dipsocoromorpha	Schizopteridae	Ogeriinae		N/A	N/A	Genbank	KJ461266	JF719827
Ogeriinae_Cameroon_2679	Dipsocoromorpha	Schizopteridae	Ogeriinae		UCR_ENT 00084970	UCR	Sanger	TBA	TBA
Ogeriinae_Cameroon_3355	Dipsocoromorpha	Schizopteridae	Ogeriinae		UCR_ENT 00084974	UCR	Sanger	TBA	TBA
Undescribed_Colombia_633	Dipsocoromorpha	Schizopteridae	Ogeriinae		UCR_ENT 00074536	SHARKEY	Illumina	TBA	TBA
Kaimon_sp_Bru_134	Dipsocoromorpha	Schizopteridae	Ogeriinae		UCR_ENT 00004816	UCR	Sanger	KF781219	TBA
Kaimon_sp_Australia_4990	Dipsocoromorpha	Schizopteridae	Ogeriinae		UCR_ENT 00119012	UCR	Illumina	TBA	TBA
cf_Ogeria_insularis_Madagascar_2085	Dipsocoromorpha	Schizopteridae	Ogeriinae		UCR_ENT 00045446	CAS	Sanger		TBA
Ogeria_sp_Thailand_1560	Dipsocoromorpha	Schizopteridae	Ogeriinae		UCR_ENT 00086442	TIGER	Sanger	TBA	TBA
Pachyplagia_sp_Australia_9130	Dipsocoromorpha	Schizopteridae	Ogeriinae		UCR_ENT 00128015	UCR	Illumina, PROBE	TBA	TBA
nr_Nannodictyus_sp_Thai_238	Dipsocoromorpha	Schizopteridae	Schizopterinae		UCR_ENT 00057524	TIGER	Sanger	KF781218	KF781254

nr_Nannodictyus_sp_Malaysia_9214	Dipsocoromorpha	Schizopteridae	Schizopterinae		N/A	UCR	Illumina	TBA	TBA	
Nannocoris_sp5_Peru_CR_349	Dipsocoromorpha	Schizopteridae	Schizopterinae		UCR_ENT 00077899	UCR	Sanger	TBA	KX810860	KU315299
Nannocoris_sp_CR_4259	Dipsocoromorpha	Schizopteridae	Schizopterinae		UCR_ENT 00116301	UCR	Illumina, PROBE	TBA	TBA	
Pinochius_sp_Cameroon_2196	Dipsocoromorpha	Schizopteridae	Schizopterinae		UCR_ENT 00087540	UCR	Illumina	TBA	TBA	
Pinochius_sp_Bru_138	Dipsocoromorpha	Schizopteridae	Schizopterinae		UCR_ENT 00004807	UCR	Sanger	KF781221	KF781256	
Pinochius_sp_Thai_245	Dipsocoromorpha	Schizopteridae	Schizopterinae		UCR_ENT 00057526	TIGER	Sanger	KF781222	KF781257	
Hoplonannus_craneae_Trinidad_2213	Dipsocoromorpha	Schizopteridae	Schizopterinae	*Corixidea* group	UCR_ENT 00084981	UCR	Sanger	KT272759	KT224610	KT272749
Hoplonannus_paenebrunneus_Trinidad_3466	Dipsocoromorpha	Schizopteridae	Schizopterinae	*Corixidea* group	UCR_ENT 00100834	UCR	Sanger	TBA	TBA	
Hoplonannus_sp_CR_82	Dipsocoromorpha	Schizopteridae	Schizopterinae	*Corixidea* group	UCR_ENT 00004790	UCR	Sanger	KF781209	KF781245	
Hoplonannus_Honduras_1218	Dipsocoromorpha	Schizopteridae	Schizopterinae	*Corixidea* group	UCR_ENT 00081695	UCR	Sanger	MF661993	MF662015	MF662054
Hoplonannus_sp_Arg_1113	Dipsocoromorpha	Schizopteridae	Schizopterinae	*Corixidea* group	UCR_ENT 00082376	UCRC	Sanger		TBA	
Voragocoris_schuhi_254	Dipsocoromorpha	Schizopteridae	Schizopterinae	*Corixidea* group	UCR_ENT 00055624	UCR	Sanger	KF781228	KF781263	
Voragocoris_Peru_206	Dipsocoromorpha	Schizopteridae	Schizopterinae	*Corixidea* group	UCR_ENT 00082340	UCR	Sanger	MF662013	MF662051	MF662089
Corixidea_sp_6683	Dipsocoromorpha	Schizopteridae	Schizopterinae	*Corixidea* group	UCR_ENT 00120065	MTEC	Illumina	TBA	TBA	
Corixidea_sp_Peru_253	Dipsocoromorpha	Schizopteridae	Schizopterinae	*Corixidea* group	UCR_ENT 00057532	UCR	Sanger	TBA	KF781246	
Corixidea_major_USA_3923	Dipsocoromorpha	Schizopteridae	Schizopterinae	*Corixidea* group	UCR_ENT 00012039	FSCA	Sanger	KT272758	KT224611	KT272747
Membracioides_sp_CostaRica_4276	Dipsocoromorpha	Schizopteridae	Schizopterinae	*Corixidea* group	UCR_ENT 00116314	UCR	Sanger	TBA	TBA	
Membracioides_sp_Peru_377	Dipsocoromorpha	Schizopteridae	Schizopterinae	*Corixidea* group	UCR_ENT 00084401	UCR	Sanger	MF661994	MF662016	MF662055
Membracioides_Colombia_478	Dipsocoromorpha	Schizopteridae	Schizopterinae	*Corixidea* group	UCR_ENT 00076304	SHARKEY	Sanger	MF661999	MF662021	MF662060
Membracioides_Colombia_528	Dipsocoromorpha	Schizopteridae	Schizopterinae	*Corixidea* group	UCR_ENT 00076278	SHARKEY	Sanger	MF662000	MF662022	MF662061
Ceratocomboides_sp_Colombia_944	Dipsocoromorpha	Schizopteridae	Schizopterinae		UCR_ENT 00081344	SHARKEY	Sanger	TBA	TBA	
Undescribed_sp_Peru_153	Dipsocoromorpha	Schizopteridae	Schizopterinae		UCR_ENT 00004806	UCR	Sanger		KF781230	
Undescribed_Colombia_3563	Dipsocoromorpha	Schizopteridae	Schizopterinae		UCR_ENT 00106838	SHARKEY	Sanger		TBA	
Undescribed_Peru_460	Dipsocoromorpha	Schizopteridae	Schizopterinae		UCR_ENT 00086128	UCR	Sanger		TBA	
Undescribed_Colombia_3564	Dipsocoromorpha	Schizopteridae	Schizopterinae		UCR_ENT 00106839	SHARKEY	Sanger	TBA	TBA	
Ceratocomboides_sp_Trinidad_1886	Dipsocoromorpha	Schizopteridae	Schizopterinae	*Schizoptera* group	UCR_ENT 00063172	UCR	Illumina	TBA	TBA	
Ceratocomboides_sp6_167_CR	Dipsocoromorpha	Schizopteridae	Schizopterinae	*Schizoptera* group	UCR_ENT 00078258	UCR	Sanger		KX810828	KU315263
cf_Ptenidiophyes_mirabilis_CR_89	Dipsocoromorpha	Schizopteridae	Schizopterinae	*Schizoptera* group	UCR_ENT 00004805	UCR	Sanger	KF781223	KF781258	
Ptenidiophyes_sp2_CostaRica_3391	Dipsocoromorpha	Schizopteridae	Schizopterinae	*Schizoptera* group	UCR_ENT 00014874	INBio	Sanger	KU315251	KX810844	KU315281
Ptenidiophyes_sp_Peru_158	Dipsocoromorpha	Schizopteridae	Schizopterinae	*Schizoptera* group	UCR_ENT 00004803	UCR	Sanger	KF781224	KF781259	
Schizoptera_Odontorhagus_stricklandi_3408_TR	Dipsocoromorpha	Schizopteridae	Schizopterinae	*Schizoptera* group	UCR_ENT 00100780	UCR	Sanger		KX810845	KU315282
Schizoptera_Od_sp_Guat_7521	Dipsocoromorpha	Schizopteridae	Schizopterinae	*Schizoptera* group	UCR_ENT 00127103	UCR	Illumina, PROBE	TBA	TBA	
Schizoptera_Odontorhagus_ansata_4871_Guat	Dipsocoromorpha	Schizopteridae	Schizopterinae	*Schizoptera* group	UCR_ENT 0009170?	FSCA	Sanger	KU315257	KX810855	KU315293
Schizoptera_Odontorhagus_sp_Colombia_923	Dipsocoromorpha	Schizopteridae	Schizopterinae	*Schizoptera* group	UCR_ENT 00081350	SHARKEY	Sanger	MF662011	MF662049	MF662087
Schizoptera_Od_sp_CostaRica_3368	Dipsocoromorpha	Schizopteridae	Schizopterinae	*Schizoptera* group	UCR_ENT 00014779	INBio	Sanger		KX810834	KU315272

Schizoptera_Od_sp_CostaRica_3384	Dipsocoromorpha	Schizopteridae	Schizopterinae	*Schizoptera* group	UCR_ENT 00014888	INBio	Sanger		TBA	
Schizoptera_Od_sp_CostaRica_3385	Dipsocoromorpha	Schizopteridae	Schizopterinae	*Schizoptera* group	UCR_ENT 00014885	INBio	Sanger		KX810837	KU315275
Schizoptera_Lophopleurum_Peru_342	Dipsocoromorpha	Schizopteridae	Schizopterinae	*Schizoptera* group	UCR_ENT 00082350	UCR	Sanger	MF662010	MF662048	
Schizoptera_Lophopleurum_sulcata_3456_TR	Dipsocoromorpha	Schizopteridae	Schizopterinae	*Schizoptera* group	UCR_ENT 00100826	UCR	Sanger	KU315253	KX810849	KU315286
Schizoptera_Lophopleurum_sp24_3458_TR	Dipsocoromorpha	Schizopteridae	Schizopterinae	*Schizoptera* group	UCR_ENT 00100828	UCR	Sanger	KU315254	KX810850	KU315287
Schizoptera_S_sp_CostaRica_3369	Dipsocoromorpha	Schizopteridae	Schizopterinae	*Schizoptera* group	UCR_ENT 00014845	INBio	Sanger		KX810835	KU315273
Schizoptera_sp_Peru_252	Dipsocoromorpha	Schizopteridae	Schizopterinae	*Schizoptera* group	UCR_ENT 00057531	UCR	Sanger	KF781227	KF781262	
Schizoptera_Schizoptera_maxima_3435_TR	Dipsocoromorpha	Schizopteridae	Schizopterinae	*Schizoptera* group	UCR_ENT 00100830	UCR	Sanger		KX810847	KU315284
Schizoptera_Schizoptera_sp_Colombia_632	Dipsocoromorpha	Schizopteridae	Schizopterinae	*Schizoptera* group	UCR_ENT 00077905	SHARKEY	Sanger	MF662012	MF662050	MF662088
Schizoptera_Zygophleps_ultima_3445_TR	Dipsocoromorpha	Schizopteridae	Schizopterinae	*Schizoptera* group	UCR_ENT 00102132	UCR	Sanger	KU315252	KX810848	KU315285
Schizoptera_Z_sp_Peru_410	Dipsocoromorpha	Schizopteridae	Schizopterinae	*Schizoptera* group	UCR_ENT 00086122	UCR	Sanger	KU315255	KX810853	KU315291
Schizoptera_sp_Peru_159	Dipsocoromorpha	Schizopteridae	Schizopterinae	*Schizoptera* group	UCR_ENT 00057522	UCR	Sanger	KF781226	KF78126	
Schizoptera_sp_6303	Dipsocoromorpha	Schizopteridae	Schizopterinae	*Schizoptera* group	UCR_ENT 00101323, UCR_ENT 00126705, UCR_ENT 00126706, UCR_ENT 00126707, UCR_ENT 00126708	FMNH	Sanger		TBA	
Schizoptera_Kophaegis_similis_2627_Cub	Dipsocoromorpha	Schizopteridae	Schizopterinae	*Schizoptera* group	UCR_ENT 00088107	UCR	Sanger	KU315245	KX810833	KU315269
Schizoptera_Od_sp_Cuba_2625	Dipsocoromorpha	Schizopteridae	Schizopterinae	*Schizoptera* group	UCR_ENT 00088105	UCR	Sanger	KU315244	KX810832	KU315268
Dundonannus_sp_Cameroon_2634	Dipsocoromorpha	Schizopteridae	Schizopterinae	*Dundonannus* group	UCR_ENT 00084186	UCR	Sanger		TBA	
Dundonannus_sp_Cameroon_2260	Dipsocoromorpha	Schizopteridae	Schizopterinae	*Dundonannus* group	UCR_ENT 00077099	UCR	Illumina	TBA	TBA	
nr_Semanganannus_Thailand_1426	Dipsocoromorpha	Schizopteridae	Schizopterinae	*Dundonannus* group	UCR_ENT 00081642	TIGER	Sanger	TBA	TBA	
Vilhenannus_sp_Cameroon_7320	Dipsocoromorpha	Schizopteridae	Schizopterinae	*Dundonannus* group	UCR_ENT 00124956	UCR	Sanger	TBA	TBA	
Machadonannus_sp_7055	Dipsocoromorpha	Schizopteridae	Schizopterinae	*Dundonannus* group	UCR_ENT 00125913	SAMC	Illumina	TBA	TBA	
Chinannus_monteverdensis_CostaRica_4256	Dipsocoromorpha	Schizopteridae	Ogeriinae		UCR_ENT 00116293	UCR	Sanger		KT272721	KT272738
Chinannus_bierigi_CR_80	Dipsocoromorpha	Schizopteridae	Ogeriinae		UCR_ENT 00004804	UCR	Sanger	KF781208	KF781243	
Chinannus_nicaraguensis_Nicaragua_6280	Dipsocoromorpha	Schizopteridae	Ogeriinae		UCR_ENT 00101300	FMNH	Sanger		KT272724	KT272734
Chinannus_communis_Colombia_508	Dipsocoromorpha	Schizopteridae	Ogeriinae		UCR_ENT 00076302	SHARKEY	Sanger		KT272719	KT272735
Chinannus_translucidus_Ecuador_127	Dipsocoromorpha	Schizopteridae	Ogeriinae		UCR_ENT 00078169	UCR	Sanger	KT272756	KT272746	KT272723
Chinannus_trinitatis_Trinidad_1915	Dipsocoromorpha	Schizopteridae	Ogeriinae		UCR_ENT 00088673	UCR	Illumina	TBA	TBA	
Chinannus_duopaxillatus_FG_46	Dipsocoromorpha	Schizopteridae	Ogeriinae		UCR_ENT 00004808	UCR	Sanger		KF781244	
Peloridinannus_Peru_269	Dipsocoromorpha	Schizopteridae	Ogeriinae		UCR_ENT 00044295	UCR	Illumina	TBA	TBA	
Ogeriinae_Cameroon_2203	Dipsocoromorpha	Schizopteridae	Ogeriinae		UCR_ENT 00087547	UCR	Illumina	KT272763	KT224613	KT272754
Ogeriinae_Cameroon_2630	Dipsocoromorpha	Schizopteridae	Ogeriinae		UCR_ENT 00088114	UCR	Illumina	KT272764	KT224612	KT272755
Ogeriinae_CostaRica_3363	Dipsocoromorpha	Schizopteridae	Ogeriinae		UCR_ENT 00014813	INBio	Illumina	TBA	TBA	
Hypsipteryx_sp_Thailand_4207	Dipsocoromorpha	Hypsipterygidae			UCR_ENT 00112812	TIGER	Illumina	TBA	TBA	
Trichotonannus_sp_Cameroon_6511	Dipsocoromorpha	Ceratocombidae	Trichotonanninae		UCR_ENT 00120713	UCR	Illumina, PROBE	TBA	TBA	

Trichotonannus_sp_Thailand_7233	Dipsocoromorpha	Ceratocombidae	Trichotonanninae		UCR_ENT 00123595	TIGER	Sanger	TBA	TBA
Stemmocrypta_antennata	Dipsocoromorpha	Stemmocryptidae			N/A	N/A	No sequence	N/A	N/A

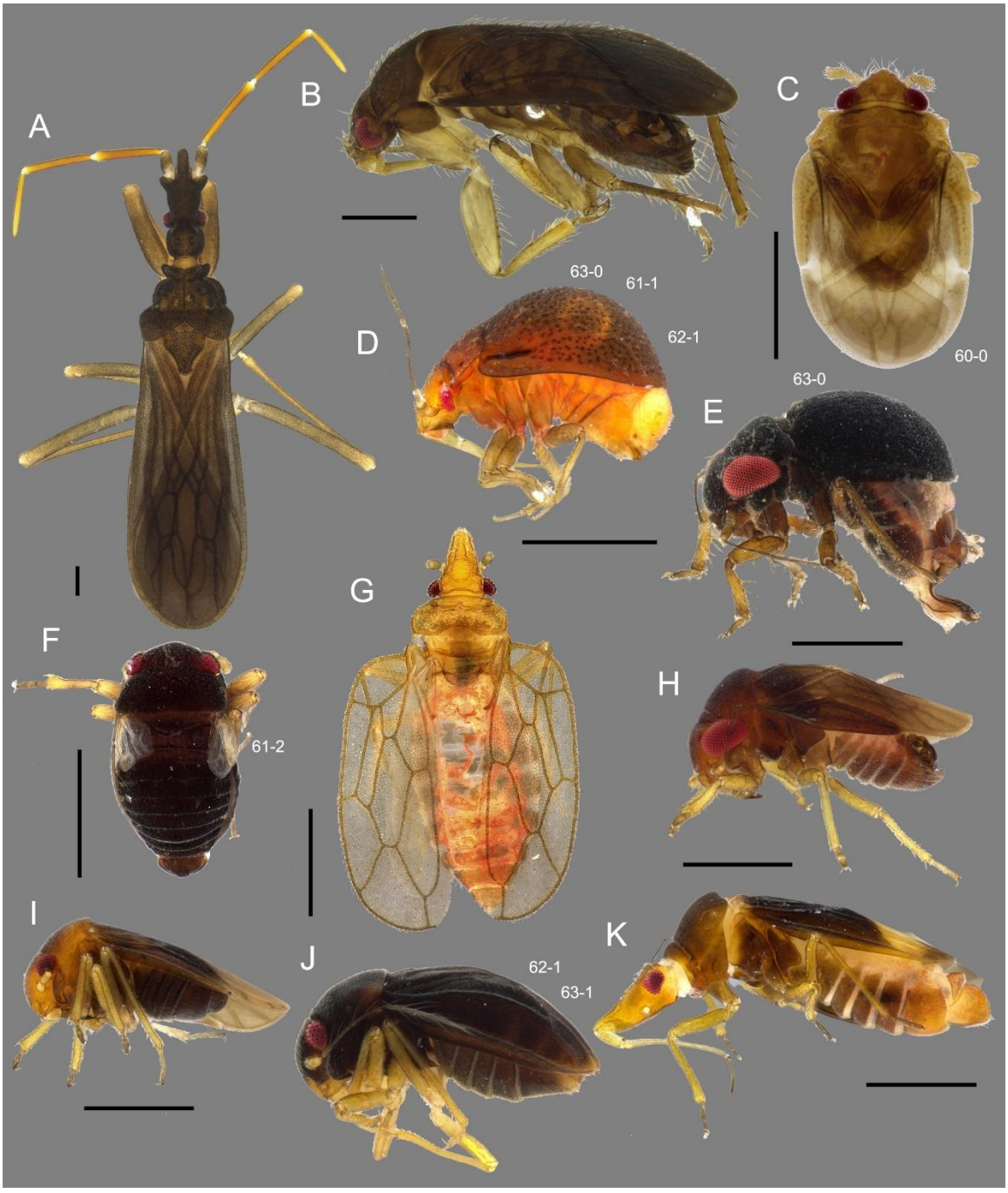
A
B
C
63-0
61-1
D
62-1
60-0
63-0
E
G
F
61-2
H
I
J
62-1
63-1
K

Figure 6.1. Habitus of Enicocephalomorpha and Dipsocoromorpha. A, Enicocephalidae (U16), dorsal view; B, *Trichotonannus* sp. (ED 7233), male, lateral view; C, Issidomimini (ED 6813), male, dorsal view; D, cf. *Kvamula-Seychellesanus* sp. (ED 2043), female, lateral view; E, *Hypselosoma* sp. (ED 3024), female, lateral view; F, cf. *Ogeria insularis* (ED 2085) female, dorsal view; G, Hypsipterigidae (ED 4207), female, dorsal view; H, *Hypselosoma* sp. (ED 2396), male, lateral view; I, cf. *Dundonannus* sp. (ED 2260), male, lateral view; J, *Schizoptera* (*Cantharocoris*) sp. (ED 3458), female, lateral view; K, *Nannocoris* sp. (ED 349), male, lateral view.

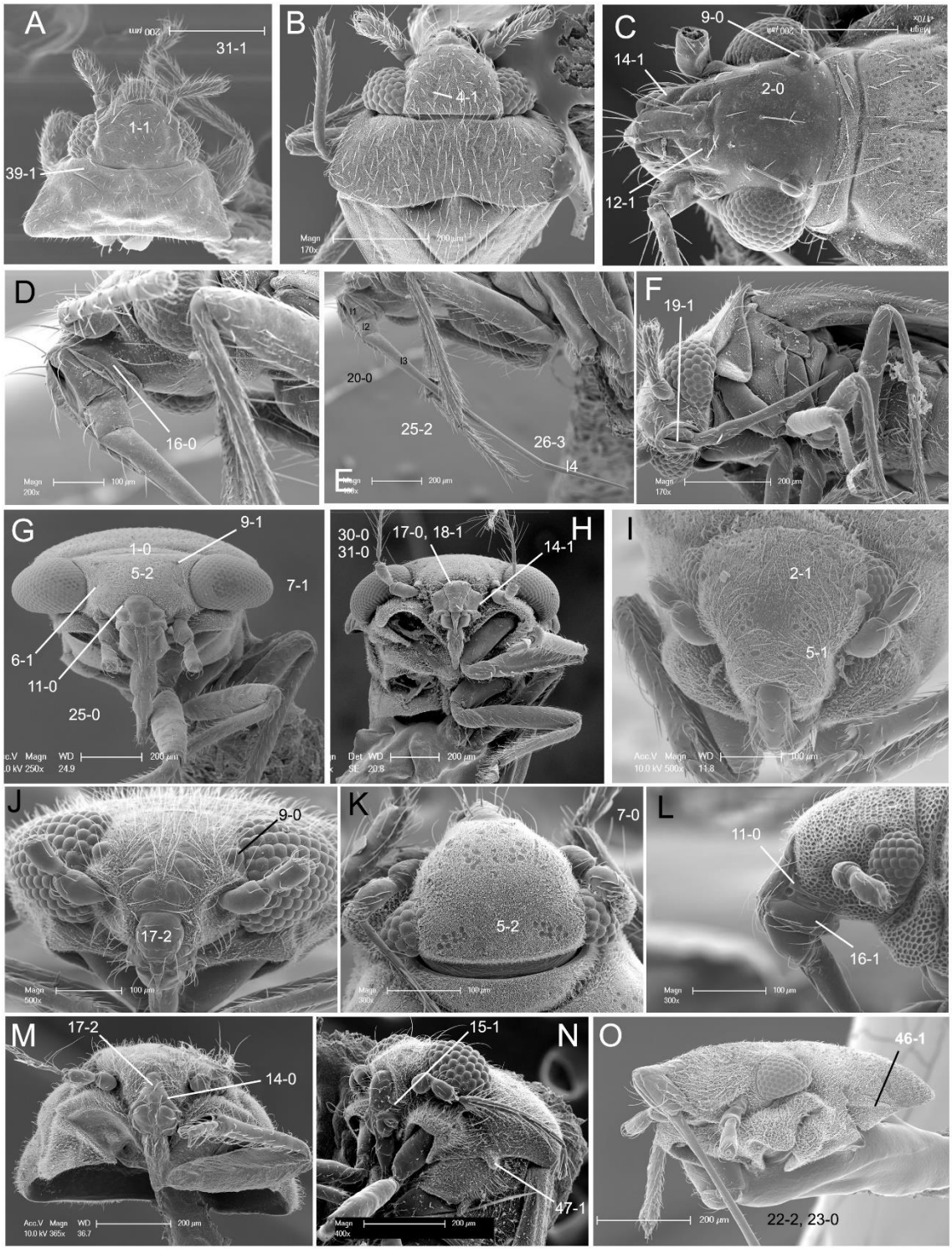
A
31-1
1-1
39-1
B
4-1
C
9-0
14-1
2-0
12-1
D
16-0
E
I1
I2
I3
20-0
25-2
26-3
I4
F
19-1
G
9-1
1-0
5-2
7-1
6-1
11-0
25-0
H
30-0
31-0
17-0, 18-1
14-1
I
2-1
5-1
J
9-0
17-2
K
7-0
5-2
L
11-0
16-1
M
17-2
14-0
N
15-1
47-1
O
46-1
22-2, 23-0

Figure 6.2. Scanning electron micrographs of selected morphological features. A, *Cryptostemma* sp., head and pronotum, dorsal view; B, *Kvamula* sp. (ED 6927), head and pronotum, dorsal view; C, *Leptonannus* sp. (ED 6781), head and pronotum, dorsal view; D, *Leptonannus* sp. (ED 6781), head, lateral view; E, *Leptonannus* sp. (ED 6781), labium and foreleg, lateral view; F, *Muatianvuaia* sp. (ED 6957), head and thorax, lateroventral view; G, *Rectilamina* sp. (ED 1451), head and prothorax, frontal view; H, *Hypselosoma* sp. (ED 5075), head and thorax, ventrofrontal view; I, *Kokeshia* sp. (ED 1416), head, frontal view; J, *Pinochius* sp. (ED 244), head, frontal view; K, *Ogeria* sp. (ED 4182), head and pronotum, dorsal view; L, near *Ceratocomboides* sp. (ED 790), head, lateral view; M, *Guapinannus* sp. (ED 5470), head and prothorax, ventrofrontal view; N, *Schizoptera* sp. (ED 496), head and thorax, lateral view; O, *Nannocoris* sp. (ED 6300), head and thorax, lateral view.

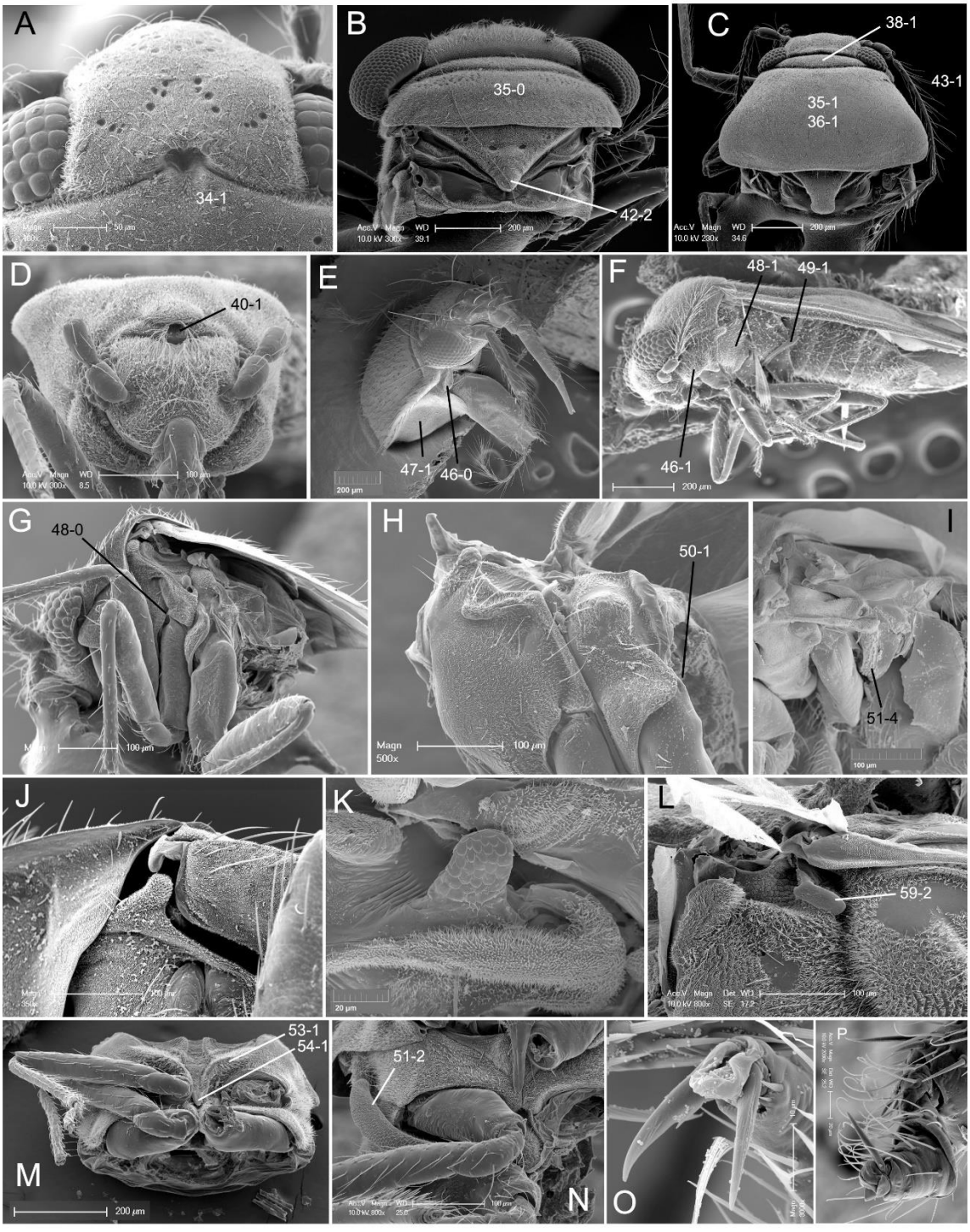
A
34-1
B
35-0
42-2
C
38-1
43-1
35-1
36-1
D
40-1
E
47-1
46-0
F
48-1
49-1
46-1
G
48-0
H
50-1
I
51-4
J
K
L
59-2
M
53-1
54-1
N
51-2
O
P

Figure 6.3. Scanning electron micrographs of selected morphological features. A, *Kaimon* sp. (ED 7203), head and pronotum, dorsal view; B, *Glyptocombus* sp. (ED 171), head and pronotum, dorsal view; C, *Odontorhagus* sp. (ED 2307), head and pronotum, dorsal view; D, Undescribed genus (ED5276), head and prothorax, frontal view; E, *Trichotonannus* sp., head and prothorax, lateral view; F, *Odontorhagus* sp. (ED 535), habitus, lateral view; G, *Kvamula* sp. (ED 6927), head and thorax, lateral view; H, *Pinochius* sp. (ED 244), meso- and metathorax, lateral view; I, *Cryptostemma* sp. (ED 3869), meso- and metathorax, lateral view; J, *Leptonannus* sp. (ED 6781), wing-to-thorax coupling structure; K, *Ceratocombus* sp. (ED 474), wing-to-thorax coupling structure; L, *Kokeshia* sp. (ED 1415), wing-to-thorax coupling structure; M, *Nannocoris* sp. (ED 6300), meso- and metathorax, ventral view; N, *Dundonannus* sp. (ED 2193), meso- and metathorax, ventral view; O, *Muatianvuaia* sp. (ED 6957), male, pretarsus of mid leg; P, *Hypselosoma* sp. (ED 5075), male, pretarsus of foreleg.

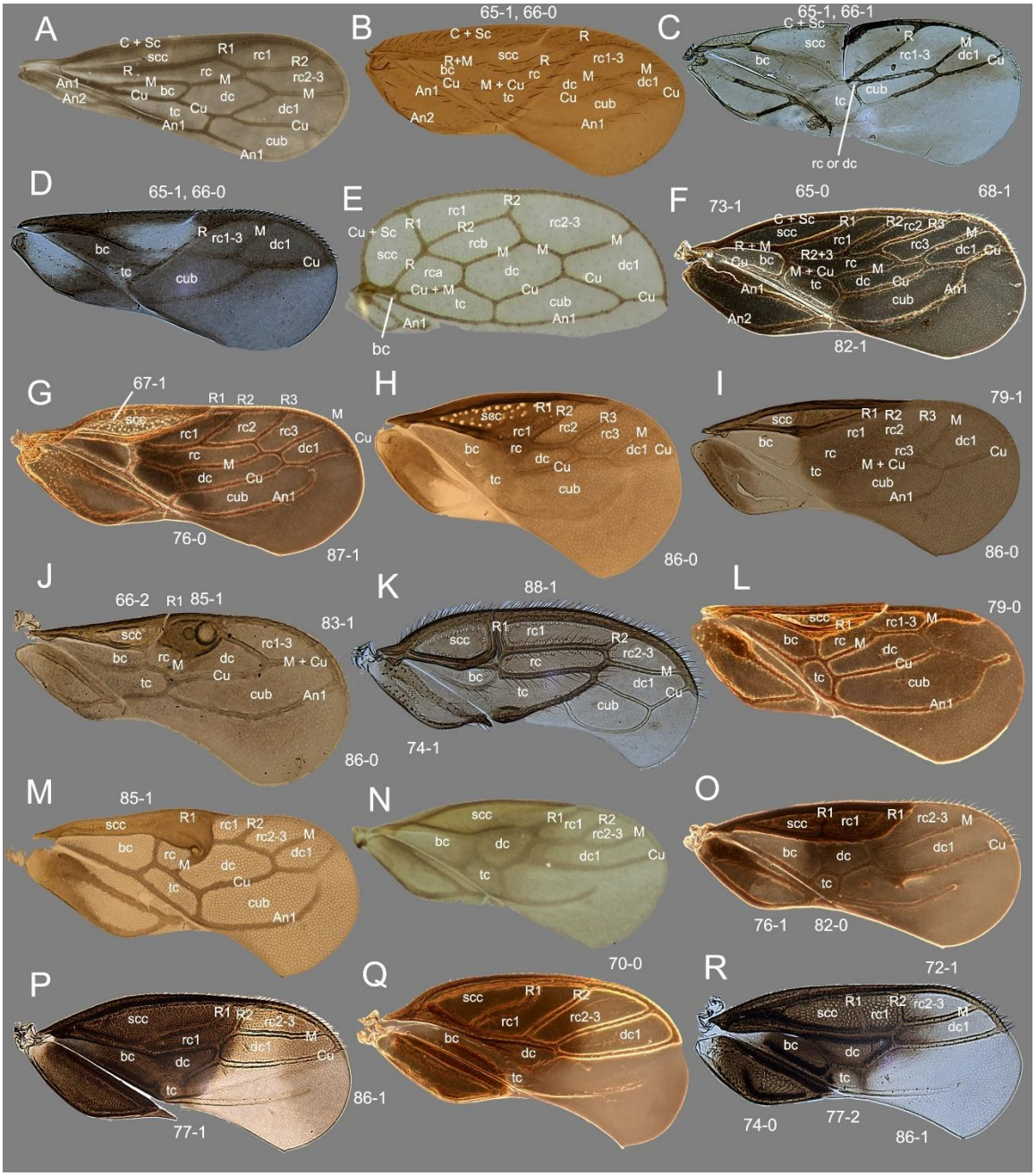

Figure 6.4. Right forewing of selected Enicocephalomorpha and Dipsocoromorpha. A, Enicocephalidae sp.; B, *Trichotonannnus* sp. (ED 6511); C, *Cryptostemma* sp. (ED 5470); D, *Ceratocombus* sp. (ED 3009); E, *Hypsipteryx ugandensis*; F, *Glyptocombus* sp. (ED 3213); G, *Rectilamina* sp. (ED 1451); H, Undescribed genus (ED 2630); I, Undescribed genus (ED 3363); J, Undescribed genus (ED 633); K, *Guapinannus* sp. (ED 5472); L, *Kokeshia* sp. (ED 1409); M, *Ogeria* sp. (ED 1560); N, *Dundonannus chiumbensis* (BMNH (E) 1496258); O, *Corixidea* sp. (ED 380); P, *Nannocoris* sp. (ED 381); Q, Pinochius sp. (ED 302); R, Schizoptera sp. (ED 923).

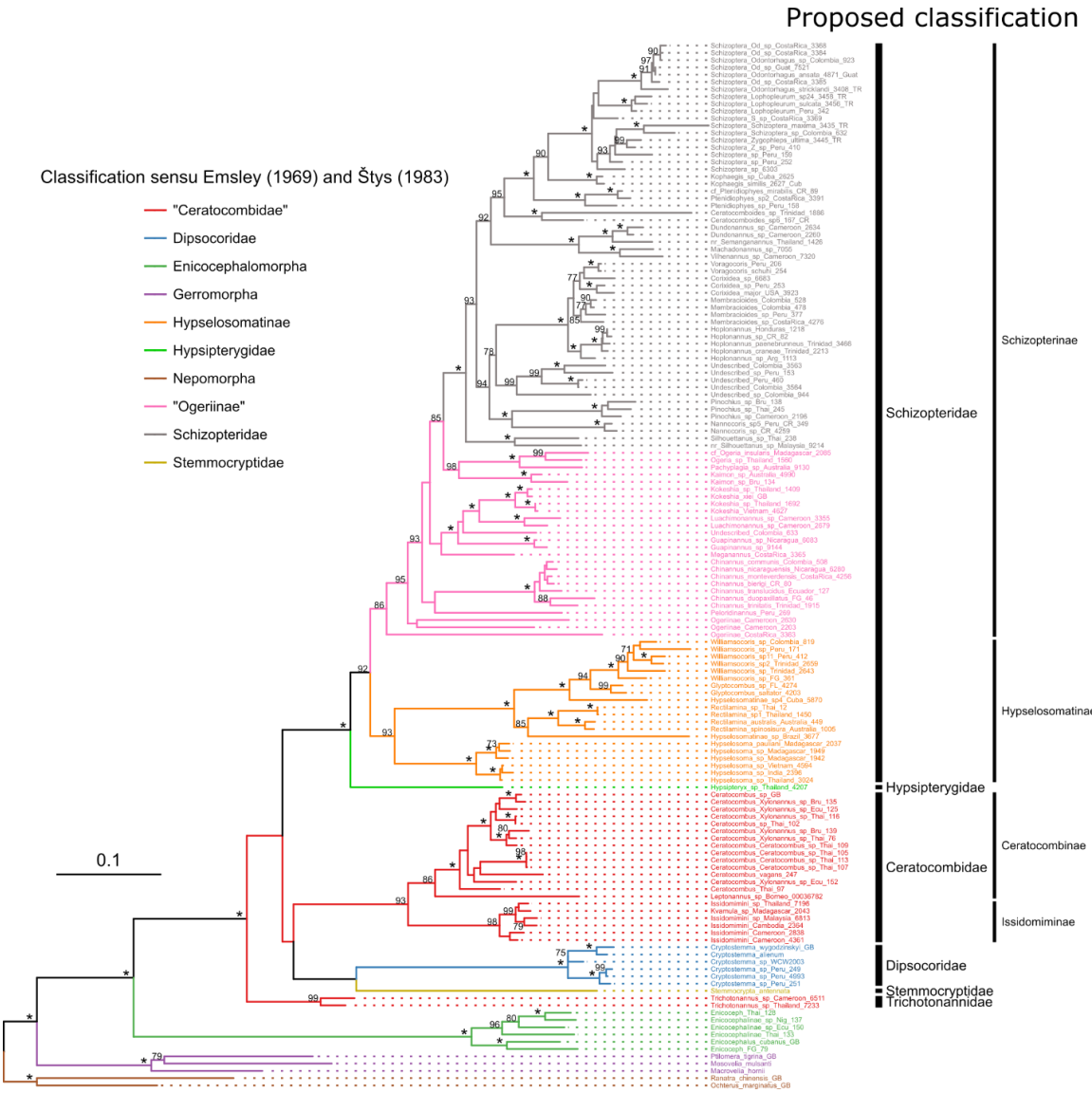

Figure 6.5. Phylogenetic reconstruction produced by a maximum likelihood analysis of the combined dataset in RAxML. Numbers at nodes indicate Rapid Bootstrap support, asterisk denotes full support, values below 70 not shown. Old classification is provided in color, with legend shown on the figure. New classification is annotated on the right.

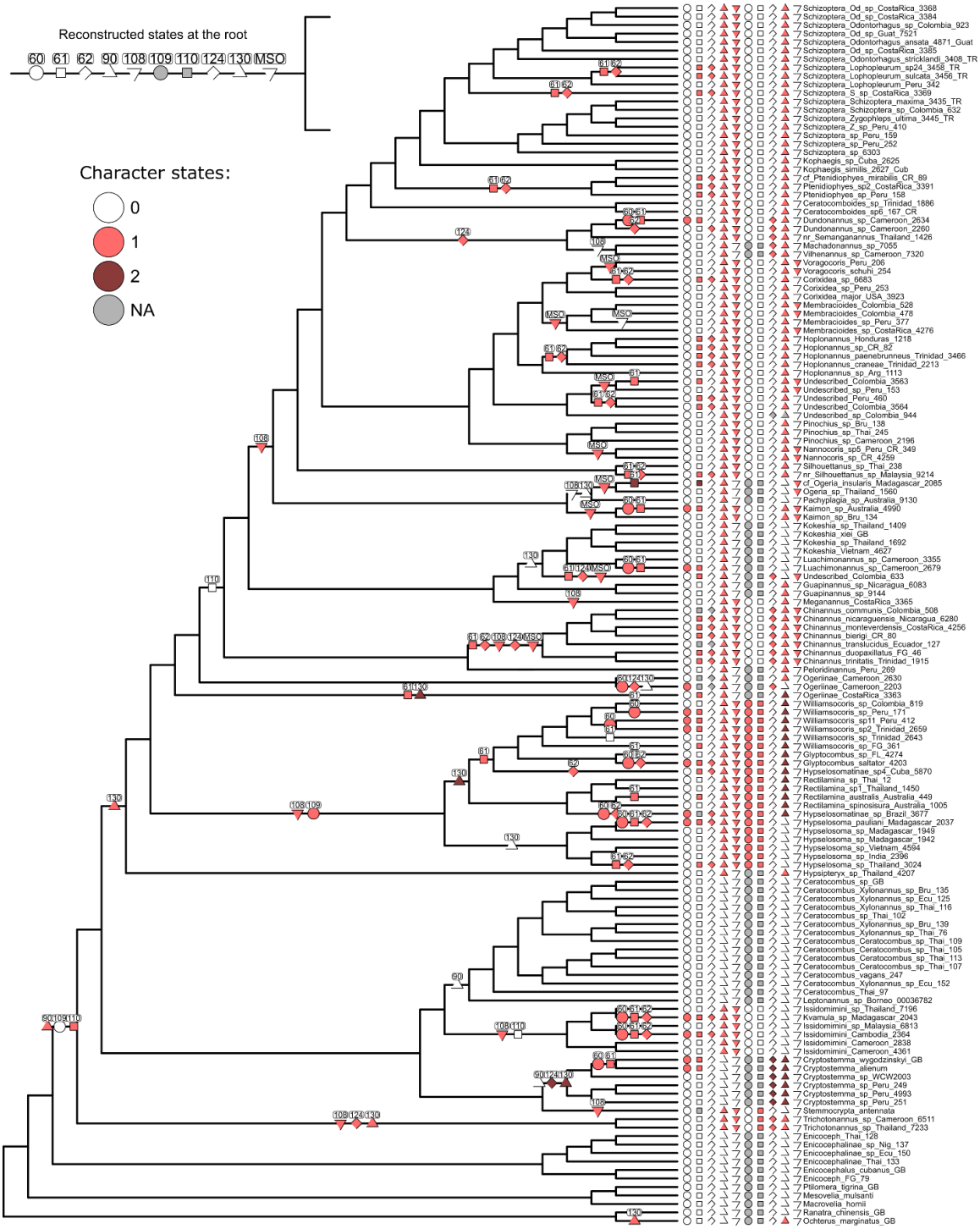

Figure 6.6. Results of the maximum likelihood ancestral state reconstruction of selected characters. Matrix of symbols on the right indicates states of terminal taxa, corresponding symbols with numbers on the phylogeny indicate reconstructed shifts.

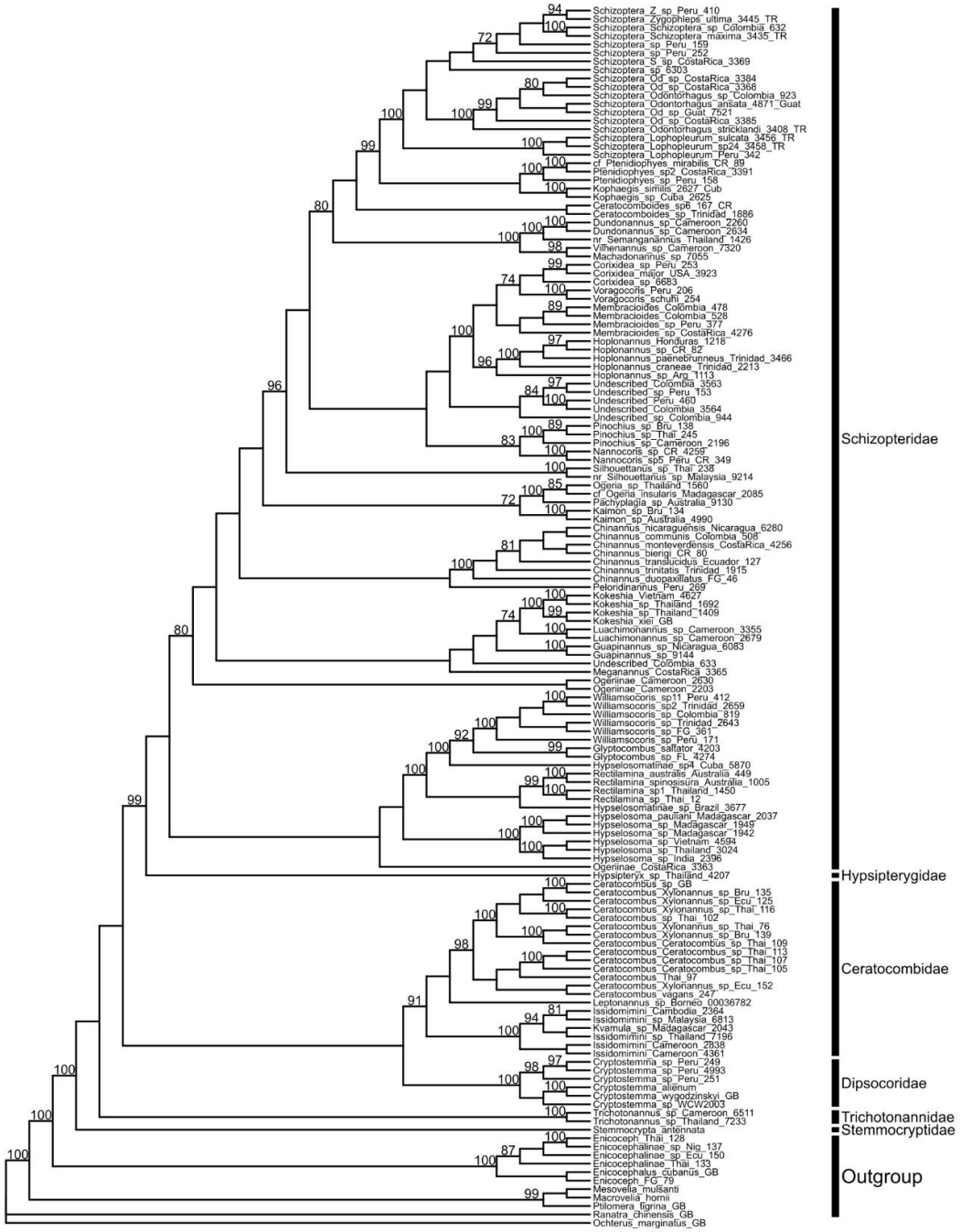

Figure 6.S1. Phylogenetic reconstruction produced by a parsimony analysis of the combined dataset in TNT. Numbers at nodes indicate bootstrap support, values below 70 not shown. New classification is annotated on the right.

Conclusion

The research done as part of this dissertation greatly improved our knowledge of the comparative morphology, phylogenetic relationships, taxonomy, and biodiversity of Dipsocoromorpha. A cost-efficient method of sequencing museum material was first tested on insects and employed to sample DNA of rarely collected minute litter bugs, greatly improving confidence in phylogenetic hypotheses generated for the *Corixidea* genus group, as well as Dipsocoromorpha as a while. Using extensive genetic datasets, phylogenetic hypotheses were proposed at shallow levels for the genus *Chinannus* and the *Corixidea* genus group, as well as on a deep level for the entire infraorder Dipsocoromorpha. Two taxonomic projects, guided by phylogenetic inference, revised two genera of Dipsocoromorpha, *Chinannus* and *Voragocoris*. Finally, the comparative study of abdominal morphology was conducted to standardize terminology and provide data for phylogenetic reconstructions and taxonomic revisions.